Tertiary tectonics and uplift of the Inner Moray Firth and adjacent areas.

Kenneth Thomson

Doctor of Philosophy
The University of Edinburgh
1993

EX BIBL. UNIV. EDINBURGH

Declaration

This thesis has been composed solely by myself. The work presented is my own except for parts of the following chapters which were jointly produced with assistance from Dr J.R. Underhill (The University of Edinburgh; Chapters 2 and 7), Dr R.R. Hillis (University of Adelaide; Chapter 3) and Dr P.F. Green and Dr R.J. Bray (Geotrack International; Chapter 4).

K. Thomson.

Contents.

Abstract. 1

Acknowledgements. 3

1. Introduction. 4

1.1 Project justification and aims. 4

1.2 Structure of the thesis. 11

1.3 Project area: a geological summary. 12

1.4 History of research in the area. 14

1.4.1 The Devonian Orcadian Basin. 14

1.4.2 The Inner Moray Firth. 14

1.4.3 The Great Glen Fault. 16

1.4.4 Uplift and erosion research. 17

1.5 Summary of the potential causes of uplift, erosion and tectonic reactivation. 19

1.5.1 Compressional mechanisms. 19

1.5.2 North Atlantic rifting mechanisms. 22

1.6 The mid-late Danian unconformity. 27

1.7 Uplift and erosion; a clarification of the terminologyand principles used. 27b

1.8 Conclusions. 28

2. Pre-Cenozoic geology. 29

2.1 Introduction. 29

2.2 Pre-Devonian geology. 29

2.3 Devonian Orcadian Basin. 33

2.4 Permo-Carboniferous ("Variscan") inversion. 35

2.5 Permo-Triassic extension. 41

2.6 Late Permian, Early Triassic and Early Jurassic thermal subsidence. 43

2.7 Toarcian-Aalenian regional uplift and Aalenian-Oxfordian thermal subsidence. 43

2.8 Upper Jurassic rifting. 47

2.9 Cretaceous thermal subsidence. 47

2.10 Cenozoic evolution of the Inner Moray Firth. 51

2.11 Conclusions. 51

3. Estimation of uplift and erosion using sonic velocity data. 53

3.1 Introduction. 53

3.2 Principles of compaction state as a measure of uplift and erosion. 53

3.3 Historical development of the methodology. 55

3.3.1 Stratigraphic unit selection. 55

3.3.2 Normal compaction relations. 57

3.3.3 Estimation of uplift and erosion. 60

3.4 Porosity-depth relations in the Hod, Tor and Kimmeridge Clay Formations. 60

3.5 Selection of stratigraphic units. 66

3.6 Selection of logging tool for compaction analysis. 68

3.7 Determination of apparent erosion. 75

3.8 Comparison of apparent erosion estimates 76

3.9 Patterns of apparent erosion. 81

3.10 Conclusions. 83

4. Estimation of uplift and erosion using apatite fission track analysis. 85

4.1 Introduction. 85

4.2 Principles of apatite fission track anlysis. 85

4.2.1 Apatite fission track dating. 85

4.2.2 Track length distributions and thermal history analysis. 88

4.3 Previous apatite fission track analyses of the Scottish Highlands. 92

4.4 Sample details and fission track analysis results. 100

4.5 Fission track ages and track lengths. 105

4.6 Fission track modelling results, Late-Cretaceous/Early Tertiary palaeotemperatures and erosion estimates. 108

4.7 Conclusions. 113

5. Estimation of uplift and erosion using geochemical analyses. 114

5.1 Introduction. 114

5.2 Vitrinite reflectance studies. 114

5.2.1 The vitrinite reflectance trend method. 114

5.2.2 Vitrinite reflectance modelling. 129

5.2.3 Onshore vitrinite reflectance evidence. 160

5.3 Evidence from biological marker molecules. 164

5.4 Clay mineralogical evidence. 176

5.5 Conclusions. 179

6. Comparison and implications of uplift estimates. 180

6.1 Introduction. 180

6.2 Comparison of erosion estimates, apparent versus total erosion. 180

6.3 Tectonic uplift versus erosion. 188

6.4 Implications for sediment decompaction and maturation modelling. 190

6.5 Implications for the burial history of the Inner Moray Firth. 191

6.6 Upper Cretaceous Chalk distribution, thermal subsidence history and basin formation models: the implications of erosion estimates. 192

6.7 Conclusions. 194

7. Tertiary structural reactivation. 196

7.1 Introduction. 196

7.2 Extensional reactivation. 196

7.3 Inversion. 202

7.4 Strike-slip reactivation: the Great Glen Fault. 207

7.5 Strike-slip reactivation: the Sutherland Terrace-Helmsdale Fault-Great Glen Fault system. 214

7.6 Regional tilting of the Inner Moray Firth. 229

7.7 Conclusions. 234

8. Potential driving mechanisims to account for structural reactivation, uplift and erosion. 236

8.1 Introduction. 236

8.2 Regional tectonic Setting. 237

8.3 Potential mechanisms. 244

8.3.1 The Iceland "hot-spot", its inflation and collapse. 244

8.3.2 North Atlantic rifting. 248

8.3.3 North Atlantic igneous activity, volcanic over/underplating. 250

8.3.4 Two-layer lithospheric compression. 250

8.3.5 Intraplate stress. 251

8.4 Discussion. 252

8.4.1 North Atlantic phenomena. 252

8.4.2 Compressional tectonics. 254

8.5 Summary of the evidence for the timing of structural reactivation, uplift and erosion in the Inner Moray Firth and Scottish Highlands. 257

8.6 Conclusions. 258

9. Summary and conclusions. 260

9.1 Introduction. 260

9.2 Summary of the findings. 260

9.2.1 Compaction analysis. 260

9.2.2 Apatite fission track analysis. 261

9.2.3 Geochemical analyses. 262

9.2.4 Structural analyses. 263

9.2.5 Tectonic uplift and the extensional origin of the Inner Moray Firth: implications of the uplift and erosion data. 264

9.2.6 Potential causes and timing of the phenomena. 265

9.3 Unresolved issues and recommendations for future research. 266

References. 269

Appendix.

Copy of paper "Controls on the development and evolution of structural styles in the Inner Moray Firth Basin." by K. Thomson and J.R. Underhill. (1993). *In:* Parker, J.R. (ed): *Petroleum Geology of North West Europe.* Geological Society, London, 1167-1178.

Abstract.

The latest Cretaceous and Tertiary saw a significant change in the tectonic regime of northwestern Europe. North Atlantic rifting over the Iceland "hot-spot" to the northwest resulted in the total separation of North America from Europe by the mid-Miocene while to the southeast the closure of the Tethyan Ocean resulted in the Alpine Orogeny which culminated by the Pliocene. Contemporaneous with these events many of the pre-existing Mesozoic basins of northwestern Europe experienced tectonic reactivation characterised by dip-slip inversion, while regional uplift of both basins and massif areas occurred.

Seismic reflection profiles and field studies indicate that the Inner Moray Firth experienced tectonic reactivation during the Tertiary, although the precise dating remains uncertain. Extensional reactivation of the pre-existing half graben bounding faults and the formation of new extensional features such as the faults forming the Sinclair Horst was the most common form of reactivation. The Great Glen Fault shows structures indicative of dextral strike-slip motion. This dextral movement combined with sinistral motion on the Helmsdale Fault resulted in the folding seen in the Sutherland Terrace (the area between the two faults) as a result of space problems. Minor inversion folds with their associated short-cut faults can also be found within the basin and attest to a period of compression. Probably the most regionally important structure within the basin is the eastward dipping mid-late Danian unconformity which provides evidence for a period of uplift and erosion in the area prior to the deposition of Cenozoic sediments.

Apatite fission track analysis of the Scottish Highlands shows that samples currently at surface experienced elevated palaeotemperatures and consequently must have been uplifted and eroded from their maximum burial-depth. Furthermore, the uplift and erosion appears to have been initiated in the Late Permian/Early Triassic, increasing in rate during the Late Cretaceous/Early Tertiary and resulting in up to 2km of post-Mesozoic erosion. Similarly, in the Inner Moray Firth compaction and geochemical analyses indicate that the Mesozoic sediments of the area have been exhumed from their maximum burial-depth by as much as 1km since the Mesozoic. Such large volumes of Cretaceous thermal subsidence deposits having been present in the basin, combined with the knowledge that the crust is thinned, implies that the recent extensional model for the formation of the basin is correct and that the earlier strike-slip model can be discounted.

Although the exact timing of some of these events is difficult to assess it appears likely that the Late Cretaceous/Early Tertiary increase in exhumation rates over the Scottish Highlands and the tectonic reactivation of the Inner Moray Firth were a direct result of the large topographic anomaly associated with the evolving mantle plume during the early stages of North Atlantic rifting and the isostatic response of thickening the crust with the associated igneous products. However, such a model cannot account for the Inner Moray Firth as, if the uplift and erosion which has been measured occurred at the mid-late Danian unconformity (a surface where some erosion obviously occurred), rapid subsidence would be required immediately before uplift in order to achieve maximum burial-depth. For the same reason differential compression of the crust and lithosphere at this time seems to be an unreasonable proposition. However, such a mechanism could potentially work if the uplift and erosion in the Inner Moray Firth occurred in the Neogene in response to changes in the spreading direction of the North Atlantic Ocean and the tectonic regime in the Alps as no rapid subsidence prior to uplift would be required. Consequently, as the flexural effects due to fluctuations in the level of intraplate stresses also appear incompatible with the data, being an order of magnitude too small and producing the wrong pattern of regional uplift, it appears possible that the Scottish Highlands and adjacent Inner Moray Firth experienced differing tectonic histories during the Cenozoic. However, until more work is carried out to confirm the magnitudes and timings of these events both within the Scottish Highlands, Inner Moray Firth and other areas the exact histories and mechanisms to produce the observed effects remain open to question.

Acknowledgements.

Like any project much is owed to the support of others and I hope that I do justice to everyone involved. Firstly, I would like to thank my supervisors John Underhill and Roger Scrutton as without them this project may not have proceeded as it did. By introducing me to Richard Hillis and Paul Green and Richard Bray of Geotrack International they initiated the major turning point in the project. Richard Hillis must be considered a major factor in this project as without him the estimation of uplift and erosion would have remained a small part of the work. Paul Green and Richard Bray of Geotrack International need to be thanked as they have provided me with a method to bring the uplift and erosion story of the Scottish Highlands into the project and recently agreed to process samples from Greenland for which Andrew Whitham and Simon Price of the Cambridge Arctic Shelf Programme must also be thanked as I collected the samples as part of their expedition. Mike Summerfield must also be thanked for his interest and for revealing to me how tectonics and apatite fission track analysis fit in with geomorphology. The vitrinite reflectance work carried out in this project would not have appeared if it were not for meeting with James Illiffe and the members of the Petroleum Science and Technology Institute's Project Hedera. Our discussion resulted in them allowing me to use their software and thereby saved me valuable time as I grappled with the complexities of writing my own programme. In addition, the conversations I had with John Marshall and Iain Scotchman on the subject must be noted as they saved me from making serious errors. Various members of the Department must also be thanked, particularly Sarah Prosser for bringing to my attention the facts about compaction synclines and for keeping the workstation running. John Dixon, Roger Hipkin and Paul Caban are thanked for their interest while particular thanks must go to Kevin Stephen, Jon Turner, Richard Davies, Jo Fleming, Chris Kay and Neil McMahon who have provided invaluable support. Shane Voss and Ian Chisholm are thanked for their assistance with the computing facilities. Shell UK Expro, Esso, Unocal, Arco, Mobil, Halliburton, Shelf Exploration, British Petroleum and GECO are acknowledged for their release of data. The British Geological Survey are thanked for extensive logistical support, in particular access to the BGS "Wellog" software and considerable help in using it from Chris J. Evans. Dick Sutherland and Martyn Stoker (British Geological Survey) are also thanked for their help. Finally, this project would not have been possible without the financial support of a Shell/Esso Studentship and the support of Larry Wakefield, Griff Cordey and Ceri Powell throughout the course of the project.

1. Introduction.

1.1 Project justification and aims.

With the rapid expansion of petroleum exploration in the North Sea and adjacent areas from the 1970s onwards it was recognised that significant tectonic reactivation of the Mesozoic basins occurred at various times during the Cenozoic. The majority of this activity was dominated by inversion of pre-existing half-grabens and uplift of intrabasinal highs (e.g. Glennie and Boegner, 1981; Cartwright, 1989; Ziegler, 1987a and b; Naylor *et. al.*, 1993; Knipe, 1993; Hinz *et. al.*, 1993; Booth *et. al.*, 1993; Boldreel and Andersen, 1993; Gowers *et. al.*, 1993; Arthur, 1993; Oudmayer and Jager, 1993). The timing of these inversion episodes revealed that, although not all the basins were active at the same times, a significant degree of synchroneity of inversion episodes existed between the basins (Ziegler, 1987a and b; **Figure 1.1**). These times corresponded to the boundaries between the tectonosequences forming the Cenozoic fill of the Northern and Central North Sea (Galloway *et. al.*, 1993). The synchroneity of these events led to the suggestion that specific plate wide events may have been the cause (e.g. Beach, 1987; Hillis, 1992; Cloetingh et. al., 1985).

During the 1980s attention was also paid to the detailed quantification of burial and exhumation histories of basins within the North Sea and their surrounding structural highs. Examination of the extent of diagenesis, compaction and organic maturation revealed that the Mesozoic sediments over large areas of the North Sea and adjacent regions are currently not at their maximum burial-depth and consequently uplift and erosion must have occurred at some time during the Cenozoic (Glennie and Boegner, 1981; Cope, 1986; Cornford, 1986; Bulat and Stoker, 1987; Hillis, 1988; Hardman *et. al.*, 1993; Knipe *et. al.*, 1993; **Figure 1.2**). In addition, the advent of apatite fission track analysis suggested that kilometres of section had been removed from the British mainland during the Cenozoic with both shelf and "massif" areas affected (Green, 1986, 1989; Bray *et. al.*, 1992; Lewis *et. al.*, 1992a and b; Green *et. al.*, 1993; **Figure 1.3**).

Although the Cenozoic structural evolution of most of the North Sea basins had been deduced by the end of the 1980s, little attention had been paid to the Inner Moray Firth. However, as uplift and erosion of parts of the North Sea and adjacent areas had been recognised, the Inner Moray Firth presented itself as a candidate for such a study as only Mesozoic and older sediments are found at seabed, possibly

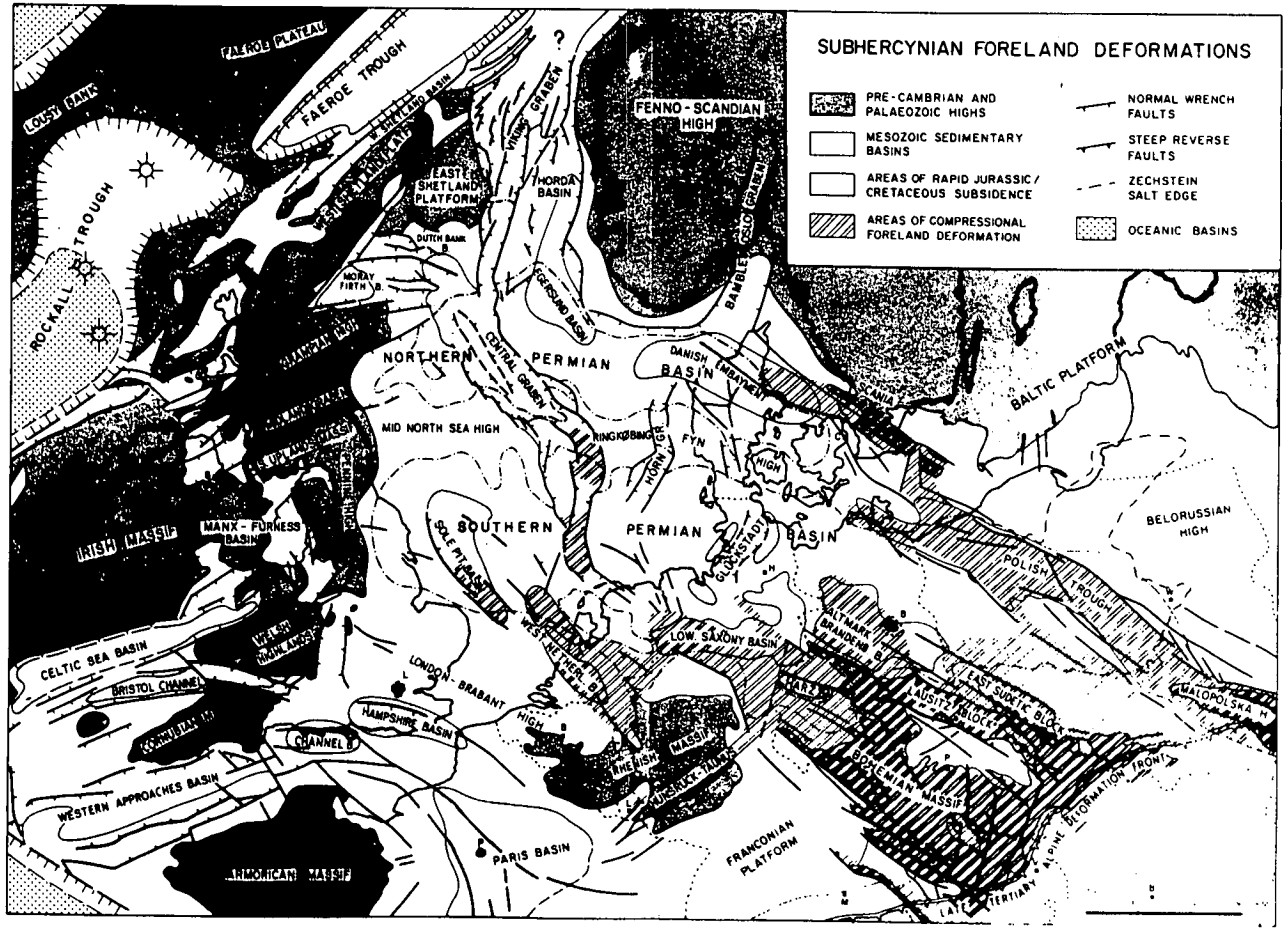

Figure 1.1(a) Map showing the extent of the "sub Hercynian" deformation phase into the Alpine Foreland (Ziegler, 1987b).

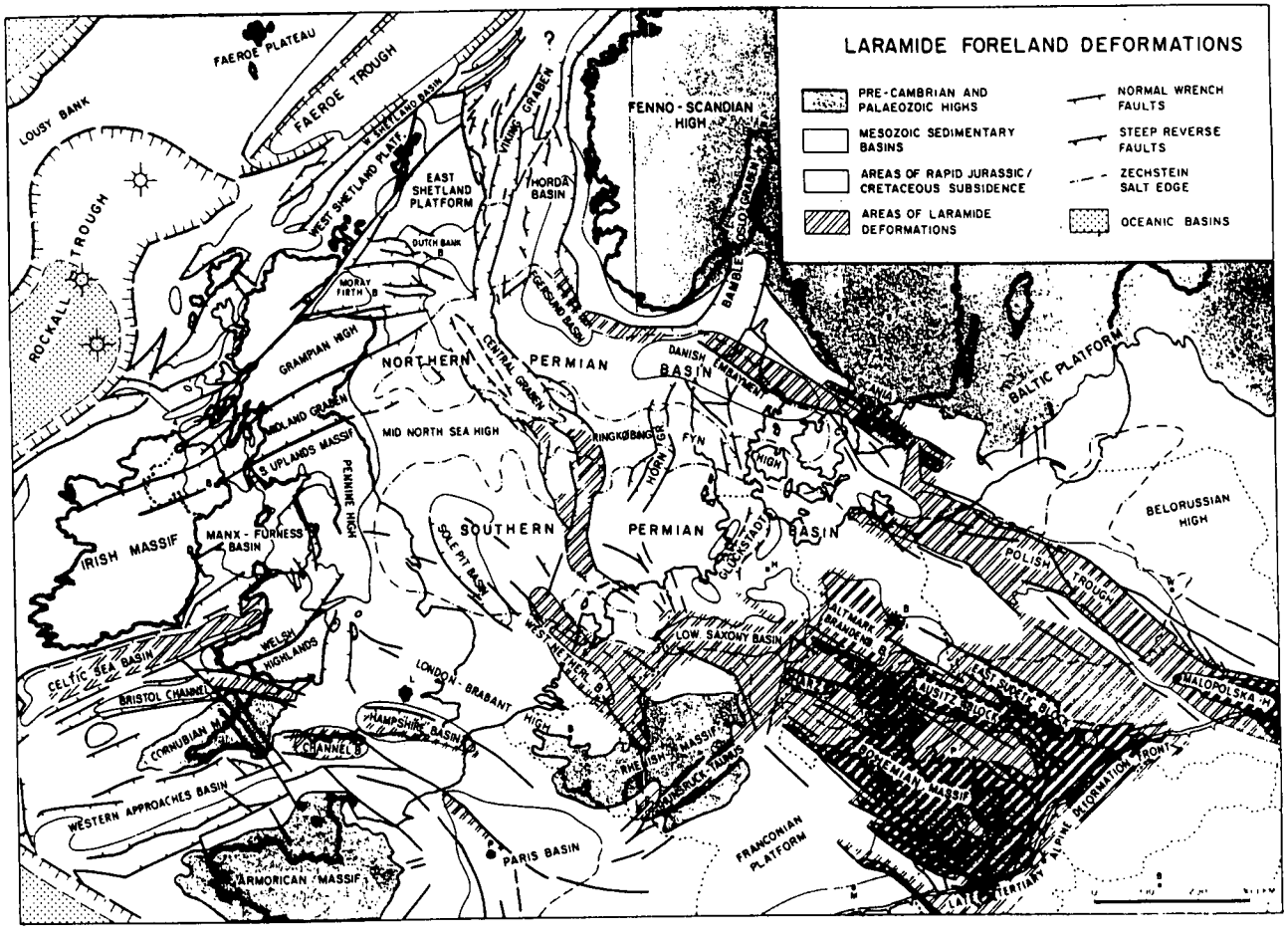

Figure 1.1(b) Map showing the extent of the "Laramide" deformation phase into the Alpine Foreland (Ziegler, 1987b).

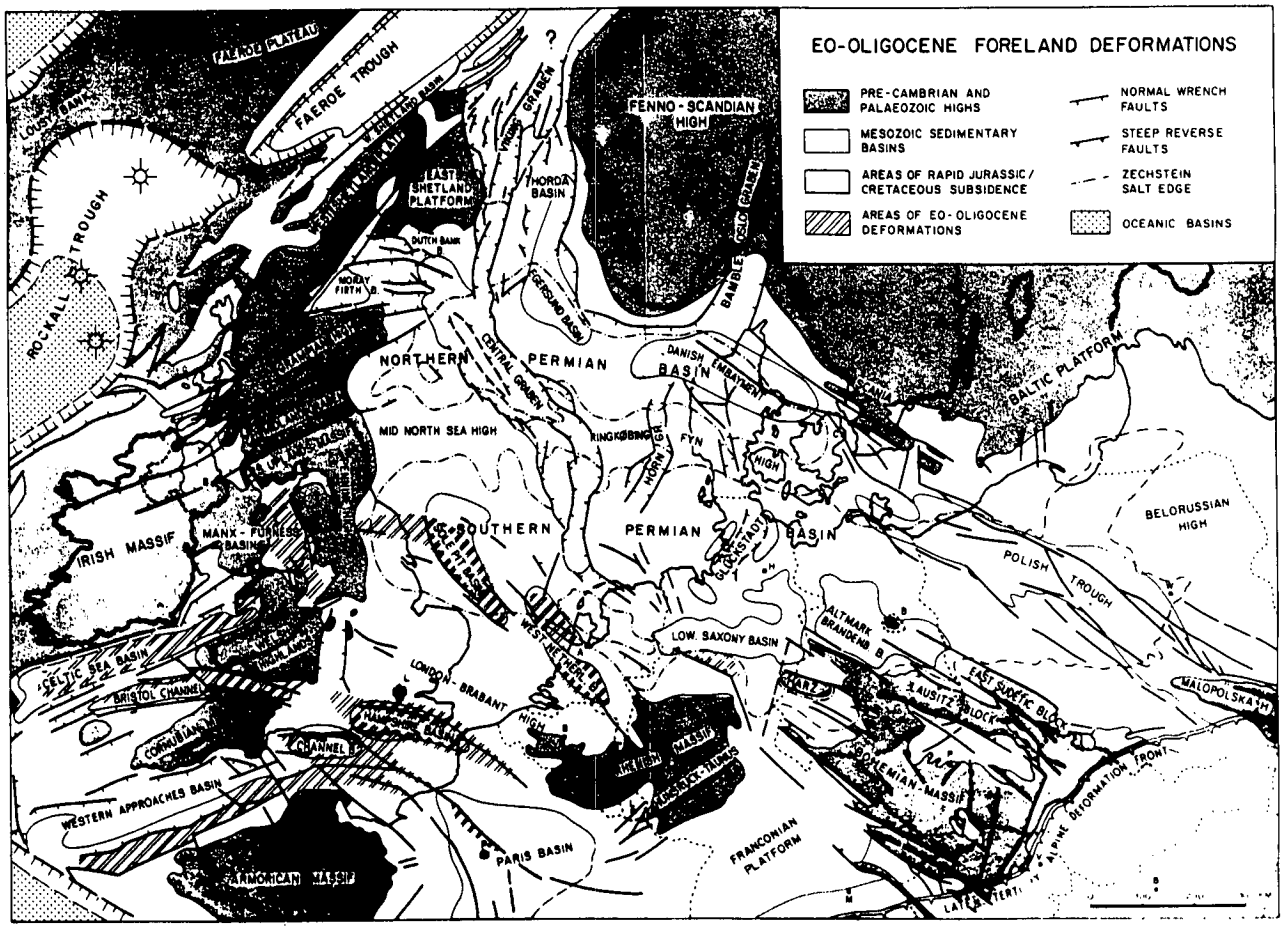

Figure 1.1(c) Map showing the extent of the Eo-Oligocene deformation phase into the Alpine Foreland (Ziegler, 1987b).

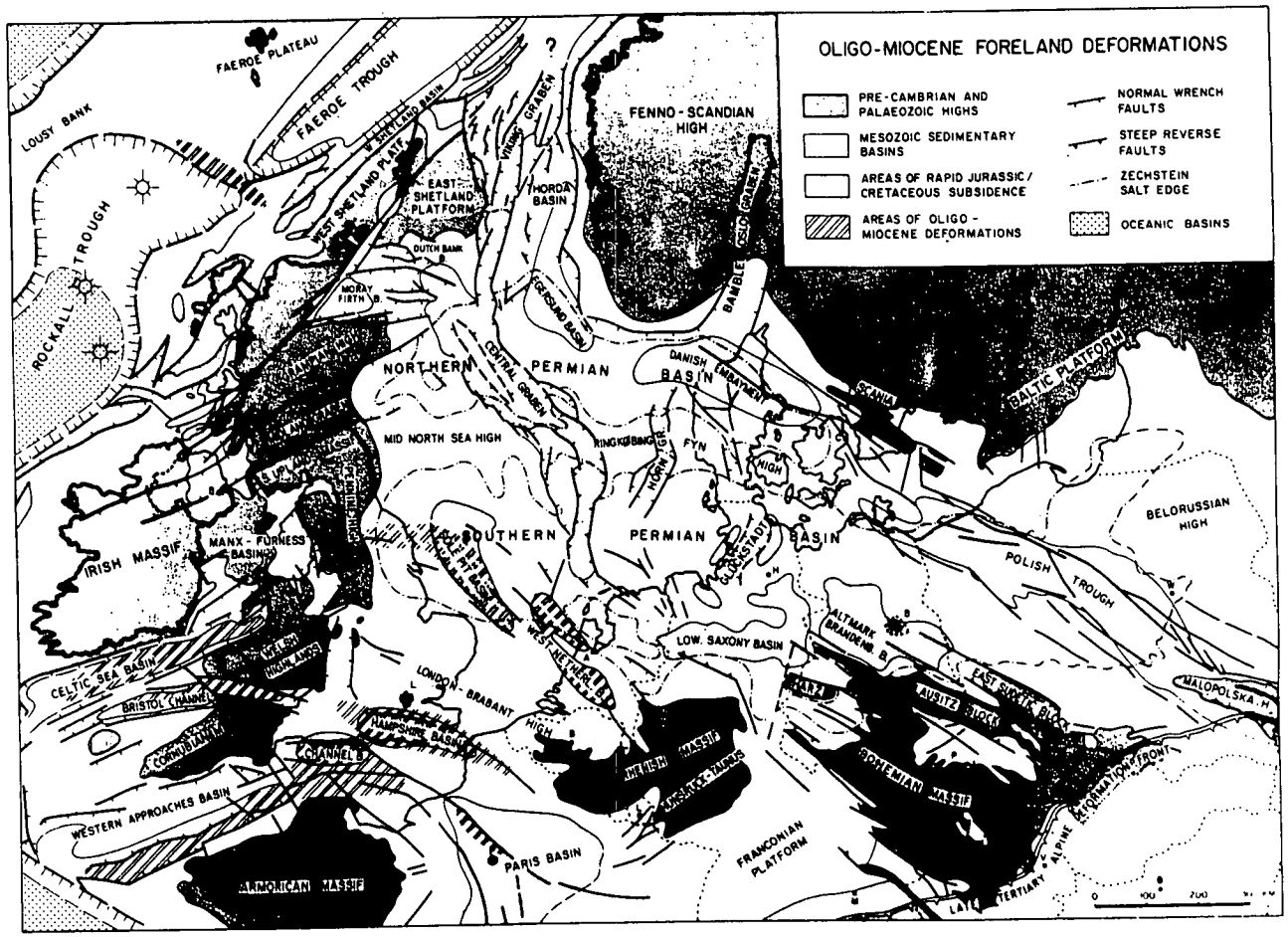

Figure 1.1(d) Map showing the extent of the Oligo-Miocene deformation phase into the Alpine Foreland (Ziegler, 1987b).

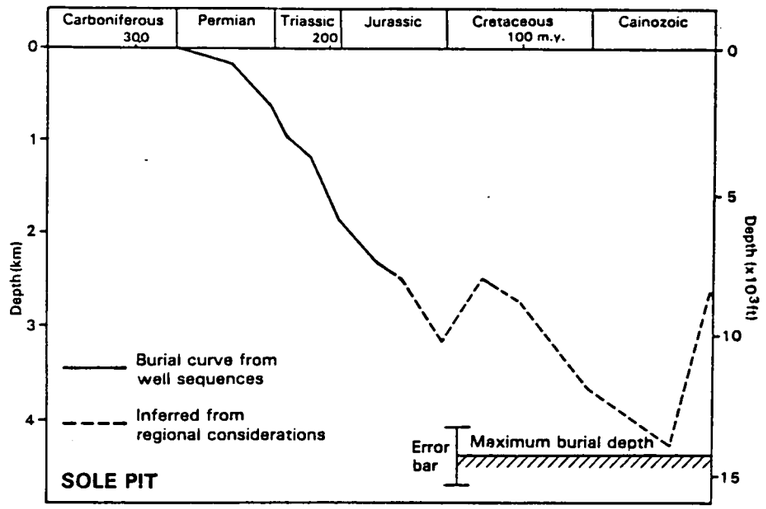

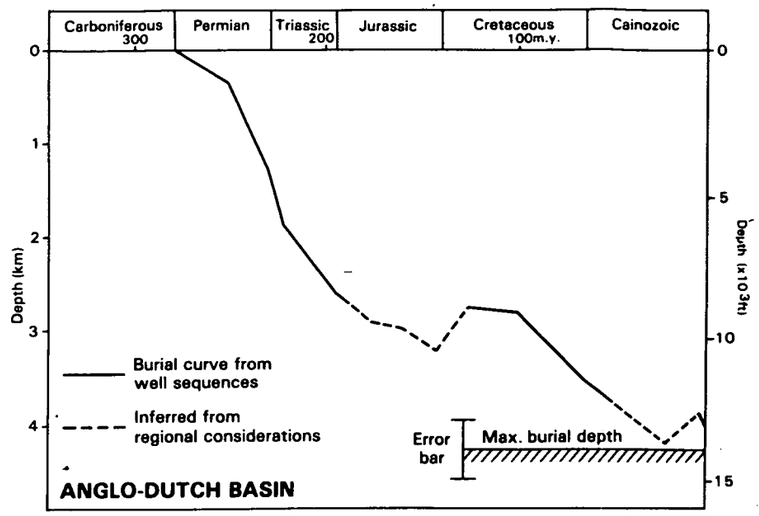

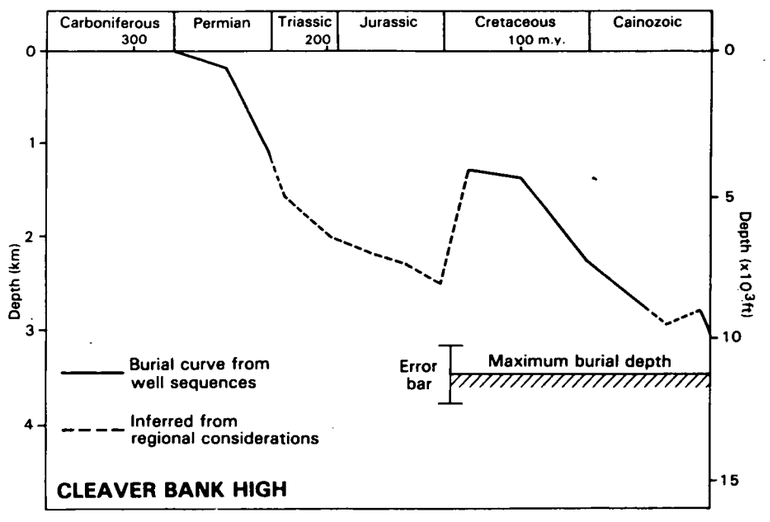

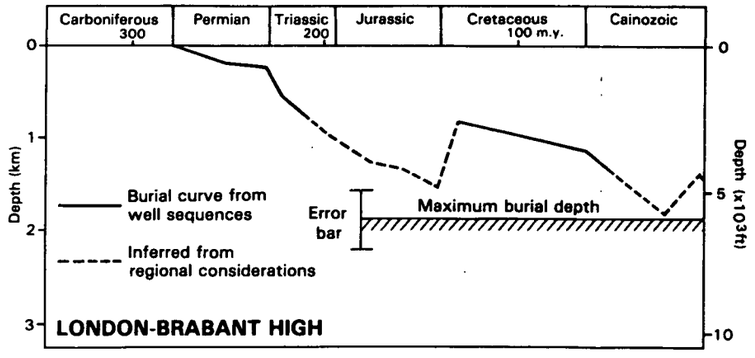

Figure 1.2 Subsidence history curves for parts of the North Sea (Bulat and Stoker, 1987). Note the periods of uplift and erosion inferred from the estimation of maximum burial-depth. Further details of this work can be found in Chapter 3.

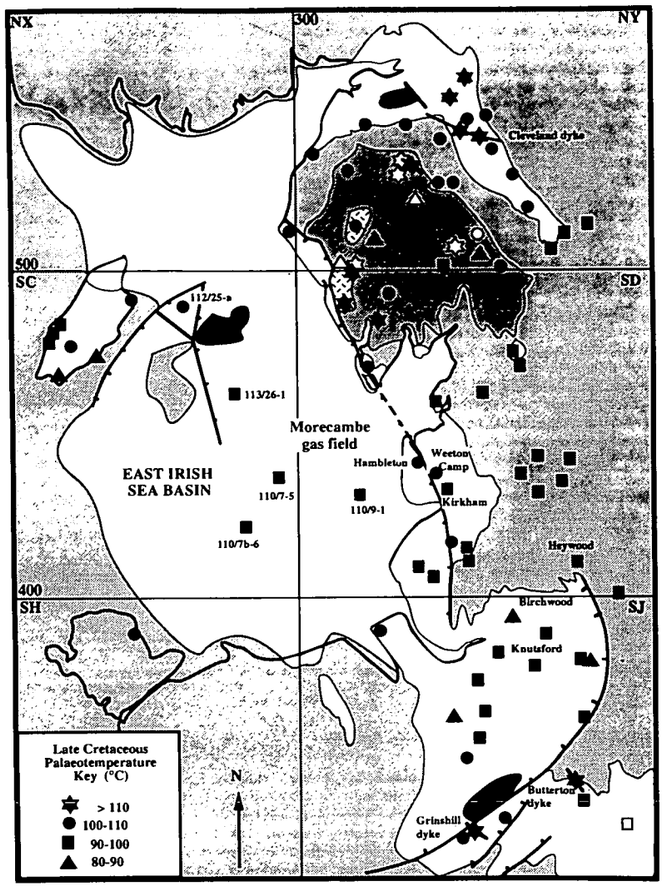

(a)

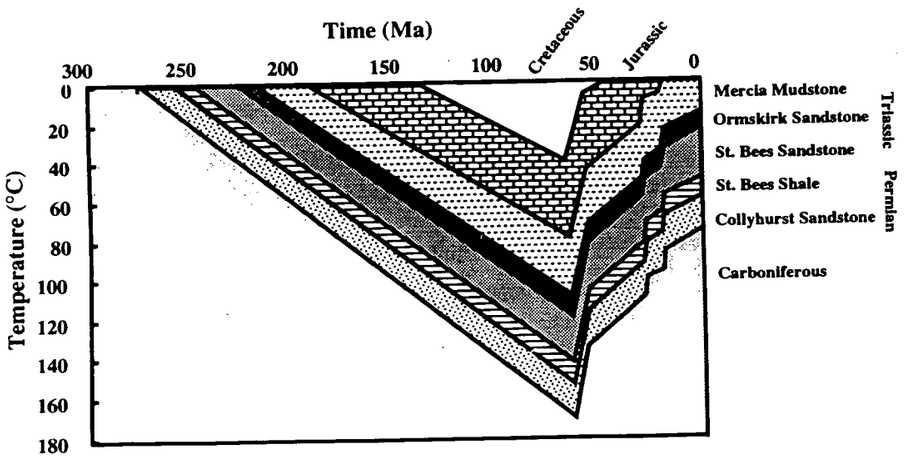

(b)

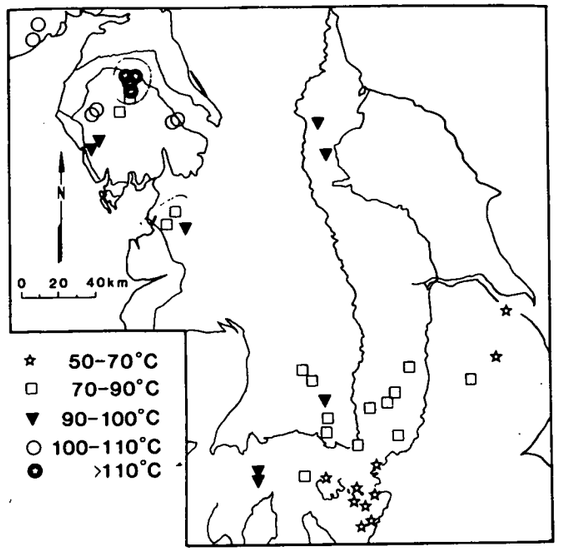

(c)

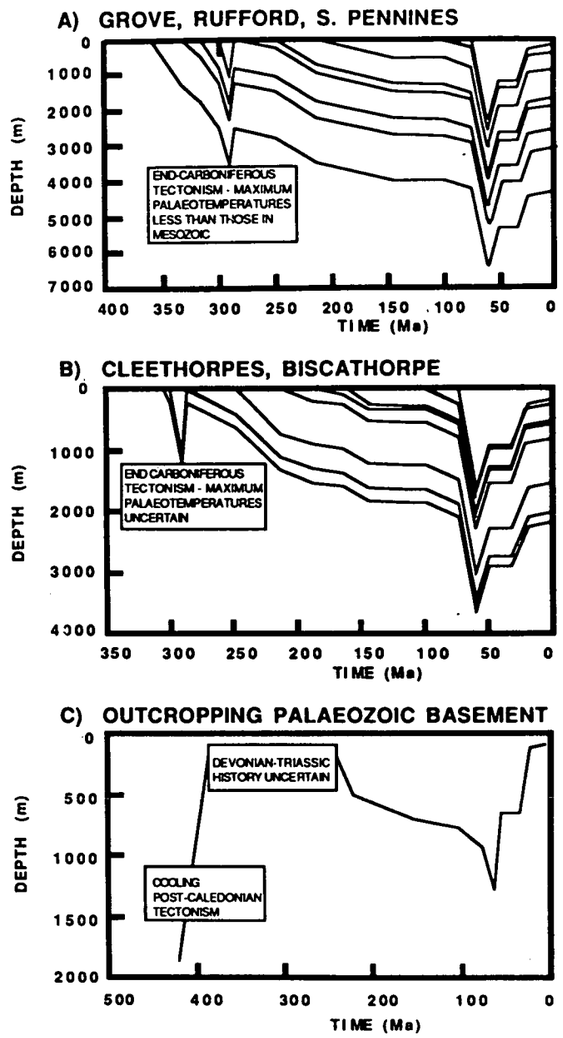

(d)

Figure 1.3 Apatite fission track analyses from northern England (Green, 1989; Lewis et. al., 1992). (a) Late Cretaceous palaeotemperatures for the localities shown indicating that the samples which are now at surface were probably buried to several kilometres depth at this time. (b) Schematic burial history for the area shown in (a) incorpating the uplift and erosion data. (c) Late Cretaceous palaeotemperatures for the localities shown. Again burial-depths of several kilometres for samples which are now at the surface are inferred. (d) Schematic burial histories for localities in (c) incorporating the uplift and erosion data.

suggesting that uplift and erosion had occurred. If uplift and erosion had occurred, Cenozoic sediments may have been present in the basin and this would contradict the traditionally accepted strike-slip basin formation model (McQuillin *et. al.*, 1982; Barr, 1985; Andrews and Brown, 1987; Bird *et. al.* 1987; Frostick *et. al.*, 1988, Roberts *et. al.*, 1990, Andrews *et. al.*, 1990) since no thermal subsidence deposits should be expected (a model over which doubt had already been suggested (Underhill, 1991a and b)).

Consequently, this project primarily aimed to determine the timing and styles of Cenozoic structural reactivation within the Inner Moray Firth and the extent, magnitude and timing of Cenozoic uplift and erosion in both the Inner Moray Firth and Scottish Highlands. This was deemed necessary as it would place the basin in its Cenozoic regional context and consequently allow the data from this area to be combined with that from other areas so that potential causes could be rigourously tested. Additionally, if extensive Mesozoic/Cenozoic thermal subsidence deposits could be shown to have been present this would require that the basin formed as a Mesozoic extensional basin, as the structural evidence was beginning to suggest (Underhill, 1991a and b). A subsidiary aim of the project was to examine the pre-Cenozoic evolution of the basin, primarily for the reasons of gaining familiarity with the previous history of the basin in case older structures or events had an effect on the period of interest, but also to check the extensional hypothesis of basin formation which was nearing completion at the time the project started. This subsidiary aim is only dealt with briefly in the thesis as a summary of the pre-Cenozoic evolution of the area (Chapter 2) but it is dealt with more fully in published material (Underhill, 1991a and b; Thomson and Underhill, 1993).

1.2 Structure of the thesis.

The thesis can be divided into four parts which deal with various aspects of the project. Firstly, Chapter 2 deals with the pre-Cenozoic evolution of the basin so that the reader has some familiarity with the basin history prior to the period of interest. This is then followed by the evidence for Cenozoic uplift and erosion in the Inner Moray Firth and Scottish Highlands in chapters 3, 4 and 5 in which compaction, apatite fission track and geochemical analyses have been applied while Chapter 6 takes the evidence from these chapters to draw some conclusions. Primarily, Chapter 6 aims to draw the uplift and erosion evidence together in a consistent manner before going on to discuss the difference between erosion and tectonic uplift, its implications for the burial history of the area and the problem of

the Inner Moray Firth supposedly being a strike-slip basin as opposed to an extensional basin with extensive thermal subsidence deposits.

The third part of the thesis (Chapter 7) looks at the evidence for extensive structural modification of the Inner Moray Firth during the Cenozoic and is based on a large seismic reflection profile database supplemented by fieldwork on the coastal exposures. It intends to document the varied nature and widespread extent of such activity before the final part of the thesis attempts to take this evidence with that from previous chapters to place the Inner Moray Firth in its regional context.

The final part of the thesis is contained in chapters 8 and 9 with chapter 8 attempting to draw the evidence from the Inner Moray Firth and Scottish Highlands together in a fashion consistent with the regional picture before attempting to explain the phenomena in this context and/or by previously proposed models. Finally, Chapter 9 summarises the progress made by the project and where the problems with the findings lie before suggesting what future work needs to be undertaken to resolve the problems which remain.

1.3 Project area: a geological summary.

Although Chapter 4 deals with the apatite fission track analysis of the Scottish Highlands, the majority of the work is based in the adjacent Inner Moray Firth which lies at the western end of the North Sea triple rift system. This area has experienced a long and complex history since the Caledonian Orogeny and the subsequent formation of the Orcadian Basin which underlies it, but the dominant structural setting developed during the Upper Jurassic with the formation of several half grabens. The basin is significantly faulted with faults generally trending east north east-west south west but a north east-south west orientation becomes dominant along its western margin **(Figure 1.4)**. The area is well-defined structurally being bounded to the north, west and south by the Wick, Helmsdale and Banff faults respectively and is bisected by the north east-south west trending Great Glen Fault, which with the Helmsdale Fault, defines the boundaries of the Sutherland Terrace **(Figure 1.4)**. The majority of the major faults in the basin are Late Jurassic half-graben bounding features but a small number of the major faults within the basin, which also have the same orientation, appear to be later structures and define features such as the Sinclair Horst (Underhill, 1991a; **Figure 1.4**).

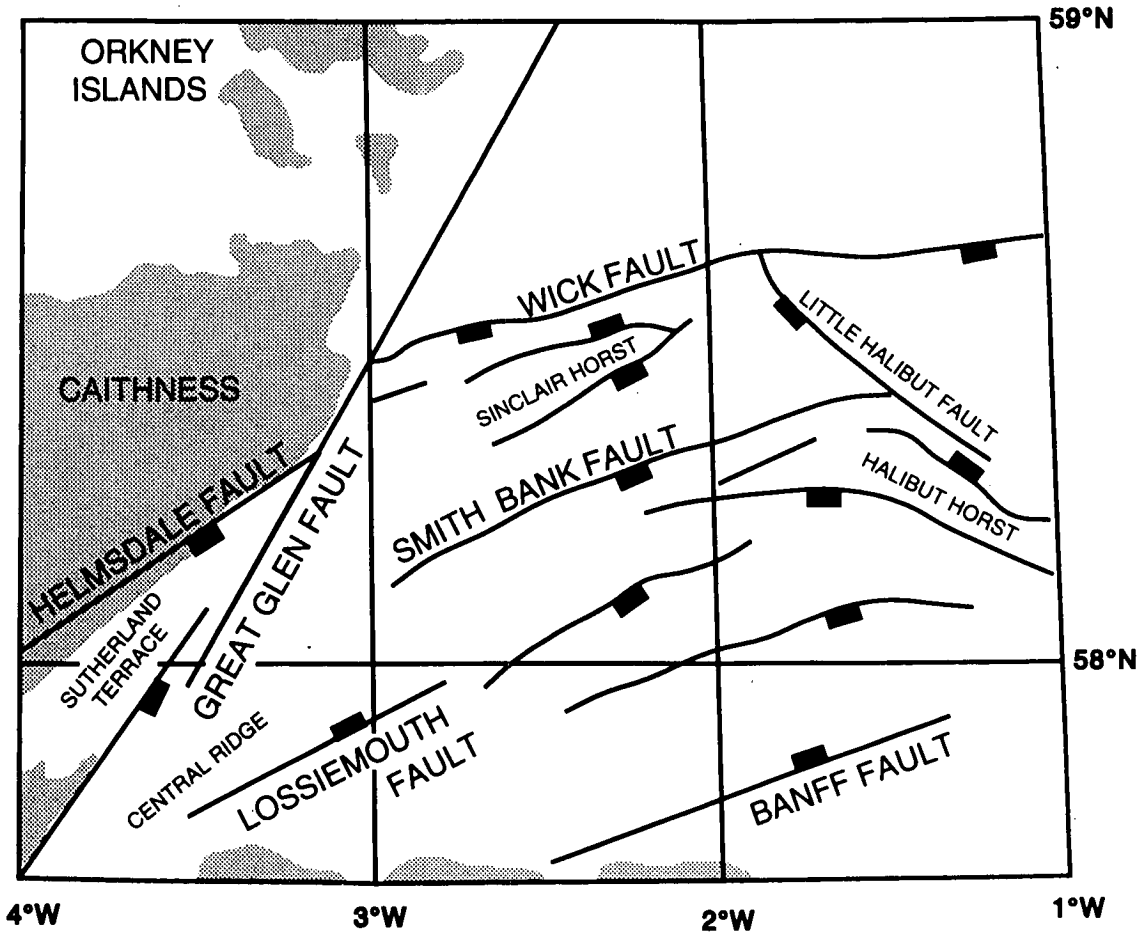

Figure 1.4 Map showing the major structural features of the Inner Moray Firth basin.

1.4 History of research in the area.

1.4.1 The Devonian Orcadian Basin.

The Orcadian Basin, which underlies the Mesozoic Inner Moray Firth basin and outcrops in Caithness, has been the subject of research for nearly two centuries with the majority of the earlier work focussing on the stratigraphy, lithology and palaeontology of the area and is described in detail by Crampton and Carruthers (1914) in the memoir for the area. Since the publication of the Caithness memoir, most attention has still remained focussed on the stratigraphy (e.g. Richardson, 1962; Miles and Westoll,1963; Donovan *et. al.*, 1973) which has been presented in detail by Mykura (1991), while recently the petroleum potential (Parnell, 1985; Trewin, 1989; Hillier and Marshall, 1992) and tectonics (McClay *et. al.*, 1986; Norton *et. al.*, 1987; Coward *et. al.*, 1989; Underhill and Brodie, 1993) have received some attention.

The limited exposure of the Old Red Sandstone onshore and its deep burial beneath thick Mesozoic/Cenozoic sequences on many offshore seismic reflection profiles has led to some ambiguity in interpreting the tectonic evolution of the Orcadian Basin. Some workers have suggested that strike-slip movement on the major tectonic linements in Scotland (e.g. the Highland Boundary, Great Glen, Melby, Nesting and Walls Boundary faults) occurred due to the oblique collision of Greenland and Europe during the Caledonian Orogeny (Trewin, 1989; Richards, 1990) and that this resulted in the localised transpression and transtension with the formation of uplifted source areas and subsiding basins. However, more recently it was proposed that extensional collapse of the overthickened crust, formed during the Caledonian Orogeny, was responsible for the formation of the basin (McClay *et. al.*, 1986; Norton *et. al.*, 1987; Coward *et. al.*, 1989).

1.4.2 The Inner Moray Firth.

Until the early 1970s the existence of a sedimentary basin beneath the Inner Moray Firth was in doubt. Prior to this time the presence of such a basin had been suggested by Arkell (1933), based on the fact that Permo-Triassic and Jurassic stratigraphies can be found at outcrop along the coastal margins. However, with the first regional gravity survey the issue remained contentious. The discovery of a significant negative gravity anomaly led Collette (1960) to suggest that a large Caledonian granite, similar to those seen in the adjacent Grampian Highlands,

accounted for this but Hallam (1965) considered that the anomaly was produced by a major Mesozoic sedimentary basin and later magnetic data (Institute of Geological Sciences, 1972) seemed to support this. During the early 1970s further seismic, gravity and drilling surveys confirmed the presence of the Mesozoic basin (Chesher *et. al.*, 1972; Chesher and Bacon, 1975; Sunderland, 1972). Smith and Bott (1975) carried out a seismic refraction survey of the Caledonian foreland, fold-belt and the North Scottish Shelf in order to determine the crustal thicknesses of these regions **(Figure 1.4b)**. Part of the survey (Line E; **Figure 1.4b**) was shot in a northwest-southeast orientation across the Inner Moray Firth, with the northern margin of the line passing over the Caithness Ridge, which marks the footwall to the basin. The survey intended to measure the thicknesses of various layers within the crust by time-term analysis based on Pg first arrivals (velocity of the first granitic layer, that is the first appearance of basement), P* (velocity at the mid-crustal Conrad discontinuity) and Pn (velocity at the Moho).However, in the case of the Inner Moray Firth line only P* and Pn were measured. The P* data could be divided into three groups from southeast to northwest with velocities of 1.10-1.38s (mean 1.28s), 1.23-1.59s (mean 1.43s) and 0.70-1.03s (mean 0.92s) respectively **(Figure 1.4b)** and could be explained by varying thicknesses (2km, 3.5km, and 0.5km) of Mesozoic cover with a velocity of 3km s^{-1} along the line length and the P* refractor at 7.4km, 6.6km and 6.6km respectively. The Pn values ranged from 2.61-3.30s from the southeast to the northwest **(Figure 1.4b)** and corresponded to Moho depths of 22.0km, 22.8km and 29.4km for the same three subdivisions as for the P* data. The two southeastern values which lie within the Inner Moray Firth are substantially lower than the 29.4km from the immediate footwall to the basin and the 26km for the Caledonian foreland suggesting that the Inner Moray Firth lies on thinned crust approximately 23km thick.

During the 1980s, as subsurface well and seismic reflection profile data became available for publication, a substantial body of work on the tectonic evolution of the Inner Moray Firth was produced (McQuillin *et. al.*, 1982; Barr, 1985; Bird *et. al.*, 1987; Roberts *et. al.*, 1990; Andrews *et. al.*, 1990). Most of this literature suggested a major role for the Great Glen Fault as a transtensional feature, on which dextral movement resulted in the development of the Inner Moray Firth. Such hypotheses ignored the work of Smith and Bott (1975) but acknowledged that of Donato and Tully (1981) who suggested that the basin lay on unthinned lithosphere and consequently could not be an extensional basin containing thermal subsidence deposits. Consequently, the structural interpretations appear to have been biased by the knowledge of the gravity interpretation of Donato and Tully (1981) and the ignorance of the work of Smith and Bott (1975). The strike-slip model for the

formation of the Inner Moray Firth was under investigation at the time the project started, with Underhill (1991a) suggesting that the basin formed by extension on the major Mesozoic half-graben bounding faults, with late-stage reactivation of the Great Glen Fault during the Cenozoic resulting in inversion and uplift of the Sutherland Terrace and Scottish Highlands.

The stratigraphy of the Jurassic in the Inner Moray Firth (and Scotland in general) has been dealt with by Sykes (1975), Andrews and Brown (1987). Andrews *et. al.* (1990), while the sedimentology of the onshore, Upper Jurassic, fault-associated " boulder beds " on the east Sutherland coast (e.g. Helmsdale Boulder Beds, Kintradwell Beds etc.) has been described by Bailey and Weir (1932), Pickering (1983), Roberts (1989) and Wignall and Pickering (1993). These suggest that the Upper Jurassic "boulder beds" formed as syn-sedimentary, fault-scarp related, submarine deposits in response to extension on the Helmsdale Fault.

For a comprehensive account of the state of the geological knowledge of the Inner Moray Firth prior to the start of the project the reader should consult Andrews *et. al.* (1990).

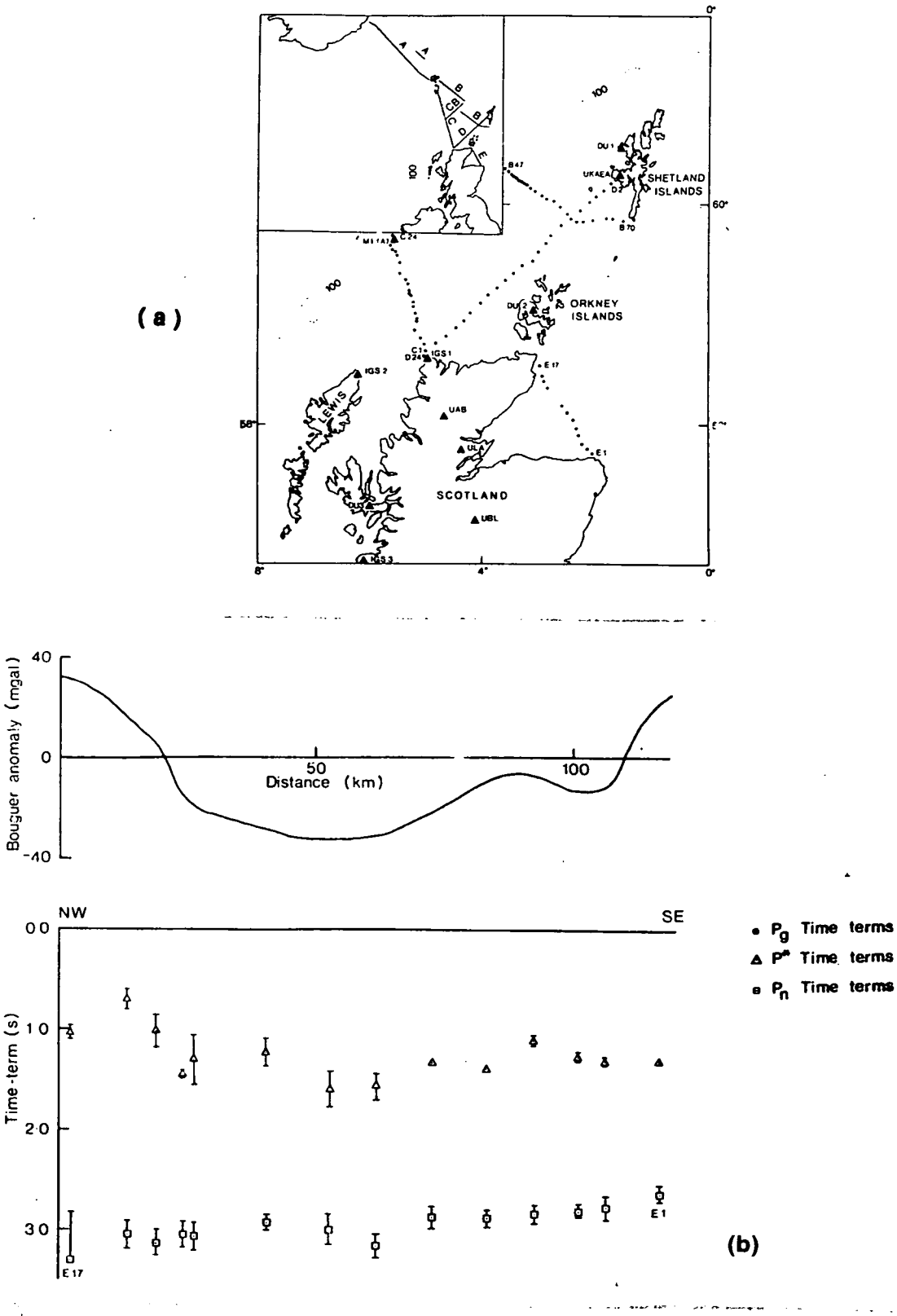

Figure 1.4b (a) Map showing the positions of shots and seismic recording stations in the North Scottish region, with overall shot lines of the North Atlantic Seismic Project shown in inset. Shots B58, B64, C3, C18 and E10-13 were misfires and are not shown. The 100fm depth contour is marked. **(b)** Time terms and Bouger anomaly profile for line E (Moray Firth). Smith and Bott (1975).

1.4.3 The Great Glen Fault.

The Great Glen Fault has long been the subject of intensive research and much controversy, with many conflicting estimates for the sense, timing and magnitude of relative movement on it. For example, the 30km or so post-Devonian dextral movement proposed by Donovan *et. al.* (1976), Garson *et. al.* (1984) and Rogers (1987) is approximately the same as the post-Carbonifereous movement proposed by Speight and Mitchell (1979) and Mesozoic/post-Mesozoic estimates listed below. However, major sinistral episodes of movement have also been proposed. As the Devonian and later strata appear to indicate approximately the same magnitude of dextral offset an incompatibility problem exists with major sinistral events proposed and consequently the Great Glen Fault remains a subject of active research. The main periods of movement suggested in the literature are listed below.

Late Silurian-Early Devonian.

100km Sinistral - Holgate (1969).

120km Sinistral - Garson and Plant (1972).

160km Sinistral - Winchester (1973).

Post-Devonian (Unspecified).

30km Dextral - Donovan *et. al.* (1976)

29km Dextral - Garson *et. al.* (1984)

25-30km Dextral - Rogers (1987)

Late Devonian.

200-300km Sinistral - Storevedt (1974)

Late Devonian-Middle Carboniferous.

104km Sinistral - Kennedy (1939)

Late Carboniferous.

2000km dextral - Van der Voo and Scotese (1981)

Post Carboniferous (Unspecified).

8km Dextral - Speight and Mitchell (1979)

Post-Triassic (Unspecified).

29km Dextral - Holgate (1969)

Mesozoic

Dextral - McQuillin *et. al.* (1982), Barr (1985), Bird *et. al.* (1987), Frostick *et. al.* (1988), Roberts *et. al.* (1990)

Post-Lower Cretaceous (probably Cenozoic).

32km Dextral - Garson and Plant (1972)

10km (approx) Dextral - Underhill (1991a), Thomson and Underhill (1993)

1.4.4 Uplift and erosion research.

It is widely believed that the western Inner Moray Firth was subject to erosion after Early Cretaceous times. Upper Cretaceous - Tertiary sediments crop out at, or near sea-bed in the eastern Inner Moray Firth, but are absent from the western Inner Moray Firth, where the youngest pre-Quaternary sediments are of Jurassic - Early Cretaceous age. The extrapolation of offshore seismic horizon geometries allowed McQuillin *et. al.* (1982) and Barr (1985) to estimate the thickness of the missing Lower Cretaceous - Tertiary sequence, and postulate that at least 650m of sediment had been stripped off the western part of the basin. Hurst (1980) similarly suggested, largely on the basis of clay mineralogy, that Middle Jurassic sediments in the vicinity of the Beatrice Field had been raised by at least 1 km with respect to the sea-bed. Duncan (1986) used a variety of biological marker molecules to constrain the burial history for the Inner Moray Firth and found that approximately 1km of sediment had been removed. Furthermore, Roberts *et. al.* (1990) suggested that interval velocity trends derived from raw velocity spectra supported a most likely estimate of erosion in the western part of the basin of approximately 300 m and at most 750 m. Recent work by Prajoga (1990) similarly estimated maximum erosion of approximately 300 m in the western Inner Moray Firth on the basis of vitrinite reflectance data.

Of all the methods applied to the determination of Cenozoic erosion in the Scottish Highlands geomorphological investigations are probably the most established (George, 1966; Watson, 1985; Hall, 1990). This evidence is based on two main sources of data. Firstly, it has been demonstrated that the Palaeogene sediments of the North Sea were sourced from the basement lithologies of both the Orkney-Shetland High and Scottish Highlands (Hartog Jager *et. al.*, 1993; Morton *et. al.*, 1993) and

that if this sediment is "backstacked" (with allowance made for the differing densities of the basement and sediment) that up to 2km of overburden has been removed from the source areas (Watson, 1985; Hall, 1990). Secondly, additional evidence is also available from the Tertiary Igneous Province. George (1966) noted that approximately 2km of roof rocks were removed from the igneous centres of Skye, Mull and Arran with erosion rates being approximately the same as currently observed in the Alps (Hall, 1990). On Morvern, zeolite zonations within the Tertiary lavas suggests that a further 1.8km of material existed above the current remains of the lava flow suggesting that the lava must have extended further into the Scottish Mainland than the current outcrop shows (Watson, 1985; Hall, 1990).

Hillier and Marshall (1992) have compiled an extensive vitrinite reflectance database from the remnants of the Orcadian Basin in Caithness, Orkney, Shetland and the margins of the Inner Moray Firth. Using the approach of Barker and Pawlewicz (1986) they have been able to estimate the maximum temperatures experienced by the samples. They suggest that the lower bounds of the temperature maxima distribution, ignoring samples which have undergone contact metamorphism, is around 100-120°C, equivalent to several kilometres of burial.

Lewis *et al.* (1992b) examined a suite of samples from the Sea of the Hebrides and adjacent areas using apatite and zircon fission track analyses. The fission track ages show two distinct populations with ages grouped around 50ma and 300ma respectively. The younger suite of samples around the Tertiary igneous centre of the Isle of Skye were interpreted as the product of thermal annealing due to the intrusion of hot igneous masses which totally annealed samples up to 8km away from its present outcrop. Although the quantification of uplift and erosion over the Skye igneous centre is difficult to constrain, Lewis *et al.* (1992b) suggest that cooling below 110°C at 52ma due to fairly constant uplift and erosion until the present day is not incompatible with the fission track evidence. Additionally; their data provides evidence for post-Cretaceous uplift and erosion for the surrounding areas. The Jurassic sediments of Skye were consistent with post-Jurassic erosion of over 1km while on the mainland, Late Cretaceous overburden was around 1-1.5km at Cape Wrath and 2km at Applecross, again suggesting post-Cretaceous erosion of 1-2km.

1.5 Summary of potential causes of uplift, erosion and tectonic reactivation.

The tectonic setting of northwestern Europe changed dramatically from the Mesozoic to the Cenozoic era to become one of compression compared to the predominantly extensional setting of the Mesozoic (Ziegler, 1987a and b; Becker, 1993). The change between these differing tectonic regimes occurred through the latest Cretaceous and Early Tertiary and is believed to be primarily due to the interaction between North Atlantic rifting to the northwest and the Alpine Orogeny to the southeast (Ziegler, 1987a and b, 1989). It is these processes which have been invoked to account for the uplift, erosion and tectonic reactivation seen in northwestern Europe. The potential causes fall into two main categories, namely those reliant upon compressional stresses resultant from Alpine Foreland tectonics (Ziegler, 1987a and b; Cloetingh *et. al.*, 1985, 1990; Beach, 1987; Hillis, 1992) or changes in the spreading characteristics of the North Atlantic Ocean (Hinz *et. al.*, 1993; Faleide *et. al.*, 1993; Boldreel and Andersen, 1993) and those related to the actual rifting of the North Atlantic between Greenland and Europe in the Palaeocene and Eocene (White, 1988; Kusznir *et. al.*, 1991, Campbell and Griffiths, 1990).

1.5.1 Compressional mechanisms.

In order to account for regional uplift of areas where there is only localized evidence of crustal compression and thickening (inversion), Hillis (1992) proposed a decoupled, two-layer model of lithospheric compression **(Figure 1.5)**. It is assumed that the entire lithosphere is under compression (due to the propagation of compressional stresses into the Alpine Foreland and/or changes in the spreading characteristics of the North Atlantic), but that compression and thickening in the lower lithosphere is decoupled, and laterally displaced, from that in the upper lithosphere **(Figure 1.5)**. Reverse movement on the pre-existing, weak crustal detachments could then result in basin inversion, indeed this was proposed as a potential mechanism for the phenomena under discussion in the "linked tectonics models" of Beach (1987; **Figure 1.6**) and Gibbs (1989), while thickening of the mantle lithosphere without accompanying thickening of the crust could then be invoked to account for the regional uplift **(Figure 1.5)**. Submersion of cold and dense mantle lithosphere into the surrounding asthenosphere would be expected to have caused an initial, isostatically-driven subsidence while subsequent warming of the lithosphere would cause uplift, and potentially extensional reactivation.

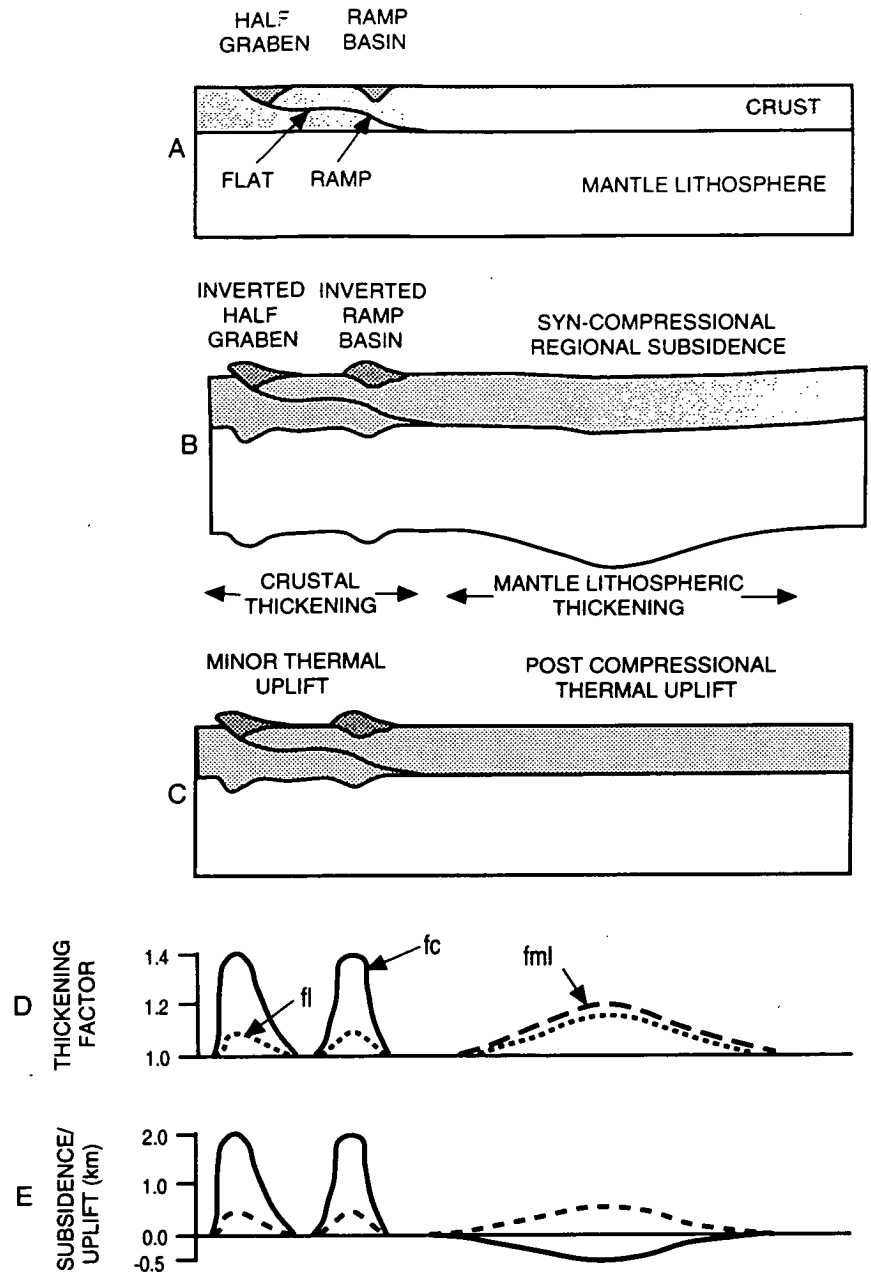

Figure 1.5 Two-layer lithospheric compression and thickening. (A) Existing sedimentary basins formed above ramps in the crustal detachment during Mesozoic extension. (B) Compression reactivates the crustal detachment causing basin inversion. Mantle lithospheric thickening is decoupled and laterally displaced from that in the crust and causes initial sibsidence. (C) The lithosphere thermally re-equilibrates to its pre-compressional level, uplifting the region of mantle lithosperic thickening. (D) Balanced distribution of lithospheric thickening similar to that illustrated schematically in A-C. The crustal thickening factor (fc- solid line) is the ratio of thickness of the deformed crust to its initial thickness. Similarily, fml is the mantle lithospheric thickening (dashed) and fl is whole lithospheric thickening (dotted). (E) Surface elevation changes associated with the distribution of lithospheric thickening shown in D, assuming local isostacy and no surface loading. Syn-compressional elevation changes are shown by the solid lines, and post-compressional, thermal uplift is shown by the dashed line (Hillis, 1992).

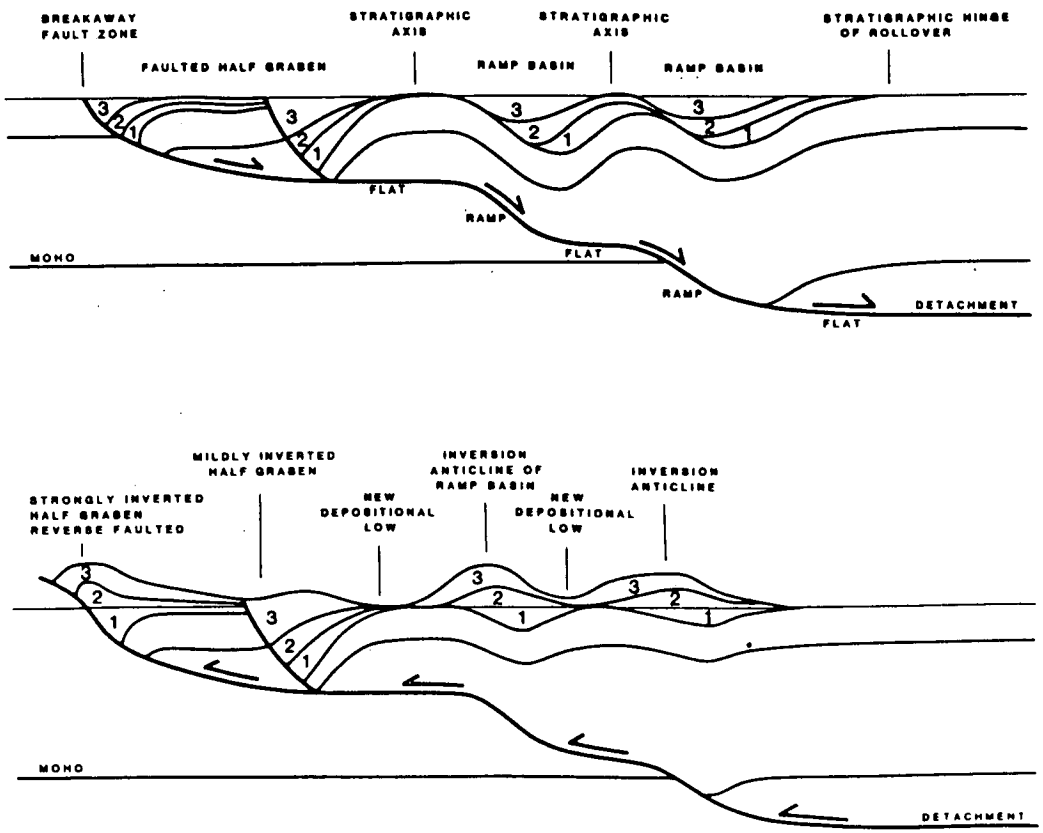

Figure 1.6 (a) Balanced section showing schematically the deformation in the hangingwall above a detachment with dip-slip movement across a flat-ramp geometry. (b) Balanced section showing schematically the effect of inversion on the geometry shown in (a), by reversed dip-slip movement (Beach, 1987). The reverse movement on such detachments with flat-ramp geometries has been proposed as a potential mechanism to propagate compressional stresses into the Alpine Foreland and consequently the inversion of the numerous Mesozoic half-grabens of northwestern Europe.

The flexural effects of small fluctuations in the stress regime within plates have been documented by several workers (e.g. Cloetingh *et. al.*, 1985; Kooi and Cloetingh, 1989; Cloetingh *et. al.*, 1990; Karner, 1986) and have been suggested as a potential mechanism to account for the uplift and erosion seen in northwestern Europe. Intraplate compressional stresses essentially act to amplify existing deflections of the lithosphere, and for example basin centres are deepened while flanks are uplifted (Cloetingh *et. al.*, 1985; Kooi and Cloetingh, 1989; Cloetingh *et. al.*, 1990; **Figure 1.7**). Hence, if the Inner Moray Firth is seen as a flank to the North Sea rift system intraplate compression (driven by Alpine and/or North Atlantic activity) could potentially generate tectonic uplift (Cloetingh *et. al.*, 1985; Kooi and Cloetingh, 1989; Cloetingh *et. al.*, 1990). Additionally, contractional structures could be expected to be developed when a basin is subjected to compressional intraplate stresses (Karner, 1986) and strike-slip deformation is also a possibility.

1.5.2 North Atlantic rifting mechanisms.

The Early Tertiary witnessed the separation of Greenland from northwestern Europe due to rifting over a mantle plume or "hot spot" to form the North Atlantic (Ziegler, 1989; White, 1988). This mantle plume had a pronounced effect on the rifting characteristics of the region and still exerts an influence. Currently the plume is situated beneath Iceland and is responsible for dynamic uplift in the area which maintains a shallow bathymetry, with Iceland maintained at approximately 2.5km above its expected elevation (White, 1988, 1989, 1992a and b; Bott, 1988). A consequence of such large uplifts over the mantle plume is the gravitational potential it induces. By elevating the crust a radial stress regime can be induced (Campbell and Griffiths, 1990; Griffiths and Campbell, 1991) and gravitational collapse, with the consequent reactivation of pre-existing faults, may occur.

Probably the most distinctive feature of the rifting process was the large amounts of volcanic products produced (up to 2 x 10^6 km^3), located in the onshore settings of Scotland, Ireland, Greenland and the Faeroes but most significantly along the rifted continental margins (White, 1988, 1989; **Figure 1.8**). For example, the Hatton Bank area contains large surface flows up to 4km thick associated with 10km of volcanic material intruded into the lower crust (White, 1988, 1989, 1992a and b; **Figure 1.9**). The potential effects of such large volumes over and underplating the continental margin are considerable, with isostatic uplift of the

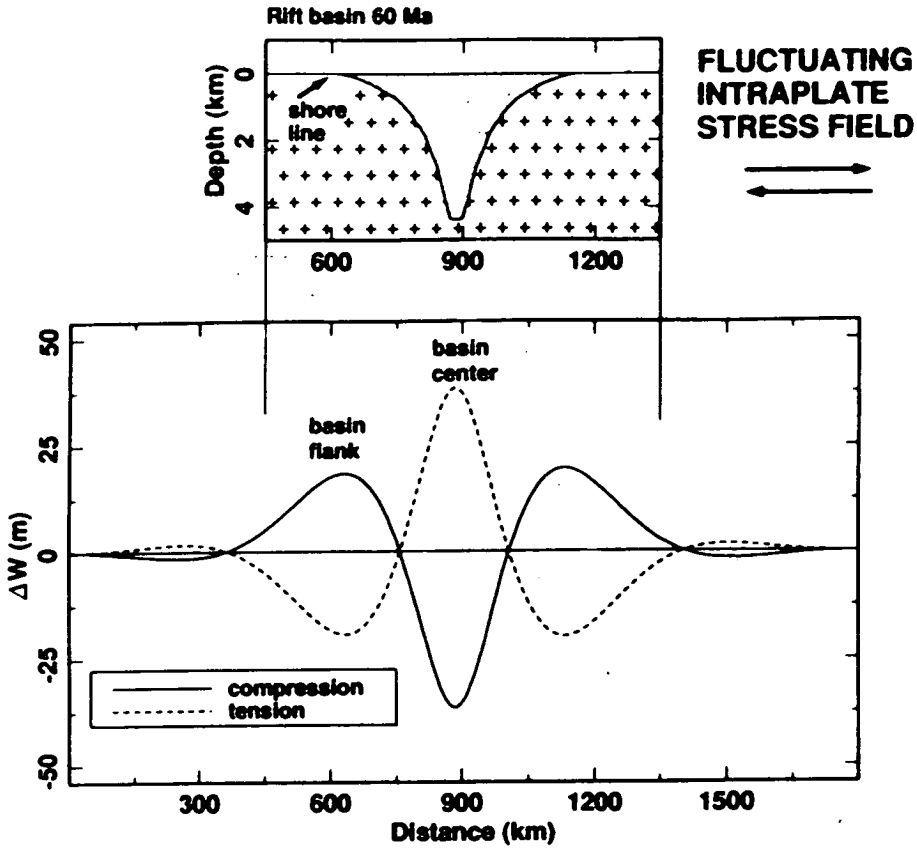

Figure 1.7 Flexural deflections at a sedimentary basin by changes in the level of intraplate stress. Sign convention: uplift is positive, subsidence is negative. Above: a 60ma old rifted basin formed by stretching. The sediments flexurally load an elastic plate. The thickness of this plate varies horizontally due to lateral changes in the temperature structure of the lithosphere. Below: the vertical deflections induced by a change to 1 kbar compression (solid curve). The flank of the basin is uplifted and the basin subsides. A change to 1 kbar tension (dashed curve) induces uplift at the basin centre and subsidence at the basin flank. The shape and magnitude of these stress-induced deflections evolve through time not only because of the increasing load, but also due to changes in the thermal structure of the lithosphere (Cloetingh *et. al.*, 1985).

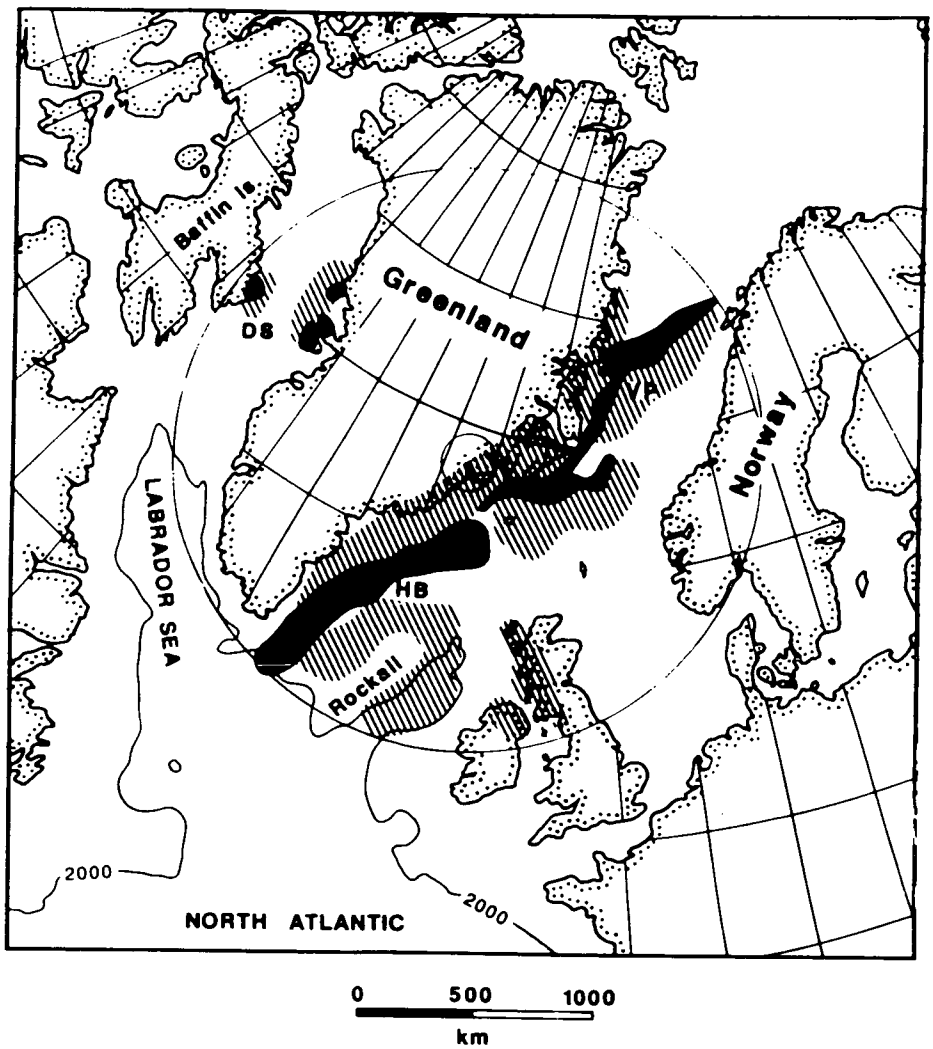

Figure 1.8 Reconstruction of the North Atlantic at magnetic anomaly 23, just after the onset of sea-floor spreading. Positions of extrusive volcanic rock are shown by solid shading, and hatching shows extent of Early Tertiary igneous activity in the region. Inferred position of the Iceland hot spot mantle anomaly is shown by the circle. DS = Davis Strait, VP = Vøring Plateau, HB = Hatton Bank. Projection is equal-area, centred on position of mantle plume. Bathymetric contours in meters (White, 1989).

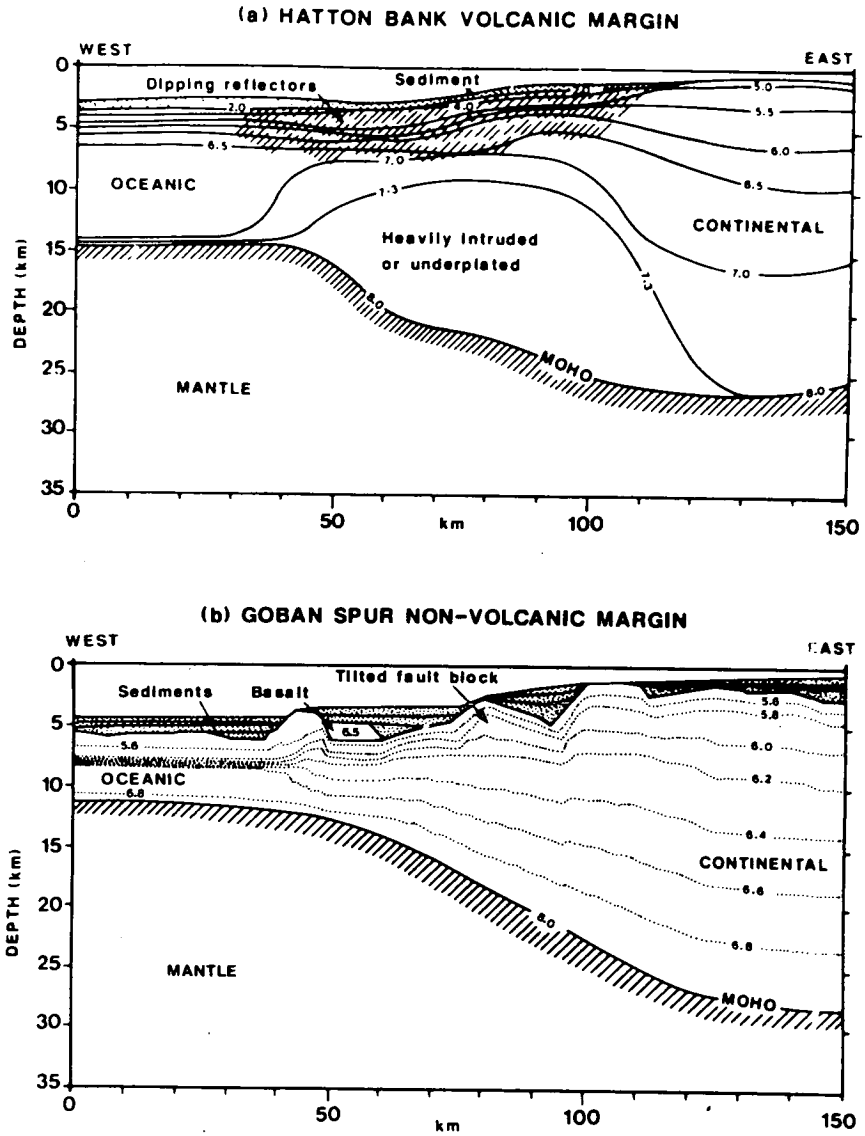

Figure 1.9 Cross-sections at the same scales with velocity contours from wide-angle seismic profiles across (a) typical volcanic margin west of Hatton Bank and (b) typical non-volcanic margin on the Goban Spur (White, 1992b). Note the large amounts of igneous under/overplating on the volcanic margin due to the rifting process occurring of the Iceland "hot-spot".

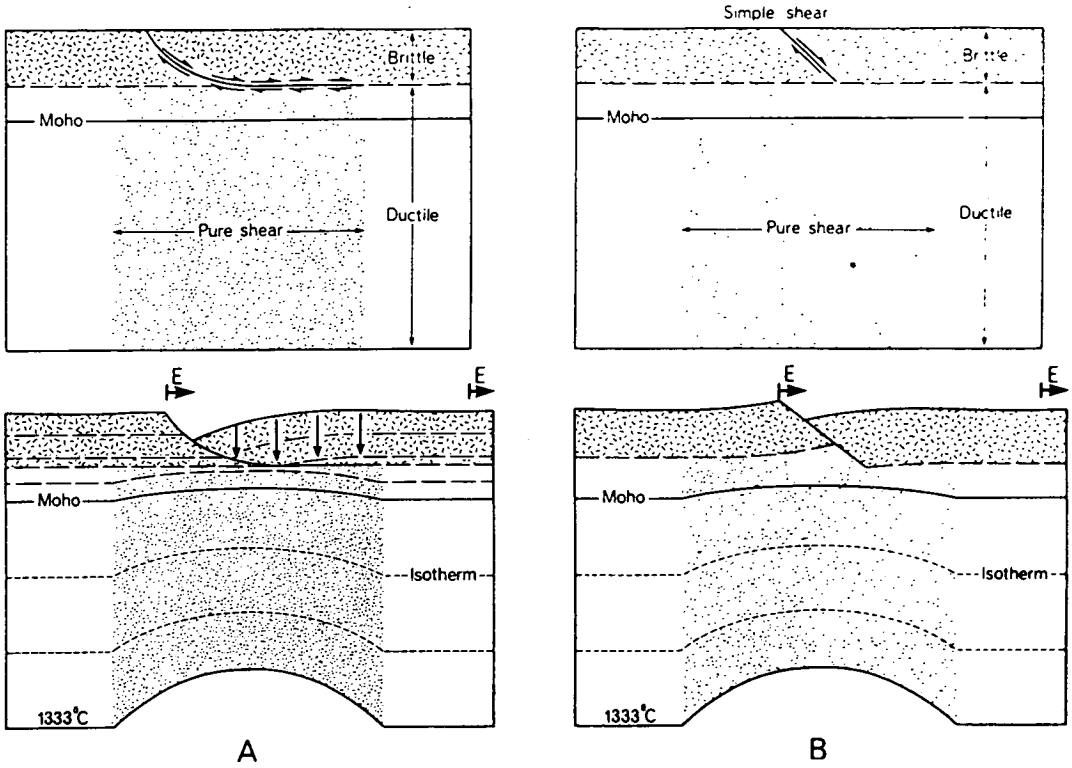

Figure 1.10 A schematic representation of lithosphere extension by faulting (simple-shear) in the upper crust and pure-shear in the lower crust and mantle (the "flexural cantilever" model), showing crustal thinning and temperature field perturbation by both simple and pure-shear. (a) listric fault, (b) planar fault (Kusznir *et. al.*, 1991). Note the flexural uplift of footwalls and the flexural downwarp of hangingwalls which is a characteristic of such models.

continental margin a distinct possibility. Furthermore, the possibility that it is unlikely that rifting occurs by pure shear (McKenzie, 1978) or simple shear (Wernicke, 1985) throughout the entire lithosphere but that these processes represent end members of potential rift types has led to the development of "flexural cantilever" models (Kusznir *et. al.*, 1991). These models assume that the upper crust has some mechanical strength, deforms by faulting and responds to loads by flexural isostasy while the lower crust and mantle deforms by pure shear **(Figure 1.10)**. The result is that upon rifting footwalls are flexurally uplifted and hangingwalls depressed **(Figure 1.10)**. Consequently, this presents another potential method of generating uplifts along continental margins and may have affected the Inner Moray Firth.

1.6 The mid-late Danian unconformity

The mid-late Danian unconformity is generally considered to be the surface where the erosion of the pre-Cenozoic units of the Inner Moray Firth occurred (Andrews *et. al.*, 1990). However, evidence for this from the Inner Moray Firth is limited as only sediments from below it (pre-Cenozoic) are preserved in the area. Further east in the Outer Moray Firth, Viking and Central grabens however, Cenozoic units are present (Andrews *et. al.*, 1990) and this has allowed the detailed examination of this potentially important surface by Stewart (1987). By using seismic stratigraphic techniques in conjunction with data from 300 wells and the associated biostratigraphic data Stewart (1987) was able to divide the Early Palaeogene of the Central North Sea (an area which included the Witch Ground Graben, Outer Moray Firth) into ten depositional sequences **(Figure 1.11)**, the boundaries between which are marked by unconformities or disconformities. Although Stewart (1987) gives a detailed account of all ten sequences it is the lower two which are of specific interest to this project as they are of Danian age and consequently may reveal information regarding the mid-late Danian unconformity.

The earliest Lower Palaeogene sequence (Sequence 1 of Stewart (1987); **Figure 1.11**) represents the Danian chalk and overlies the higher velocity Cretaceous chalks, the lateral equivalents of which are preserved in the Inner Moray Firth. The upper surface commonly forms an unconformity which can be resolved on seismic reflection profiles (Stewart, 1987; **Figure 1.11**). This erosional surface can be shown to have significant topography with deep incisions as a result of channelling and canyon cutting associated with the development of Late Danian and

Early Thanetian submarine-fan sequences which are particularly pronounced in the South Halibut Trough (Outer Moray Firth).

Overlying the Danian chalk are the Late Danian and Early Thanetian submarine-fans which form the second sequence of Stewart (1987; **Figure 1.11**), the internal seismic character of which is generally chaotic, although broad mounded structures are locally present. However, on the basis of seismic reflector character combined with well data Stewart (1987) was able to divide this sequence into a basal debris-flow deposit consisting of reworked Cretaceous and Early Danian Chalk with both reworked and contemporaneous faunas, an overlying submarine-fan sandstone containing fauna only from the time of deposition (Late Danian-Early Thanetian) and finally a hemipelagic mudstone of Early Thanetian age.

The boundary between the lower two sequences of Stewart (1987) occurs in the latter half of the Danian and as the upper surface of the underlying sequence is heavily incised and the basal deposits of the upper sequence contain debris-flows, the clasts of which were derived from the previous units, it is clearly an unconformity of some significance. It is on these ground that the erosion of the Inner Moray Firth has been associated with this mid-late Danian unconformity.

1.7 Uplift and erosion; a clarification of the terminology and principles used.

As a major aim of this project was to quantify the magnitude of uplift and erosion in the Inner Moray Firth and the Scottish Highlands (Chapters 3, 4, 5 and 6) it is necessary to clarify the terminology and principles which apply in such cases. The intrinsic problem with all techniques which measure "uplift" (e.g. apatite fission track analysis, geochemical modelling and compaction analyses) is that the reference frame for such techniques is not the same as that required for the study of uplift of regions due to tectonism (England and Molnar, 1990). Such techniques have a reference frame set at the topographic (land) surface and consequently only measure the uplift of rocks with respect to that surface (Brown, 1991), whereas uplift in the true sense (i.e. tectonic uplift of a terrane) involves the uplift of the surface with respect to a fixed datum, that is the geoid. However, sea level is thought to approximate for this over short periods. Consequently, a differentiation between these two measurements needs to be made.

Uplift of a surface with respect to either the geoid or sea level involves work done against gravity as the potential energy of the material forming the terrane is increased (England and Molnar, 1990; Brown, 1991). As work against gravity has be to invoked to raise the surface, a force is required, and hence tectonism can be invoked. Thus, when uplift of a surface is discussed, the thesis uses the terms **uplift** or **tectonic uplift.** As techniques such as apatite fission track analysis have their reference frame set at the surface and not at the geoid/sea level they are incapable of measuring **uplift** or **tectonic uplift** directly and so different terminologies are required (Brown, 1991). As such techniques measure the uplift of rocks with respect to the surface (i.e. they measure the decrease in burial-depth that has occurred) the sample under consideration must either rise to the surface or have the overburden removed from above it. As the removal of overburden is generally the most common way to bring a sample to the surface, the measured decrease in burial-depth is referred to as **erosion** in this thesis. **Erosion** is taken to involve all surface processes which remove both solid particulate matter and dissolved loads carried in the fluvial systems of an area (also referred to as denudation by other workers (e.g. Brown *et. al.*, 1993)). The term **erosion** is further qualified in some contexts as **total erosion** and **apparent erosion** depending on whether the technique involved is measuring the full extent of the erosion that occurred or the amount which has not been subsequently reversed by additional burial. In addition, as such a process results in the reversal of the burial process it is sometimes referred to **exhumation** in the thesis. However, in parts of the thesis, particularly where previous research is documented and techniques are initially described with the intention of measuring **erosion** and from that **tectonic uplift**, the term **uplift and erosion** has been used. Such a term implies that although an attempt is being made to isolate **tectonic uplift, erosion** is measured first.

Now that it is clarified that the important parameter for this project, and any other involving tectonic forces, is **uplift** or **tectonic uplift**, attention can be paid to the relationship between it and the **erosion/exhumation** as determined by the various techniques applied to the Inner Moray Firth and Scottish Highlands. Although it is generally assumed that changes in erosional activity are intrinsically linked to changes in surface elevation this is not necessarily the case. For example, long term climatic changes can result in long term changes in the **erosive** potential over an area by, for example, changing the amount of water entering the system, which can **erode** and transport solid and dissolved loads or by raising the mean surface temperature and hence, increasing the rates of chemical weathering. Furthermore, the rate of **erosion** is dependent not upon the elevation of an area but more directly

to the local gradient so that **uplifted** areas can be maintained at extremely high elevations with little **erosion** providing that the area has little local relief while low-lying areas can experience extremely high **erosion** rates with no **tectonic uplift** if the local relief is sufficiently variable. Consequently, a major **erosive** episode may be unrelated to **tectonic uplift** of the surface.

In order to determine whether **tectonic uplift** of a terrane has occurred it is necessary to gather more information than the techniques which measure **erosion** can provide. The crucial factor in determining whether **tectonic uplift** has occurred, and to quantify such an event, is to be in possession of data which can fix the surface elevations of an area before and after the **erosive** event (Brown, 1991). For example, if it is possible to determine that 1km of material was **eroded** from an area which had an initial elevation of 200m and a final elevation of 0m (sea level) then it can be confidently assumed that the **erosive** episode was unrelated to a **tectonic uplift** phase. The reduction of the topography down from 200m to sea level would result in the removal of not just the material immediately between the old and new surfaces (200m of rock) but approximately five times the amount (1km) due to the isostatic rebound of the crust as it was unloaded (assuming an average crustal density of 2.7 gcm^{-3}). However, if the situation was one of 1km of **erosion** and the surface at sea level before and after **erosion** then the erosive event can be directly linked to to 200m of **tectonic uplift**. As the initial surface elevation is zero, **uplifting** the surface by 200m and eroding the topography back down to sea level would result in 1km of **erosion** before a steady state elevation back at sea level could be achieved, again as a result of isostatic rebound. Consequently, the combination data documenting **erosion** with palaeodatum markers, such as marine sediments, provides the only satisfactory method of determining whether **tectonic uplift** has occurred.

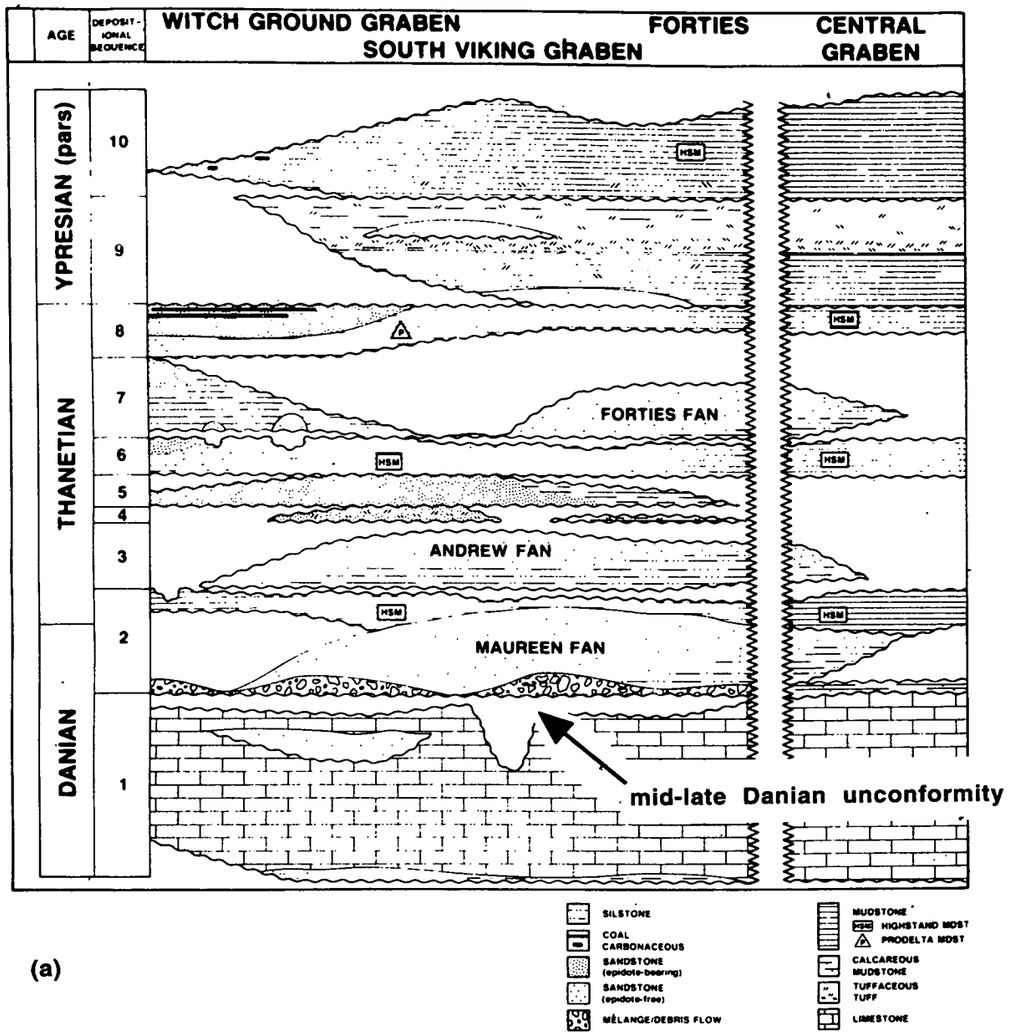

(a)

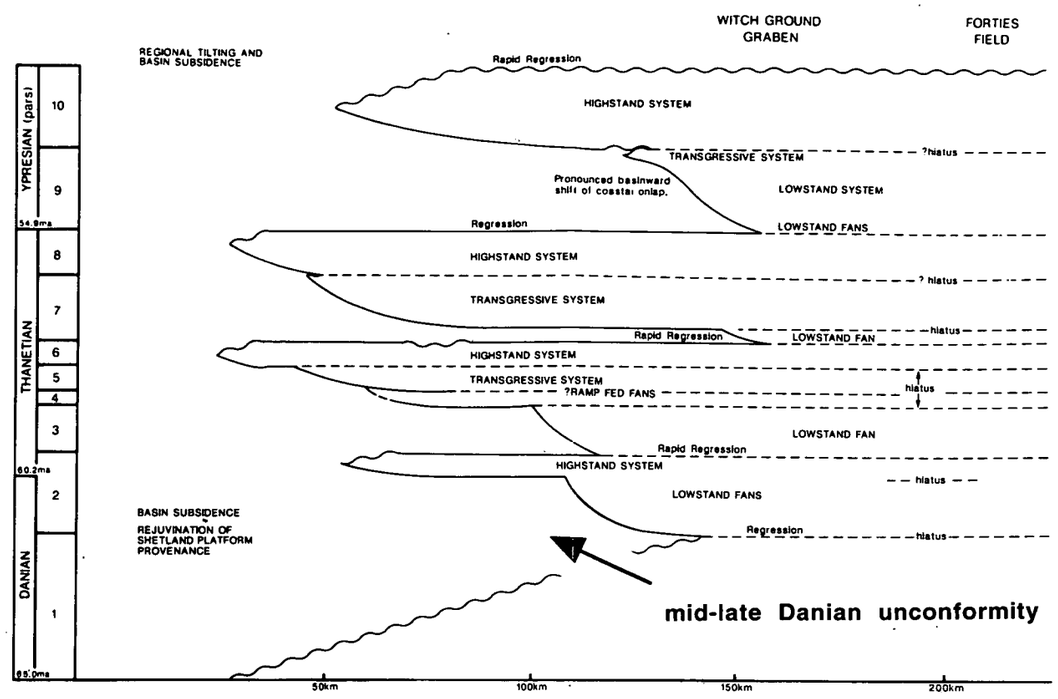

(b)

Figure 1.11 (a) Composite chronostratigraphic diagram for the Early Palaeogene of the central North sea. **(b)** Coastal onlap curve for the Early Palaeogene of the central North Sea. The diagram shows the relative onlap position of each of the ten described depositional sequences and the depositional systems operating within each. The terms 'highstand' and 'lowstand' refer only to the relative position of sea level. Stewart (1987). Note the mid-late Danian unconformity.

1.8 Conclusions.

(1) Significant tectonic reactivation of the Mesozoic basins of northwestern Europe occurred at various times during the Cenozoic with the inversion of pre-existing half-grabens and uplift of intrabasinal highs the dominant structural styles. Although not all the basins were active at the same times, a significant degree of synchroneity of the various inversion episodes and the deposition of the Cenozoic sediments existed, suggesting that specific plate-scale events may have been responsible. Additionally, the 1980s saw the detailed quantification of the burial and exhumation histories of both the basins and surrounding structural highs, revealing that substantial volumes of overburden had been removed from both areas at various times during the Cenozoic.

(2) Although by the end of the 1980s the Cenozoic structural evolution of most of the North Sea basins had been deduced, little attention had been paid to the Inner Moray Firth. In addition, as uplift and erosion of parts of the North Sea and adjacent areas had been recognised, the Inner Moray Firth presented itself as a candidate for such a study as if uplift and erosion had occurred, Cenozoic sediments may have been present in the basin and this would contradict the traditionally accepted strike-slip basin formation model in which no thermal subsidence deposits should be expected.

(3) The project primarily aimed to determine the timing and styles of Cenozoic structural reactivation within the Inner Moray Firth and the extent, magnitude and timing of Cenozoic uplift and erosion in both the Inner Moray Firth and Scottish Highlands. This was deemed necessary as it would place the basin in its Cenozoic regional context and consequently allow the data from this area to be combined with that from other areas so that potential causes of the observed effects could be rigourously tested. A subsidiary aim of the project was to examine the pre-Cenozoic evolution of the basin to check the newly emerging extensional hypothesis of basin formation against the traditionally accepted strike-slip origin of the basin.

(4) The tectonic setting of northwestern Europe changed dramatically in the Cenozoic to one of compression compared to the predominantly extensional setting of the Mesozoic and is believed to be primarily due to the interaction between North Atlantic rifting to the northwest and the Alpine Orogeny to the southeast. It is these processes which have been invoked to account for the uplift, erosion and tectonic reactivation seen in northwestern Europe. The potential causes fall into two main categories, namely those reliant upon the transmission of compressional stresses and those related to the rifting of the North Atlantic between Greenland and Europe.

2. Pre-Cenozoic geology.

2.1 Introduction.

In order to gain a full picture of the Tertiary evolution of the Inner Moray Firth, it is first necessary to understand the basin's preceding complex history. Consequently, this chapter is intended to document the major tectonic events that have occurred in the area. It shall draw mainly on published material but some details which were discovered whilst studying the basin will also be included.

2.2 Pre-Devonian geology.

The pre-Devonian geology of the Inner Moray Firth and surrounding areas consists entirely of basement type rocks (Anderton *et. al.*, 1979; Andrews *et. al.*, 1990). Onshore these units are widely exposed at outcrop but offshore evidence is limited. Although the basement can be recognised on deep seismic reflection profiles little is known in detail due to the limited number of wells penetrating it. However, enough evidence exists from both onshore exposures and the limited offshore data to divide the basement into four main types: Lewisian Gneiss, Moine, Dalradian and Caledonian Granite (Andrews *et. al.*, 1990).

The Lewisian Gneiss is restricted to small inliers immediately west of the Great Glen Fault in Easter Ross. They have received little attention except for the work of Rathbone and Harris (1980) who documented four phases of ductile deformation within them. Each of these events has been taken by them to correspond to the major metamorphic/orogenic events which affected the Gneiss up to and including the Caledonian Orogeny. Within the outcrop no brittle deformation is evident (Rathbone and Harris, 1980; Underhill and Brodie, 1993), but along their margins brittle tectonic linements can be found trending north-south to north east-south west **(Figure 2.1)**. Additionally, recent work (Underhill and Brodie, 1993) has demonstrated that the Rosemarkie inlier is fault-bounded and forms the hangingwall to a thrust over the Devonian cover rocks. This has led Underhill and Brodie (1993) to suggest that the inliers form the cores of north-plunging, thrust-related hangingwall anticlines, produced during Permo-Carboniferous ("Variscan") inversion of the Orcadian basin, and similar to the structural geometries seen in Devonian thrust-related anticlines in the same area, but at a deeper structural level.

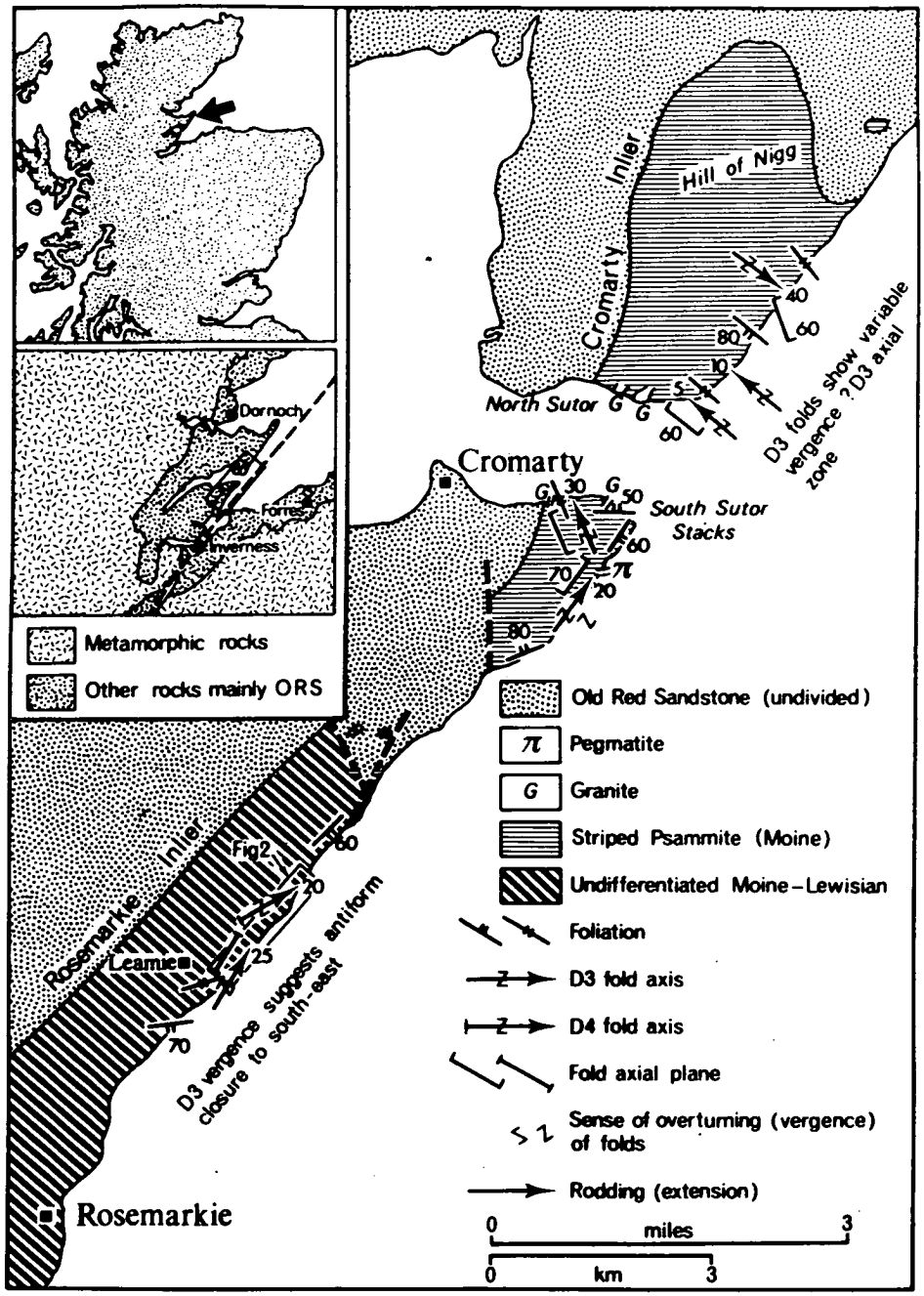

Figure 2.1 Geological map of the Moinian and Lewisian inliers at Rosemarkie and Cromarty (Rathbone and Harris, 1980).

The Moinian metasediments can be found to the north of the Great Glen Fault and are composed of psammitic and pelitic schists of Precambrian age. The rocks have suffered a long and complex deformation history, probably being first metamorphosed during the Precambrian Grenville Orogeny and subsequently deformed during the 'Morarian' metamorphic event (late Precambrian) and the Caledonian Orogeny (Anderton *et. al.*, 1979).

Of the Precambrian basement units in the Inner Moray Firth, the Dalradian is probably the most common (Andrews *et. al.*, 1990). Apart from outcrop on the Scottish Mainland it has been penetrated by several wells offshore. The earliest part of the Dalradian is formed by the Grampian Group and consists almost entirely of psammite. The overlying Appin and Argyll groups are formed of interbedded limestones, quartzites and pelitic schists and the top of the succession, the Southern Highland Group, contains metagreywackes, volcanoclastics and locally intruded basic sills. The Dalradian was deformed and metamorphosed during the Caledonian Orogeny (Anderton *et. al.*, 1979).

The Moine and Dalradian were intruded by large granitic bodies during two separate phases of the Caledonian Orogeny. This has led to the subdivision of the Caledonian granites into the 'Older' granites which were intruded around 470ma and the 'Newer' granites, intruded between the Late Silurian and Early Devonian (430-400ma). The granites are widespread onshore, forming a large proportion of the Grampian Highlands and have been discovered offshore, with wells have penetrating granite on the western flank of the Smith Bank High and in the Halibut Horst area, while Dimitropolis and Donato (1981) have postulated the existence of a granitic body under the Central Ridge and Bartholomew *et. al.* (1993) in the footwall to the Wick Fault **(Figure 2.2)**. However, as no wells have been drilled through the Central Ridge or the footwall to the Wick Fault these suggestions cannot be proved. The presence of granites in the footwall of the Helmsdale Fault (Helmsdale Granite), beneath the Smith Bank High, Halibut Horst and possibly the Central Ridge and Wick Fault suggests that they may have been the controlling factors in their development as palaeohighs during Kimmeridgian rifting **(Figure 2.2)**.

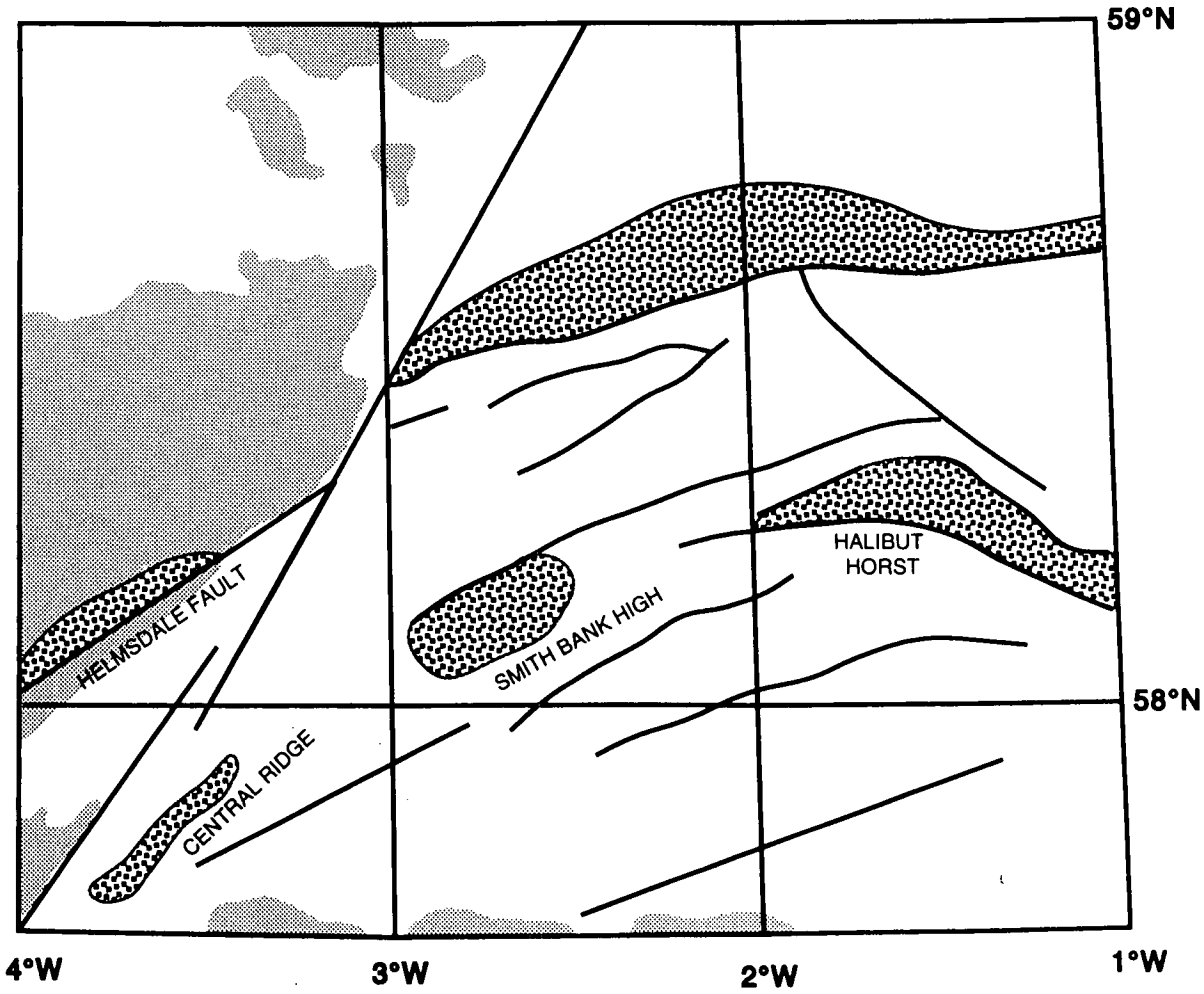

Figure 2.2 Location of known and proposed Caledonian Granites relative to major structural highs which developed during Kimmeridgian rifting. The immediate footwall to the Helmsdale Fault contains the Helmsdale Granite while both the Smith Bank High and Halibut Horst are known to be underlain by granites. Additionally, Dimitropoulos and Donato (1981) have proposed that a granite underlies the Central Ridge.

2.3 Devonian Orcadian Basin.

Following the Caledonian Orogeny a major depositional phase began during the Devonian, producing the Orcadian Basin. This basin extended from at least its present western outcrop in Scotland to western Norway **(Figure 2.3)** and consists of predominantly terrestrial sediments (Andrews *et. al.*, 1990). Traditionally, the stratigraphy of the basin fill has been divided into the Lower, Middle and Upper Old Red Sandstone Groups, approximately corresponding to the Early, Middle and Late Devonian/Early Carboniferous respectively and is essentially based on structural grounds as they are commonly separate by unconformities (Coward *et. al.*, 1989; Trewin, 1989). The Lower Old Red Sandstone consists of predominantly fanglomeratic deposits of limited distribution resting on an irregular Moinian palaeotopography (Trewin, 1989). The Middle and Upper Old Red Sandstones, which can overstep the Lower Old Red Sandstone to rest on the Moinian topography, consist of thick lacustrine muds and sands which become more fluvio-lacustrine towards the top (Trewin, 1989).

The limited exposure of the Old Red Sandstone onshore and the fact that on many offshore seismic reflection profiles have it buried beneath thick Mesozoic/Cenozoic sequences has led to some ambiguity as the the tectonic evolution of the basin. Consequently, two potential (though not mutually exclusive) models have been proposed for the development of the basin: a strike-slip model and an orogenic collapse model. A strike-slip model has been proposed in which many of the major tectonic linements in Scotland (e.g. the Highland Boundary, Great Glen, Melby, Nesting and Walls Boundary faults) underwent sinistral motion due to the oblique collision of Greenland and Europe during the Caledonian Orogeny (Trewin, 1989; Richards, 1990). This would have resulted in the localised transpression and transtension and the consequent formation of uplifted source areas and subsiding basins. The proposed magnitudes of movement on the faults is large, with upto 2000km of sinistral displacement suggested for the Great Glen Fault (Van der Voo and Scotese, 1981). However, such large displacements are now generally discounted due to palaeogeographic reconstructions showing that no more than 29km of dextral, post-Devonian displacement can be accommodated on the Great Glen Fault (Rogers, 1987; Rogers *et. al.*, 1989) and consequently, the strike-slip model for the formation of the Orcadian Basin may be considered inappropriate.

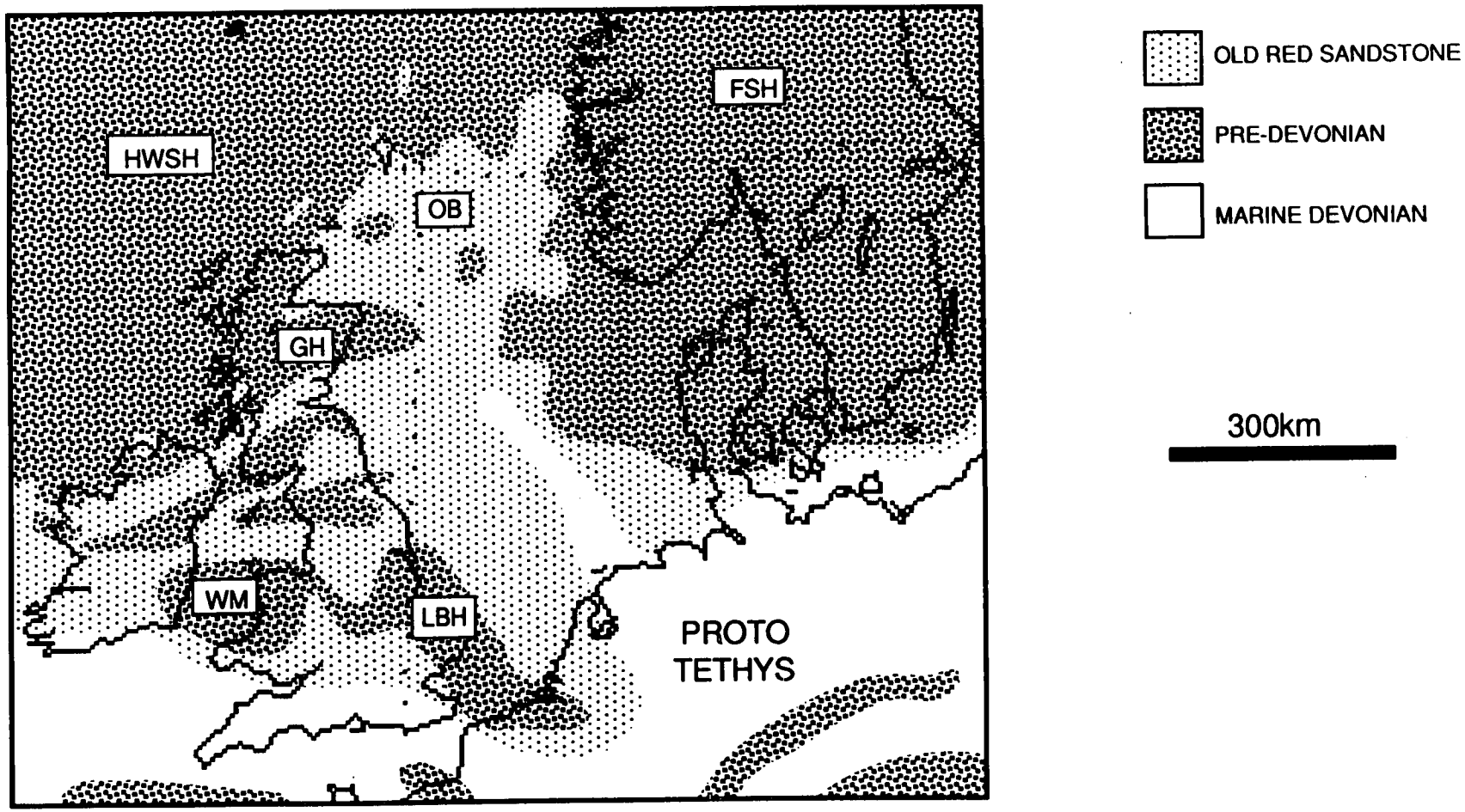

Figure 2.3 Maximum extent of continental Old Red Sandstone and marine Devonian sediments of Proto-Tethys. FSH = Fenno-Scandian High, GH = Grampian High, HWSH = Hebridies West Shetland High, LBH = London-Brabant High, OB = Orcadian Basin, WM = Welsh Massif. (After Glennie, 1990).

In view of the doubt cast upon the strike-slip model by geological constraints a more reasonable model for the formation of the basin is the extensional collapse of the overthickened crust formed during the Caledonian Orogeny (McClay *et. al.*, 1986; Norton *et. al.*, 1987; Coward *et. al.*, 1989). For example, in the Inner Moray Firth, the onshore exposures at Pennan **(Figure 2.4)** show two eastward dipping normal faults which separate Lower and Middle Old Red Sandstone from the Dalradian basement. Furthermore, the Old Red Sandstone deposits can be shown to thicken towards the faults, suggesting that the faults were active during their deposition (Coward *et. al.*, 1989). In the West Orkney Basin seismic reflection profiles show half grabens developed containing Middle Old Red Sandstone deposits which can be traced directly onshore (Coward *et. al.*, 1989). These half grabens developed due to the formation of eastward dipping normal faults which detach along reactivated Caledonian thrusts **(Figure 2.5)**. However, in Caithness, faulting appears to be less important with the only normal faulting appearing around the basin margins, with the majority of the basin fill being deposited in a passive tectonic enviroment (Coward *et. al.*, 1989). Consequently, although the evidence appears to suggest orogenic collapse as the mechanism for the formation of the Orcadian Basin further work is required to prove this conclusively.

2.4 Permo-Carboniferous ("Variscan") inversion.

Seismic data from the Inner Moray Firth highlight a significant unconformity within the Late Palaeozoic succession largely defined by truncation of underlying reflectors and onlap of subsequent units as previously identified and documented by Roberts *et. al.* (1990) and Underhill and Brodie (1993) **(Figure 2.6)**. Data from the Beatrice area (UKCS license block 11/30) and onshore in Easter Ross suggest that the dominant structural style beneath this unconformity consists of eroded thrust bounded, hangingwall anticlines (Underhill and Brodie, 1993; **Figure 2.7**). These apparently record a phase of Permo-Carboniferous ("Variscan") contractional deformation prior to partial peneplanation and Permian sedimentation **(Figure 2.8)**. As such, these structural styles are analogous to those formed during basin inversion in nearby areas (e.g. Coward *et. al.*, 1989; Astin, 1990; Seranne, 1992).

Although the most well defined data for this deformation comes from onshore exposures, some supporting evidence exists from recent, good quality seismic data from the Beatrice area which shows the overlying succession draping a well defined topography **(Figure 2.8)**, which maybe interpreted to have been partially created

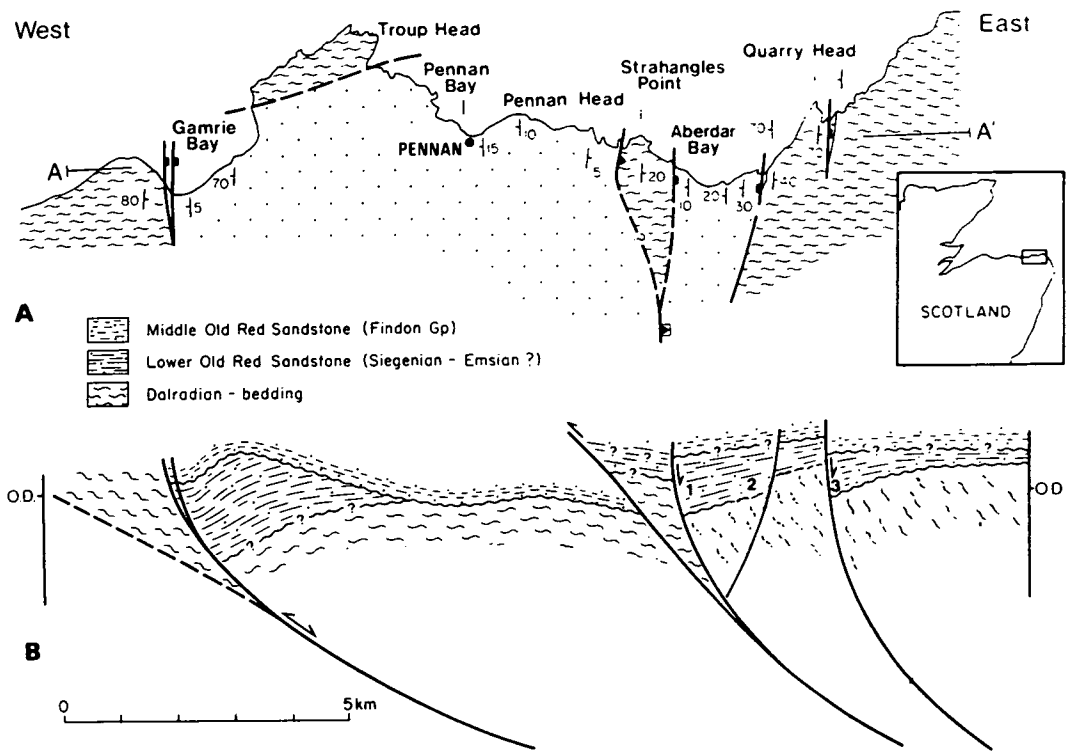

Figure 2.4 A, Map of the Pennan coast showing location of Devonian basins and bounding faults. Devonian shown by coarse stipple. B, Section through the Pennan half-graben. The Lower Old Red Sandstone fill is a growth sequence, which is unconformably overlain by Middle Old Red Sandstone. The basin has been inverted by reactivation of the bounding faults, possibly in the Permo-Carboniferous (Coward *et. al.*, 1989).

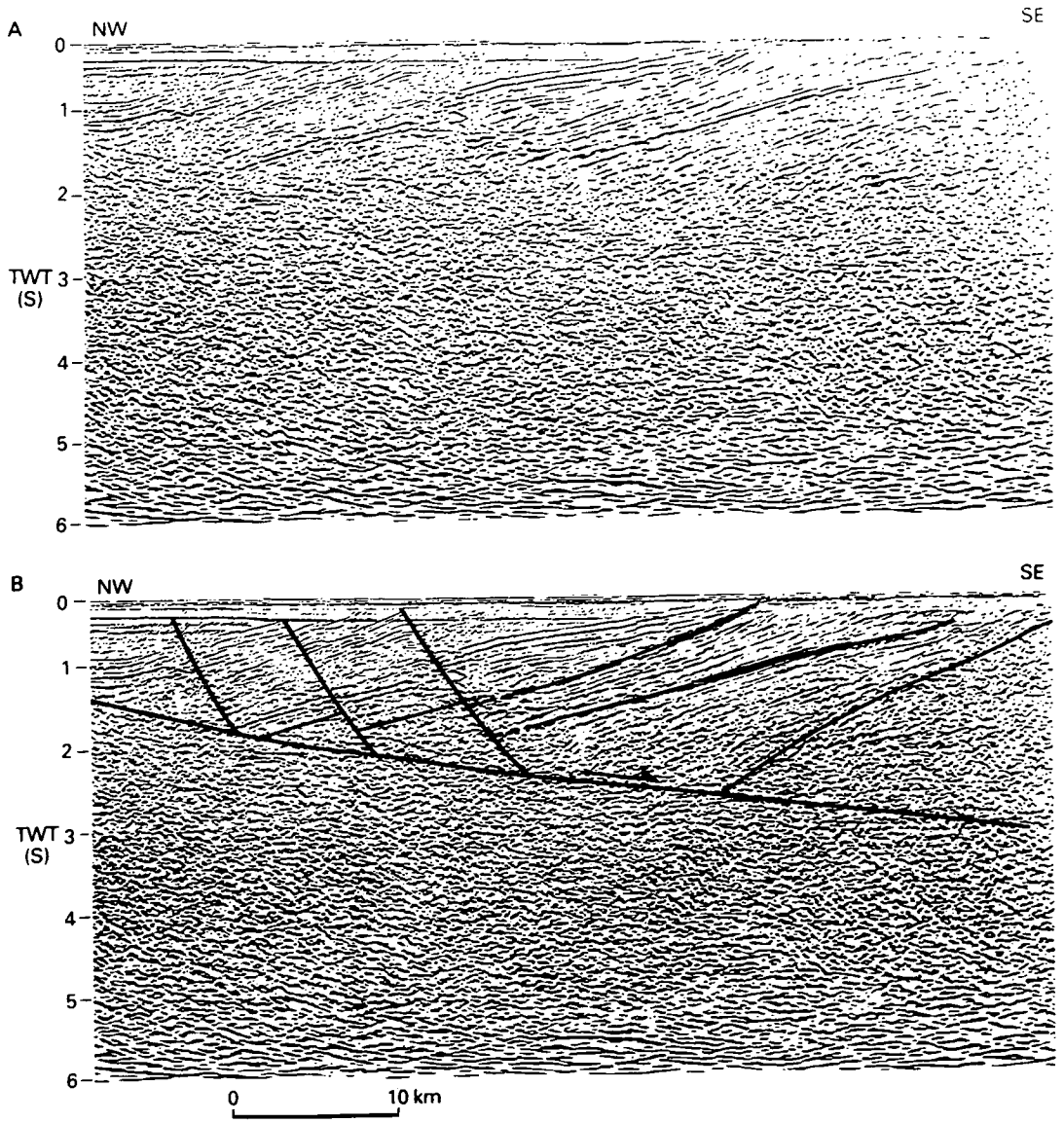

Figure 2.5 A, Seismic profile showing changing onlap directions through time, central West Orkney Basin. B, Structural interpretation of A showing steeply dipping normal faults which decouple on a shallowly dipping, reactivated Caledonian thrust (Coward *et. al.*, 1989).

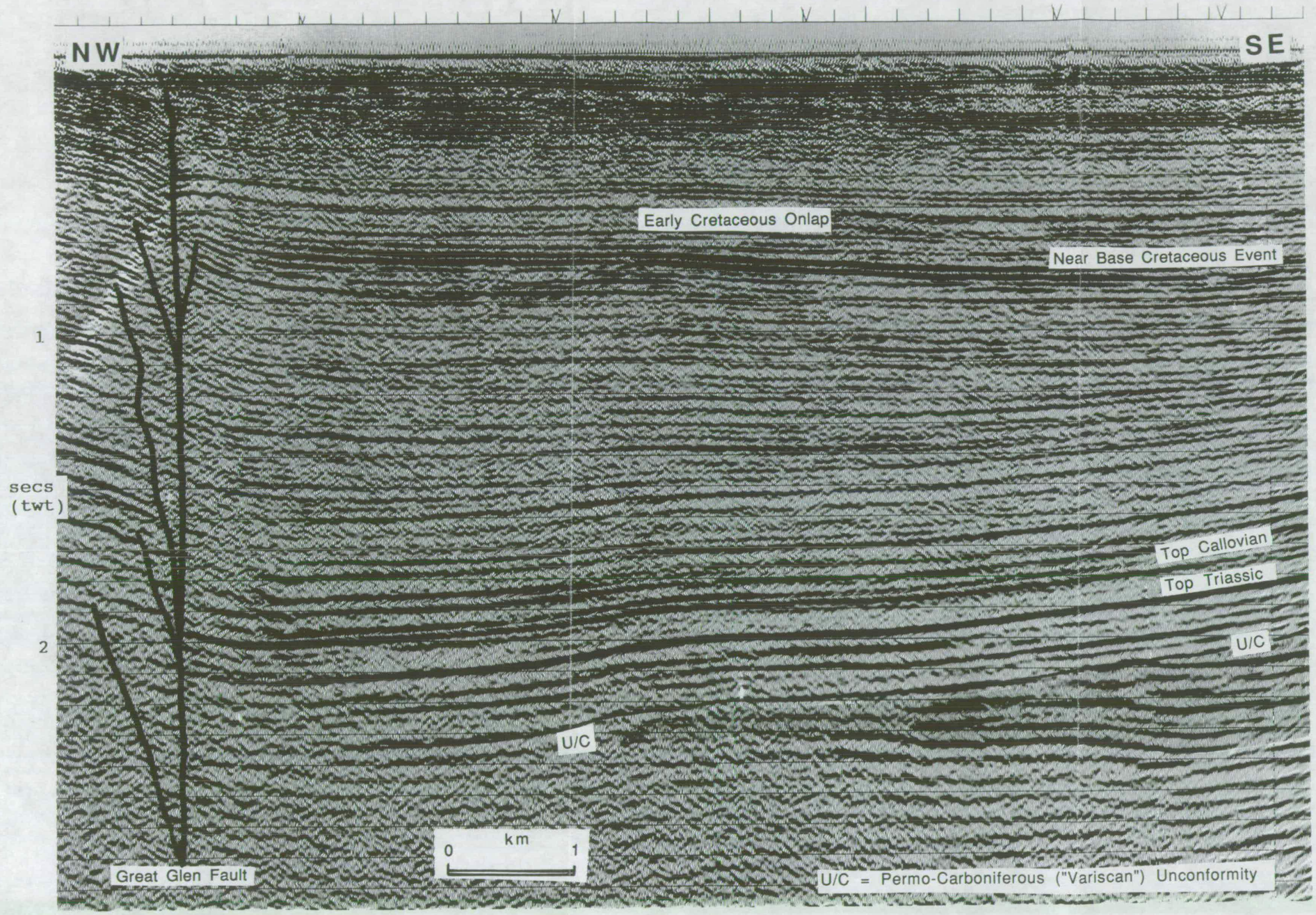

Figure 2.6 Seismic reflection profile highlighting the Permo-Carboniferous "Variscan" unconformity (U/C) defined largely by truncation of underlying strata which separates deformed Devonian sequences from the overlying Permian red beds (Thomson and Underhill, 1993).

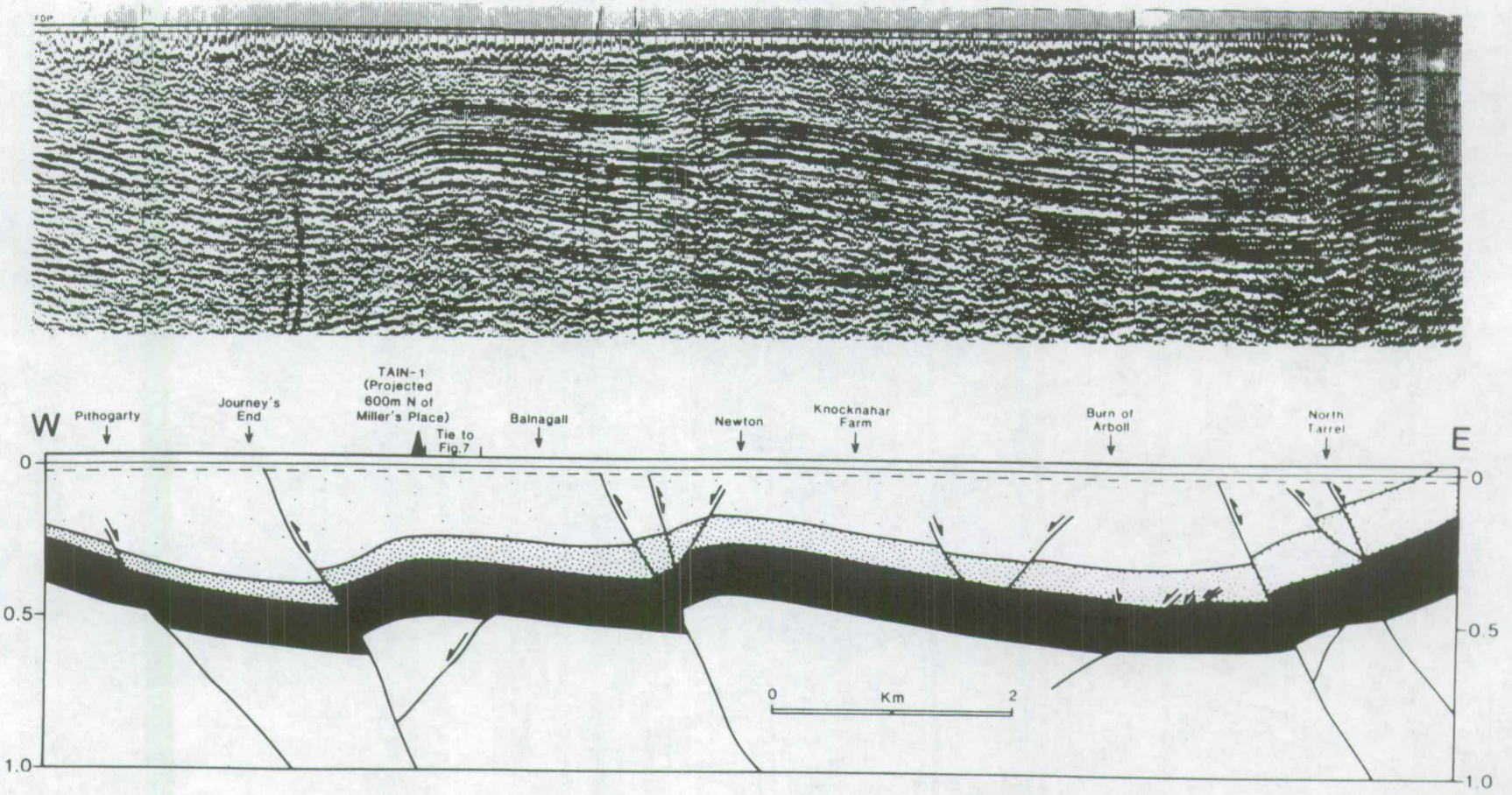

Figure 2.7 Approximately W-E trending seismic dip section (a) and line-drawing interpretation (b). The line highlights the occurrence of hangingwall anticlines in association with faults. Structural relations suggest that they result from the contractional reactivation of steeply-dipping faults that had previously experienced extension (Underhill and Brodie, 1993).

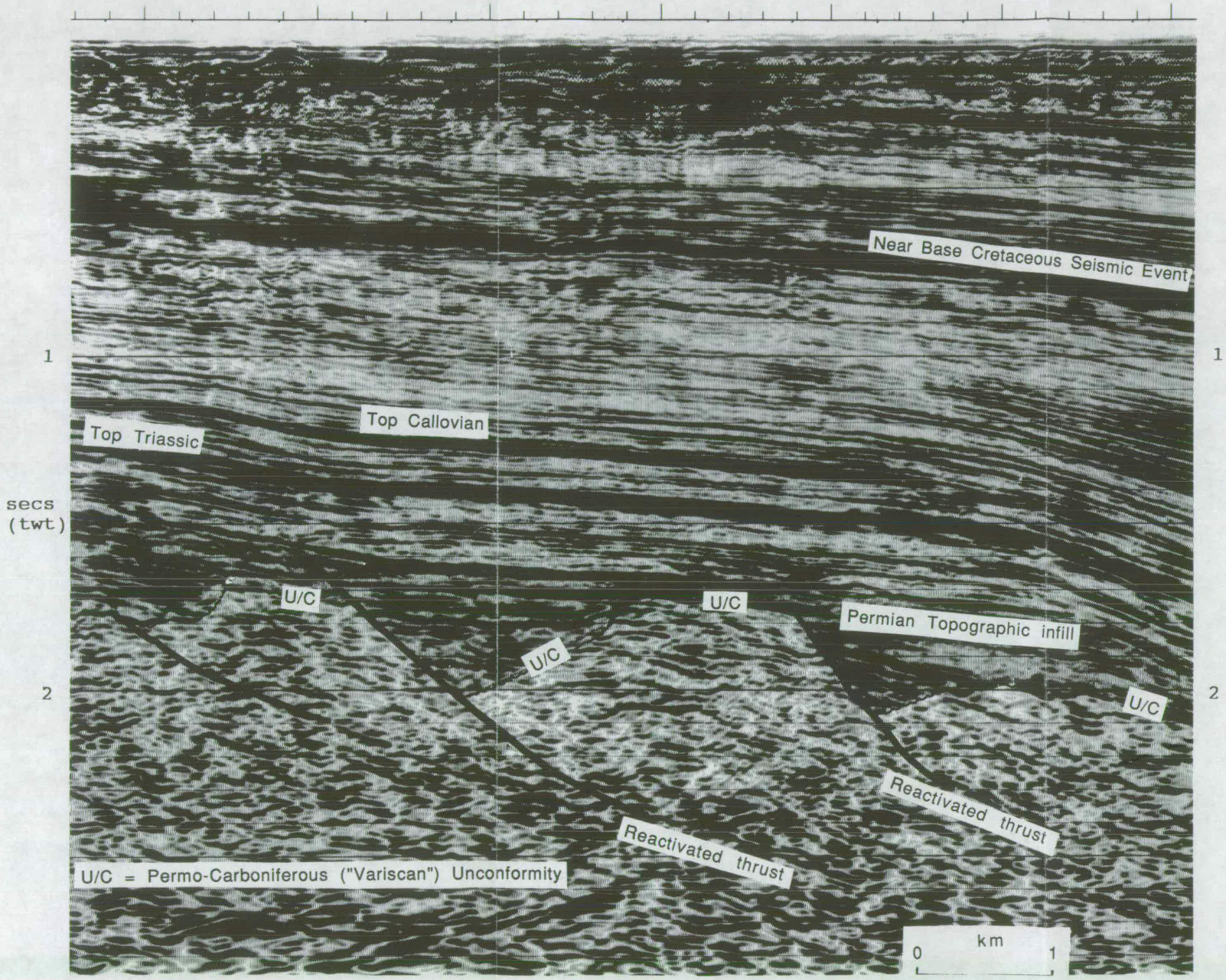

Figure 2.8 Offshore seismic line from the area southwest of the Beatrice Field (UKCS license block 11/30b) highlighting the close association of Late Palaeozoic (i.e. Permo-Carboniferous) contractional structures with reactivated extensional faults below the level of the unconformity which separates the Permian and Late Palaeozoic sequences. The attitude of the Permian strata (i.e. lack of divergent reflections) in the reactivated sub-basin suggests that syn-rift deposition was minor relative to late-stage (post-rift) topographic infill (Underhill and Brodie, 1993; Thomson and Underhill, 1993).

by renewed Permian extension following the inversion episode. Additionally, the extreme shallowing in the dip of the Lossiemouth Fault with depth has led to the suggestion that it too may well be the remnant of a reactivated Caledonian low-angle thrust at depth (Andrews *et. al.*, 1990). This suggestion seems highly likely in view of the fact that some seismic reflection profiles show what may well be a thrust-related hangingwall anticline developed in Devonian sediments **(Figure 2.9)**. If this is the case then it may well be possible that the Lossiemouth Fault developed as an extensional feature during the Devonian and was then subsequently reactivated first as a "Variscan" contractional feature and later as an extensional fault.

As it is likely that the Early Devonian deformation in the Inner Moray Firth was controlled by active rifting (McClay *et.al.*, 1986; Coward *et.al.*, 1989), it is possible that many of the contractional features described above also represent reactivated normal faults. However, it remains unclear whether contractional deformation is always closely associated with syn-sedimentary faults and the extent to which truncation by the unconformity has occurred within the pre-Permian sequence. Consequently, the exact stratigraphic level expected beneath the unconformity may be highly variable across the Inner Moray Firth and it is possible that significant amounts of Devonian and possibly thick Carboniferous sections will be found locally. Hence, Late Carboniferous successions are likely to be preserved in some areas where the unconformity had significant topography.

2.5 Permo-Triassic extension.

Permian successions within the Inner Moray Firth are hard to separate from other red bed sequences because of the lack of distinctive palaeontological markers and their lack of seismic character (Thomson and Underhill, 1993). Despite these limitations, the lowest units occurring above the prominent Variscan unconformity show varying degrees of stratigraphic thickening on the seismic data. Although this can generally be explained by the passive infill of remnant thrust-related topography, the occurrence of some thickening appears to occur adjacent to reactivated extensional faults **(Figure 2.8)**, indicating a minor component of early, syn-sedimentary tectonic control (Underhill and Brodie, 1993; Thomson and Underhill, 1993).

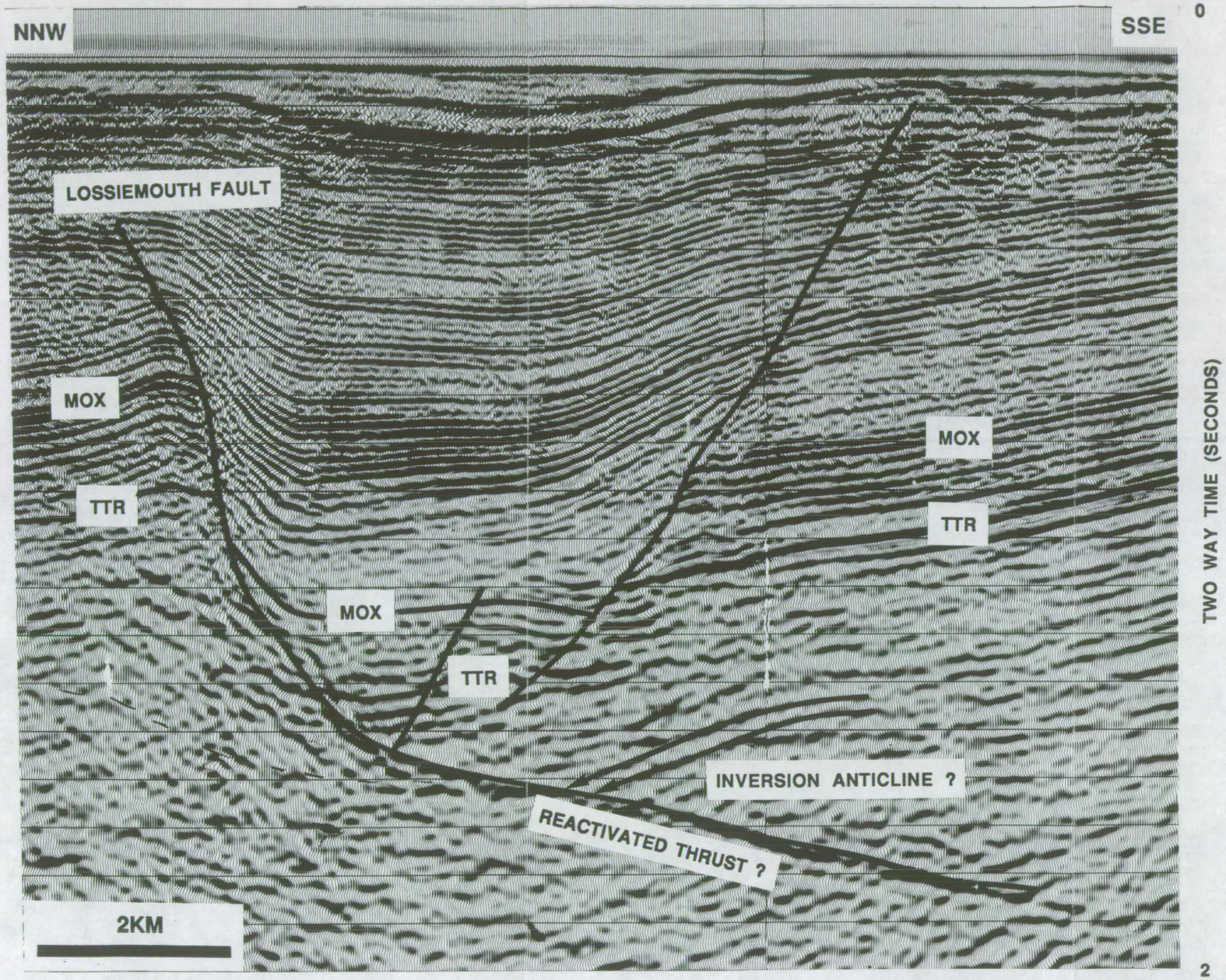

Figure 2.9 Seismic reflection profile of the Lossiemouth Fault. Note that the fault flattens rapidly with depth and that the reflectors above it appear to be folded down towards the fault suggesting that the fault may be a reactivated "Variscan" thrust with an inversion anticline above it. BCRT = Base Cretaceous, MOX = Mid Oxfordian Unconformity and TTR = Top Triassic.

2.6 Late Permian, Early Triassic and Early Jurassic thermal subsidence.

The subdivision of later Permian and Triassic is hampered because Zechstein sequences are also often dominated by reddened sandstones similar to Triassic, Permian, Carboniferous and Devonian strata. Despite these problems, the seismic data show that Late Permian and Triassic sequences are largely dominated by concordant reflectors and broad basin-wide westerly thickening packages with little or no variation adjacent to faults (Underhill, 1991a; Thomson and Underhill, 1993). In contrast to Frostick *et. al.* (1988), the data currently available from wells are too sparse to allow a detailed model to be proposed for Permo-Triassic tectonics and sedimentation. However, the Triassic sequences generally appear to have been laid down in a basin experiencing broad-based subsidence following an earlier extensional episode. As such, they probably represent a phase of thermal subsidence following the minor Permian rifting (*contra* Frostick *et. al.*, 1988). The absence of abrupt thickening across and along the Great Glen Fault again suggests that it played a negligible role in controlling basin development at this time (*contra* Frostick *et. al.*, 1988).

The top of the Triassic succession is marked by the most prominent seismic reflector in the area. Its onshore equivalent is represented by the Stotfield Cherty Rock, a significant silcrete horizon marking a notable break in sedimentation (Naylor *et. al.*, 1989). Overlying Early Jurassic units also consist of relatively thin concordant sequences which show gradual thickening towards the Scottish mainland with maximum thicknesses in the Sutherland Terrace area (Andrews and Brown, 1987; Andrews *et. al.*, 1990; Underhill, 1991a and b; Thomson and Underhill, 1993). These Early Jurassic sequences are interpreted to represent continued gentle, thermal subsidence following the Permian rifting event.

2.7 Toarcian-Aalenian regional uplift and Aalenian-Oxfordian thermal subsidence.

Evidence for a regional phase of uplift affecting the Inner Moray Firth during the Late Toarcian-Early Aalenian due to a regional doming event in the North Sea comes from stratigraphic information beyond the level of seismic resolution. These data show that a series of regional "mid-Cimmerian" unconformities occur throughout the Middle Jurassic. The earliest and most significant of these unconformities occurs throughout the area, truncates Lower Jurassic successions

including the Orrin Formation and shows progressive onlap of Bathonian-Oxfordian sequences towards the east (Underhill and Partington, 1993a and b; Stephen *et. al.* 1993).

Although regional doming has not had any significant control on structural styles at a seismic scale, documentation and understanding of its cause and effects has significance for the subsequent development of important structural styles (e.g. in the Late Jurassic rift episode). Regional mapping of the temporal and spatial variation of this event shows that similar relations exist over a wide area in the North Sea, which has been interpreted to be the result of regional doming ("Central North sea Dome"; Hallam and Sellwood, 1976; Ziegler, 1982, 1990a and b) above a warm, diffuse and transient plume head (Underhill and Partington, 1993a and b; **Figure 2.10**). Evidence that progressive shallowing occurred during the Late Toarcian (i.e. Orrin Formation in the Inner Moray Firth; Stephen *et. al.*, 1993) suggests that uplift may have begun in the Lower Jurassic. Stratigraphic evidence suggests that the unconformity reached its maximum areal extent and hence, that the dome reached its climax during the Late Bajocian-Early Kimmeridgian (Underhill and Partington, 1993a and b; **Figure 2.10**) perhaps following a renewed phase of Early Bajocian uplift which created another relatively widespread erosive unconformity.

Most significantly for the subsequent development of diagnostic structural styles in the Inner Moray Firth, the stratigraphic data suggest that the trilete North sea rift system already had an expression during the Middle Jurassic prior to the period of volcanism and most significant rifting. In the rift arms, significant deflection of the extent of maximum flooding may be seen along each of the regions subsequently characterised by significant syn-sedimentary extension, suggesting that the Inner Moray Firth and Viking Graben formed topographic depressions prior to the onset of half-graben development (Underhill and Partington, 1993a and b; **Figure 2.11**). This suggests that lithospheric thinning and differential subsidence had already occurred along subsequent axes of deformation during uplift of the dome and persisted throughout the phase of subsidence resulting from decay of this domal uplift.

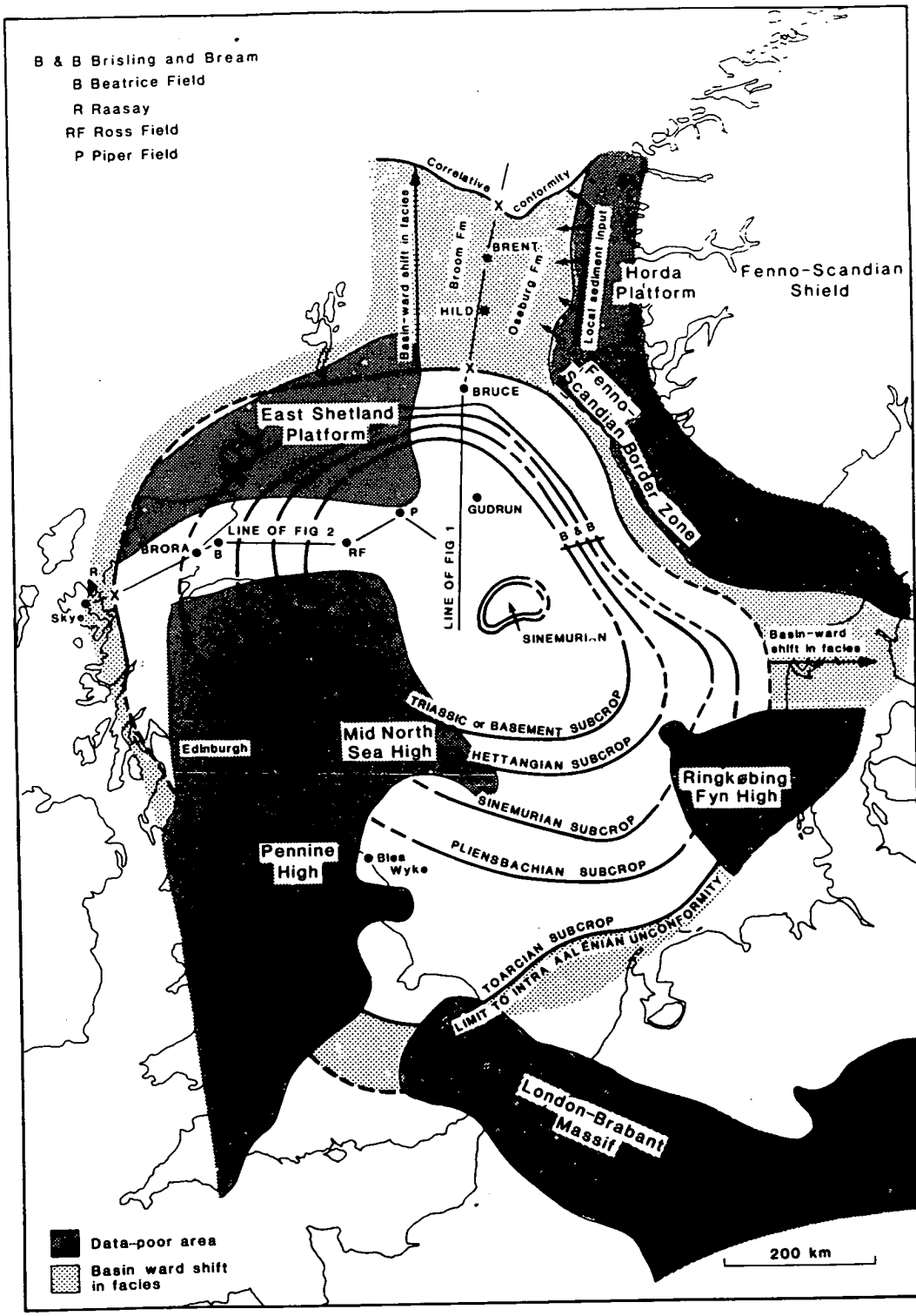

Figure 2.10 Plot of the limit to stratigraphies truncated beneath the "Mid Cimmerian Unconformity". The map is dominated by the bulls-eye distribution of subcropping units interpreted to result from regional doming centred upon the North Sea triple junction (Underhill and Partington, 1993a and b).

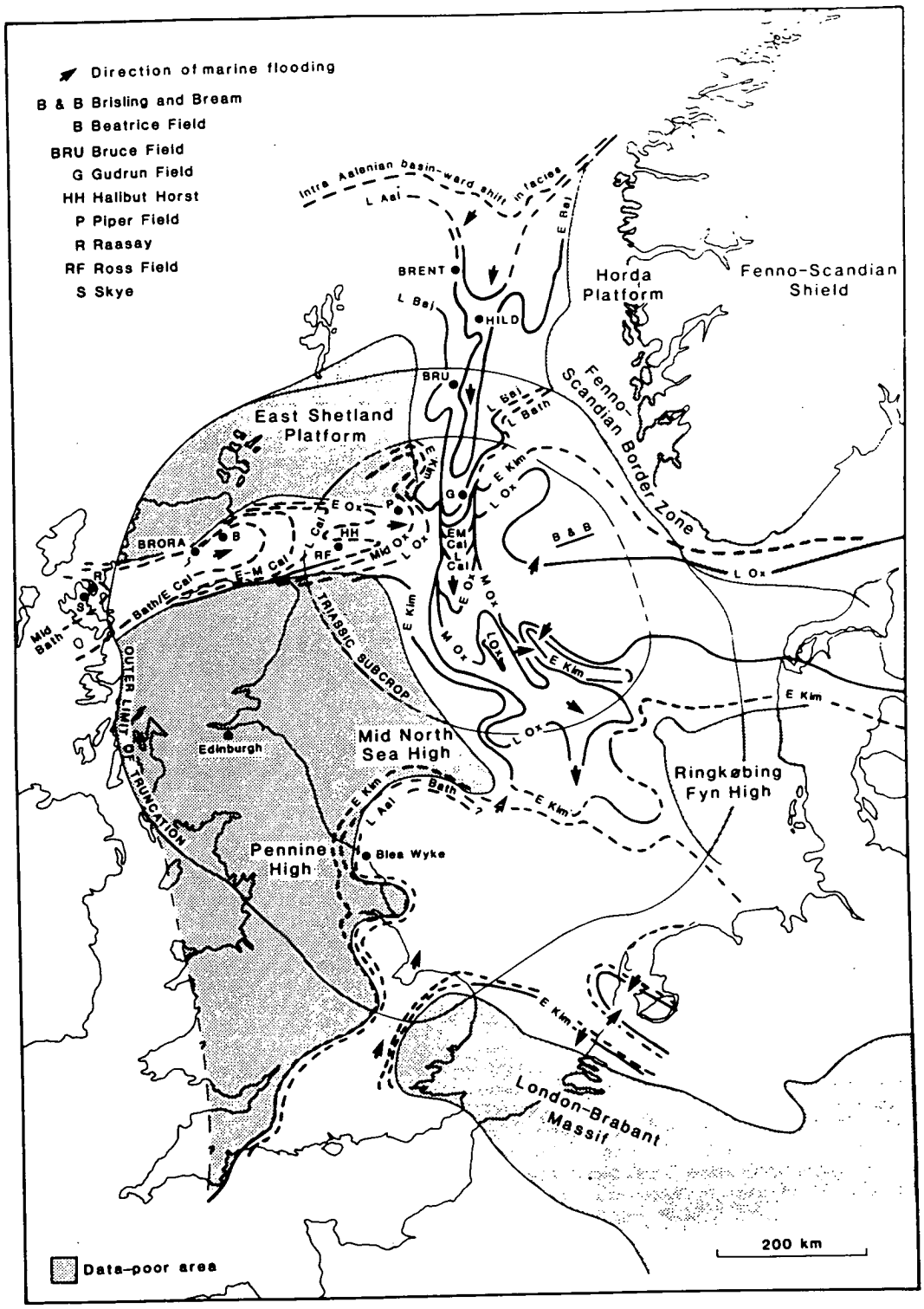

Figure 2.11 Plot of the limits to stratigraphic markers onto "Mid Cimmerian Unconformity" surface showing the progressive central onlap throughout the Middle-Late Jurassic (Underhill and Partington, 1993a and b).

2.8 Upper Jurassic rifting.

A drastic change in structural styles and basin architecture characterises the Late Jurassic of the Inner Moray Firth. Seismic data demonstrate the development of numerous classic half-graben across the area, interpreted to result from dip-slip extension (Underhill, 1991a and b; Thomson and Underhill, 1993). This phase of extension was the most significant for the development of potential hydrocarbon bearing footwall structures adjacent to active extensional faults **(Figure 2.12)**.

The duration of demonstrable syn-sedimentary fault activity may be gauged from the occurrence of divergent seismic reflector geometries and sedimentary evidence from onshore successions. These relations suggest that the area was initially deformed by continuous fault block rotation but was subsequently dominated by passive sedimentary infill of topography created during discrete rift episodes (characterised by onlapping reflectors) during the Late Kimmeridgian (Underhill, 1991b) in a similar fashion to that seen elsewhere (e.g. the Brae area in the South Viking Graben; Turner *et. al.*, 1987) and East Greenland (Surlyk, 1978).

The Kimmeridgian is capped by the second most prominent seismic reflector seen in the area: the "Base Cretaceous Event". As such, it is convenient to use this regional marker to define a distinct seismic package. However, in reality, this event does not appear to represent an unconformity but rather a condensed section (Rawson and Riley, 1982), which lies beyond the level of seismic resolution. Furthermore, it appears to have formed in response to a drastic change in water circulation patterns (Rattey and Hayward, 1993), rather than a particularly significant change in tectonic deformation and structural styles.

2.9 Cretaceous thermal subsidence.

Early Cretaceous sequences are preserved and well-imaged above the "Base Cretaceous Event". They are largely characterised by well defined onlapping reflectors, which show progressive onlap towards the basin's margins **(Figure 2.13)**. Passive infill of well-defined Jurassic half-grabens occurred with evidence for significant shifts in depocentre location (compared to the Kimmeridgian) to areas adjacent to the Wick and Little Halibut faults (Andrews *et. al.*, 1990; Roberts *et. al.*, 1990). The Late Cretaceous Chalk sequence can similarly seen to drape most of the pre-existing topography and although commonly demonstrating passive onlap onto

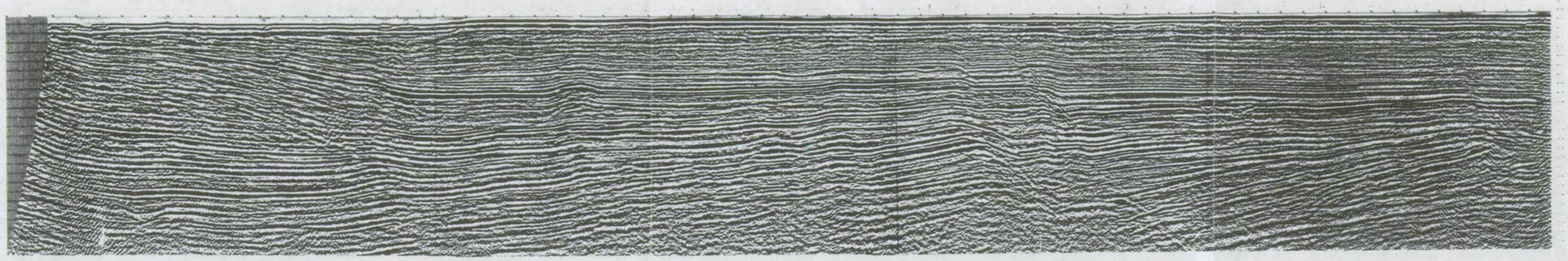

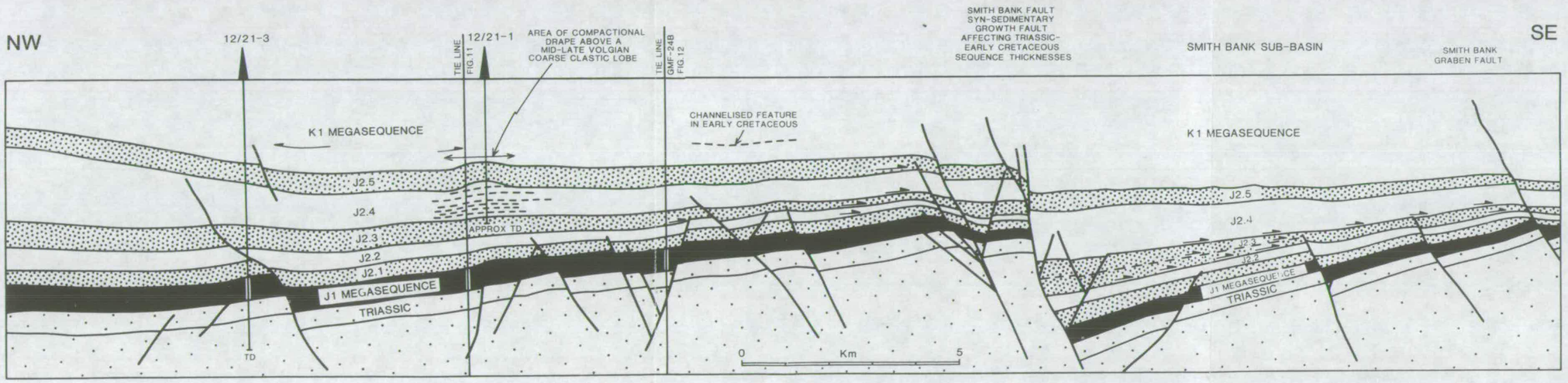

Figure 2.12(a) Seismic reflection profile and interpretation from the Inner Moray Firth. The interpretation shows the syn-rift Upper Jurassic megasequence (J2) subdivided into 5 sequences (J2.1-2.5). As can be seen these sequences thicken to varying degrees towards the major Upper Jurassic half-graben bounding faults (Underhill, 1991b).

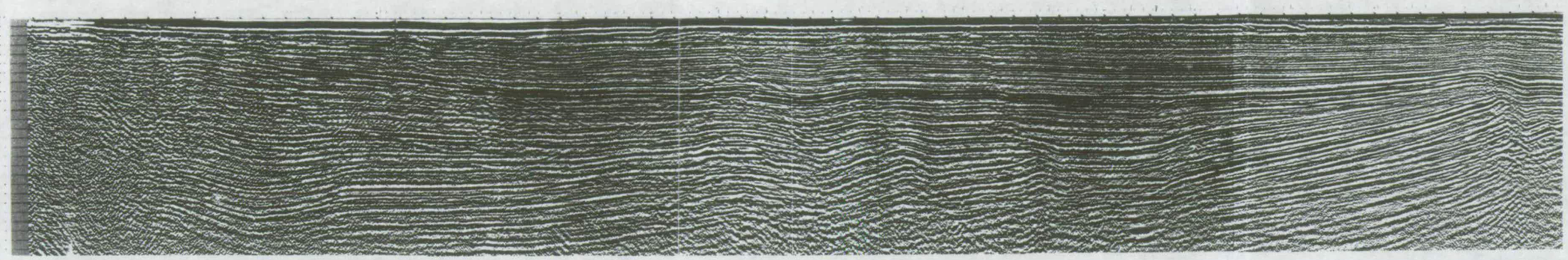

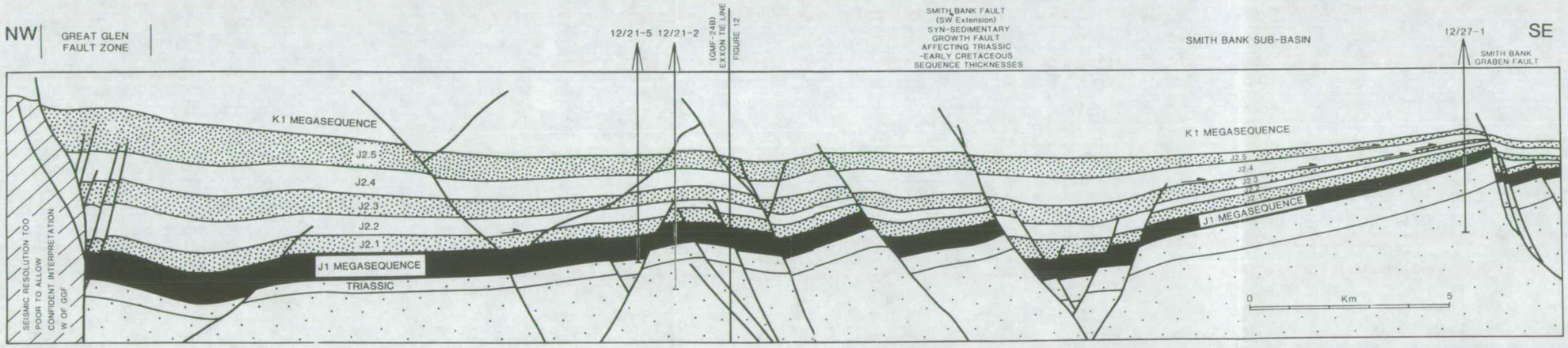

Figure 2.12(b) Seismic reflection profile and interpretation from the Inner Moray Firth. The interpretation shows the syn-rift Upper Jurassic megasequence (J2) subdivided into 5 sequences (J2.1-2.5). As can be seen these sequences thicken to varying degrees towards the major Upper Jurassic half-graben bounding faults (Underhill, 1991b).

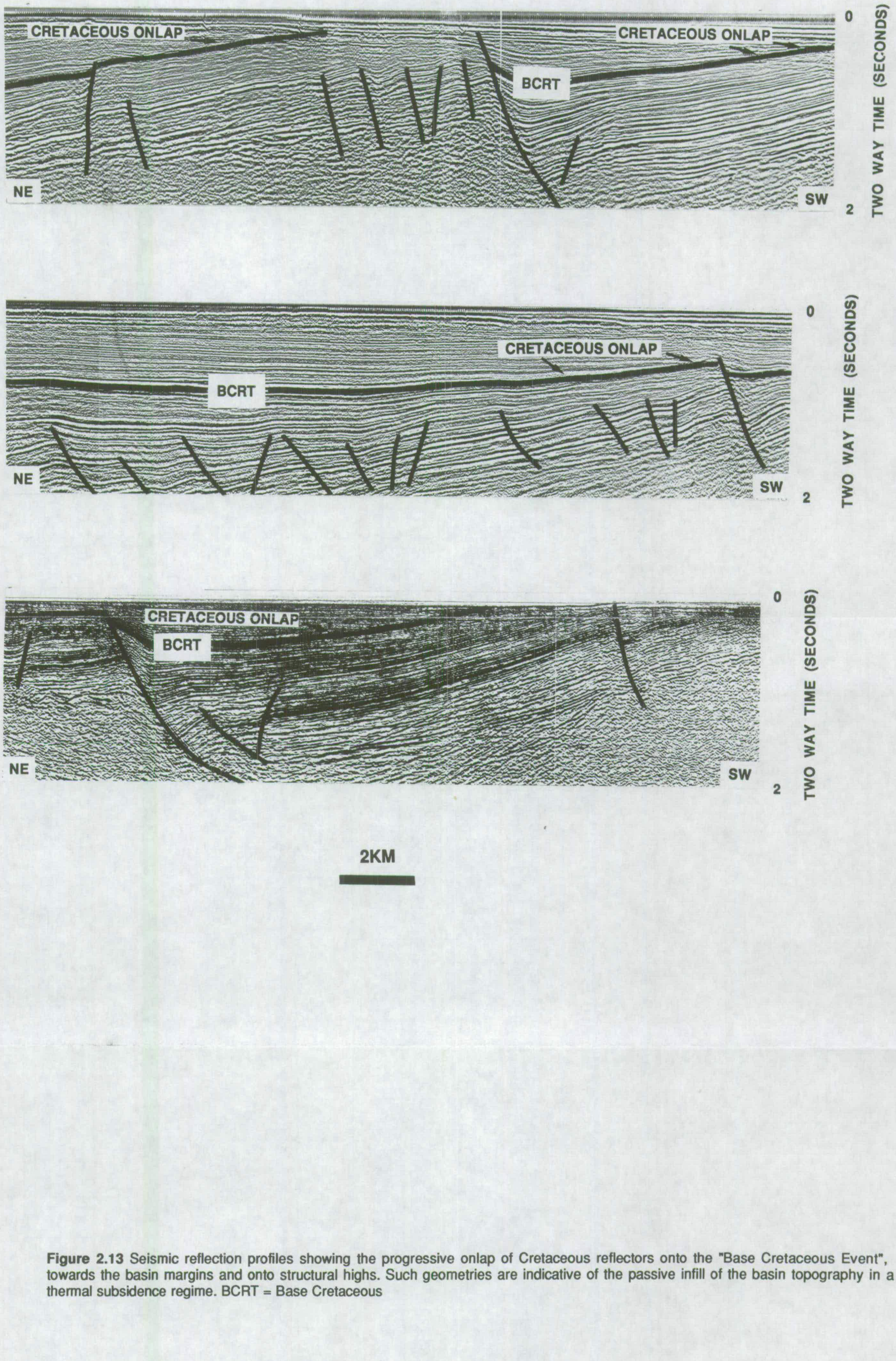

Figure 2.13 Seismic reflection profiles showing the progressive onlap of Cretaceous reflectors onto the "Base Cretaceous Event", towards the basin margins and onto structural highs. Such geometries are indicative of the passive infill of the basin topography in a thermal subsidence regime. BCRT = Base Cretaceous

basement highs, it is only occassionally interupted by unconformities (Andrews *et. al.*, 1990). The lack of evidence for divergent reflectors within the Cretaceous seismic sequences is suggestive of a passive infill of a pre-existing topography. Such an interpretation is supported by palaeontological evidence which suggests that the basin was underfilled at this time (Thomson and Underhill, 1993). Consequently, it seems most plausible that the area was undergoing a phase of thermal subsidence following the Late Jurassic rift episode.

2.10 Cenozoic evolution of the Inner Moray Firth.

This chapter has demonstrated that the Inner Moray Firth has experienced a long and complex history of deformation since the Caledonian Orogeny and up to the end of the Mesozoic. Both extensional and compressional tectonics and uplift and erosion have been involved and some of the phases of deformation appear to have been partly influenced by pre-existing structures (e.g. the locations of the major Late Jurassic half-graben bounding faults is potentially related to the to the position of the Caledonian granites in the basin). It is the intention of the rest of this thesis to describe the events which occurred during the last phase of deformation to have occurred in this basin, i.e. during the Cenozoic. It will be demonstrated that uplift leading to the removal of kilometres of stratigraphy occurred and that the pre-existing structural elements of the basin were reactivated. Additionally, attempts will be made to place these phenomena in their regional context and suggest the causes which brought them about.

2.11 Conclusions.

(1) The limited exposure and well data from the Inner Moray Firth seems to suggest that the basement consists of Lewisian Gneiss, Moine, Dalradian and Caledonian granites. Additionally, the limited data indicates that some of the later structure of the basin may have been influenced by the contrasting basement lithologies, particularly the occurrence of Caledonian granites beneath the structural highs may suggest they controlled the location of rifting in the basin.

EX BIBL UNIV. EDINBURGH

(2) Following the Caledonian Orogeny the area experienced subsidence and sedimentation, probably due to orogenic collapse, during the Devonian and Early Carboniferous. Although again evidence is limited, both onshore and offshore data suggest active rifting occurred at least locally and particularly during the earlier stages of the collapse process and that thermal subsidence became more common later. This was then followed contractional deformation during the Permo-Carboniferous "Variscan" inversion. This process can be seen offshore on seismic reflection profiles and at outcrop onshore and is characterised by thrusting with associated hangingwall anticlines.

(3) Renewed extension characterised the Permian with the reactivation of some contractional structures as normal faults. Subsequent Permo-Triassic and Early Jurassic deposition occurred in a broad basin driven by thermal subsidence with little evidence for syn-sedimentary activity.

(4) Toarcian-Aalenian regional doming interrupted Early Jurassic gentle subsidence as a result of the rise of a warm and diffuse, transient plume head below the North Sea triple junction. Although its effects lie below seismic resolution, well-based stratigraphic studies show that it led to sub-lithospheric thinning in the Inner Moray Firth, which had major significance for later Jurassic tectonism.

(5) Differential subsidence characterised Aalenian-Late Oxfordian times prior to the onset of significant Kimmeridgian extension, which largely followed the course of the earlier thinned crust and created numerous, syn-sedimentary half-graben analogous to those seen in the Viking Graben and Greenland.

(6) Subsequent Early Cretaceous sedimentation appears to have occurred in a gently subsiding, underfilled basin with progressive onlap onto its margin, which is interpreted to be the result of thermal subsidence which probably continued into Late Cretaceous times.

(7) From the Caledonian Orogeny to the end of the Mesozoic the Inner Moray Firth experienced a series of both extensional and compressional deformation phases with each subsequent phase overprinting the previous styles and partly reactivating older structures. The following chapters will deal with the Cenozoic evolution of the basin and demonstrate that not only were the pre-existing structures reactivated but that the basin experienced significant uplift and erosion.

3. Estimation of apparent erosion using sonic velocity data.

3.1 Introduction.

This chapter deals with the estimation of apparent erosion in the Inner Moray Firth using sonic velocity as a measure of compaction. A dataset of 37 exploration wells was used, (**Table 3.1**; of which two remain in confidence). The majority of the wells were available in digital format whilst the remainder were traditional paper logs. Important new findings arise from the analysis of this data and it is intended to prove that apparent erosion was extensive and reached over 1km in magnitude. Later chapters will provide additional data to confirm these findings and deal with the implications.

3.2 Principles of compaction state as a measure of uplift and erosion.

The increasing loss of porosity with increased burial-depth and the accompanying increase in velocity is a commonly observed geological phenomenon (e.g. Jankowsky, 1962; Lang, 1978). As the loss of primary porosity is generally considered to be an irreversible process, any formation which has been exhumed from its maximum burial-depth will exhibit lower porosities than would be expected for its current burial-depth. Wyville *et al.* (1956) demonstrated that interval velocity is inversely proportional to porosity and consequently exhumed formations will have higher than expected interval velocities for their current burial-depth. This simple geological phenomenon forms the basis of the method described in this chapter.

As depth-controlled compaction of sediments is also hard to reverse, formations which are above their greatest burial-depth will normally be overcompacted with respect to their present burial-depth (e.g. Magara, 1976; Lang, 1978; Bulat and Stoker, 1987; Wells, 1990; Rogers *et al.*, 1991; Jensen and Schmidt, in press). The amount of erosion of such overcompacted sediments from their maximum burial-depth is given by the displacement, along the depth axis, of the observed compaction trend from the normal (undisturbed) trend **(Figure 3.1)**. Examples of uplifted and eroded sediments displaying lower porosities (higher velocities) than expected for their current burial-depth are shown in **Figures 3.5 and 3.12**. In both figures the points represent porosity-depth pairs for individual

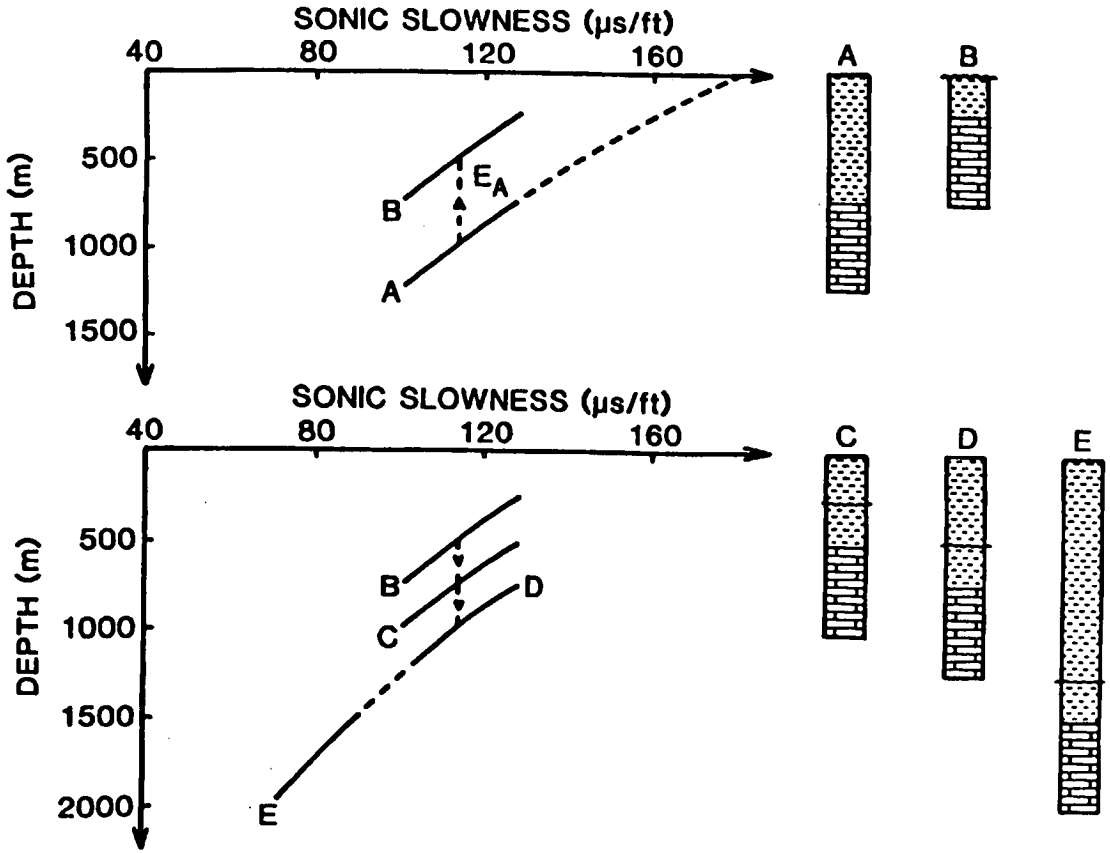

Figure 3.1 Schematic representation of porosity evaluation in a chalk sequence during burial (A), subsequent uplift (B), and post-uplift burial (C,D and E). The apparent erosion is the amount of erosion (EA) not reversed by subsequent subsidence. It can be measured by the displacement along the depth axis, of the porosity/depth (or in this case sonic slowness/depth) relation of the uplifted sequence (B or C) from that of a reference or normally-compacted sequence (A,D or E).

wells and plot above the normal (expected) porosity-depth (velocity-depth) relation. As these points represent wells which have lower porosities (higher velocities) than expected they can be interpreted as being exhumed from their maximum burial-depth.

3.3 Historical development of the methodology.

Historically the estimation of uplift and erosion from compaction state has been mainly confined to the Southern North Sea (Marie, 1975; Glennie and Boegner, 1981; Bulat and Stoker, 1987) and only recently the method has been applied to other areas (Hillis, 1988 and 1991; Wells, 1990; Rogers *et al.*, 1991; Jensen and Schmidt, in press). Regardless of when and where the work was carried out however, the method employed has remained essentially the same, relying on a few basic principles. The main factors which have been considered to be important when estimating uplift and erosion from compaction data are the selection of stratigraphic units and the determination of normal compaction trends. This section details these factors, their respective effects on uplift and erosion estimates and how the method has developed.

3.3.1 Stratigraphic unit selection.

The selection of stratigraphic units is determined by their ease of identification in wells, lateral continuity and lithological homogeneity (Bulat and Stoker, 1987). The ease of identification is of particular importance. If boundaries between stratigraphic units are difficult to define it is hard to guarantee that selected stratigraphic units are being picked correctly. This will affect the mean porosity value for the interval and the compaction gradient. Such problems have the potential to produce substantial errors in uplift and erosion estimates.

Lateral continuity is desirable as the wider the geographical spread of data, the greater the opportunity to assess the regional scale of uplift and erosion. Additionally, the geographical spread aids the determination of any variation in the regional magnitude. It is widely recognised that inverted areas experience more erosion than non-inverted areas (Bulat and Stoker, 1987; Hillis, 1991). Consequently, if the data is confined to local areas the magnitude determined can be misleading as to general regional value. This is significant where inverted and non-inverted areas show substantial uplift and erosion, with higher values located over inverted parts of the basin (as illustrated in **Figure 3.2**).

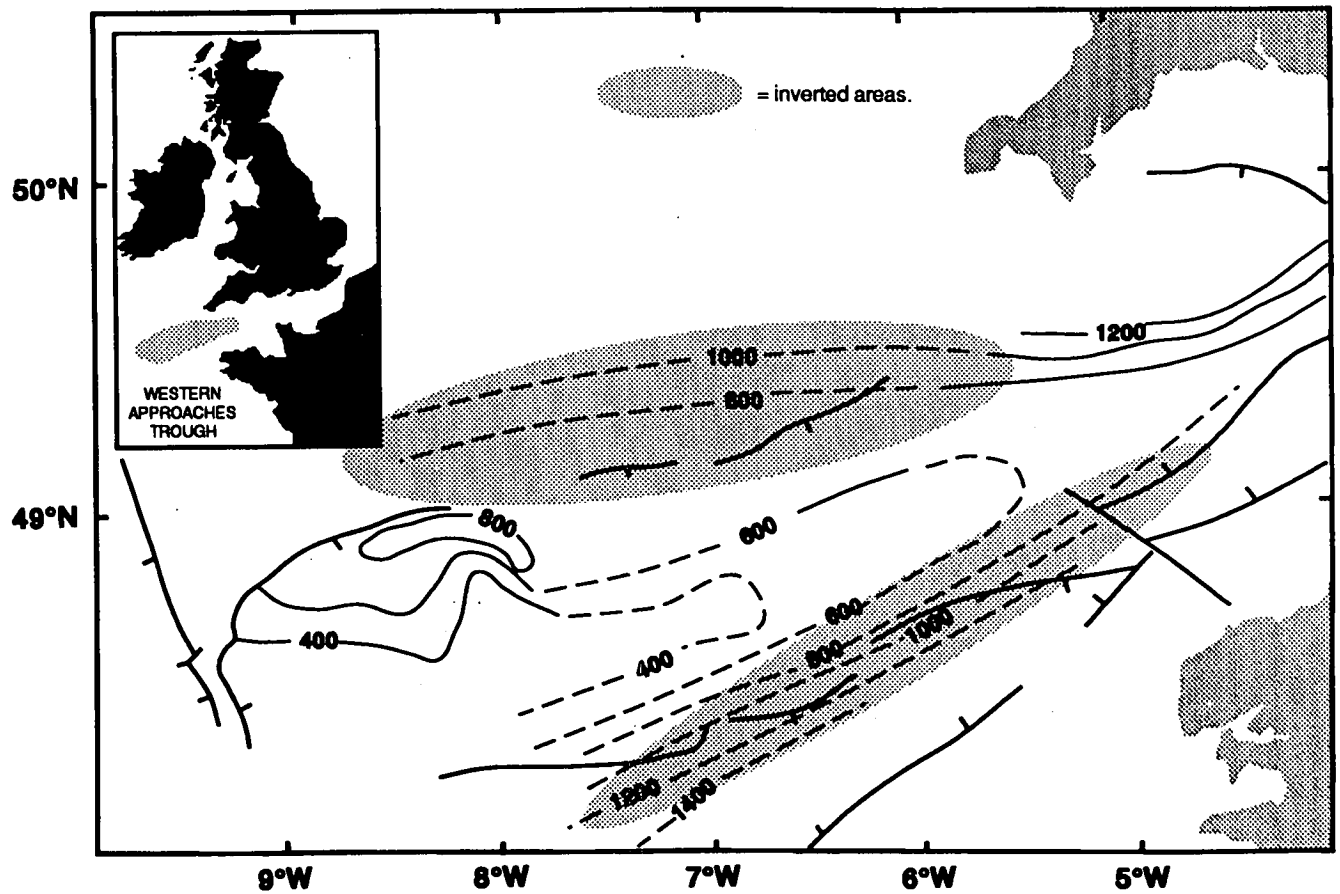

Figure 3.2 Uplift and erosion map for the Western Approaches Trough (After Hillis, 1988 & 1991). Contours represent uplift and erosion in metres and demonstrate that both inverted and non-inverted areas have experienced significant uplift and erosion. The highlighted areas represent inverted areas and show that although uplift and erosion affected inverted and non-inverted areas the inverted areas experienced more severe uplift and erosion.

The vertical and lateral lithological consistency of the units is important. If a normal compaction trend is to be geologically meaningful then it must deal with stratigraphic intervals which are vertically and laterally homogeneous. Vertical inhomogeneity results in the compaction relation within a particular stratigraphic unit being continuously variable while lateral inhomogeneity results in the inconsistency of compaction characteristics from well to well. Traditionally shales have been used due to their fairly homogeneous nature (Marie, 1975; Glennie and Boegner, 1981) and more recently chalks for the same reason (Hillis, 1991).

The choice of the number of stratigraphic units to analyse obviously depends on the local circumstances in the above variables. However, it has been common practice to analyse one unit (e.g. the Bunter Shale in the case of the Southern North Sea studies; Marie, 1975; Glennie and Boegner, 1981). This approach is now being superseded by the analysis of multiple stratigraphic units as developed by Bulat and Stoker (1987). Analysis of several stratigraphic units has advantages as the process allows several values for uplift and erosion for a particular well to be determined **(Figure 3.3)** and the consistency of estimates between formations to be assessed statistically (Bulat and Stoker, 1987 and **Figure 3.4**). Such control on uplift and erosion estimates may highlight more than one uplift and erosion episode as units below a particular unconformity may have consistently higher uplift and erosion values than those above it.

3.3.2 Normal compaction relationships.

The estimation of uplift and erosion has always involved the definition of a normal compaction relation, as uplift and erosion is defined as the vertical displacement of a porosity-depth (velocity-depth) point from this trend. Marie (1975) and Glennie and Boegner (1981) defined the normal compaction trend by least-squares regression of velocity-depth data from wells sited in non-inverted areas. This implicitly assumes that uplift and erosion only affected inverted areas. However, as observed by Bulat and Stoker (1987) and Hillis (1991) uplift and erosion can be significant where no inversion can be found **(Figures 3.2 and 3.3)**.

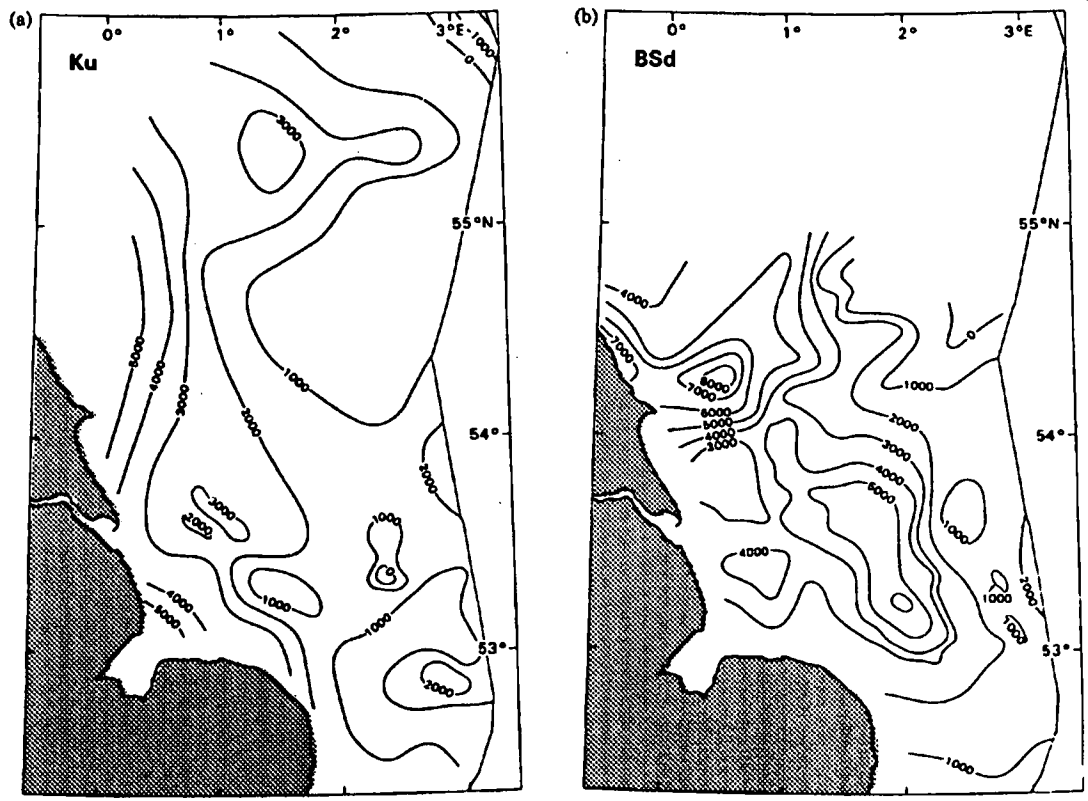

Figure 3.3 Apparent uplift maps of (a) Upper Cretaceous (Ku), (b) Bunter Sandstone Formation (BSd). Contour interval in feet. The analysis of multiple stratigraphic units allows the isolation of multiple uplift and erosion episodes. For example, the significantly greater uplift and erosion values for the Bunter Sandstone compared to the Upper Cretaceous results from the older formation experiencing uplift and erosion during the Late Jurassic-Early Cretaceous and mid-Tertiary whilst the Upper Cretaceous only experienced mid-Tertiary uplift and erosion. The combined effect of two uplift and erosion episodes on the older formation results in larger uplift and erosion values than for the Upper Cretaceous (After Bulat and Stoker, 1987).

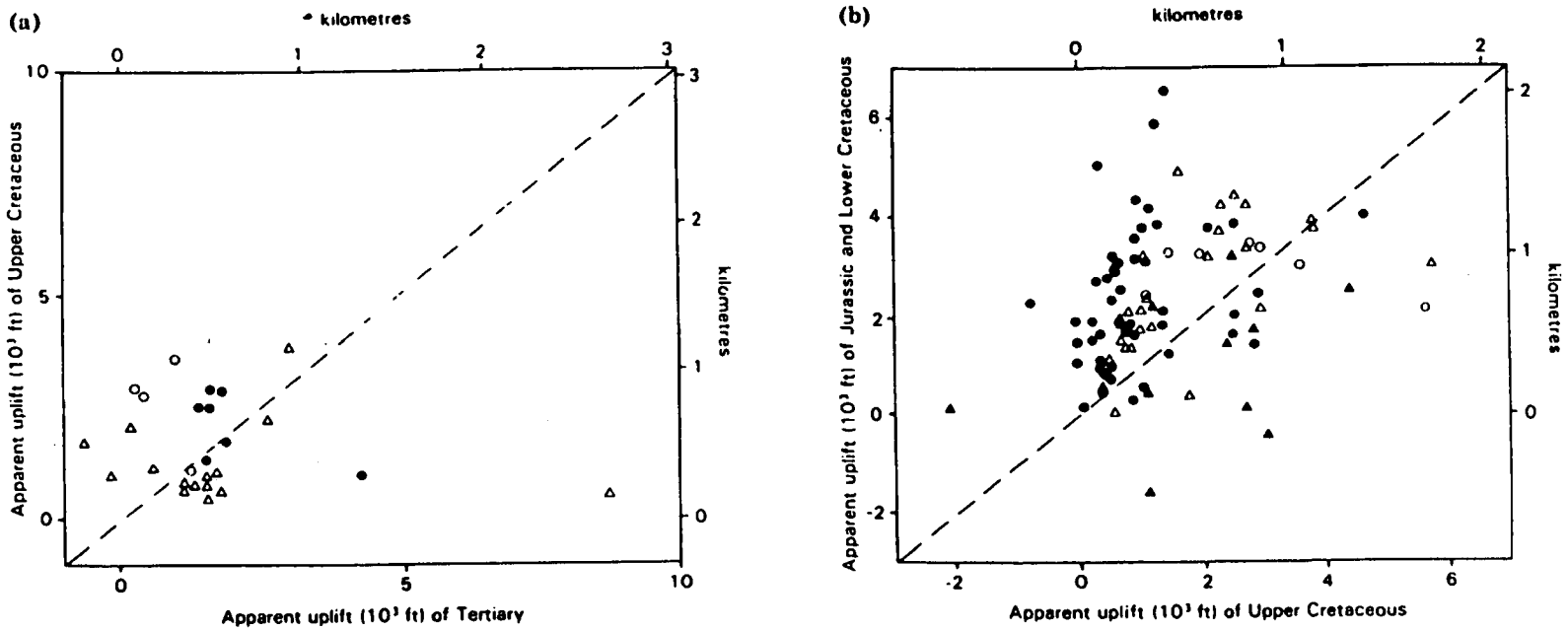

Figure 3.4 Apparent uplift cross-plots: (a) Upper Cretaceous against Tertiary and (b) Jurassic and Lower Cretaceous against Upper Cretaceous. Such plots allow the comparison of uplift and erosion estimates from different formations to test whether the estimates are statistically similar or may be different due to several erosional episode (After Bulat and Stoker, 1987).

In order to overcome the problem that non-inverted areas can also be eroded Bulat and Stoker (1987) suggested that the normal compaction relation should be defined as the lower porosity/velocity bound of the dataset, with consideration for points which are obviously erroneous **(Figure 3.5)**. This approach has been further refined by Hillis (1991) where the normal compaction gradient is first determined. This gradient is found by regressing velocity against depth for the formation under investigation in each well and then pooling the data to produce an average compaction gradient for that formation. This gradient is then placed through the well which has the highest velocity (lowest porosity) for its burial depth with reference to the gradient **(e.g. Figure 3.12)**.

3.3.3 Estimation of uplift and erosion.

Uplift and erosion has always been defined as the vertical displacement of the porosity-depth relation for a particular formation in a well from the normal relation for that formation (Marie, 1975; Glennie and Boegner, 1981; Bulat and Stoker, 1987; Hillis, 1991). In the following sections this definition has been followed and the techniques described follow those of Hillis (1991). With the use of multiple stratigraphic units and a normal compaction trend based on the observed trends within the formations it is believed that the method can be used with greater confidence than more traditional methods such those of Marie (1975) and Bulat and Stoker (1987).

3.4 Porosity-depth relations in the Kimmeridge Clay, Hod and Tor Formations.

Figure 3.6 shows plots of porosity versus depth for the Kimmeridge Clay, Hod and Tor Formations (sonic slowness is taken as a measure of porosity (Wyville *et al.*)) from the Inner Moray Firth. The apparent lack of correlation of porosity and depth can be resolved by considering individual wells. All sequences, regardless of their present burial-depth, show a relatively consistent porosity reduction with depth but have widely differing surface intercept values. The steady depth controlled decrease in porosity (as expressed by sonic slowness) is clearly apparent in the Kimmeridge Clay Formation of well 11/25-1 **(Figure 3.7)**.

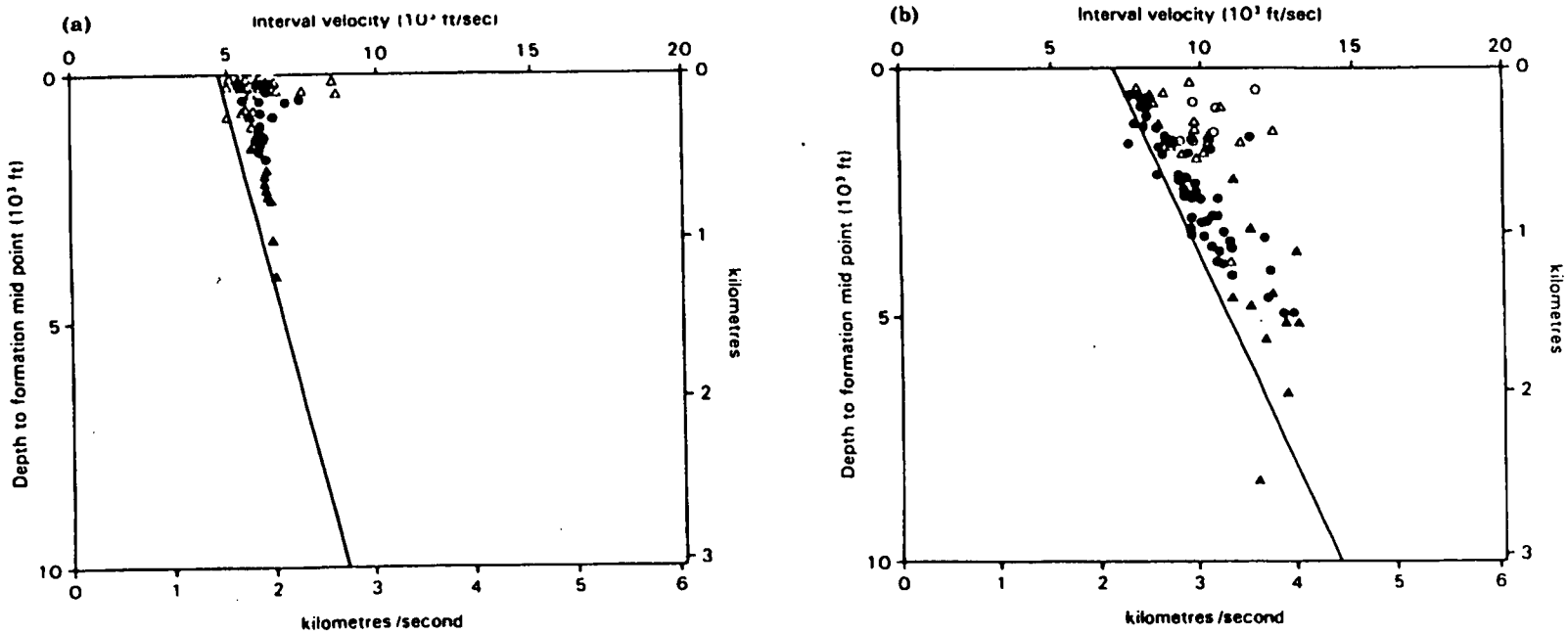

Figure 3.5 Interval velocity against depth to formation mid-point cross-plots: (a) Tertiary and (b) Upper Cretaceous. The normal compaction relation is also shown. Uplifted and eroded wells have higher velocities (lower porosities) than expected for their current burial-depth and consequently plot above the normal compaction relation. The magnitude of uplift and erosion experienced by the well is equal to the vertical displacement of the velocity-depth point from the normal compaction trend (After Bulat and Stoker, 1987).

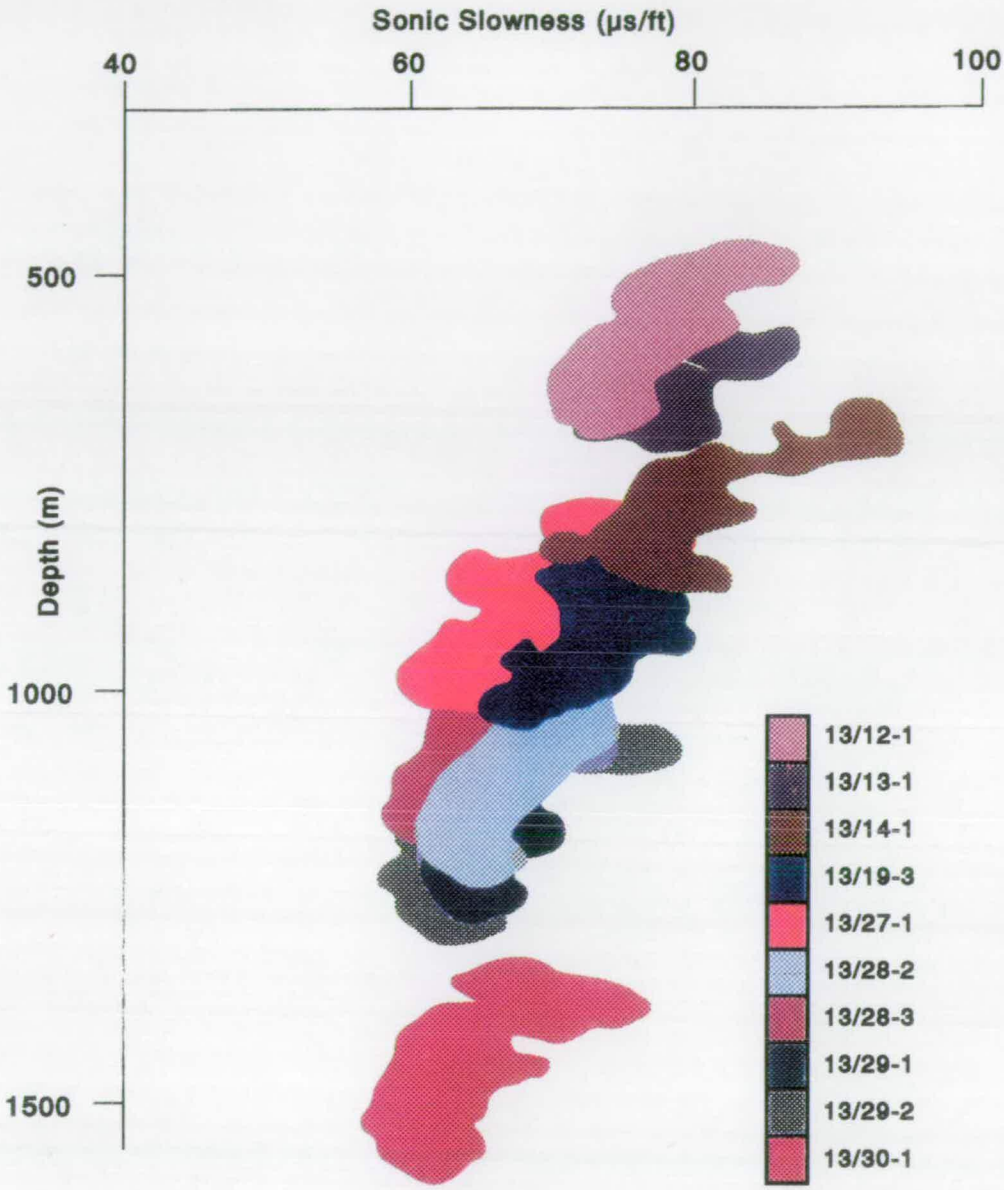

Figure 3.6(a) Sonic slowness/depth plots for the Tor Formation. The plot shows where there are more than ten points in an area of 1.2 µs/ft x 20m for the selected wells (the depth interval between points is 0.15m and was interpolated from the 6" logging depth interval).

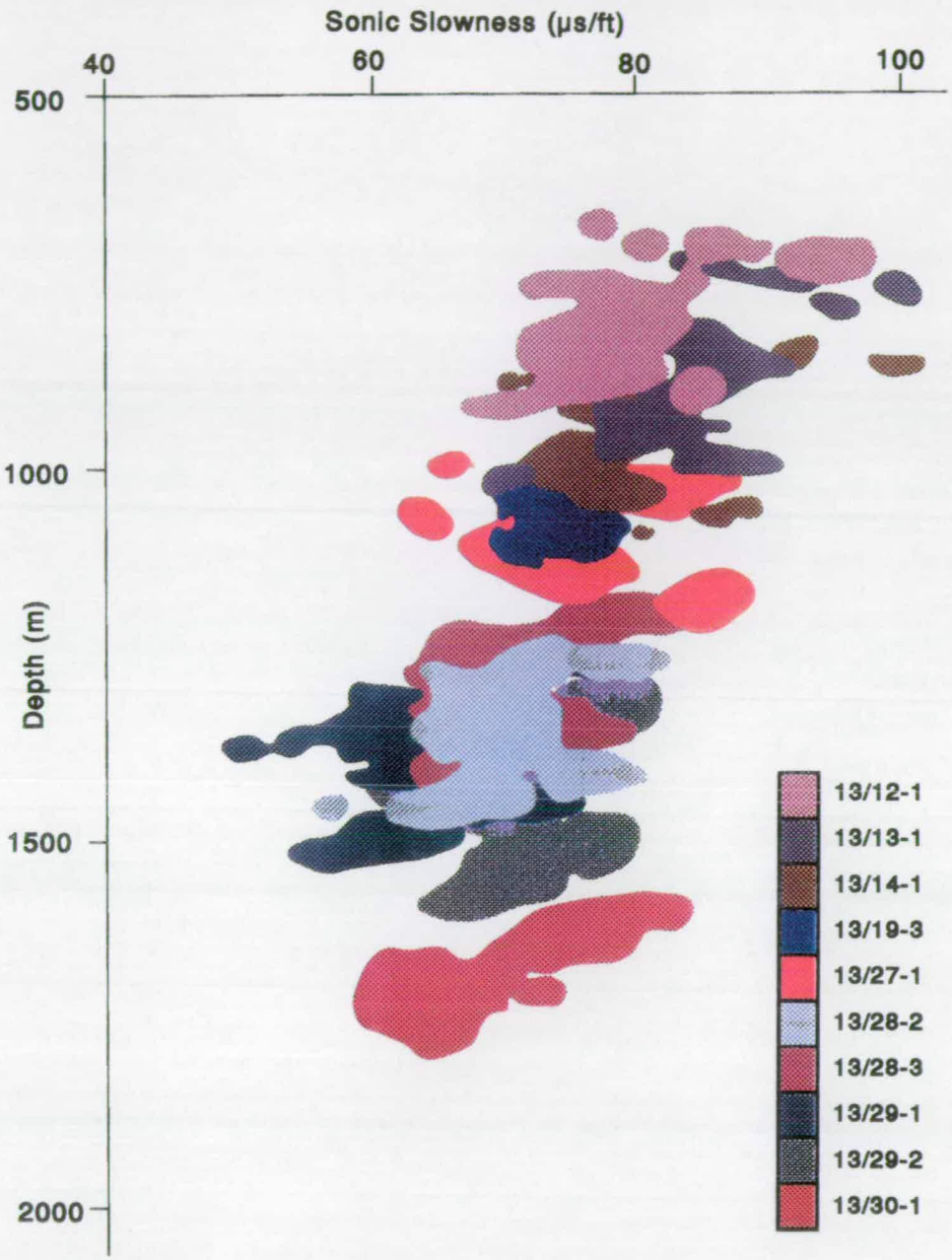

Figure 3.6(b) Sonic slowness/depth plots for the Hod Formation. The plot shows where there are more than ten points in an area of 1.2 µs/ft x 20m for the selected wells (the depth interval between points is 0.15m and was interpolated from the 6" logging depth interval).

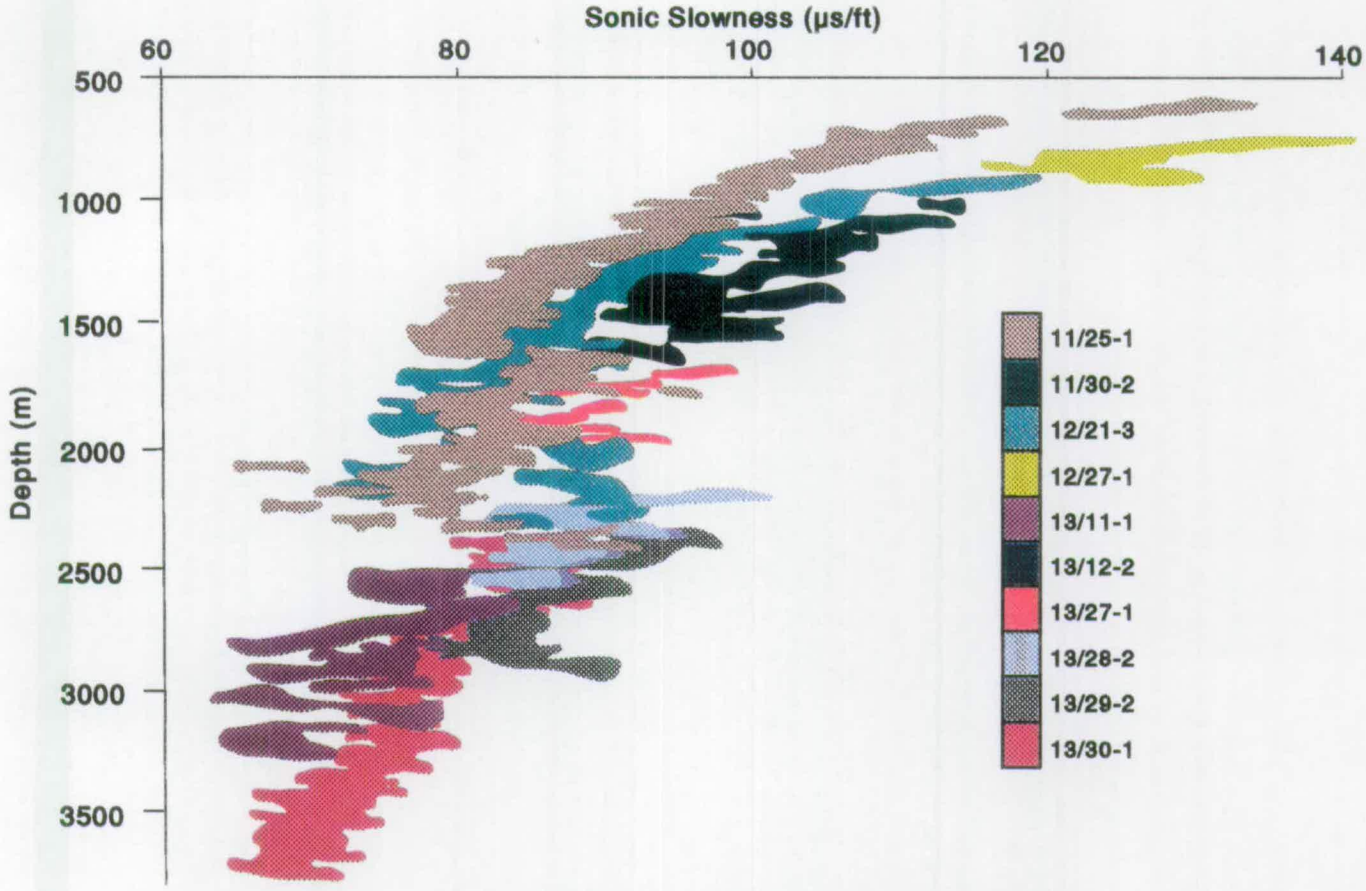

Figure 3.6(c) Sonic slowness/depth plots for the Kimmeridge Clay Formation. The plot shows where there are more than ten points in an area of 1.2 µs/ft x 20m for the selected wells (the depth interval between points is 0.15m and was interpolated from the 6" logging depth interval).

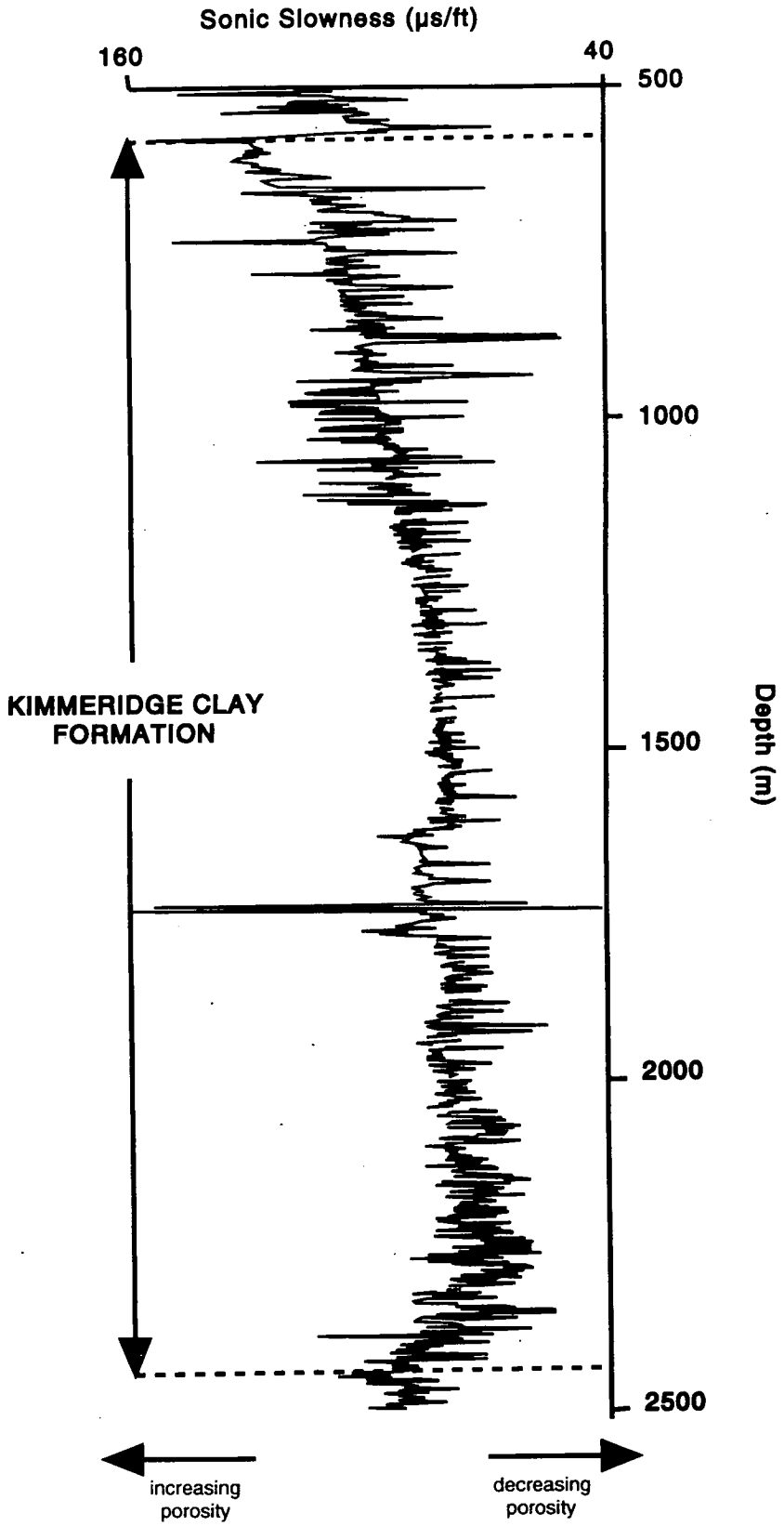

Figure 3.7 Sonic slowness (μs/ft) log for the Kimmeridge Clay Formation in well 11/25-1. The sonic slowness log (taken as a measure of porosity) shows a progressive loss of porosity with burial-depth.

Least-squares regression lines have been calculated for the Kimmeridge Clay, Hod and Tor Formations in the wells for which digital data were available for both linear porosity-linear depth and log porosity-linear depth and the correlation co-efficients obtained. In all cases the coefficients were highly significant with the linear relations being slightly better. As all the wells show a steady reduction in porosity with depth **(Figure 3.6)**, similar to that observed in the Western Approaches Trough by Hillis (1988), it is argued that the wide scatter with respect to depth is due to varying amounts of uplift and erosion in the Inner Moray Firth, which displaced the porosity-depth trend in individual wells from the normal undisturbed trend (c.f. Hillis, 1988).

3.5 Selection of stratigraphic units.

Stratigraphically-equivalent units which exhibit a vertically- and laterally-consistent relationship between depth and compaction (as expressed for example by sonic velocity) are required for the analysis of maximum burial-depth. Sonic log data indicate that of the major stratigraphic units generally encountered in exploration wells in the Inner Moray Firth, only the Chalk and the Kimmeridge Clay exhibit a reasonably consistent increase in velocity with depth **(Figure 3.8)**. The absence of significant bulk lateral facies variation within the Chalk and Kimmeridge Clay of the Inner Moray Firth suggests that depth/compaction relations should also be laterally consistent **(Figure 3.8)**.

Shales such as the Kimmeridge Clay have been widely used in the analysis of maximum burial-depth and it is widely accepted that burial-depth is the principal control on their compaction (e.g. Jankowsky, 1962; Marie, 1975; Glennie and Boegner, 1981; Jensen and Schmidt, in press). Hillis (1991) used chalk porosity to quantify Tertiary erosion on the SW UK Continental Shelf and discussed possible sedimentological/diagenetic causes of overcompaction of the Chalk of the SW UK Continental Shelf, but argued that there was no such plausible explanation for the observed regional variation in bulk (average formation) compaction. In this study, it is assumed, as argued by Scholle (1977) and Hillis (1991), that on a regional scale, burial-depth is the primary control on chalk compaction.

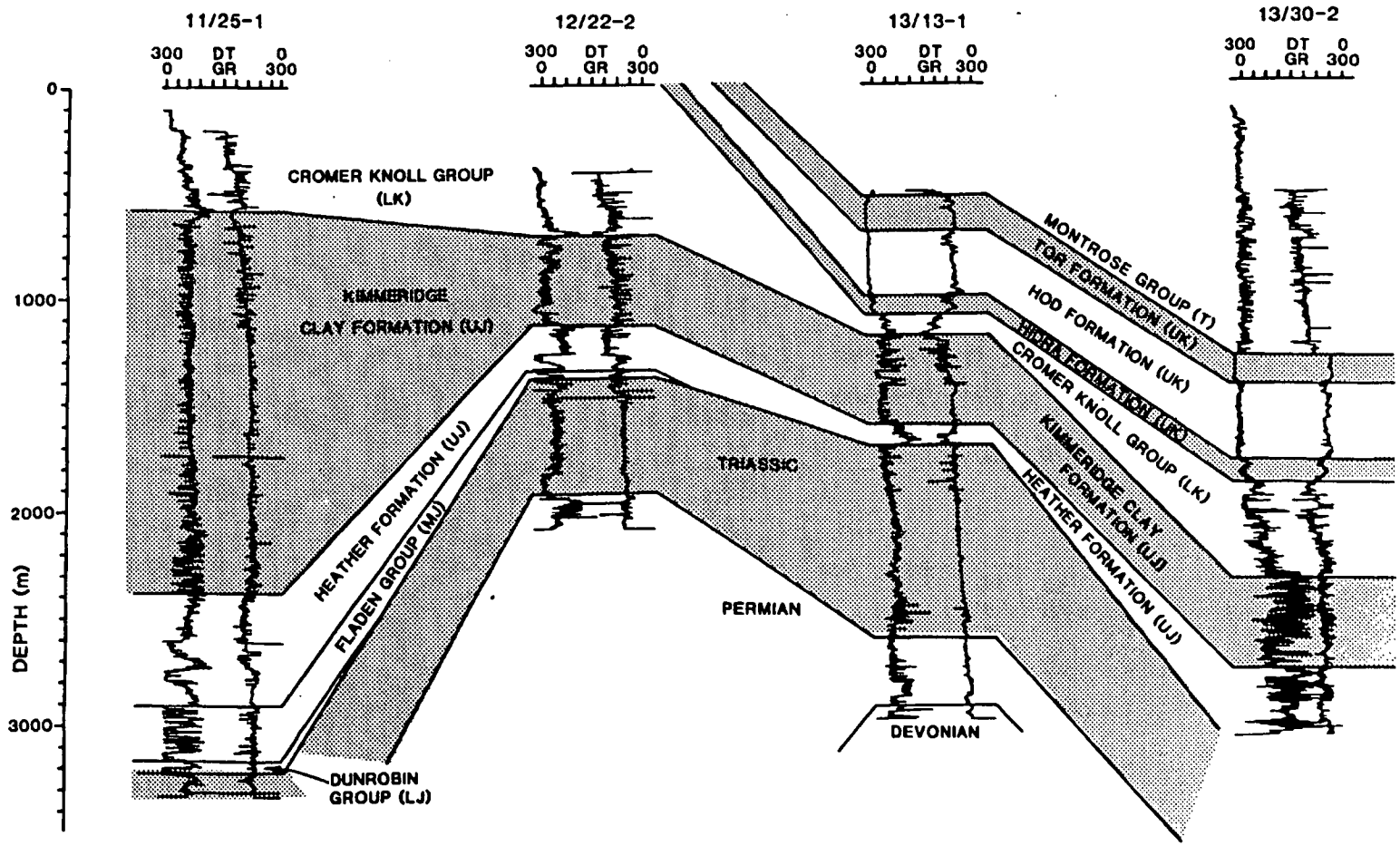

Figure 3.8 Correlation of total natural gamma ray (GR, API units, left hand trace) and Sonic slowness (DT, μs/ft, right-hand trace). Well locations shown in Figure 3.11.

On the basis of sonic and gamma ray log character, the Chalk of the Inner Moray Firth can be readily divided, into the Hidra, Plenus Marl, Hod and Tor Formations of Deegan and Scull (1977; **Figure 3.9**). The Danian, Ekofisk Formation appears to be largely absent from the Inner Moray Firth. The Hidra and Plenus Marl Formations, equivalent to the Cenomanian Lower Chalk of traditional Chalk stratigraphy of southern Britain (cf. Rawson *et al.* 1978), show variable shale content as expressed by the gamma ray log **(Figure 3.9)** and were not used in this study. The Hod and Tor Formations are equivalent to the Turonian-Maastrichtian Middle and Upper Chalks of Rawson et al. (1978). Although the sonic character of the Hod and Tor Formations is internally consistent, a discontinuity marks their mutual boundary **(Figure 3.9)** and the two formations were analysed separately in this study. The Kimmeridge Clay Formation, as used in this study, follows the definition of Deegan and Scull (1977) and is shown in **Figure 3.10**.

3.6 Selection of logging tool for compaction analysis

The sonic tool measures the shortest time for a compressional wave to travel through the formation adjacent to the borehole wall. The first sonic pulse to arrive will normally circumvent any vugular or fracture (secondary) porosity developed in the formation (Merkel, 1981). Hence where secondary porosity is widely developed, the sonic log-derived porosity is too low (Schlumberger, 1987). Although the primary porosity of chalks is strongly controlled by burial-depth-related processes (i.e. physical and chemical compaction of Taylor and Lapré, 1987), secondary porosity development is largely depth-independent, being controlled by processes such as fracturing and jointing (Watts, 1983). Hence, the insensitivity of the sonic log to secondary porosity is considered advantageous over other basic porosity tools (i.e. density and neutron) in burial-depth analysis of chalk lithologies.

Since porosity expresses the compactional state of the sedimentary rocks. Sonic velocities may be converted to porosities as demonstrated by Hillis (1991) for his quantification of Tertiary erosion on the SW UK Continental Shelf. Similarly, velocities in the Hod and Tor Formations were converted to porosity using the Raiga-Clemenceau *et al.* (1988) relation. The resultant values of apparent erosion were all within 100 m of those determined directly from velocity data. However, as porosity estimates were based on velocity data, it is to be expected that the porosity-based and velocity-based estimates should be similar. Consequently little credibility can be

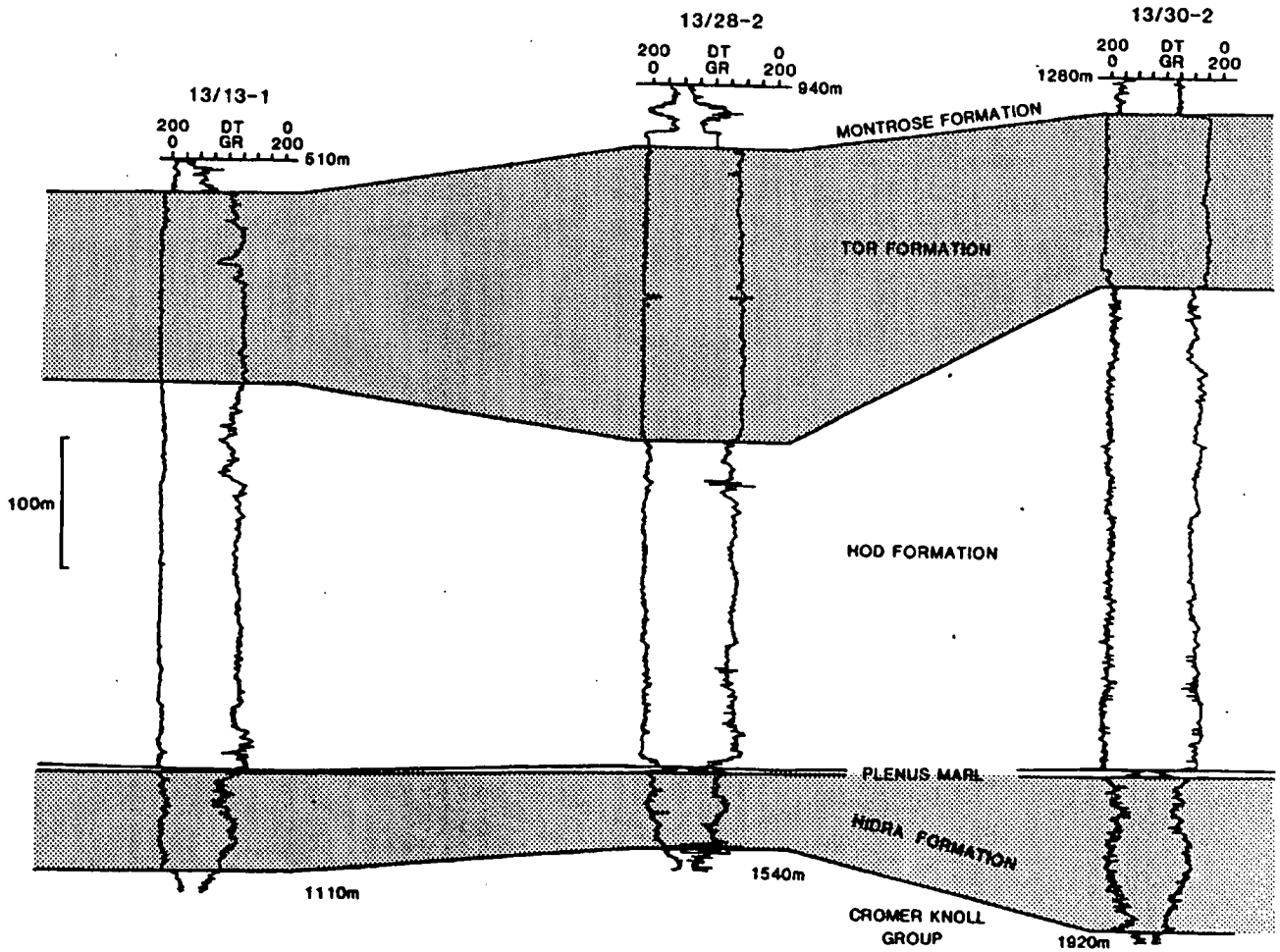

Figure 3.9 Correlation of total gamma ray (GR, API units, left-hand trace) and sonic slowness (DT, μs/ft, right-hand trace) for the Hod and Tor Formations. Well locations shown in Figure 3.11.

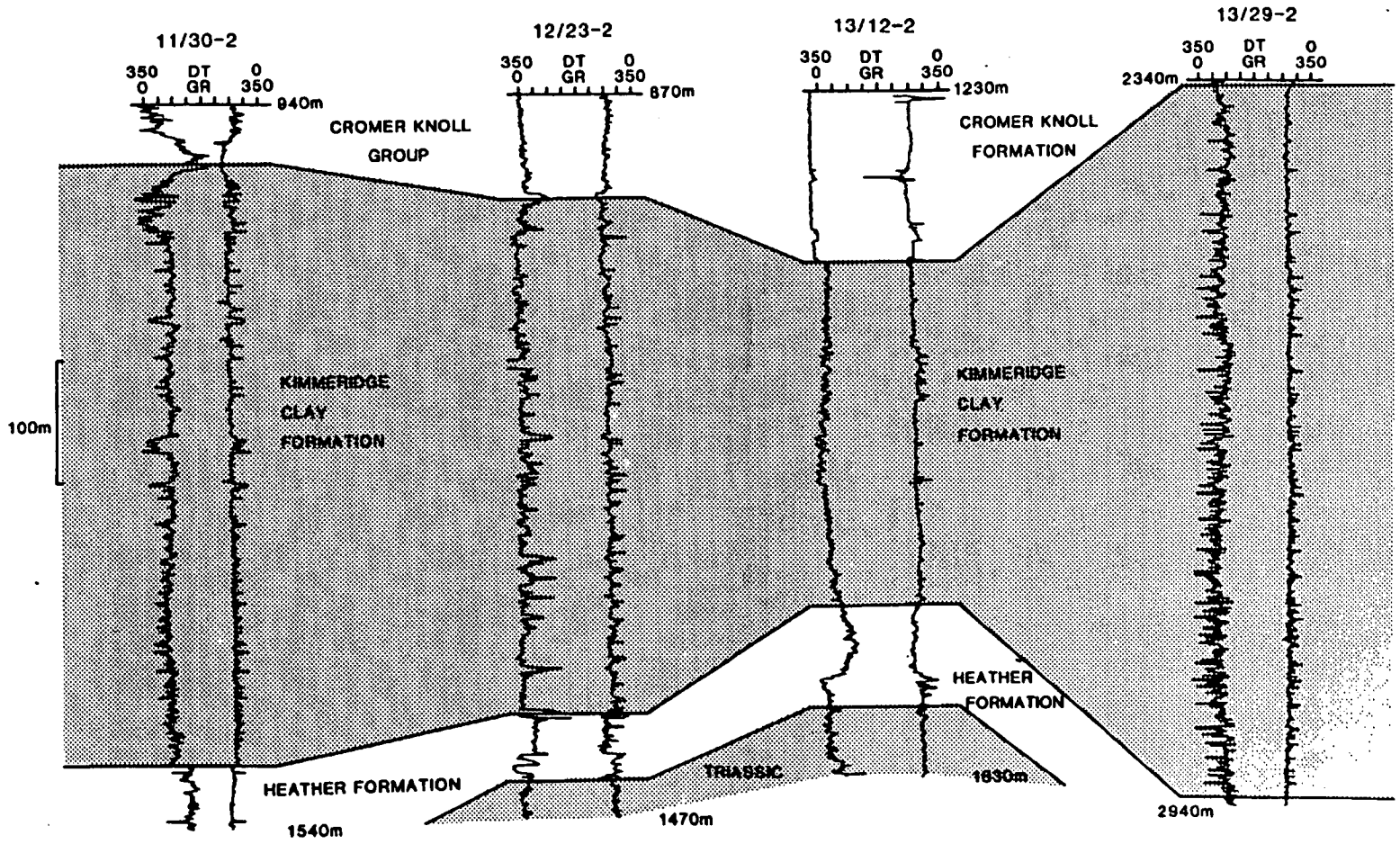

Figure 3.10 Correlation of total gamma ray (GR, API units, left-hand trace) and sonic slowness (DT, μs/ft, right-hand trace) for the Kimmeridge Clay Formation. Well locations shown in Figure 3.11.

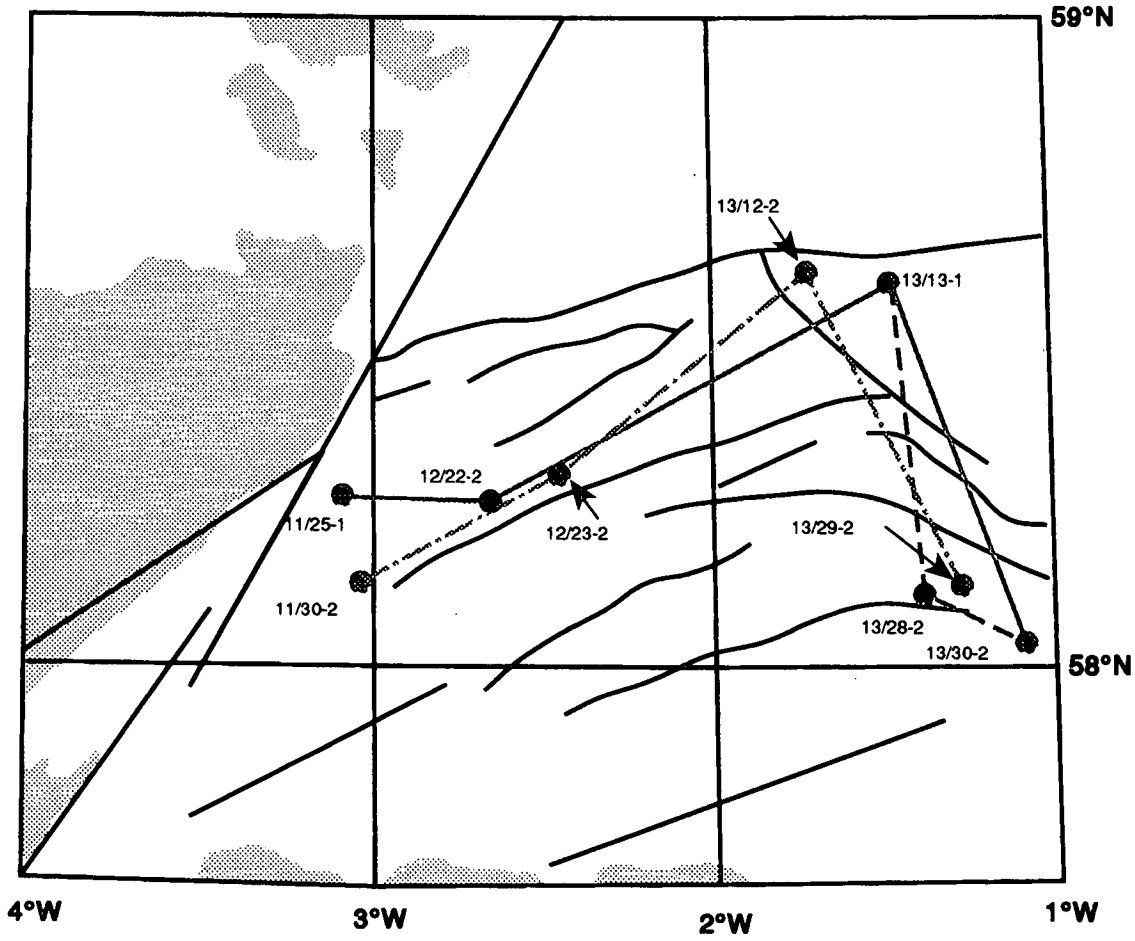

Figure 3.11 Map showing locations of wells in figures 3.8, 3.9 and 3.10. Solid line represents Figure 3.8, dashed line represents Figure 3.9 and dashed-dot line represents Figure 3.10.

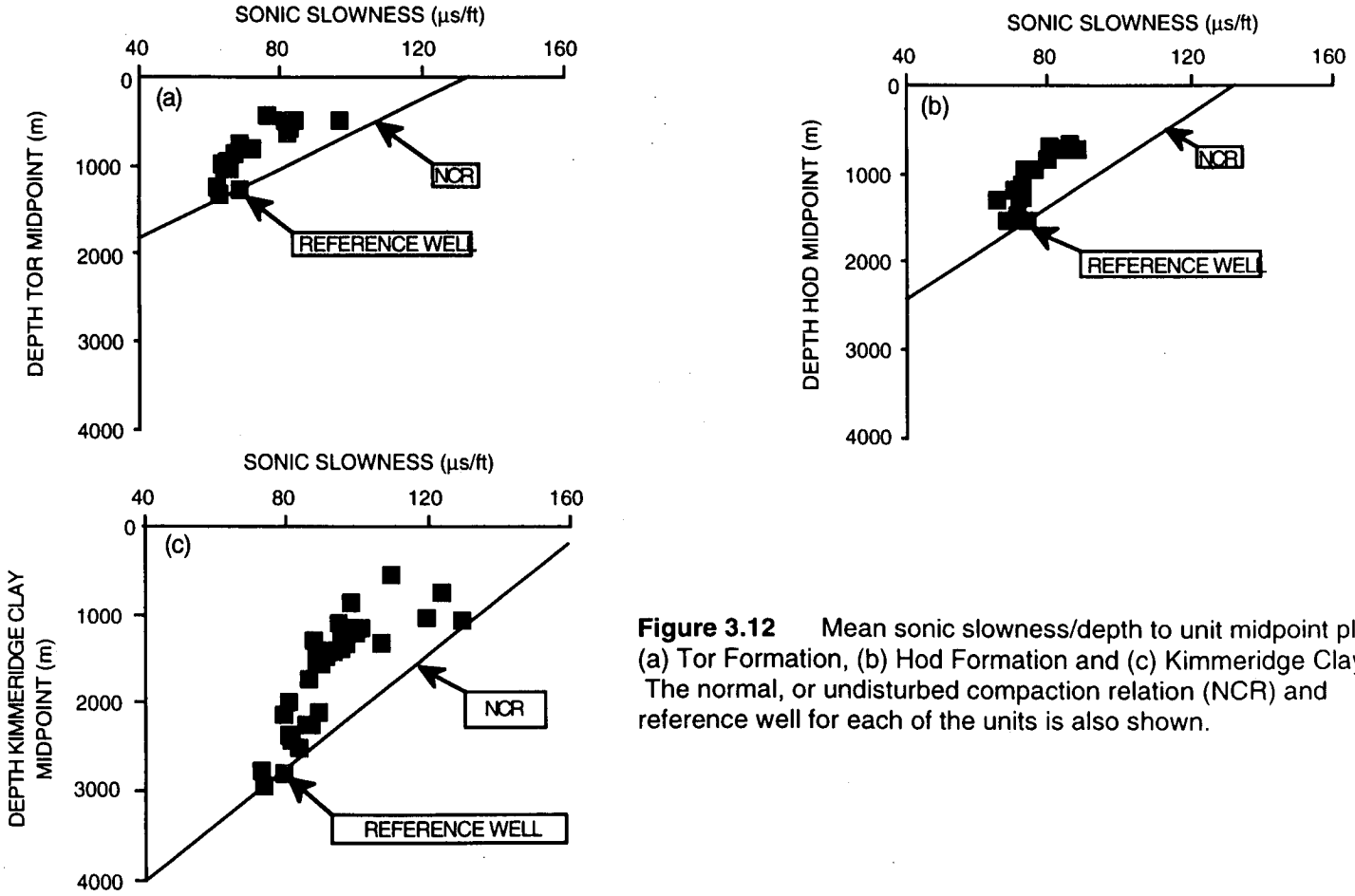

Figure 3.12 Mean sonic slowness/depth to unit midpoint plots for (a) Tor Formation, (b) Hod Formation and (c) Kimmeridge Clay Formation. The normal, or undisturbed compaction relation (NCR) and reference well for each of the units is also shown.

Table 3.1 Depth to midpoint and mean sonic slowness for the Kimmeridge Clay, Hod and Tor Formations. (bsb: below sea-bed)

Well	Kimmeridge Clay Fm		Hod Fm		Tor Fm	
	mean slowness (µs/ft)	formation midpoint (m bsb)	mean slowness (µs/ft)	formation midpoint (m bsb)	mean slowness (µs/ft)	formation midpoint (m bsb)
11/25-1	88.2	1400				
11/30-1	106.6	1333				
11/30-2	97.1	1159				
11/30-3	99.7	1204				
11/30-4	100.9	1159				
11/30-5	99.7	1210				
12/21-2	95.5	1280				
12/21-3	88.5	1516				
12/21-5	93.4	1406				
12/22-2	98.3	855				
12/23-2	94.8	1083				
12/24-2	79.3	2128				
12/27-1	123.8	744				
12/27-2	119.7	1044				
12/28-1	91.5	1419				
12/29-1	91.3	1461				
13/11-1	72.5	2760				
13/12-1	80.2	2352	80.6	669	75.9	445
13/12-2	95.2	1377				
13/13-1	96.6	1333	83.0	715	81.0	499
13/14-1			79.7	825	82.4	580
13/17-1	90.0	1560	88.0	710	84.0	476
13/18-1	129.6	1054	86.2	651	96.8	478
13/19-1			86.0	691	82.0	634
13/19-3			73.7	942	71.7	802
13/22-4			72.6	1129	67.0	863
13/27-1	86.1	1716	75.9	948	68.7	735
13/28-2	85.6	2241	71.8	1205	63.1	970
13/28-3	88.9	2115	70.7	1183	64.8	959
13/29-1	87.0	2241	71.7	1254	64.1	995
13/29-2	83.6	2500	65.6	1293	65.8	1026
13/29-3			72.8	1264	64.5	1038
13/30-1	73.3	2932	68.4	1518	62.8	1316
13/30-2	80.8	2430	70.9	1478	61.7	1236
13/30-3	78.8	2798	74.1	1533	68.5	1277

Table 3.2 Linear sonic slowness-linear depth and log sonic slowness-linear depth gradients for the Kimmeridge Clay, Hod and Tor Formations in individual wells and the mean for each unit.

	Kimmeridge Clay Fm. gradient		Hod Fm. gradient		Tor Fm. gradient	
Well	linear	log	linear	log	linear	log
11/25-1	-0.0197	-0.00009				
11/30-1						
11/30-2	-0.0307	-0.00013				
11/30-3	-0.0284	-0.00012				
11/30-4	-0.0051	-0.00002				
11/30-5	-0.0091	-0.00003				
12/21-2	-0.0132	-0.00006				
12/21-3	-0.0268	-0.00011				
12/21-5						
12/22-2	-0.0746	-0.00033				
12/23-2	-0.0498	-0.00023				
12/24-2	-0.0120	-0.00007				
12/27-1	-0.0570	-0.00020				
12/27-2						
12/28-1	-0.0421	-0.00020				
12/29-1	-0.0371	-0.00018				
13/11-1	-0.0106	-0.00006				
13/12-1	-0.0357	-0.00018	-0.0546	-0.00029	-0.0502	-0.00029
13/12-2	-0.0262	-0.00011				
13/13-1	-0.0731	-0.00031	-0.0531	-0.00028	-0.1179	-0.00060
13/14-1			-0.0599	-0.00032	-0.0957	-0.00048
13/17-1						
13/18-1						
13/19-1						
13/19-3			-0.0191	-0.00010	-0.0365	-0.00022
13/22-4						
13/27-1	-0.0369	-0.00019	0.0153	0.00010	-0.0669	-0.00041
13/28-2	-0.0141	-0.00008	-0.0185	-0.00012	-0.0389	-0.00027
13/28-3	-0.0451	-0.00022	-0.0294	-0.00018	-0.0262	-0.00018
13/29-1	-0.0456	-0.00023	-0.0218	-0.00013	-0.0074	-0.00005
13/29-2	-0.0227	-0.00012	-0.0117	-0.00007	-0.0578	-0.00036
13/29-3						
13/30-1	-0.0119	-0.00007	-0.0906	-0.00056	-0.0441	-0.00030
13/30-2	-0.0247	-0.00008	-0.0282	-0.00017	-0.0178	-0.00012
13/30-3						
Average Gradient	-0.0031	-0.00014	-0.0614	-0.00019	-0.0383	-0.00030

placed in the porosity data as confirmatory evidence for the magnitude of uplift and erosion based on velocity data. As shales do not have the relatively simple monomineralic matrix of chalks, and it is not possible to determine their absolute porosity from the basic porosity logs, this study estimated the magnitude of uplift and erosion based on velocity data as the measure of compaction.

3.7 Determination of apparent erosion

The tops and bases of the Kimmeridge Clay, Hod and Tor Formations were consistently picked from squashed plots of the sonic and gamma ray logs **(Figures 3.9 and 3.10)**. The mean slowness of the resultant intervals was determined from digital sonic log data. Mean slowness calculated in this way is the reciprocal of interval velocity, and sonic log calibration was checked with reference to continuous velocity (check shot) log data. **Table 3.1** lists the mean slowness and depth to formation midpoint (below sea-bed) for the Kimmeridge Clay, Hod and Tor Formations in the wells used in this study. The gradient of the slowness/depth relationship in each formation was determined by averaging the gradient derived by linear, least-squares, best-fit regression of slowness on depth (i.e. slowness as dependent variable) for individual wells (the gradients for individual formations in individual wells and the average gradient for each formation (as shown in **Table 3.2**). The mean gradient from all wells where a given formation is encountered is shown on **Figure 3.12**.

The well with the lowest velocity (highest slowness) for its burial-depth, with allowance for the mean slowness/depth gradient, was taken as the reference well from which apparent erosion for the other wells was calculated **(Figure 3.12)**. Well 13/30-3 is the reference well for the Kimmeridge Clay, Hod and Tor Formations. Apparent erosion for a given well is the vertical displacement of its slowness/depth trend from that of the reference well. This can be defined more rigorously as the vertical displacement of the mean slowness/depth gradient between the mean slowness/depth value of the reference well and the well under consideration. Apparent erosion (E_A) can be estimated graphically from the plots of slowness against depth to formation midpoint **(Figure 3.12)**. However, in practice, it was determined numerically using the equation:

$$E_A=((\Delta t_U-\Delta t_R)/m)-d_U+d_R$$

where **m** is the mean gradient of the slowness/depth relation;

Δt_U and Δt_R are the mean slownesses of the well under consideration and the reference well respectively;

d_U and d_R are the depths of the formation midpoints (below sea-bed) of the well under consideration and the reference well respectively;

The resultant apparent erosion values are given in **Table 3.3** and have been plotted and contoured in **Figure 3.13**.

Log slowness/linear depth gradients were also calculated for each of the formations **(Table 3.2)**. These generally show a similar or slightly poorer fit to the data than the linear relations. Apparent erosion values based on the log slowness/linear depth relations were calculated and are similar to those based on the linear relations (**Table 3.3**).

If the reference well is above its maximum burial-depth then the apparent erosion magnitudes determined will be consistently underestimated by the amount of apparent erosion in the vicinity of the reference well. Slowness/depth relations in the Kimmeridge Clay, Hod and Tor Formations in the Outer Moray Firth (UKCS Quadrant 14) were also analysed in an attempt to assess whether the reference well used was currently at its maximum burial-depth. Facies variation (in the Chalk from the Inner to the Outer Moray Firth) and possible local overpressure (in the Kimmeridge Clay of the Outer Moray Firth) preclude unequivocal determination of whether the reference well is above its maximum burial-depth. However, if the reference well is above its maximum burial-depth it is at most by a few hundred metres.

3.8 Comparison of apparent estimates

Apparent erosion values from the Kimmeridge Clay, Hod and Tor Formations (derived from the linear sonic slowness-depth gradient) were plotted against each other in order to check their consistency (**Figure 3.14**; cf. Bulat and Stoker, 1987). Least-squares, best-fit, linear relations between the apparent erosion values and associated co-efficients of correlation were determined by regression of apparent erosion values from the deeper formation on the shallower formation (**Table 3.4**; the choice of dependent variable is arbitary in this case). The t-statistic of the co-efficients of correlation were calculated and tested against the

Table 3.3 Apparent erosion values derived from the linear sonic slowness-linear depth and log sonic slowness-linear depth analyses of the Kimmeridge Clay, Hod and Tor Formations.

	Kimmeridge Clay Fm. apparent erosion (m)		Hod Fm. apparent erosion (m)		Tor Fm. apparent erosion (m)	
Well	linear	log	linear	log	linear	log
11/25-1	1099	1059				
11/30-1	577	553				
11/30-2	1056	1011				
11/30-3	926	884				
11/30-4	934	895				
11/30-5	921	879				
12/21-2	986	940				
12/21-3	972	932				
12/21-5	926	880				
12/22-2	1296	1248				
12/23-2	1204	1158				
12/24-2	654	651				
12/27-1	617	692				
12/27-2	449	494				
12/28-1	975	930				
12/29-1	937	892				
13/11-1	239	289				
13/12-1	402	393	693	675	694	690
13/12-2	897	851				
13/13-1	894	851	582	561	539	540
13/14-1			561	544	430	433
13/17-1	895	852	455	434	503	510
13/18-1	105	227	561	540	261	310
13/19-1			527	505	385	388
13/19-3			601	602	419	416
13/22-4			443	449	451	454
13/27-1	849	815	537	530	545	545
13/28-2	340	308	389	339	420	435
13/28-3	361	320	440	457	399	408
13/29-1	297	260	342	352	375	386
13/29-2	146	122	465	516	311	317
13/29-3			304	310	325	335
13/30-1	41	84	164	194	80	96
13/30-2	303	291	138	153	182	202
13/30-3	0	0	0	0	0	0

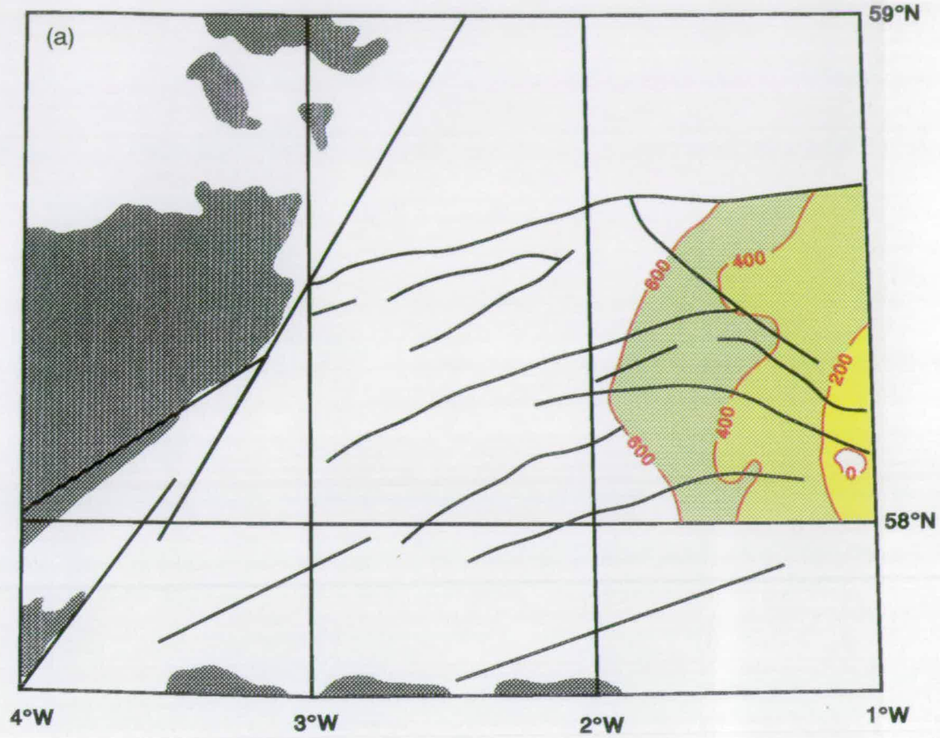

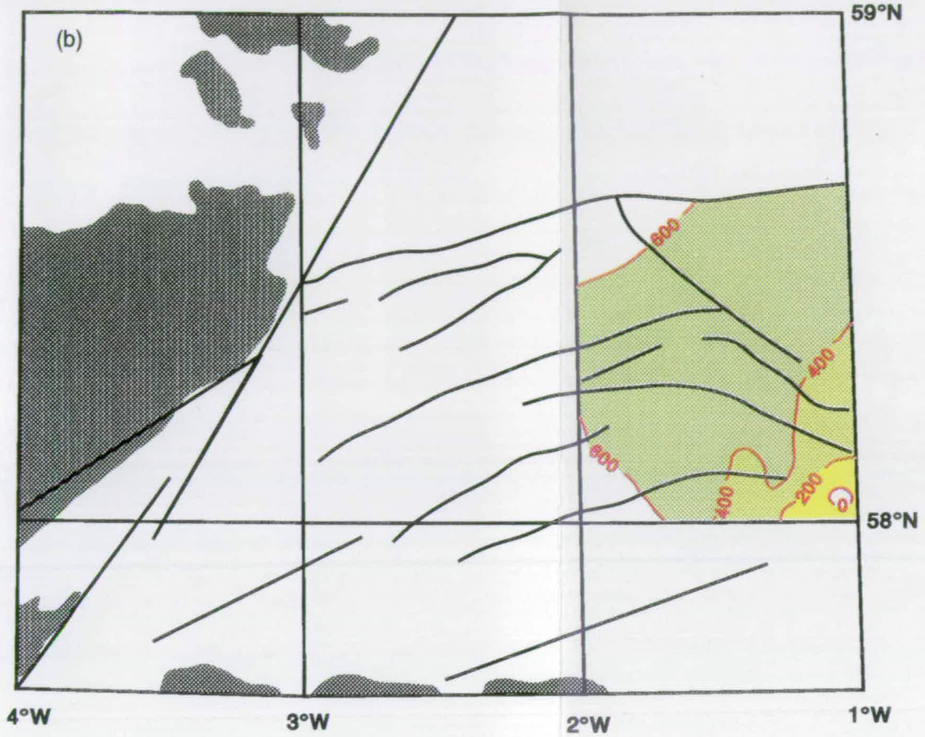

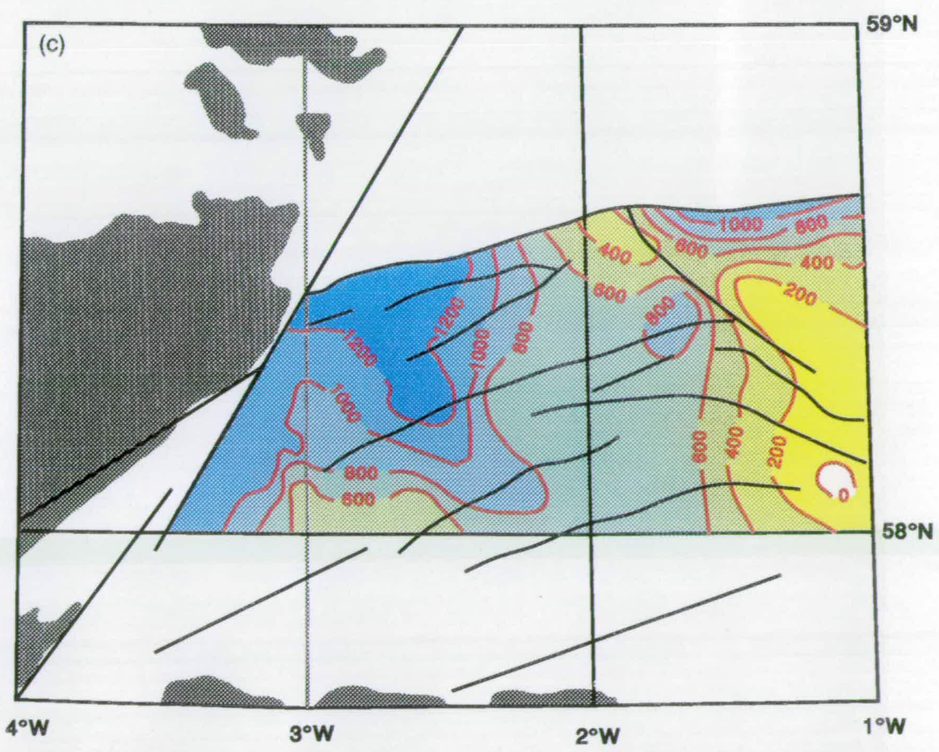

Figure 3.13 Maps of Apparent erosion for the Inner Moray Firth (a) Tor Formation (b) Hod Formation (c) Kiimmeridge Clay Formation. All maps show a progressive increase in uplift and erosion to the west and the map for the Kimmeridge Clay Formation (c) demonstrates that erosion reached a maximum of approximately 1.2 km in the region of the Wick-Great Glan Fault intersection. This erosional maxima coincides with the only inversion structure present in the basin.

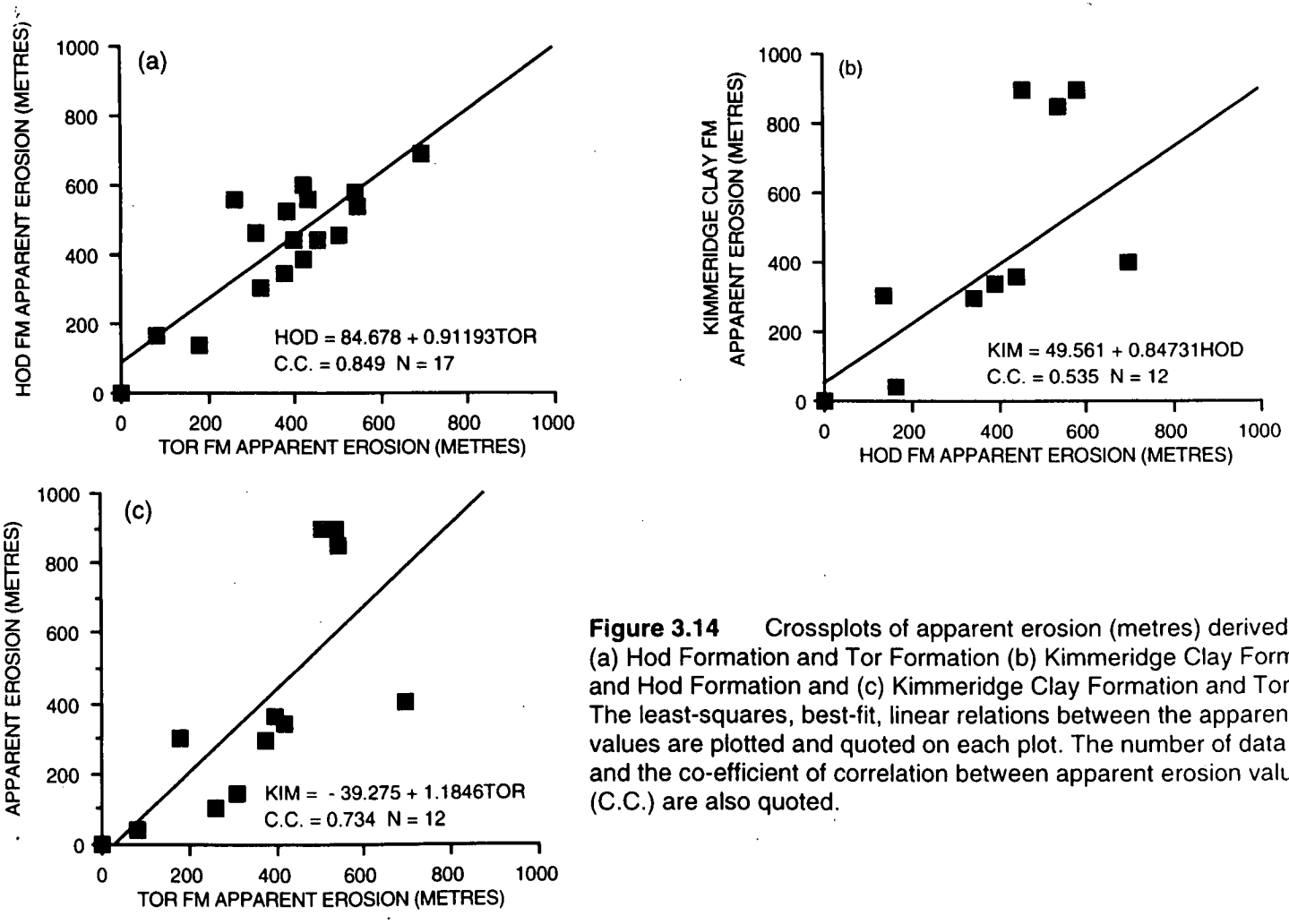

Figure 3.14 Crossplots of apparent erosion (metres) derived from (a) Hod Formation and Tor Formation (b) Kimmeridge Clay Formation and Hod Formation and (c) Kimmeridge Clay Formation and Tor Formation. The least-squares, best-fit, linear relations between the apparent erosion values are plotted and quoted on each plot. The number of data points (N) and the co-efficient of correlation between apparent erosion values (C.C.) are also quoted.

Table 3.4 Correlation between apparent erosion results (E_A) from the Kimmeridge Clay, Hod and Tor Formations. N is the number of wells with both formations. H_O is the null hypothesis that the correlation coefficient (cc) is from a population the mean of which is zero.

FORMATIONS	N	cc between E_A values from the two formations	t-statistic	confidence level at which H_O can be rejected		
				95.00%	99.50%	99.95%
Hod/Tor	17	0.849	4.07	Y	Y	Y
Kimmeridge/Tor	12	0.734	3.50	Y	Y	N
Kimmeridge/Hod	12	0.535	2.00	Y	N	N

one-tailed Student's t-distribution in order to determine whether the co-efficients of correlation were significant (e.g. Till, 1974). There is a less than 0.05% chance that the co-efficient of correlation between apparent erosion values determined from the Hod and Tor Formations comes from a population of co-efficients with a mean value of zero. This probability is less than 0.5% chance that the co-efficient of correlation between apparent erosion values determined from the Hod and Tor Formations come from a population of co-efficients with a mean value of zero. This probability is less than 0.5% in the case of the apparent erosion values from the Kimmeridge Clay and Tor Formations and 5% from the Kimmeridge Clay and Hod Formations **(Table 3.4)**.

It is unlikely that a sedimentological and/or diagenetic mechanism, such as those discussed by Bulat and Stoker (1987) and Hillis (1991), mechanism could account for similar amounts of overcompaction in the carbonate and clastic formations analysed in the Inner Moray Firth. In the absence of an alternative explanation, the fact that the correlation between the results of apparent erosion from the three formations are all statistically significant supports the argument that burial at depth beyond that currently observed is responsible for overcompaction of the Hod, Tor and Kimmeridge Clay Formations.

3.9 Patterns of apparent erosion.

Figure 3.15 shows a contoured plot of uplift and erosion for the Inner Moray Firth based on the results obtained in Section 3.6. This section briefly discusses the pattern of uplift and erosion, and as the data from the Hod and Tor formations is limited, is based on the map based on the Kimmeridge Clay Formation. **Figure 3.15** shows clearly that the magnitude of uplift and erosion is at a maximum of approximately 1.2 km in the western part of the basin and gradually decreases to the east reaching a minimum value in the vicinity of the Inner Moray Firth/Outer Moray Firth transition. Additionally the data yield evidence to the relationship between uplift and erosion and crustal compression. As crustal compression is a likely source of uplift and erosion (as discussed in Chapter 11) it would expected that uplift and erosion would be localised to these areas. However, in the Inner Moray Firth compression is of relatively minor magnitude and of insufficient areal extent to be responsible (see Chapter 10). Crustal compression however does seem to be centred on the local erosional maxima in block 12/16,

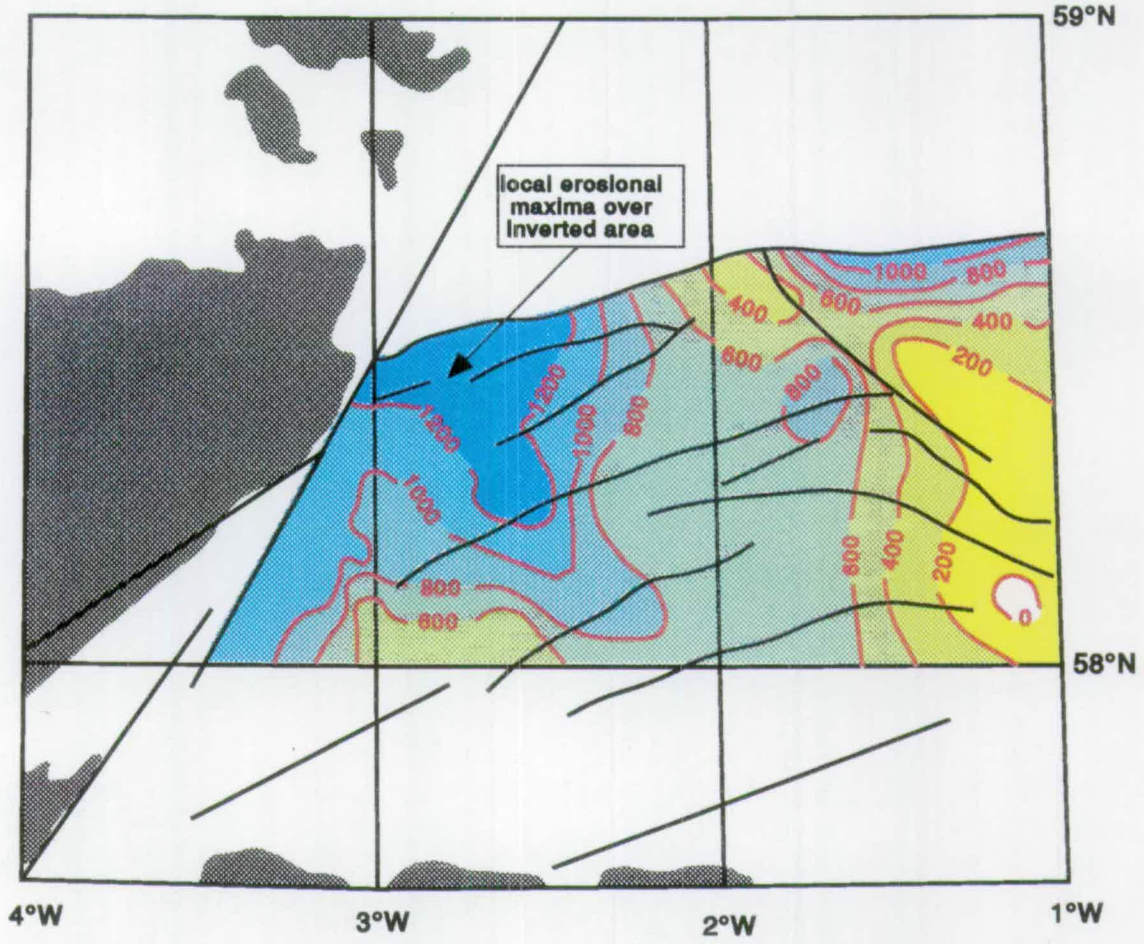

Figure 3.15 Map of apparent erosion for the Inner Moray Firth based on sonic slowness in the Kimmeridge Clay Formation.

where the only documented inversion structure in the basin is present **(Figure 3.15)**. Additionally, there is evidence (discussed in Chapter 10) for strike-slip transpression in the Sutherland Terrace area. The Sutherland Terrace is outwith the area where data are available but the contour pattern suggests that another local maxima may also exist. These findings are similar to those observed by Hillis (1988 and 1991) and may suggest that uplift and erosion is generally more widespread than the distribution of areas of crustal compression.

3.10 Conclusions.

(1) As the formations analysed show a steady decrease in porosity (as expressed by sonic slowness) with increasing burial-depth in all wells it appears most likely that the principal control on porosity, and its reduction, is the amount of overburden present above the formation. As overburden increases, porosity is progressively reduced and the amount of overburden directly controls the amount of porosity reduction. However, when individual formations are analysed from all the wells where they are present the porosity values show a wide spread with burial-depth and a range of surface intercept values. Such a spread of porosity values suggests that the formations in the Inner Moray Firth are overcompacted with respect to their present burial-depth. Overcompaction can be interpreted as a result of uplift and erosion from maximum burial-depth resulting in the porosity-depth relation of the formation under consideration being displaced vertically from the normal trend. The widespread in porosity values for individual formations can then be attributed to varying degrees of uplift and erosion in the Inner Moray Firth. In wells where a formation is exhumed significantly the displacement of the porosity-depth relation is large (e.g. 11/25-1) whilst in wells which have experienced little exhumation the displacement is smaller (e.g. 13/30-1). As the Upper Cretaceous Chalk has been affected by uplift and erosion the erosive event must have occurred after its deposition (i.e. during the Tertiary).

(2) Estimates of apparent erosion from the Inner Moray Firth show a general increase to the west reaching approximately 1.2 km. The general pattern also shows little influence from pre-existing structures suggesting that uplift and erosion was largely controlled by a more regional phenomenon. However, the local erosional maxima in the northwestern part of the basin resides over the only inversion structure of Tertiary age yet to be found in the basin. This may suggest that the higher values found in this area are directly related to the extra erosion caused by this local compressive event.

(3) The similarity of apparent erosion estimates in the Kimmeridge Clay, Hod and Tor Formations, and their statistical significance suggests that the overcompaction they experienced must have been the result of a effect common to the history of all three formations. As both clastic and carbonate lithologies were examined it is unlikely that a common diagenetic process could have been involved. Additionally, the chances of a common sedimentological phenomenon having the same effect must be discounted. Consequently, uplift and erosion from maximum burial-depth appears to be the most probable explanation of the overcompaction.

4. Estimation of uplift and erosion using apatite fission track analysis.

4.1 Introduction.

Having demonstrated that there is evidence for considerable uplift of the Inner Moray Firth from sonic velocities, this chapter deals with the estimation of uplift and erosion of the adjacent onshore areas of the Scottish Highlands using apatite fission track analysis. The results presented are interpreted as showing that the Scottish Highlands has experienced uplift and erosion since Late Permian/Early Triassic with a significant post-Cretaceous component. Significantly, the post-Cretaceous component for the onshore samples will also be shown to have the same general regional trend as described in Chapter 3 for the Inner Moray Firth.

4.2 Principles of apatite fission track analysis.

4.2.1 Apatite fission track dating.

Apatite fission track analysis (AFTA) has been developed as a radiometric technique for the determination of the low temperature (< 125°C) thermal history of rocks (Green *et al.*, 1989a). Unlike other radiometric techniques which depend on alpha particle decay, apatite fission track analysis relies on the spontaneous fission of ^{238}U into two highly charged fission fragments. These fragments travel in opposite directions through the host crystal and create a linear zone of damage known as a fission track. Such fission tracks are recognised as randomly orientated tubes intersecting a polished surface of the host crystal after chemical etching (Green, 1986; shown schematically in **Figure 4.1**).

The spontaneous fission decay of one ^{238}U atom results in the production of one fission track. Consequently, the rate of fission track production depends on the ^{238}U content of the apatite grain and the rate of decay. If a randomly orientated surface is taken through a host crystal then the chances of a fission track intersecting that surface depends on the length of the fission track (Green, 1988). Consequently, the areal density of fission tracks intersecting a randomly orientated, polished and etched surface through a host crystal is a function of the uranium content, distribution of etchable track lengths and time.

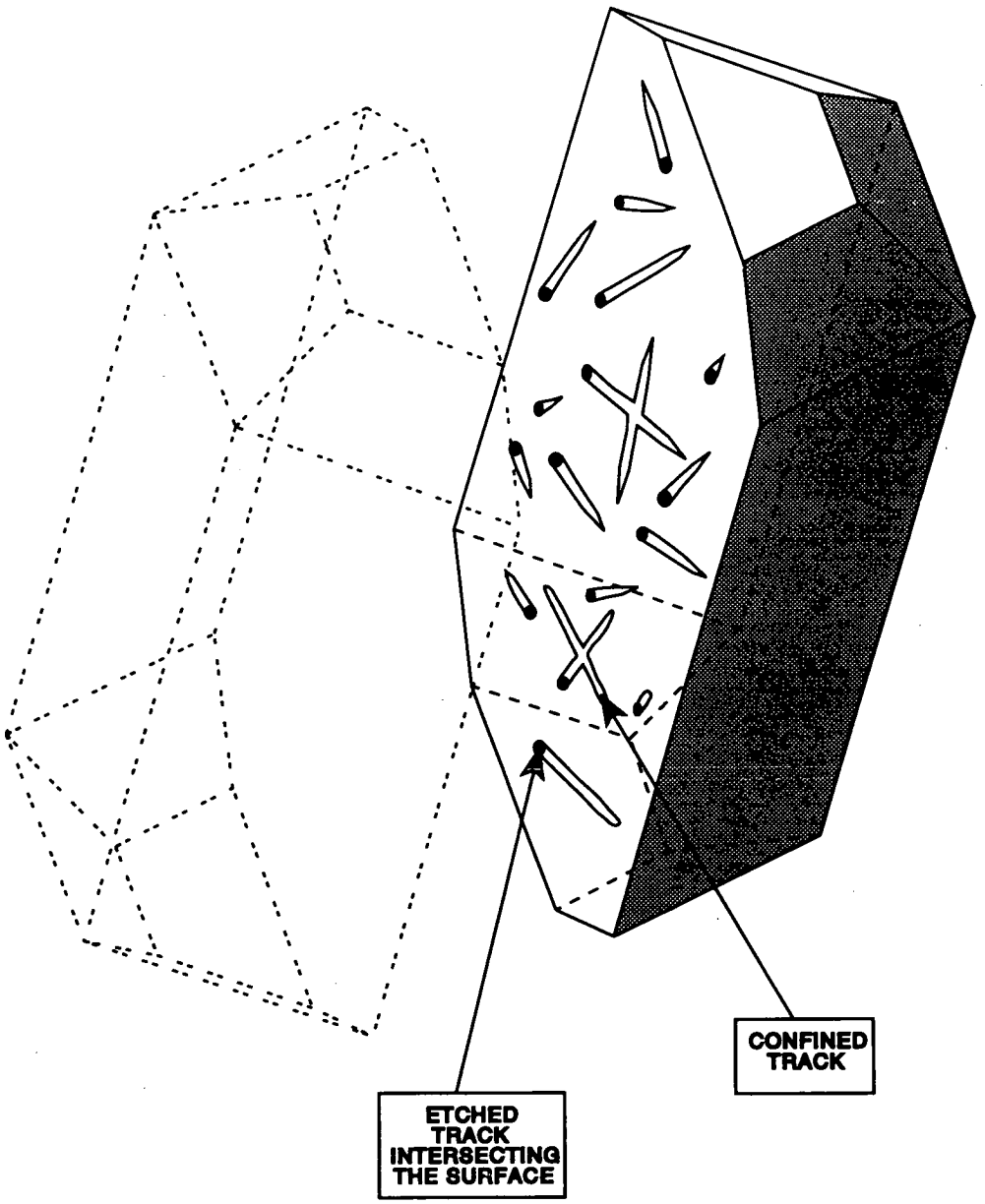

Figure 4.1 Schematic representation of a polished and etched surface through an apatite grain. Etched fission tracks intersecting the surface are shown as well as confined tracks embedded in the grain. Tracks intersecting the surface may be used to determine the fission track age of the sample while the confined tracks allow the track length distributions to be determined (After Brown et al., 1993)

Fission track ages are calculated by the measurement of the areal distribution of spontaneous fission tracks, and those subsequently induced by thermal neutron irradiation, that intersect the polished and etched surface of several individual apatite grains within a sample. The spontaneous track density provides a measure of the amount of ^{238}U that has undergone spontaneous fission while the induced tracks allow the determination of the ^{238}U still present. The dates are calibrated against age standards using a technique know as the "zeta calibration method" (Hurford and Green, 1983). For individual samples the pooled ages of the individual grains are generally quoted with a statistical measure of the age distribution.

As previously stated, the areal density of fission tracks intersecting a randomly oriented, polished and etched surface is a function of track length. Consequently, the apatite fission track age is also dependent upon this parameter. At formation, the etchable track length in apatite is approximately 16±1μm (Gleadow *et al.*, 1986). However, after formation fission tracks are thermally annealed which results in the reduction in track length as the damage to the host crystal lattice is repaired. Since the etchable track length decreases as a result of thermal annealing, the fission track age determined from such a sample is dependent upon its thermal annealing history. The thermal annealing process is primarily controlled by the maximum temperature experienced by the tracks and to a lesser extent by the duration of heating (Green *et al.*, 1989b). Both laboratory experimentation and the analysis of samples from wells where the thermal history is well constrained by other methods has enabled the development of mathematical models for the prediction of fission track ages and track length distributions and is discussed in Green *et al.* (1989b).

On time scales of 1-10 Ma apatite fission tracks progressively shorten from the initial length of 16±1μm with increasing temperature and become completely annealed at temperature in excess of 110±10°C. Consequently, the apparent fission track age of a sample is reduced systematically with continued thermal annealing, and may eventually be reduced to zero at sufficiently high temperatures. As a result of this process it is possible to date the time at which a samples passed through the 110±10°C on the return path to lower temperatures as the fission track "clock" has been reset to zero. This provides a tool to estimate the timing of uplift and erosion episodes.

The rate of thermal annealing increases non-linearly with temperature. Tracks anneal at very slow rates below 60°C and the rate increases significantly above this temperature. The temperature range between 60°C and that at which tracks completely anneal is referred to as the partial annealing zone. Additionally, the rate of annealing is dependent upon the chemical composition of the apatite grain, particularly the chlorine/fluorine ratio (Green *et al.*, 1989b). At any given temperature the fluorine rich apatite grains anneal at higher rates than chlorine-rich grains. This composition dependent annealing behaviour can provide information as to the maximum temperature experienced by a sample.

4.2.2 Track length distributions and thermal history analysis.

The distribution of apatite fission track lengths is normally estimated by measuring the lengths of horizontal, confined tracks (Green *et al.*, 1989a). Such tracks are those which are completely contained within the host mineral grain but have been etched by etchant penetrating along cracks or other tracks which intersect the surface. This process is obviously biased towards longer track lengths but is the most reproducible and direct method for estimating the track length distribution (Green *et al.*, 1989b). As tracks are generated continuously, each individual track experiences a different portion of the total thermal history of the apatite grain. Consequently, the total distribution of track lengths with the fission track age represents an integrated record for the thermal history within the temperature range where tracks are preserved. Over geological heating times this temperature is approximately 110±10°C. As the fission track age will only date the time when the sample last reached this temperature, providing the sample passed rapidly through the partial annealing zone to temperatures below 60°C and has not been significantly reheated, the distribution of track lengths is important in understanding the thermal evolution of the sample and the meaningful interpretation of the fission track age.

The importance of track length distributions to the understanding of the thermal history of a sample may be illustrated by the use of three modelled examples **(Figure 4.2)**. In case A, the cooling history represents that of a volcanic rock with rapid cooling and no reheating above 30-40°C. The fission track age will closely approximate that of the time eruption and the fission track lengths are near their initial value at 14-15μm and a standard deviation of 1μm. This simple distribution of track lengths clearly mirrors the simple thermal history of the sample. For a more complex thermal history such as shown in case B, where the sample cooled

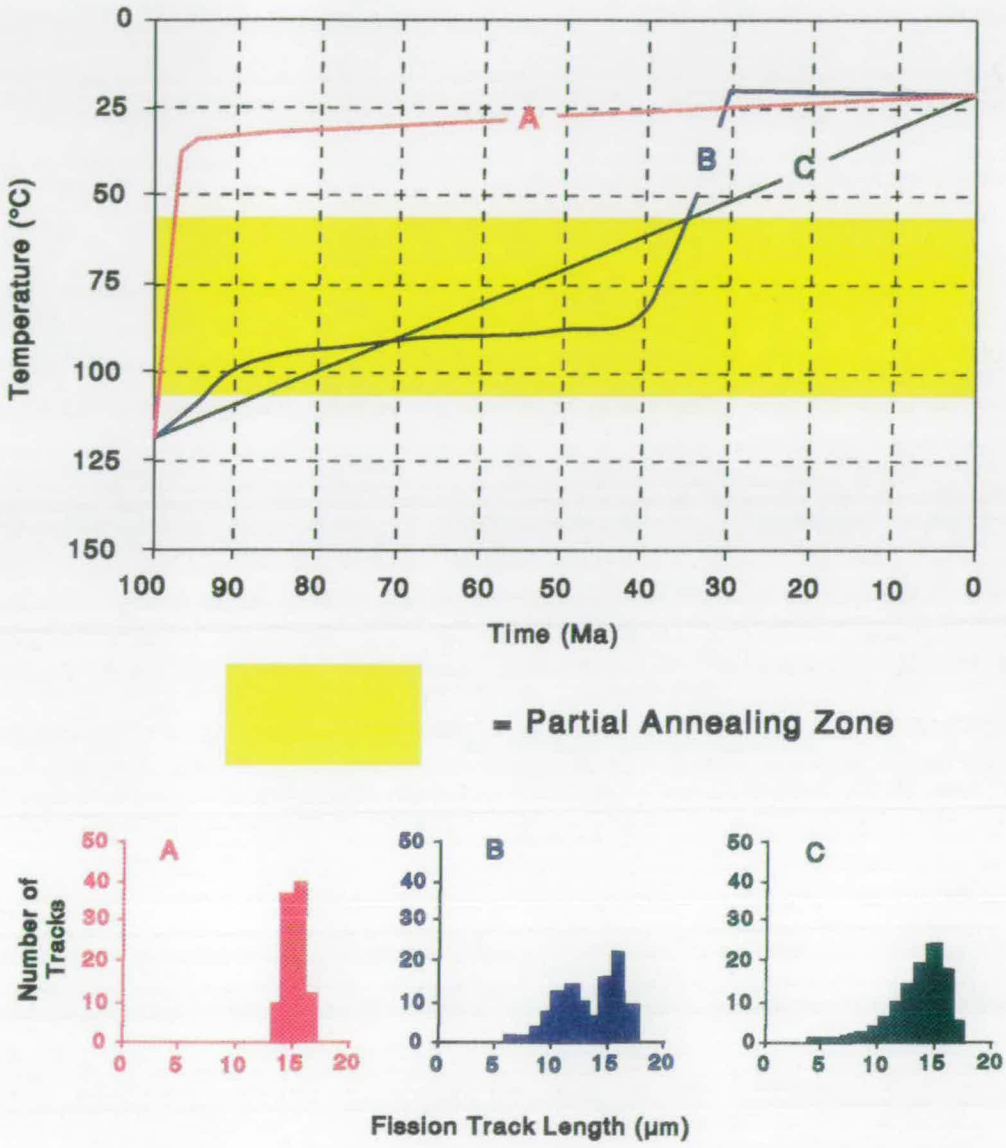

Figure 4.2 Hypothetical fission track length distributions for three possible uplift histories. For rapid cooling from above 110±10°C to below 60°C the fission tracks suffer very little annealing and consequently long track lengths are preserved and the track length distribution is narrow (Case A). Cooling from above 110±10°C and prolonged residency at temperatures above 60°C results in substantial track annealing and consequently reduced track lengths. After cooling to below 60°C these shorter tracks are preserved and as new longer tracks form a bimodal track length distribution results (Case B). For steady cooling from above 110±10°C to surface temperatures a track length distribution skewed towards longer tracks is produced (Case C). The oldest tracks suffer substantial annealing while progressively younger tracks suffer less so, with the youngest tracks having their full lengths preserved (After Brown et al., 1993).

below 110°C but remained at high temperatures for an extended period before rapid cooling, the track distribution is more complex. Those tracks formed prior to the final cooling phase will have been annealed and consequently shortened while the later tracks produced after the cooling phase will preserve their maximum length. This results in a bimodal track length distribution. The fission track age will be significantly younger than the time when the sample passed through 110°C as some of the annealed tracks will be too short to intersect the etched surface and so the areal track density and the fission track age will be reduced. Finally, in case C the sample cools relatively slowly and at constant rate from above 110°C to the surface. In such a case the track lengths have a wide distribution reflecting the slowly changing thermal regime but is skewed towards the younger, longer track lengths.

Green (1986) demonstrated how the integration of fission track ages with track length distributions can be used to determine the low temperature thermal history of Northern England. In his study of the Palaeozoic intrusions of the area he recognised that the apatite fission track ages varied from 45-279 Ma, significantly younger than the age of the intrusions (384-468 Ma). These anomalously low fission track ages were interpreted as being the result of thermal annealing reducing track lengths and consequently the fission track age. Detailed examination of plots of confined track length distributions for some of the samples **(Figure 4.3 (b))** reveals that two distinct types of track length distributions are present, samples 58 and 67 from the Carrock Fell area having long track lengths and small standard deviations and the remainder showing greater degrees of spread within the data and shorter average track lengths.

The relation between track length distributions, fission track age and standard deviation of track length distributions shows a progressive decrease in track length and increase in standard deviation with increasing fission track age **(Figure 4.3 (c))**. In all the samples a peak is present in the longer track length (13-16μm) range but with increasing age a second population of tracks appears creating a bimodal distribution of track lengths best shown in Green's samples 45 and 52. Such a spread of track lengths led Green (1986) to interpret the data as a combination of two distinct track length populations (schematically summarized in **Figure 4.3 (d)**). The shorter tracks represent the older population which has undergone thermal annealing, reducing both track length and fission track age whilst the longer tracks form the younger population produced after rapid cooling.

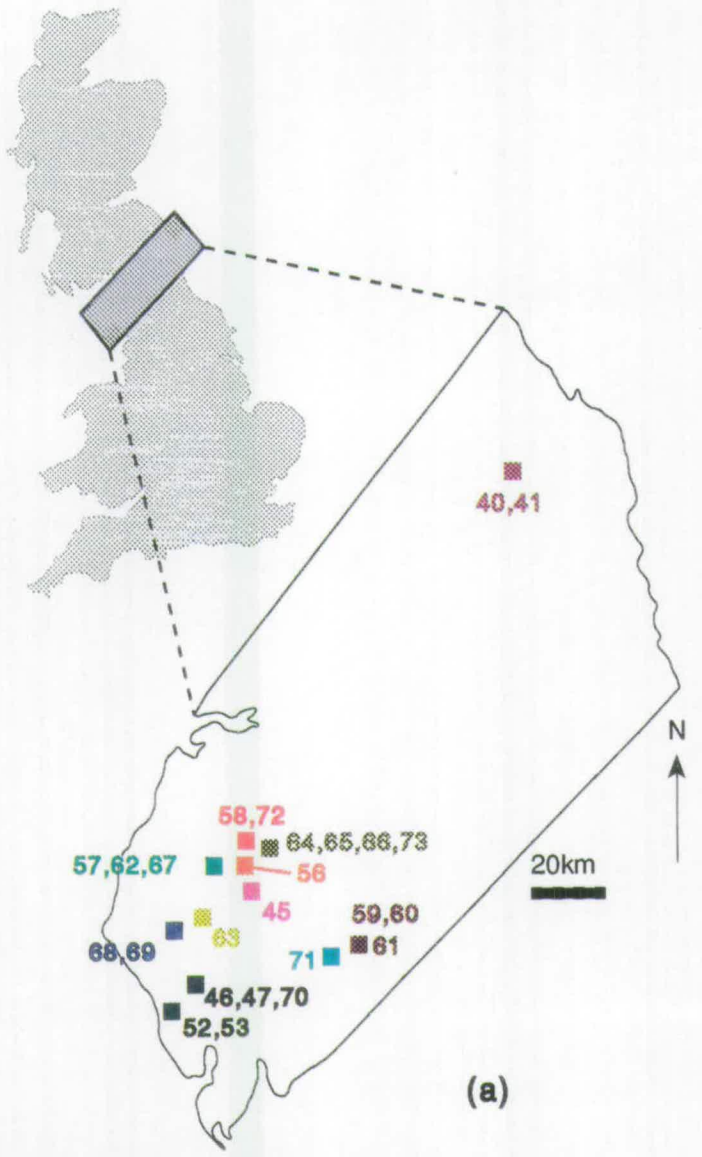

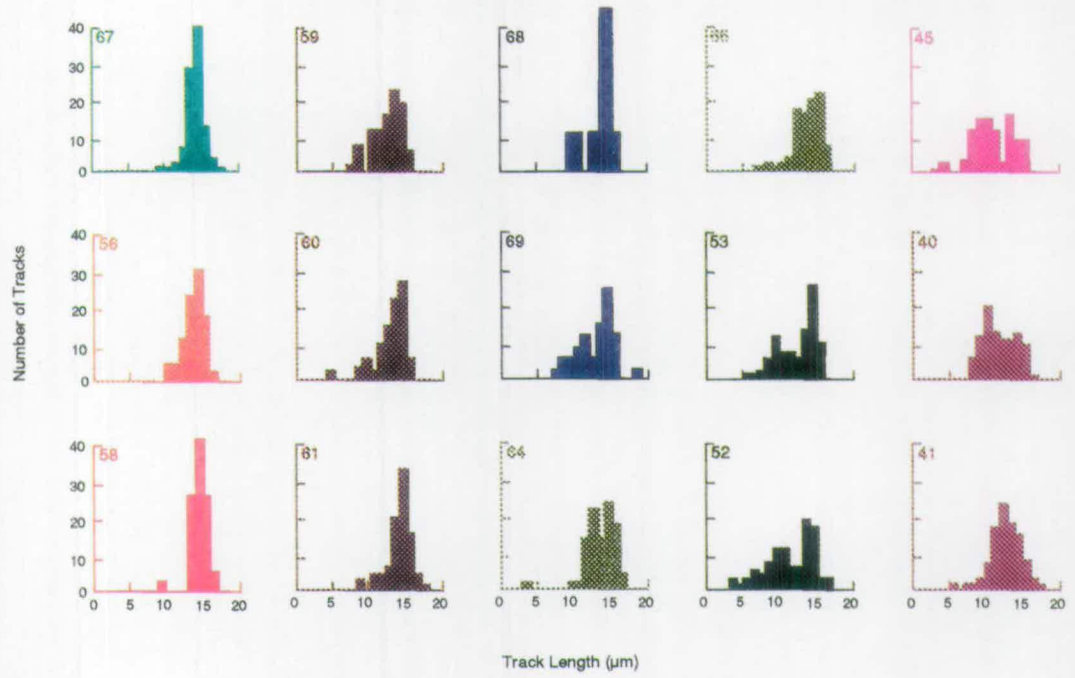

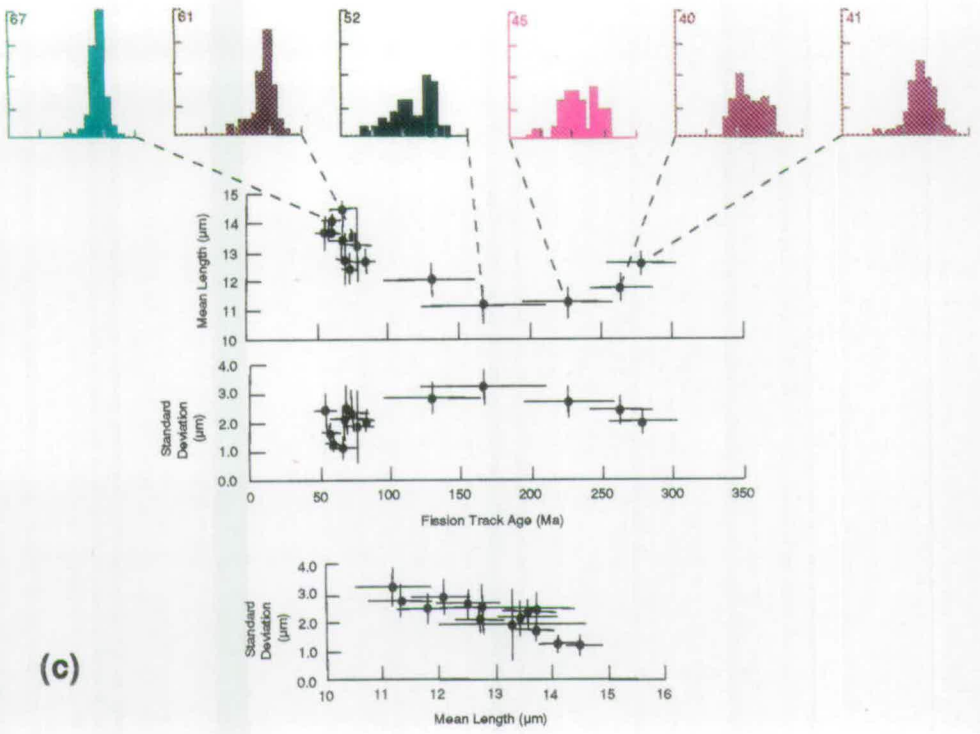

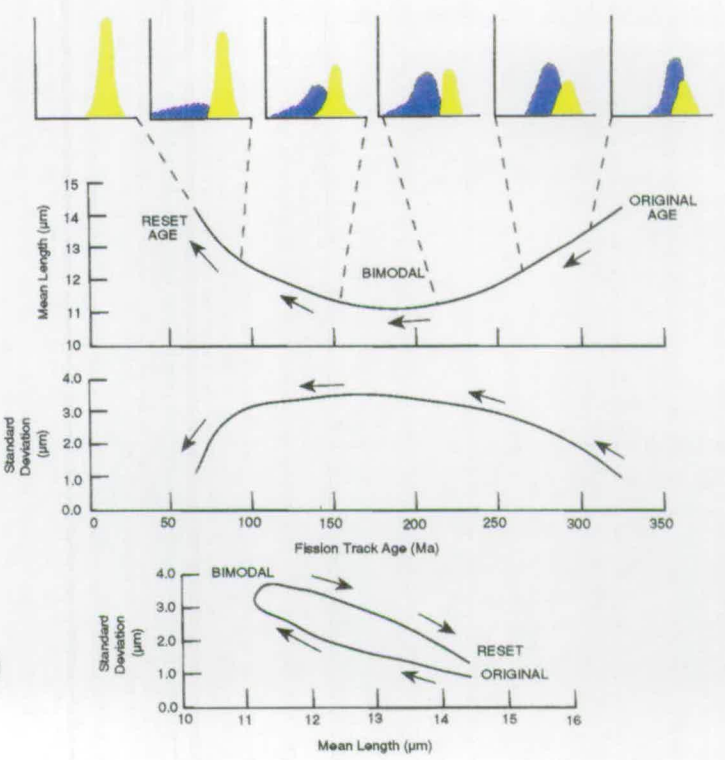

Figure 4.3 Apatite fission track analysis of the Palaeozoic intrusions of Northern England by Green (1986). (a) Location of samples studied. (b) Distribution of confined tracks from 15 localities which show that some samples have long tracks with narrow distributions while the majority show varying degrees of annealing resulting in shorter track lengths and wider distributions. (c) Interrelationship between mean track length, standard deviation of the distribution of track lengths and fission track age. The trends are interpreted as indicating a partial to complete overprint of pre-existing tracks as explained in (d). Length distributions corresponding to selected data points are shown , illustrating the transition from minor partial overprint (right) to total overprint (left). (d) Schematic explanation of the trends in (c). The length distributions are seperated into their two components. Shorter distributions represent those tracks produced prior to 60Ma and have beer thermally annealed while the longer peak represents the tracks formed since 60Ma and have not been thermally annealed du to experiencing lower temperatures.

The above data from Green (1986) shows a marked similarity to the hypothetical models shown in **Figure 4.2**. The Carrock Fell samples are analogous to case A in that at some time after post-intrusion cooling and before 60 Ma they were buried to sufficient depth to achieve temperatures in excess of 125°C and became totally annealed. At 60 Ma however the Carrock Fell area experienced rapid uplift and erosion and passed through the partial annealing zone quickly to reside at temperatures of less than 50°C ever since. The rapid passage through the partial annealing zone resulted in long track lengths being preserved and the fission track age closely mirrors the age of uplift. The remainder of the samples experienced essentially the same history as Carrock Fell but did not achieve temperatures in excess of 125°C. For example, the Cheviot Granite (Green's samples 40 and 41) achieved a temperature maximum of 80-90°C and consequently resided within the partial annealing zone prior to uplift. At these temperatures the fission tracks were not totally annealed. Consequently, although track lengths were reduced the fission track "clock" was not totally reset prior to uplift. Upon uplift and erosion at 60Ma the shorter shorter tracks forming the older population were still present, and when combined with the newer longer tracks produced a bimodal track length distribution. Samples such as those from the Cheviot Granite are directly analogous to case B **(Figure 4.2)**.

Like apatites, zircons also contain ^{238}U that can undergo spontaneous fission decay and produce fission tracks. The behavior of zircon fission tracks has been shown to be essentially similar to that of apatite fission tracks but annealing occurs at higher temperatures (Lewis *et al.*, 1992b). However, as the annealing temperatures of zircons are so high that suitable geological situations with which laboratory experiments can be compared have not been found, the annealing kinetics of zircon fission tracks are poorly understood. Currently the annealing temperature of zircons is believed to be approximately 200°C with the partial annealing zone between 160-200°C (Lewis *et al.*, 1992b).

4.3 Previous apatite fission track analyses of the Scottish Highlands.

Previous apatite fission track studies of Scotland have to date only dealt with the low temperature thermal history of Caledonian Granites (Hurford, 1977) and the thermal effects of the Tertiary igneous complex of the Isle of Skye, west of the Moine Thrust (Lewis *et al.*, 1992b). This section is intended to provide a brief overview of this work so that comparisons can be made with it in later sections.

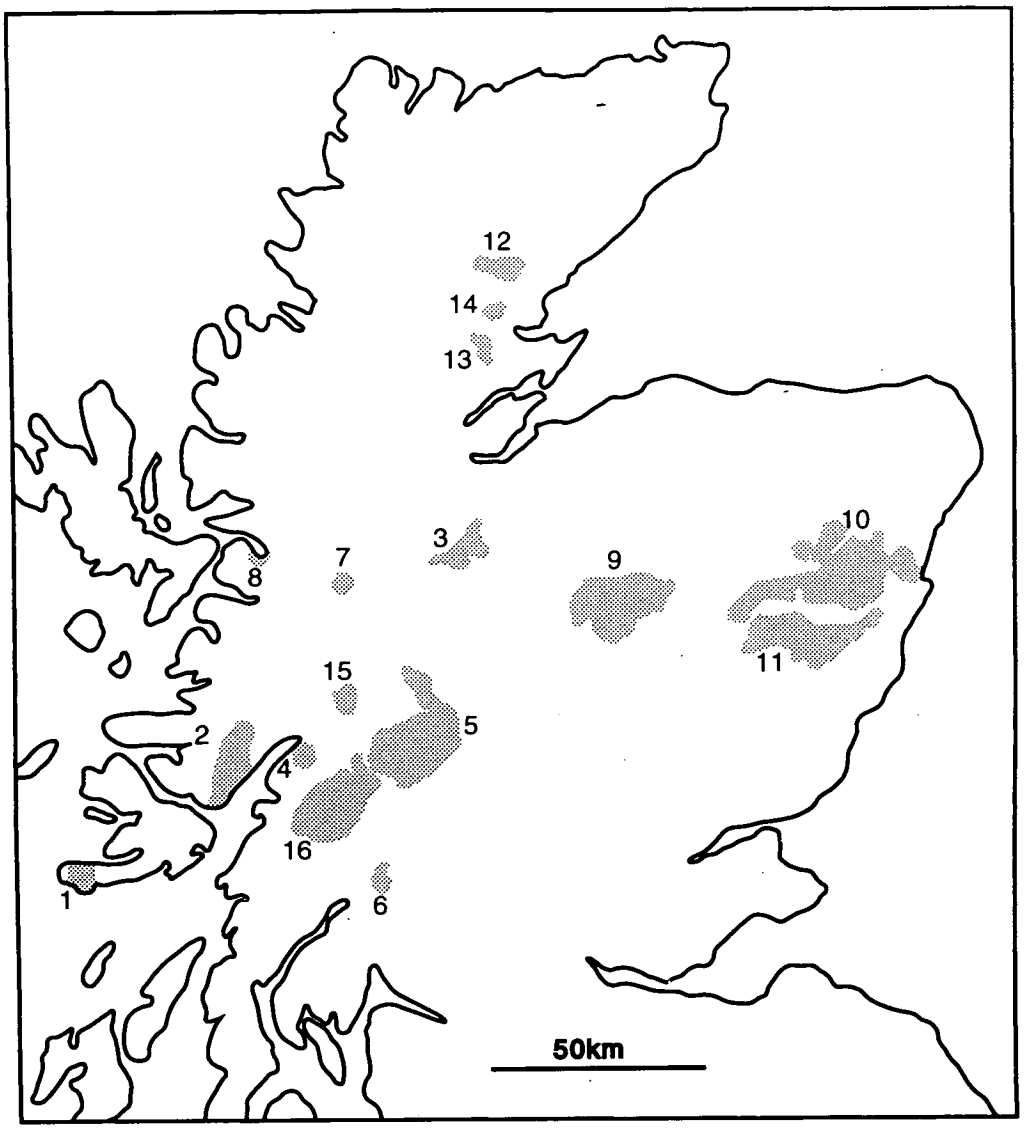

Figure 4.4 Location of the granites studied by Hurford (1977) using apatite and zircon fission track analyses.

Table 4.1 Apatite fission track dating results from Caledonian newer and last granites, from the Scottish Highlands (After Hurford, 1977).

INTRUSION (see **Figure 4.4**)	FISSION TRACK DATE (Ma)
1 Ross of Mull	275±16
2 Strontian	235±15 248±30 235±36 231±24 231±21
3 Foyers	268±30 275±11
4 Ballachulish/ Kentallen	169±7 193±11 274±13
5 Moor of Rannoch	241±13 228±12
6 Glen Fyne	235±15 278±30 286±14
7 Cluanie	225±17 240±18 382±23
8 Ratagan	288±17 275±16 272±12
9 Cairngorm	297±21
10 Hill of Fare	244±13 235±13
11 Kincardine	186±20 209±13
12 Rogart	258±13 258±13 255±14 256±13 256±13 257±11
13 Fearn	283±15 262±17
14 Migdale	217±14 225±13
15 Ben Nevis	237±24
16 Ben Cruachan/ Ben Starav	298±17 245±23 297±32 301±17

The post-intrusion history of sixteen of the "newer and last granites" of the Caledonian orogeny were examined by Hurford (1977). The samples were collected from both the Grampian and Northern Highlands, with the majority of the data from the Grampians **(Figure 4.4)**. Both apatite, sphene and zircon fission track data was collected and the apatite data is shown in **Table 4.1**. In all cases the apatite fission track ages were discordant with the radiometric ages of the granites, being substantially younger at between 200-300Ma. Such a discordancy in apatite fission track ages was interpreted as being the result of thermal annealing of fission tracks and the consequent reduction in fission track age. As neither measurements of track length nor single grain ages were made, this dataset is difficult to interpret and consequently Hurford (1977) states that it is not possible to deduce whether the fission track age represents the time of cooling below 100°C if the samples were completely annealed.

Potential thermal histories for this dataset were suggested by Hurford (1977). It was suggested that the samples may have been partially, or even totally, annealed by subsequent thermal events and supports this argument by stating that the Permian mineralisation around Strontian has K/Ar ages of 230±6Ma, similar to the apatite fission track age of 235±8Ma for the Strontian Granite. The final proposed cause of the reduced apatite fission track age was that the granites experienced slow cooling and resetting during one or more thermal events. The vague nature of these interpretations is to expected as the dataset did not include track length and single grain age data with which modelling of the thermal history could be undertaken as the data was collected before the technique was popularised and the crucial importance of these parameters realised.

Lewis *et al.* (1992b) examined a suite of samples from the Sea of the Hebrides and adjacent areas **(Figure 4.5)** using apatite and zircon fission track analyses. The fission track ages **(Table 4.2)** show that both the apatite and zircon data fall into two distinct populations with ages grouped around 50Ma and 300Ma respectively (some of apatite data is shown in **Figure 4.6** to illustrate this). The older population with fission track ages are comparable with those of Hurford (1977). Additionally, Lewis *et al.* (1992b) noticed that within these older populations the single grain age distributions for samples have tails which extend to 500Ma and beyond reflecting sourcing from the older Hebridian Craton **(Figure 4.7)**.

Table 4.2 Apatite and zircon fission track data from the Sea of the Hebrides and adjacent areas (After Lewis *et al.*, 1992b).

Sample	Locality	Age (Ma)	Track length (μm)
Apatites.			
Mainland.			
SKY 166	Carn Breac	288.87±17.44	11.41±0.24
SKY 167	Milton	303.69±25.84	11.80±0.27
SKY 171	Cruarg	286.16±24.17	10.57±0.30
SKY 175	Inverbain	279.39±11.62	11.93±0.15
SKY 178	Rhutoin	306.07±30.32	11.19±0.26
SCOT 300	Kinlochbervie	263.47±17.66	12.13±0.39
SCOT 302	Gualin House	302.18±17.40	12.67±0.15
SCOT 304	Durness	374.62±27.58	11.66±0.93
Raasay.			
SKY 161	North Raasay	293.06±19.64	11.99±0.30
SKY 315	Beinn na Leac	52.60±6.00	14.12±0.23
SKY 317	Rubha na Leac	47.01±3.22	12.03±1.39
SKY 318	Fearns Rd	53.30±3.90	13.46±0.31
SKY 319	Eyre	69.80±0.32	12.94±0.32
SKY 320	Eyre	47.87±2.88	12.61±0.60
Skye.			
SKY 308	Bearrercaig Bay	357.12±27.21	12.16±0.15
SKY 327	Ob Lusa	53.49±4.35	12.30±0.64
SKY 329	Skulamus	47.20±3.70	13.50±0.30
SKY 330	Drumfearn	49.70±3.80	13.18±0.23
SKY 331	Loch na Dal	72.80±6.60	13.05±0.63
SKY 337	Loch Buidhe	53.85±3.75	10.58±0.99
SKY 341	Beinn nan Charn	47.10±3.30	14.21±0.65
SKY 350	Camasunary	52.37±3.91	13.15±0.35
SKY 358	Strathaird	56.93±5.13	13.47±0.66
Lewis/Harris.			
LEW 292	Northton, Harris	281±16.83	13.31±0.11
LEW 294	Tarbert, Harris	290.57±57	13.05±0.16
LEW 298	Eye Peninsula, Lewis	292.42±17.95	12.48±0.30
Zircons.			
Skye.			
GE	Western Red Hills	51.90±2.70	
MG	Western Red Hills	48.40±2.50	
BDME	Western Red Hills	51.00±3.40	
LAE1	Western Red Hills	45.80±4.30	
LAE2	Western Red Hills	45.90±3.50	
NPF	Western Red Hills	46.90±3.00	
GBMDE	Eastern Red Hills	53.10±3.70	
AFE	Eastern Red Hills	49.70±2.20	
BADE	Eastern Red Hills	47.50±2.60	
BNC	Eastern Red Hills	49.00±2.60	
CSE	Eastern Red Hills	53.60±3.60	
BERR/AS	Craeg Strollamus	44.40±3.30	
BERR/ELG	Elgol	62.70±3.90	

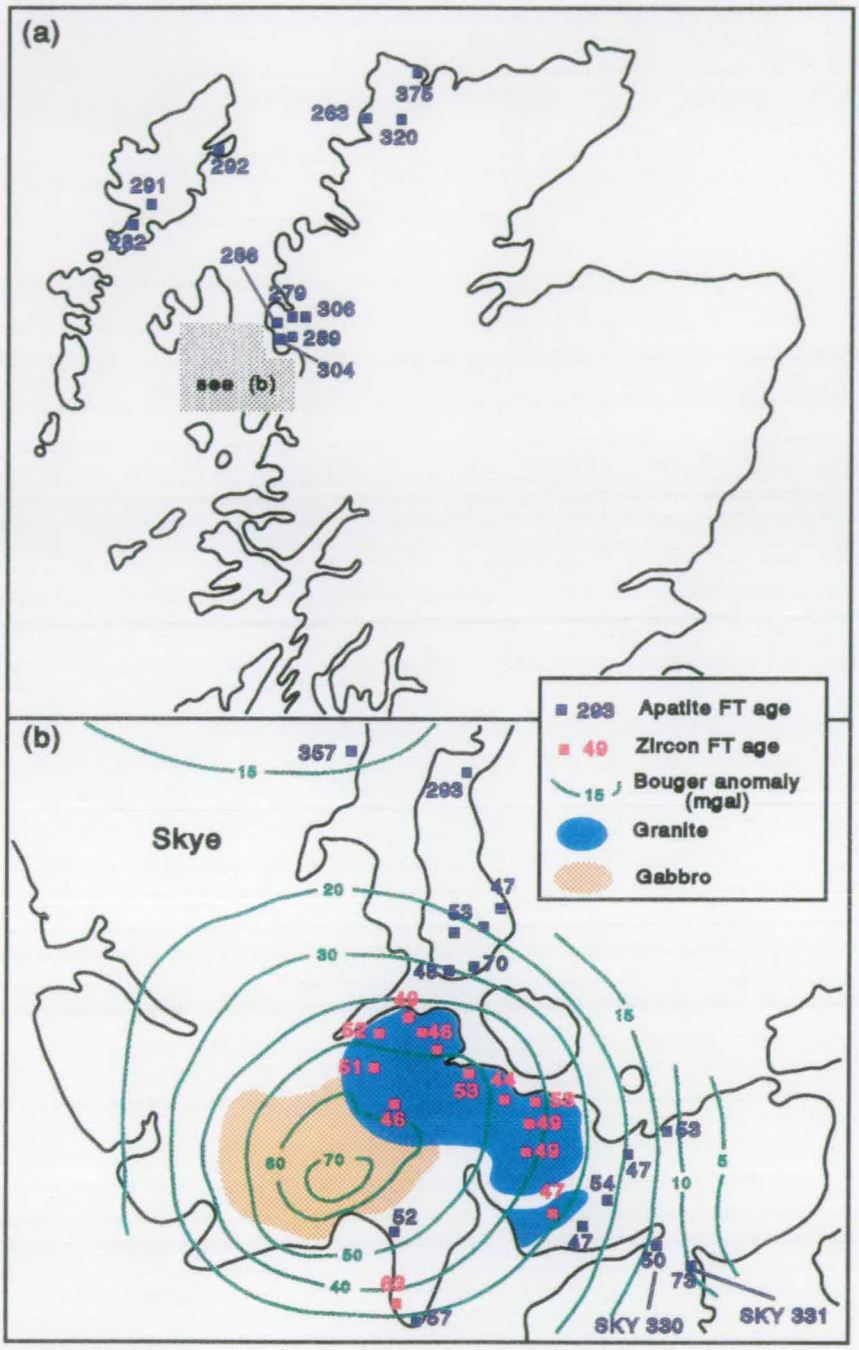

Figure 4.5 Apatite and zircon fission track analyses by Lewis et al. (1992). (a) Location of samples with fission track ages. (b) Relationship between fission track ages and the Bouger anomaly around Skye. All samples within the 15mgal contour show that the igneous centre completely annealed them whilst samples beyond 20km samples seem unaffected. Between these limits partial annealing occurred. Samples SKY 330 and SKY 331 which are discussed in the text are highlighted.

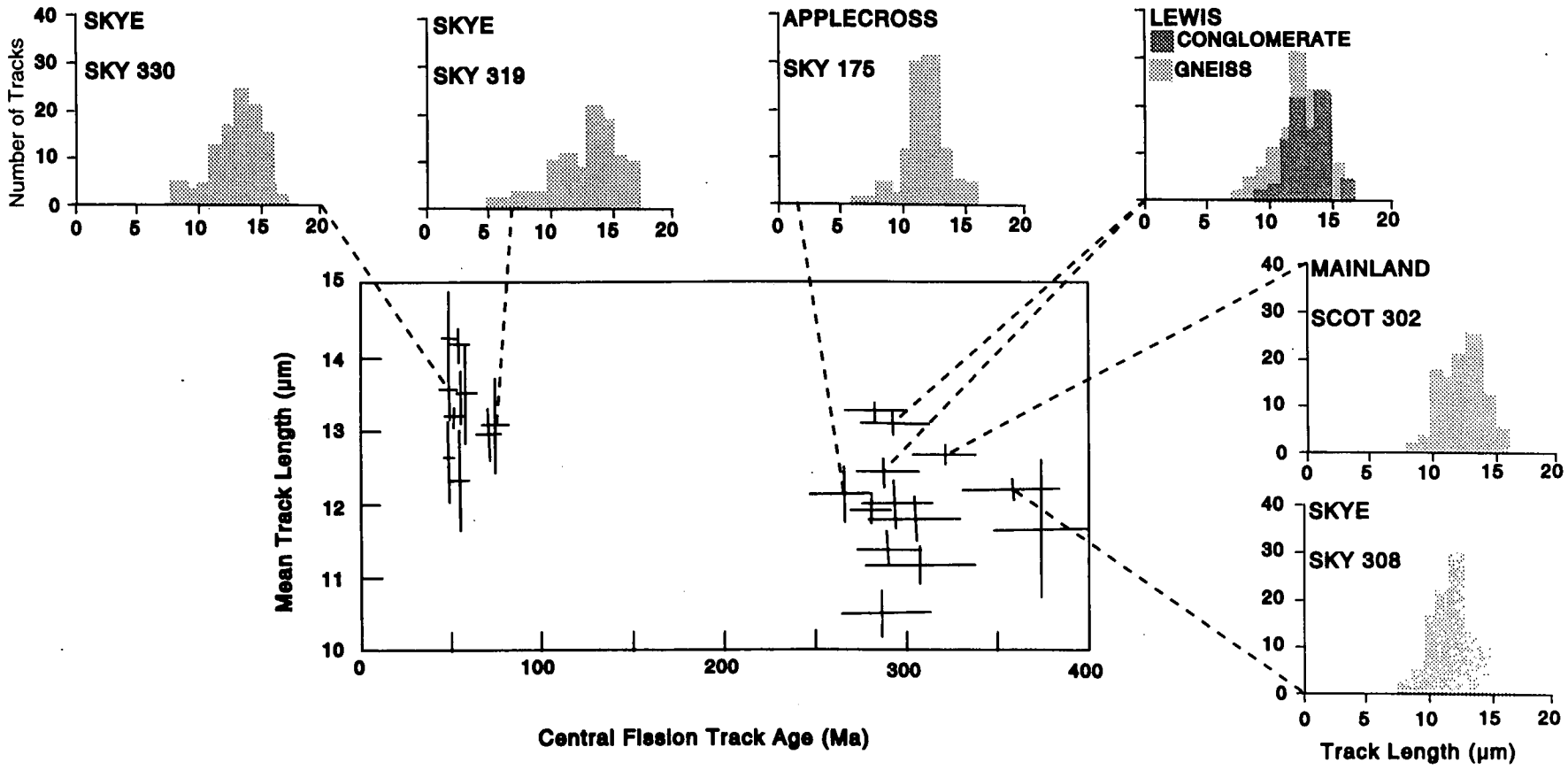

Figure 4.6 Plot of mean track length (µm) against mean fission track age (Ma) and plots track length distributions for the samples analysed by Lewis et al. (1992). The data shows that for the area two distinct populations exist with a younger set (~50ma) which experienced the thermal effects of the Skye igneous centre and those with age between 250-400Ma which underwent burial and slow exhumation unaffected by the igneous activity.

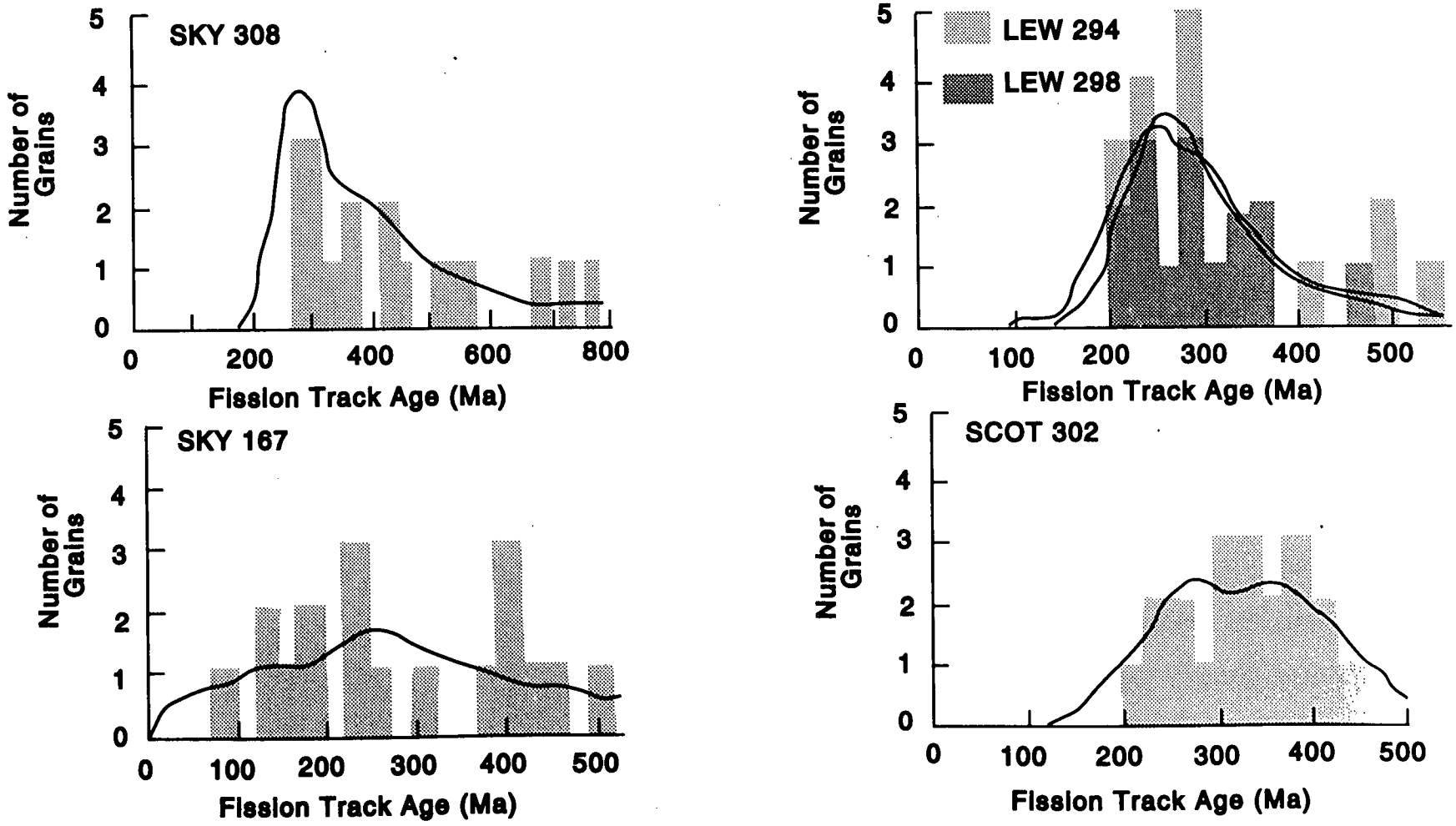

Figure 4.7 Plots single grain fission track age distributions by Lewis et al. (1992). All the plots have tails reaching 500Ma and beyond, consistent with the Hebridian Craton being a major source of sediment for the area.

The younger population of fission track ages have both apatite and zircon ages all within error of each other at approximately 50Ma and track lengths around 13μm, suggestive of some annealing. These samples can be explained when their position is plotted relative to the bouger anomaly map of the area **(Figure 4.5)**. As can seen the anomaly is related to the presence of the Tertiary igneous complex and all samples which lie within the 15mgal contour have been totally annealed. An example of such a sample is SKY 330 **(Figure 4.8)** which has a fission track age of 49.7±3.8Ma. However, samples which lie outwith the 15mgal contour, such as SKY 331 (near the 10mgal contour) are only partially annealed with SKY 331 having a fission track age of 73±7Ma **(Figure 4.8)**. Consequently, the younger suite of samples around the Tertiary igneous centre of the Isle of Skye can be readily interpreted as the product of thermal annealing due to the intrusion of hot igneous masses which totally annealed samples upto 8km away from its present outcrop.

Although the quantification of uplift and erosion over the Skye igneous centre is difficult to constrain as the apatites and zircons were completely annealed, Lewis *et al.* (1992b) suggest that cooling below 110°C at 52Ma due to fairly constant uplift and erosion until the present day is not incompatible with the fission track evidence. Additionally, their data provides evidence for post-Cretaceous uplift and erosion for the surrounding areas. The Jurassic sediments of Skye which have not been affected by igneous heating contain Precambrian apatite grains which could not have experienced temperatures in excess of 50°C since deposition. This is consistent with post-Jurassic (Tertiary?) erosion of over 1km. On the mainland, Late Cretaceous overburden was around 1-1.5km at Cape Wrath and 2km at Applecross, again suggesting post-Cretaceous erosion of 1-2km.

4.4 Sample details and fission track analysis results.

A total of twenty-one samples were collected from the Scottish Highlands for apatite fission track analysis. The samples came from a variety of stratigraphic levels including both proterozoic basement (Torridonian and Moinian rocks) and Phanerozoic (Devonian and Permo-Triassic) sediments. The locations of the samples are shown in **Figure 4.9** and the sample details in **Table 4.3**. The samples were then analysed by Geotrack International and the fission track ages, corrected ages and mean track lengths determined **(Table 4.4)**.

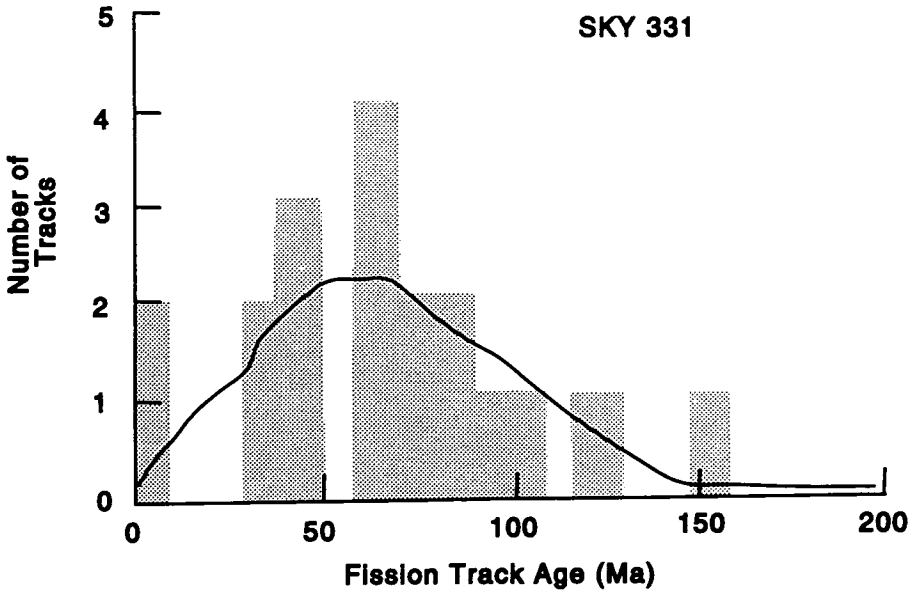

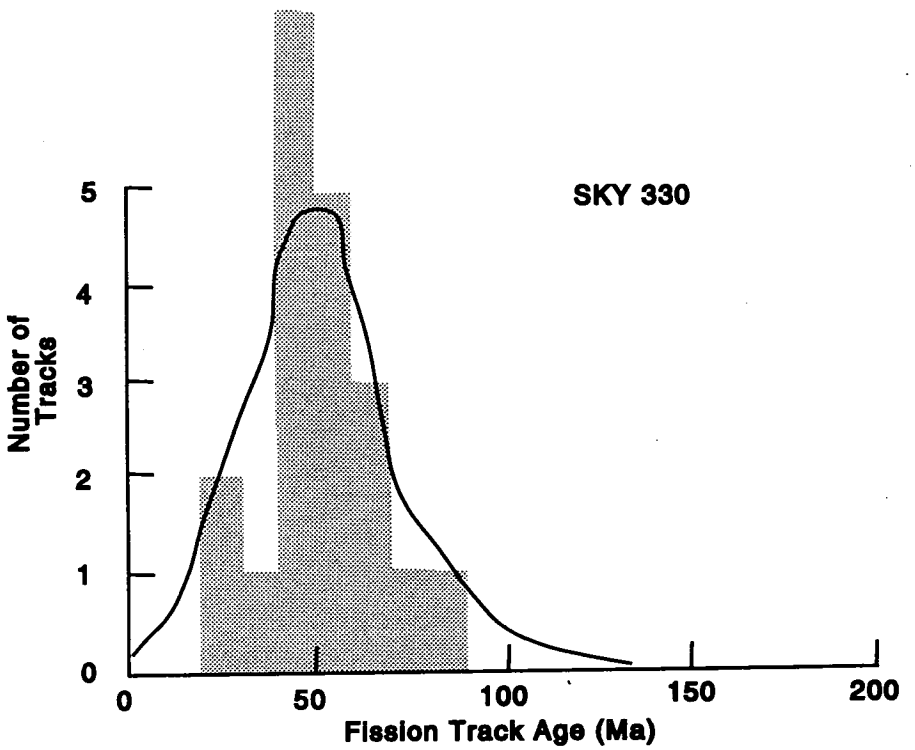

Figure 4.8 Single grain age distributions for samples SKY 331 and SKY 330. SKY 331 is situated outwith the 15mgal contour and the wide ranges in individual grain ages reflects the partial annealing that it experienced. SKY 330 with the much tighter distribution and mean age around 50Ma has experienced total annealing due the thermal effects of the igneous centre and lies within the 15mgal contour.

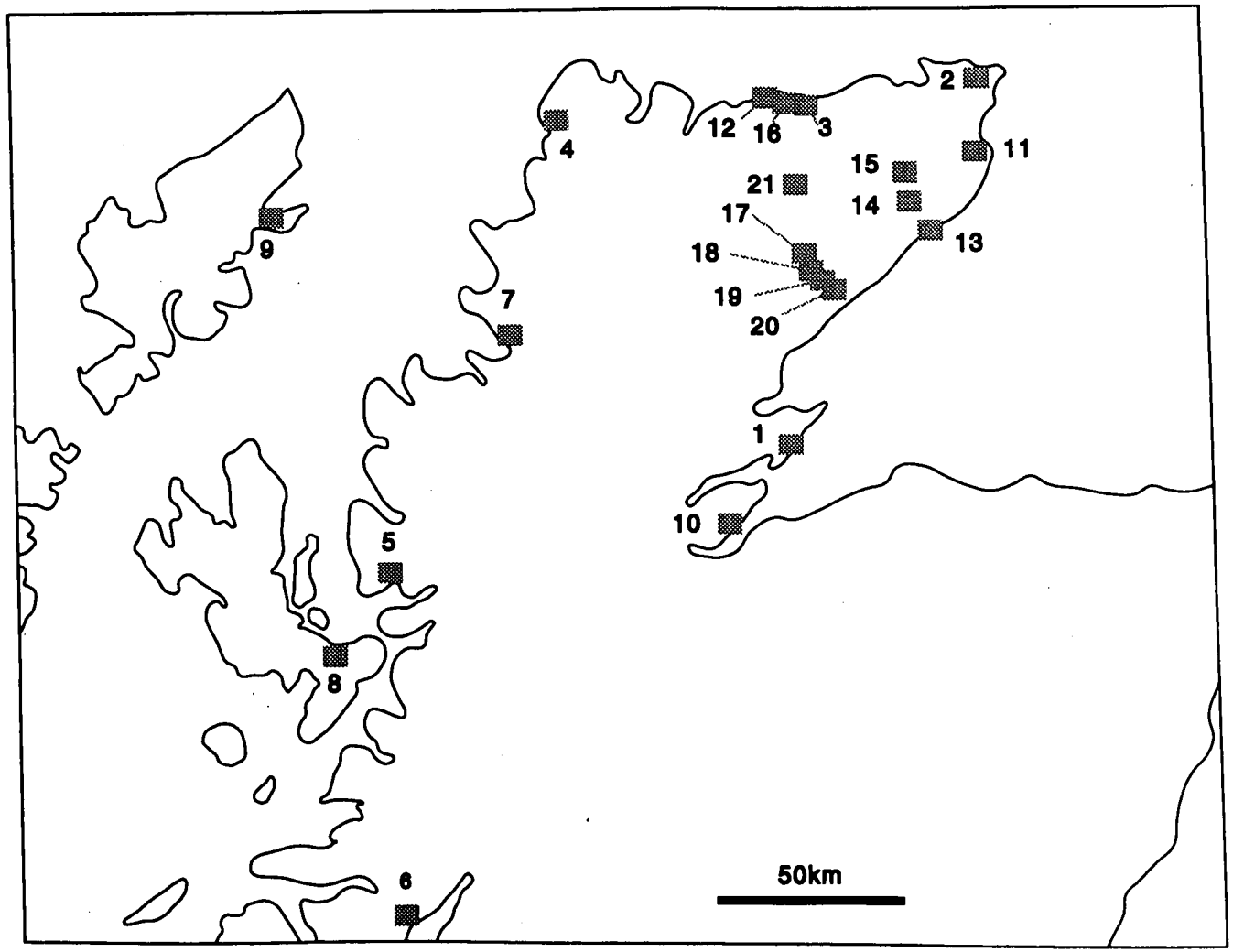

Figure 4.9 Location of samples collected for apatite fission track analysis in this study.

Table 4.3 Locations, stratigraphic details and apatite yields for the samples analysed by apatite fission track analysis.

Sample Number	Grid Reference	Stratigraphic Subdivision	Stratigraphic age (Ma)	Apatite yield*
1	NH 853737	Middle Old Red Sandstone	386-377	excellent
2	ND 325433	Middle Old Red Sandstone	386-377	excellent
3	NC 959660	Middle Old Red Sandstone	386-377	excellent
4		Torridonian Sandstone	1100-600	excellent
5	NG 835424	Torridonian Sandstone	1100-600	excellent
6		Middle Old Red Sandstone	386-377	excellent
7	NH 211899	Torridonian Sandstone	1100-600	very poor
8	NG 170824	Torridonian Sandstone	1100-600	excellent
9	NB 145932	Permo-Triassic	290-208	excellent
10	NH 680550	Middle Old Red Sandstone	386-377	excellent
11	ND 358546	Middle Old Red Sandstone	386-377	excellent
12	NC 835654	Middle Old Red Sandstone	386-377	excellent
13	ND 192321	Middle Old Red Sandstone	386-377	excellent
14	ND 182406	Middle Old Red Sandstone	386-377	excellent
15	ND 182406	Middle Old Red Sandstone	386-377	excellent
16	NC 176444	Moine	>460	excellent
17	NC 876285	Moine	>460	excellent
18	NC 900245	Moine	>460	excellent
19	NC 903220	Moine	>460	poor
20	NC 940190	Moine	>460	excellent
21	NC 893440	Moine	>460	excellent

* Yield based on quantity of apatite suitable for age determination. Excellent: >20 grains; very good: approximately 20 grains; good: 15-20 grains; fair: 10-15 grains; poor: 5-10 grains; very poor: <5 grains.

Table 4.4 Fission track ages, corrected ages, stratigraphic ages and mean track lengths for the samples analysed.

Sample Number	Fission Track Age (Ma)	Corrected Age (Ma)	Stratigraphic Age (Ma)	Mean Track length (μm)
1	265.0±12.4	315	386-377	12.03±0.19
2	213.6±15.7	234	386-377	13.04±0.16
3	185.5±7.9	193	386-377	13.74±0.15
4	176.4±15.7	203	1100-600	12.41±0.24
5	184.2±17.4	205	1100-600	12.85±0.20
6	182.1±11.7	205	386-377	12.70±0.14
7	131.8±26.7	149	1100-600	12.60±0.42
8	51.0±4.3	54	1100-600	13.47±0.26
9	212.1±16.0	250	290-208	12.11±0.28
10	272.0±19.6	319	386-377	12.18±0.18
11	222.9±13.5	236	386-377	13.47±0.17
12	225.3±18.4	250	386-377	12.85±0.17
13	180.2±11.8	199	386-377	12.93±0.21
14	182.2±7.8	198	386-377	13.12±0.15
15	186.2±8.7	207	386-377	12.85±0.22
16	235.0±12.2	259	>460	12.98±0.17
17	170.5±12.1	184	>460	13.25±0.16
18	169.5±8.3	185	>460	13.07±0.22
19	114.9±34.0		>460	
20	171.4±10.4	180	>460	13.61±0.45
21	213.2±10.4	252	>460	12.09±0.26

4.5 Fission track ages and track lengths.

Examination of the data contained in **Table 4.4** yields information regarding the thermal history of the samples. Firstly, it can be seen that both the fission track and corrected ages are substantially lower than the stratigraphic ages at around 200-300Ma (c.f. Hurford, 1977; Lewis *et al.*, 1992b). This would suggest that thermal annealing has been an important process during the life of the samples. Indeed, the magnitude of the age reduction may suggest that the samples have been totally annealed and that the ages represent a first approximation (with caution regarding duration of residency in the partial annealing zone) of the age at which the samples passed through the 110±10°C isotherm into lower temperature domains. The mean track lengths and their distributions also show evidence of substantial annealing. This evidence is based on the fact that all the samples have shortened track lengths, ranging between 12 and 14μm and possess large standard deviations of 1.3-2.6μm. This is substantiated when mean track length is plotted against fission track age **(Figure 4.10)**, as the majority of the data appears to define a broad envelope of decreasing mean track length with increasing fission track age. Such a distribution is compatible with the older samples passing through the 110±10°C isotherm first and then spending longer in the partial annealing zone. The younger samples probably passed through the 110±10°C isotherm later and then escaped the partial annealing zone more quickly. Complimentary with this interpretation is the evidence from **Figure 4.11** which shows standard deviation plotted against mean track length. As can be seen there is a general trend of increasing standard deviation with decreasing track length. As previously mentioned, the older samples generally have shorter track lengths and this may be attributable the longer residency in the partial annealing zone. The longer the period of residency in the partial annealing zone the greater the variation in track length should be, and consequently the larger the standard deviation. As **Figure 4.11** shows a general increase in standard deviation with decreasing track length it appears possible that the older samples entered the partial annealing zone first and probably spent longer in it before entering the low rate annealing zone below the 60°C isotherm.

Within the dataset under discussion one notable exception exists. Sample 8 from the Isle of Skye consists of Torridonian Sandstone similar to other samples. The fission track age is extremely young at around 50Ma (c.f. Lewis *et al.*, 1992b). This sample obviously has experienced a different thermal history to the rest of the dataset and it is most probably related to the Skye Tertiary igneous centre. The

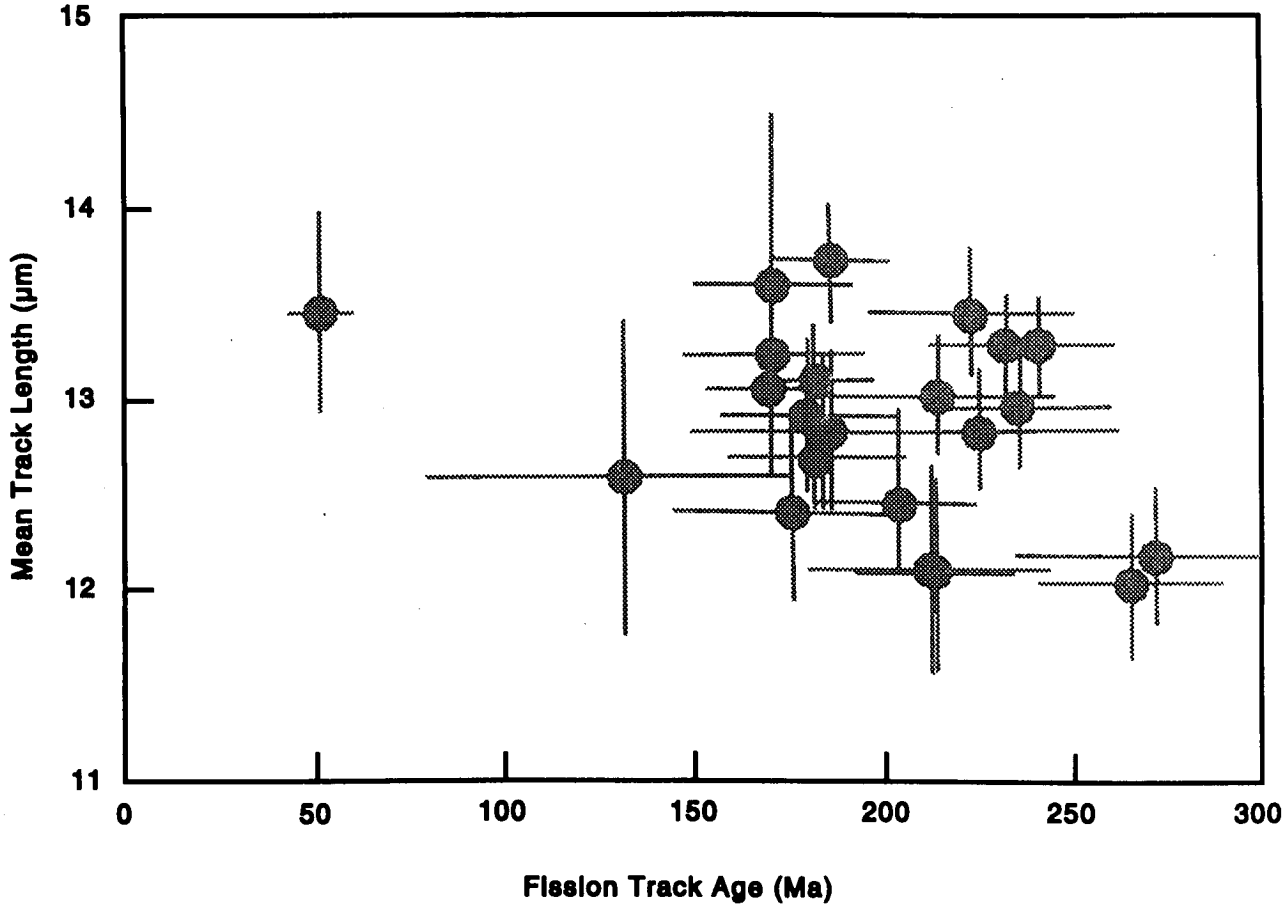

Figure 4.10 Plot of mean fission track length against fission track age for the samples shown in Figure 4.9. As all samples have track lengths below 15µm the samples must have experienced thermal annealing at some point in their history. The sample at 50ma differs from the remainder as it has experienced Tertiary thermal heating beyond 110±10°C due to its proximity to the Skye igneous centre.

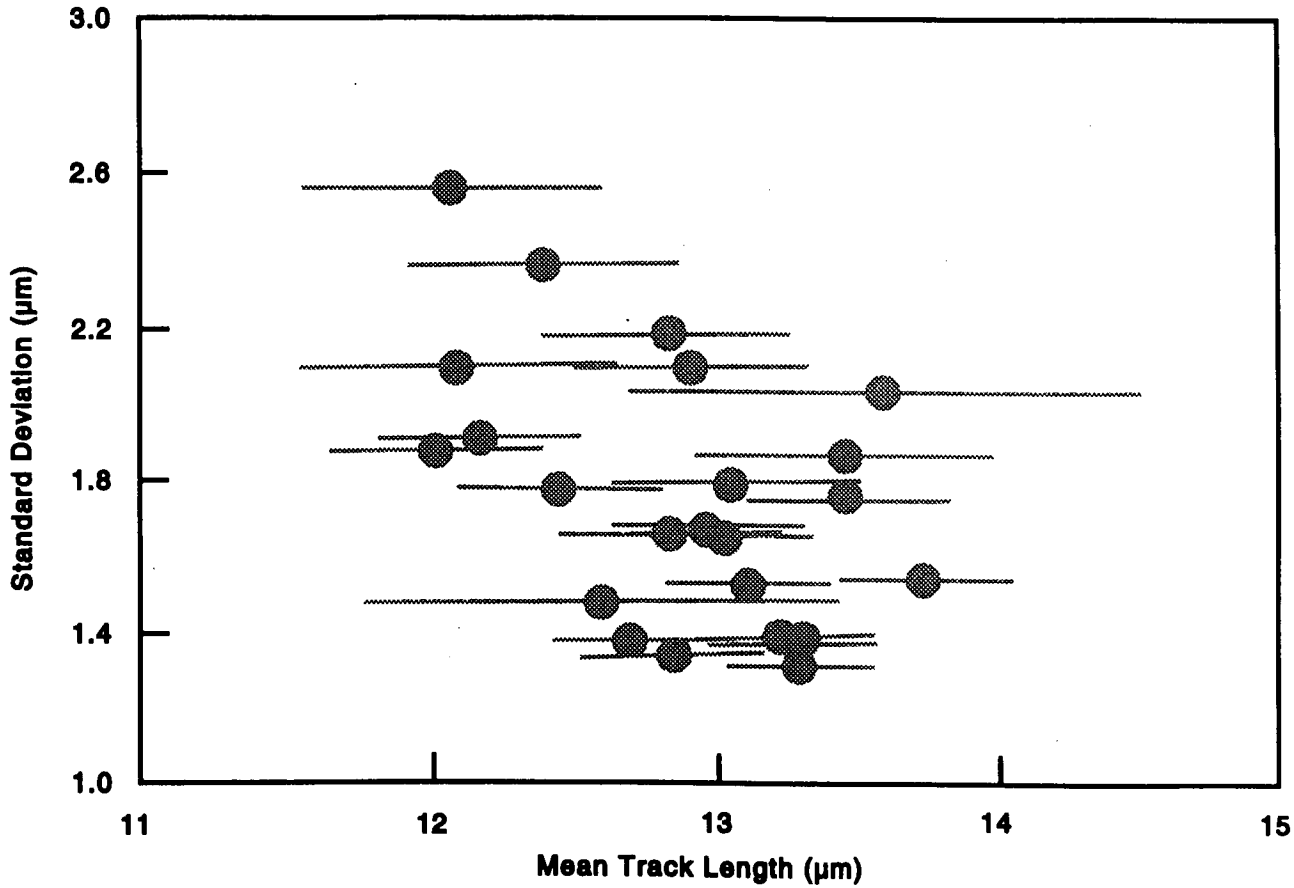

Figure 4.11 Plot of standard deviation against mean fission track length for the samples shown in Figure 4.9. The samples show a progressive increase in standard deviation with decreasin mean track length. This can be attributed to the greater degree of thermal annealing experienced by the shorter track length samples. As annealing progresses and new tracks are produced the oldest tracks shorten and combined with the new tracks to produce a greater range of track lengths within the grains. With more severe annealing tracks are reduced more and so the spread ot track lengths is increased.

extremely high heatflows in this area most likely caused complete annealing of the sample and as the area cooled the fission track age recorded when the sample cooled below 110±10°C, as proposed by Lewis *et al.* (1992b). The relative rapidity of cooling compared to the slow exhumation that probably affected the other samples has resulted in the sample having track lengths amongst the longest in the entire dataset and a reasonably small standard deviation (compared to the dataset under discussion) of 1.8μm. Obviously as this datapoint was affected by adversely high heatflows not related directly to burial-depth it cannot be used in the quantification of uplift and erosion and has been disregarded for regional interpretations.

4.6 Fission track modelling results, Late Cretaceous/Early Tertiary palaeotemperatures and erosion estimates.

Modelling of the fission track ages and mean track lengths/track length distributions was also undertaken in order to assess the timing of samples passing through the 110±10°C isotherm, quantify the burial/erosion history and estimate the post-Cretaceous component of uplift and erosion. This process and the results derived from it must be taken with some caution as without any stratigraphic control on the burial history the modelling must be taken as being poorly constrained.

It appears that all the samples (except samples 8 and 9) passed through the 110±10°C isotherm between 350-250Ma (**Table 4.5**; c.f. Hurford, 1977) and since then have undergone fairly continuous uplift. Sample 8 as previously mentioned was so overprinted with the Tertiary igneous signature that its history prior to this time cannot be assessed while sample 9 appears to have undergone burial until the Tertiary when it was exhumed. All the samples require an increase in the rate of erosion around 60Ma, though in most cases this is only a minor deflection in the uplift and erosion path. However, samples 4 and 9 require a more substantial deflection. These findings seem consistent with the geological history of the area. Firstly, the prolonged exhumation history is consistent the the Scottish Highlands being the main source of sediments for the North Sea and a major contributor to the Minches basin, as suggested by Watson (1985). The steady and prolonged exhumation would allow the area to supply sediment throughout the Mesozoic and Cenozoic. Secondly, the increased rate of exhumation around the Cretaceous-Tertiary boundary reflects the rapid increase in sediment influx into the North Sea at this time (Parker, 1975; Rochow, 1981; Galloway *et. al.*, 1993; Hartog Jager *et. al.*, 1993; Morton *et. al.*, 1993). Finally as sample 9 is part of the fill of the Minches Basin, and was probably buried not only by Jurassic but also

Table 4.5 Timing of cooling below 110°C, temperature at 60Ma and the magnitude of post-Cretaceous erosion derived from apatite fission track analysis.

Sample Number	Timing of cooling below 110°C (Ma)	Palaeotemperature at 60Ma (°C)	Post-Cretaceous erosion (m)
1		60	1667
2	300	40	1000
3	300	30	667
4	300	70	2000
5	300	60	1667
6	300	50	1333
7	225	60	1667
8	60	>110	
9		80	2333
10		60	1667
11	300	20	333
12	350	50	1333
13	250	40	1000
14	250	40	1000
15	250	40	1000
16	350	40	1000
17	250	40	1000
18	250	40	1000
19	250		
20	250	40	1000
21	300	50	1333

Cretaceous sediments, it seems unlikely that erosion would have brought it to surface until the initiation of faster erosion rates in the Early Tertiary.

Fission track modelling also provided evidence as to the palaeotemperatures experienced by the samples around the Cretaceous-Tertiary boundary (60Ma) **(Table 4.5)**. With the exceptions of samples 8 (Tertiary igneous affected sample) and 9 (Minches Basin), all the samples appear to have reached temperatures at or below 60°C (the lower temperature bound of the partial annealing zone). Sample 9 at this time was still within the partial annealing zone but may have been in the early stages of exhumation. The palaeotemperatures show a westward increase **(Figure 4.12)** with minimum values around the Inner Moray Firth margins and a maxima around the Skye igneous complex. Other local maxima probably exist close to the other Tertiary igneous complexes but the limited sample density means they could not be resolved. **Figure 4.12** also shows that if the effects of Tertiary igneous activity are discounted that the palaeotemperature maximum probably lay to the west of the outer Hebrides. This may suggest that uplift and erosion is the prime cause of the observed palaeotemperature trend as the data shows the same westward increase as the erosion data for the Inner Moray Firth. To test this hypothesis the palaeotemperature data (sample 8 excluded) was converted into the amount of erosion **(Table 4.5)** by assuming a surface temperature of 10°C and a geothermal gradient of 30°C/km (the choice of temperatures/thermal gradients being arbitary but geologically reasonable) and contoured in **Figure 4.13**. The contour map shown in **Figure 4.13** shows a high degree of compatibility with that for the Inner Moray Firth **(Figure 3.15)** with post-Cretaceous erosion of around 1-1.2km in the region of the Wick/Great Glen Fault intersection. As with **Figure 3.15**, **Figure 4.13** show a general increase in erosion to the west, reaching over 2km in the Outer Hebrides, consistent with the 2km estimate for the maximum burial-depth of Triassic conglomerate on the Isle of Lewis (Lewis *et al.*, 1992b). Additionally, the estimates of Late Cretaceous burial-depths for Cape Wrath (1-1.5km) and Applecross (2km) by Lewis *et al.* (1992b) are consistent with the post-Cretaceous uplift and erosion estimates in **Figure 4.13**.

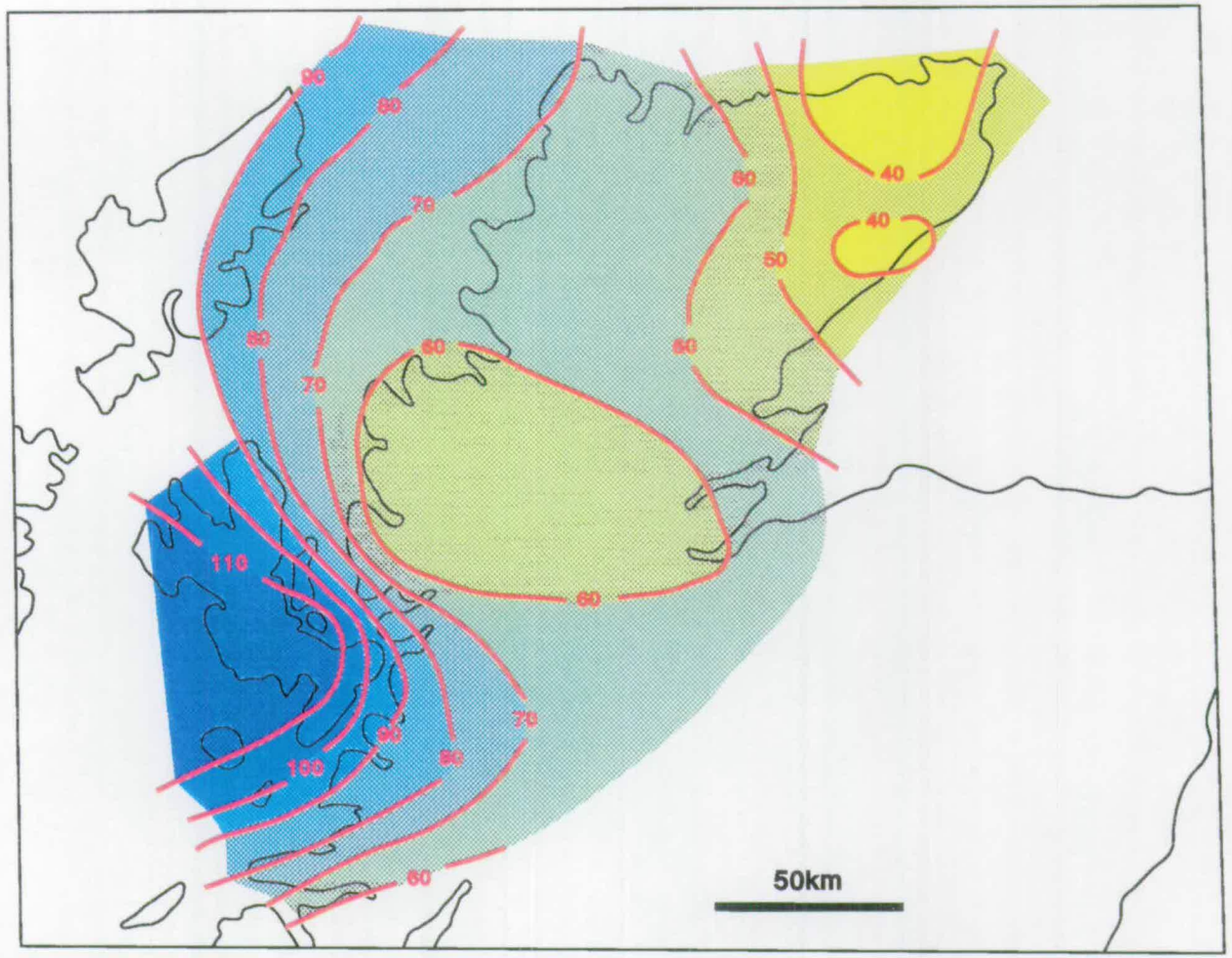

Figure 4.12 Late Cretaceous/Early Tertiary palaeotemperature map for the Scottish Highlands. The map shows a progressive increase in temperature to the west, and on such a regional scale it is probably due to burial at depths greater than currently observed. The "bullseye" around the Skye igneous centre is an exception to this regional trend and reflects the high heatflows from the intrusive bodies in the area, as observed by Lewis et al. (1992).

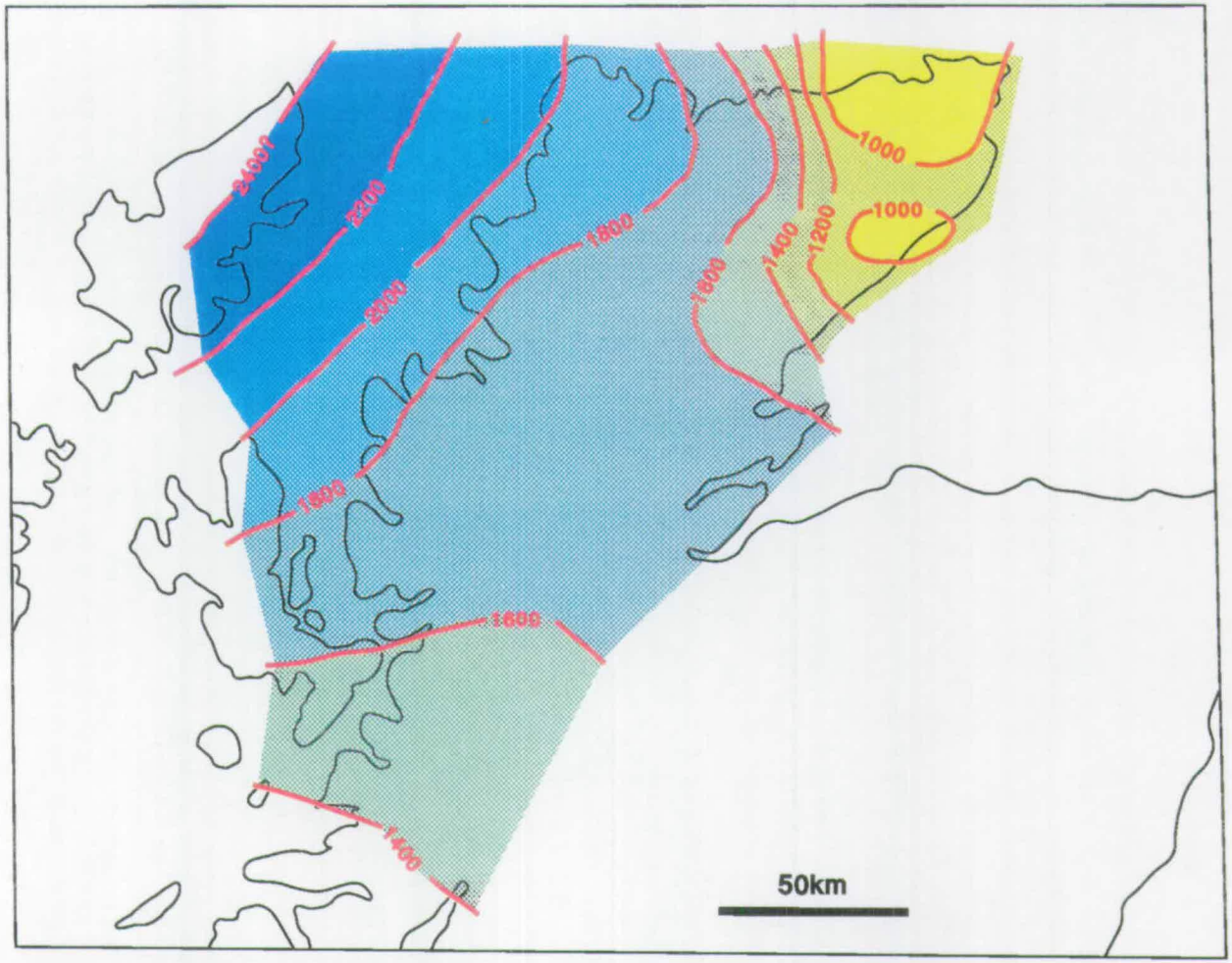

Figure 4.13 Tertiary/post-Tertiary uplift and erosion map for the Scottish Highlands. The map shows a progressive increase in the amount of erosion to the west, as observed in the Inner Moray Firth (Figure 3.15) and values along the Inner Moray Firth margin are compatible with those shown on the map. The amount of erosion gradually increases to a maximum of over 2km aroud the Minches Basin and the Outer Hebrides.

4.7 Conclusions.

(1) The dramatic reduction in apatite fission track ages compared to the stratigraphic ages, and reduction in track lengths suggests that thermal annealing was an important process in the history of the Scottish Highlands. As thermal annealing is primarily controlled by the maximum temperature experienced by the samples, the data suggests that these samples which are now at the surface have experienced significantly higher temperatures during their history. In the case of sample 8 the higher temperatures can be confidently related to the thermal effects of the Skye igneous centre and although no evidence is preserved, earlier thermal events cannot be ruled out. The remainder of the samples from the Scottish Highlands appear unaffected by Tertiary igneous activity and consequently the higher temperatures experienced by them can be confidently ascribed to burial at depths greater than currently observed. Consequently, as the samples are now at the surface they must have experienced uplift and erosion.

(2) Fission track ages and modelling suggest that the Scottish Highlands experienced fairly continuous uplift and erosion since the Late Permian/Early Triassic. Such an interpretation is consistent with the Scottish Highlands sourcing sediments for the North Sea and Sea of the Hebrides during the Mesozoic and Cenozoic. Indeed, the increase in uplift and erosion rates around the Late Cretaceous/Early Tertiary compares favourably with the rapid deposition of Tertiary fans and turbidites in the North Sea. Consequently, their appears to be a link between the rates of exhumation for the Scottish Highlands and the deposition in the North Sea.

(3) Fission track modelling of the Late Cretaceous/Early Tertiary palaeotemperatures show a general increase to the west, similar to the uplift and erosion pattern observed for the Inner Moray Firth. Additionally these palaeotemperatures highlight the localised thermal effects of the Tertiary igneous centres which appear to only totally anneal samples within 10km of the centres.

(4) When Late Cretaceous/Early Tertiary palaeotemperatures are converted to uplift and erosion values their magnitudes can be shown to be of the same scale and regional trend as observed for the Inner Moray Firth. Along the margins of the Inner Moray Firth fission track estimates of 1-1.2km near the Wick/Great Glen Fault intersection are consistent with those seen offshore while to the west estimates increase to over 2km in the Outer Hebrides. The evidence for post-Cretaceous uplift and erosion from the Outer Hebrides to the Inner Moray Firth-Outer Moray Firth transition suggests a regional mechanism(s) is responsible.

5. Estimation of uplift and erosion using geochemical analyses.

5.1 Introduction.

This chapter deals with the estimation of uplift and erosion in the Inner Moray Firth using a variety of geochemical methods. It is intended to demonstrate that geochemical analyses can provide (in most cases) consistent evidence for the removal of up to 1km of sediment from the area from the Late Cretaceous onwards.

5.2 Vitrinite reflectance studies.

Vitrinite reflectance is a widely quoted, quantifiable measure of organic maturation. Such a measure is often referred to when detailing the source rock potential of an area and can also be used to constrain models of the burial history. Consequently, vitrinite reflectance measurements can be used to estimate the amount of missing stratigraphy at unconformities. This section deals with the use of vitrinite reflectance data from both the Inner Moray Firth and Scottish Highlands in the analysis of their exhumation histories.

5.2.1 The vitrinite reflectance trend method.

Pearson and Watkins (1983) state that for the majority of wells in the North Sea the interpolated vitrinite reflectance (Ro %) value for the sea-bed is 0.2%. Consequently, this value may be taken as the depositional vitrinite reflectance value for the area and if higher values occur at sea-bed, uplift and erosion may have occurred. The vitrinite reflectance trend method, as used for southern offshore Norway (Jensen and Schmidt, in press) and for the Irish Sea (Hardman *et. al.*, 1993; Naylor *et. al.*, 1993), relies on the fact that vitrinite reflectance increases irreversibly with time and temperature. At deposition, surface vitrinite reflectance values are believed to be 0.2% and intersection of the $\log_{10}$ vitrinite reflectance/depth trend with the 0.2% value should be at zero burial-depth in non-uplifted wells and at negative burial-depths if uplift and erosion has occurred **(Figure 5.1)**. The amount of section removed from the location of a well is equal to the negative burial-depth at the surface vitrinite reflectance value of 0.2% **(Figure 5.2)**. For the quantification of Neogene uplift in southern offshore

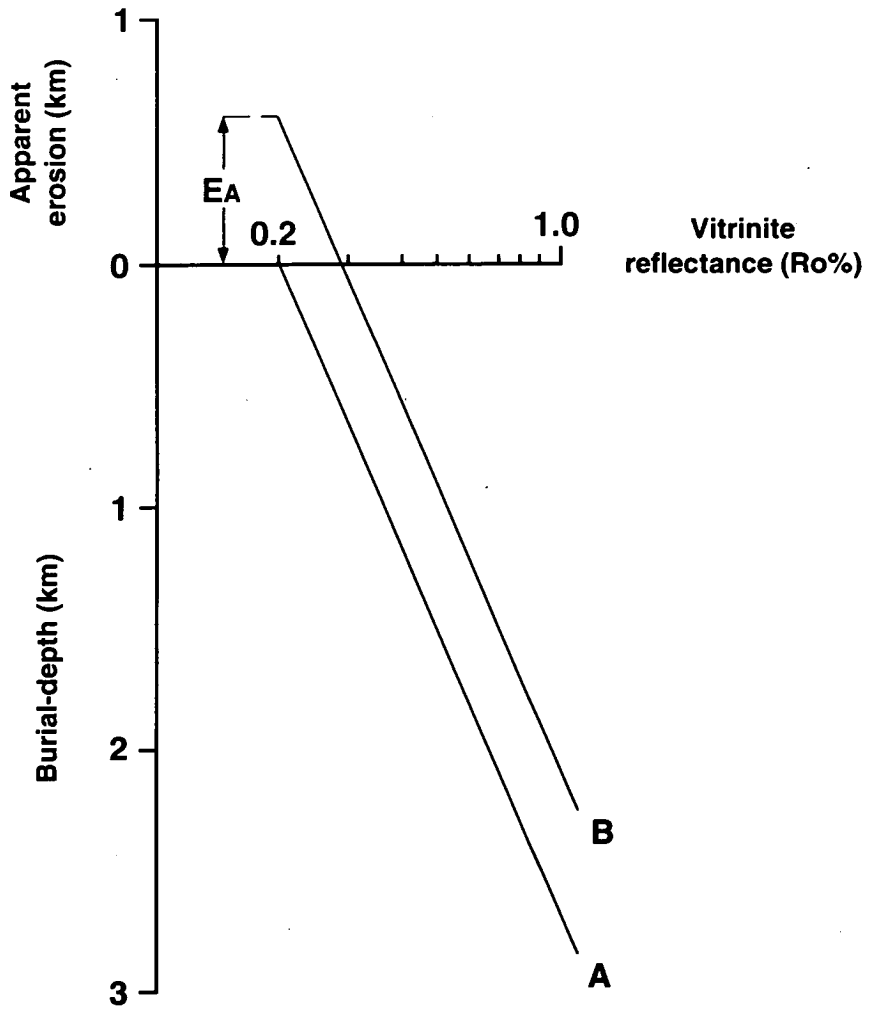

Figure 5.1 Determination of apparent erosion magnitude from vitrinite reflectance data. Burial-depth/ log10 vitrinite reflectance relations regress to linear equations. For wells at their maximum burial burial-depth (A) the trend line crosses the surface deposition value (0.2%) at the present surface. Uplifted and eroded wells (B) have trend lines which intersect the surface depositional value at negative burial-depths. The magnitude of erosion (EA) is equal to the magnitude of the negative burial-depth at the surface depositional value.

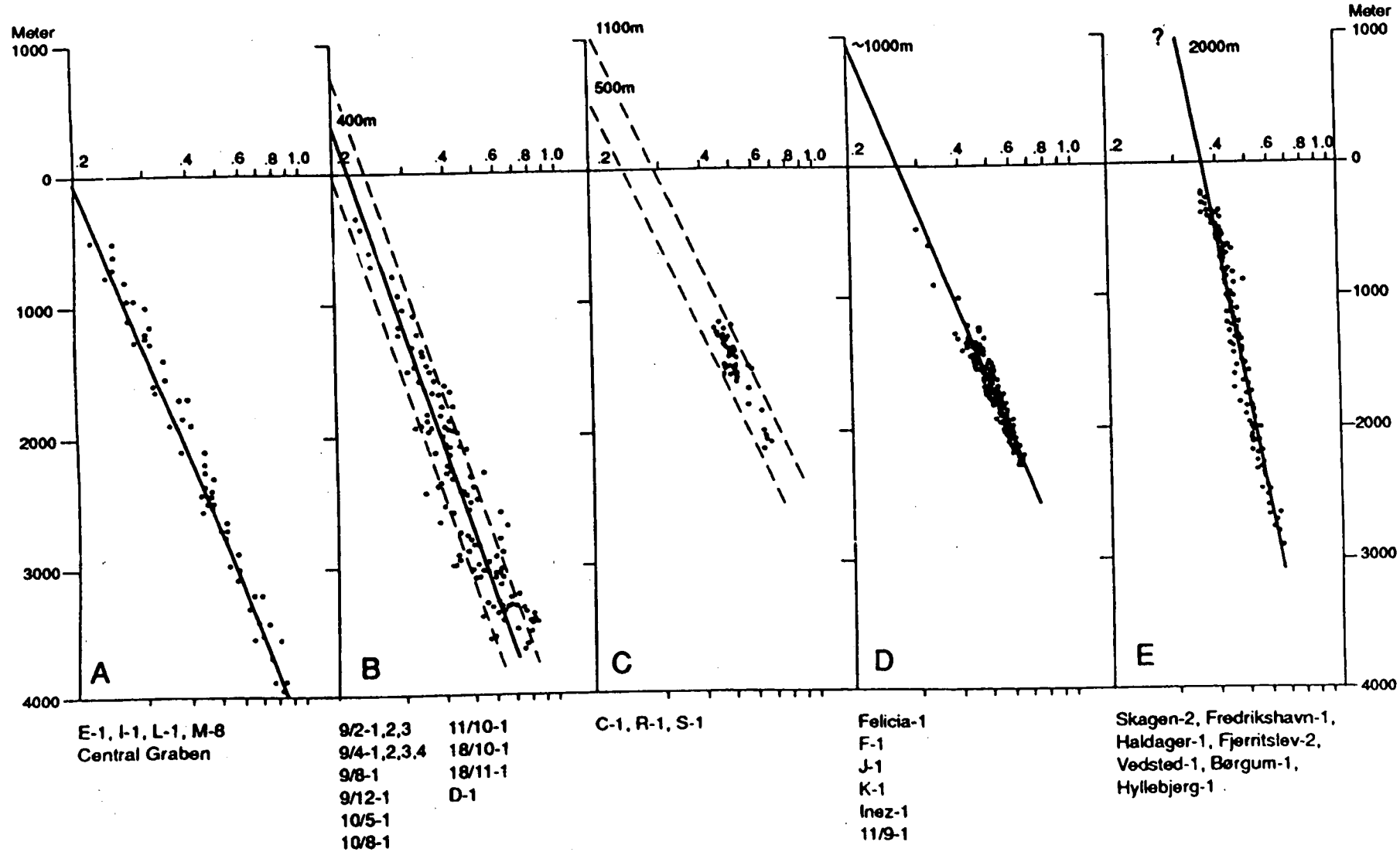

Figure 5.2 Vitrinite reflectance-depth data for southern offshore Norway grouped according to geographical position. The surface intercepts are at vitrinite reflectance values in excess of 0.2% suggesting that uplift and erosion has occurred in the area. The magnitudes of uplift and erosion are also shown. After Jensen and Schmidt (in press).

Table 5.1 Comparison of Neogene uplift and erosion estimates for southern offshore Norway by sonic velocity analysis and the vitrinite reflectance trend method (Jensen and Schmidt, in press). As can be seen the results compare favourably with each other suggesting that the vitrinite reflectance trend method can be readily applied to the estimation of uplift and erosion.

Well	Uplift and erosion estimates derived from sonic velocity analysis (m)	Uplift and erosion estimates derived from the vitrinite reflectance trend method (m)
9/2-1	250-500	400
9/2-2	200-500	400
9/4-1	0-200	400
9/4-3	100-400	400
9/4-4	100-300	400
9/8-1	100-300	400
9/12-1	200-400	400
10/5-1	500-1000	400
10/8-1	500-1000	400
11/10-1	500-1000	400
D-1	0-200	400
F-1	600-1300	1000
Felicia-1	800-1200	1000
Inez-1	200-700	1000
K-1	700-1300	1000

Norway, the vitrinite reflectance estimates of Jensen and Scmidt (in press) compared favourably with their estimates derived from compaction based studies similar to those described in Chapter 3 **(Table 5.1)**. This section intends to apply the same methodology to the estimation of uplift and erosion from the vitrinite reflectance data of the ten offshore wells contained within Prajoga (1990) and four onshore localities given in Scotchman (1991).

In order for the vitrinite reflectance trend method to be applied to the Inner Moray Firth it must first be established that vitrinite reflectance increases with depth. Consequently, the vitrinite reflectance-depth data of Prajoga (1990) was plotted and found to show this trend **(Figure 5.3)**. Such an observation is in direct contradiction to Pearson and Watkins (1983) who state *"All % Ro values lie between 0.30 and 0.45 with no clear depth-related trend."* (see **Figure 5.5**). However, Pearson and Watkins (1983) contradict themselves by suggesting that the vitrinite reflectance-depth data for well 12/24-1 may be compatible with the steady increase in vitrinite reflectance with depth **(Figure 5.6)**, with the trend of the data from the well intercepting the surface at 0.2%, suggesting that no uplift occurred in the vicinity of the well. Despite the uncertainty in the statements of Pearson and Watkins (1983), the data used in this study **(Figure 5.3)** shows clearly that vitrinite reflectance increases with depth and consequently, that the vitrinite reflectance trend method can be applied to the area.

In practice, current burial-depth was plotted against $\log_{10}$ vitrinite reflectance and a best-fit, least-squares, linear regression of burial-depth against $\log_{10}$ vitrinite reflectance was produced **(Figure 5.7)**. **Table 5.2** shows the vitrinite reflectance-depth data, the resultant equations and correlation co-efficients. For each well, the amount of section removed was calculated using the equation of the general form:

$$E = -(m \log_{10} 0.2 + c)$$

where **E** is the amount of section missing;
m is the gradient of the burial-depth/$\log_{10}$ vitrinite reflectance relation;
c is the intercept of the burial-depth/vitrinite reflectance relation on the burial-depth axis;

The uplift and erosion estimates are shown in **Table 5.2(b)**.

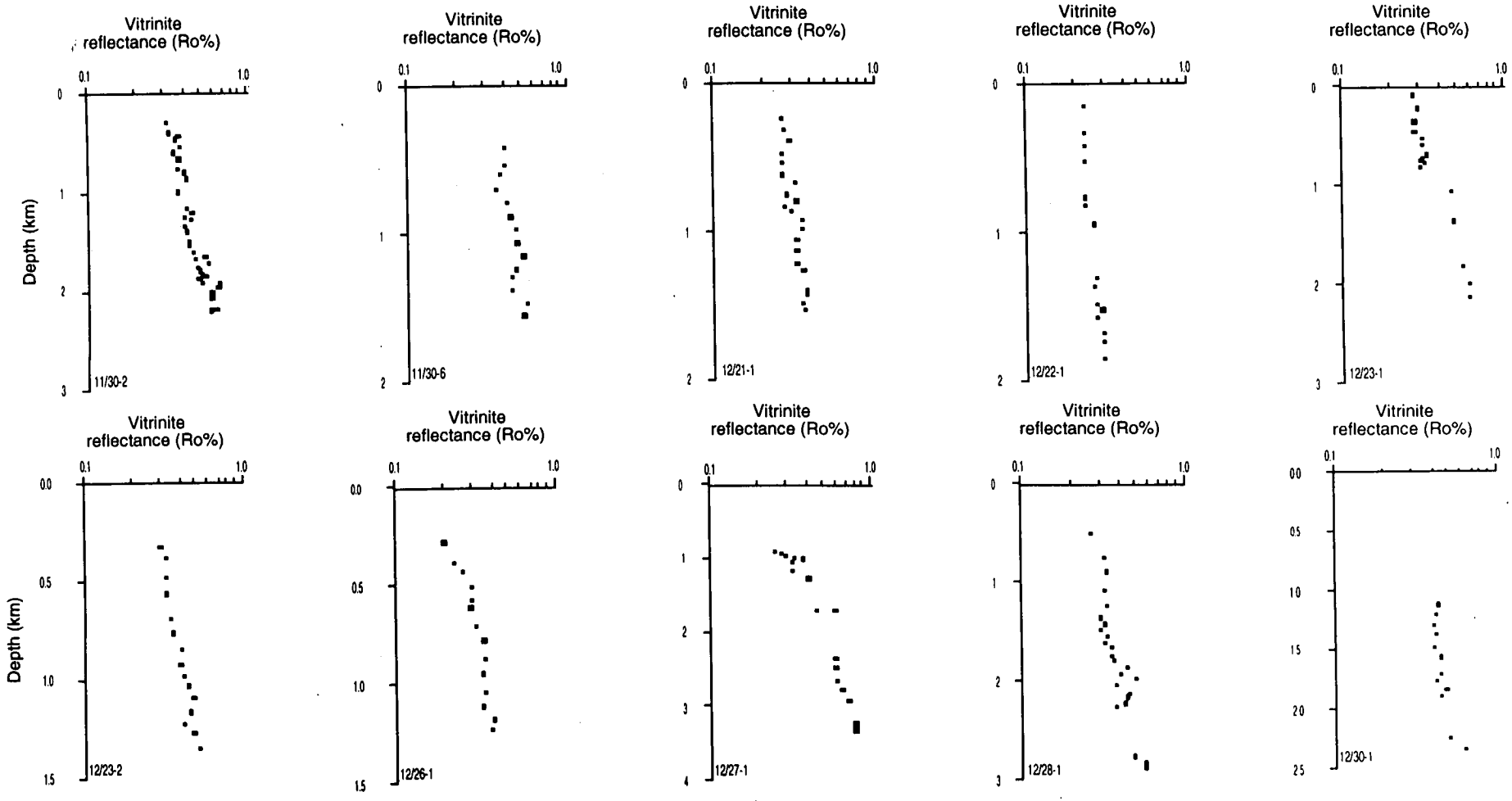

Figure 5.3 Plots of vitrinite reflectance (Ro%) (logarithmic scale) against burial-depth for ten wells in the Inner Moray Firth (well locations shown in Figure 5.4). All plots show a progressive increase in vitrinite reflectance with burial-depth and consequently these wells are amenable to analysis by the vitrinite reflectance trend method as described by Jensen and Schmidt (in press).

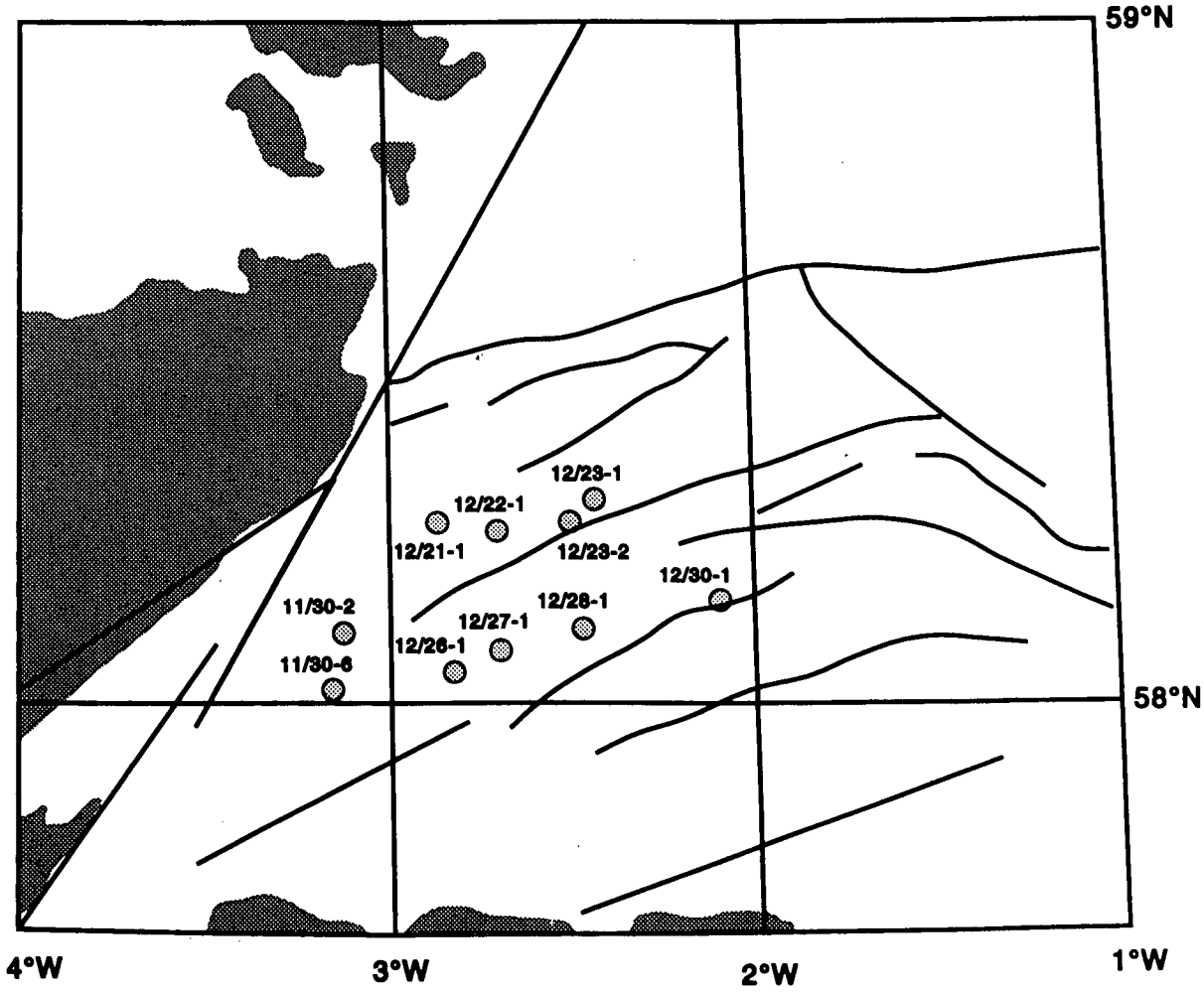

Figure 5.4 Wells location map for the vitrinite reflectance data used by Prajoga (1990) and this study.

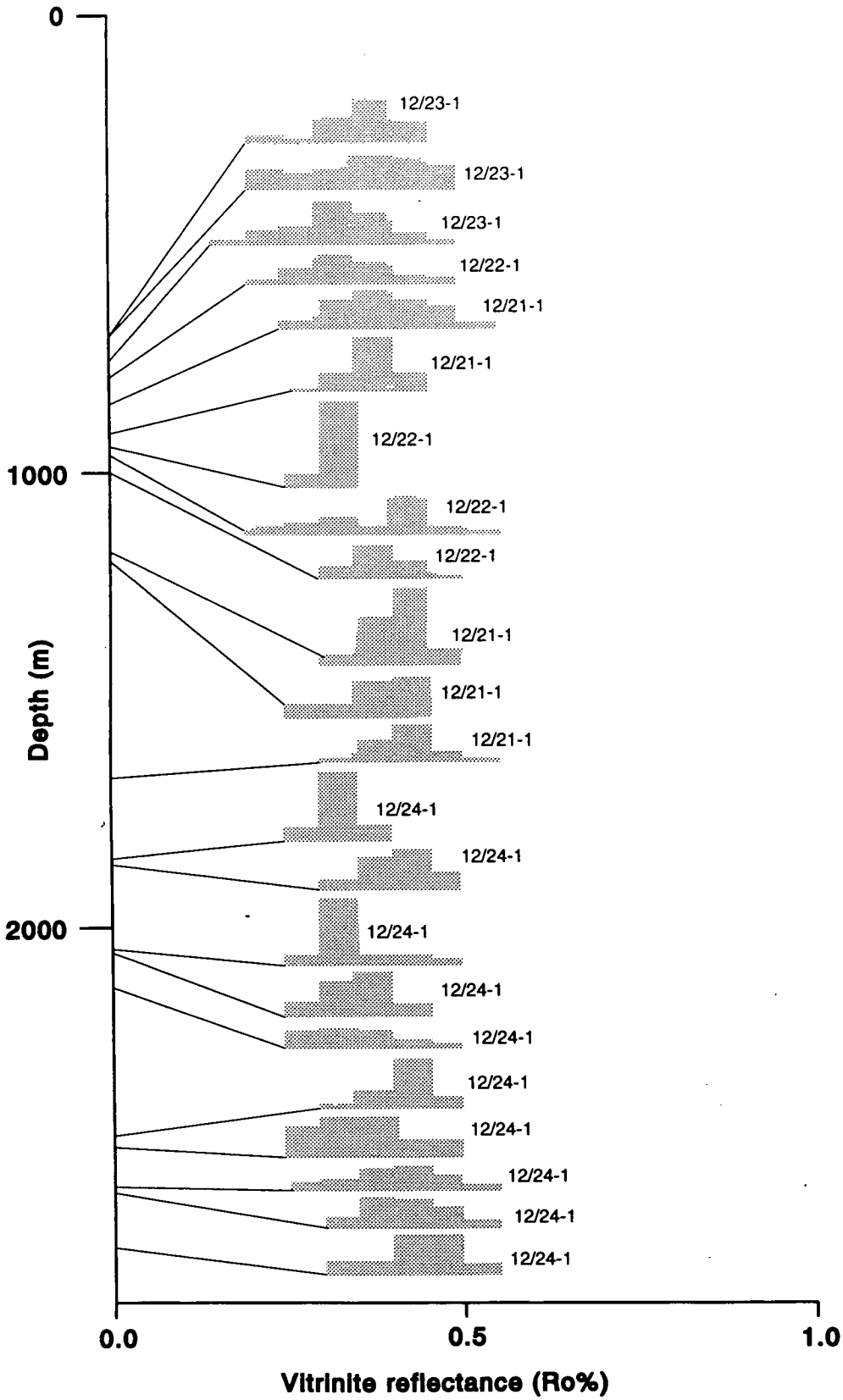

Figure 5.5 Composite vitrinite reflectance-depth profile for the Inner Moray Firth. Although no clear depth related trend can be observed for the whole dataset when individual wells are considered such a trend can be identified. After Pearson and Watkins (1983).

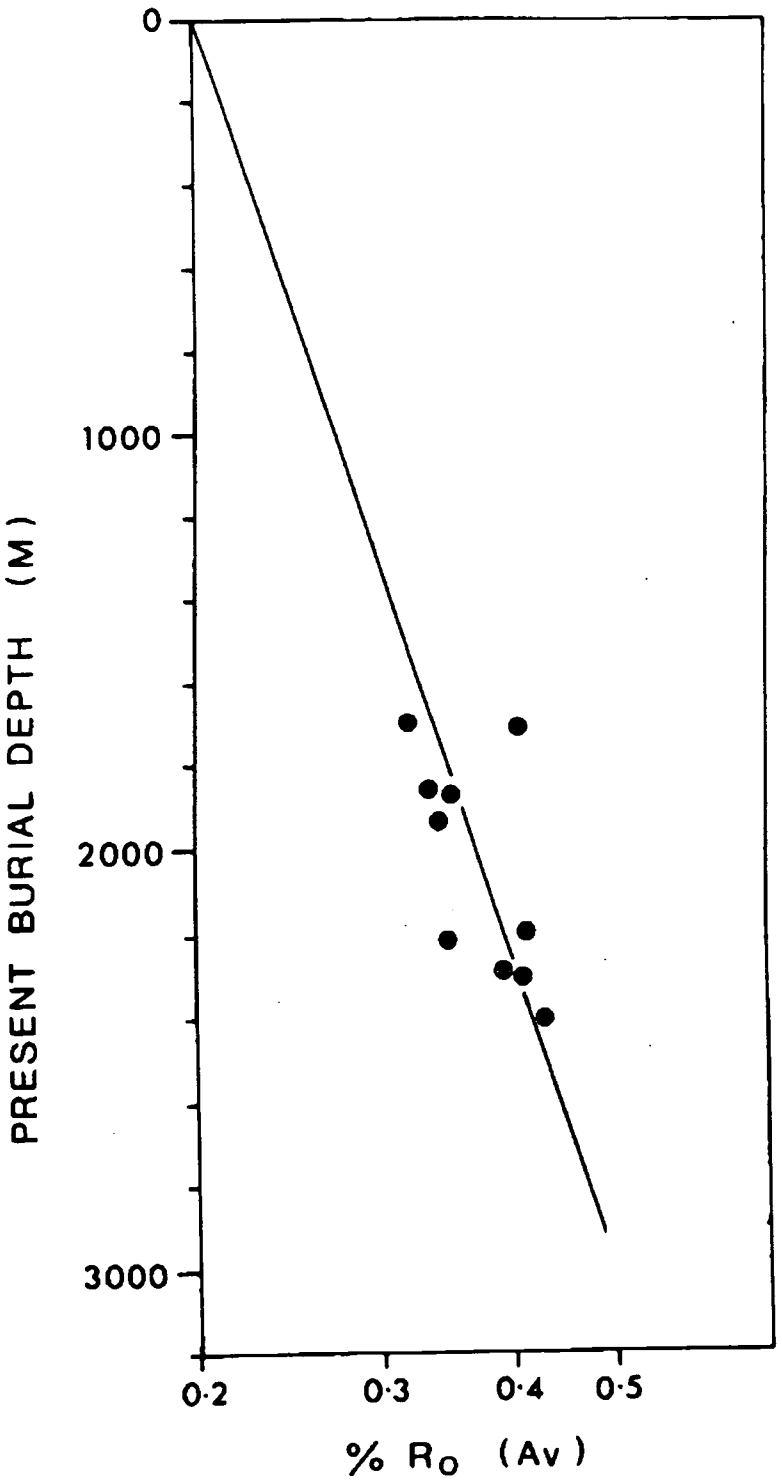

Figure 5.6 Vitrinite reflectance-depth plot for well 12/24-1. The well shows a progressive increase in vitrinite reflectance with increasing burial-depth. After Pearson and Watkins (1983).

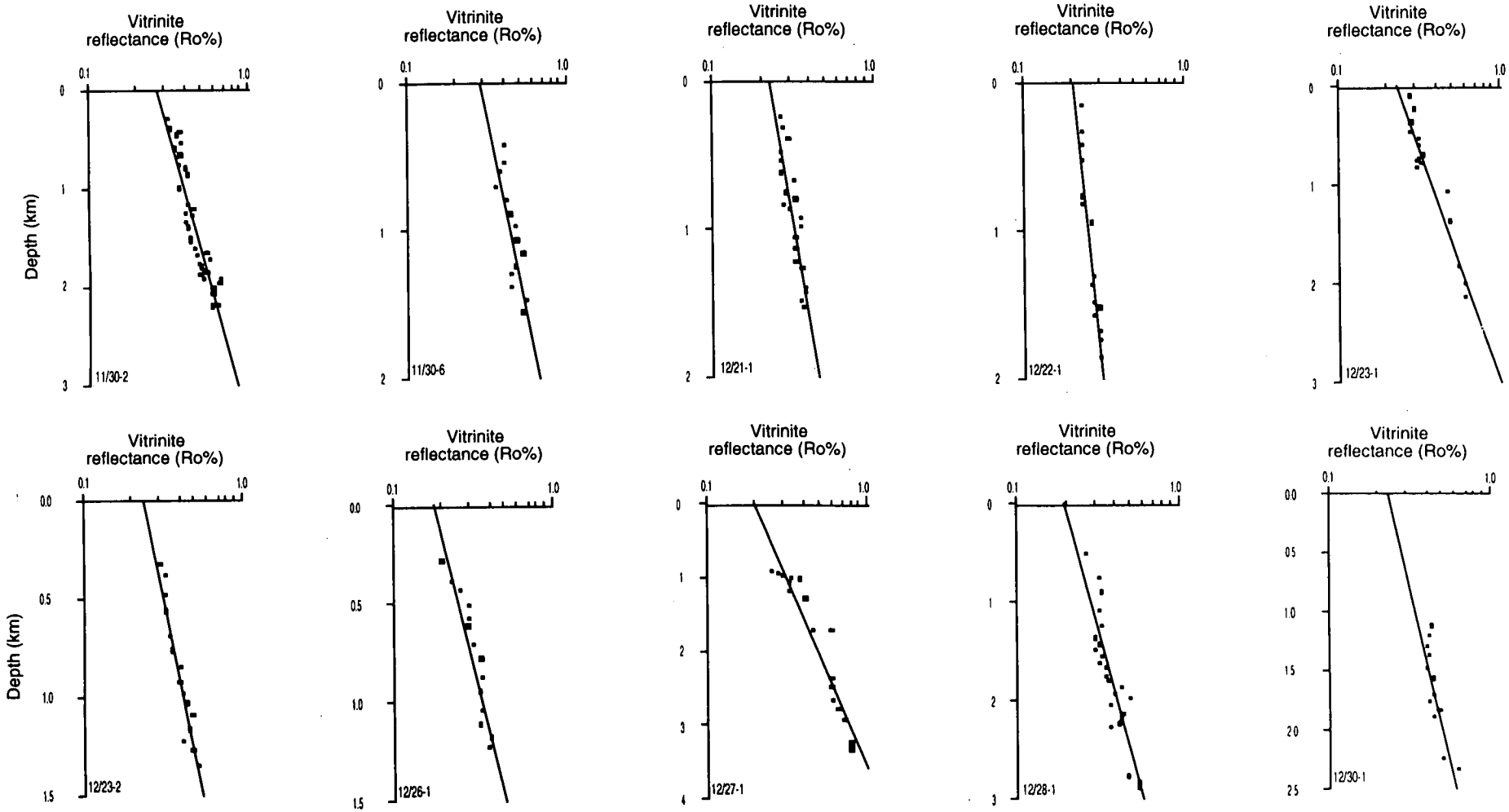

Figure 5.7 Vitrinite reflectance (Ro%) (logarithmic scale) plots against present burial-depth for ten wells in the Inner Moray Firth. Least-squares best-fit regressions are also shown and demonstrate that the surface intercept vitrinite reflectance value exceeds 0.2% for most of the wells, suggesting that they have experienced uplift and erosion. Well locations shown in Figure 5.4 and the details of the regression lines for each well in Table 5.2(b).

Table 5.2(a) Vitrinite reflectance (Ro%) burial-depth data used by Prajoga (1990) and this study for ten wells in the Inner Moray Firth.

11/30-2

Depth (m)	Ro (%)	Depth (m)	Ro (%)	Depth (m)	Ro(%)	Depth (m)	Ro(%)
283	0.31	850	0.41	1509	0.42	1871	0.49
381	0.32	991	0.36	1600	0.45	1901	0.51
411	0.37	1143	0.41	1631	0.53	1924	0.66
442	0.35	1204	0.44	1661	0.46	1943	0.65
553	0.38	1234	0.39	1692	0.56	1992	0.59
585	0.34	1265	0.43	1749	0.48	2046	0.59
655	0.37	1353	0.39	1779	0.50	2166	0.63
747	0.36	1387	0.41	1810	0.51	2176	0.59
777	0.39	1478	0.42	1840	0.53	2203	0.57

11/30-6

Depth (m)	Ro (%)	Depth (m)	Ro (%)	Depth (m)	Ro(%)	Depth (m)	Ro(%)
500	0.40	859	0.41	1225	0.52	1554	0.54
622	0.40	951	0.43	1317	0.46	1628	0.52
677	0.38	1042	0.46	1372	0.44	2396	0.61
768	0.35	1134	0.47	1463	0.44	2469	0.67

12/21-1

Depth (m)	Ro (%)	Depth (m)	Ro (%)	Depth (m)	Ro(%)	Depth (m)	Ro(%)
317	0.26	756	0.31	1003	0.34	1347	0.35
402	0.27	829	0.28	1070	0.34	1481	0.37
463	0.29	873	0.32	1134	0.32	1512	0.37
555	0.26	905	0.27	1210	0.32	1570	0.34
616	0.26	946	0.30	1295	0.38	1612	0.36
695	0.26						

12/22-1

Depth (m)	Ro (%)	Depth (m)	Ro (%)	Depth (m)	Ro(%)	Depth (m)	Ro(%)
152	0.23	157	0.23	762	0.23	914	0.30
244	0.23	488	0.23	823	0.27	944	0.30
290	0.23	549	0.26	838	0.29	1006	0.30
335	0.23	731	0.27	869	0.27		

12/23-1

Depth (m)	Ro (%)	Depth (m)	Ro (%)	Depth (m)	Ro(%)	Depth (m)	Ro(%)
168	0.27	610	0.31	823	0.30	1432	0.47
305	0.29	677	0.31	853	0.32	1890	0.55
445	0.28	777	0.33	884	0.30	2073	0.60
539	0.28	808	0.31	1143	0.46	2210	0.60

Table 5.2(a) continued.

12/23-2

Depth (m)	Ro (%)	Depth (m)	Ro (%)	Depth (m)	Ro(%)	Depth (m)	Ro(%)
402	0.30	767	0.34	1056	0.41	1301	0.41
463	0.32	844	0.35	1112	0.44	1353	0.48
554	0.32	923	0.40	1164	0.47	1423	0.51
646	0.32	996	0.39	1240	0.45		

12/26-1

Depth (m)	Ro (%)	Depth (m)	Ro (%)	Depth (m)	Ro(%)	Depth (m)	Ro(%)
274	0.20	564	0.30	866	0.36	1109	0.34
381	0.23	610	0.29	945	0.34	1178	0.40
427	0.26	701	0.31	1036	0.36	1224	0.39
503	0.30	777	0.35				

12/27-1

Depth (m)	Ro (%)	Depth (m)	Ro (%)	Depth (m)	Ro(%)	Depth (m)	Ro(%)
900	0.25	1052	0.32	1682	0.45	2758	0.65
930	0.27	1158	0.32	2362	0.58	2911	0.71
960	0.29	1265	0.40	2469	0.58	3216	0.77
977	0.33	1679	0.58	2643	0.60	3320	0.78
1006	0.38						

12/28-1

Depth (m)	Ro (%)	Depth (m)	Ro (%)	Depth (m)	Ro(%)	Depth (m)	Ro(%)
495	0.26	1409	0.31	1790	0.36	2156	0.43
739	0.31	1470	0.30	1851	0.43	2217	0.41
876	0.33	1531	0.33	1912	0.39	2247	0.37
1074	0.31	1592	0.31	1973	0.49	2750	0.47
1226	0.33	1653	0.34	2034	0.37	2811	0.54
1348	0.30	1729	0.34	2110	0.44	2872	0.55

12/30-1

Depth (m)	Ro (%)	Depth (m)	Ro (%)	Depth (m)	Ro(%)	Depth (m)	Ro(%)
1116	0.42	1366	0.41	1691	0.44	1881	0.44
1196	0.41	1466	0.40	1751	0.41	2236	0.50
1286	0.40	1551	0.44	1821	0.47	2316	0.62

Table 5.2(b) Table of the regression data for burial-depth against vitrinite reflectance for wells in the Inner Moray Firth. The estimates of erosion derived from the burial-depth vitrinite reflectance data are also shown.

WELL	Gradient of the burial-depth/ $\log_{10}$ vitrinite reflectance relation	Intercept on the burial-depth axis of the burial-depth/$\log_{10}$ vitrinite reflectance relation	Correlation coefficient for burial-depth / $\log_{10}$ vitrinite reflectance regression	Uplift and erosion estimate (m)
11/30-2	5943	-3424	0.918	730
11/30-6	5354	-2890	0.802	850
12/21-1	6413	-4175	0.871	310
12/22-1	5566	-3814	0.933	80
12/23-1	4746	-3003	0.962	310
12/23-2	4238	-2606	0.955	360
12/26-2	3284	-2423	0.912	-130
12/27-1	5073	-3581	0.951	-40
12/28-1	6305	-4478	0.881	-70
12/30-1	5825	-3698	0.824	370

Table 5.3 Table of onshore vitrinite reflectance data and erosion estimates derived from it. Uplift and erosion estimated using the burial-depth/vitrinite reflectance relation for the combined data of wells 11/30-2 and 11/30-6 (m= 5963, c= 3343).

Location	Vitrinite reflectance values (Ro%)	Average vitrinite reflectance (Ro%)	Uplift and erosion estimate (m)
Ballintore/Ethie	0.38	0.38	840
Brora	0.26, 0.35, 0.36, 0.43	0.35	620
Lothbeg Point	0.41	0.41	1030
Portgower	0.45, 0.49	0.47	1390

For the onshore localities, the approach taken has been slightly different. As all the onshore data comes from the surface measurements it is impossible to produce a burial-depth/vitrinite reflectance relation. Consequently, the burial-depth/vitrinite reflectance relation for the combined data from wells 11/30-2 and 11/30-6 **(Table 5.3)** was used to calculate the maximum burial-depth for the average vitrinite reflectance value at each locality. The two wells were chosen as they are the closest to the onshore localities. As the datapoints are currently at the surface , the maximum burial-depth equals amount of section removed and was calculated using the equation:

$$E = (m \log_{10} Ro_{(mean)}) + c$$

where **E** is the amount of section missing;
m is the gradient of the burial-depth/$\log_{10}$ vitrinite reflectance relation;
$\mathbf{Ro_{(mean)}}$ is the mean vitrinite reflectance value for the outcrop locality;
c is the intercept of the burial-depth/vitrinite reflectance relation on the burial-depth axis;

The data, equation details and erosion estimates are shown in **Table 5.3.**

The results contained in **Tables 5.2 and 5.3** suggest that the Inner Moray Firth experienced uplift and erosion. However, compared to the results from sediment compaction (Chapter 3) and apatite fission track analysis (Chapter 4) the results are less internally consistent. For the offshore data a wide range of uplift and erosion estimates were produced, ranging between -130 and 850m. However, the majority of the results have the same order of magnitude as seen in chapters 3 and 4. Wells 11/30-2 and 11/30-6 give results directly comparable with those derived from compaction, with values around 700-900m. Four other wells (12/21-1, 12/23-1, 12/23-2 and 12/30-1) yield lower values around 300m, but still with the same order of magnitude as results from compaction analysis. The remaining four wells (12/22-1, 12/26-1, 12/27-1 and 12/28-1) are substantially different from the compaction evidence with values near zero and even negative and it appears that for these wells at least the method breaks down. For the onshore data the results are consistent with both the compaction and apatite fission track analyses and consequently some confidence could possibly be placed in them. On balance it appears that the vitrinite reflectance trend method, although more erratic in this study than for Jensen and Schmidt (in press), provides some supportive evidence for uplift and erosion in the Inner Moray Firth with a magnitude of hundreds of metres.

5.2.2 Vitrinite reflectance modelling.

Over the last 30 years there has been a concerted effort to produce mathematical models that can predict the extent of organic metamorphism as measured for example by vitrinite reflectance (Wood, 1988). Since the seminal work of Lopatin (1971) a variety of potential models have been developed which all share the same basic elements in that they attempt to reconcile the extent of organic metamorphism with the effects of time and temperature (the effects of which are linear and exponential respectively). Such models can be applied to the estimation of the amount of missing stratigraphy at an unconformity by modelling the preserved stratigraphy with the inclusion of possible amounts of missing section. This enables the production of possible vitrinite reflectance values which can be compared with the actual observed values. This section deals with the estimation of the amount of Tertiary uplift and erosion in the Inner Moray Firth using such techniques for the ten wells shown in **Figure 5.4**.

The majority of the models in current use fall into two distinct classes which either calculate a time temperature integral for the sediments under consideration or apply chemical kinetics. The time temperature integral (TTI) method was developed by Lopatin (1971) and Waples (1980) and assumes that the rate of the maturation reaction doubles for a 10°C increase in temperature. The models calculate the time temperature integral for distinct stratigraphic intervals by dividing its temperature history into 10°C intervals and multiplying the time spent in that temperature range by the rate factor for that interval. For every 10°C increase in temperature the rate factor doubles and is generally taken as unity for the interval 100-110°C. The interval TTI value (i.e. the time temperature integral for a particular stratigraphic interval) is then the sum of the TTI values for the individual 10°C intervals experienced by the stratigraphic interval under consideration **(Figure 5.8)**. The interval TTI values can then be compared with maturity indicators such as vitrinite reflectance as numerous equations have been developed for the conversion of TTI values into vitrinite reflectance (Ro%) or other maturity indicies.

The second family of widely used maturation models fall into the realm of chemical kinetics. These models attempt to describe the process of maturation in terms of the Arrhenius equation:

$$k = A \exp(-E/RT)$$

DEPTH[1] (m)	TEMPERATURE[2] (°C)	TIME[3] (my BP)	TIME[4] (duration in my)	RATE FACTOR[5]	TTI[6] (interval)	TTI[7] (total)
0	10–20	100	9	1/512	0.0176	0.0176
250	20–30	91	10	1/256	0.0391	0.0567
500	30–40	81	4	1/128	0.0313	0.0880
750	40–50	77	14	1/64	0.2188	0.3068
1000	50–60	63	18	1/32	0.5625	0.8693
1250	60–70	45	14	1/16	0.8750	1.7443
1500	70–80	31	31	1/8	3.8750	5.6193
1750	80–90	0	—	1/4		
2000	90–100			1/2		
2250	100–110			1.0		
				2.0		

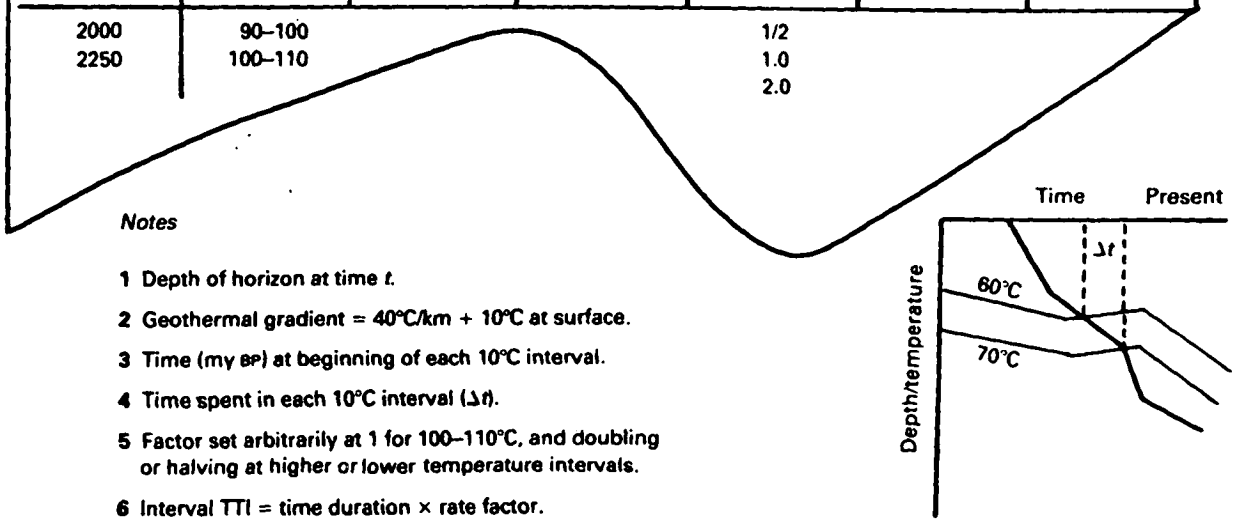

Notes

1 Depth of horizon at time *t*.

2 Geothermal gradient = 40°C/km + 10°C at surface.

3 Time (my BP) at beginning of each 10°C interval.

4 Time spent in each 10°C interval (Δt).

5 Factor set arbitrarily at 1 for 100–110°C, and doubling or halving at higher or lower temperature intervals.

6 Interval TTI = time duration × rate factor.

7 Running total of interval TTI values.

Figure 5.8 Schematic representation of the calculation of TTI values using the approach of Lopatin/Waples. The models calculates the time temperature integral for distinct stratigraphic intervals by dividing its temperature history into 10°C intervals and multiplying the time spent in each temperature zone by an appropriate rate factor. The interval TTI value (i.e. the time temperature integral for a particular stratigraphic interval) is then the sum of the TTI values for the individual 10°C interval experienced by the stratigraphic interval under consideration. After Comford (1990).

where **k** is the reaction rate (million years^{-1});

A is the pre-exponential factor (million years^{-1});

E is the activation energy (kilojoules/mole);

R is the gas constant (kilojoules/mole/K);

T is the temperature (K).

For these models a wide range of activation energies and pre-exponential factors have been reported which generally attempt to fit a single value for each of these valiables to the shape of the pyrolysis S-2 peak for any one sample (Cornford, 1990; **Figure 5.9**). However, the use of the Arrhenius equation in such a way assumes that the reaction kinetics are first-order and that there is a simple precursor/product relationship when in reality the process is more complex. Firstly, the modelling described above assumes that a single chemical reaction is involved when in reality there are several interrelated reactions involved (Sweeney *et al.*, 1987; **Figure 5.10**). Additionally each kerogen type has a variety of chemical bonds which require a range of activation energies to be used (Burnham and Sweeney, 1989; **Figure 5.11**). Consequently, a new generation of models have been developed which apply these kinetic refinements. One such model has been developed by The Petroleum Science and Technology Institute's Project Hedera which applies the model described by Sweeney (1990), used by Bray *et al.* (1992; **Figure 5.12**), Hardman *et. al.* (1993) and this study.

The vitrinite reflectance-depth data for the ten wells used in the previous section was combined with the stratigraphic breakdown used by Prajoga (1990) as the input data for the modelling package developed by Project Hedera. The package then chose default thermal conductivities, compaction/decompaction algorithms and variables based on the input lithologies. The present day heatflow for the wells was calculated by the software using the present corrected bottom hole temperatures and the thermal conductivities of the input lithologies. As no palaeoheatflow data was available the initial set up for each well kept the palaeoheatflow constant at the present value and assumed no unconformity was present in order to test the suitability of of the heatflow assumptions. For wells 11/30-2, 11/30-6, 12/23-2 and 12/30-1 this produced a reasonable match with the data. However, for the remainder of the wells this proved unsuitable with predicted vitrinite reflectance values far above those observed. Consequently, the heatflows were reduced in an attempt to produce a better fit but in all cases the heatflows could not be lowered sufficiently to produce a reasonable fit. For example, well 12/28-1 **(Figure**

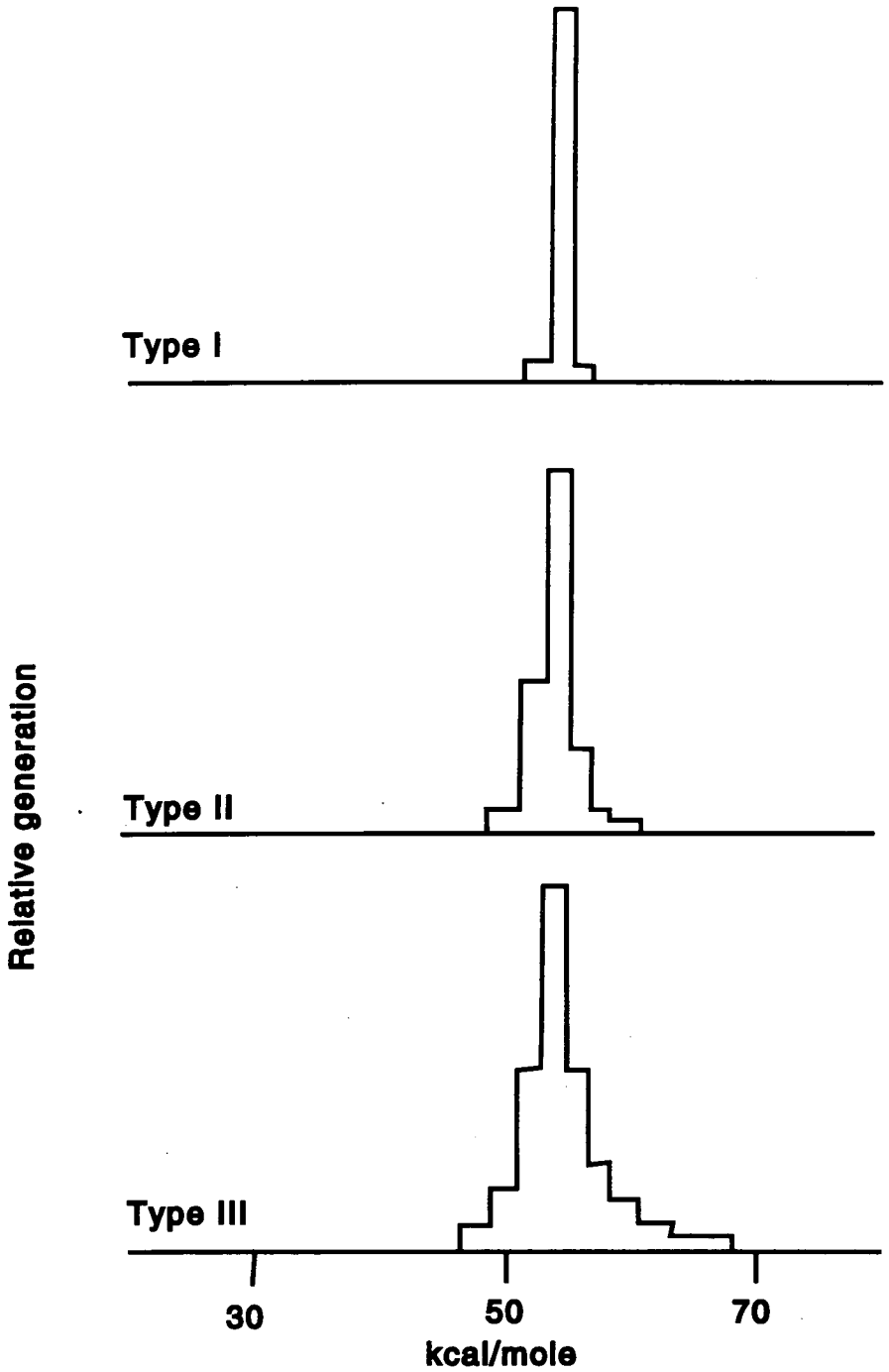

Figure 5.9 Plots of the distributions of activation energies for various kerogen types. Each kerogen type has a differing distribution of activation energies and the modelling of their kinetics by a single activation energy must be considered a gross simplification. Consequently, the latest maturation models incorporate a range of either discrete or continuous activation energies in an attempt to produce more realistic results. After Cornford (1990).

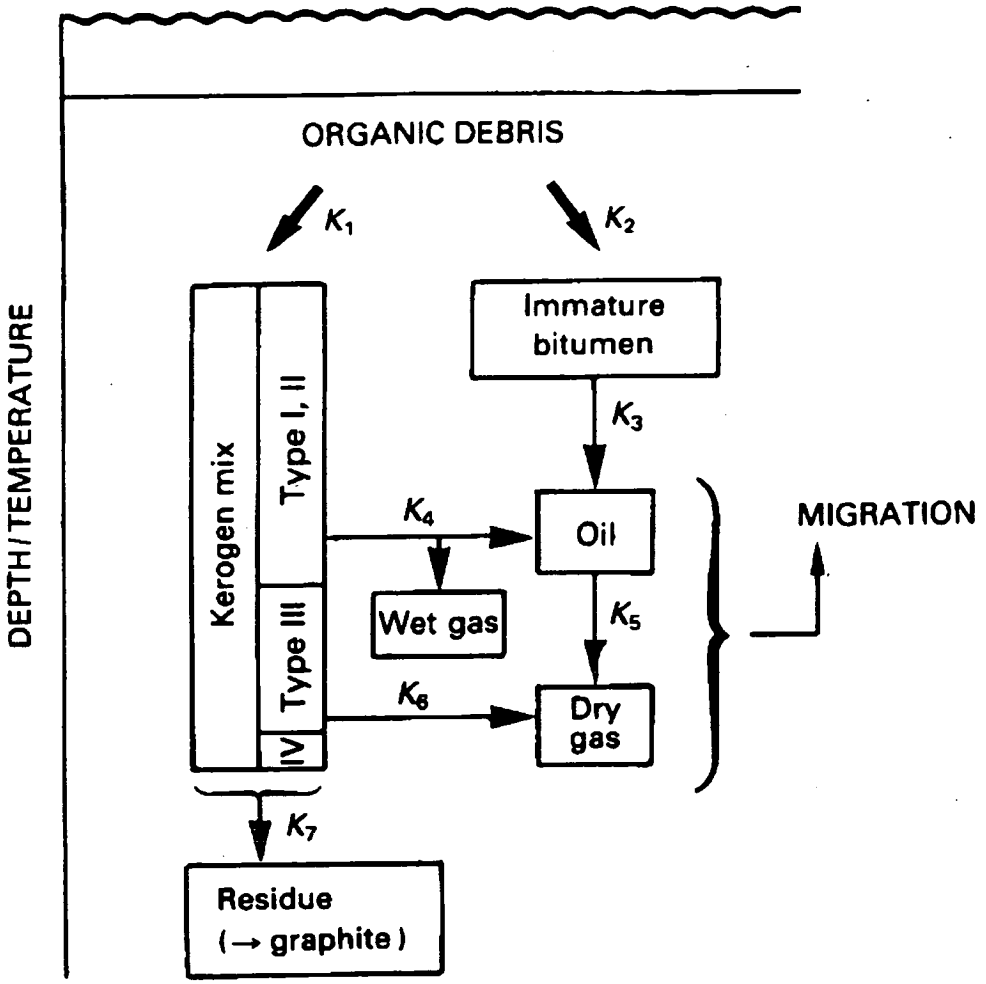

Arrhenius equation: $K = A_e^{-Ea/RT}$

Figure 5.10 Schematic representation of the variety of reactions involved in the organic maturation process. Traditionally the modelling of such processes for comparison with maturity indicators such as vitrinite reflectance relied on the production of one rate constant k and one set of constants for input into the Arrhenius equation. This vastly simplified approach is now being superceded by models which use a range of rate constants and activation energies in order to attempt to mirror geological reality. After Cornford (1990).

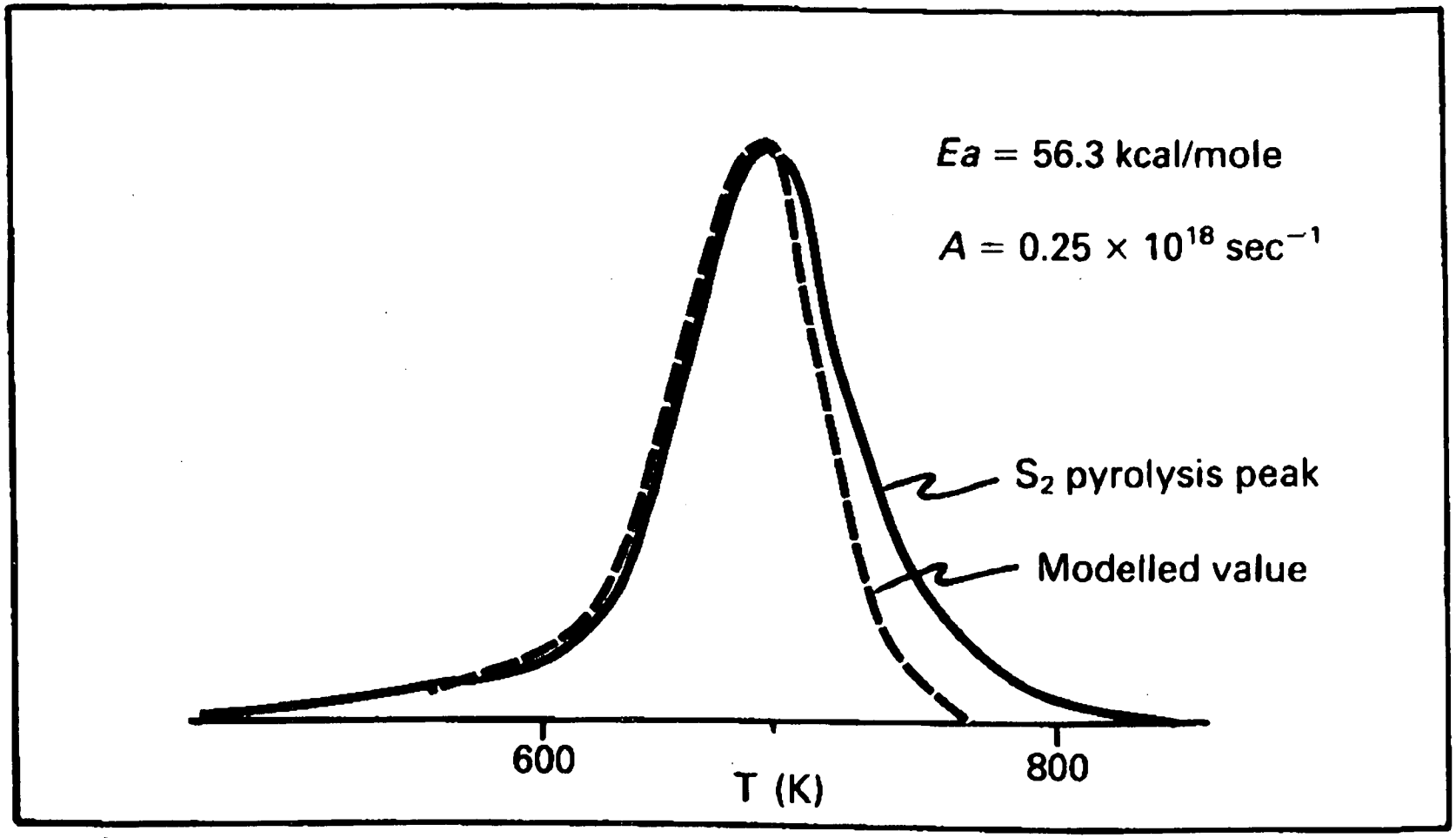

Figure 5.11 Activation energies and Arrhenius factors can be determined by matching a model to the Rock Eval S-2 pyrolysis curve. In this case the fit is reasonable but cannot be improved. Improvements upon this situation can be achieved by using a range of activation energies and Arrhenius factors in any kinetic model. After Cornford (1990).

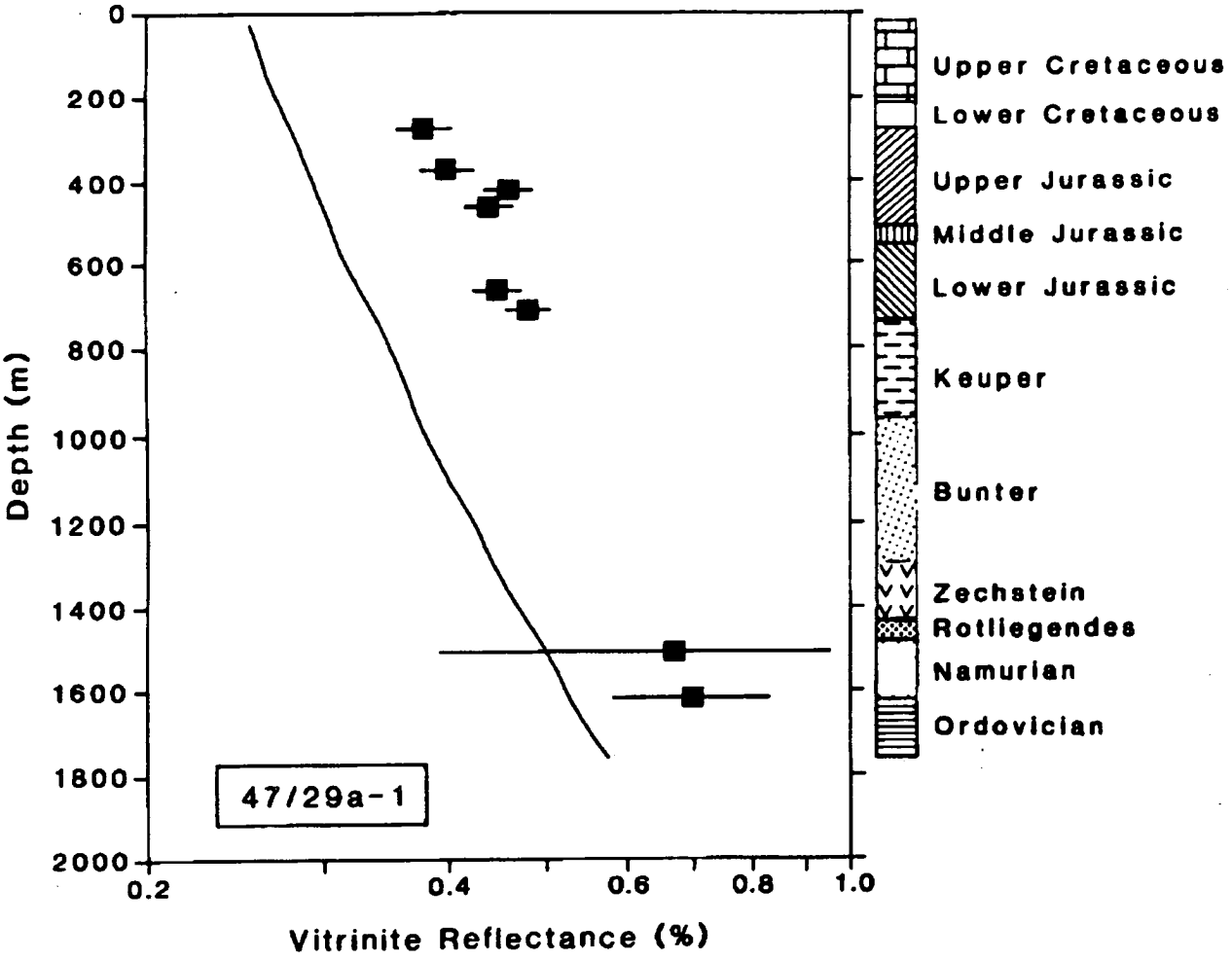

Figure 5.12 Vitrinite reflectance-depth data and modelled profile for Southern North Sea well 47/29a-1. The modelled profile was generated using the kinetic model of Burnham and Sweeney (1989) and Sweeney (1990) and assumed that no sediments were missing. As can be seen the modelled profile substantially under-predicts the extent of vitrinite reflectance and is consistent with the interpretation that the samples have experienced burial to depths greater than currently observed and subsequent uplift and erosion to their burial-depths. After Bray et al. (1992).

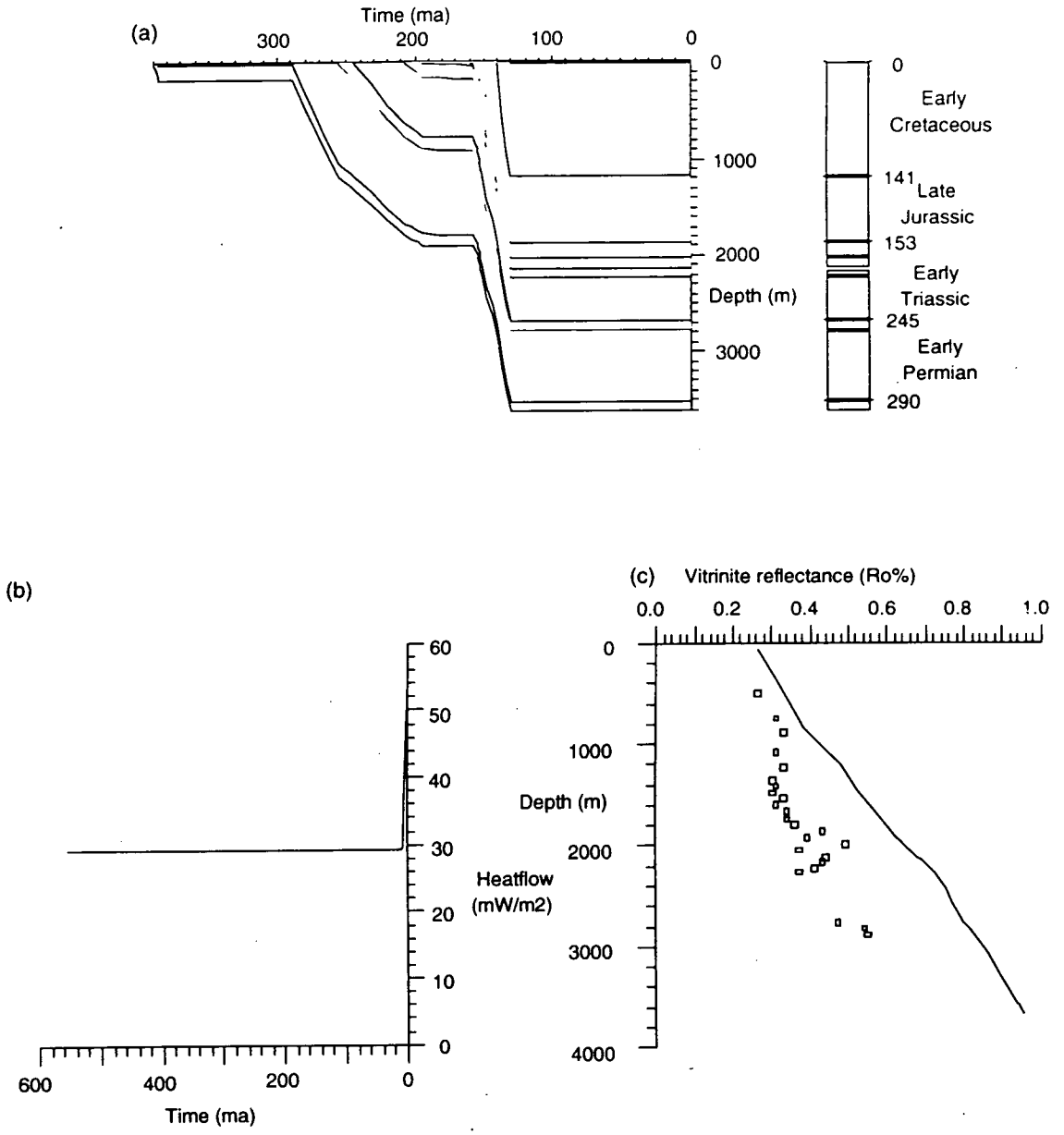

Figure 5.13 Vitrinite reflectance modelling of well 12/28-1. By keeping the preserved stratigraphy and including no extra deposition for the unconformity (a) it can be shown that the palaeoheatflow (b) cannot be lowered sufficiently rapidly or by sufficient magnitude for the predicted vitrinite reflectance values to match those observed (c).This suggests that the input data is insufficient to accurately model the well and consequently uplift and erosion.

5.13) could not have the heatflow lowered rapidly enough or by sufficient magnitude (30 mW/m^2 being a geologically reasonable minimum; J. Illiffe, *pers. comm.*) to get the predicted vitrinite reflectance values to approach that observed. As a result these wells were not included in the study.

For wells 11/30-2, 11/30-6, 12/23-2 and 12/30-1, which appeared suitable for the estimation of uplift and erosion, extra stratigraphy was introduced at an unconformity of mid-late Danian age as such unconformity exists in the basin (Chapter 7) and apatite fission track analysis suggests an increase in erosion rates over the Scottish Highlands at approximately this time. This extra stratigraphy was adjusted in 500m steps in order to gain a sense of the approximate amount of stratigraphy removed. In three of the wells (11/30-2, 11/30-6 and 12/23-2) the unconformity is present at sea-bed and represents approximately a 100ma time break. Consequently, two types of depositional/erosional histories were developed and are shown schematically in **Figure 5.14**. The first type of history assumed that deposition continued from the time of the last recorded sedimentation until 60ma and that the sediments were then removed at a constant rate between 60ma and the present day **(Figure 5.14(a))**. For the second potential history the depositional phase upto 60ma is the same but the sediments are then removed in 10ma and for the remaining 50ma the sea-bed represents an hiatal surface **(Figure 5.14(b))**. For well 12/30-1, where sediments are present above the unconformity the burial/erosional history is better constrained and the unconformity was modelled as equal periods of deposition and erosion **(Figure 5.14(c))**.

Assuming that no unconformity exists, the model predicted vitrinite reflectance values broadly in agreement with those observed for well 11/30-2 **(Figure 5.15(a))**. The predicted values for the upper 1km fall near the centre of the data, possibly fractionally on the lower side **(Figure 5.15 (a)iii)** while below 1km the predicted values appear too large. The misfit below 1km can be explained as the model assumes instantaneous heating and consequently for units which are rapidly deposited (as is the case for the data here, **Figure 5.15(a)iiii)** the modelled increase in temperature occurs too quickly compared to geological reality and hence predicts higher maturities. With 500m of steady deposition until 60ma and then steady erosion to the present day the fit to the upper 1km is improved while little change is seen below 1km **(Figure 5.15(b)iii)** and with 1000m input into the model the predicted maturities for the upper 1km bound the upper end of the vitrinite reflectance data with little change below 1km **(Figure 5.15(c)iii)**. Consequently, it appears that steady deposition of approximately

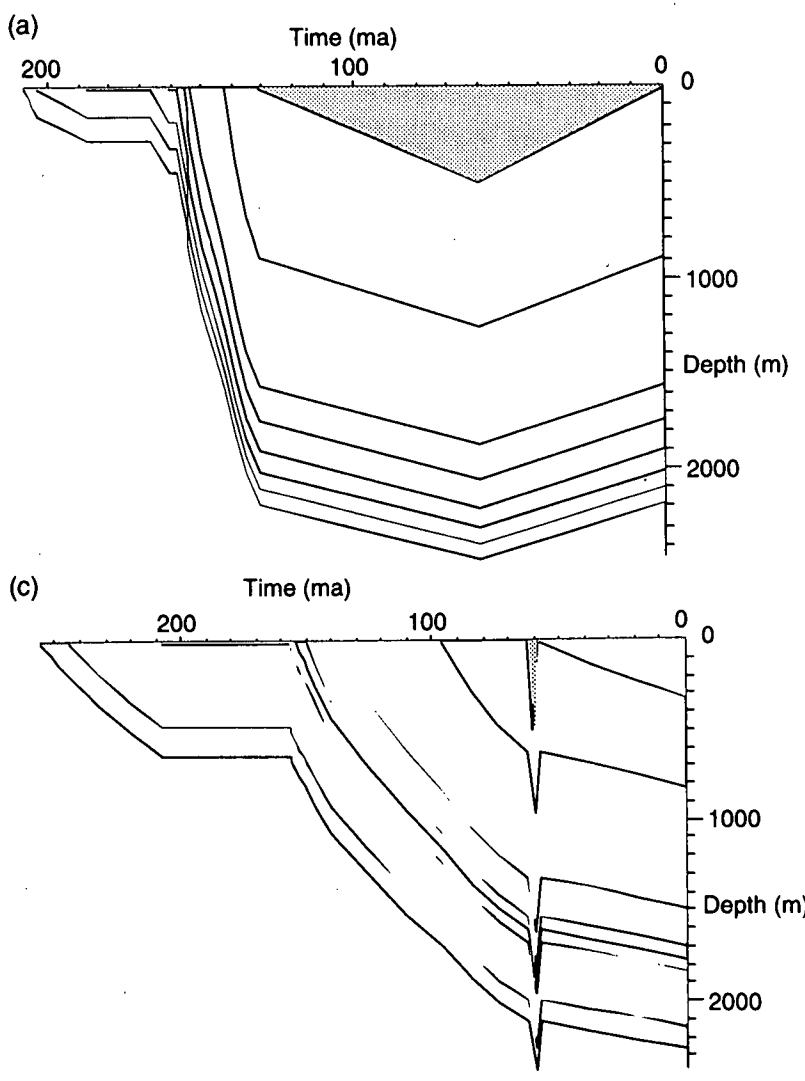

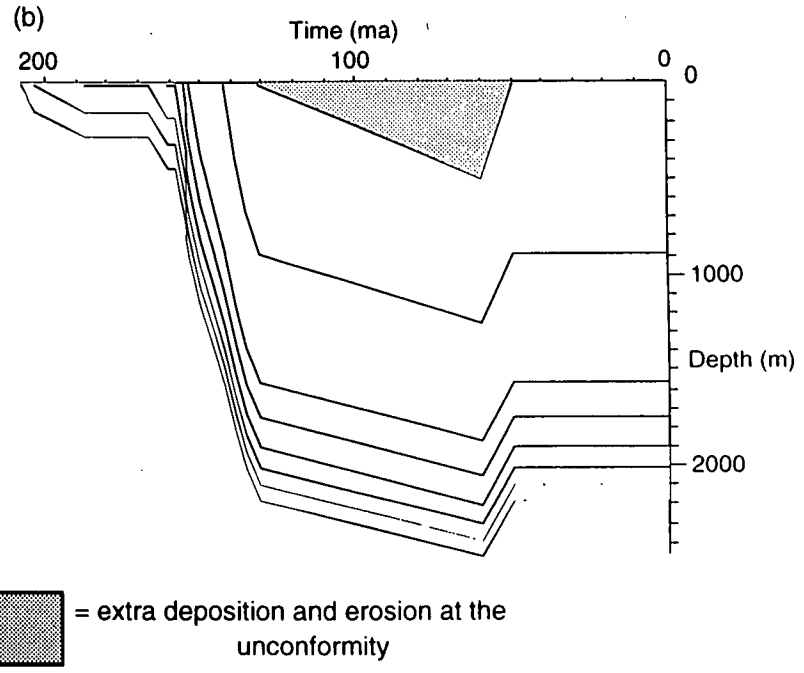

= extra deposition and erosion at the unconformity

Figure 5.14 Potential deposition/erosion types . (a) The extra sediments accumulate at a constant rate from the time of the last recorded sediments to 60ma. The sediments are then removed at a constant rate to the present day. (b) Deposition from the time of the last recoeded sediments until 60ma at a constant rate followed by the removal of the extra section in 10ma. From 50ma to the present day the sea-bed represents an hiatus. (c) In this case where sediments are preserved both above and below the unconformity the extra stratigraphy is deposited during half the timespan of the unconformity and then totally removed during the other half.

Figures 5.15, 5.16 and 5.17 Estimation of uplift and erosion using vitrinite reflectance modelling for wells 11/30-2, 11/30-6 and 12/23-2 respectively. (a) The effect of assuming no unconformity on the prediction of the extent of vitrinite reflectance. (b) Modelling assumes that deposition continued from the time of the last recorded sedimentation until 60ma and that 500m of extra stratigraphy accumulated. This was then followed by uplift and erosion of 500m of section at a constant rate from 60ma to the present day. (b) Modelling assumes that deposition continued from the time of the last recorded sedimentation until 60ma and that 1000m of extra stratigraphy accumulated. This was then followed by uplift and erosion of 1000m of section at a constant rate from 60ma to the present day. (c) In this case an extra 500m of stratigraphy accumulated from the time of last preserved sedimentation until 60ma and that this extra stratigraphy was then removed by 50ma, the sea-bed representing an hiatus from 50ma onwards. (d) An extra 1000m of stratigraphy accumulated from the time of last preserved sedimentation until 60ma and that this extra stratigraphy was then removed by 50ma, the sea-bed representing an hiatus from 50ma onwards. (i) The modelled burial/erosion history with the extra sediments lost at the unconformity highlighted. (ii) Plot of palaeoheatflow against time which was used to produce the predicted vitrinite reflectance values. (iii) A plot of vitrinite reflectance versus depth with the datapoints for that well and the computer generated vitrinite reflectance/depth profile. (iiii) A plot of vitrinite reflectance versus sample age with the datapoints for that well and the computer generated vitrinite reflectance/depositional age profile.

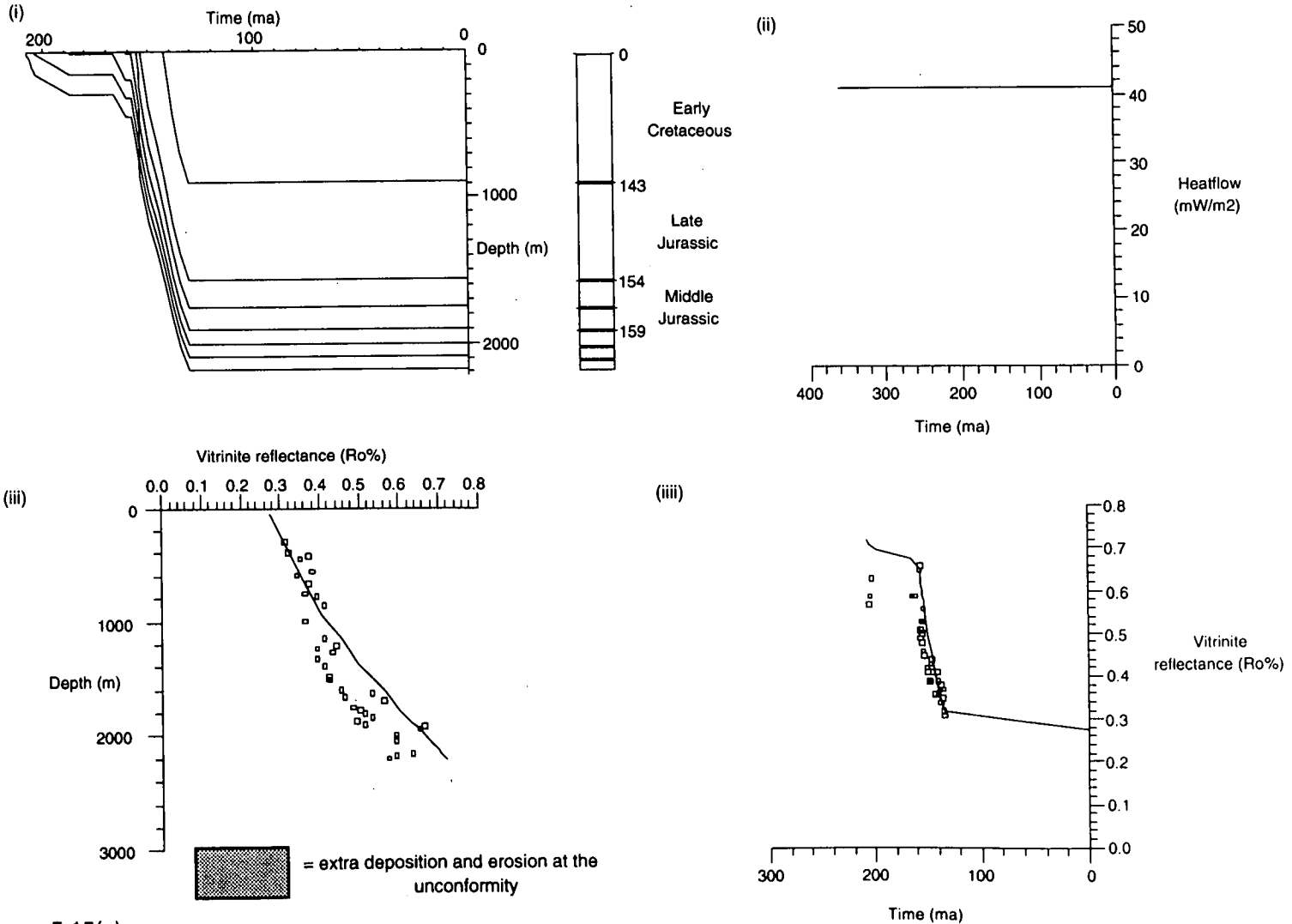
(i)
Time (ma)
200
100
0
0
1000
2000
Depth (m)
0
143
154
159
Early Cretaceous
Late Jurassic
Middle Jurassic
(ii)
50
40
30
20
10
0
400
300
200
100
0
Heatflow (mW/m2)
Time (ma)
(iii)
Vitrinite reflectance (Ro%)
0.0 0.1 0.2 0.3 0.4 0.5 0.6 0.7 0.8
0
1000
2000
3000
Depth (m)
= extra deposition and erosion at the unconformity
(iiii)
0.8
0.7
0.6
0.5
0.4
0.3
0.2
0.1
0.0
300
200
100
0
Time (ma)
Vitrinite reflectance (Ro%)

Figure 5.15(a)

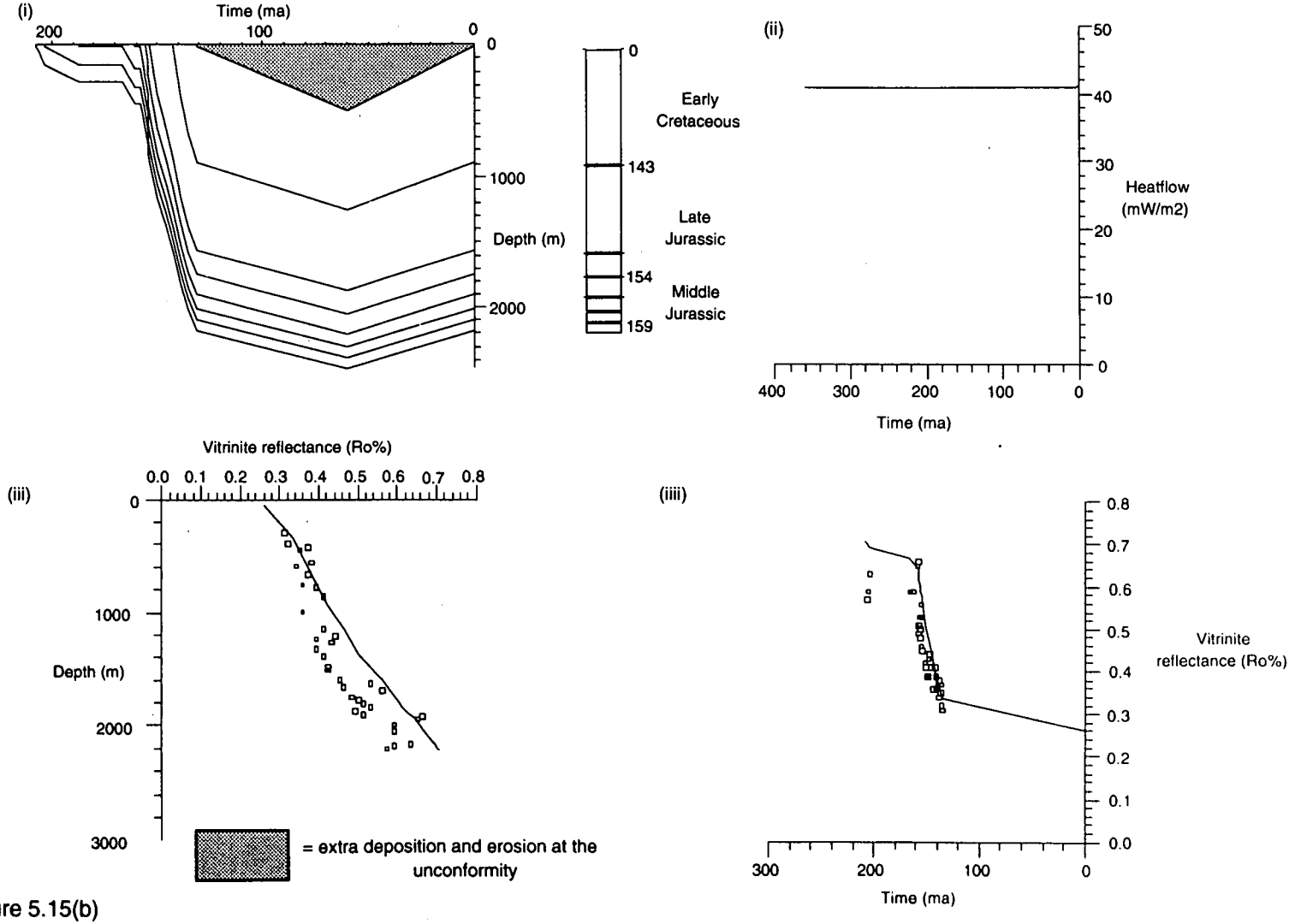
(i)
Time (ma)
200
100
0
0
1000
2000
Depth (m)
0
143
154
159
Early Cretaceous
Late Jurassic
Middle Jurassic
(ii)
50
40
30
20
10
0
400
300
200
100
0
Time (ma)
Heatflow (mW/m2)
(iii)
Vitrinite reflectance (Ro%)
0.0 0.1 0.2 0.3 0.4 0.5 0.6 0.7 0.8
0
1000
2000
3000
Depth (m)
= extra deposition and erosion at the unconformity
(iiii)
0.8
0.7
0.6
0.5
0.4
0.3
0.2
0.1
0.0
300
200
100
0
Time (ma)
Vitrinite reflectance (Ro%)

Figure 5.15(b)

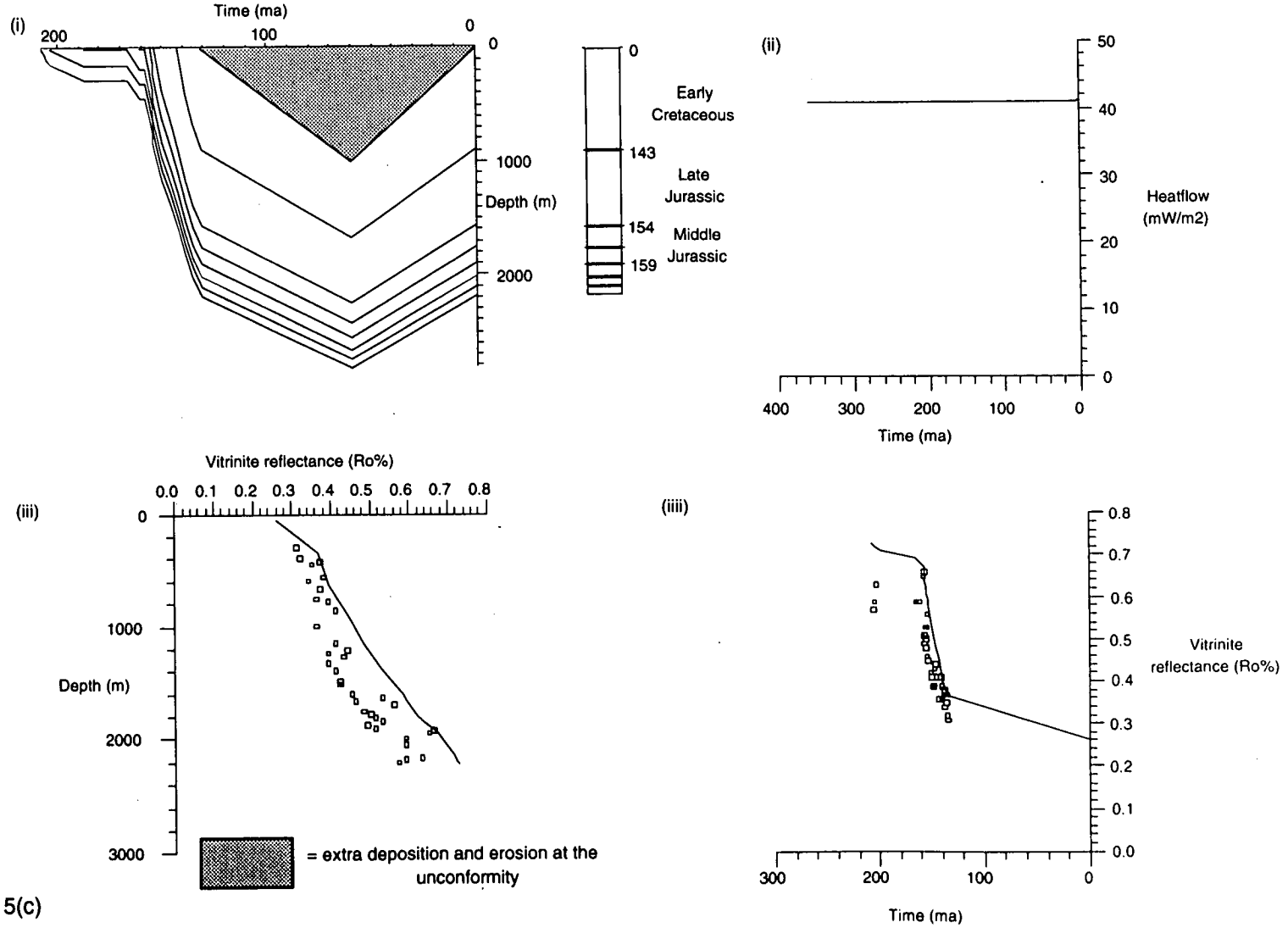
(i)
Time (ma)
200
100
0
0
1000
2000
Depth (m)
0
143
154
159
Early Cretaceous
Late Jurassic
Middle Jurassic
(ii)
50
40
30
20
10
0
400
300
200
100
0
Time (ma)
Heatflow (mW/m2)
(iii)
Vitrinite reflectance (Ro%)
0.0 0.1 0.2 0.3 0.4 0.5 0.6 0.7 0.8
0
1000
2000
3000
Depth (m)
= extra deposition and erosion at the unconformity
(iiii)
0.8
0.7
0.6
0.5
0.4
0.3
0.2
0.1
0.0
300
200
100
0
Time (ma)
Vitrinite reflectance (Ro%)

Figure 5.15(c)

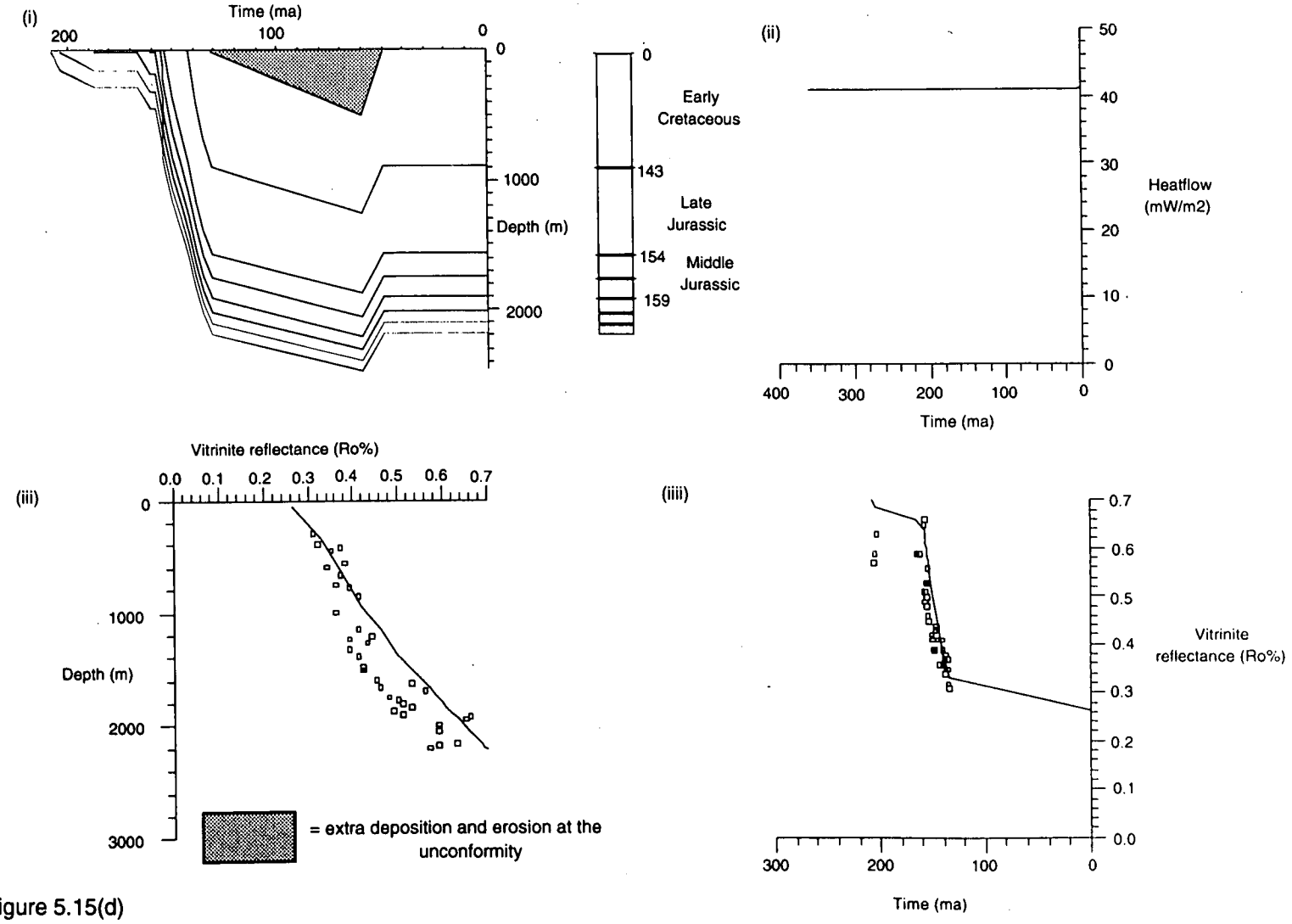
(i)
Time (ma)
200
100
0
0
1000
Depth (m)
2000
0
Early Cretaceous
143
Late Jurassic
154
Middle Jurassic
159
(ii)
50
40
30
20
10
0
Heatflow (mW/m2)
400
300
200
100
0
Time (ma)
(iii)
Vitrinite reflectance (Ro%)
0.0 0.1 0.2 0.3 0.4 0.5 0.6 0.7
0
1000
Depth (m)
2000
3000
= extra deposition and erosion at the unconformity
(iiii)
0.7
0.6
0.5
0.4
0.3
0.2
0.1
0.0
Vitrinite reflectance (Ro%)
300
200
100
0
Time (ma)

Figure 5.15(d)

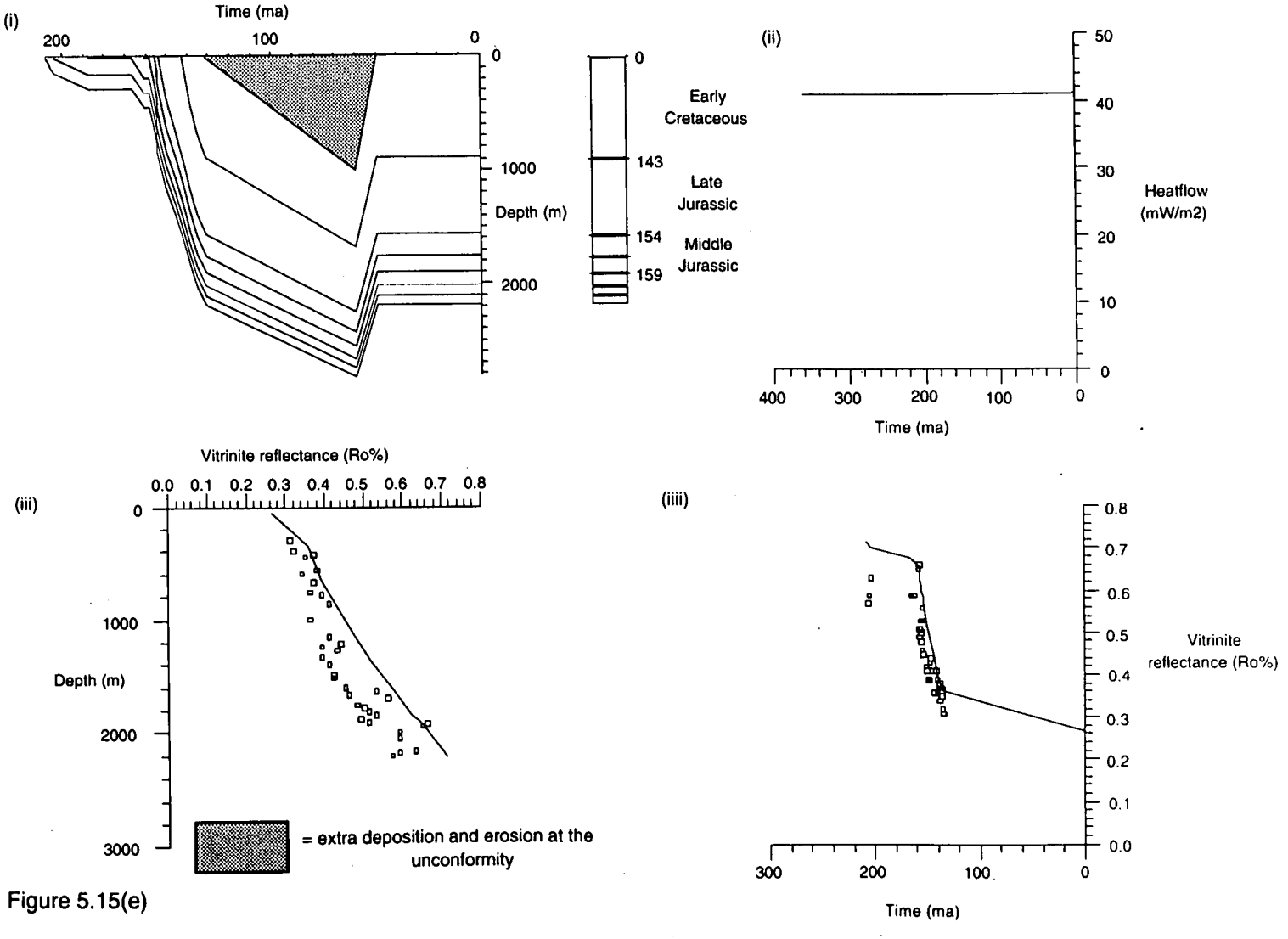
(i)
Time (ma)
200
100
0
0
1000
2000
Depth (m)
0
143
154
159
Early Cretaceous
Late Jurassic
Middle Jurassic
(ii)
50
40
30
20
10
0
400
300
200
100
0
Time (ma)
Heatflow (mW/m2)
(iii)
Vitrinite reflectance (Ro%)
0.0 0.1 0.2 0.3 0.4 0.5 0.6 0.7 0.8
0
1000
2000
3000
Depth (m)
= extra deposition and erosion at the unconformity
(iiii)
0.8
0.7
0.6
0.5
0.4
0.3
0.2
0.1
0.0
300
200
100
0
Time (ma)
Vitrinite reflectance (Ro%)

Figure 5.15(e)

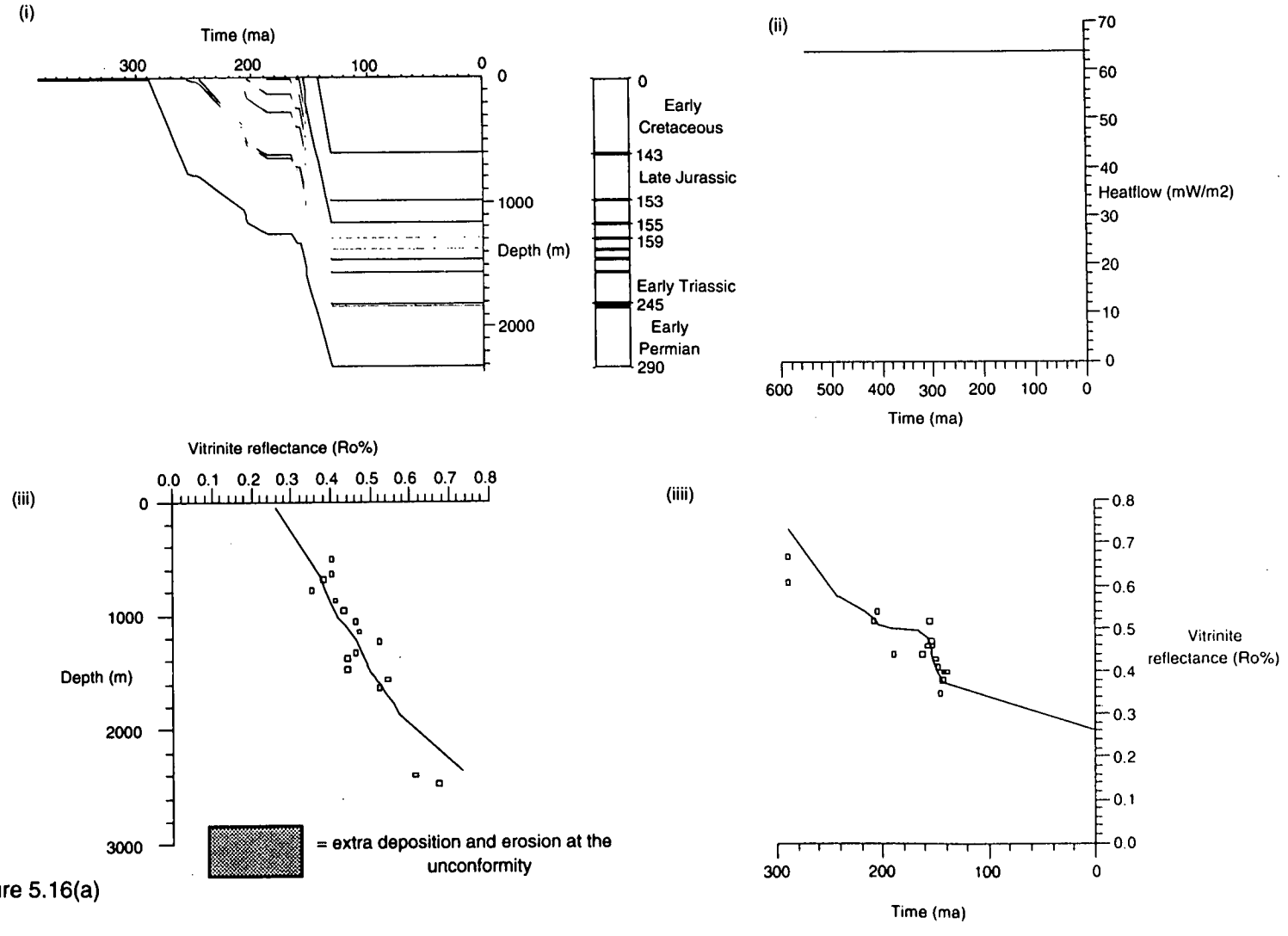
(i)
Time (ma)
300
200
100
0
0
1000
2000
Depth (m)
0
Early Cretaceous
143
Late Jurassic
153
155
159
Early Triassic
245
Early Permian
290
(ii)
70
60
50
40
30
20
10
0
Heatflow (mW/m2)
600
500
400
300
200
100
0
Time (ma)
(iii)
Vitrinite reflectance (Ro%)
0.0
0.1
0.2
0.3
0.4
0.5
0.6
0.7
0.8
0
1000
2000
3000
Depth (m)
= extra deposition and erosion at the unconformity
(iiii)
0.8
0.7
0.6
0.5
0.4
0.3
0.2
0.1
0.0
Vitrinite reflectance (Ro%)
300
200
100
0
Time (ma)

Figure 5.16(a)

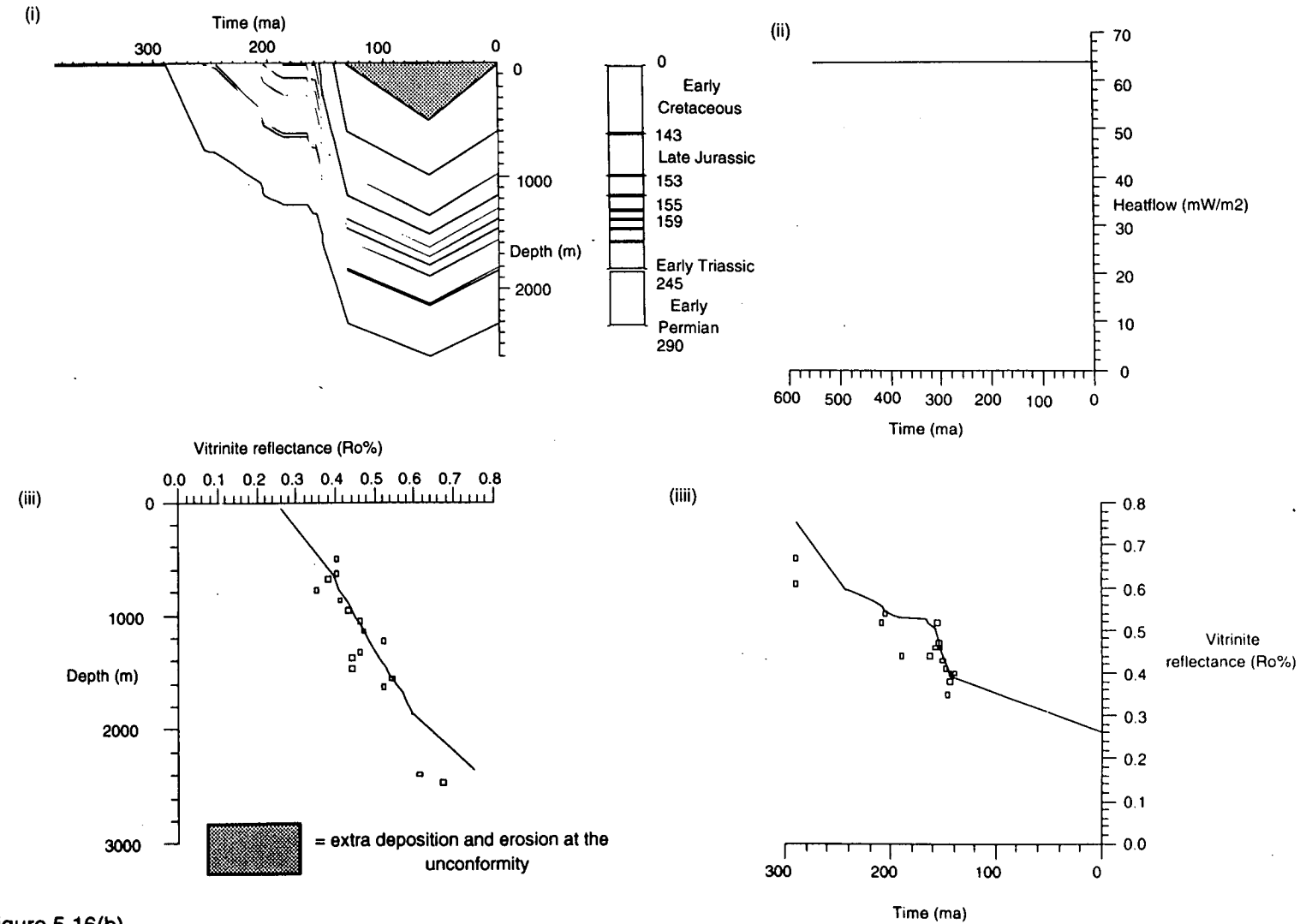
(i)
Time (ma)
300
200
100
0
0
1000
2000
Depth (m)
0
Early
Cretaceous
143
Late Jurassic
153
155
159
Early Triassic
245
Early
Permian
290
(ii)
70
60
50
40
30
20
10
0
Heatflow (mW/m2)
600
500
400
300
200
100
0
Time (ma)
Vitrinite reflectance (Ro%)
0.0
0.1
0.2
0.3
0.4
0.5
0.6
0.7
0.8
(iii)
0
1000
2000
3000
Depth (m)
= extra deposition and erosion at the unconformity
(iiii)
0.8
0.7
0.6
0.5
0.4
0.3
0.2
0.1
0.0
Vitrinite reflectance (Ro%)
300
200
100
0
Time (ma)

Figure 5.16(b)

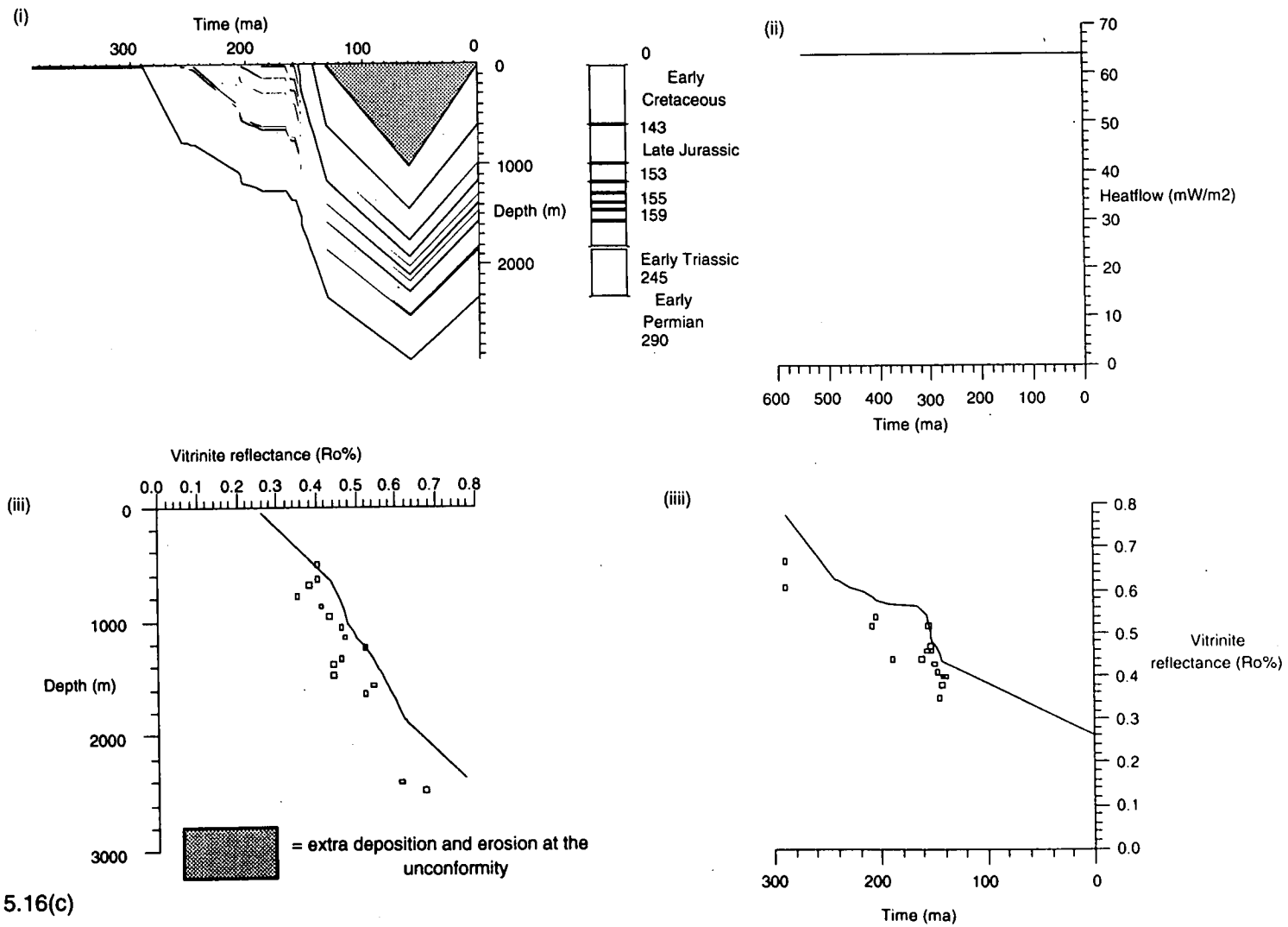
(i)
Time (ma)
300
200
100
0
0
1000
2000
Depth (m)
0
Early
Cretaceous
143
Late Jurassic
153
155
159
Early Triassic
245
Early
Permian
290
(ii)
70
60
50
40
30
20
10
0
Heatflow (mW/m2)
600
500
400
300
200
100
0
Time (ma)
Vitrinite reflectance (Ro%)
0.0
0.1
0.2
0.3
0.4
0.5
0.6
0.7
0.8
(iii)
0
1000
2000
3000
Depth (m)
= extra deposition and erosion at the unconformity
(iiii)
0.8
0.7
0.6
0.5
0.4
0.3
0.2
0.1
0.0
Vitrinite
reflectance (Ro%)
300
200
100
0
Time (ma)

Figure 5.16(c)

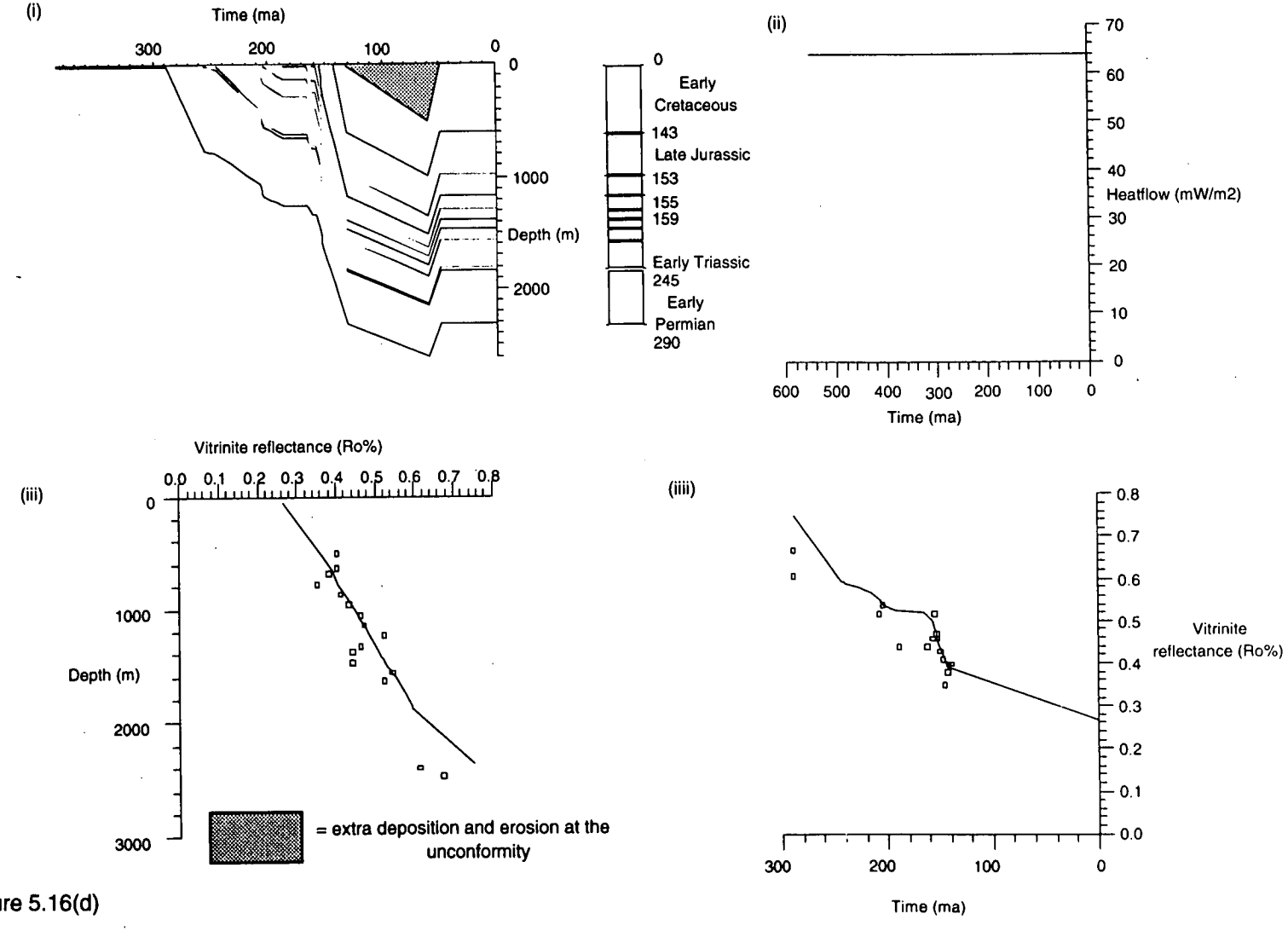
(i)
Time (ma)
300
200
100
0
0
1000
2000
Depth (m)
0
Early
Cretaceous
143
Late Jurassic
153
155
159
Early Triassic
245
Early
Permian
290
(ii)
70
60
50
40
30
20
10
0
Heatflow (mW/m2)
600
500
400
300
200
100
0
Time (ma)
(iii)
Vitrinite reflectance (Ro%)
0.0
0.1
0.2
0.3
0.4
0.5
0.6
0.7
0.8
0
1000
2000
3000
Depth (m)
= extra deposition and erosion at the unconformity
(iiii)
0.8
0.7
0.6
0.5
0.4
0.3
0.2
0.1
0.0
Vitrinite reflectance (Ro%)
300
200
100
0
Time (ma)

Figure 5.16(d)

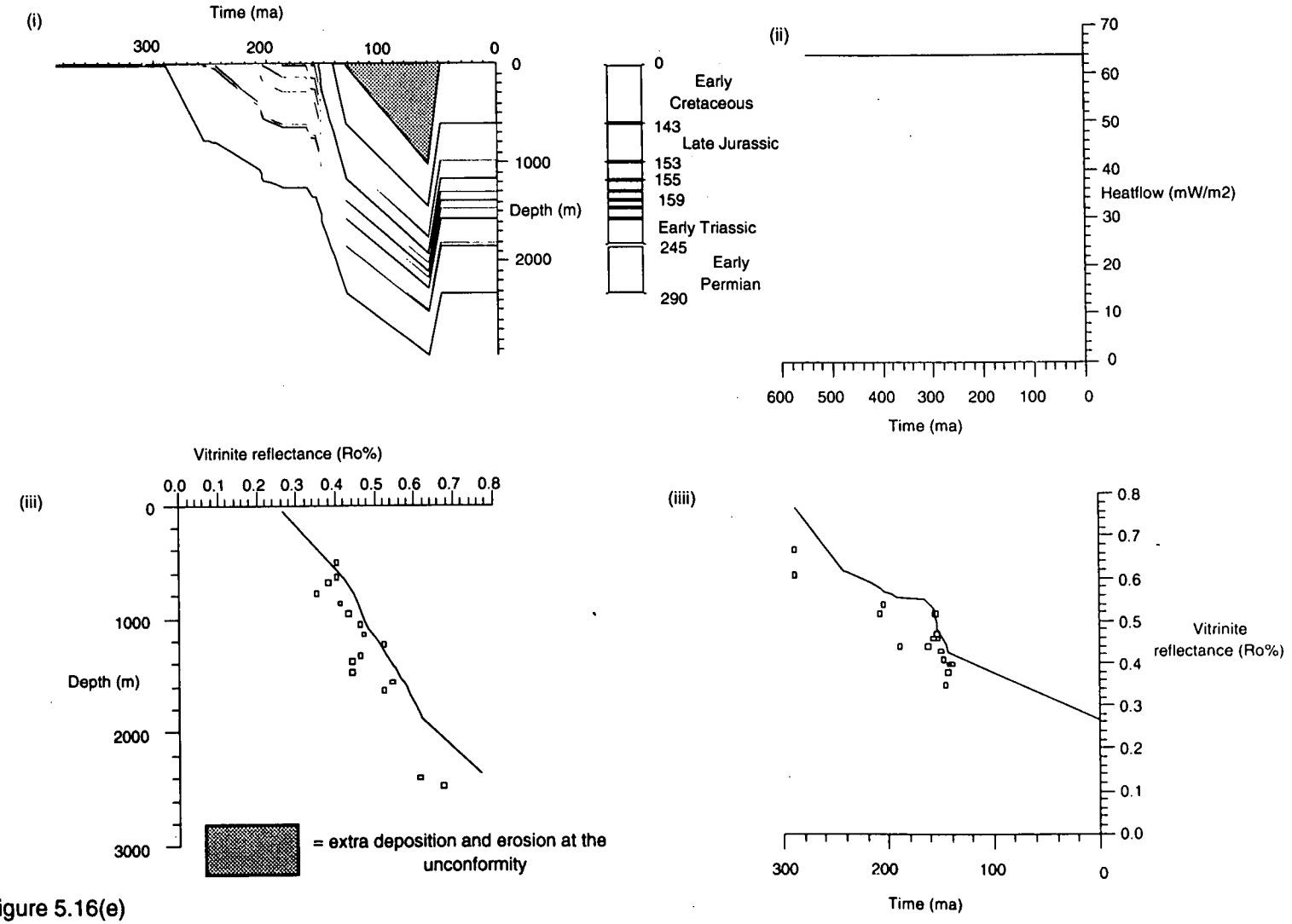
(i)
Time (ma)
300
200
100
0
0
1000
2000
Depth (m)
0
Early Cretaceous
143
Late Jurassic
153
155
159
Early Triassic
245
Early Permian
290
(ii)
70
60
50
40
30
20
10
0
Heatflow (mW/m2)
600
500
400
300
200
100
0
Time (ma)
(iii)
Vitrinite reflectance (Ro%)
0.0
0.1
0.2
0.3
0.4
0.5
0.6
0.7
0.8
0
1000
2000
3000
Depth (m)
= extra deposition and erosion at the unconformity
(iiii)
0.8
0.7
0.6
0.5
0.4
0.3
0.2
0.1
0.0
Vitrinite reflectance (Ro%)
300
200
100
0
Time (ma)

Figure 5.16(e)

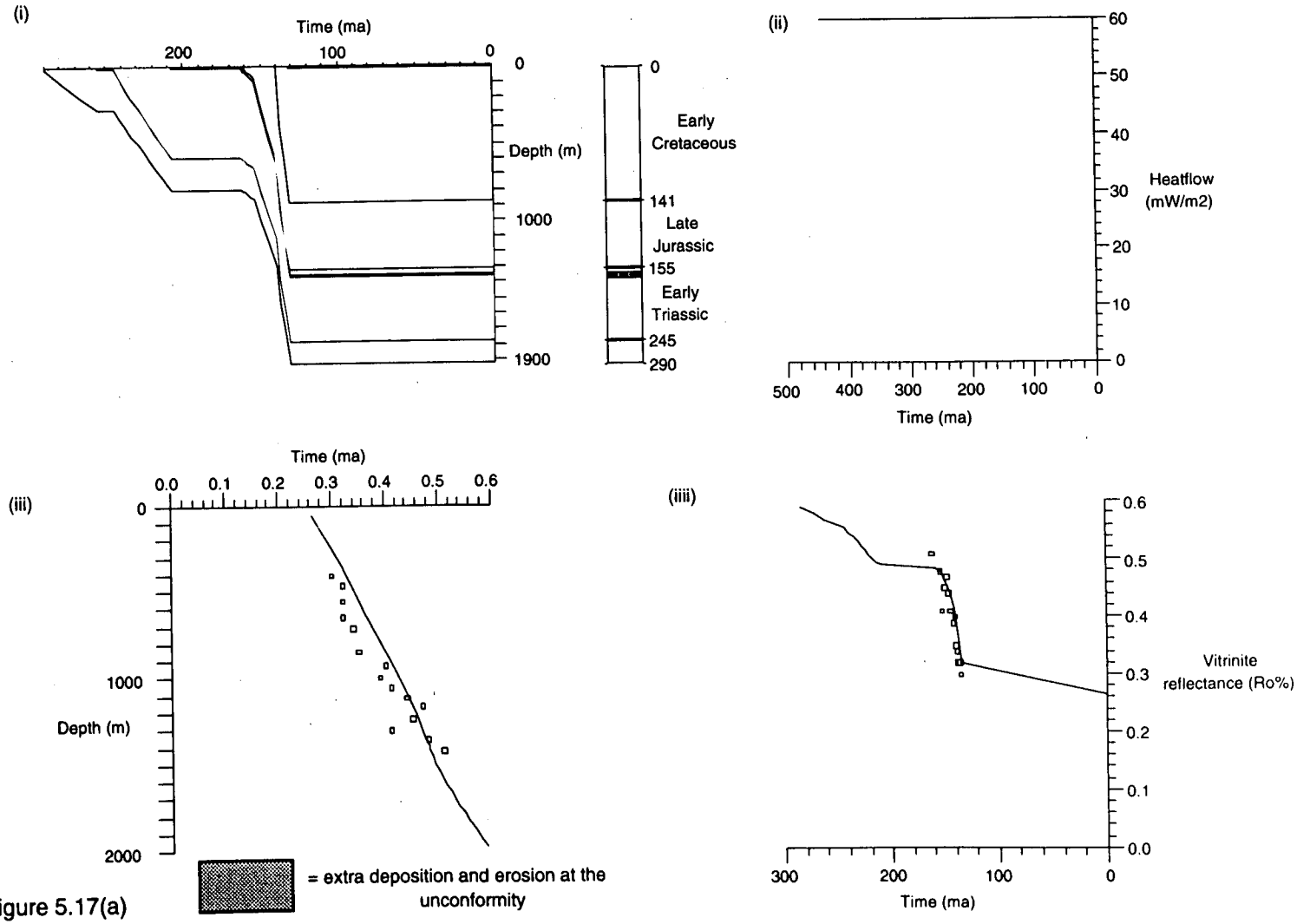
(i)
Time (ma)
200
100
0
0
Depth (m)
1000
1900
0
Early
Cretaceous
141
Late
Jurassic
155
Early
Triassic
245
290
(ii)
60
50
40
30
20
10
0
Heatflow
(mW/m2)
500
400
300
200
100
0
Time (ma)
(iii)
Time (ma)
0.0
0.1
0.2
0.3
0.4
0.5
0.6
0
1000
Depth (m)
2000
= extra deposition and erosion at the
unconformity
(iiii)
0.6
0.5
0.4
0.3
0.2
0.1
0.0
Vitrinite
reflectance (Ro%)
300
200
100
0
Time (ma)

Figure 5.17(a)

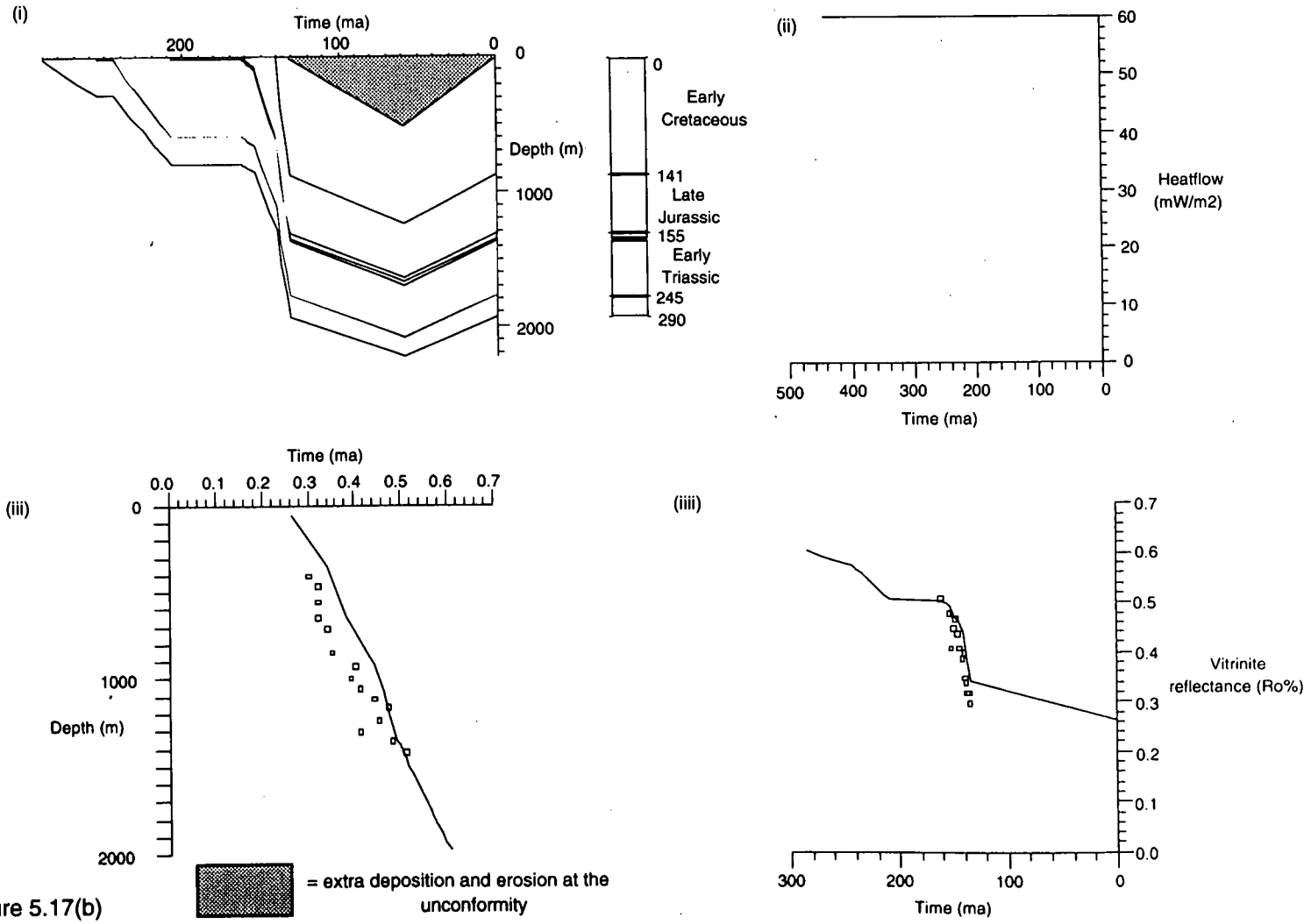
(i)
Time (ma)
200
100
0
0
Depth (m)
1000
2000
0
Early Cretaceous
141
Late Jurassic
155
Early Triassic
245
290
(ii)
60
50
40
30
20
10
0
Heatflow (mW/m2)
500
400
300
200
100
0
Time (ma)
(iii)
Time (ma)
0.0
0.1
0.2
0.3
0.4
0.5
0.6
0.7
0
1000
Depth (m)
2000
(iiii)
0.7
0.6
0.5
0.4
0.3
0.2
0.1
0.0
Vitrinite reflectance (Ro%)
300
200
100
0
Time (ma)
= extra deposition and erosion at the unconformity

Figure 5.17(b)

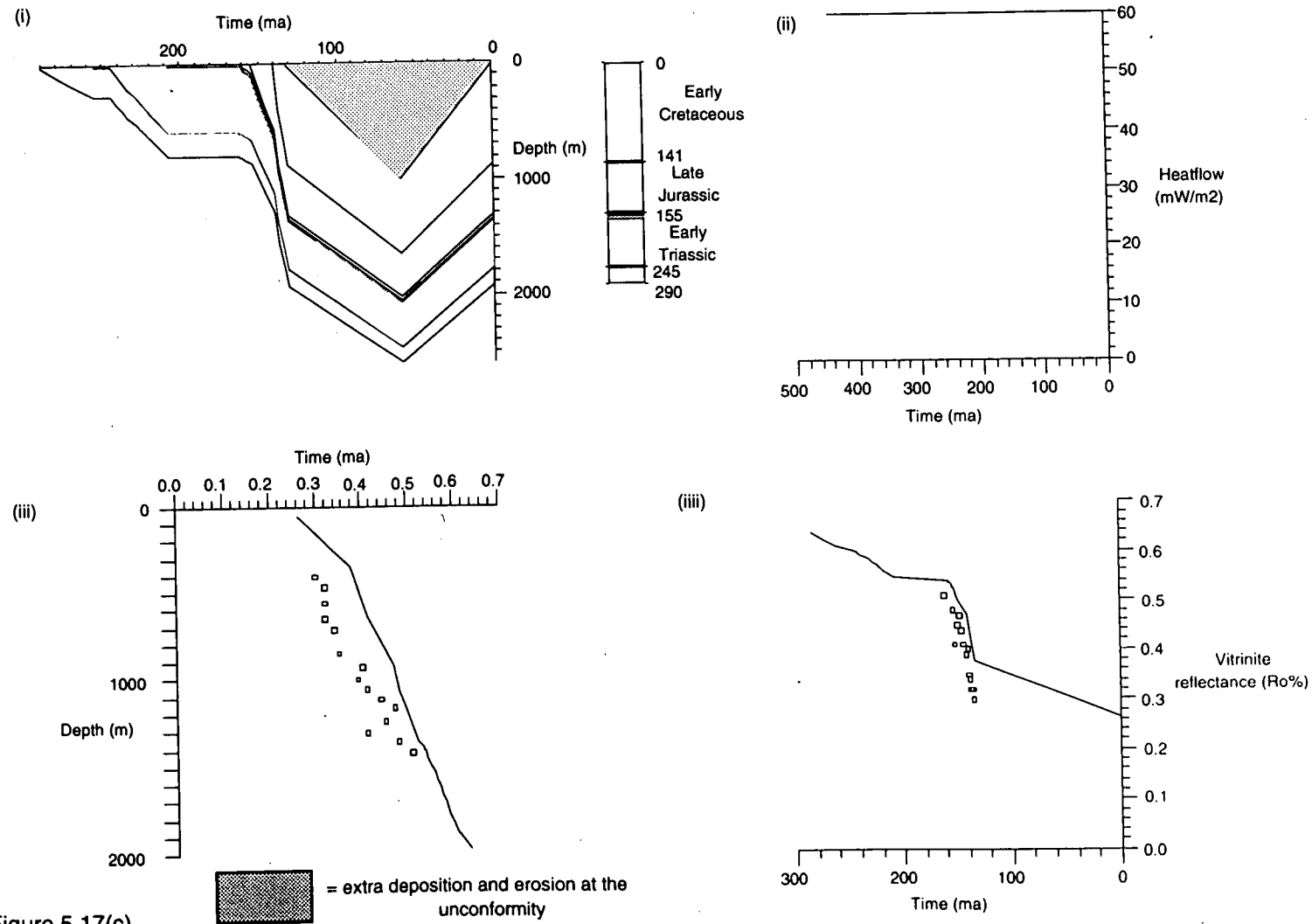
(i)
Time (ma)
200
100
0
0
Depth (m)
1000
2000
0
Early
Cretaceous
141
Late
Jurassic
155
Early
Triassic
245
290
(ii)
60
50
40
30
20
10
0
Heatflow
(mW/m2)
500
400
300
200
100
0
Time (ma)
(iii)
Time (ma)
0.0
0.1
0.2
0.3
0.4
0.5
0.6
0.7
0
1000
Depth (m)
2000
(iiii)
0.7
0.6
0.5
0.4
0.3
0.2
0.1
0.0
Vitrinite
reflectance (Ro%)
300
200
100
0
Time (ma)
= extra deposition and erosion at the
unconformity

Figure 5.17(c)

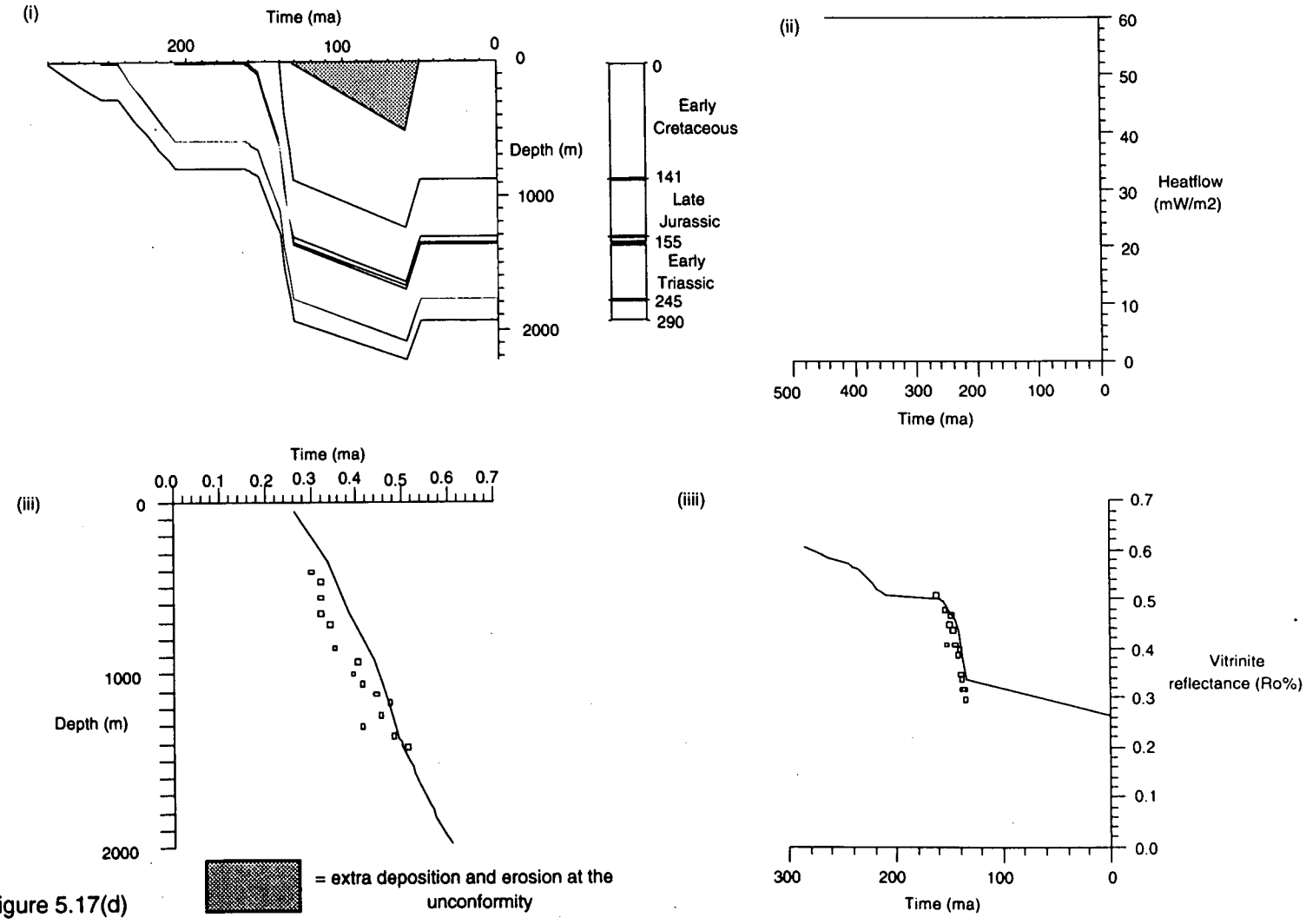
(i)
Time (ma)
200
100
0
0
Depth (m)
1000
2000
0
Early
Cretaceous
141
Late
Jurassic
155
Early
Triassic
245
290
(ii)
60
50
40
30
20
10
0
Heatflow
(mW/m2)
500
400
300
200
100
0
Time (ma)
(iii)
Time (ma)
0.0
0.1
0.2
0.3
0.4
0.5
0.6
0.7
0
1000
Depth (m)
2000
(iiii)
0.7
0.6
0.5
0.4
0.3
0.2
0.1
0.0
Vitrinite
reflectance (Ro%)
300
200
100
0
Time (ma)
= extra deposition and erosion at the
unconformity

Figure 5.17(d)

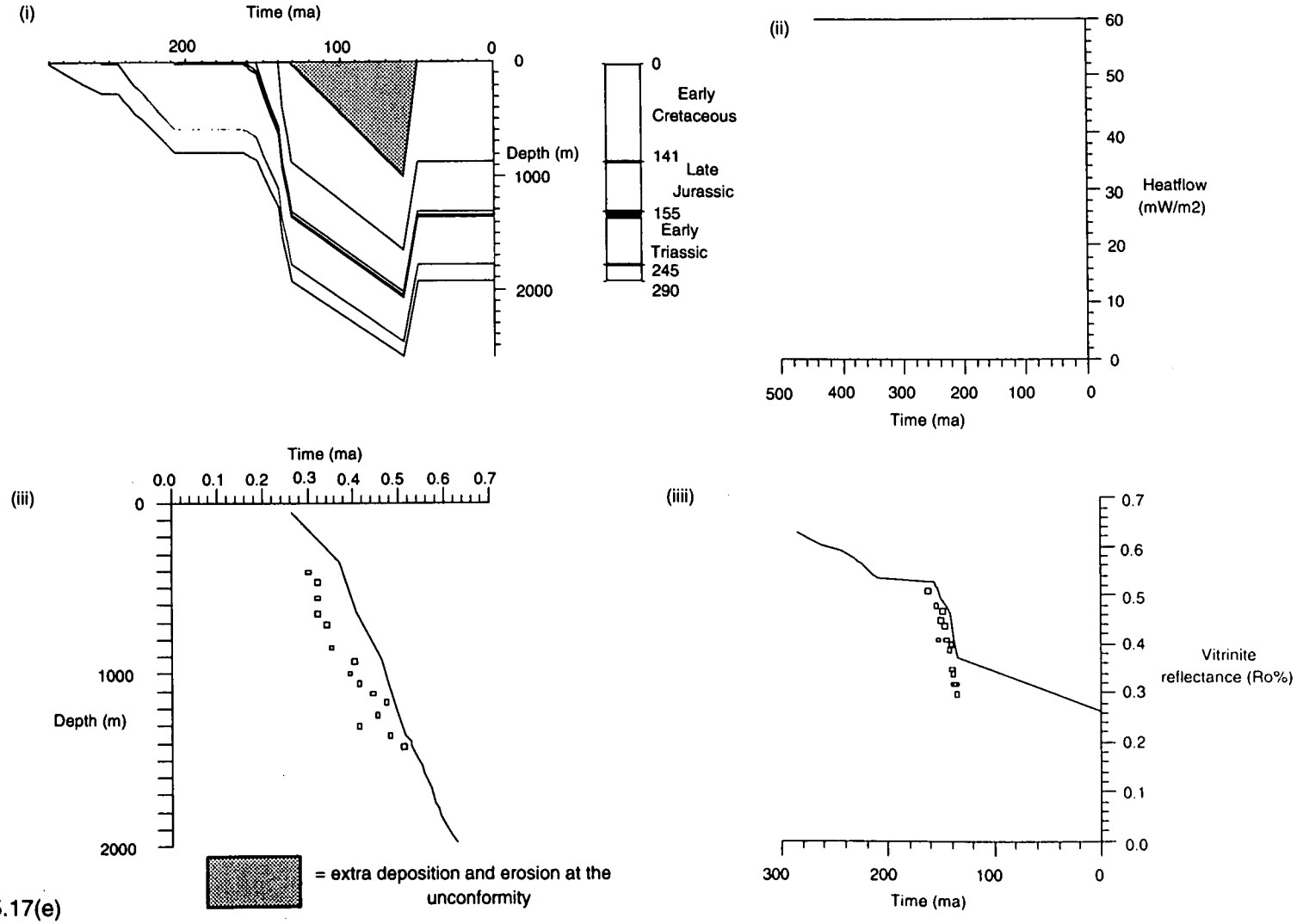
(i)
Time (ma)
200
100
0
0
Depth (m)
1000
2000
0
Early
Cretaceous
141
Late
Jurassic
155
Early
Triassic
245
290
(ii)
60
50
40
30
20
10
0
Heatflow
(mW/m2)
500
400
300
200
100
0
Time (ma)
(iii)
Time (ma)
0.0
0.1
0.2
0.3
0.4
0.5
0.6
0.7
0
1000
Depth (m)
2000
= extra deposition and erosion at the
unconformity
(iiii)
0.7
0.6
0.5
0.4
0.3
0.2
0.1
0.0
Vitrinite
reflectance (Ro%)
300
200
100
0
Time (ma)

Figure 5.17(e)

500m of extra sediment until 60ma, followed by steady erosion to the present day (as shown by **Figure 5.15(b)i**) is consistent with the observed vitrinite reflectance data. The results of modelling similar amounts of extra stratigraphy but with a 50ma hiatus at the sea-bed are similar to those described above. With 500m of extra stratigraphy input into the model **(Figure 5.15(d)i)** the fit to the upper 1km is extremely good, again with little alteration to the predicted maturities below 1km **(Figure 5.15(d)iii)**. With 1000m of extra stratigraphy the effects appear the same as before **(Figure 5.15(e)iii)** with predicted maturities for the upper 1km being at the higher end of the dataset and with little difference at depths greater than 1km. Again it appears that approximately 500m of missing stratigraphy is consistent with the observed vitrinite reflectance values. However, as two different forms of uplift history can produce similar results the accuracy of vitrinite reflectance modelling must be questioned and the exact nature of the uplift and erosion history has still be resolved.

In the case of well 11/30-6 **(Figure 5.16(a))**, the model predicts vitrinite reflectance values which agree well with the data when no missing stratigraphy is included. However, with the inclusion of 500m of missing section both potential burial histories provide better fits with the data **(Figures 5.16(b and d))**. As with 11/30-2 the inclusion of 1000m of missing stratigraphy **(Figures 5.16 (c and e))** results in predicted maturities which are too high and lie at slightly higher vitrinite reflectance values than observed. Again it can be suggested that the vitrinite reflectance data is consistent with approximately 500m of erosion.

For well 12/23-2 the predicted maturities with no missing stratigraphy fall slightly higher than the actual data, particularly in the upper (younger) part of the section **(Figure 5.17(a)iii)**. However, as the present day heatflow cannot be altered and the section was rapidly deposited **(Figure 5.17(a)iiii)** the fit can be considered reasonably tolerable. With the inclusion of 500m of erosion **(Figures 5.17(b and d))** the predicted maturities even deviate from the lower part of the section and with 1000m of missing stratigraphy the predicted maturities are far too great **(Figure 5.17(c and e))**. This seems to suggest that the amount of missing stratigraphy (if any is missing at all) is certainly less that 500m.

Figure 5.18 Estimation of uplift and erosion using vitrinite reflectance modelling for well 12/30-1. (a) The effect of assuming no unconformity on the prediction of the extent of vitrinite reflectance. (b) Modelling assumes that deposition continued from the time of the last recorded sedimentation until the middle of the timespan the unconformity represents and that 500m of extra stratigraphy accumulated prior to uplift and erosion of 500m of section at a constant rate to the time of deposition of the first sediments above the unconformity. (c) Modelling assumes that deposition continued from the time of the last recorded sedimentation until the middle of the the timespan the unconformity represents and that 1000m of extra stratigraphy accumulated prior to uplift and erosion of 1000m of section at a constant rate to the time of deposition of the first sediments above the unconformity. (i) The modelled burial/erosion history with the extra sediments lost at the unconformity highlighted. (ii) Plot of palaeoheatflow against time which was used to produce the predicted vitrinite reflectance values. (iii) A plot of vitrinite reflectance versus depth with the datapoints for that well and the computer generated vitrinite reflectance/depth profile. (iiii) A plot of vitrinite reflectance versus sample age with the datapoints for that well and the computer generated vitrinite reflectance/depositional age profile.

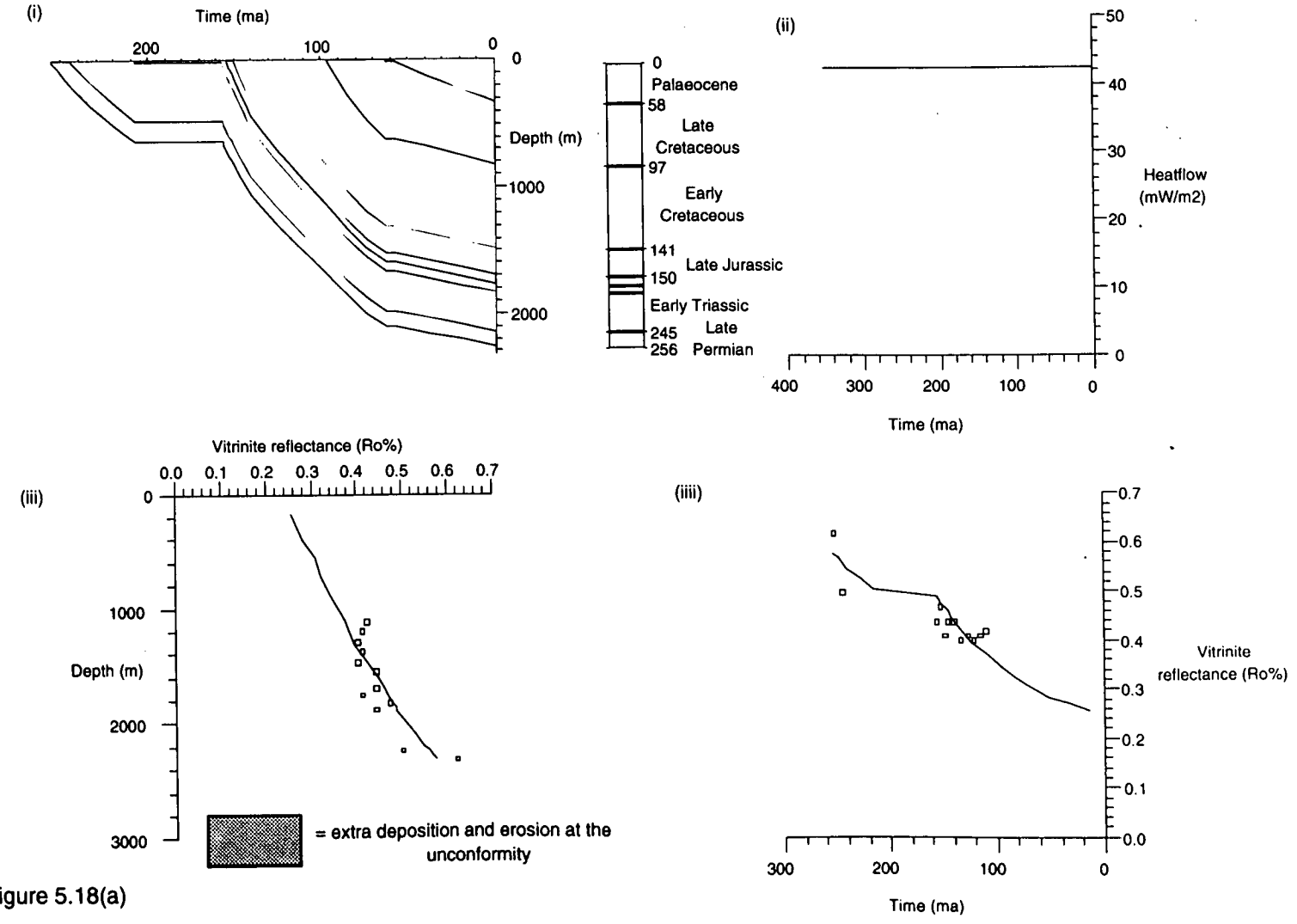
(i)
Time (ma)
200
100
0
0
Depth (m)
1000
2000
0
Palaeocene
58
Late
Cretaceous
97
Early
Cretaceous
141
Late Jurassic
150
Early Triassic
245
Late
256
Permian
(ii)
50
40
30
20
10
0
Heatflow
(mW/m2)
400
300
200
100
0
Time (ma)
(iii)
Vitrinite reflectance (Ro%)
0.0
0.1
0.2
0.3
0.4
0.5
0.6
0.7
0
1000
Depth (m)
2000
3000
= extra deposition and erosion at the
unconformity
(iiii)
0.7
0.6
0.5
0.4
0.3
0.2
0.1
0.0
Vitrinite
reflectance (Ro%)
300
200
100
0
Time (ma)

Figure 5.18(a)

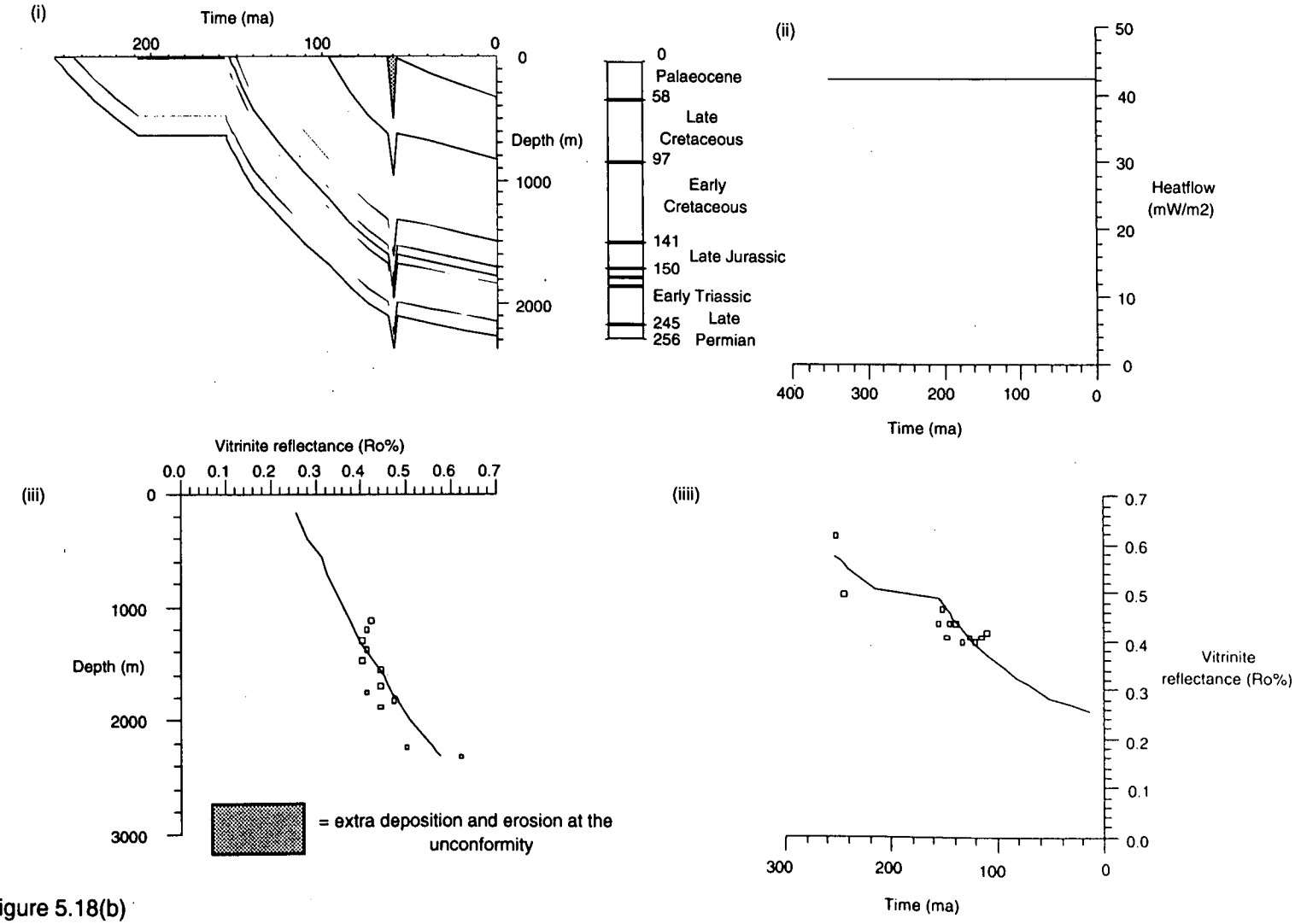
(i)
Time (ma)
200
100
0
0
Depth (m)
1000
2000
0
Palaeocene
58
Late
Cretaceous
97
Early
Cretaceous
141
Late Jurassic
150
Early Triassic
245
Late
256
Permian
(ii)
50
40
30
20
10
0
Heatflow
(mW/m2)
400
300
200
100
0
Time (ma)
(iii)
Vitrinite reflectance (Ro%)
0.0
0.1
0.2
0.3
0.4
0.5
0.6
0.7
0
1000
2000
3000
Depth (m)
= extra deposition and erosion at the unconformity
(iiii)
0.7
0.6
0.5
0.4
0.3
0.2
0.1
0.0
Vitrinite
reflectance (Ro%)
300
200
100
0
Time (ma)

Figure 5.18(b)

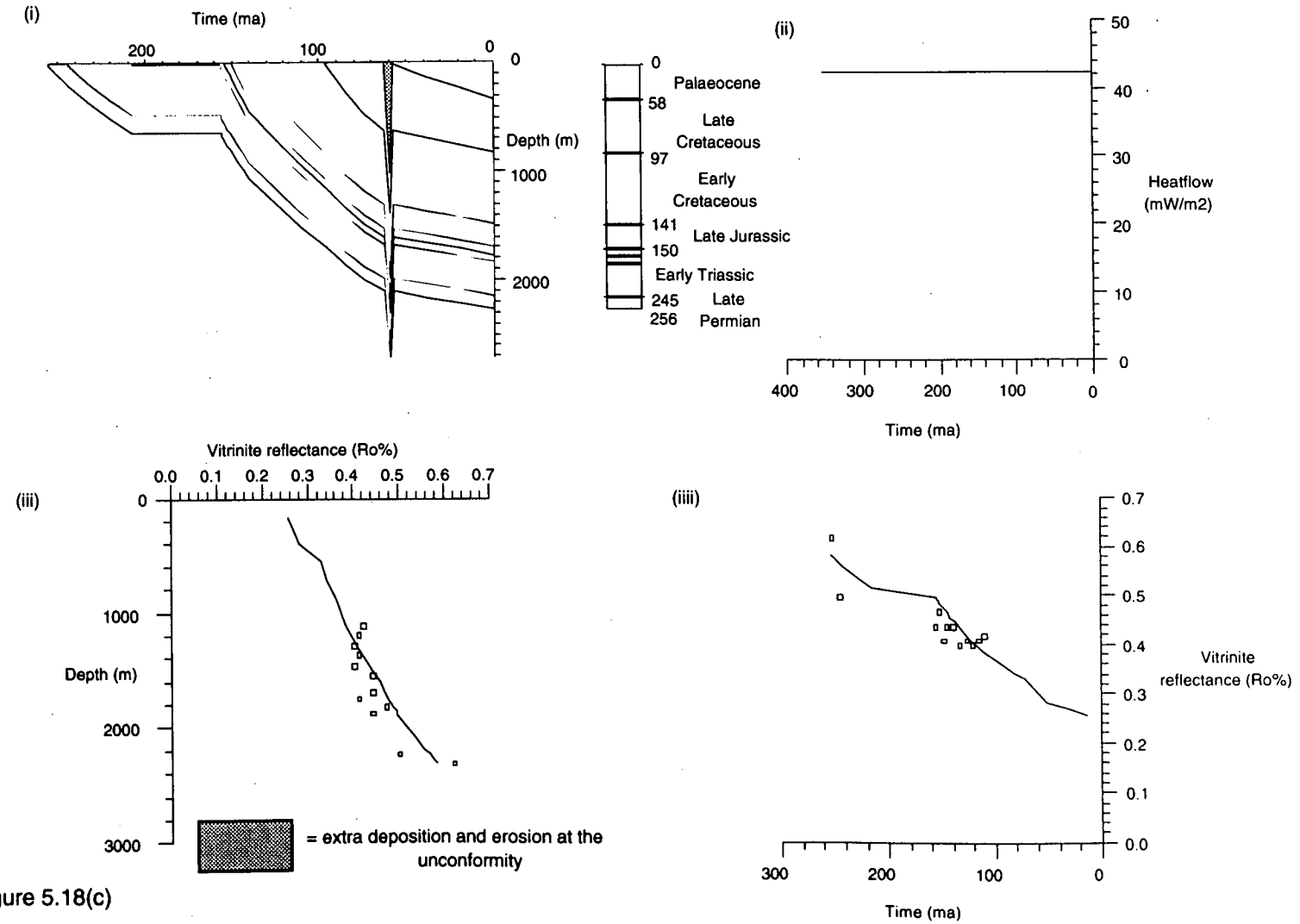
(i)
Time (ma)
200
100
0
0
Depth (m)
1000
2000
0
Palaeocene
58
Late
Cretaceous
97
Early
Cretaceous
141
Late Jurassic
150
Early Triassic
245
Late
256
Permian
(ii)
50
40
30
20
10
0
Heatflow
(mW/m2)
400
300
200
100
0
Time (ma)
(iii)
Vitrinite reflectance (Ro%)
0.0
0.1
0.2
0.3
0.4
0.5
0.6
0.7
0
1000
Depth (m)
2000
3000
= extra deposition and erosion at the
unconformity
(iiii)
0.7
0.6
0.5
0.4
0.3
0.2
0.1
0.0
Vitrinite
reflectance (Ro%)
300
200
100
0
Time (ma)

Figure 5.18(c)

With the greater stratigraphic control on the unconformity in well 12/30-1 it should be expected that a more accurate picture emerges. However, the picture seems equally vague with the effects of assuming no missing stratigraphy and 500m of missing stratigraphy producing equally good fits **(Figures 5.18(a and b))**. However, the inclusion of 1000m of erosion predicts maturities far in excess of that observed **(Figure 5.18(c))**. Consequently, it appears that the extent of erosion in well 12/30-1 lies somewhere between 0 and 500m. The potential cause of the similarity of results when assuming 0 and 500m of missing section is that the time during which the extra 500m potentially accumulated was extremely short and consequently the additional heating effects were minimalised and so hard to detect.

The results described above seem to give a rough indication that uplift and erosion occurred in the Inner Moray Firth after the Late Cretaceous. Although not conclusive and unable to provide quantifiable estimates of the amount of missing stratigraphy it is encouraging that the estimates are of the same order of magnitude as those derived from compaction analysis, apatite fission track analysis and the vitrinite reflectance trend method. In his studies Prajoga (1990) also attempted to estimate the amount of missing stratigraphy and produced estimates for all ten wells **(Table 5.4)**. However, careful examination of the predicted and actual vitrinite reflectance values shows that in most cases his predicted vitrinite reflectance values are far too large compared to the data **(e.g. Figure 5.19)** and consequently the estimates of the amount of missing stratigraphy must be considered dubious. As Prajoga's (1990) model overestimated maturity and proposes lower estimates of the amount of missing section compared to the modelling described above it can be seen that if a reasonable fit with the data was achieved no missing stratigraphy may be required by the Lopatin-type model. Consequently, it appears that the Lopatin type models are potentially less rigorous than the new generation of kinetic models.

5.2.3 Onshore vitrinite reflectance evidence.

Hillier and Marshall (1992) have compiled an extensive vitrinite reflectance database from the remnants of the Orcadian Basin in Caithness, Orkney, Shetland and the margins of the Inner Moray Firth **(Figure 5.20)**. Using the approach of Barker and Pawlewicz (1986) they have been able to estimate the maximum temperatures experienced by the samples. They suggest that the lower bounds of the temperature maxima distribution, that is ignoring samples which have undergone contact metamorphism, is around 100-120°C. This suggests the removal

Table 5.4 Uplift and erosion estimates for ten wells in the Inner Moray Firth. The estimates were derived from a Lopatin-type TTI model. After Prajoga (1990).

Well	Uplift and erosion estimate (m)
11/30-2	198
11/30-6	274
12/21-1	244
12/22-1	213
12/23-1	91
12/23-2	122
12/26-1	168
12/27-1	168
12/28-1	61
12/30-1	91

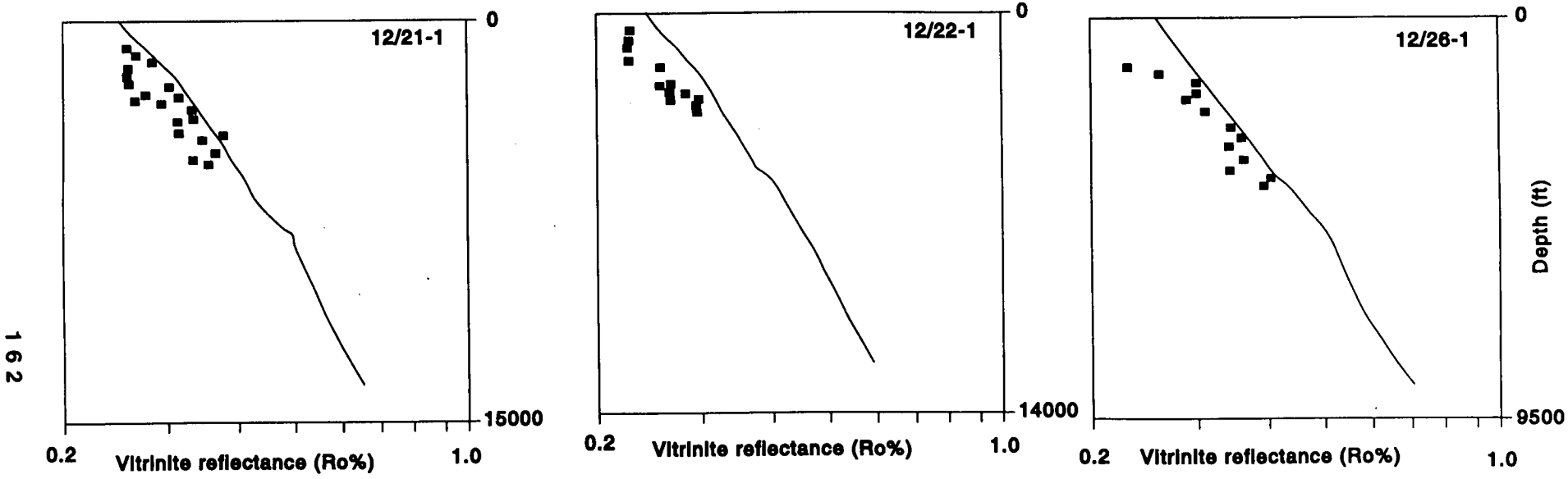

Figure 5.19 Comparison of vitrinite reflectance -depth data and modelled vitrinite reflectance profiles for three wells in the Inner Moray Firth (Prajoga, 1990). The modelled profiles show higher maturities than exist in reality and consequently place doubt on the estimates of uplift and erosion derived from them.

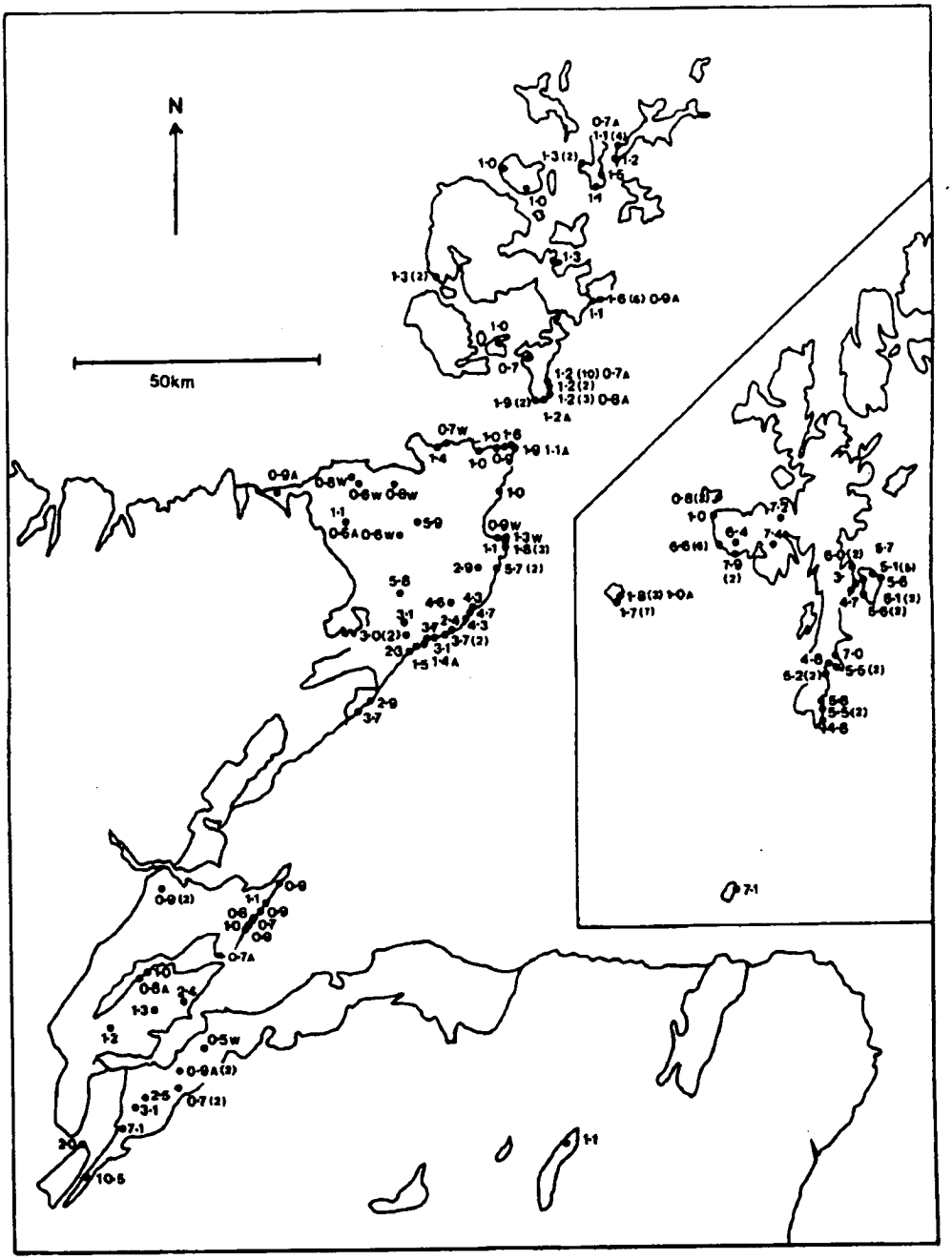

Figure 5.20 Vitrinite reflectance database for the Orcadian Basin (Hillier and Marshall, 1992). The vitrinite reflectance values are generally higher than those observed offshore and suggest greater burial-depths, and hence uplift and erosion than seen in the Inner Moray Firth.

of several kilometres of section and is consistent with apatite fission track data which suggests that samples experienced temperatures in excess of 110°C prior to the Late Permian/Early Triassic.

5.3 Evidence from biological marker molecules.

The use of biological marker molecules is common for constraining the burial history of basins. For the Inner Moray Firth such a study has been carried out by Duncan (1986) for eleven wells **(Figure 5.21)** and allowed the estimation of uplift and erosion by a variety of methods. This section briefly reviews this work for the sake of completeness and so that comparisons may be drawn with the work already documented.

The first approach exploited by Duncan (1986) is based on the isomerisation and aromatisation characteristics of steranes and hopanes and was devised by MacKenzie and McKenzie (1983). Unlike vitrinite reflectance, the reactions involved are truely unimolecular and obey first-order reaction kinetics. Consequently, the modelling of such processes can be considered as more accurate than the modelling of the complex reactions involved in the section 5.2.2. The method exploits the fact that for both steranes and hopanes the aromatisation reaction proceeds at a higher rate than isomerisation at elevated temperatures but with increasing age both reactions occur at lower temperatures. The consequence of the two separate reactions involved having differing kinetic properties is that for a particular thermal history the relative extents of both reactions can be used to "fingerprint" the thermal history **(Figure 5.22)**.

If the isomerisation-aromatisation data for the Inner Moray Firth **(Figure 5.23)** are compared with the schematic representation in **Figure 5.22** it can be seen that both reaction types have made moderate progress but it cannot be confirmed whether the reactions took a high temperature-low time or low temperature-high time pathway (Duncan, 1986). However, when the data is compared with modelled values based on the preserved stratigraphy with a range of realistic heatflows it can be seen that the actual data has higher than expected aromatisation values. Duncan (1986) attributes this to two possible causes. Firstly, as more aromatisation has occurred than predicted by the model it is conceivable that the samples have experienced higher temperatures than the model predicts (c.f. **Figure 5.22**) and consequently that the samples have experienced uplift and erosion from their

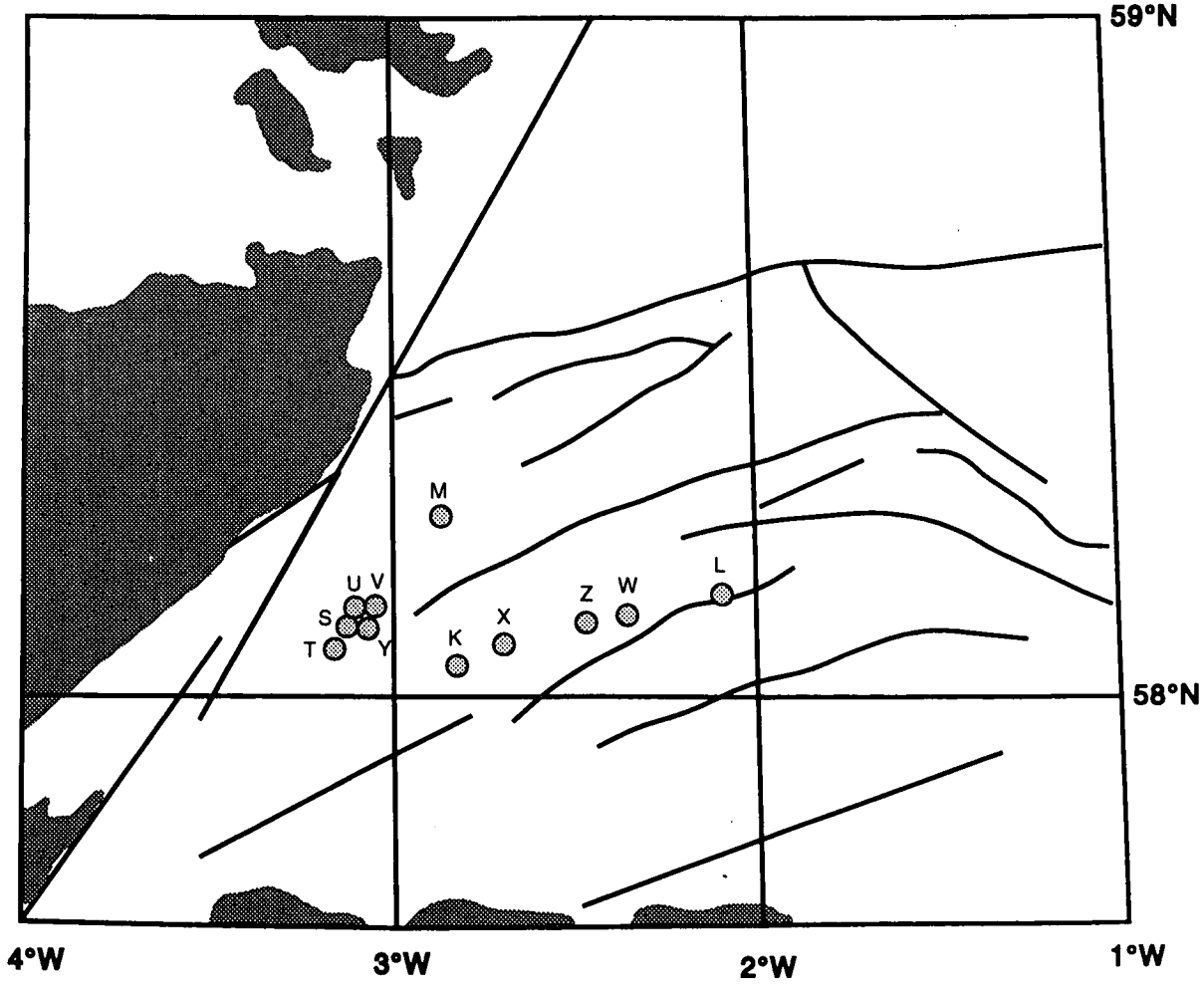

Figure 5.21 Location of wells with geochemical marker molecule data used by Duncan (1986).

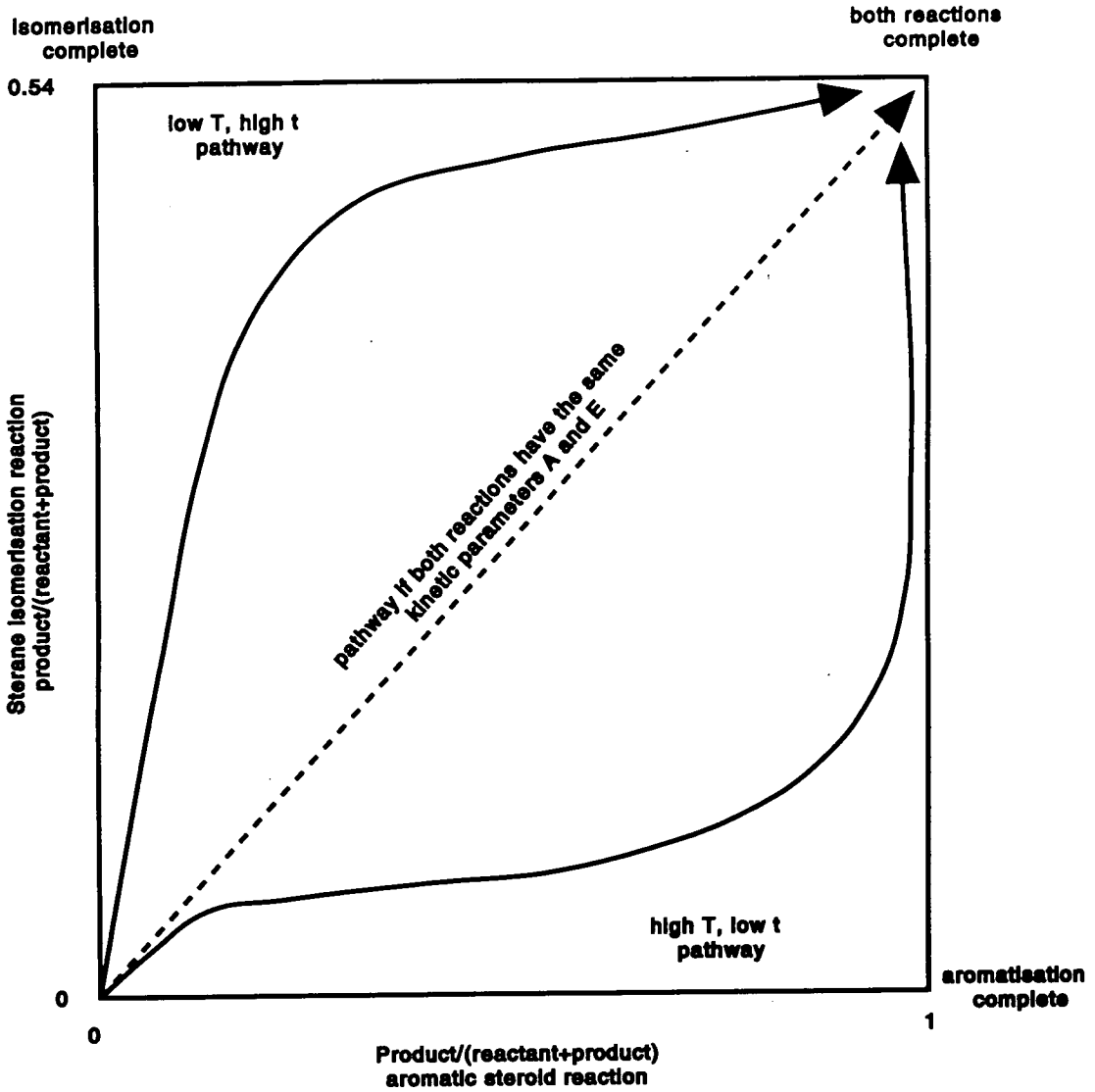

Figure 5.22 Summary of possible pathways on an aromatisation/isomerasation diagram for different thermal histories (Duncan, 1986). For high temperatures the aromatisation reaction initially proceeds at a higher rate than isomerisation and so samples will plot to the right of the diagram. For lower average temperatures and longer time spans isomerisation proceeds at a higher rate and so samples plot to the left.

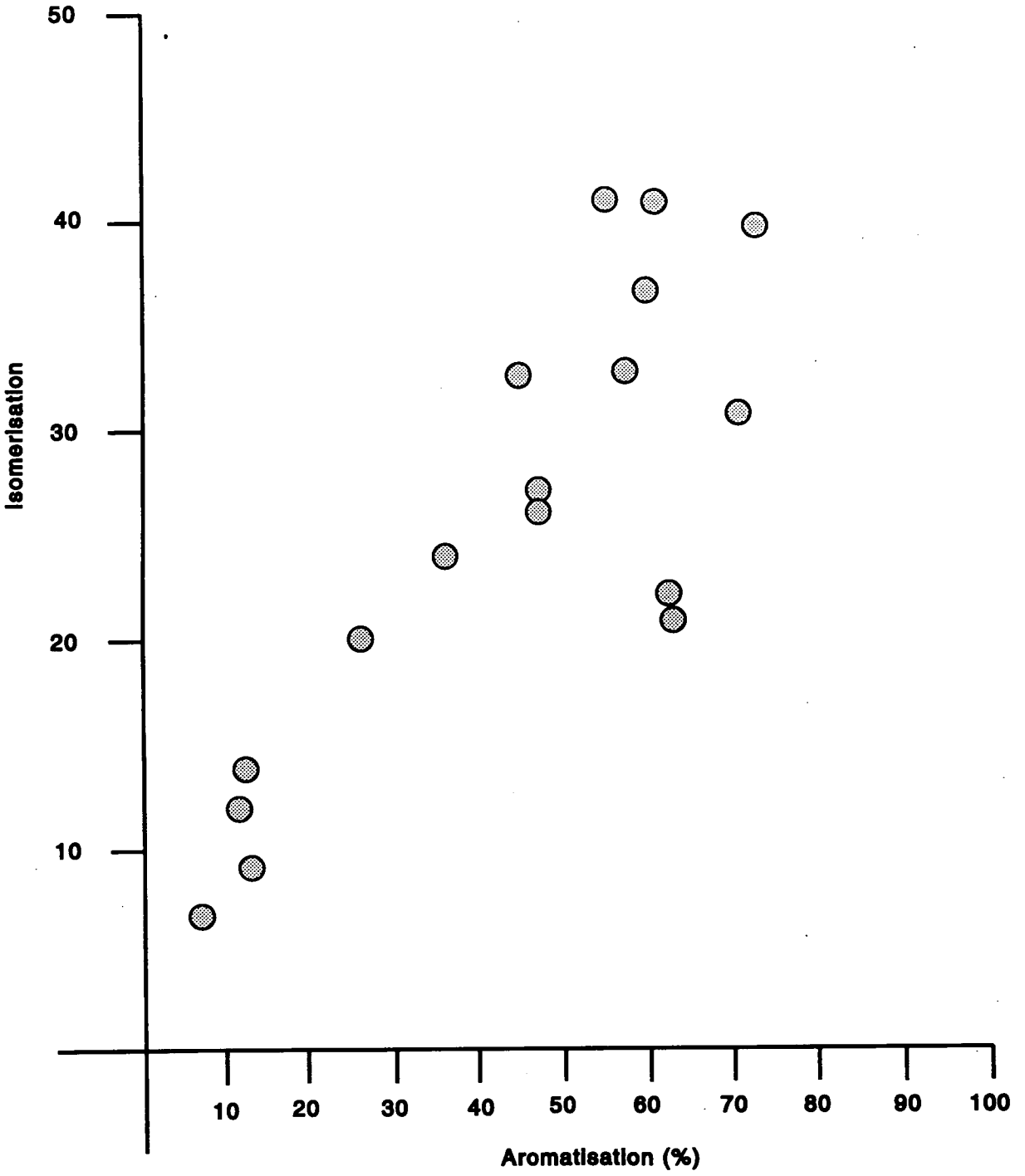

Figure 5.23(a) Aromatisation/isomerisation plot for the Inner Moray Firth. The extent of steroid hydrocarbon isomerisation is plotted as a function of steroid hydrocarbon aromatisation. After Duncan (1986).

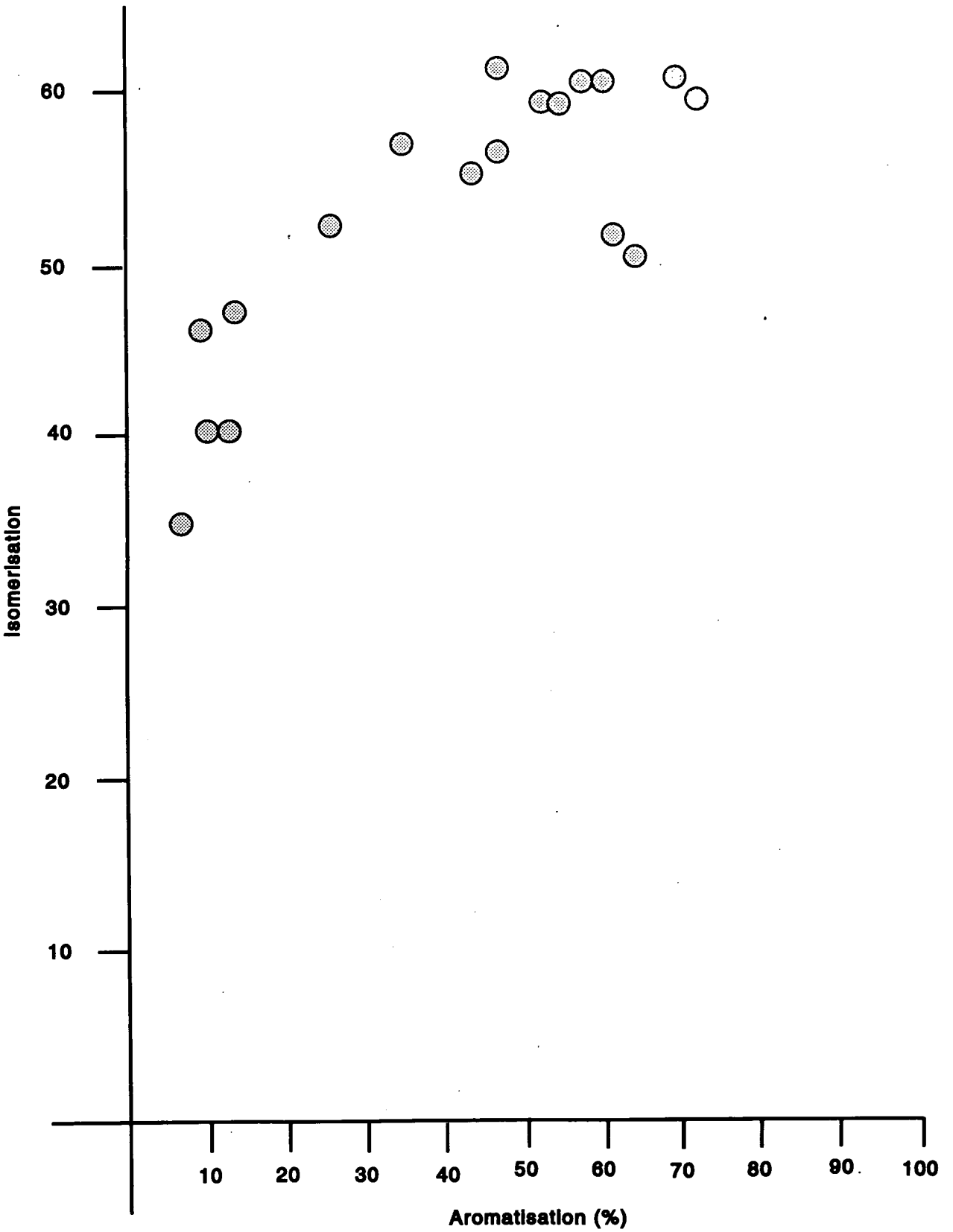

Figure 5.23(b) Aromatisation/isomerisation plot for the Inner Moray Firth. The extent of hopane hydrocarbon isomerisation is plotted as a function of steroid hydrocarbon aromatisation. After Duncan (1986).

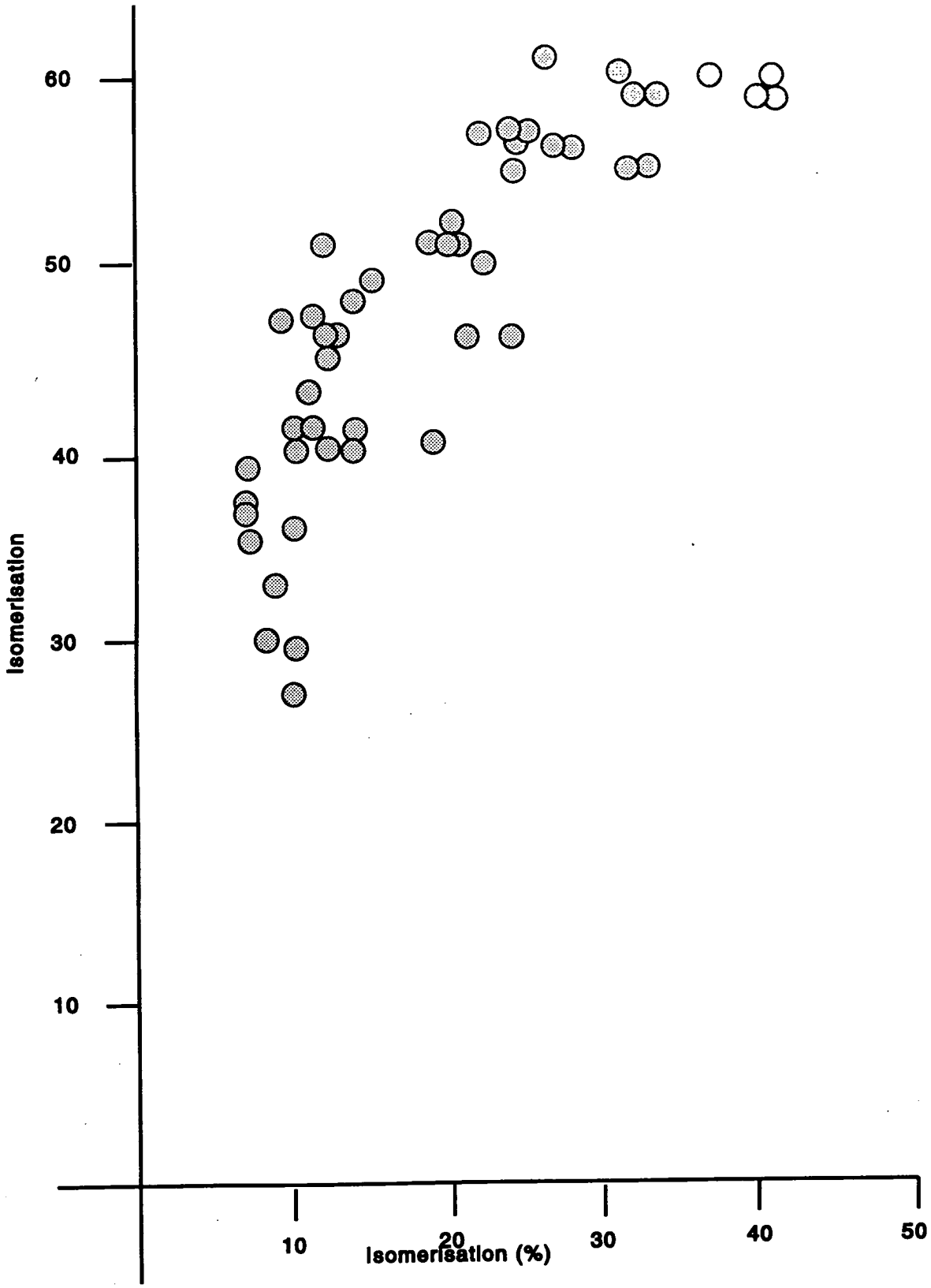

Figure 5.23(c) Aromatisation/isomerisation plot for the Inner Moray Firth. The extent of hopane hydrocarbon isomerisation is plotted as a function of steroid hydrocarbon isomerisation. After Duncan (1986).

maximum burial-depth. The other potential cause of the substantial shift in the data from the predicted values is that the extent of aromatisation is overestimated and Duncan (1986) provides some evidence for this.

As the aromatisation data appears to be in doubt Duncan (1986) also plotted the extent of sterane isomerisation against present temperature and compared it with predicted values **(Figure 5.24)**. As can be seen, the data shows a substantial horizontal translation with higher than predicted isomerisation for current burial-depths. The majority of the data lies within an 11°C wide sigmoidal envelope and the horizontal translation can be explained by the cooling of the samples from their maximum temperature, that is they have been uplifted and eroded from their maximum burial-depth. For the majority of the samples Duncan (1986) suggests 830±160m of erosion while for wells T and K, which lie further from the predicted values, 1000m and >1000m respectively.

The sterane and hopane isomerisation data was also analysed by Duncan (1986) in a less rigorous manner based on the fact that the isomerisation reactions of both molecule types have differing activation energies and so proceed at differing rates under the same thermal conditions. The result is that the maximum palaeotemperature, and hence the amount of section removed, by comparing the reaction extents. The results of such an analysis for the Inner Moray Firth are shown in **Table 5.5**. Although this method is vastly simplified compared to the previous one, and the estimates of removed section decrease with depth, it is encouraging that the results are of the same order of magnitude and so can be taken as confirmatory evidence for the amount of section lost.

For well X Duncan (1986) was not in the possession of any sterane or hopane isomerisation data and consequently resorted to the determination of uplift and erosion by modelling pristane isomerisation kinetics. The principle of modelling pristane kinetics is that the (6R,10S) mesopristane molecule progressively alters into a 1:1 mixture of (6R,10R) and (6S,10S) pristane enantiomers in a way that is describable using the Arrhenius equation. As can be seen in **Figure 5.25**, this reaction has not yet reached completion with approximately 57% mesopristane still present. Consequently, this well is still amenable to modelling. The modelling procedure applied the Arrhenius equation to the pristane data in order to assess the maximum temperatures experienced by the samples. In this case the choice of activation energy and pre-exponential factor was complex as a variety have been proposed. However, Duncan (1986) gives detailed arguments for the choice of the

Table 5.5(a) Maximum palaeotemperatures and uplift and erosion estimates derived from the analysis of sterane and hopane isomerisation data (Duncan, 1986). The results are based on the analysis of individual samples.

Depth (m)	Maximum palaeotemperature (°C)	Present temperature (°C)	Uplift and erosion estimate (m)*
1740	123.0	66.0	1500
1929	123.0	73.0	1316
1673	113.0	63.0	1316
1829	113.0	69.5	1145
1888	113.0	72.0	1079
1888	113.0	72.0	1079
1625	104.0	62.0	1105
1560	98.0	60.0	1000

Table 5.5(b) Maximum palaeotemperatures and uplift and erosion estimates derived from the analysis of sterane and hopane isomerisation data (Duncan, 1986). The results are based on incremental values determined every 61m.

Depth (m)	Maximum palaeotemperature (°C)	Present temperature (°C)	Uplift and erosion estimate (m)*
1951	129.0	74.0	1447
1890	121.0	72.0	1289
1829	115.0	69.5	1197
1768	111.0	67.0	1158
1707	107.5	65.0	1118
1646	96.0	62.5	881

* estimates assume a geothermal gradient of 38°C/km

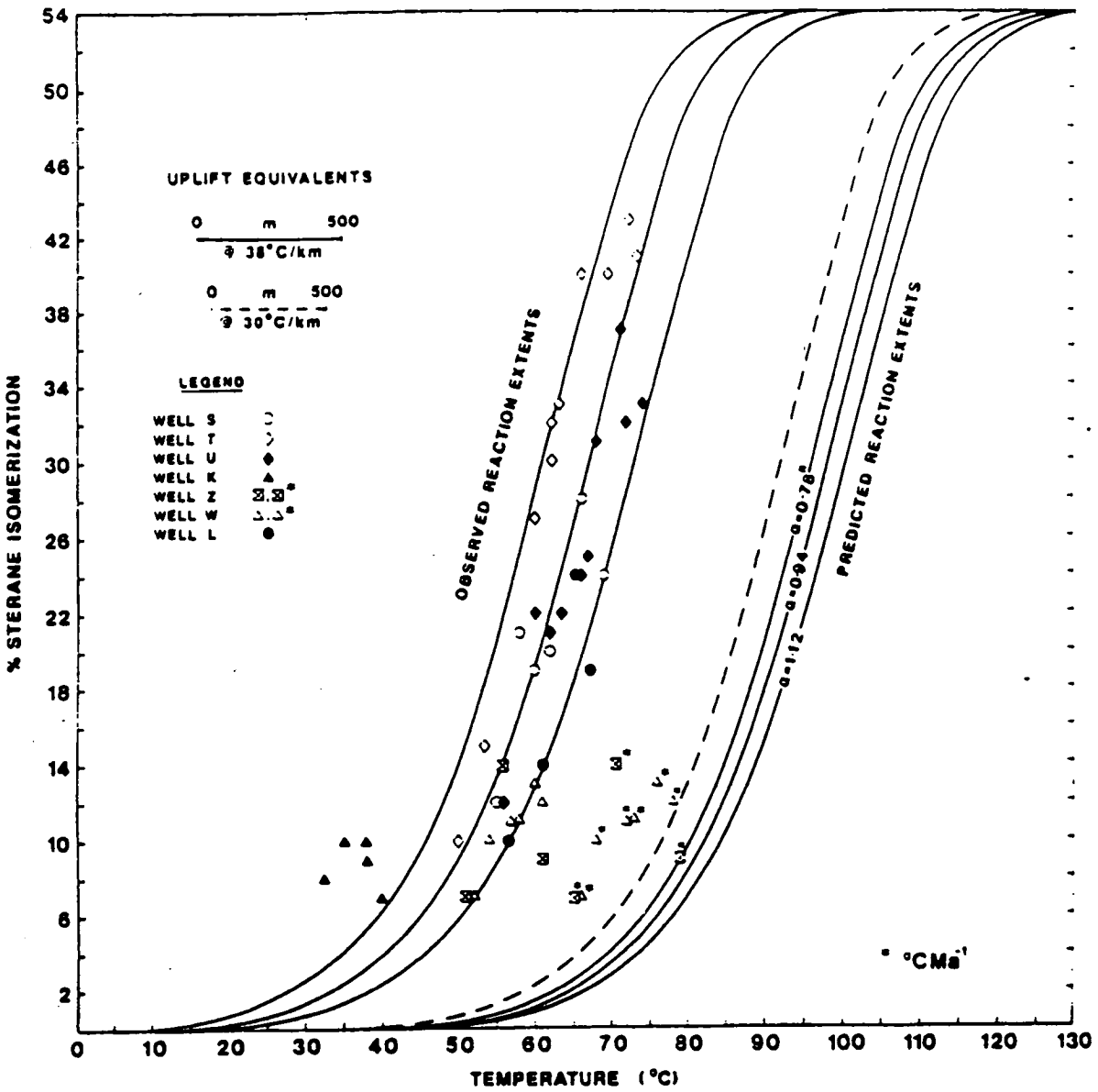

Figure 5.24 Sterane isomerisation plotted as a function of temperature for the Inner Moray Firth. Predicted reaction extent curves were computer generated using appropriate activation parameters and heating rates and mapped onto the dataset. All solid curves were constructed assuming a constant geothermal gradient of 38°C/km. The heating rate for the broken curve is based on a geothermal gradient of 30°C/km. Asterisked symbols correspond to samples calibrated using a geothermal gradient typical of the Beatrice suite geothermal gradients. All datapoints show higher than expected isomerisation extents than preicted for their current temperature and consequently uplift and erosion from their maximum burial-depth can be inferred. After Duncan (1986).

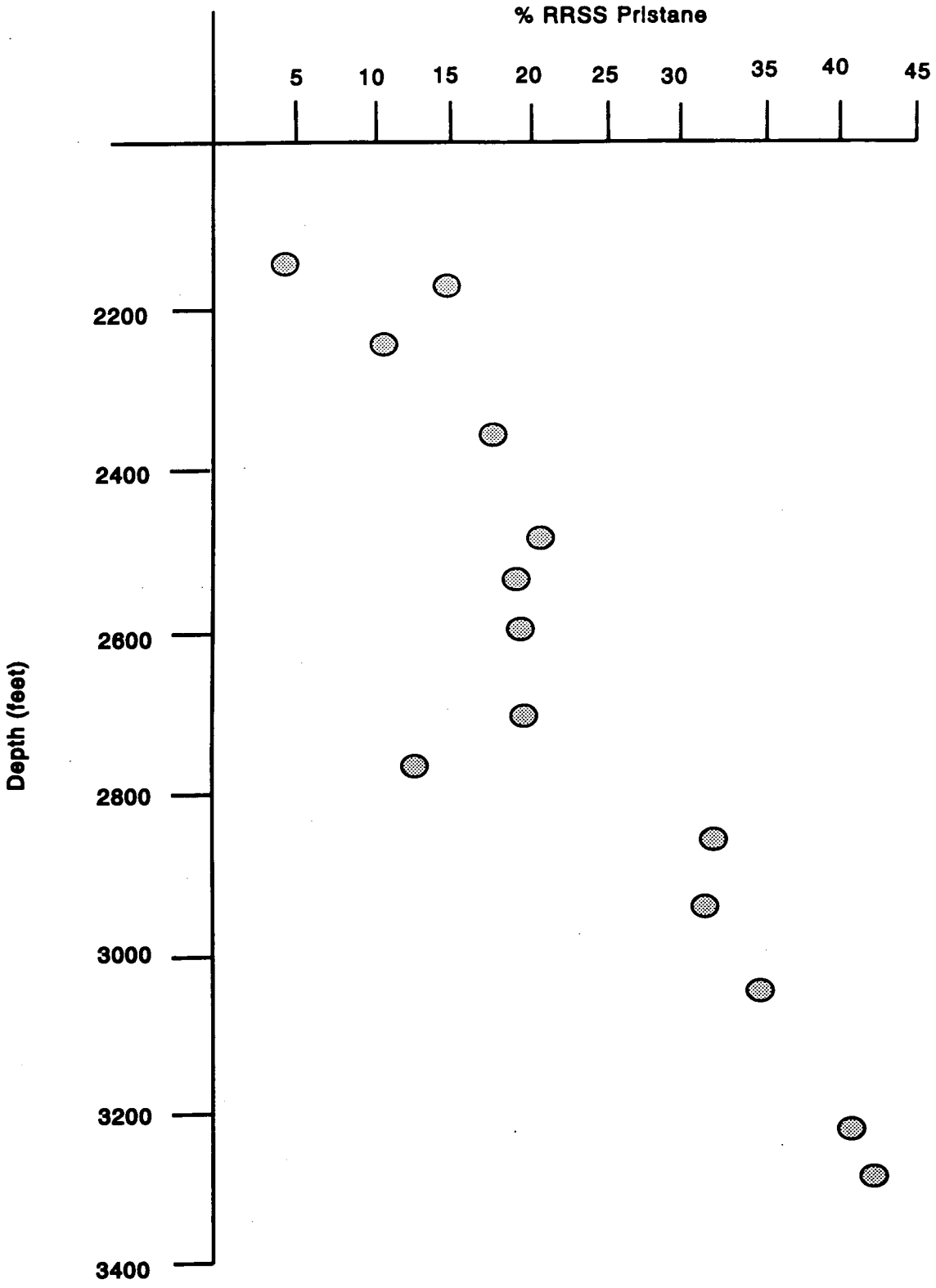

Figure 5.25 Extent of pristane isomerisation as a function of burial-depth for well X (Duncan, 1986). The extent of isomerisation shows a steady depth related increase but has not yet reached completion with 57% mesopristane still present in the deepest samples.

Table 5.6(a) Estimation of uplift and erosion by the application of the Arrhenius equation to pristane chemical kinetics. The estimates assume an activation energy (E) of 116 kj/mole, pre-exponential factor (A) of 154 s^{-1} and a geothermal gradient of 38°C/km. After Duncan (1986).

Depth (m)	% RRSS pristane	Present temperature (K)	Predicted maximum temperature (K)	Temperature difference (K)	Uplift and erosion estimate (m)
662.0	14.6	302.76	331.37	28.61	752.9
683.4	10.6	303.57	328.48	24.91	655.5
716.9	17.7	304.84	333.20	28.36	746.3
756.5	21.1	306.35	335.04	28.69	755.0
772.4	19.4	306.95	334.18	27.23	716.6
791.3	19.9	307.67	334.39	26.72	703.2
825.4	20.0	308.96	334.48	25.52	671.6
846.5	13.1	309.77	330.35	20.58	541.6
872.3	32.7	310.75	340.43	29.68	781.0
897.3	32.0	311.70	340.15	28.45	748.7
929.6	35.7	312.93	341.84	28.91	760.8
982.1	41.5	314.92	344.76	29.84	785.3
1001.3	42.8	315.65	345.53	29.88	786.3

Table 5.6(b) Estimation of uplift and erosion by the application of the Arrhenius equation to pristane chemical kinetics. The esimates assume an activation energy (E) of 91 kj/mole, pre-exponential factor (A) of 0.074 s^{-1} and a geothermal gradient of 38°C/km. After Duncan (1986).

Depth (m)	% RRSS pristane	Present temperature (K)	Predicted maximum temperature (K)	Temperature difference (K)	Uplift and erosion estimate (m)
662.0	14.6	302.76	318.26	15.50	407.9
683.4	10.6	303.57	314.87	11.30	297.4
716.9	17.7	304.84	320.4	15.56	409.5
756.5	21.1	306.35	322.58	16.23	427.1
772.4	19.4	306.95	321.56	14.61	384.5
791.3	19.9	307.67	321.81	14.14	372.1
825.4	20.0	308.96	321.91	12.95	340.8
846.5	13.1	309.77	317.05	7.28	191.6
872.3	32.7	310.75	328.95	18.20	478.9
897.3	32.0	311.70	328.62	16.92	445.3
929.6	35.7	312.93	330.63	17.70	465.8
982.1	41.5	314.92	334.12	19.20	505.3
1001.3	42.8	315.65	335.04	19.39	510.3

two separate activation energy/pre-exponential factors sets used in the study. The results of applying the two differing activation energy/pre-exponential factor sets to the determination of maximum palaeotemperature are shown in **Table 5.6**. As can be seen for both possible sets of reaction constants the predicted maximum palaeotemperatures are in excess of the present temperatures. This suggests that these samples have experienced uplift and erosion from their maximum burial-depth, the magnitudes of which are also shown. In both cases the estimated loss of section is of the same order of magnitude as previously derived from other chemical measurements, compaction data and apatite fission track analyses and although the two potential estimates differ from each other they are both internally consistent.

The variety of methods for analysing the extent of the reactions for geochemical marker molecules documented here show convincing evidence for the loss of up to 1km of sediment from the Inner Moray Firth after the Late Cretaceous. The consistency of estimates between the methods can be ascribed to the simple nature of the reactions under consideration and consequently the relative ease with which they can be modelled compared to vitrinite reflectance with it's more complex kinetics and precursor-product relationships. Consequently, these estimates can be taken with some confidence as realistic estimates of the amount of section lost.

5.4 Clay mineralogical evidence.

The progressive transformation of the composition of clays and clay minerals with increased burial-depth and temperature is a well understood phenomenon (Curtis, 1980; Hower, 1981). For example, the progressive transformation of smectite through illite/smectite mixed layer clays to illite has been extensively studied (Hower, 1981) and has been applied to the determination of the maximum burial-depth experienced in the Beatrice oilfield (UKCS lincense block 11/30) and hence the determination of the amount of uplift and erosion by Hurst (1980). In his study, Hurst (1980) noted that the Lower Cretaceous sediments currently at sea-bed in well 11/30-1 contain clays with 75% smectite which is compatible with a maximum palaeotemperature upto 55°C **(Figure 5.26)**. Clearly, as the sea-bed currently has a temperature of 11°C the only plausible explanation for this is that the excess temperature was attained by burial to depths greater than currently observed. By assuming that present geothermal gradient is applicable to the past, Hurst (1980) suggested that the excess temperature could be accounted for by the deposition and subsequent post-Early Cretaceous removal of 1.25km of sediment. As

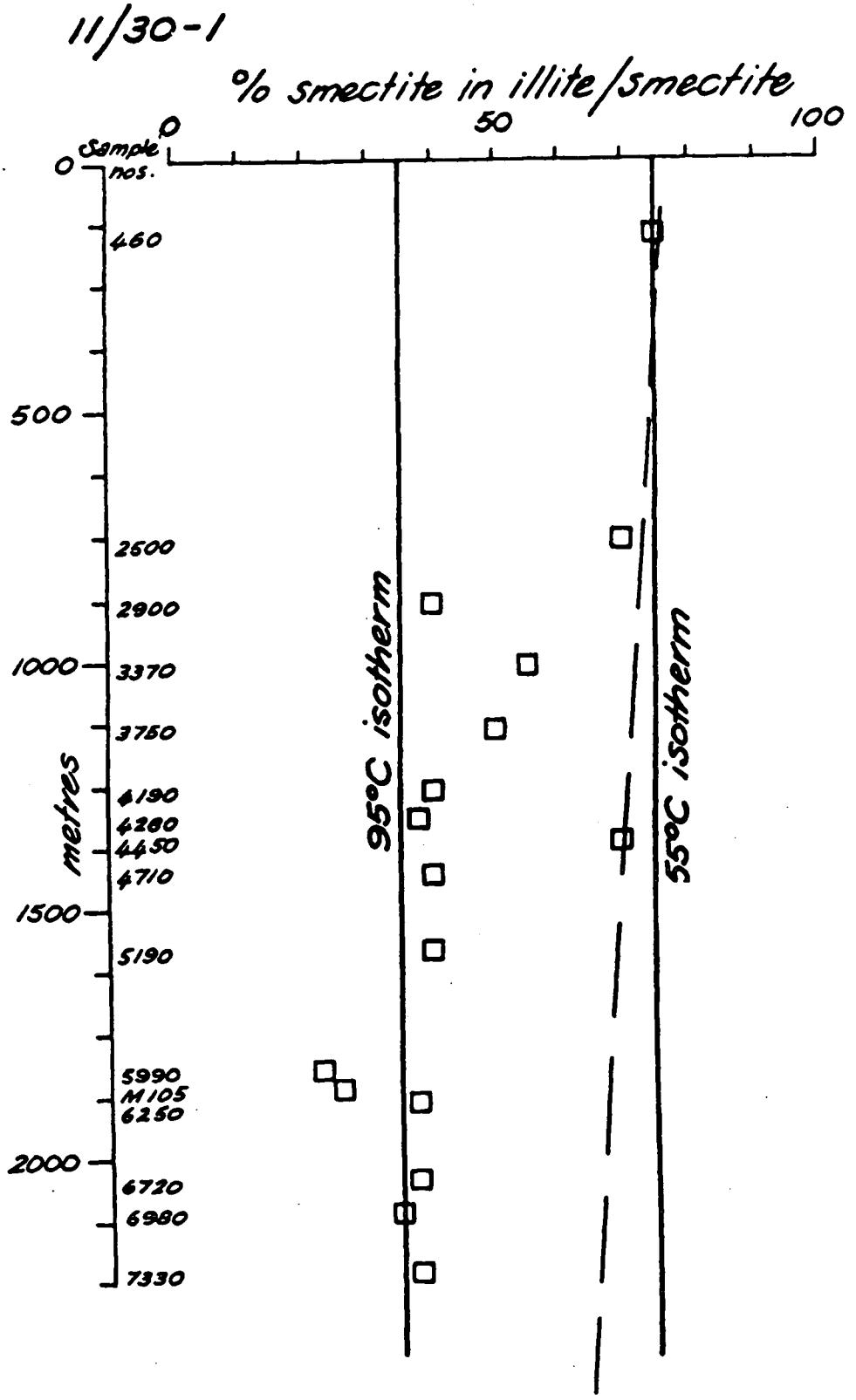

Figure 5.26 Plot of %smectite in illite/smectite mixed layer clays for well 11/30-1. The dashed line represents the geothermal gradient derived from the amount of smectite present in the clays and suggests surface temperaures higher than currently observed. Consequently, uplift and erosion can be inferred. After Hurst (1980).

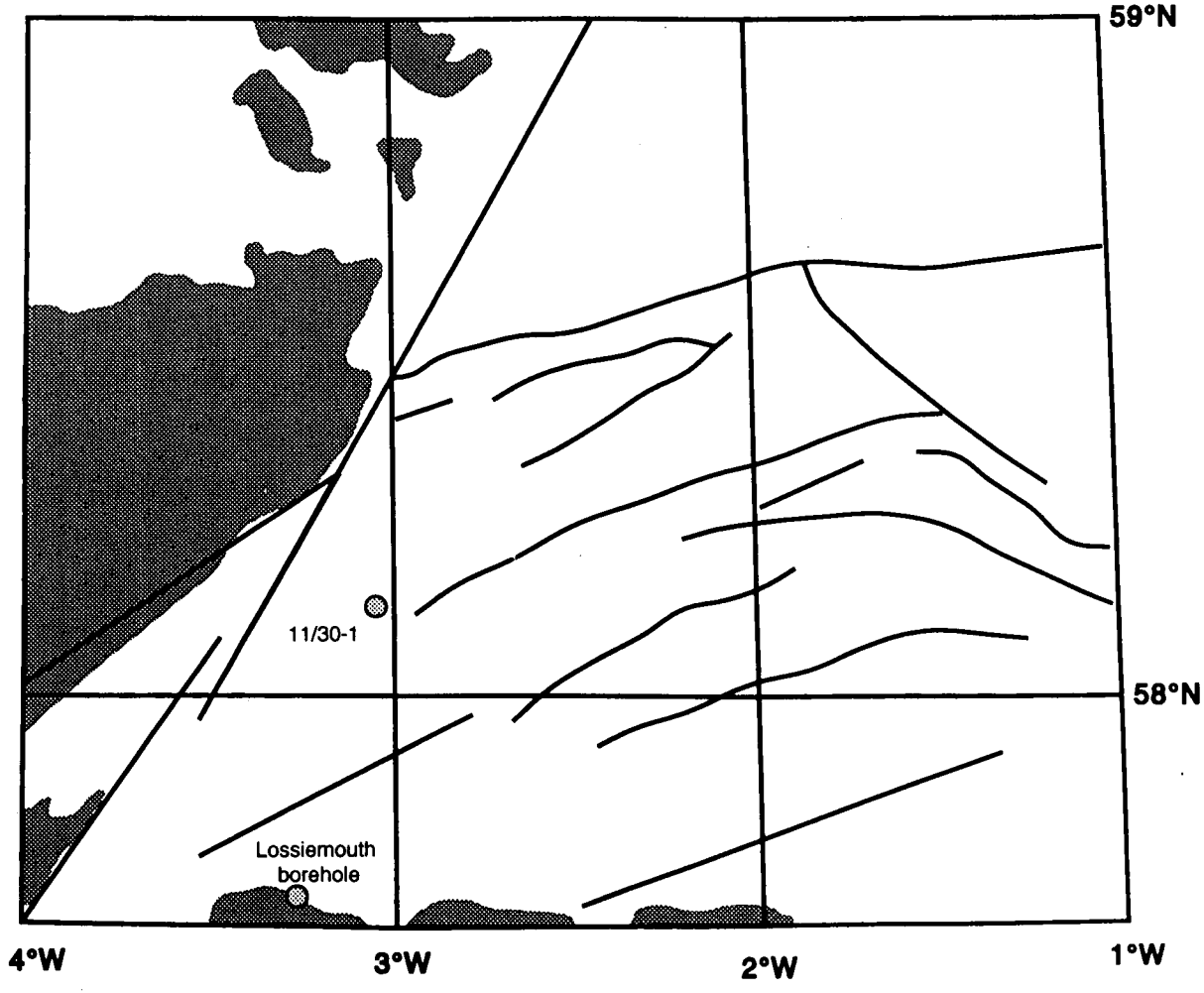

Figure 5.27 Location of clay mineralogical data used by Hurst (1980 and 1985).

with the previous methods (described earlier), the results are in agreement with compaction and apatite fission track analyses. Results with a similar order of magnitude (3km) have been derived for the Lossiemouth borehole **(Figure 5.27)** by Hurst (1985) where he states that the illite+chlorite assemblage in the shales is typical of maximum temperatures >90°C. However, Hurst (1985) also states that the spore colouration indices for the same area only suggest a temperature maximum of 60°C (2km of erosion). Consequently, even though there is doubt regarding the extent of erosion in the Lossiemouth area both estimates are of the same order of magnitude as those previous noted.

5.5 Conclusions.

(1) The geochemical data cited in this chapter provides consistent evidence for uplift and erosion in the Inner Moray Firth after the Late Cretaceous. The variety of methods employed suggests that uplift and erosion was of the order of 100s of metres and in some cases suggests that it may have exceeded 1km. Although the results can differ significantly between the methods, the overall picture can be taken with some confidence.

(2) Although capable of estimating the magnitude of uplift and erosion, modelling is unable to constrain the detailed uplift and erosion history of the basin. For example, the vitrinite reflectance modelling has shown that radically differing uplift and erosion paths can be fitted to the same dataset without the alteration of any other variables. Consequently, it is as yet not possible to determine the detailed history of uplift and erosion history of the basin and consequently suggest detailed models for its occurrence.

(3) The greater range in uplift and erosion estimates derived from vitrinite reflectance compared to the other methods described in this and previous chapters shows that vitrinite reflectance must be used with caution and preferably in conjunction with other techniques. The variation in the vitrinite reflectance estimates is in all probability due to the fact that the models currently employed do not match the complexities which exist in reality. Unlike the analysis of geochemical marker molecules which have simple kinetics, the kinetics of vitrinite reflectance are more detailed and probably not fully understood at present.

6. Comparison and implications of uplift and erosion estimates.

6.1 Introduction.

The previous three chapters have documented a substantial body of evidence suggesting that uplift and erosion occurred in the Inner Moray Firth after the Cretaceous. This chapter intends to clarify what each method was measuring and draw comparisons between their results in order to show that they are reasonably consistent. Additionally, the distinction between erosion and uplift will be discussed in relation to this data and the implications of these results.

6.2 Comparison of erosion estimates: apparent erosion versus total erosion.

In order for a meaningful comparison to be made of the data contained in the previous three chapters it must first be clarified what each method is measuring. In all cases the methods attempt to quantify the amount of stratigraphy removed from the area, that is erosion. Previously, the data has been referred to as uplift and erosion estimates but in reality all the methods measure either the amount of erosion that occurred or the amount of erosion that has not been reversed by subsequent burial and although uplift can be inferred (see section 6.3), the measurements do not directly reflect the true extent of uplift in the area.

As the methods measure differing physical/chemical properties, care must be taken in comparing the data. Firstly, the measurements based on sonic velocity data (Chapter 3) do not necessarily measure the full extent of erosion in the area because they rely on the measurement of overcompaction with respect to present burial-depth. Subsequent post-erosional burial will increase burial-depth and consequently reduce overcompaction with respect to present burial-depth and can eventually return the sediments to the normal compaction relation. Consequently, these estimates have been referred to as apparent erosion estimates. Apparent erosion is equal to the height above maximum burial-depth (with respect to sea-bed/land surface) of a given stratigraphic unit **(Figure 3.1)**. It is not necessarily the same as the amount of erosion that occurred when the unit was exhumed from its maximum burial-depth (total erosion). If renewed burial follows erosion, the magnitude of apparent erosion is reduced by the amount of that subsequent burial

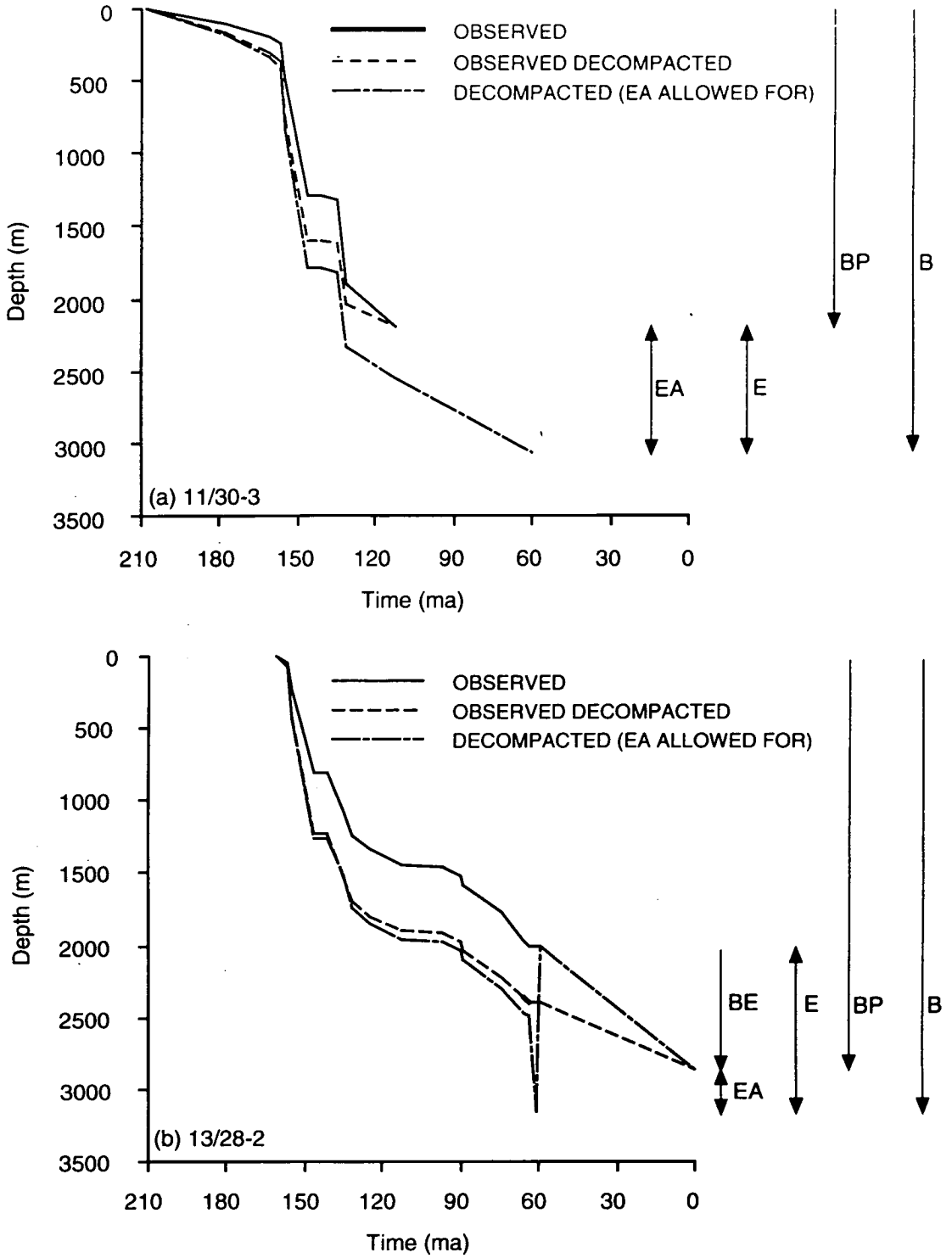

Figure 6.1 Present observed (solid) and decompacted burial histories for the base Jurassic in wells (a) 11/30-3 and (b) 13/28-2. The dashed plot is corrected for compactional effects without consideration of Danian erosion, whereas the dash and dot plots for both wells have been corrected for compaction with allowance for Danian erosion. The decompaction procedure was based on that of Sclater and Christie (1980). Ages were taken from the operator's composite logs and geochronologically calibrated using the timescale of Harland et. al. (1989). In both wells maximum burial-depth (B) equals present burial-depth (BP) plus apparent erosion (EA), i.e. B=EA+BP. In 11/30-3, there was no post-erosional burial, apparent erosion (EA) equals the erosion that occurred at he time the rocks were exhumed. However, in well 13/28-2 erosion at the time of exhumation equals apparent erosion (EA) plus the post-erosional burial (BE), i.e. E=EA+BE.

(Figures 3.1 and 6.1). Although overburden weight caused by burial following erosion does not cause further compaction until a unit exceeds its greatest burial-depth, the apparent erosion becomes smaller as the unit approaches its maximum burial-depth (Hillis, 1991).

In the western Inner Moray Firth Basin, where Jurassic - Lower Cretaceous sedimentary rocks crop out at or near the sea-bed, apparent erosion is equal to the magnitude of total erosion. The magnitude of apparent erosion decreases eastwards, under the cover of Tertiary sediments **(Figure 3.15)**. This means that apparent and total erosion are not necessarily the same in this area as an unconformity of mid-late Danian age exists within the Inner Moray Firth (Chapter 7), and this corresponds to the time of increased erosion rates over the Scottish Highlands. Therefore, it is possible that the exhumation from maximum burial-depth occurred at this time. Assuming Danian uplift and erosion, the correction for the effects of post-Danian burial gives total erosion estimates which not decrease significantly eastwards **(Figures 6.1 and 6.2(b) and Table 6.1)**. In the case of the reference well, since the apparent erosion is zero, it can only be said that erosion is less than the magnitude of post-Danian burial. However, it seems unlikely that erosion drops suddenly to zero in the vicinity of the reference well and may be closer to the maximum possible value than to zero if the assumption of Danian uplift is correct. Unfortunately, due to the thickness of the assumed post-erosional sequence, the extent to which Danian erosion may have extended into the Outer Moray Firth Basin and even the Viking and Central Grabens cannot be assessed.

Recently it has been proposed that the uplift and erosion episode responsible for the overcompaction with respect to present burial-depth in the Inner Moray Firth may have occurred during the Neogene (Becker, 1993). This time corresponds to the uplift and inversion of a number of basins in northwestern Europe (Jansen and Schmidt, in press; Japsen, 1993; Booth *et. al.*, 1993) and consequently seems a viable alternative to Danian erosion. As no Neogene/post-Neogene sediments are present in the Inner Moray Firth, Neogene uplift and erosion cannot be conclusively proved. However, if it is assumed that such a erosive episode occurred the apparent erosion estimates **(Figure 6.2(a))** are the same as the total erosion estimates **(Figure 6.2(c))** as no post-erosional burial would have reversed the overcompaction with respect to burial-depth. Hence, two possible patterns of total erosion appear possible. If Danian uplift and erosion is the cause, then approximately 1km of sediment was removed from most of the Inner Moray Firth and erosion extended at least into the Outer Moray Firth and possibly the Central and Viking Grabens However, if Neogene uplift was responsible then

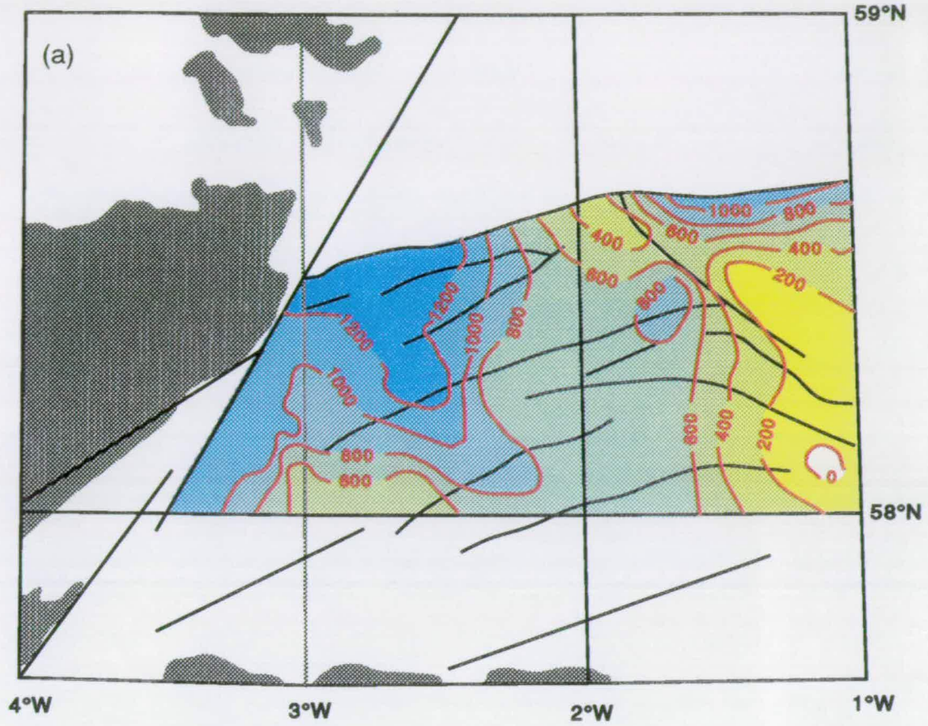

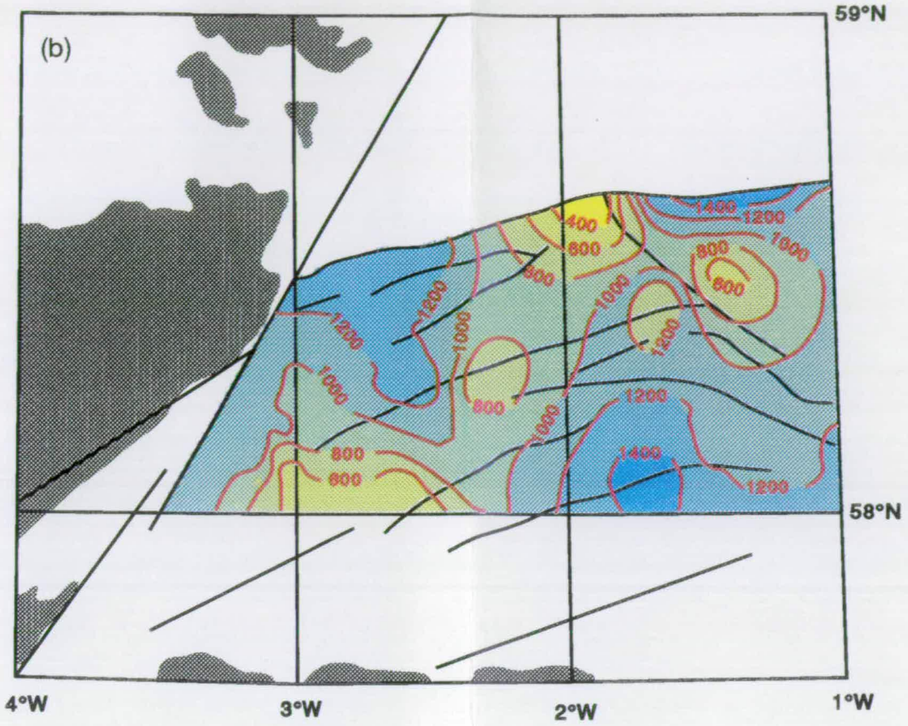

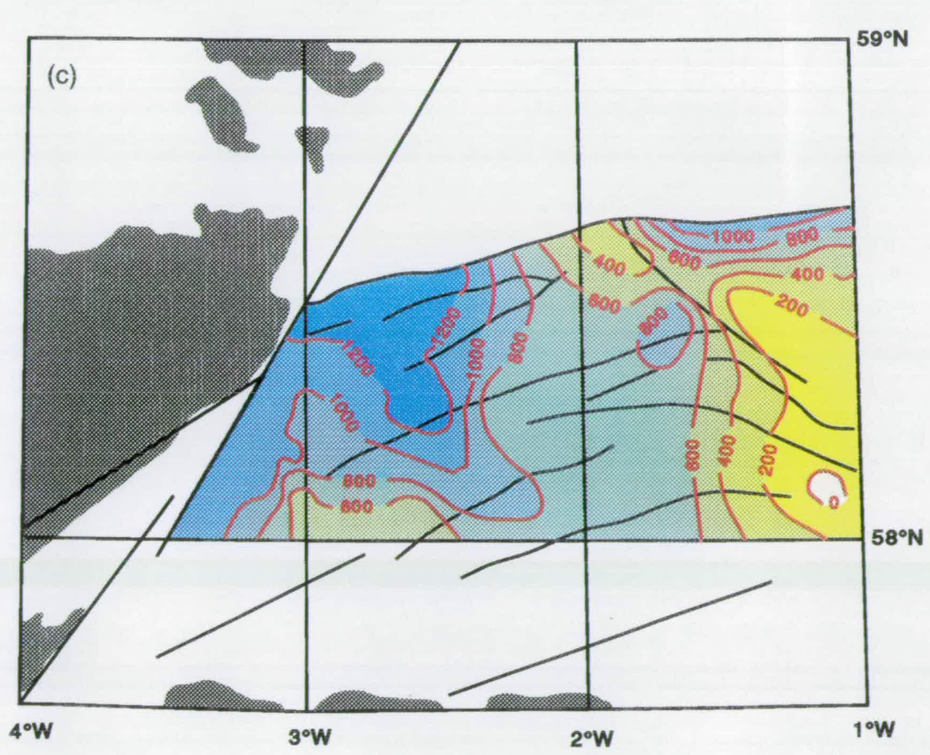

Figure 6.2 (a) Map of apparent erosion for the Inner Moray Firth based on sonic slowness in the Kimmeridge Clay Formation (i.e. the height above maximum burial-depth that has not been subsequently reversed by post-erosional burial). (b) Total erosion map assuming Palaeocene (Danian) uplift was responsible (i.e. apparent erosion plus the amount of post-erosional burial). (c) Total erosion map assuming Neogene uplift. Note that as no post-Neogene burial has taken place the total erosion map is the same as the apparent erosion map and that uplift and erosion values in the east are less than if Paleocene uplift is assumed.

Table 6.1 Apparent and total erosion (assuming Danian uplift) estimates fro the Inner Moray Firth based on the compaction evidence documented in Chapter 3.

Well	Kimmeridge Clay Fm		Hod Fm		Tor Fm	
	apparent erosion (m)	total erosion (m)	apparent erosion (m)	total erosion (m)	apparent erosion (m)	total erosion (m)
11/25-1	1099	1099				
11/30-1	577	577				
11/30-2	1056	1056				
11/30-3	926	926				
11/30-4	934	934				
11/30-5	921	921				
12/21-2	986	986				
12/21-3	972	972				
12/21-5	926	926				
12/22-2	1296	1296				
12/23-2	1204	1204				
12/24-2	654	654				
12/27-1	617	617				
12/27-2	449	449				
12/28-1	975	993				
12/29-1	937	957				
13/11-1	239	239				
13/12-1	402	692	693	983	694	984
13/12-2	897	1187				
13/13-1	894	1300	582	986	539	943
13/14-1			561	1036	430	905
13/17-1	895	1289	455	849	503	897
13/18-1	105	532	561	988	261	688
13/19-1			527	1074	385	1505
13/19-3			601	1318	419	1136
13/22-4			443	1259	451	1267
13/27-1	849	1498	537	1186	545	1194
13/28-2	340	1187	389	1236	420	1267
13/28-3	361	1172	440	1251	399	1210
13/29-1	297	1149	342	1194	375	1227
13/29-2	146	1054	465	1373	311	1219
13/29-3			304	1342	325	1363
13/30-1	41	1240	164	1363	80	1279
13/30-2	303	1477	138	1312	182	1356
13/30-3	0	1208	0	1208	0	1208

erosion reached a maximum of 1km in the west of the basin and gradually decreases eastwards to zero near the Outer Moray Firth boundary.

Apatite fission track analysis (Chapter 4) provides information as to the thermal history of a sample and is a temperature-based system as opposed to the mechanical compaction described in Chapter 3. Unlike compaction-based analyses, it is possible to determine the full extent of an erosive episode even if burial has occurred subsequently. As the modelling of fission track ages and track length distributions produces estimates of palaeotemperatures and palaeotemperature changes these can be related to distinct heating and cooling events. Additionally, as fission track data can in some cases provide palaeogeothermal gradient data, it is possible to distinguish between cooling by erosive episodes and cooling due to a lowering of the thermal state of the area **(Figure 6.3)**. In this case no palaeogeothermal gradient evidence was available. However, the widespread nature of the elevated temperatures and their compatibility with compaction data from the adjacent Inner Moray Firth suggests erosion was the prime cause of the cooling. Consequently, the uplift and erosion estimates (given in Chapter 4) can be taken as the true extent of erosion for the Scottish Highlands (i.e. total erosion).

The vitrinite reflectance data (documented in Chapter 5) was analysed by two distinct methods. Firstly, the vitrinite reflectance trend method relied on the progressive increase in vitrinite reflectance with depth and the fact that surface measurements should be 0.2%. This method can be considered analogous to the compaction studies (Chapter 3) as it effectively measures overmaturity with respect to present burial-depth while the compaction method measures overcompaction with respect to present burial-depth. Consequently, the estimates of uplift and erosion are apparent erosion estimates and not necessarily total erosion estimates. However, for all the wells except 12/30-1 no post-erosional sediments are present and consequently these apparent erosion estimates are also total erosion estimates. For well 12/30-1 the apparent erosion estimate needs to be corrected for post-erosional burial. Unfortunately, unlike compaction which does not proceed when sediments are above their maximum burial-depth, the maturation process continues and consequently the vitrinite reflectance-depth trend has been subsequently modified by post-erosional burial. this means that the apparent erosion estimate for well 12/30-1 .cannot be adjusted to become the total erosion estimate and the best that can be said is that total erosion must have been at least as much as apparent erosion.

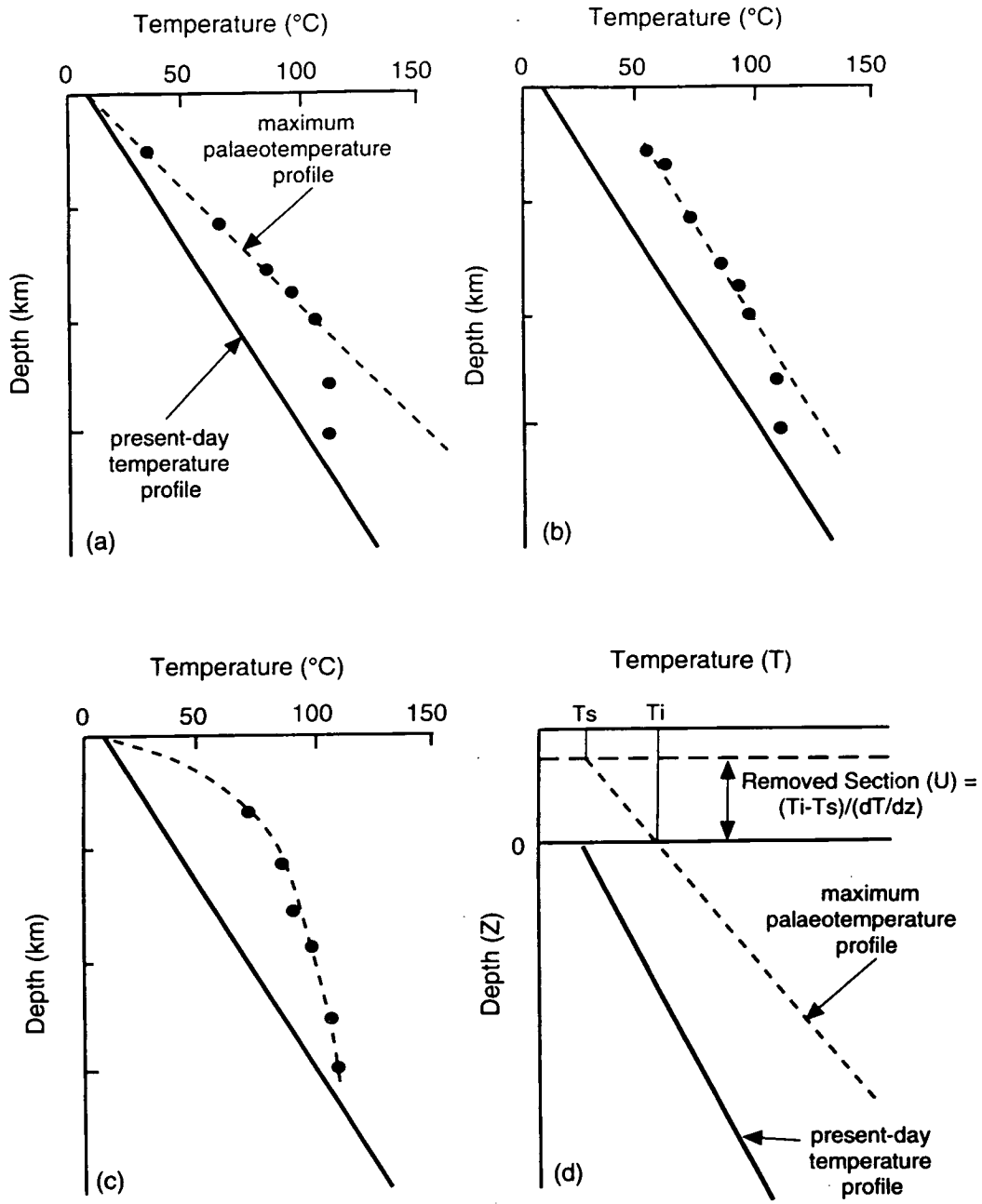

Figure 6.3 Hypothetical cases to illustrate estimation of palaeogeothermal gradients and the cause of heating and subsequent cooling, from palaeotemperature profiles. In each case a palaeotemperature profile derived from apatite fission track analysis is shown, and the data indicate that the section has been hotter in the past; (a) Shows a case where heating is caused by increased basal heatflow in the past. The paleotemperature estimates show an increased palaeogeothermal gradient; (b) Shows a case where heating in the past was caused by deep burial prior to cooling by uplift and erosion. The palaeotemperature estimates show a profile similar to the gradient of the present-day profile, and thus do not allow an explanation of heating in terms of increased heat flow. In this case the amount of removed section can be estimated by dividing the amount of cooling by the geothermal gradient; (c) Shows a case in which heating in the past was due to the passage of heated fluid through the shallow part of the section. The palaeotemperature estimates show a palaeogeothermal gradient which is lower than the present value; (d) Illustrates the method of calculating the removed section in the general case where heating was due to a combination of deeper burial and increased palaeogeothermal gradient. After Bray et. al. (1992).

For the modelling of vitrinite reflectance extra stratigraphy was added to the model and subsequently removed in order to represent the lost section. The estimates of erosion in this case are total erosion estimates. The same can be said for the majority of the work carried out by Duncan (1986) as a similar technique was applied to different maturity indicators. However, in the case of pristane isomerisation the difference between present and expected temperatures were used to measure of erosion. Technically these are apparent erosion estimates as if post-erosional burial has occurred the present temperature would be greater than that immediately after erosion. However, as no post-erosional burial has occurred apparent erosion estimates obtained from the pristane data are the same as total erosion estimates.

Once the difference between apparent and total erosion is established, and apparent erosion converted to total erosion, a direct comparison between the differing methods can be made. The compaction-based estimates vary between 400 and 1400m if Danian uplift is assumed, and show no regional trend. Local maxima occur to both the west and east. If Neogene uplift is assumed then estimates vary between 0 and 1200m decreasing steadily eastwards. These values compare well with the apatite fission track analyses of the Scottish Highlands as around the Inner Moray Firth margins the estimates are generally about the same (c.f. **Figures 6.2 and 4.13**).The Neogene estimates compare particularly well as they show the same westward increase in estimates as the Scottish Highlands data. Therefore, these datasets are mutually supportive for the existence of Tertiary erosion although the Scottish Highlands data suggests the Late Cretaceous/Early Tertiary for the onset of erosion while the Inner Moray Firth suggests that the erosive episode could be Danian or Neogene.

Less conclusive, but supportive evidence can be gained from vitrinite reflectance studies. Offshore, the vitrinite reflectance trend method produces estimates of the right order of magnitude but generally smaller than seen in the compaction data **(Table 5.2b)**. Although the data also shows no geographical trend it cannot be seen to support the Danian erosion as the fragility of a method which produces negative erosion estimates means that it must be used with a large degree of caution. Onshore, the vitrinite reflectance trend method produces estimates more closely resembling those seen from both compaction and apatite fission track analyses **(Table 5.3)**. As for the modelling of vitrinite reflectance data, the estimates of erosion are less well constrained, but seem to suggest around 500m of stratigraphy may have been removed. Consequently, it appears that vitrinite

reflectance data can provide supportive evidence for both the compaction and apatite fission track analyses but it is generally less consistent than them.

Finally the geochemical evidence of Duncan (1986) seems to suggest the removal of 500-1500m of section from the Inner Moray Firth, possibly decreasing eastwards. As such estimates were determined by examining a variety geochemical processes, their self consistence and similarity with compaction and apatite fission track analyses suggest that these values must be close to the actual amount of erosion that occurred in the area.

The data discussed here, and presented in the previous three chapters, all seems to suggest that up to 1.5km of stratigraphy was removed from the Inner Moray Firth since the Cretaceous and that the Scottish Highlands were also affected, but to a larger degree. Some of the implications of this large scale, regional erosion will be discussed in the following sections. The potential methods for the generation of such an erosive episode will be dealt with in Chapter 8 after the structural and tectonic evidence (Chapter 7) has been dealt with.

6.3 Tectonic uplift versus erosion.

England and Molnar (1990) and Brown (1991) have highlighted the distinction between three different measures of "uplift": uplift of the surface with respect to the geoid; uplift of rocks with respect to the surface (i.e. erosion); and the displacement of rocks with respect to the geoid. Of these three quantities only surface uplift is associated with work done against gravity and hence, this is the relevant value for studies of tectonic controls on uplift **(Figure 6.4)**.

Since only regional uplift of the earth's surface with respect to the geoid (as opposed to erosion, or the uplift of rocks with respect to the geoid) demonstrates work done against gravity, it is necessary to prove regional surface uplift to invoke isostatic forces requiring uplift (England and Molnar, 1990). As in the Inner Moray Firth marine, or near-marine sediments were deposited before and after erosion, it seems reasonable to infer that erosion was associated with uplift of rocks with respect to the geoid (which here approximates sufficiently well to sea-level), as opposed to base-level change. Since erosion and hence the inferred uplift of rock in the Inner Moray Firth occurred over some 10^4 km^2 with the eroded material not being deposited within the Inner Moray Firth regional uplift of the surface is inferred. For the Scottish Highlands the long-lived nature of the erosive episode

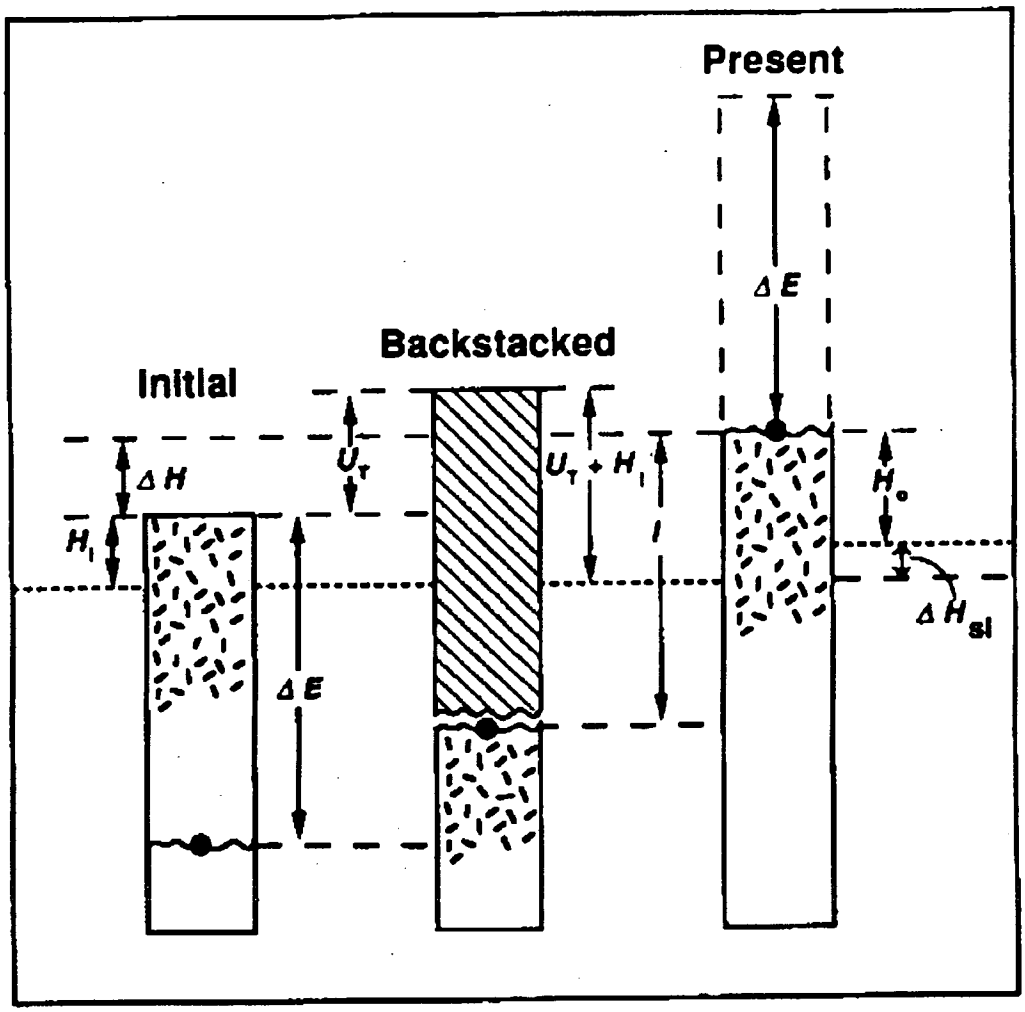

Figure 6.4 Summary diagram of the relation between the various components of uplift histories. UT is the tectonic uplift component, I is the isostatic rebound component, Ho is the present-day elevation of the mean surface, E is the mean section removed by erosion, H is the net change in surface elevation, Hi is the elevation of the initial mean surface and Hsl is the change in sea level relative to initial sea-level. After Brown (1991).

(Late Permian/Early Triassic onwards) would tend to suggest that for a substantial part of this time, surface elevations were fairly constant and that the uplift of rocks with respect to the surface was due to erosion, the widespread nature of the erosion again suggests regional uplift of the surface. This seems particularly true for the Late Cretaceous/Early Tertiary onwards when erosion rates appear to increase and the most feasible way to achieve this is to invoke tectonic driving forces.

If uplifted crust is eroded, isostatic rebound resulting from gravitational unloading will amplify the initial (tectonic) uplift (U_T) according to the relation:

$$U_E = U_T \quad \frac{r_m}{(r_m - r_s)} ,$$

where U_E is the total magnitude of erosion;

r_m is the density of the mantle (approximately 3.3 gcm^{-3});

r_s is the density of the eroded sediment (approximately 2.2 gcm^{-3}).

Hence, the erosion of 1km in the Inner Moray Firth and up to 2km in the Scottish Highlands requires a tectonic uplift of only $\frac{1}{3}$ km and $\frac{2}{3}$ km respectively.

6.4 Implications for sediment decompaction and maturation modelling.

Sediment decompaction is a widely performed technique which aims to restore the original thickness of buried and compacted stratigraphic units (e.g. Sclater and Christie, 1980; Falvey and Deighton, 1982). In order to restore the original thickness of a stratigraphic unit its normal porosity/depth relation must be determined. Restored thicknesses are calculated from the porosity increase as the unit is raised from its present burial-depth, up the normal porosity/depth relation, to the surface. In areas such as the Inner Moray Firth, where sediments are not at their maximum burial-depth, this procedure is more complex than in areas where sediments are at their maximum burial-depth. Firstly, a normal porosity/depth relationship will not simply be an average one for the area. It should be determined only from wells at their maximum burial-depth. Secondly, a unit must be added to the observed stratigraphy in order to allow for the effect of the eroded sediments. Units deposited prior to the erosion will decompact more (i.e. increase in thickness more) than if allowance is not made for the eroded sediments. Furthermore, if the sequence is not at its maximum burial-depth then the units deposited after erosion (in this case the Tertiary) will not cause further compaction of the older units (in

this case the pre-Tertiary). For example, in the eastern Inner Moray Firth, pre-Tertiary units acted as compaction basement during Tertiary burial associated with deposition of the post-erosional sequence if Danian erosion is assumed **(Figure 6.1)**.

A burial-history plot for sediments not at their maximum burial-depth which allows for erosion predicts greater palaeo-burial depth for any unit deposited prior to erosion than a plot that ignores erosion **(Figure 6.1)**. Hence, combining any given model of palaeo-heatflow with a burial-history plot for potential hydrocarbon source that allows for erosion will predict a higher level of organic maturity than the same palaeo-heatflow model combined with a subsidence plot that does not account for erosion.

6.5 Implications for the burial history of the Inner Moray Firth.

The evidence that units in the Inner Moray Firth are not at their maximum burial-depth has an even more profound effect on the modelling of pre-erosional subsidence of the basin than the implications for the sediment decompaction procedure. Since units were exhumed from their maximum burial-depth during the Tertiary, they must have attained their maximum burial-depth prior to this time. The actual magnitude of burial prior to Tertiary times equals the observed burial plus the apparent erosion **(Figures 3.1 and 6.1)**. Hence Cenozoic, post-rift subsidence in the Inner Moray Firth was both of greater magnitude, and more rapid than suggested by the preserved stratigraphy.

The results of this thesis suggest that eastwards thickening of Upper Cretaceous and Tertiary post-rift sediments deposited during the thermal phase of basin subsidence in the Inner Moray Firth Basin is largely the result of post-depositional erosion (*contra* Roberts *et al.*, 1990). The previous interpretation (Roberts *et. al.*, 1990) relied on the strike-slip model for the formation of the basin and so predicted no Cretaceous and Tertiary thermal subsidence in the Inner Moray Firth, while areas to the east, which had been formed by extension, underwent thermal subsidence.The resultant effects of these differing subsidence regimes was suggested to be a general easterly tilting of the Moray Firth and the erosion of sediments in the western Inner Moray Firth (Roberts *et. al.*, 1990).

6.6 Upper Cretaceous Chalk distribution, thermal subsidence history and basin formation models: the implications of erosion estimates.

The evidence that 1km of sediment is missing from the Inner Moray Firth has profound implications for the depositional history of the area, the manner in which it subsided and ultimately challenges previously proposed models for the formation of the basin. As 1km of sediment was removed at some time during the Tertiary, and the current sea-bed consists of Upper Jurassic and Lower Cretaceous sediments, the removed section must have consisted of Lower Cretaceous, Upper Cretaceous and possibly Tertiary sediments. As the Cretaceous sediments preserved in the western and eastern Inner Moray Firth consist of onlapping deposits which drape pre-existing topography (Thomson and Underhill, 1993) and have depocentre locations different from the Jurassic (Andrews *et. al.*, 1990; Roberts *et. al.*, 1990), they have been interpreted as being the result of thermal subsidence (Thomson and Underhill, 1993). Consequently, it seems reasonable to assume that the missing 1km of stratigraphy in the Inner Moray Firth consists of similar thermal subsidence deposits. This contrasts with many previous interpretations which suggest that the Inner Moray Firth did not undergo Mesozoic thermal subsidence on account of its being an isostatically uncompensated strike-slip basin (McQuillin *et. al.*, 1982; Barr, 1985; Bird *et. al.*, 1987; Roberts *et. al.*, 1990). This suggestion is based on the regional gravity interpretation of Donato and Tully (1981) which shows a residual negative gravity anomaly over the Inner Moray Firth **(Figure 6.5)** which in turn has to be taken to imply that the basin lies on unthinned lithosphere and formed as a result of upper crustal extension. Although the presence of such an anomaly cannot be disputed, the interpretation is open to question particularly in the light of seismic refraction studies which indicate that the area has experienced significant crustal thinning (Smith and Bott, 1975) and the structural evidence presented in previous chapters. Indeed, the magnitude of crustal thinning (23km) is comparable with that seen in the Witch Ground Graben (Andrews *et. al.*, 1990). Consequently, as the Inner Moray Firth must have undergone Mesozoic thermal subsidence it appears that the previously proposed models of a strike-slip origin for the basin must be discarded.

As it appears likely that thermal subsidence deposits existed in the eastern Inner Moray Firth during the Upper Cretaceous, at the same time that the adjacent Scottish Highlands were undergoing erosion, it is possible to suggest what the depositional pattern may have been. Firstly, as Chalk was being deposited in the Outer Moray Firth (Andrews *et. al.*, 1990) it appears highly likely that such deposits must have occurred further east. Additionally, as the Scottish Highlands

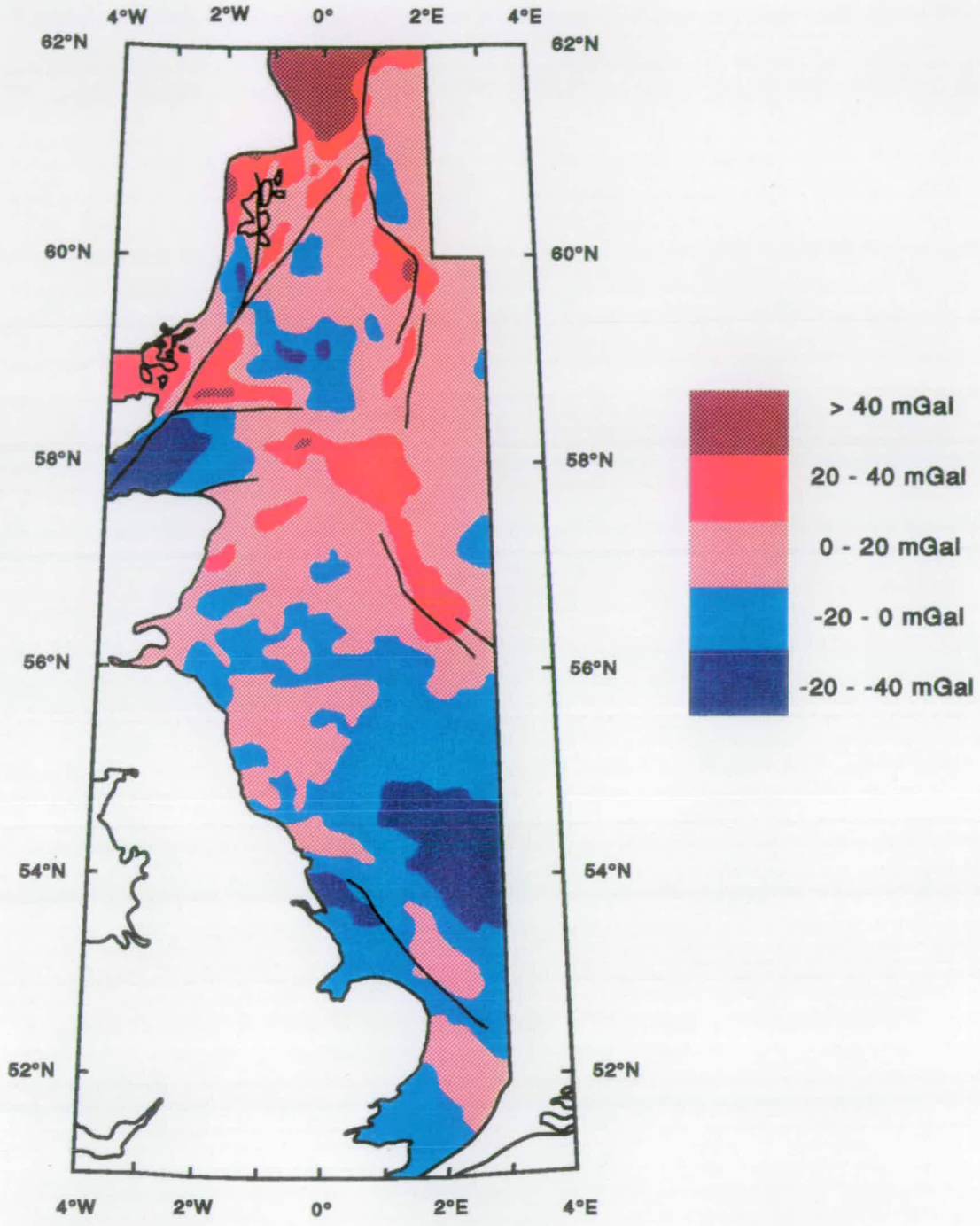

Figure 6.5 Simplified Bouger anaomaly map of the UK North Sea (Donato and Tully, 1981). Note the large negative anomaly over the Inner Moray Firth. This has been taken as evidence that the basin lies on unthinned continental lithosphere and consequently could not have formed as an extensional basin. However, seismic refraction studies (Smith and Bott, 1975) show that the lithosphere is thinned and consequently lithospheric extension appears to be responsible for the presence of the basin.

were shedding sediment, which in view of the lithologies was most likely to be sandy in composition, it is conceivable that some of it must have reached the basin. A picture therefore emerges of sand-rich deposits along the basin margins and finer grained sediments distal (eastward) to it which eventually merged with the chalk in the west. Such an interpretation also questions the history of the Helmsdale Fault. As the Inner Moray Firth was undergoing subsidence at the same time as the Scottish Highlands were being uplifted and eroded a transition zone or surface is required to accommodate these relative movements. This could be achieved by locally flexing the crust but it appears more likely that the Helmsdale Fault could have been active as a normal fault. This would then suggest that the fault had been active more or less continuously during the Upper Jurassic, Cretaceous and Early Tertiary (see next chapter).

6.7 Conclusions.

(1) A substantial body of evidence exists to suggest that a maximum of approximately 1.5km of sediment was removed by erosion from the Inner Moray Firth and that this either occurred at the mid-late Danian unconformity or during the Neogene. If the erosion occurred in the Danian then it was fairly constant over the entire area with local maxima both in the western and eastern parts of the basin and may have even affected the Viking and Central Grabens. However, if erosion occurred in the Neogene then it decreased towards the east, reaching zero close to the Outer Moray Firth. Additionally, evidence from the Scottish Highlands suggests a similar amount of erosion occurred along the basin margins and that this increased to the west reaching approximately 2km over the Outer Hebridies.

(2) The large regional extent of the erosive episode would tend to imply that surface uplift and consequent erosion was responsible as opposed to a sea level change. As surface uplift with respect to the geoid represents quantifiable work done against gravity it is necessary to invoke tectonic forces to drive it. Consequently, the erosive episode must have been tectonically driven. In order to remove 1km of sediment from the Inner Moray Firth and up to 2km from the Scottish Highlands the tectonically driven uplift must have been approximately $\frac{1}{3}$ km and up to $\frac{2}{3}$ km respectively.

(3) As Upper Jurassic and Lower Cretaceous sediments are present at the sea-bed and up to 1km of sediments were removed from the area during the Tertiary, the removed sediments must have been Cretaceous and possibly Tertiary in age. The preserved Cretaceous sediments in both the Inner and Outer Moray Firth drape pre-existing topography and show prominent onlap patterns indicative of thermal subsidence deposits. Consequently, it can be assumed that the removed stratigraphy was probably deposited in a thermal subsidence regime and consequently the area must have contained in excess of 1km of thermal subsidence deposits. The presence of such a large thickness of thermal subsidence deposits is incompatible with the previously proposed strike-slip models for basin formation. Consequently, it appears most likely that the basin formed as result of extension and the consequent thermal subsidence provided space for the now missing stratigraphy.

(4) Apatite fission track analysis of the Scottish Highlands suggests that the area was experiencing uplift and consequent erosion during the Cretaceous, at the same time as the Inner Moray Firth was subsiding. Such differential movement requires a transitional zone or surface to accommodate it and consequently it appears possible that the Helmsdale Fault may have been active at this time. Additionally, as the Scottish Highlands were shedding clastic detritus it is highly likely that some of this reached the Inner Moray Firth. Consequently, it seems possible that clastic sedimentation occurred in the western Inner Moray Firth during the Upper Cretaceous while chalk was deposited to the east, the western limit of chalk deposition lying west of it's current subcrop.

7. Tertiary structural reactivation.

7.1 Introduction.

Seismic reflection profiles in the Inner Moray Firth **(Figure 7.1)** show that many of the major structural elements of the area experienced localised reactivation after the Cretaceous as part of the regional events already documented. Indeed, some show faults cutting through Cretaceous sediments to sea-bed. This chapter intends to document the varied styles of structural reactivation seen in the Inner Moray Firth so that they can be combined with the erosion estimates previously described to test potential models which could account for the phenomena (Chapter 8).

7.2 Extensional reactivation.

Of all the reactivation styles in the Inner Moray Firth extension appears to be the most common, with the majority of this activity was centred on the pre-existing Upper Jurassic half-graben bounding faults (e.g. the Wick, Smith Bank and Lossiemouth faults). As these faults cut through to sea-bed, their histories must have included a period of late-stage activity. Where Tertiary sediments are preserved, seismic sections **(Figure 7.2)** show that some of this activity must have occurred at least in the Early Tertiary.

However, whether this late-stage activity was tectonically-driven is open to question in the light of observations that the majority of seismic sections across the major half-graben bounding faults show shallow synclinal structures present in their hangingwall basin fills **(Figure 7.3)** and steeply upturned beds immediately adjacent to the faults (Prosser, 1991). Such geometries can be readily interpreted as being the result of differential compaction over an irregular half-graben topography (Thomson and Underhill, 1993). By backstripping and decompacting the basin fill Prosser (1991) was able to demonstrate that the geometries in the areas of the Lossiemouth and Smith Bank faults could be accounted for by the process of compaction **(Figure 7.4)**. As such geometries can be seen on seismic sections across most of the major Mesozoic extensional structures within the basin, and in outcrop at Dun Glas (Grid Reference ND 057172; **Figure 7.5**), it can be readily appreciated that compaction could have accounted for the majority of the fault activity in the area. However, as the modelling undertaken by Prosser (1991) contains large potential margins of error and did not decompact the chosen units from

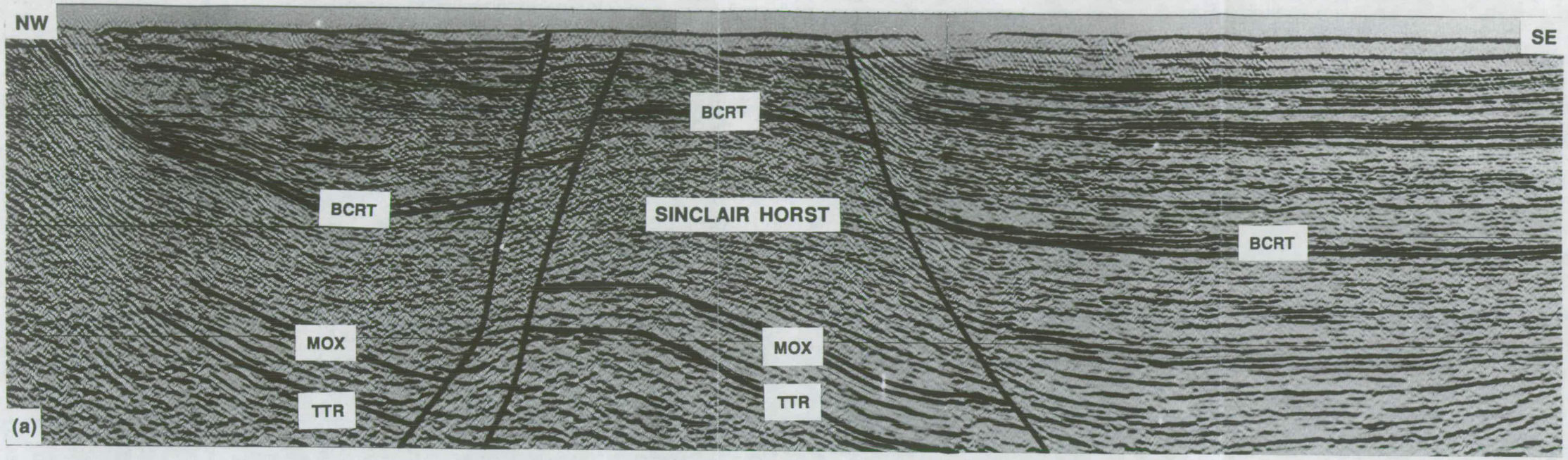

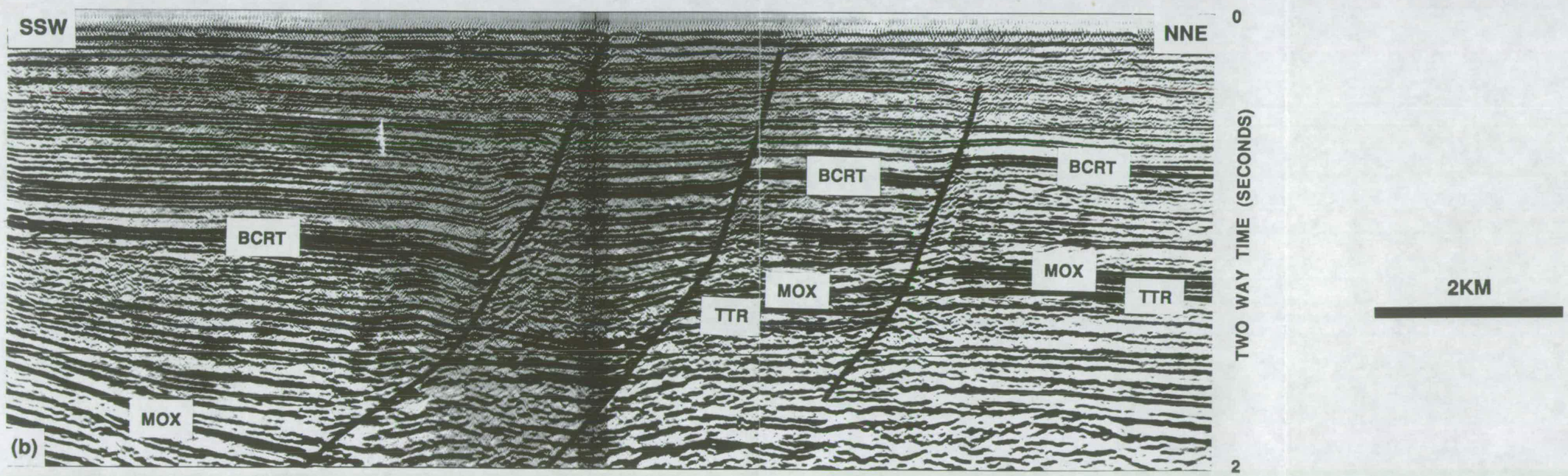

Figure 7.1 Seismic reflection profiles (locations shown in **Figure 7.7**) showing Mesozoic faults which have been subsequently reactivated to cut through Cretaceous sediments to sea bed. BCRT = Base Cretaceous, MOX = Mid Oxfordian Unconformity and TTR = Top Triassic.

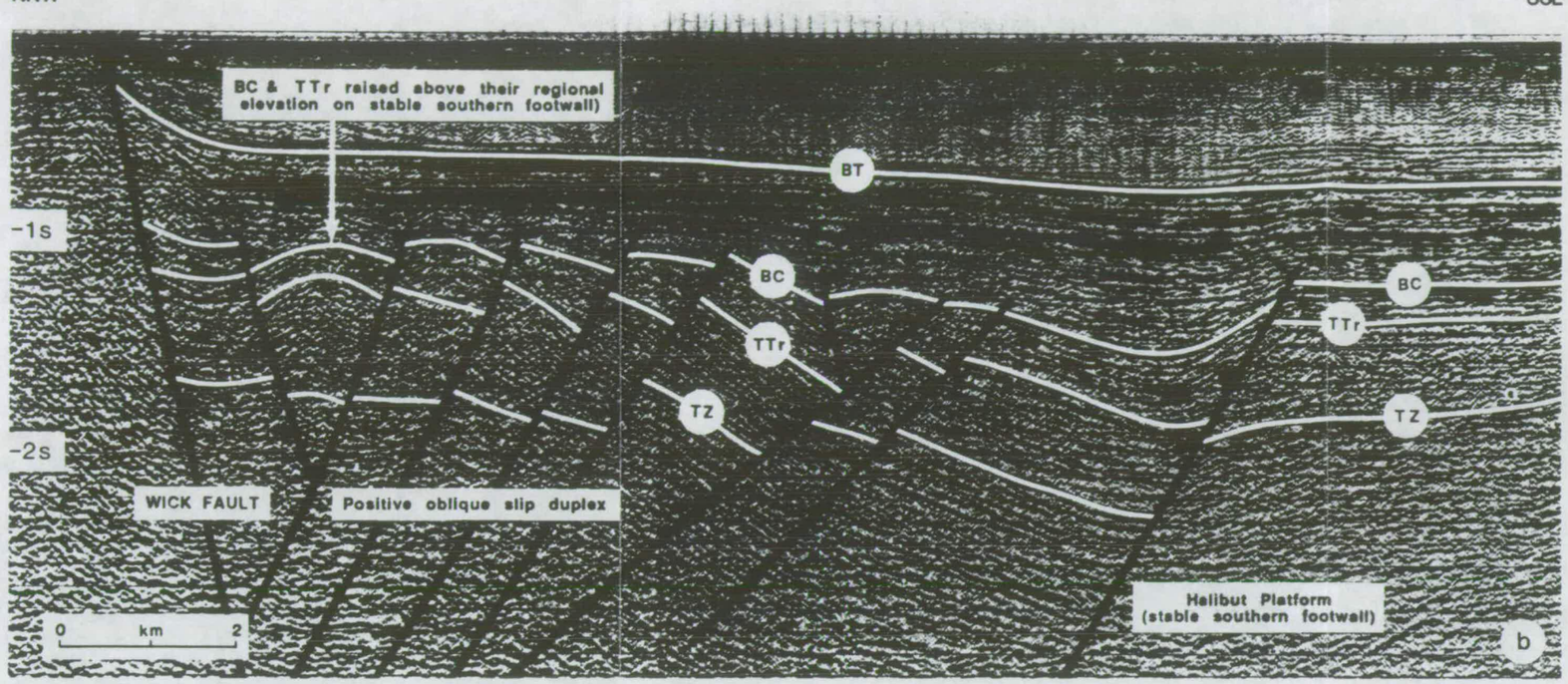

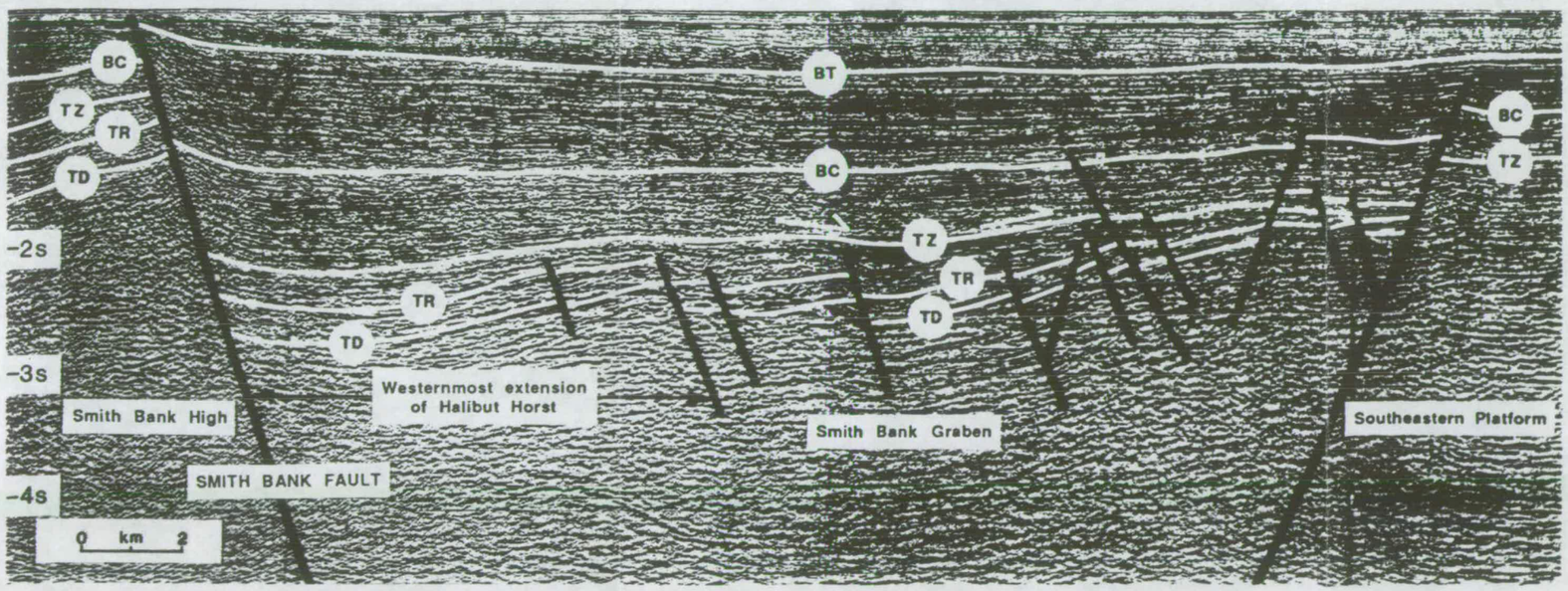

Figure 7.2 Seismic reflection profiles from the eastern Inner Moray Firth (Roberts *et. al.*, 1990). The lines show that both the Wick and Smith Bank faults affect the base of the Tertiary and consequently must have experienced some activity during the Early Tertiary or later.

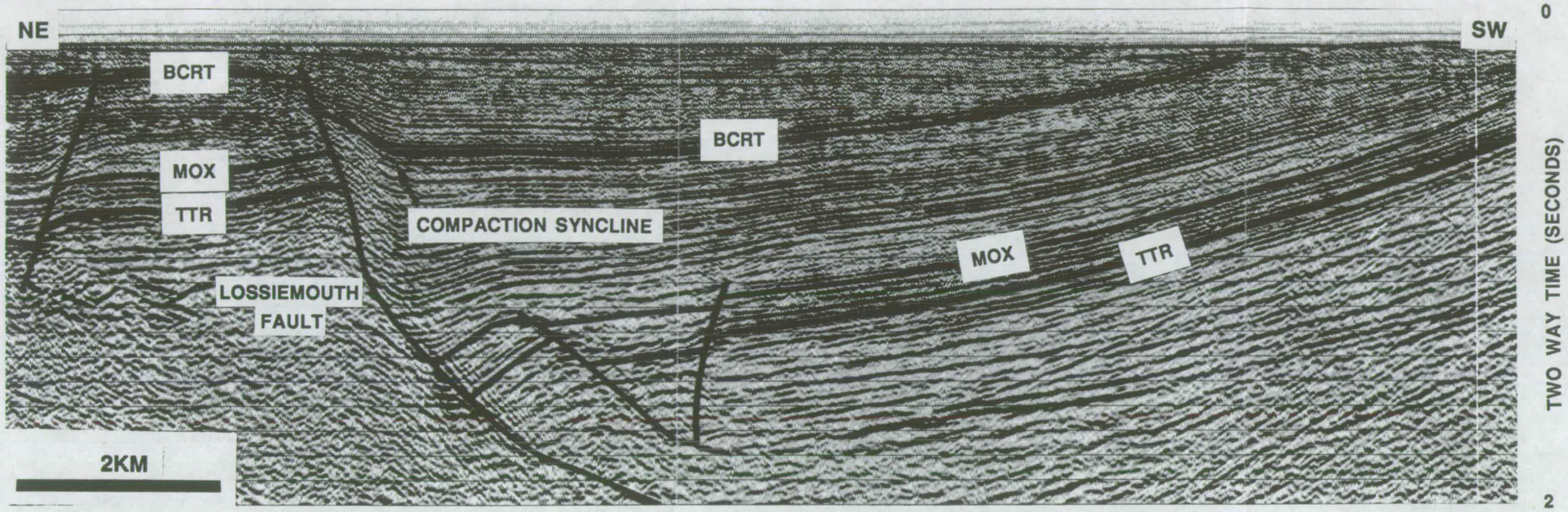

Figure 7.3 Seismic reflection profile (location shown in **Figure 7.7**) across the Lossiemouth Fault showing a hangingwall syncline formed as a result of differential compaction of the half graben fill. BCRT = Base Cretaceous, MOX = Mid Oxfordian Unconformity and TTR = Top Triassic.

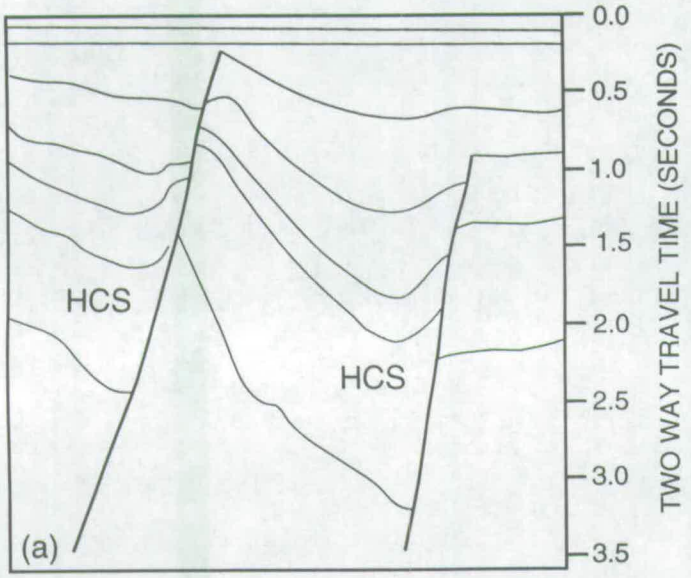

Figure 7.4 Origin of hangingwall compaction synclines. (a) Sketch of a seismic reflection profile of the Smith Bank Fault showing prominent hangingwall compaction synclines (HCS). (b) Depth-converted and progressively backstripped with allowance for compactional effects the same profile shows that the prominent compaction synclines are gradually reduced in magnitude and can eventually be removed. This suggests that the synclinal structures seen in the hangingwall of most of the major half-graben bounding faults in the Inner Moray Firth are compatible with compaction being the main cause. Additionally, the majority of the post-Cretaceous activity on these faults may also be caused by compactional effects (After Prosser, 1991).

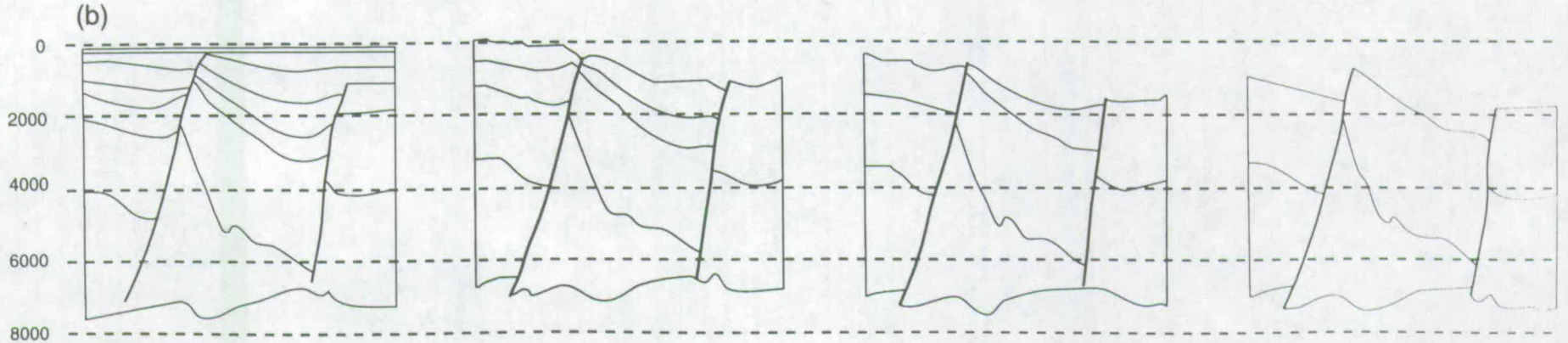

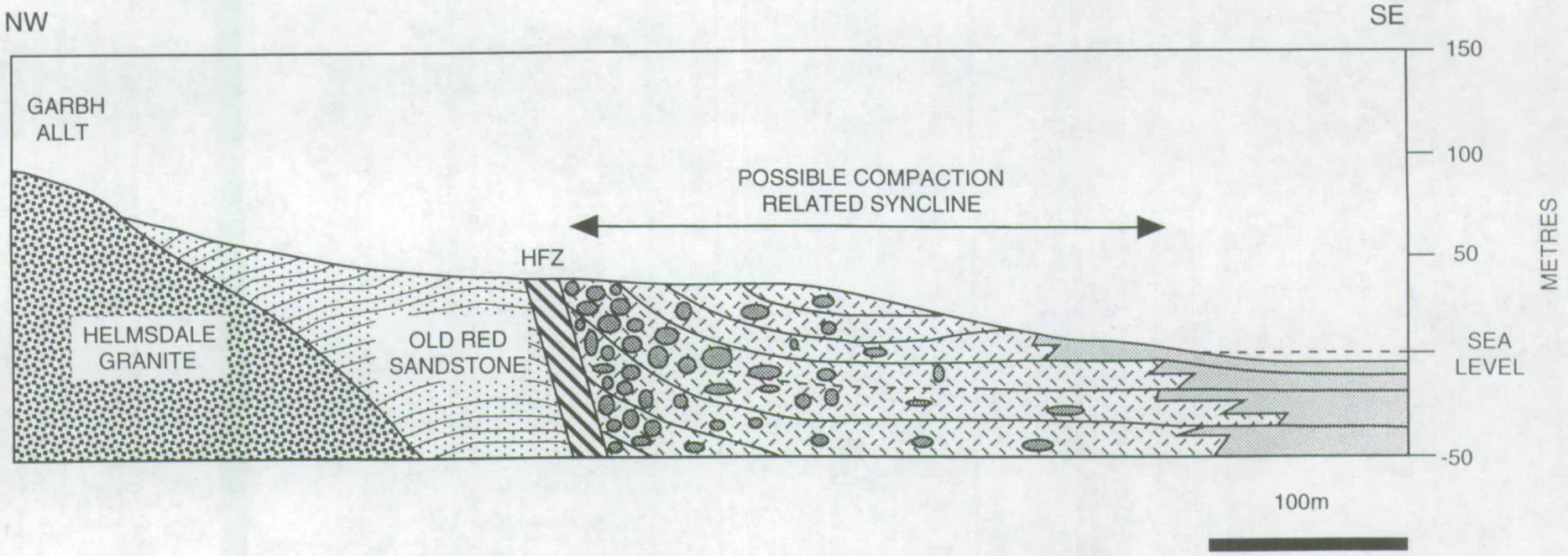

Figure 7.5 Cross-section across the Helmsdale Fault Zone (HFZ) highlighting the increase in the unusually steep dip to beds immediately adjacent to the fault, believed to be the result of compaction. After MacDonald (1985).

their maximum burial-depth, and so underdecompacted them (see Section 6.4), a substantial tectonic component cannot be ruled out.

To further complicate the picture a second population of extensional faults exists **(Figure 7.6)** which form the Sinclair Horst **(Figure 7.7)**. Although such faults have similar orientations to the major half-graben bounding faults, seismic reflection profiles **(Figure 7.6)** demonstrate that these faults are neither syn-rift nor compaction-related. They displace syn-rift and thermal subsidence deposits by similar amounts and show no compaction synclines. These faults must have been active after the Cretaceous as they displace Cretaceous sediments and no signs of earlier activity are evident. Hence, these faults probably formed as a new population of post-Cretaceous faults which were tectonically-driven, suggesting that some of the activity on the faults with obvious compaction components may have had a tectonic origin.

7.3 Inversion.

Most discussions of the evolution of the Inner Moray Firth ignore the existence of compressional structures (McQuillin *et. al.*, 1982; Barr, 1985; Andrews and Brown, 1987; Bird *et. al.*, 1987; Frostick *et. al.*, 1988, Roberts *et. al.*, 1990, Andrews *et. al.*, 1990). However, Underhill (1991 a and b) and Thomson and Underhill (1993) have documented the presence of inversion structures close to the intersection of the Great Glen and Wick faults **(Figure 7.8)**. The inversion structures include a hangingwall anticline and an associated "short-cut" fault. As compressional stresses increased, buttressing against the footwall resulted in the development of the "short-cut" fault. As Cretaceous sediments are affected by the inversion and the associated faults cut through to seabed the inversion must have occurred after Cretaceous times.

Probably the most significant inversion structure seen in the Inner Moray Firth is the large fold in UKCS license block 11/25 **(Figure 7.9)**. This fold displaces Cretaceous sediments showing that it must have formed after this time. To the west the fold is bounded by the Great Glen Fault, while to the east it is limited by a late stage extensional fault **(Figure 7.9)**. This fault cuts through to sea-bed and although it dips steeply towards the Great Glen Fault close to the surface, it flattens out rapidly with depth. The fold appears to have formed as a result of extension on the late stage fault causing the basin fill between it and the Great Glen Fault to be

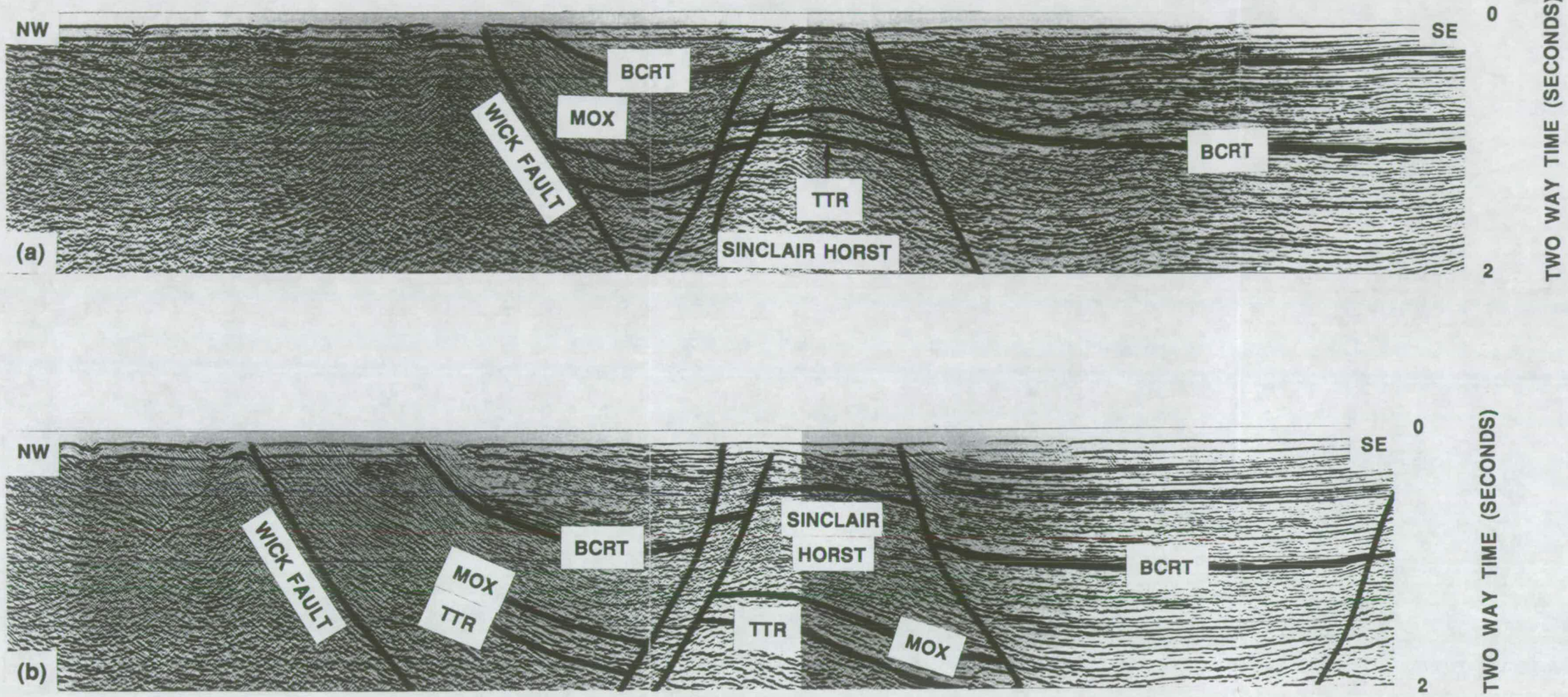

Figure 7.6 Seismic reflection profiles (locations shown in **Figure 7.7**) across the Sinclair Horst. As no discernible thickening across these faults exists, and there are no compaction geometries, it appears likely that they are not syn-sedimentary structures but form a new population of post-Cretaceous faults formed during the reactivation of the basin. BCRT = Base Cretaceous, MOX = Mid Oxfordian Unconformity and TTR = Top Triassic.

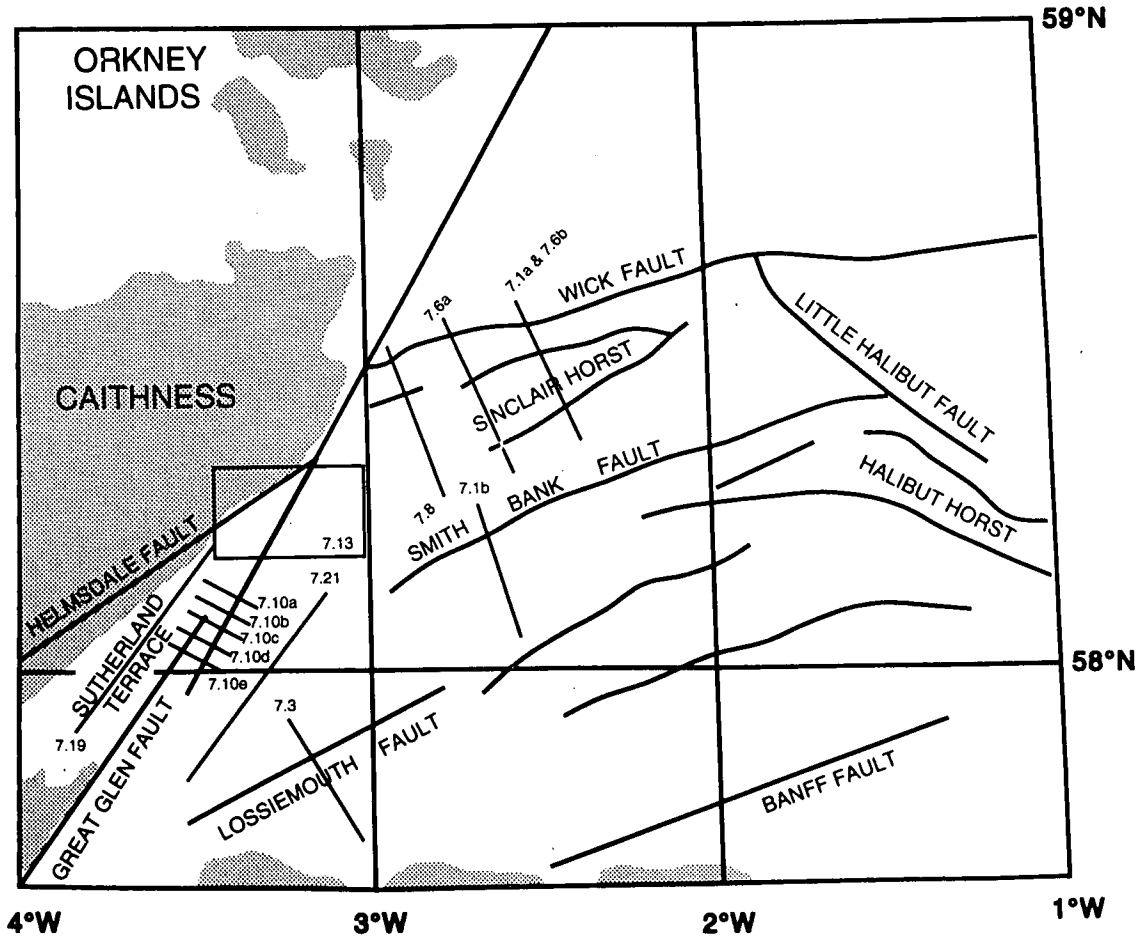

Figure 7.7 Map showing the locations of seismic reflection profiles in other figures.

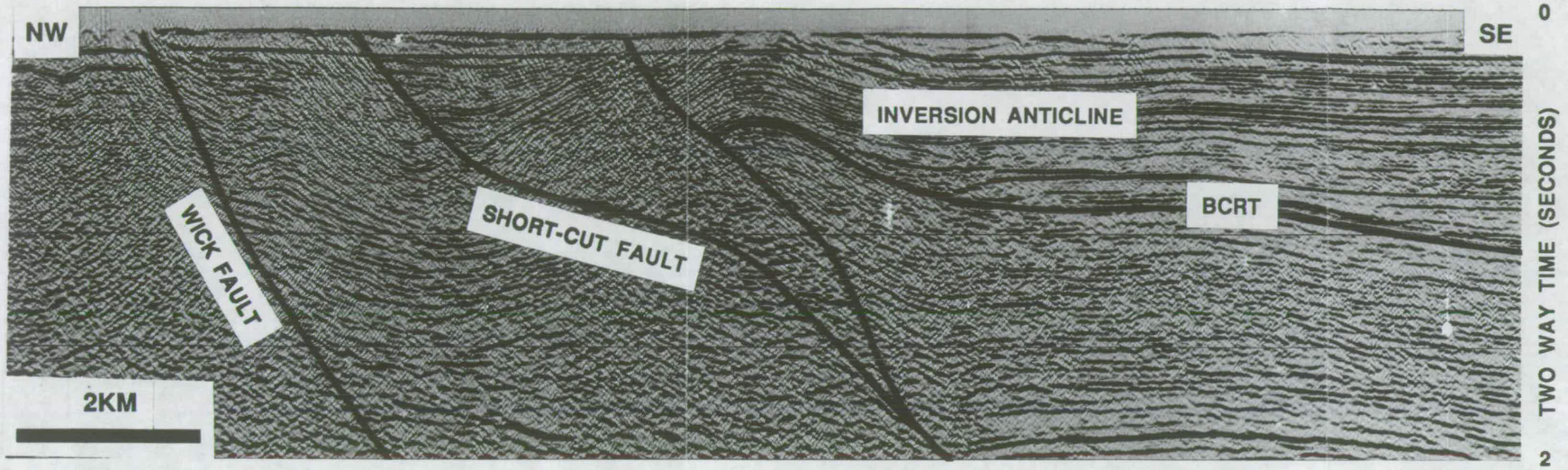

Figure 7.8 Seismic reflection profile (location shown in **Figure 7.7**) showing an inversion-related hangingwall anticline and associated short-cut fault in the region of the Wick/Great Glen Fault intersection. BCRT = Base Cretaceous

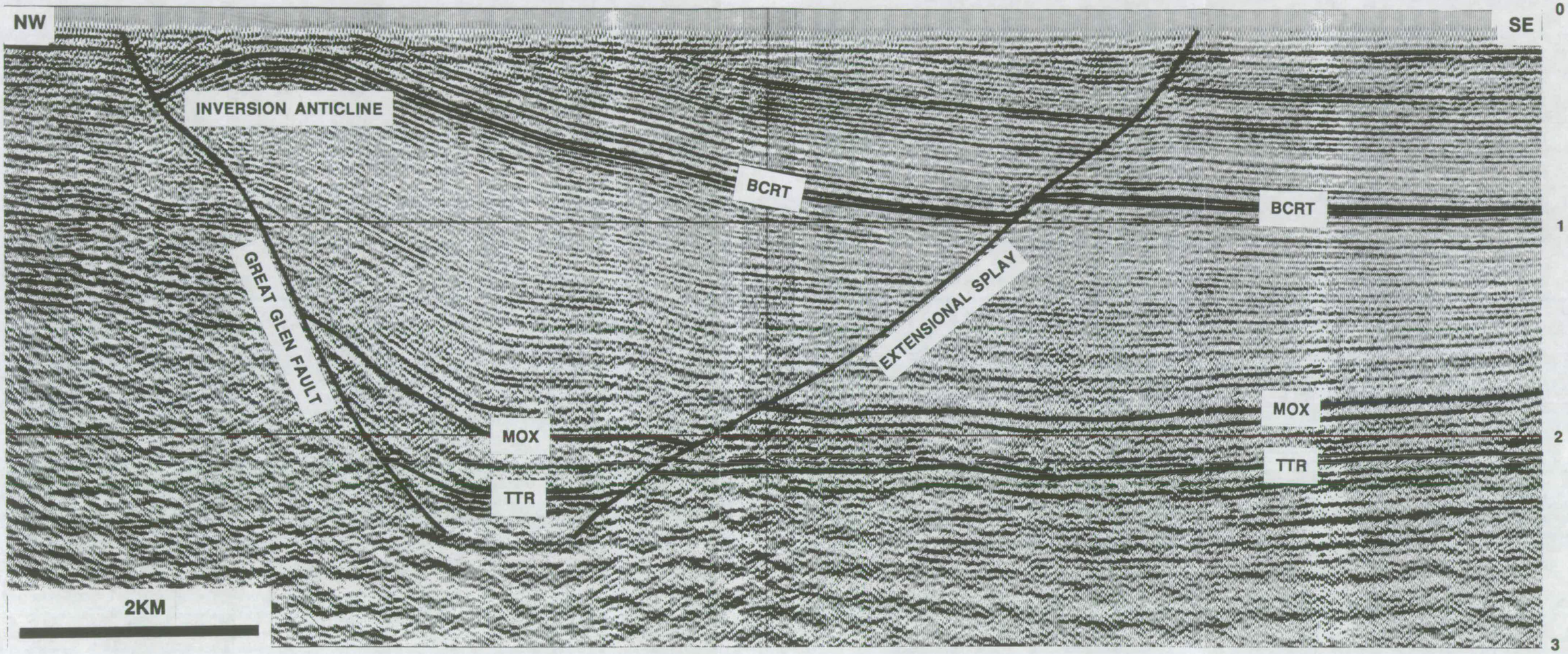

Figure 7.9 Seismic reflection profile (location shown in **Figure 7.13**) showing a major inversion fold between the Great Glen Fault and a major extensional splay to it. BCRT = Base Cretaceous, MOX = Mid Oxfordian Unconformity and TTR = Top Triassic.

transported to the west (i.e. towards the Great Glen Fault). As the Great Glen Fault formed a barrier to the westward advance of the basin fill, the fold developed as the basin fill accumulated against it. Additionally, it appears highly likely that the extensional fault which was responsible for the folding was controlled by the Great Glen Fault. The rapid convergence of the two faults at depth would suggest that they are linked and consequently that the extensional fault is an extensional splay to the Great Glen Fault, similar to those produced in sand-box studies (Naylor *et. al.*, 1986). Consequently, it seems possible that the inversion fold in UKCS license block 11/25 was the result of a complex interaction between splays of the Great Glen Fault.

7.4 Strike-slip reactivation: the Great Glen Fault.

The most significant Tertiary fault activity within the Inner Moray Firth occurs along the narrow Great Glen Fault zone **(Figure 7.10)**. Stratigraphic relations on seismic profiles demonstrate that it was active after the Early Cretaceous. It displays typical "flower structures" (sensu Harding,1990; **Figure 7.11**) with "helicoidal" geometries similar to those described from sand-box experiments (Naylor *et. al.*, 1986; Koopman *et. al.*, 1987; Arthur, 1993) and suggestive of strike-slip movement **(Figure 7.12)**. The overall sense of movement can be shown to have a down to the south-east component **(Figure 7.10)** but the isopach evidence is insufficient to suggest whether the strike-slip component was dextral or sinistral (Thomson and Underhill, 1993). However, detailed examination of the step-overs between splays along the fault can provide evidence as to the sense of strike-slip motion. In UKCS license block 11/25 the splays step to the left **(Figure 7.13)** and between them contain compressional structures such as the "box fold" shown in **Figure 7.14**. Gamond (1987) showed that compressional step-overs occur when the overall sense of movement along the shear zone is opposite to the stepping sense (i.e. right-lateral shear with left stepping faults or left-lateral shear with right stepping faults; **Figure 7.15**) and consequently it can be deduced that the overall sense of movement on the Great Glen Fault must have been dextral in order to produce compression between left stepping splays **(Figure 7.13)**.

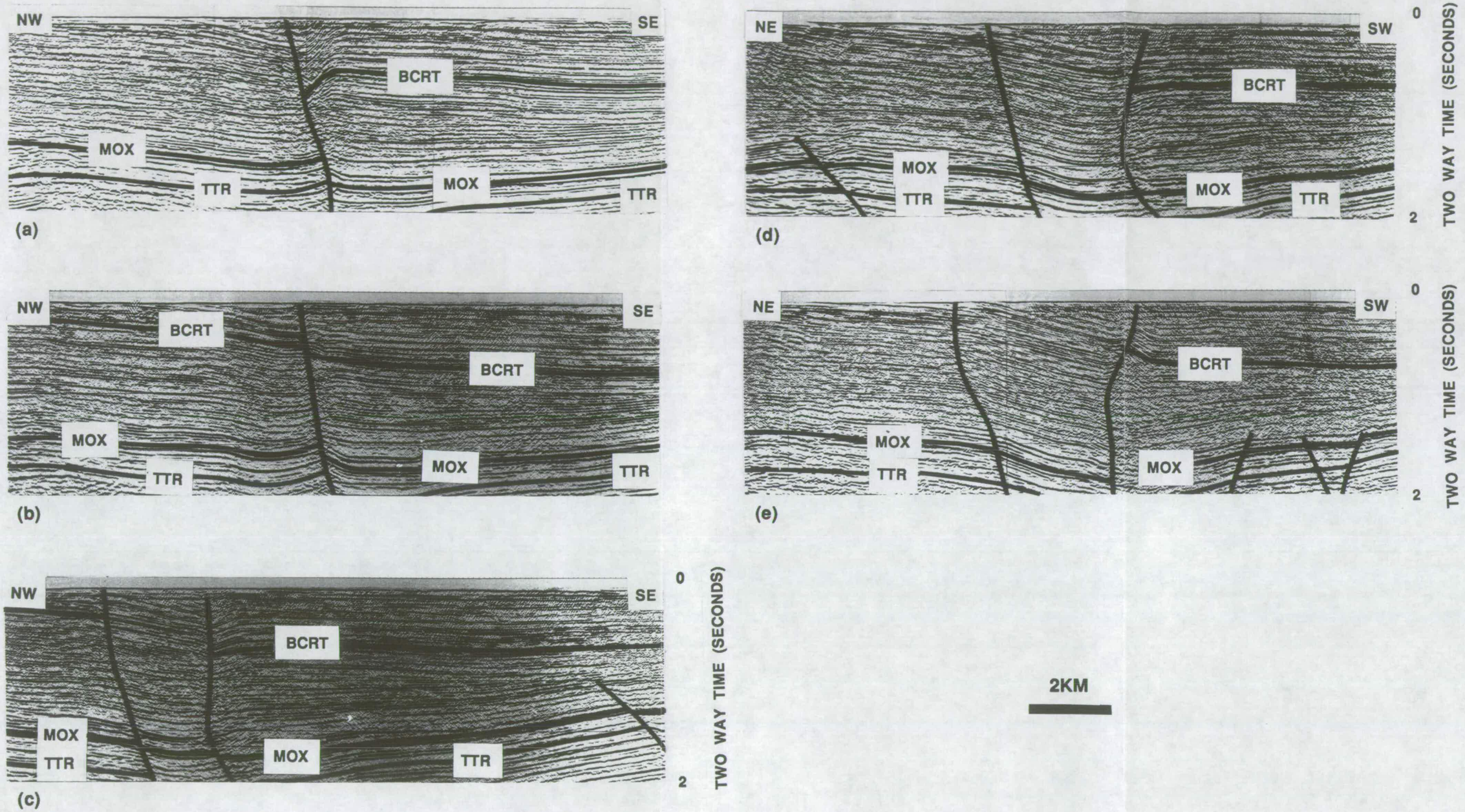

Figure 7.10 Seismic reflection profiles (locations shown in **Figure 7.7**) across the Great Glen Fault. The helicoidal and flower structure geometries shown are indicative of strike-slip movement. BCRT = Base Cretaceous, MOX = Mid Oxfordian Unconformity and TTR = Top Triassic.

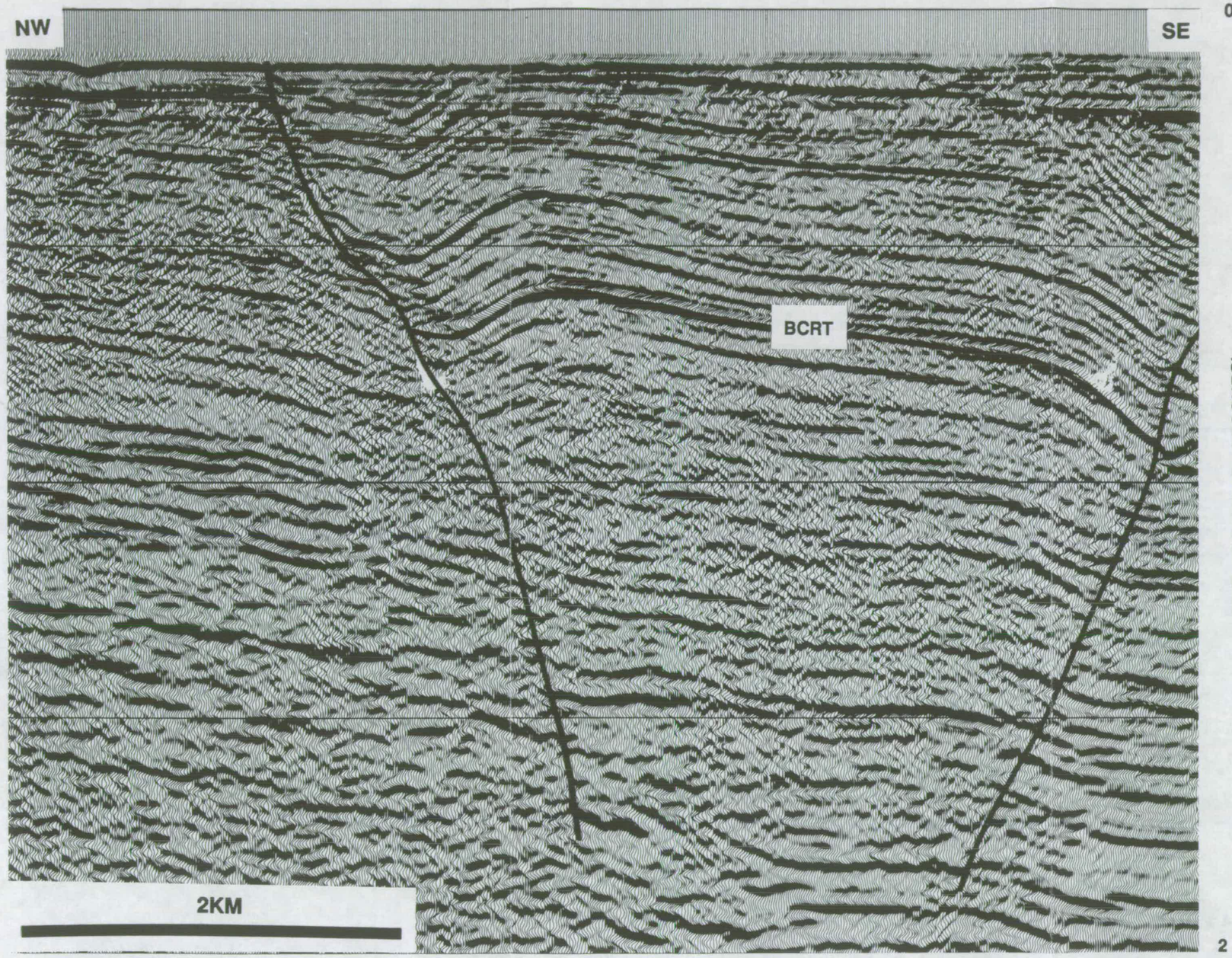

Figure 7.14 Seismic reflection profile (location shown in **Figure 7.13**)showing the box-fold between left-stepping splays of the Great Glen Fault. As the fold is clearly the product of compression the sense of movement on the individual splays is dextral **(Figure 7.15)**. BCRT = Base Cretaceous.

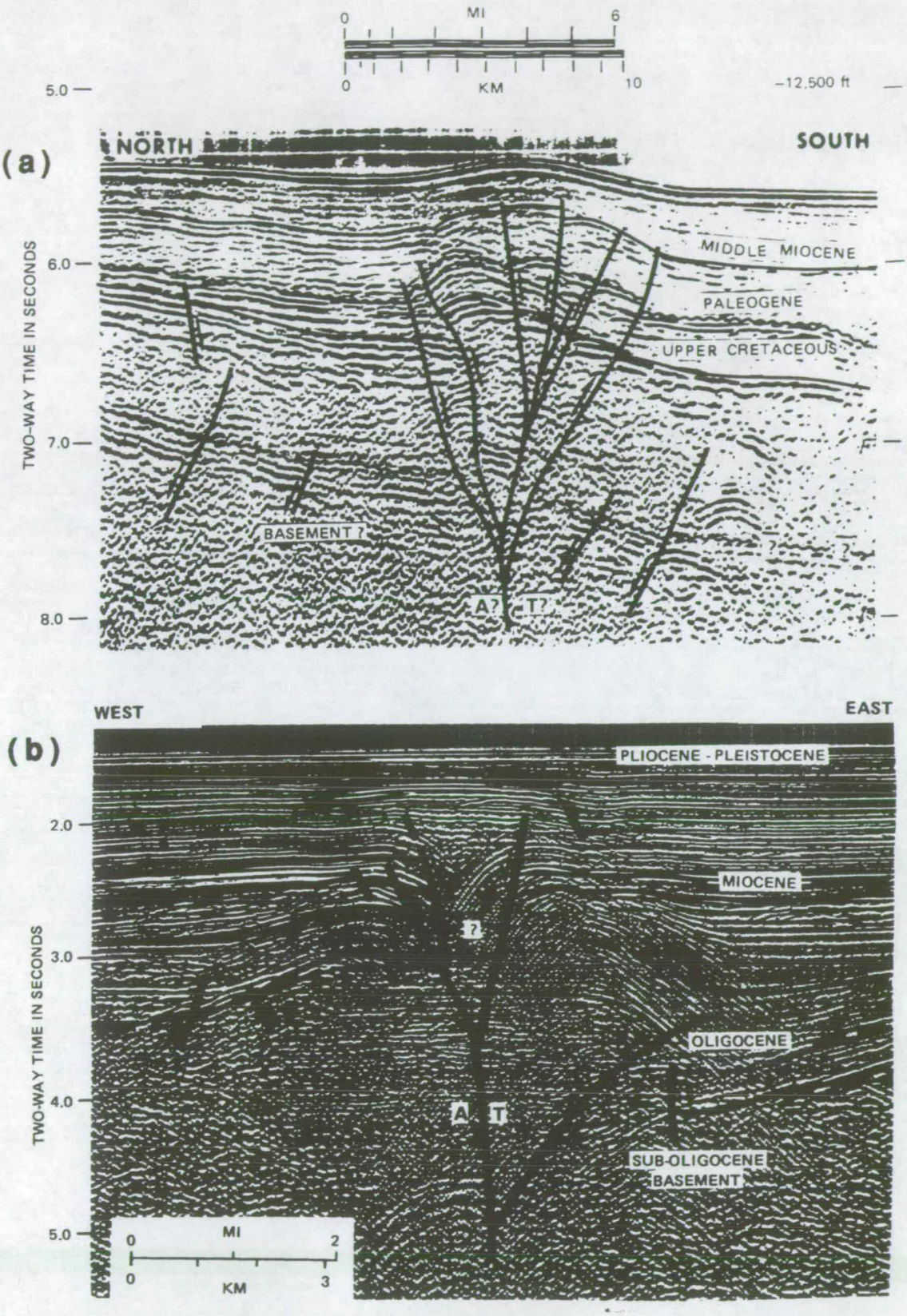

Figure 7.11 Seismic reflection profiles across strike-slip faults (Harding, 1990). (a) shows an example of a positive flower structure while (b) shows a negative flower structure. A = away from viewer, T = towards viewer.

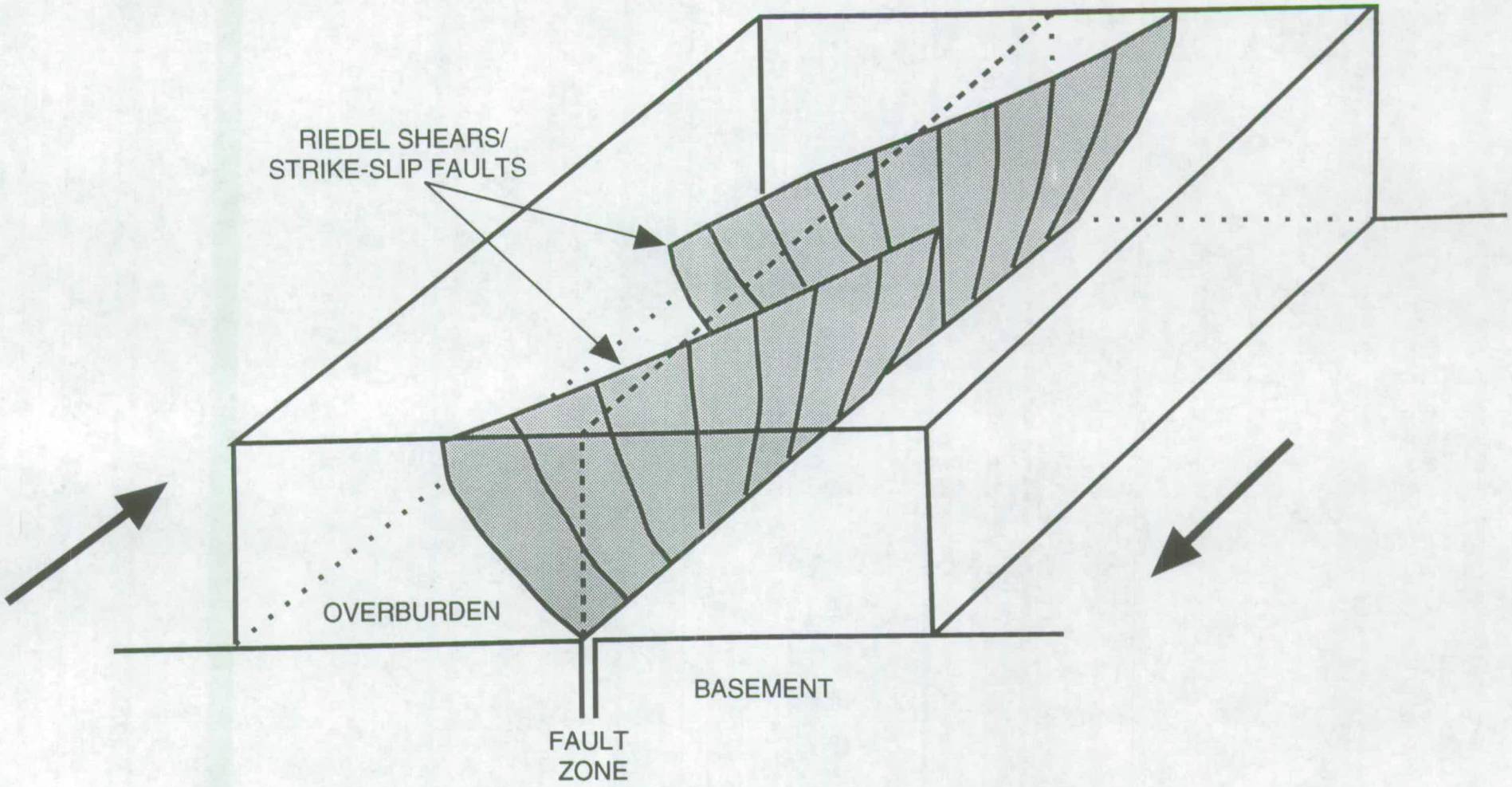

Figure 7.12 Helicoidal geometries produced in sand-box experiments simulating strike-slip deformation. The faults/shears produced bear a marked similarity to the geometries seen on seismic reflection profiles of the Great Glen Fault in the Inner Moray Firth, suggesting strike-slip movement occurred on the fault. After Naylor et. al. (1986).

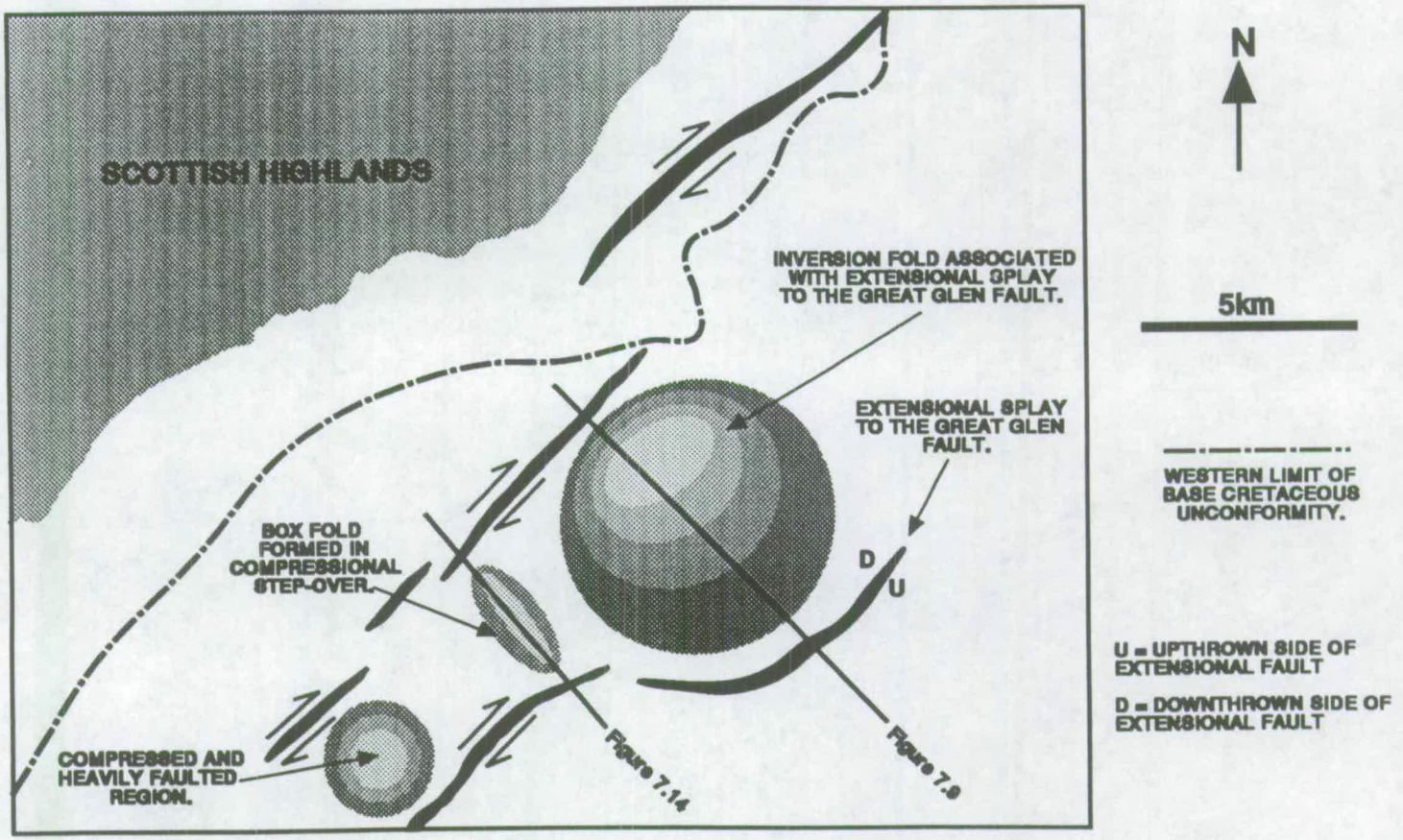

Figure 7.13 Map of the structures affecting the Base Cretaceous in the region of UKCS license block 11/25. The most significant feature in the area is the large inversion fold and its associated extensional fault. The fold appears to be the result of extension on this fault, which is probably an extensional splay to the Great Glen Fault, this resulted in the transport of the hangingwall material towards the Great Glen Fault where it was prevented from further westward movement and consequently became folded. Note that the Great Glen Fault consists of several strands which predominantly step to the left. Such left-stepping strands show compressional structures between them, such as the box-fold shown, which is indicative of dextral displacement on the strands (Garnond, 1987).

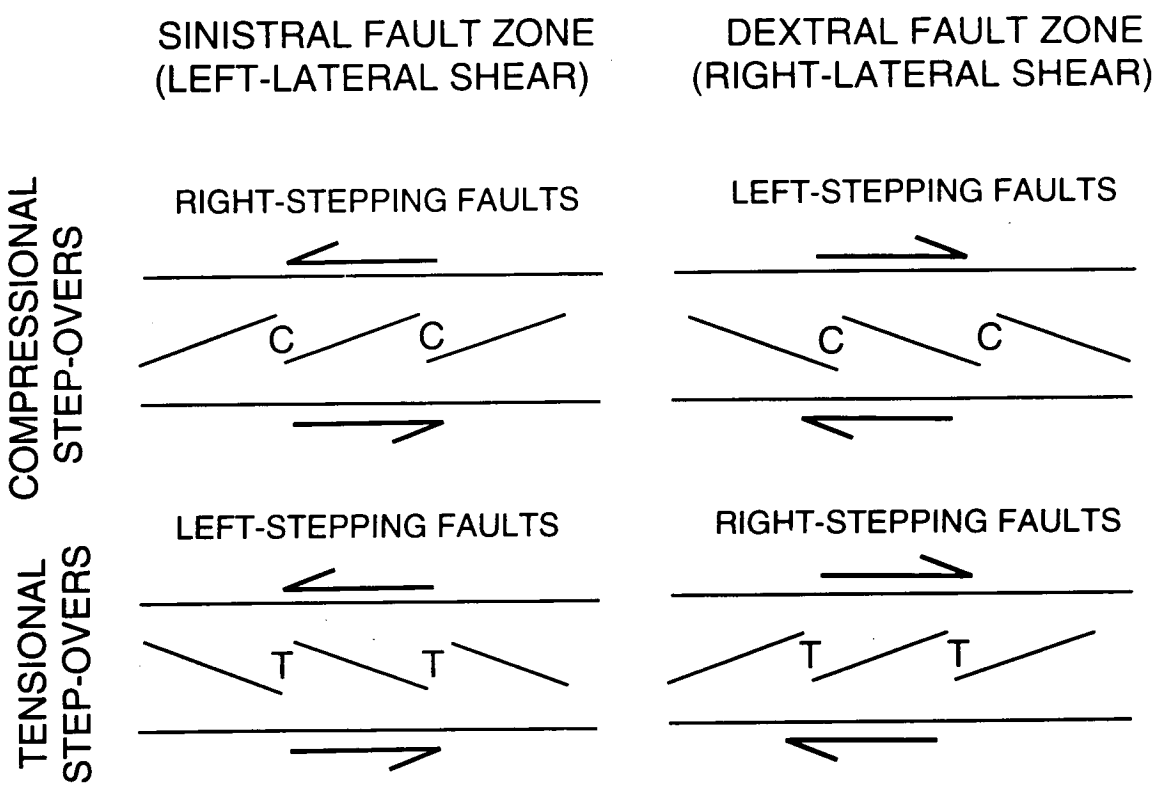

Figure 7.15 The stress state of step-overs in strike-slip/shear zones. Compression occurs between step-overs when the stepping sense is opposite to the shear sense (i.e. left-stepping faults in a dextral shear zone or right-stepping faults in a sinistral shear zone). Tension occurs between faults when they step in the same sense as the shear zone (i.e. left-stepping faults in a sinistral shear zone or right-stepping faults in a dextral shear zone). After Gamond (1987).

7.5 Strike-slip reactivation: the Sutherland Terrace-Helmsdale Fault-Great Glen Fault System.

The Sutherland Terrace is a fault-bounded wedge at the western margin of the Inner Moray Firth with the Helmsdale Fault as its western boundary **(Figure 7.7)**. To the northeast the Helmsdale Fault merges with the Great Glen Fault, the western boundary to the Sutherland Terrace, and to the southwest it passes onshore at Dun Glas resulting in a small fault bounded coastal exposure of the folded Kimmeridgian basin fill **(Figure 7.16)** between Dun Glas and Kintradwell.

The strike of the beds generally varies between north-south and east north east-west south west **(Figure 7.17)**, generally following the coastline. To the north the beds dip away from the Helmsdale Fault (i.e. to the south), but in the area of Kintradwell (Grid Reference NC 925074) the dip direction is reversed **(Figure 7.17)**. The folds also show a slight asymmetry with the northeastern limbs being slightly shorter than the southwestern limbs **(Figure 7.17)**. Substantial variations in the angle of dip can be found along the section with the beds steepening towards the northeast, that is as the coastal exposure becomes closer to the Helmsdale Fault. At Dun Glas (Grid Reference ND 057172), where the exposure is closest to the Helmsdale Fault, the dips can exceed 45° **(Figure 7.18)** while in the Kintradwell area dips are around 20°. The extreme steepening of the dip towards the Helmsdale Fault can be explained in terms of differential compaction (Prosser, 1991 and Section 7.2) which causes the beds to steeply dip away from the Helmsdale Fault before returning to horizontal through a hangingwall compaction syncline. This also explains the northerly dip at Kintradwell, as the boulder beds are further from the Helmsdale Fault, they probably lie on other limb of a hangingwall compaction syncline. Such an interpretation contradicts that of Roberts (1989) who suggested that the northerly dip at Kintradwell may have been the product of oblique strike-slip on the Helmsdale Fault during the Late Jurassic.

A marked variation in fold wavelength can be seen onshore with wavelengths between 400m to 2000m. Again, as with the variation in angle of dip a pattern can be recognised with wavelength decreasing to the northeast **(Figure 7.17)**. Such a pattern could possibly suggest that the amount of compression increases to the northeast, that is towards the Helmsdale/Great Glen Fault intersection. One notable exception is the Rubha na Gaoithe syncline (Grid Reference NC 993116) where the beds can be seen to turn around in less than 100m. The direction of plunge of the fold axes falls into two categories, plunging either to the southeast or northwest. Such

Figure 7.16 Photographs showing the folding of the onshore Kimmeridgian deposits of the Sutherland Terrace. The folding is interpreted to be the result of space problems within the Sutherland Terrace due to dextral and sinistral strike-slip movement on the Great Glen and Helmsdale faults respectively.

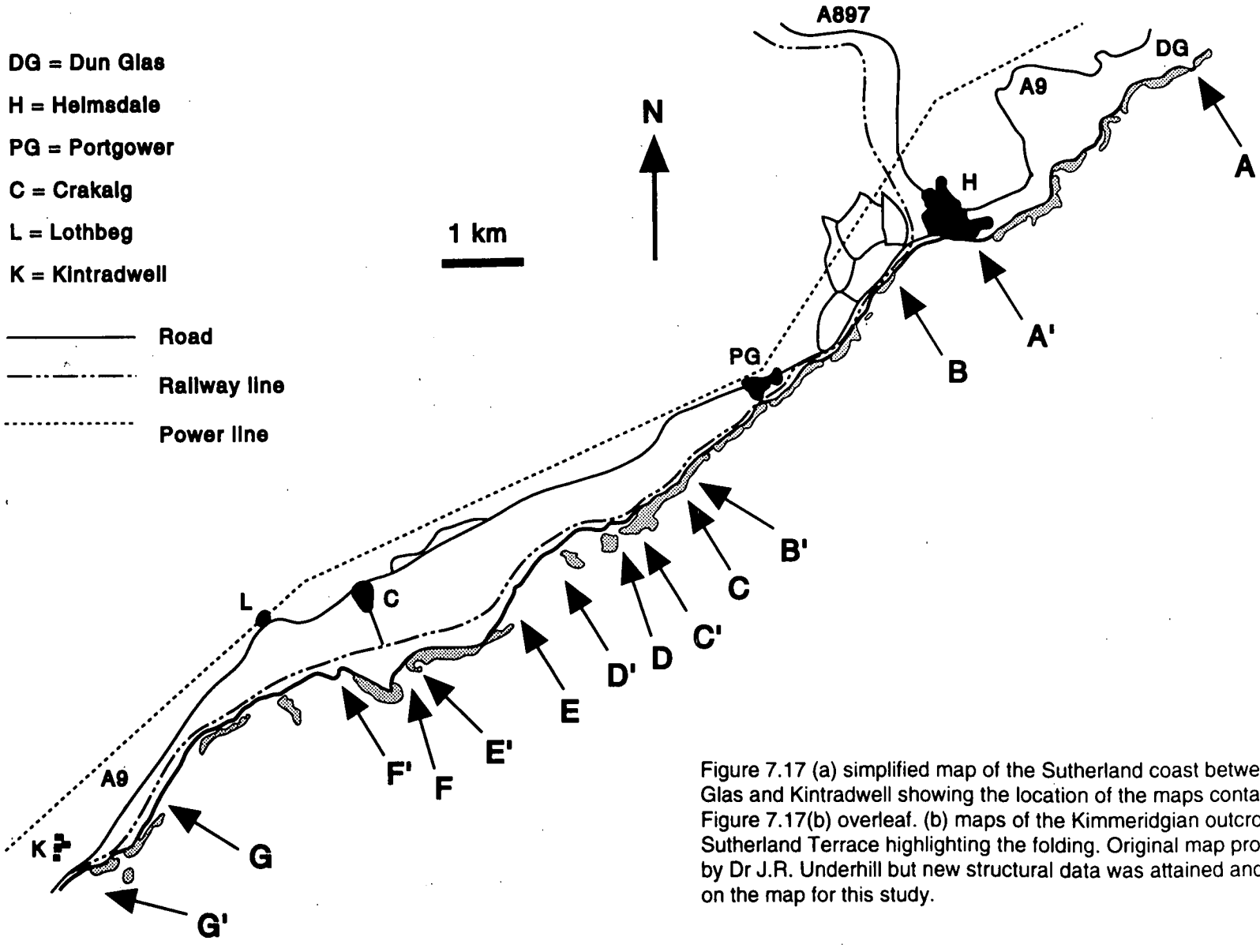

Figure 7.17 (a) simplified map of the Sutherland coast between Dun Glas and Kintradwell showing the location of the maps contained in Figure 7.17(b) overleaf. (b) maps of the Kimmeridgian outcrop in the Sutherland Terrace highlighting the folding. Original map produced by Dr J.R. Underhill but new structural data was attained and posted on the map for this study.

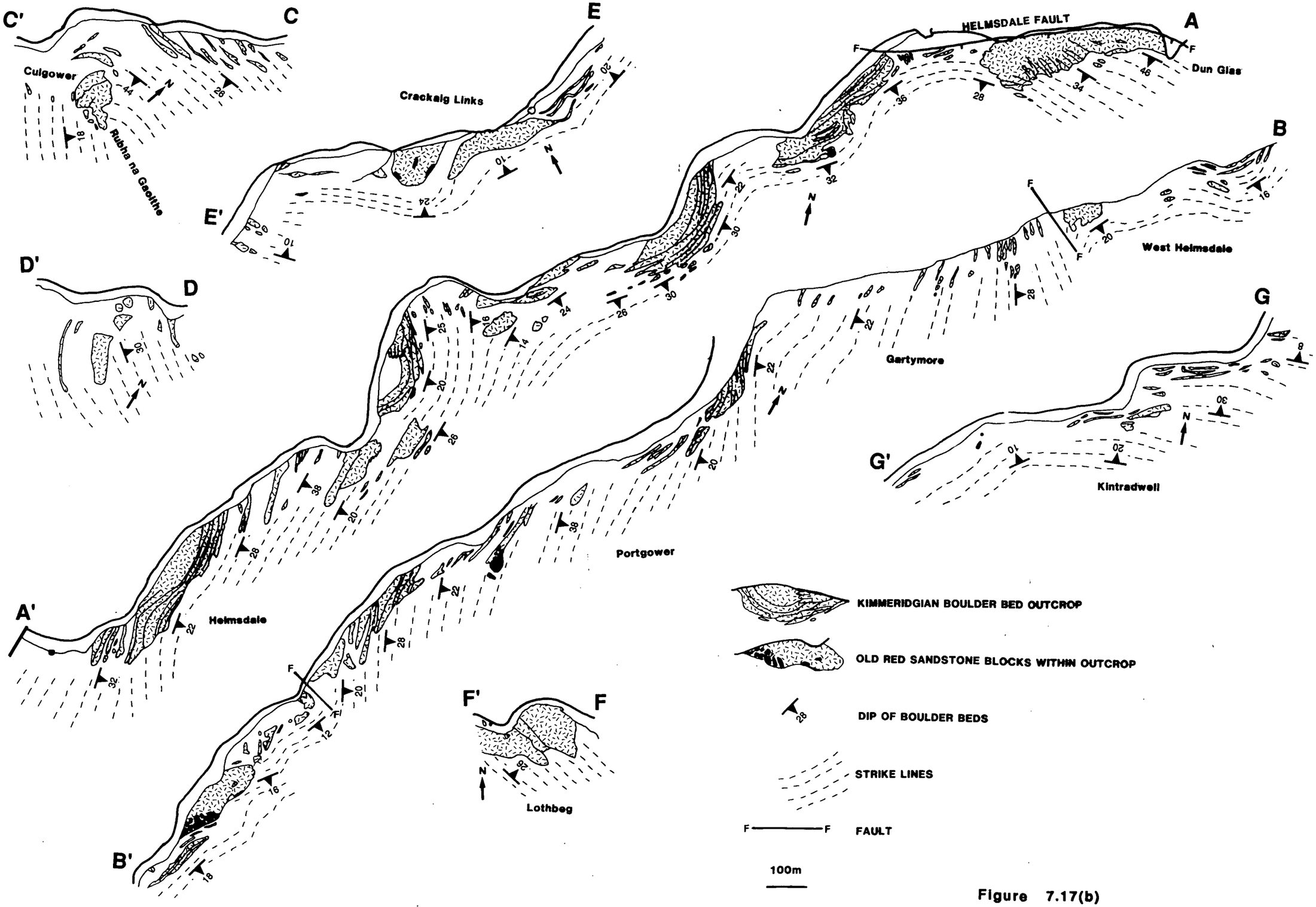
C'
C
Culgower
Rubha na Gaoithe
E
Crackaig Links
E'
HELMSDALE FAULT
A
F
Dun Glas
B
West Helmsdale
D'
D
G
Gartymore
G'
Kintradwell
A'
Helmsdale
B'
Portgower
F'
Lothbeg
KIMMERIDGIAN BOULDER BED OUTCROP
OLD RED SANDSTONE BLOCKS WITHIN OUTCROP
DIP OF BOULDER BEDS
STRIKE LINES
FAULT
100m

Figure 7.17(b)

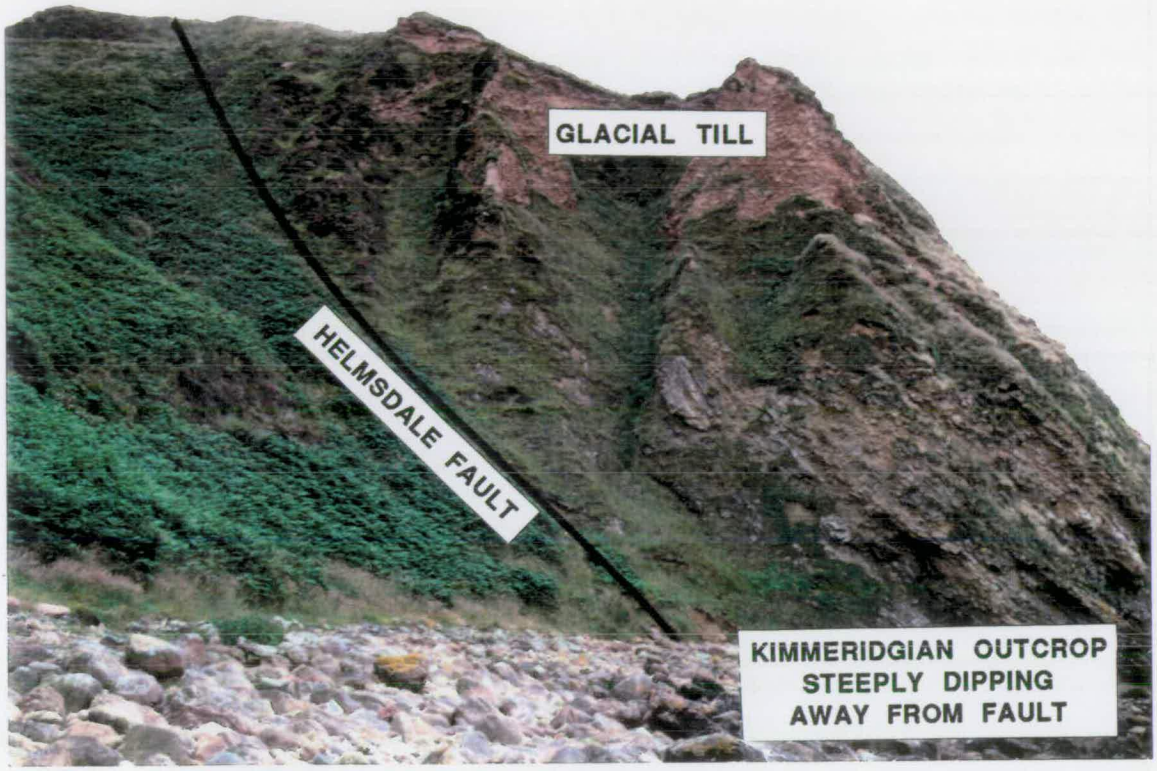

Figure 7.18 The Helmsdale Fault and associated Kimmeridgian outcrop at Dun Glas (Grid Reference ND 057171). Note the extreme steepening of the Kimmeridgian outcrop adjacent to the Helmsdale Fault. This is interpreted as a result of differential compaction of the Kimmeridgian syn-rift deposits against a rigid footwall buttress.

orientations are not tne direct product of folding but also depend of the position of the exposure relative to the hangingwall compaction syncline. As previously noted the beds dip away from the Helmsdale Fault in the northeast and towards it in the southwest by virtue of their position on the compaction syncline. With fold axes at high angles to the Helmsdale Fault, and beds dipping away from it in the northeast, the folds would be expected to plunge away from the fault (southeastwards) while folds in the southwest would plunge towards it (northwestwards). This proposed pattern suggests that fold plunge directions depend on the initial orientation of the bedding.

Seismic reflection profiles from the offshore part of the Sutherland Terrace show the Kimmeridgian section is folded **(Figure 7.19)**. Comparison of such sections with geological cross sections constructed from the onshore exposures **(Figure 7.20)** shows a distinct similarity between the structural patterns. However, the structural similarity is only present within the Sutherland Terrace with seismic reflection profiles to the east showing no folding **(Figure 7.21)**. This would seem to suggest that the folding is the result of a local tectonic regime peculiar to the Sutherland Terrace.

The local stress field orientation can be determined from the orientation of the folding in the Sutherland Terrace. On a stereographic projection the fold axis marks the position of intermediate compressive stress (σ_2), while the minimum compressive stress (σ_3) lies at the point of intersection of the axial plane with the great circle to the bedding poles. The principal compressive stress (σ_1) is at 90° to both the minimum and intermediate stress axes, providing that the system is orthogonal **(Figure 7.22)**. Stereographic projections produced from the structural data collected suggests that the intermediate compressive stress axis was orientated northwest-southeast **(Figure 7.23)**, although significant scatter in the positions of the fold axes allows a error of ± 30°. As previously noted, the folds plunge either to the northwest or southeast depending on their position relative to the hangingwall compaction syncline. Consequently, it is difficult to ascertain whether σ_2 was horizontal at the time of folding or plunged either to the northwest or southeast. The minimum compressive stress (σ_3) appears to be steeply inclined, if not vertical, at around 70° to either the northwest or southeast and so it would seem reasonable to suggest that it was near vertical for all practical purposes **(Figure 7.23)**. Assuming that σ_2 was near horizontal and σ_3 near vertical, the principal compressive stress (σ_1) must also have been horizontal if the stress system was orthogonal. As to the orientation of σ_1 it can be seen that it is roughly

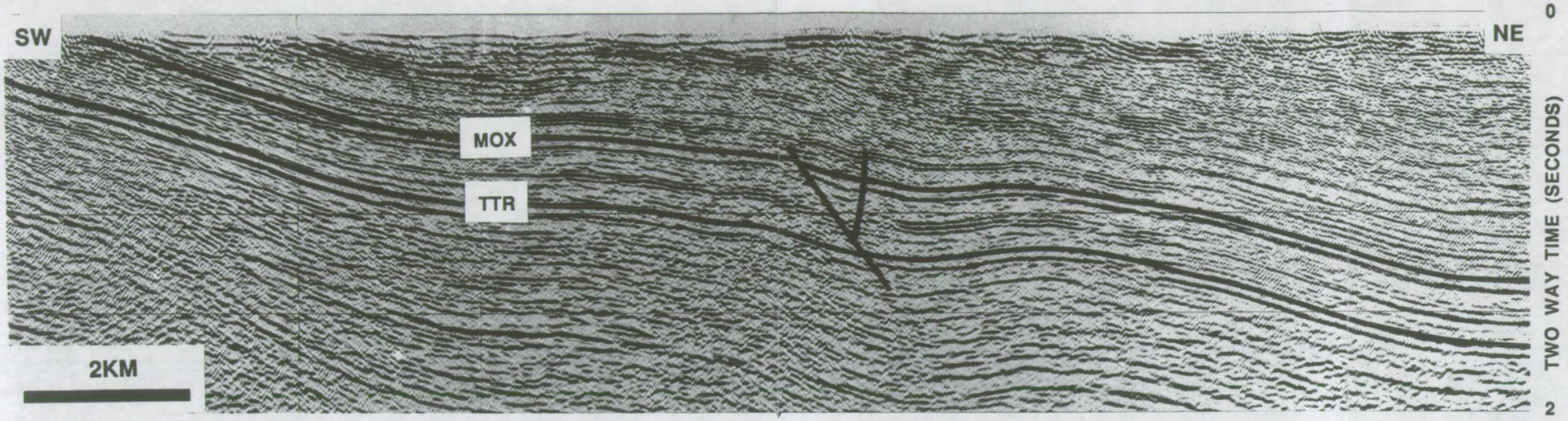

Figure 7.19 Seismic reflection profile (location shown in **Figure 7.7**) from the Sutherland Terrace showing the folded nature of the sediments, similar to cross sections from the coastal exposure between Dun Glas and Kintradwell **(Figure 7.20)**. MOX = Mid Oxfordian Unconformity and TTR = Top Triassic.

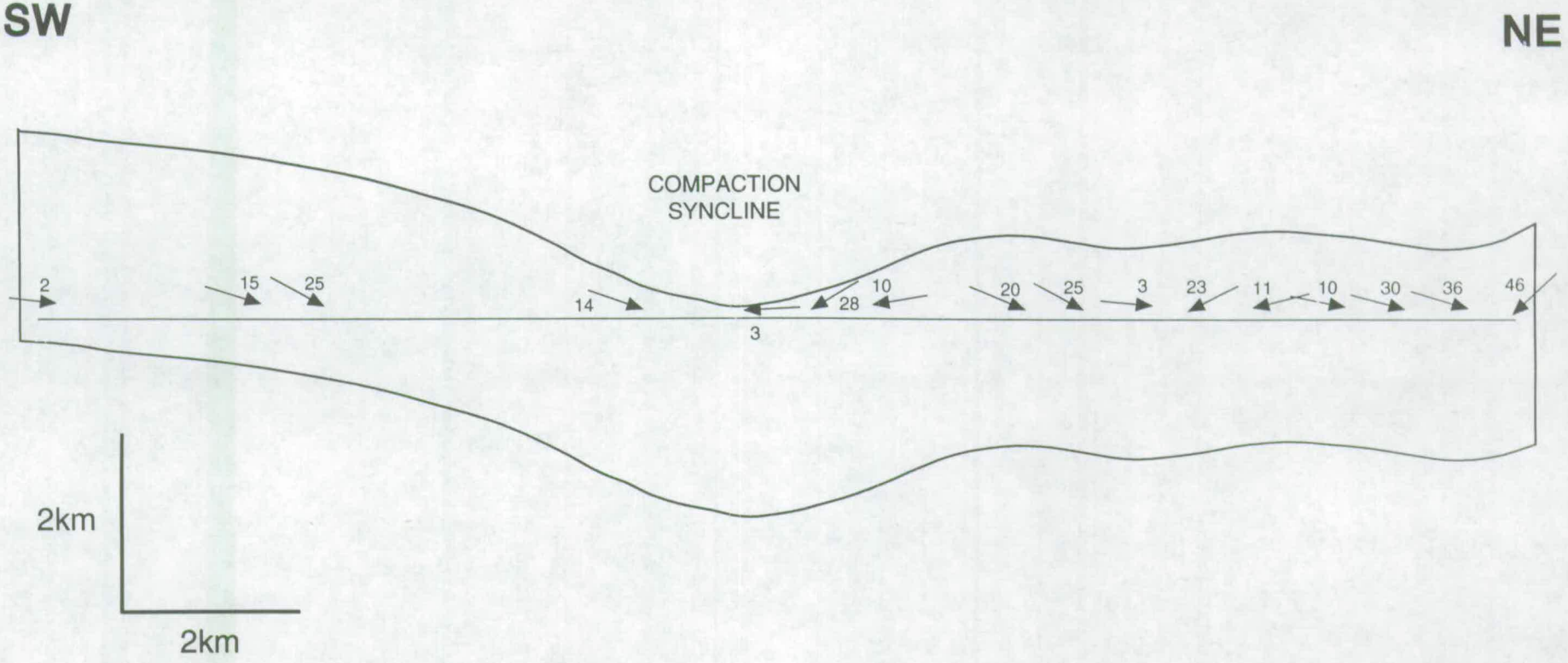

Figure 7.20 Simplified geological cross section of the Kimmeridgian "boulder beds" exposed onshore between Dun Glas and Kintradwell. Note the folding, the most prominent of which is the large compaction syncline marked. The section shows a similarity to offshore seismic reflection profiles.

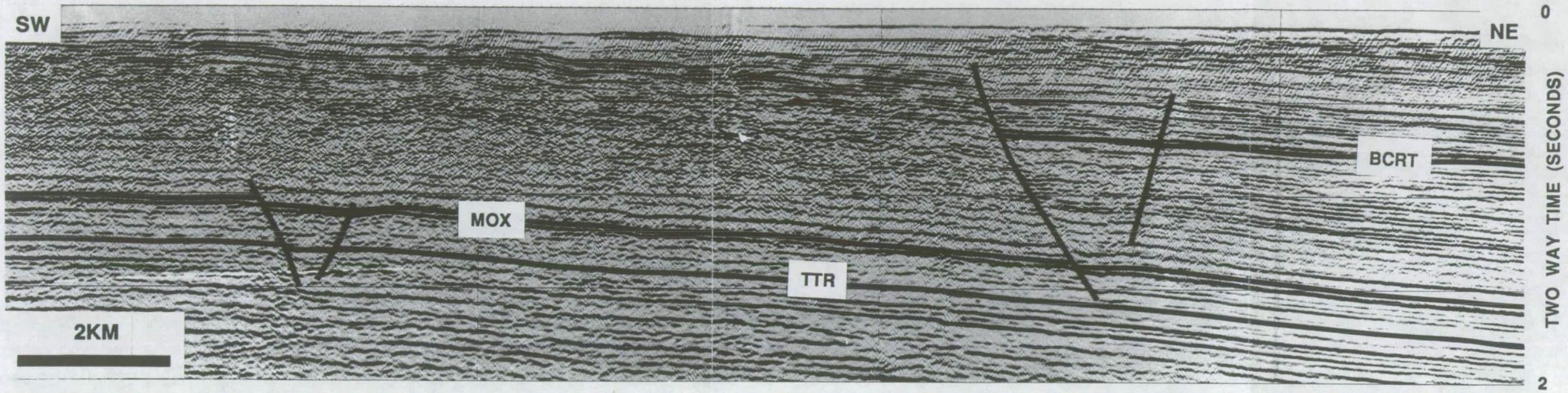

Figure 7.21 Seismic reflection profile (location shown in **Figure 7.7**) parallel to **Figure 7.19** but outwith the Sutherland Terrace. Note that no folding is present as the folding is restricted to the Sutherland Terrace. BCRT = Base Cretaceous, MOX = Mid Oxfordian Unconformity and TTR = Top Triassic.

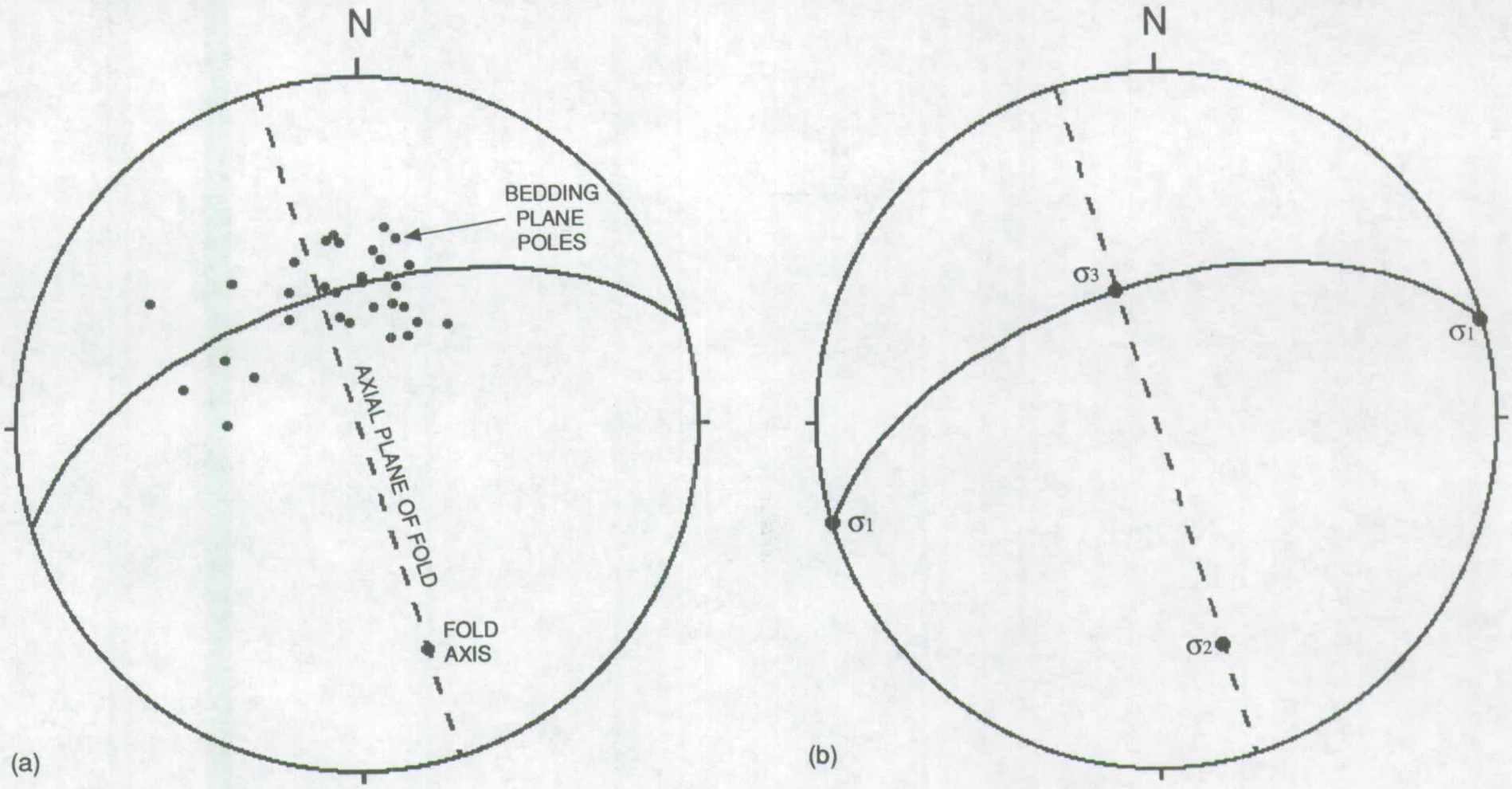

Figure 7.22 Determination of the orientation of stress axes from stereographic projections of folds. (a) Stereographic projection of poles to bedding of a fold with best-fit great circle, axial plane and fold axis. (b) The fold axis marks the location of the intermediate compressive stress ($\sigma 2$) while the minimum compressive stress ($\sigma 3$) lies at the intersection of the axial plane with the best-fit great circle to the bedding poles. The principle compressive stress ($\sigma 1$) lies at 90° to both the intermediate and minimum compressive stress axes.

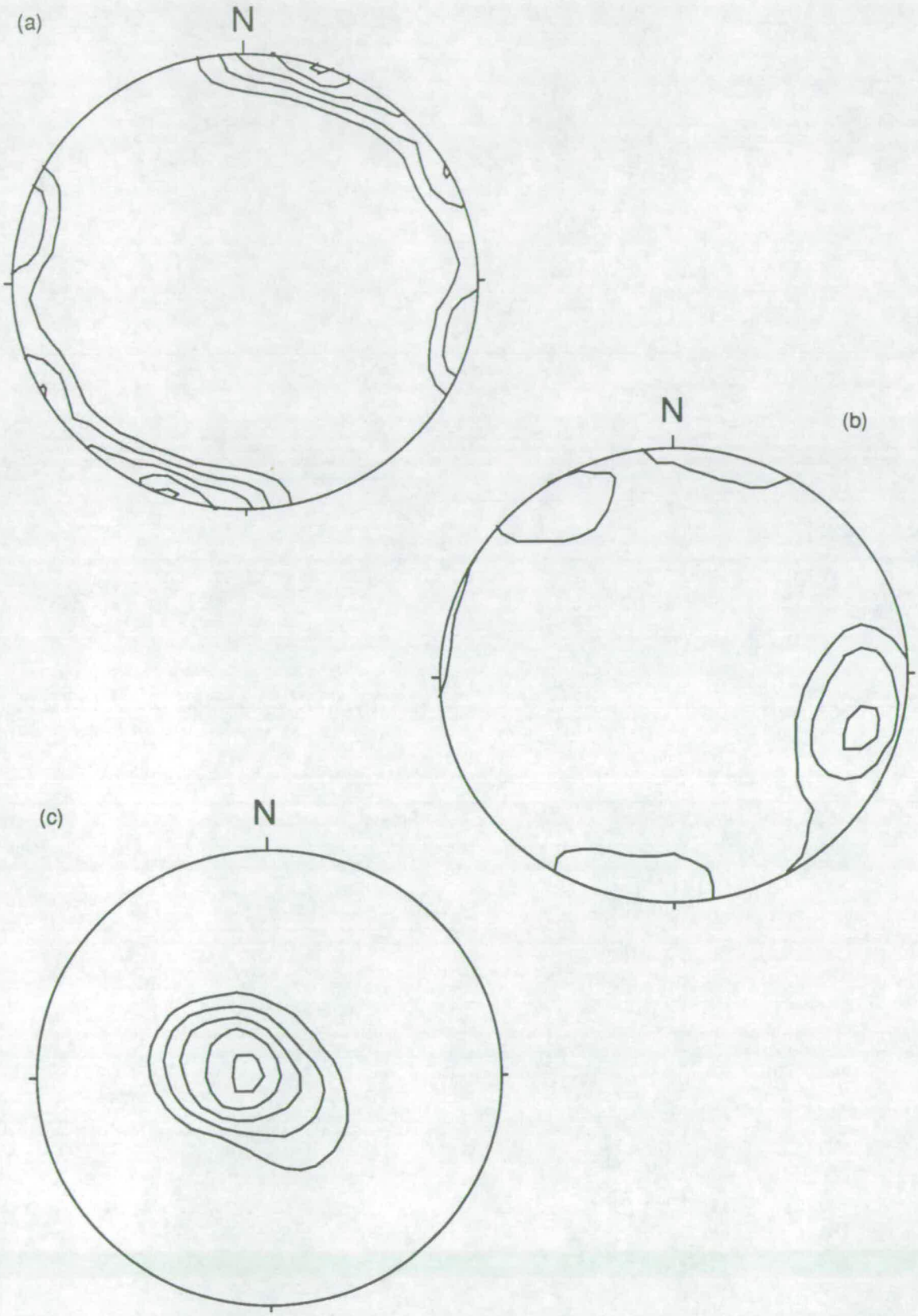

Figure 7.23 Contoured stereographic projections of stress axes for the Sutherland Terrace based on fold orientations. (a) The orientation of the principal compressive stress ($\sigma 1$) which trends approximately northeast-southwest. (b) The intermediate compressive stress ($\sigma 2$) which trends approximately northwest-southeast. (c) The minimum compressive stress ($\sigma 3$) which is near vertical.

northeast-southwest **(Figure 7.23)**, at 90° to the other axes. Again, the margin of error would be around 30°, the same as for the σ_2, as any change in the orientation of one axis in the σ_1-σ_2 plane has the same effect on the other. In addition, it must be noted that if σ_2 and σ_3 are not truly vertical and horizontal respectively then σ_1 will also be inclined.

Any proposed kinematic model for the origin of the folding seen in the Sutherland Terrace must take into account the following facts. Firstly the axes trend at high angles to the Helmsdale Fault thus discounting the possibility of this being a case of dip-slip inversion with contraction across the Helmsdale Fault. Such a situation requires movement of the hangingwall up the Helmsdale Fault and the generation of fold axes parallel/subparallel to it. The fold axes also trend at high angles to the Great Glen Fault which also discounts the possibility of these folds being wrench or forced parallel folds as described by many workers (Christie-Blick and Biddle, 1985; Harding *et. al.*, 1985; Little, 1992; Naylor *et. al.*, 1986; Sylvester, 1988; **Figure 7.24**).

The orientation of the principal stress axes suggests that the principal compressive stress was near horizontal and at an oblique angle to both the Helmsdale and Great Glen faults. This would suggest that the faults could not have acted in a purely dip-slip fashion and that strike-slip, possibly with a minor dip-slip component was the predominant style of movement at the time of folding. The general decrease in fold wavelength to the northeast, towards the Helmsdale-Great Glen Fault intersection, would indicate that compression was greater to the northeast. Combining this with the fact that the folding is only found in the Sutherland Terrace would suggest that the folding was a response to space problems in the area. All these factors suggest that the folding could not have occurred as a classical dip-slip inversion event or in response to straightforward strike-slip motion. Instead, it appears that the tectonic regime is similar to that described for strike-slip fault wedges (Christie-Blick and Biddle, 1985; **Figure 7.25**). Based on the available data it is possible to propose that the folding was the result of dextral strike-slip movement on the Great Glen Fault and probably a component of sinistral motion on the Helmsdale Fault. Such a tectonic regime would produce accommodation space problems in the Sutherland Terrace as it moved into the smaller area towards the intersection of the two faults **(Figure 7.26)**. As a result, folds could then develop across the area with axes at high angles to both faults.

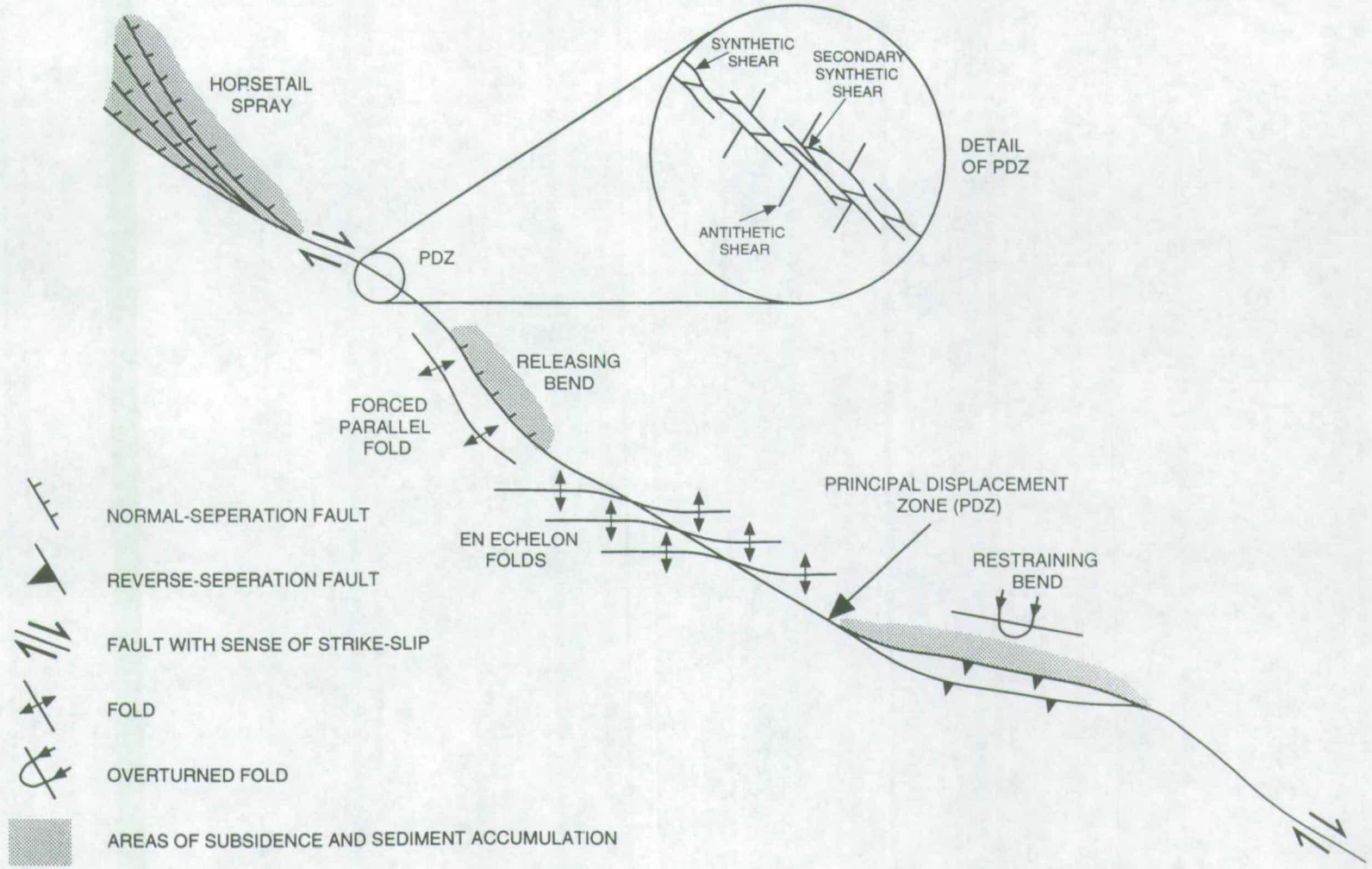

Figure 7.24 The spatial arrangement of structures associated with an idealised dextral strike-slip fault. After Christie-Blick and Biddle (1985).

Figure 7.25 Summary of the possible outcomes when two strike-slip faults merge to produce a fault-bounded wedge. Depending upon the relative slip senses and how the faults merge relative to each other a variety of possibilities exist, with the wedge either subsiding or being subject to uplift and compression. After Christie-Blick and Biddle (1985).

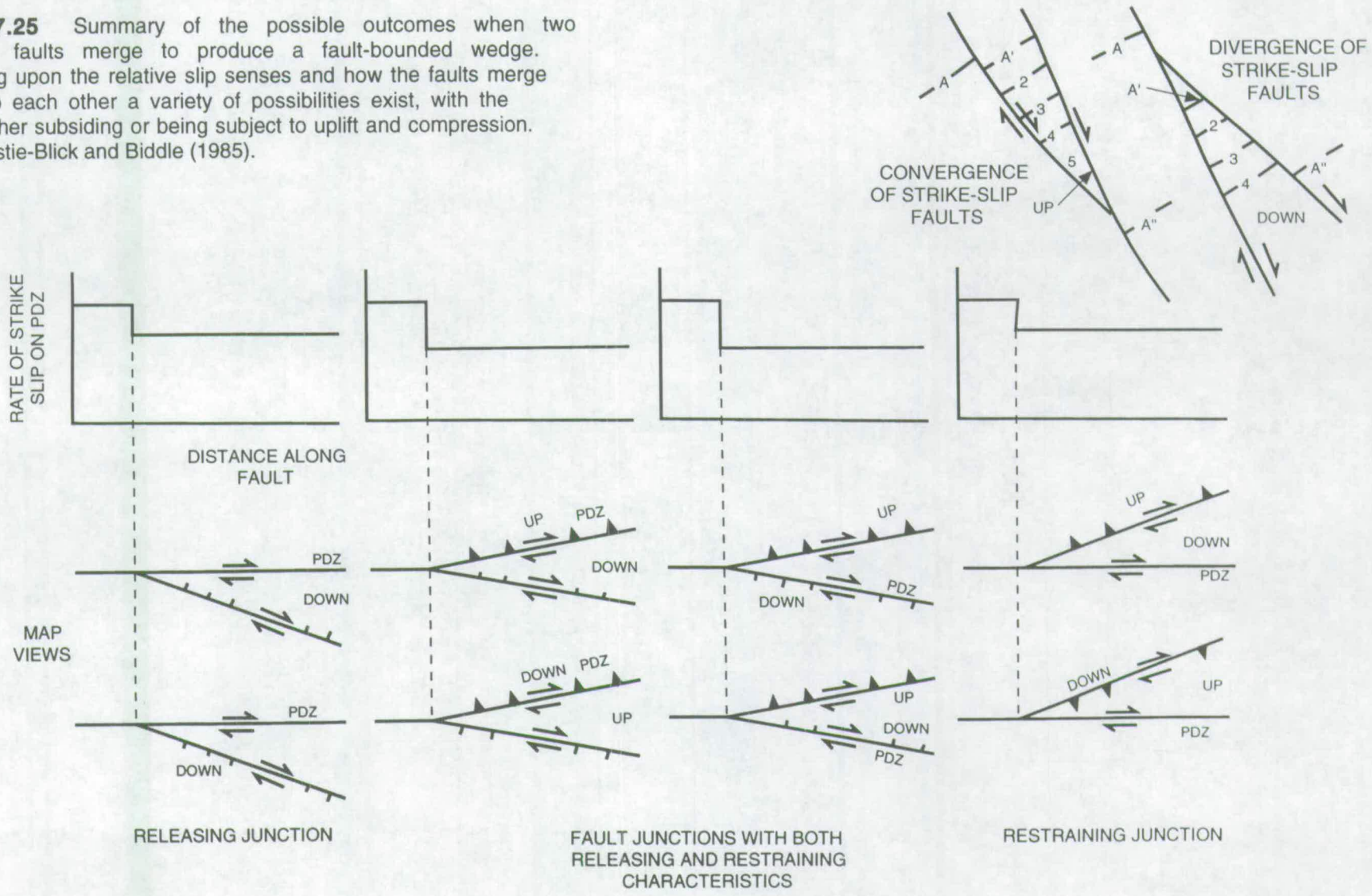

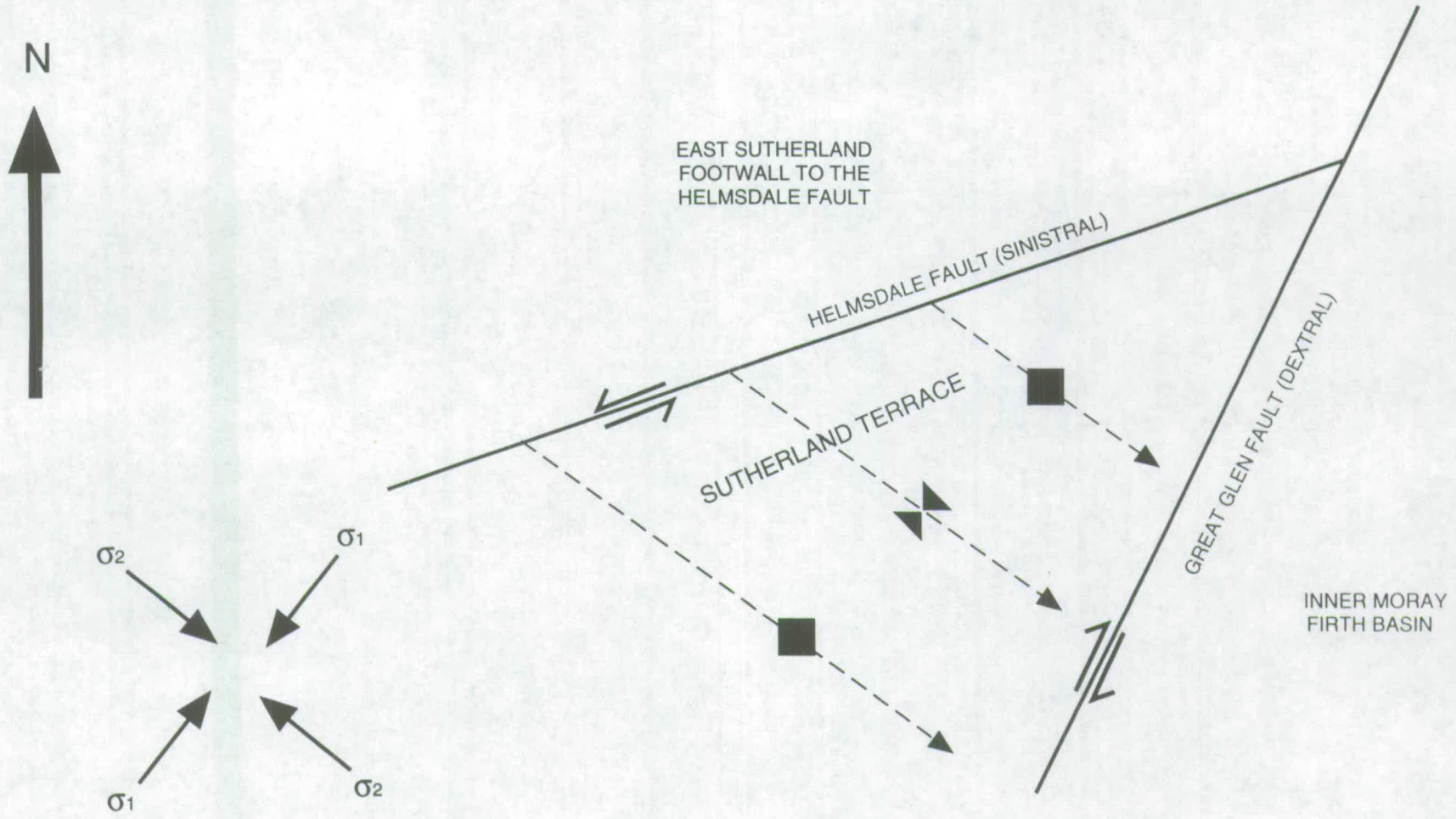

Figure 7.26 Schematic representation of the generation of folds within the Sutherland Terrace. Dextral strike-slip motion on the Great Glen Fault and sinistral motion on the Helmsdale Fault resulted in a localised stress regime of northeast-southwest compression and consequently resulted in the generation of northwest-southeast orientated folds.

The degree of folding in the Sutherland Terrace is relatively small. If the dating of this movement is correct then the amount of Tertiary dextral strike-slip motion on the Great Glen Fault must be limited. If the movement on the fault was excessive, it would be more likely that the folds would be tight and may even have developed small scale thrusts. However, offshore seismic reflection data does not show any really excessive compression towards the apex of the Sutherland Terrace. Consequently, it is proposed that Tertiary movement was limited to around 10km. Such an estimate of Tertiary movement on the Great Glen Fault is probably compatible with the 29km of dextral movement proposed by Holgate (1969) based on the Tertiary dykes of Mull. In addition, several other estimations of similar magnitude and slip sense have been made which have poorly constrained dates. Post Devonian estimates include 30km (Donovan *et. al.*, 1976), 29km (Garson *et. al.*, 1984) and 25-30km (Rogers, 1987; Rogers *et. al.*, 1989). Speight and Mitchell (1979) suggest that 8km of post Carboniferous movement has occurred **(Figure 7.27)** and 32km of post Lower Cretaceous movement is suggested by Garson and Plant (1972).

7.6 Regional Tilting of the Inner Moray Firth.

Both seismic profiles **(Figure 7.28)** and geological maps **(Figure 7.29)** of the seabed show that the stratigraphy at seabed in the Inner Moray Firth progressively youngs eastward with Tertiary units are only present at the Outer Moray Firth/Inner Moray Firth boundary **(Figures 7.28 and 7.29)**. The regional tilting of the basin as seen on seismic data, combined with evidence from chapters 3, 4, 5 and 6 shows that the pre-Cenozoic units are no longer at their maximum burial-depth and that the outcrop pattern is due to uplift and erosion during the Tertiary, followed by gentle burial **(Figure 6.1(b))**, the magnitude of which increased to the east **(Figure 7.30)**. Furthermore, a major unconformity can be seen separating the uplifted Upper Cretaceous Chalk sequences from the Tertiary Montrose Group which overlies the unconformity in the far eastern Inner Moray Firth, Outer Moray Firth and Central Graben regions (Parker, 1975; Rochow, 1981). This unconformity has been dated as mid-late Danian (Andrews *et. al.*, 1990) and it's relationship with the uplifted Mesozoic units suggests that it may be the surface where the erosion documented in Chapters 3, 4, 5 and 6 took place.

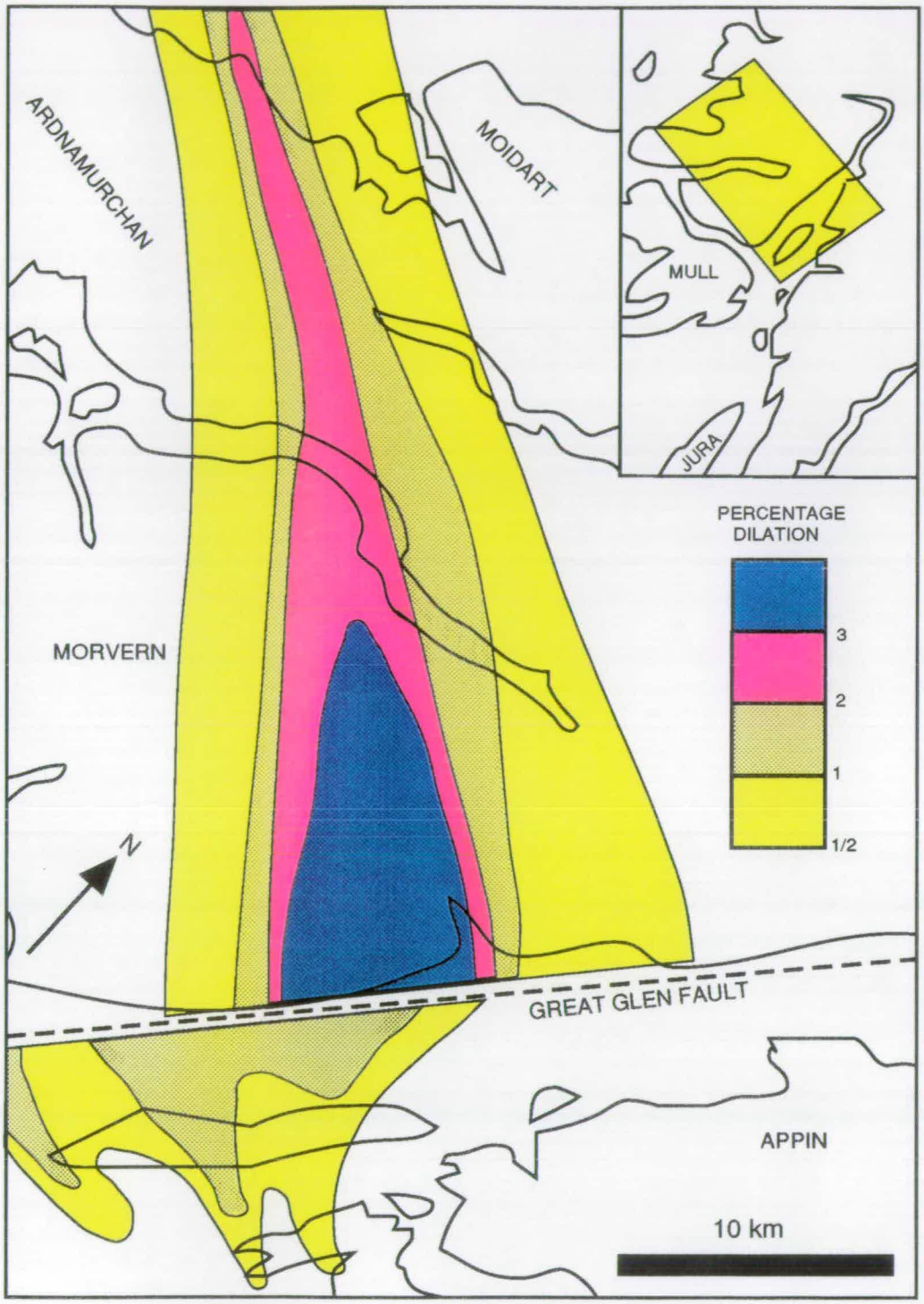

Figure 7.27 Contour map of the percentage crustal dilation resulting from the intrusion Permo-Carboniferous dykes in Argyll. The contours show a dextral offset of approximately 8km across the Great Glen Fault. After Speight and Mitchell (1979).

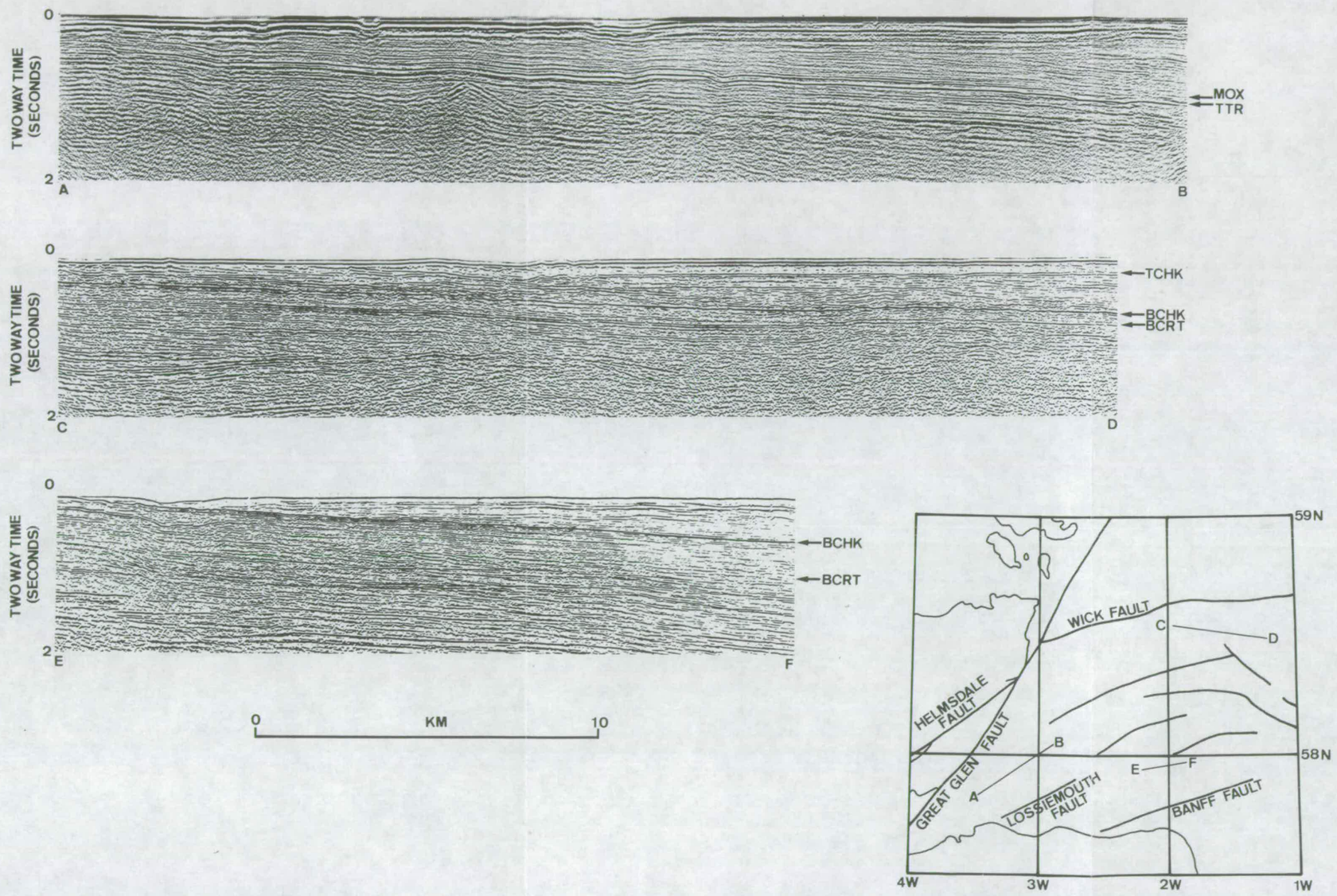

Figure 7.28 Seismic reflection profiles showing tilted eastward dipping pre-rift, syn-rift and thermal subsidence deposits. Note that progressively younger units crop out at, or near sea-bed from west to east. TCHK = Top Chalk, BCHK = Base Chalk, BCRT = Base Cretaceous, MOX = Mid Oxfordian Unconformity and TTR = Top Triassic.

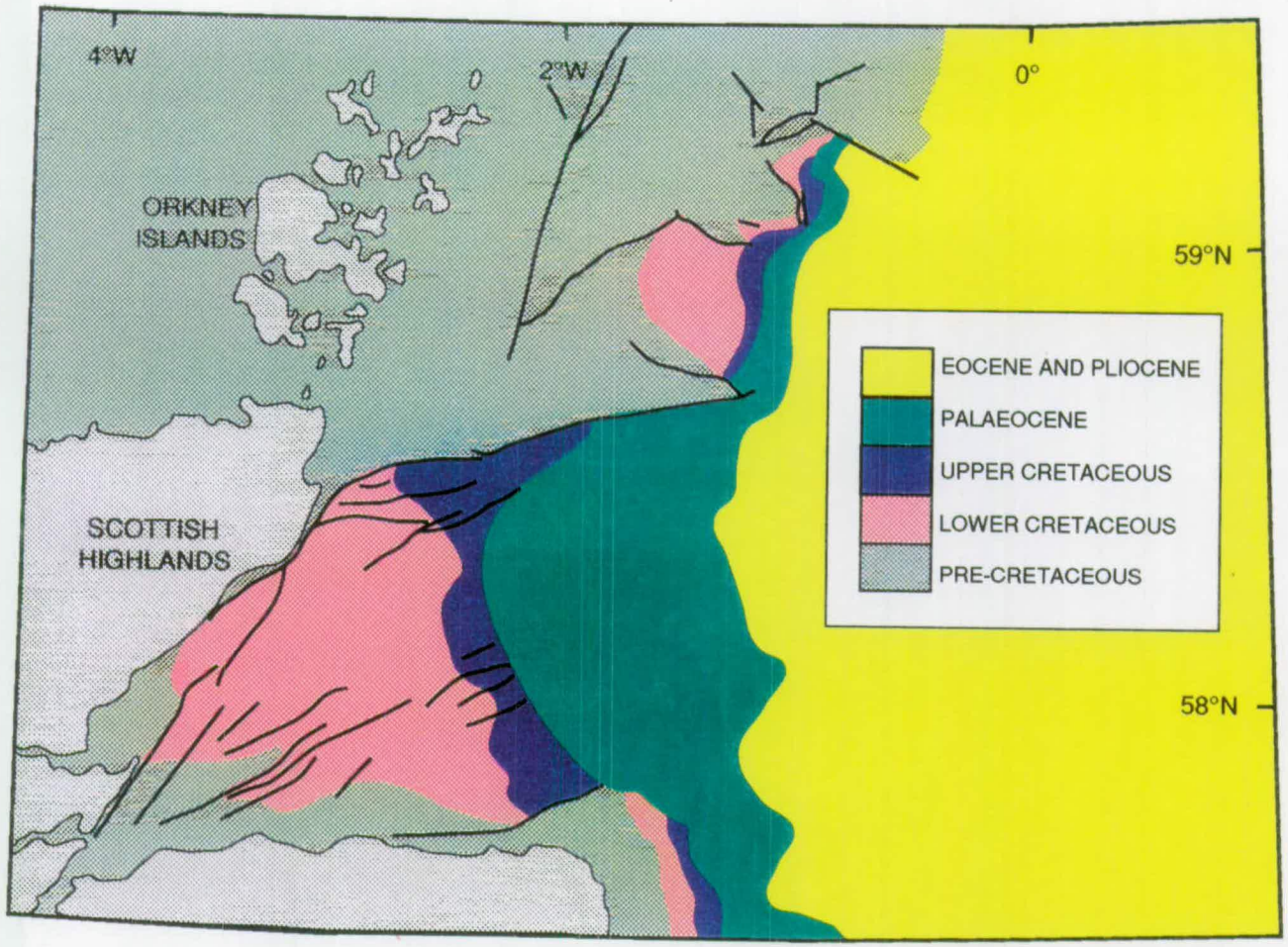

Figure 7.29 Pre-Quaternary geological subcrop map of the Inner Moray Firth and adjacent areas (After Andrews et. al.; 1990). The map shows a progressive increase in the age of the subcrop to the east. This is interpreted as the result of Late Cretaceous/Early Tertiary uplift and erosion followed by progressive Tertiary burial, the magnitude of which increases to the east.

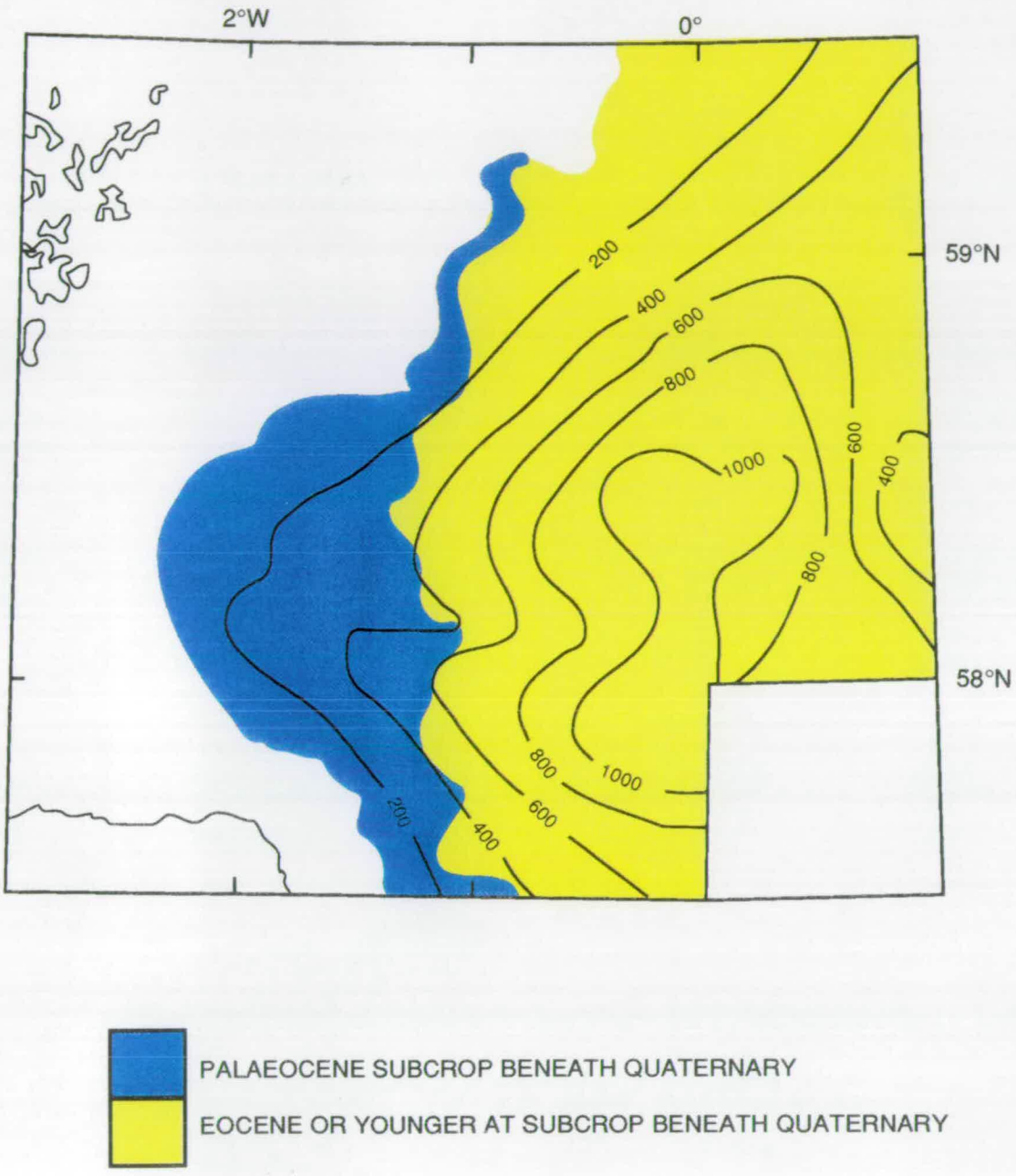

Figure 7.30 Distribution and generalised thickness of Palaeocene and Eocene strata in the Moray Firth, based on well data only (After Andrews et. al., 1990). Note the progressive increase in Tertiary thicknesses to the east.

7.7 Conclusions.

(1) Both seismic reflection profiles and field studies indicate that substantial structural modification of the Inner Moray Firth occurred after the Cretaceous, probably during the Early Tertiary. A variety of structural styles can be demonstrated involving extensional, compressional and strike-slip tectonics suggesting a complex interaction of the stress field with local pre-existing structures, many of which were reactivated.

(2) Although compactional effects mask a substantial proportion of any extensional, tectonic reactivation of pre-existing half-graben bounding faults it appears that a tectonic component cannot be ruled out in all areas. This appears to be particularly reasonable when the existence of the extensional faults forming the Sinclair Horst is considered. As these faults are clearly new tectonic features and have the same general trend as the pre-existing extensional structures, reactivation of the older features would seem possible.

(3) The presence of inversion geometries at the Wick/Great Glen Fault intersection attests to a period of compression within at least a localised part of the Inner Moray Firth since the Cretaceous. Whether this period of compression was basin wide or a local expression of the regional stress field which caused contemporaneous extension and strike-slip movements on other faults remains unanswered. However, in the case of the inversion structure seen in UKCS license block 11/25 the compression which generated the folding can be ascribed with a high level of probability to the strike-slip activity of the Great Glen Fault.

(4) Detailed examination of the Great Glen Fault can demonstrate that it was active after the Cretaceous and that the predominant style of movement was strike-slip. The sense of movement has a down to the southeast component and compressional step-overs indicate that the lateral sense of movement was dextral. The dextral sense of movement is compatible with previous interpretations based on field mapping which suggest that during the Tertiary the fault experienced dextral strike-slip.

(5) Further evidence for dextral strike-slip activity on the Great Glen Fault comes from the folding seen in the Sutherland Terrace. The orientation of these folds is incompatible with them being generated as dip-slip inversion structures and they were probably the result of dextral movement on the Great Glen Fault and sinistral movement on the Helmsdale Fault. Such opposing slip senses would lead to

compression in the Sutherland Terrace due to space problems and would be capable of generating the fold orientations observed.

(6) The most widespread structural phenomenon in the Inner Moray Firth is the gentle tilting of the basin to the east and of all the structural styles it is probably the most regionally significant. This tilting seen on seismic reflection profiles is the structural manifestation of the regional uplift and erosion and subsequent Tertiary subsidence described in the previous chapters. The data shows a significant regional unconformity separating the uplifted Mesozoic from Cenozoic units which is dated as mid-late Danian. Consequently, it seems possible that the uplift and erosion previously documented occurred during the mid-late Danian.

8. Potential driving mechanisms to account for structural reactivation, regional uplift and erosion.

8.1 Introduction.

This chapter investigates the potential mechanisms which might account for the phenomena described in the previous chapters. Firstly, the tectonic reactivation which includes extension, inversion and strike-slip deformation (Chapter 7) will be addressed. The activity is almost certainly Tertiary in age as the faults can be seen to cut through Cretaceous sediments to seabed, and in the far eastern Inner Moray Firth Tertiary sediments are affected, but the exact timing is uncertain.

The uplift and erosion documented in chapters 3, 4 and 5 also needs explaining and here the dating can in some cases be more precise. For the Scottish Highlands the apatite fission track analysis (Chapter 4) indicates that uplift and erosion rates increased during the Late Cretaceous/Early Tertiary and consequently the event(s) responsible for this must have occurred around this time. However, for the Inner Moray Firth the evidence is more ambiguous. In Chapter 7 it was noted that the basin was tilted to the east and that a significant unconformity of mid-late Danian age appears associated with this. With the presence of such an unconformity, it would seem reasonable to suggest that the uplift and erosion documented in chapters 3 and 5 occurred at this time. However, (Becker, 1993) has suggested that uplift in the Inner Moray Firth occurred during the Neogene, the same time as that for other areas of the North Sea (Boldreel and Andersen, 1993; Booth, 1993; Japsen, 1993; Jensen and Schmidt, in press) and this date cannot be discounted outright as any evidence for post-Palaeocene sedimentation would have been removed by erosion.

With regard to the patterns of uplift and erosion, both areas show a progressive westward increase with maximum values for the Inner Moray Firth of approximately 1km and 2km for the Scottish Highlands. As any proposed tectonic mechanism must generate sufficient uplift to result in the erosion that is known to have taken place and this places further constraints on any causal mechanism. Erosion of up to 1km in the Inner Moray Firth and up to 2km in the Scottish Highlands requires a tectonic uplift of $\frac{1}{3}$ km and $\frac{2}{3}$ km respectively.

The following sections will deal with the possible mechanisms and events which may be responsible for the above phenomena. However, before such an undertaking can be made the regional tectonic setting of the Inner Moray Firth and Scottish Highlands from the Late Cretaceous onwards needs to be investigated.

8.2 Regional tectonic setting.

The tectonic setting of northwestern Europe changed dramatically in the Cenozoic era due to the interaction between North Atlantic rifting to the northwest and the Alpine Orogeny to the southeast (Ziegler, 1987a and b, 1989). This resulted in the stress regime changing to one of compression compared to the predominantly extensional setting of the Mesozoic era (Ziegler, 1987a and b; Becker, 1993).

Prior to the Cenozoic, sea-floor spreading was in progress along the Mid-Atlantic Ridge, south of the Charlie-Gibbs Fracture Zone, and in the Labrador Sea (Ziegler, 1989; Becker, 1993; Knott *et. al.*, 1993; **Figure 8.1**). However, during the Palaeocene, sea-floor spreading was initiated to the northeast forming the Reykjanes, Aegir and Mohns Ridges which led to the separation of Greenland from northwestern Europe **(Figure 8.2)**, with eventual total separation of Europe from North America by the mid-Miocene. With the extinction of the Labrador Sea spreading axis in the Oligocene, the North Atlantic spreading direction changed from northwest-southeast in the Palaeocene to east-west in the Oligocene and Neogene (Becker, 1993).

While the above events occurred in the Atlantic Ocean, the Tethyan Ocean was progressively closing in a process which would culminate in the Alpine Orogeny (Ziegler, 1987a and b; Becker, 1993; Knott *et. al.*, 1993). The earliest significant deformation occurred during the Late Turonian-Early Senonian "sub Hercynian" phase as subduction began when the orogenic front met the Helvetic Shelf of the eastern Central and Eastern Alps and the Carpathians (Ziegler, 1987a and b). At the same time the western Central and Western Alps did not experience subduction but some oceanic material was obducted onto the foreland (Ziegler, 1987a and b). Following this period of deformation, a quiescent phase developed until the Palaeocene "Laramide" phase of deformation **(Figure 8.3)**, as a result of collision between the Penninic nappe system and the Helvetic Shelf in the Western Alps. While subduction developed in the Western Alps during the Eocene, the development of the Alpine Foredeep and Molasse Foreland Basin commenced and was concluded by

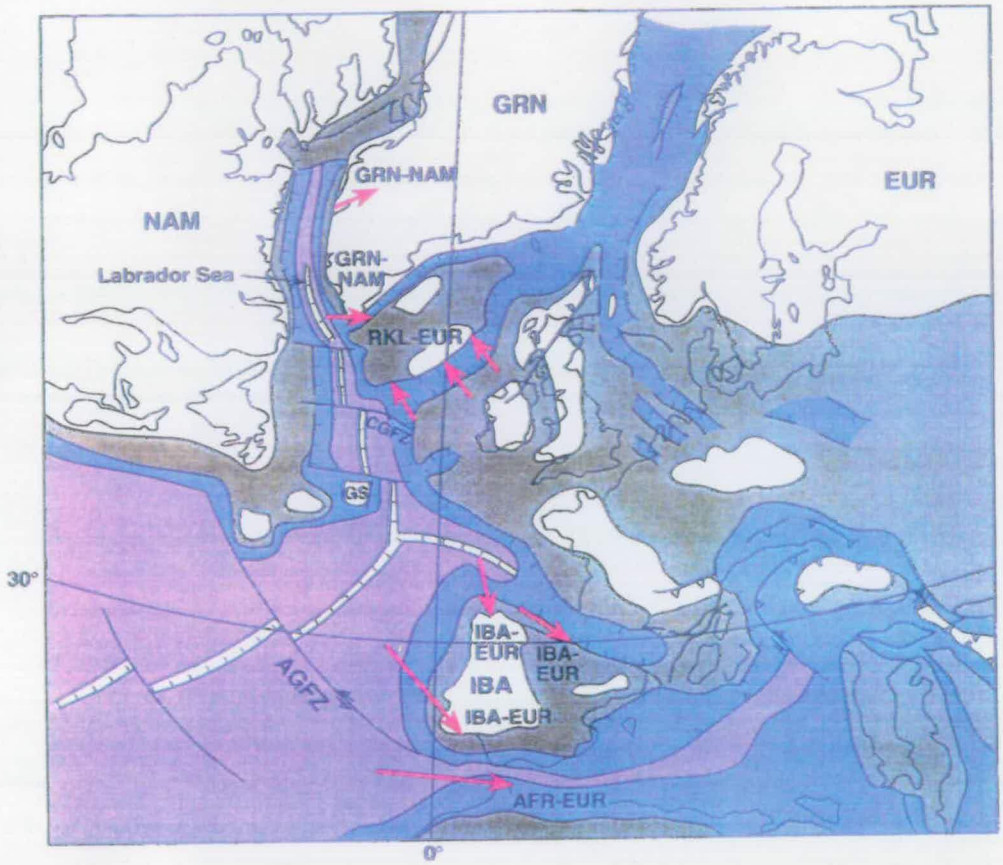

Figure 8.1 Plate reconstruction of the North Atlantic area for the Late Cretaceous (Santonian) showing that sea-floor spreading was in progress in the Labrador Sea and south of the Charlie Gibbs Fracture Zone but not between Greenland and northwestern Europe. NAM - North America, GRN - Greenland, EUR - Europe, IBA - Iberia, RKL - Rockall, AFR - Africa, ADR - Adria, CGFZ - Charlie-Gibbs Fracture Zone, AGFZ - Azores-Gibraltar Fracture Zone (Knott *et. al.*, 1993).

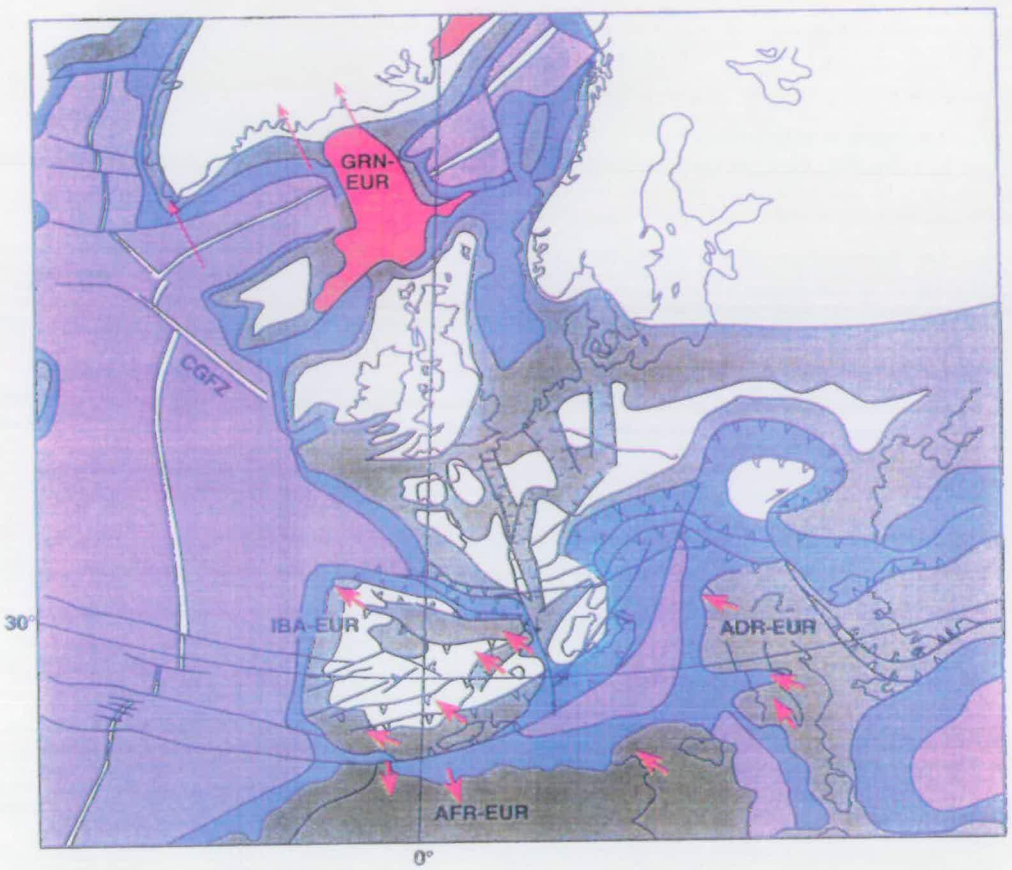

Figure 8.2 Plate reconstruction of the North Atlantic area for the Eocene (Bartonian). Note the sea-floor spreading between Greenland and northwestern Europe and the large amounts of volcanic products in the area. NAM - North America, GRN - Greenland, EUR - Europe, IBA - Iberia, RKL - Rockall, AFR - Africa, ADR - Adria, CGFZ - Charlie-Gibbs Fracture Zone, AGFZ - Azores-Gibraltar Fracture Zone (Knott *et. al.*, 1993).

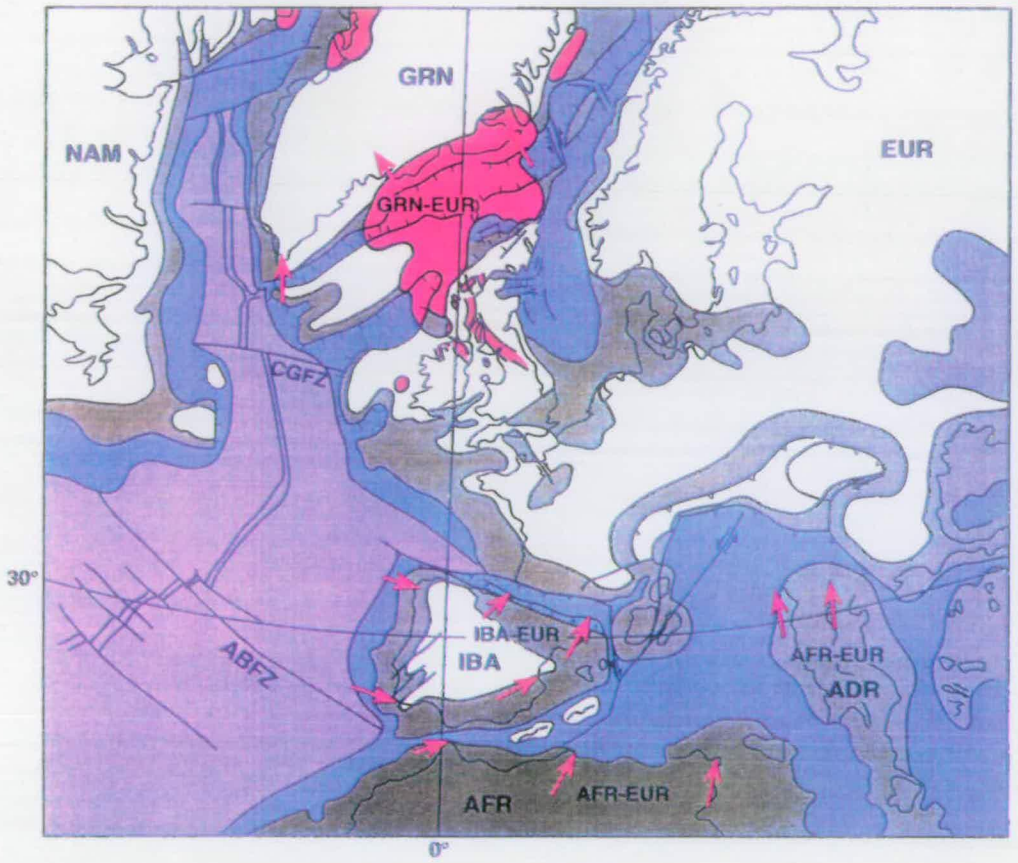

Figure 8.3 Plate reconstruction of the North Atlantic area for the Palaeocene (Thanetian) showing extensive volcanism between Greenland and northwestern Europe and the Laramide deformation developing to the south. NAM - North America, GRN - Greenland, EUR - Europe, IBA - Iberia, RKL - Rockall, AFR - Africa, ADR - Adria, CGFZ - Charlie-Gibbs Fracture Zone, AGFZ - Azores-Gibraltar Fracture Zone (Knott *et. al.*, 1993).

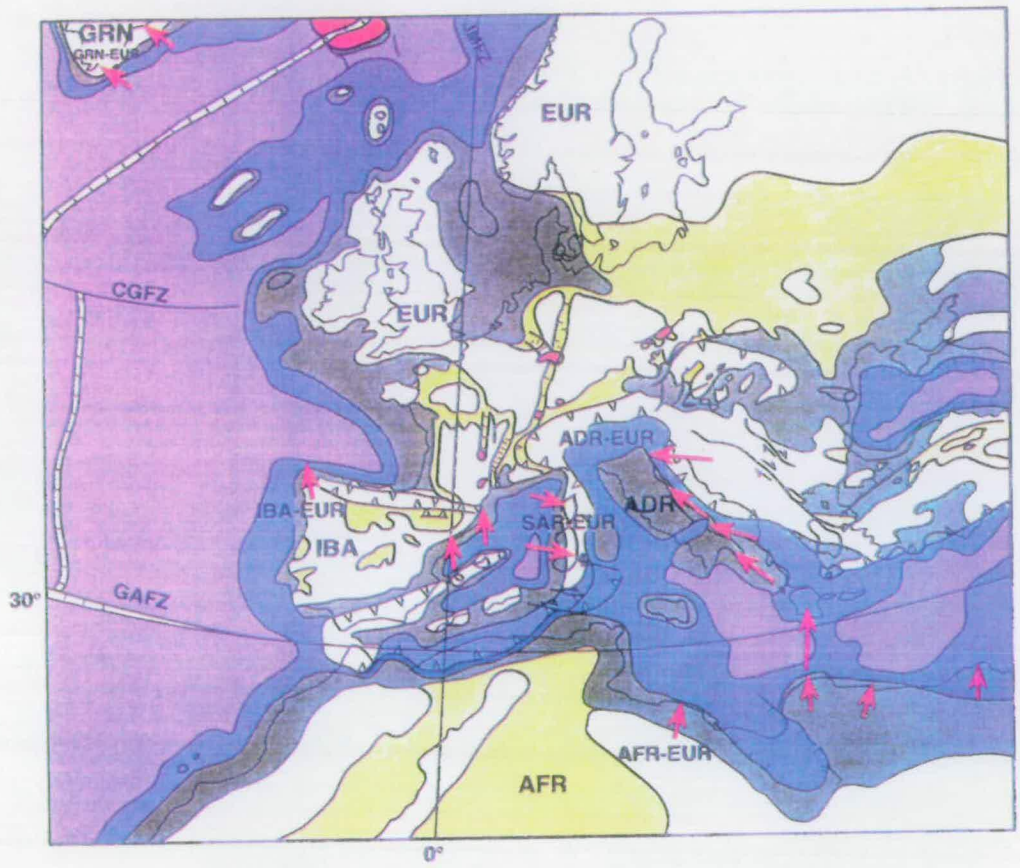

Figure 8.4 Plate reconstruction of the North Atlantic area for the Miocene (Burdigalian) showing extensive sea-floor spreading between Greenland and northwestern Europe and the extensive deformation in the Alpine Foreland by this time. NAM - North America, GRN - Greenland, EUR - Europe, IBA - Iberia, RKL - Rockall, AFR - Africa, ADR - Adria, CGFZ - Charlie-Gibbs Fracture Zone, AGFZ - Azores-Gibraltar Fracture Zone (Knott *et. al.*, 1993).

the Oligo-Miocene (Homewood *et. al.*, 1986; Pfiffner, 1986). This process resulted from the loading of the European craton by the Austro-Alpine and Penninic nappes which had been obducted onto it. Finally the Alpine Orogeny culminated in the Miocene and Pliocene **(Figure 8.4)**, with the imbrication of the Helvetic nappes, uplift of the external basement massifs of the Swiss and French Alps and the folding of the Jura Mountains and external chains of the Western Alps.

Contemporaneous with both of the processes described above significant structural reactivation occurred in northwestern Europe with the structural inversion of many pre-existing basins (**Figure 8.5**; Ziegler, 1987a and b; Bevan, 1984; Glennie and Boegner, 1981; Hillis, 1988, Cartwright, 1989; Naylor *et. al.*, 1993; Knipe, 1993; Hinz *et. al.*, 1993; Booth *et. al.*, 1993; Boldreel and Andersen, 1993; Gowers *et. al.*, 1993; Arthur, 1993; Oudmayer and Jager, 1993) and accompanying regional uplift of both the basins and structural highs (Green, 1986, 1989; Lewis *et. al.*, 1992a and b; Bray *et. al.*, 1992; Cope, 1986; Hillis, 1988, 1991; Bulat and Stoker, 1987; Japsen, 1993; Jensen and Schmidt, in press). These events have traditionally been attributed to the effects of either the opening of the North Atlantic Ocean during the Early Tertiary (White, 1988, 1989, 1992a, 1992b) or the effects of the changing stress regime within northwestern Europe due to the Alpine Orogeny (Beach, 1987 Ziegler, 1987a and b; Gibbs, 1989), changes in the spreading direction of the North Atlantic (Hinz *et. al.*, 1993; Faleide *et. al.*, 1993, Booth *et. al.*, 1993; Boldreel and Andersen, 1993) or a combination of the two (Cartwright, 1989; Ziegler, 1989; Hillis, 1992; Lewis *et. al.*, 1992a; Green *et. al.*, 1993).

It is the intention of the rest of this chapter to place the phenomena previously described for the Inner Moray Firth and Scottish Highlands into this regional context and thereby attempt to discover the potential driving mechanisms that may be responsible.

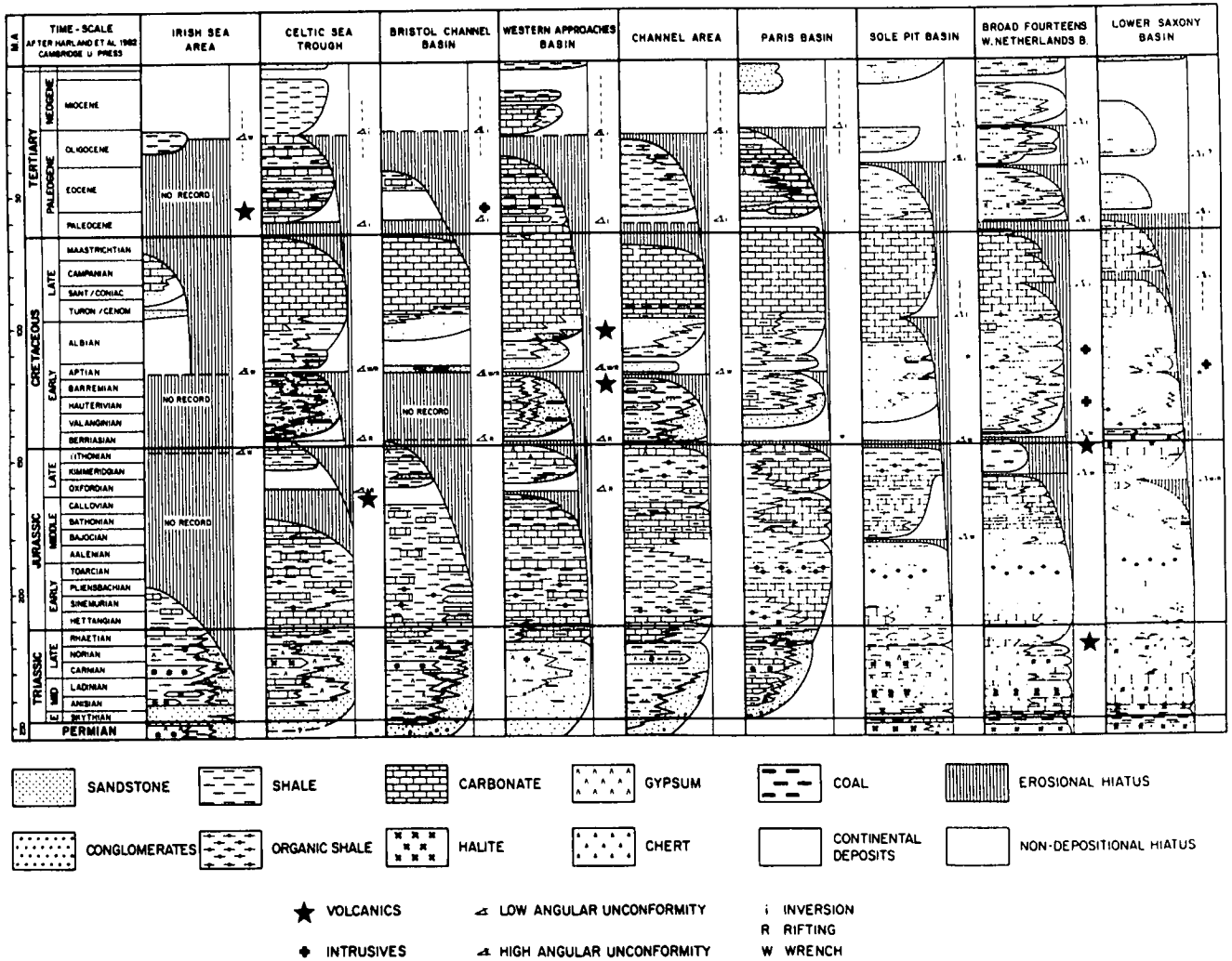

Figure 8.5 Time-stratigraphic correlation chart for parts of northwestern Europe from the Late Permian to the present-day. Note the high level of correlation between basin for the several uplift and inversion episodes that characterise the Late Cretaceous and Tertiary (Ziegler, 1987b).

8.3 Potential mechanisms.

8.3.1 The Iceland "hot-spot", its inflation and collapse.

Greenland separated from northwestern Europe in the Early Tertiary due to rifting over a mantle plume or "hot-spot" to form the North Atlantic (Ziegler, 1989; White, 1988) with seafloor spreading commencing around 57-55ma (White, 1992b; **Figures 8.2 and 8.3**). This mantle plume had a pronounced effect on the rifting characteristics of the region and still exerts an influence to this day. Currently, the plume is situated beneath Iceland and is associated with thermal, gravitational and geoidal anomalies (White, 1988, 1989; Bott, 1988; **Figure 8.6**). Indeed, the presence of the plume beneath Iceland is responsible for dynamic uplift in the area which maintains a shallow bathymetry, causing Iceland to be approximately 2.5km above its expected elevation (White, 1988, 1989, 1992a and b; Bott, 1988). It is thus important to assess how such rifting over a mantle "hot-spot" could have affected the Inner Moray Firth and Scottish Highlands. In order to do so, it is essential to understand the mechanics of rifting and plume interaction and evolution.

Igneous petrological data suggests that the material forming the Iceland "hot-spot" consists of asthenospheric material approximately 200°C hotter than normal (White, 1988 and 1989) and that it rose through the mantle as a plume due to its buoyancy relative to the normal temperature mantle that surrounds it **(Figure 8.7)**. Furthermore, the effects of plume initiation need to be addressed as although the "hot-spot" is currently in a steady-state and its effects are well understood, at the time of interest the plume and associated "hot-spot" were rapidly developing as it rose to eventually impinge on the base of the lithosphere. Campbell and Griffiths (1990) and Griffiths and Campbell (1991) have, by modelling plume initiation, been able to deduce the effects of an anomalously hot mass as it rose from depth to eventually impinge on the base of the lithosphere. They suggest that the material produces uplift of the surface 10-20ma prior to eruption of the volcanics **(Figure 8.8)**. Additionally, their results imply that unless crustal thinning (rifting) had already taken place by other means, volcanism does not commence until uplift has ceased as the plume would be too deep to decompress sufficiently to generate melt. Furthermore, the modelling shows that while volcanism starts above the plume, and the central uplift collapses, the surrounding areas can still become uplifted for a further 20-60ma **(Figure 8.8)** due to the plume head spreading laterally as it meets the base of the lithosphere and producing a spreading thermal anomaly which generates uplift **(Figure 8.8)**. A consequence of such large uplifts

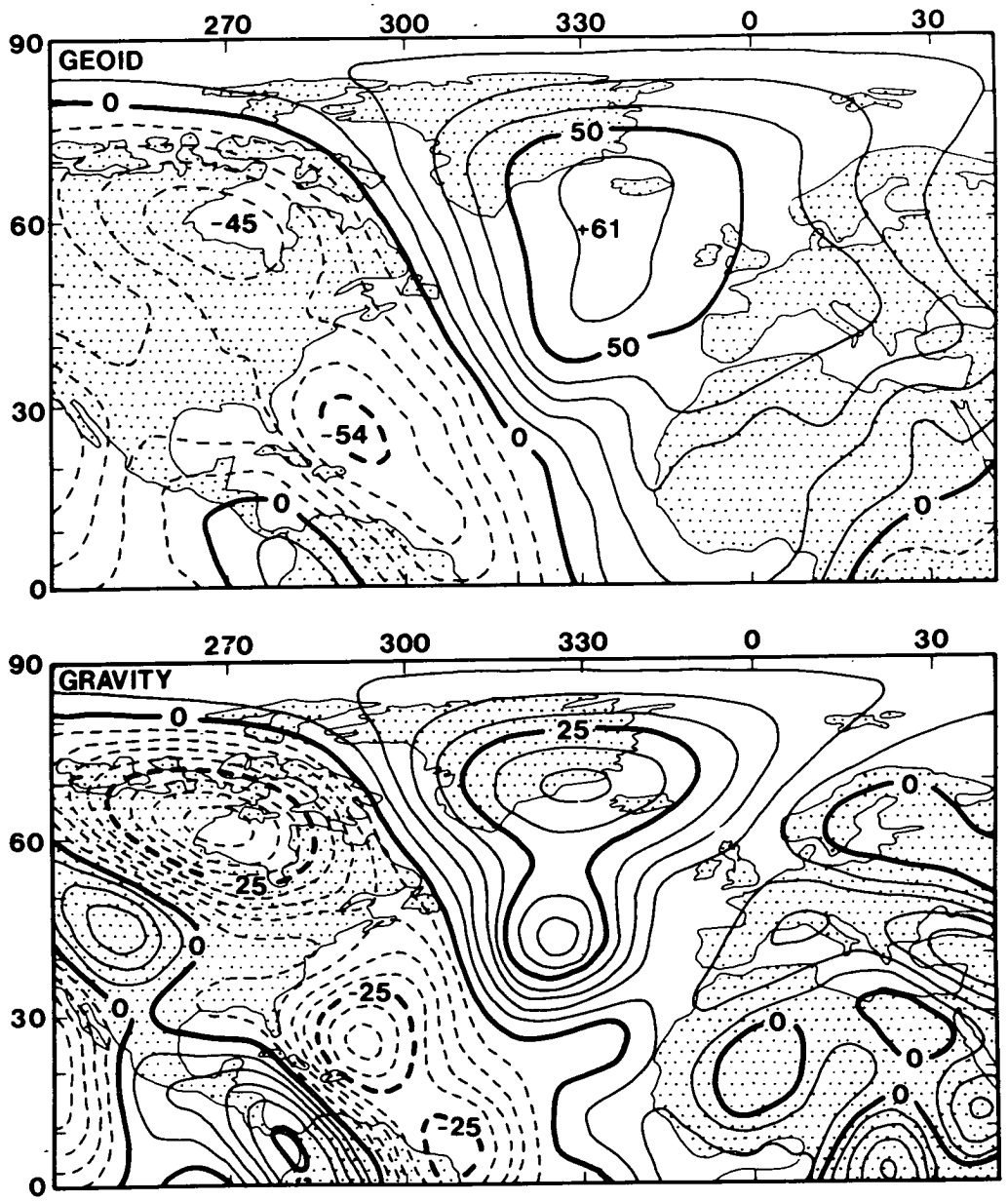

Figure 8.6 Geoidal and gravity anomalies of the North Atlantic (Bott, 1988). Note the significant anomalies centred over Iceland which are manifestations of the mantle plume situated beneath it.

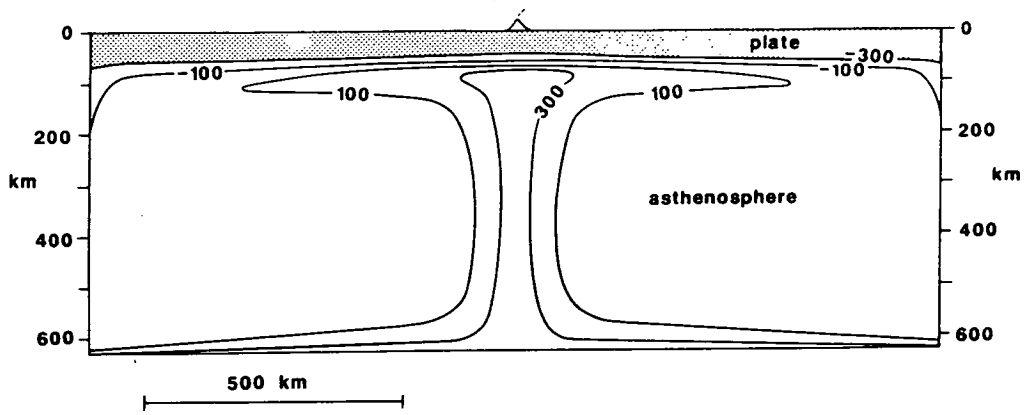

Figure 8.7 Cross-section of the temperature structure through the mantle plume beneath the Cape Verde Rise (White, 1988). Note the narrow rising mantle plume at the centre and the broad, mushroom-shaped head of hot asthenosphere material deflected laterally by the overlying plate. Plume volcanism occurs only above the rising central plume.

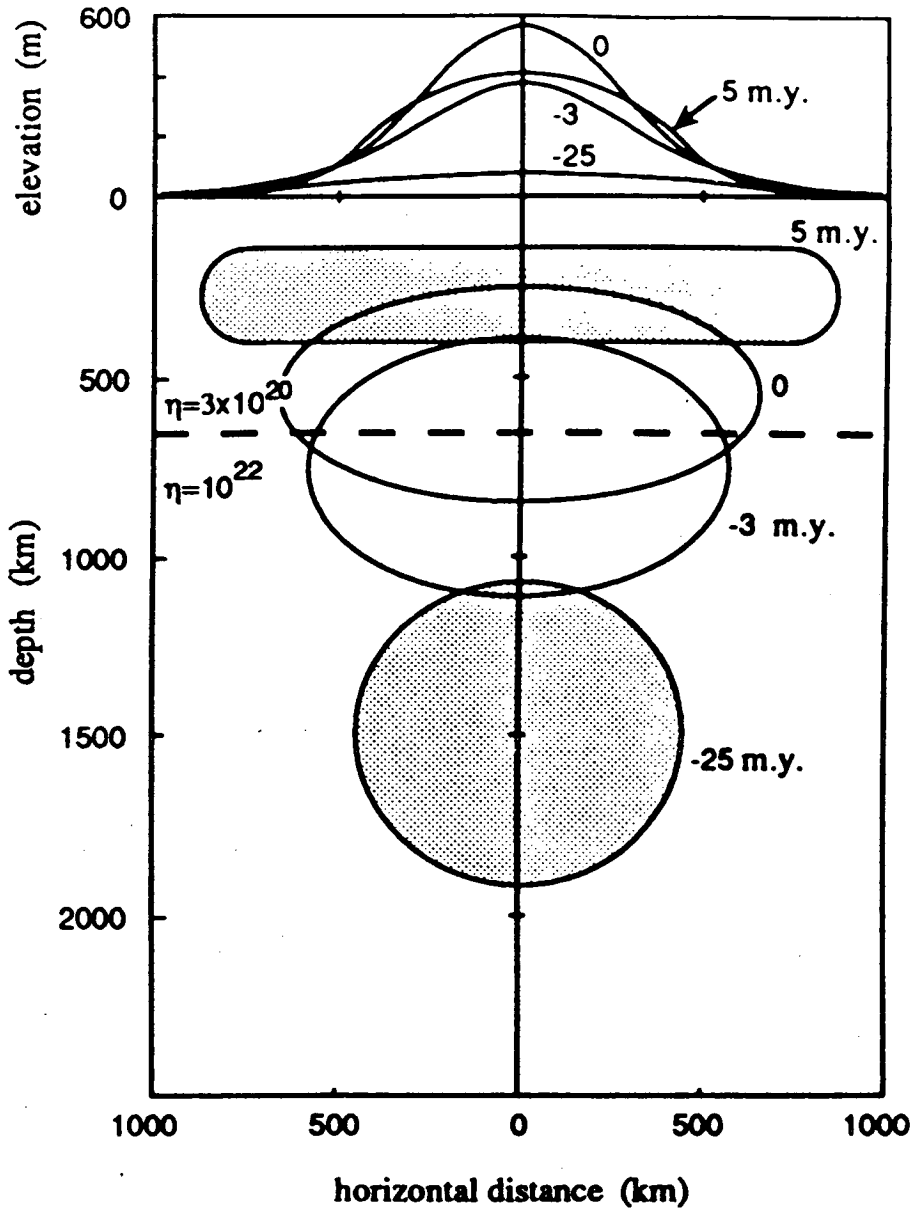

Figure 8.8 Diagram showing the main dimensions predicted for the heads of starting plumes and the shapes of the surface uplift scaled from laboratory experiments. Horizontal spreading occurs in the upper mantle. Effects of plume enlargement due to entrainment and source influx during the plume ascent are allowed for, but any effects of a continuing input from the source during the spreading are neglected (Griffiths and Campbell, 1991).

over the mantle plume is the gravitational potential it induces. By elevating the crust a radial stress regime can be induced and rifting may result (Campbell and Griffiths, 1990; Griffiths and Campbell, 1991). This has been postulated as the cause of the east-west extension in the Faeroes Basin (Knott *et. al.*, 1993) and may explain the northeast-southwest extension suggested by England (1988) for northwest Britain, as such an orientation is roughly tangental to the proposed topographic anomaly induced by the thermal anomaly **(Figure 8.9)**. Furthermore, analogue models of domes (Dixon, 1975; Withjack and Schiener, 1982) have shown that strike-slip motion could be induced around them, and this presents the possibility, providing they can be scaled-up, that the strike-slip movement on the Great Glen Fault may have occurred by a similar mechanism.

8.3.2 North Atlantic rifting.

The effects of the rifting process itself may have potential influences on the Inner Moray Firth and adjacent areas. The recognition that it is unlikely that rifting occurs by pure shear (McKenzie, 1978) or simple shear (Wernicke, 1985) throughout the entire lithosphere but that these processes represent end members of potential rift types has led to the development of "flexural cantilever" models (Kusznir and Egan, 1989; Weissel and Karner, 1989; Kusznir *et. al.*, 1991; Roberts and Yielding, 1991). In such models it is assumed that the upper crust has some mechanical strength, that it deforms by faulting (simple shear) and responds to loads by flexural rather than Airy isostasy while the lower crust and mantle deforms by pure shear **(Figure 1.10)**. The result is that upon rifting the crustal loading is altered and this results in the flexural uplift of footwalls and flexural downwarp of hangingwalls **(Figure 1.10)**. Consequently, this presents a potential method of generating uplifts along continental margins and may have an effect on the regional uplift seen in the Scottish Highlands and Inner Moray Firth if they are seen as lying on a "megafootwall" to the North Atlantic.

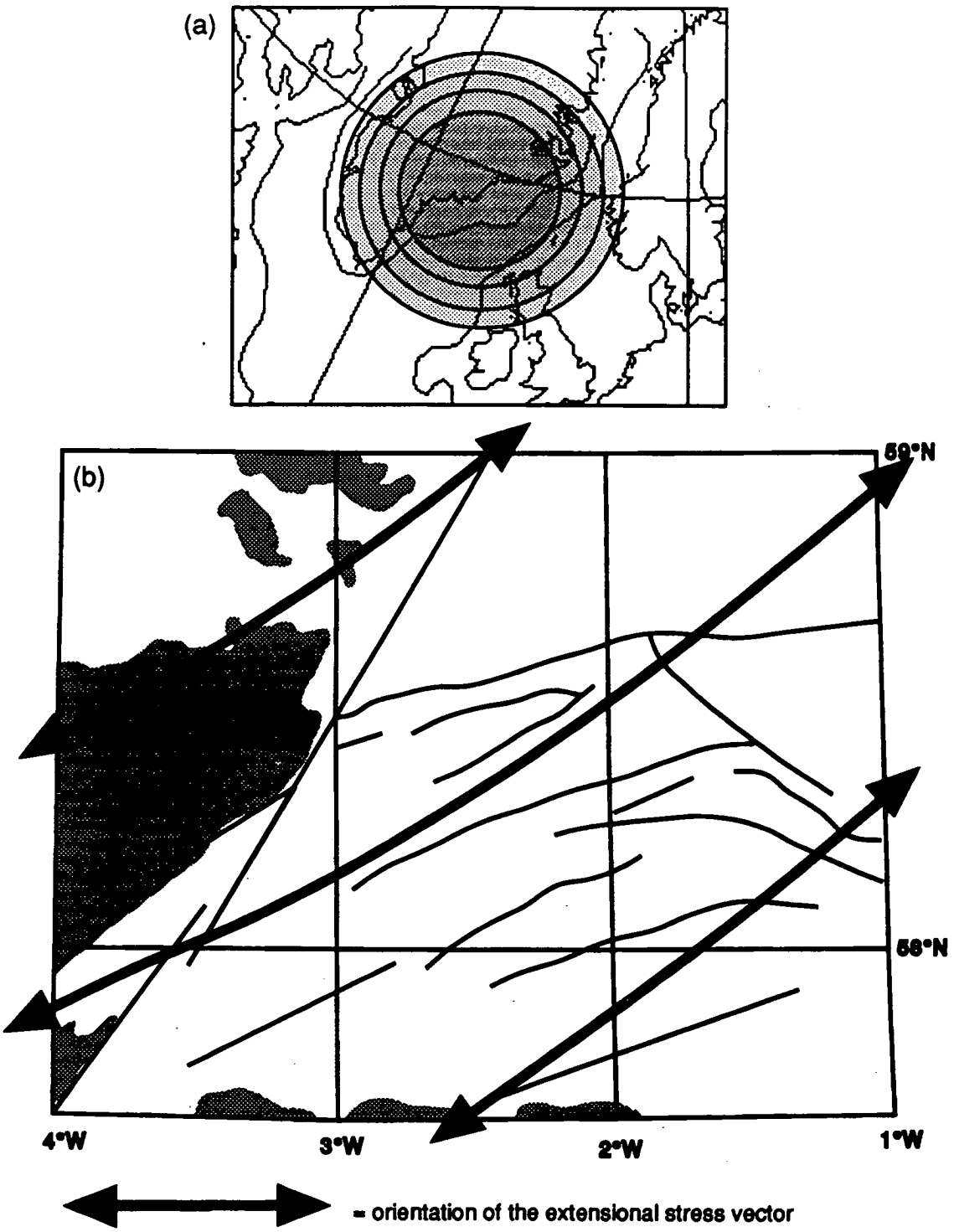

Figure 8.9 (a) Plate reconstruction for the North Atlantic at 60ma. The concentric circles are centred on the approximate position of the Iceland "hot-spot" at that time (White, 1989) and consequently indicate that the topographic anomaly. (b) The resultant circumferential collapse would result in an northeast-southwest orientation of the extensional stress vector over the Scottish Highlands and Inner Moray Firth, consistent with that proposed by England (1988).

8.3.3 North Atlantic igneous activity, volcanic over/underplating.

The most distinctive feature of the rifting process was the large amounts of volcanic products produced. The North Atlantic contains up to 2 x 10^6 km^3 of volcanics, located in the onshore settings of Scotland, Ireland, Greenland and the Faeroes but most significantly along the rifted continental margins (White, 1988, 1989; **Figure 1.8**). The rifted continental margins are particularly significant, with large surface flows such as the 4km thick pile seen on the Hatton Bank and the large amounts (10km thick) intruded into the lower crust (White, 1988, 1989, 1992a and b; **Figure 1.9**). The potential effects of such large volumes of igneous material being added to the continental margin are considerable, with evidence suggesting that after rifting some parts remained elevated, even to the present day as an isostatic response to thickening the continental margins.

8.3.4 Two-layer lithospheric compression.

Regional uplift of a basin which only shows localised inversion (as seen in the Inner Moray Firth) has also been described in the East Midlands Shelf (Green, 1989), and in the Western Approaches Trough (Hillis, 1991). In order to account for regional uplift of areas where there is only localized evidence of crustal compression, Hillis (1992) proposed a decoupled, two-layer model of lithospheric compression **(Figure 1.5)**. This model is discussed here to see if it could account for the regional uplift of the Inner Moray Firth.

It is clear from the inversion structures in the Inner Moray Firth that the (upper) crust was under local compression in Tertiary times. Hillis' (1992) model assumes that the entire lithosphere is under compression, but that compression and thickening in the lower lithosphere is decoupled, and laterally displaced, from that in the upper lithosphere **(Figure 1.5)**. Reverse movement on the pre-existing, weak crustal detachments, extension on which had formed the basins may have caused the basin inversion (c.f. Beach, 1987; Gibbs, 1989), while thickening of the mantle lithosphere without accompanying thickening of the crust could then be invoked to account for the regional uplift **(Figure 1.5)**. Submersion of cold, dense mantle lithosphere into the surrounding asthenosphere would have caused an initial, isostatically-driven subsidence. Subsequent warming of the lithosphere would have caused uplift, and potentially the extensional reactivation (Chapter 7). Hence, thickening of the mantle lithosphere without thickening of the overlying crust (which is concentrated in the inversion axes) can account for the initial subsidence

then uplift of uninverted areas inferred from compaction data (Chapters 3 and 6; **Figure 1.5**).

The amount of mantle lithospheric thickening required to produce 1/3 km of tectonic uplift can be easily determined from the curves of Sandiford and Powell (1990) which are paramaterized in terms of thickening factors, f (reciprocal of extension factor, ß). In the absence of crustal thickening a mantle lithospheric thickening factor (f_{ml}) of 1.1 will generate the inferred subsidence then uplift. It could be proposed that mantle lithospheric compression and thickening is balanced by crustal compression and thickening in inverted areas within the Inner Moray Firth. This can potentially fit the data as in the inverted areas crustal thickening alone would lead to an initial uplift (no prior subsidence) and relatively minor subsequent thermal uplift **(Figure 1.5)**. In the inverted areas, where pre-erosional units crop out at sea-bed, there is no evidence of burial immediately prior to erosion.

8.3.5 Intraplate stress.

The predominant stress field of northwest Europe changed from one of extension to one of compression during Late Cretaceous/Early Tertiary due to combination of Atlantic rifting to the northwest and Alpine collision to the south (Ziegler 1987a; 1987b). Intraplate compressional stresses essentially act to amplify existing deflections of the lithosphere, and for example basin centres are deepened while flanks are uplifted (Cloetingh *et. al.*, 1985; Kooi and Cloetingh, 1989; Cloetingh *et. al.*, 1990; **Figure 1.7**). Hence, if the Inner Moray Firth is seen as a flank to the North Sea rift system intraplate compression could generate tectonic uplift.

8.4 Discussion.

8.4.1 North Atlantic phenomena.

Taken as a whole the phenomena previously described can explain some features seen in the Inner Moray Firth and adjacent areas. Firstly, the presence of the large topographic swell over the Iceland "hot-spot" and the proposed extension it induces (Campbell and Griffiths, 1990; Griffiths and Campbell, 1991) may explain the extensional reactivation seen in the basin. An east-west to northeast-southwest orientated extension (Knott *et. al.*, 1993; England, 1988) could induce oblique dextral extension on most of the normal faults in the basin as they trend east north east-west south west **(Figure 8.10)** and may have been able to reactivate the Great Glen Fault. Additionally, the analogue models of domes (Dixon, 1975; Withjack and Schiener, 1982) seem to provide a potential mechanism for the strike-slip motion on the Great Glen Fault, providing that the process can work at these larger scales. As there is no real age constraint of the timing of the structural reactivation, except that it is Tertiary in age, it would seem logical to place the timing of this activity as contemporaneous with the doming. Campbell and Griffiths (1990) and Griffiths and Campbell (1991) have shown that maximum uplift occurs 10-20ma before the volcanism and as the main phase of volcanic activity occurred during the Late Palaeocene-Early Eocene this would conveniently place the tectonic reactivation in the Late Cretaceous and Early Palaeocene (Danian). The large scale tilting of the basin also seems to fit this picture with the dome producing uplift and erosion, the products of which were deposited in the Outer Moray Firth and Central Grabens as Palaeocene and Eocene deltas, slope fans and turbidites (Parker, 1975; Rochow, 1981; Galloway *et. al.*, 1993) to produce the geometries currently seen on seismic reflection profiles. However, the inversion seen in UKCS license block 12/16 cannot be readily explained by such a mechanism.

With regard to the uplift and erosion histories of Inner Moray Firth and Scottish Highlands the correlation is more ambiguous. The slight increase in erosion rates over the Scottish Highlands during the Late Cretaceous/Early Tertiary appears to correlate well with the initiation of the plume and rifting. Indeed, the progressive increase in post-Cretaceous erosion to the west seems to strengthen the argument because the Outer Hebridies are marginally closer to the plume and nearer the continental margin. This proximity to the continental margin will also increase the expected uplift as the igneous underplating will probably be more significant than in eastern Scotland while the potential effects of rift flank uplift, as predicted by the "flexural cantilever" model may also play a role. However, in the

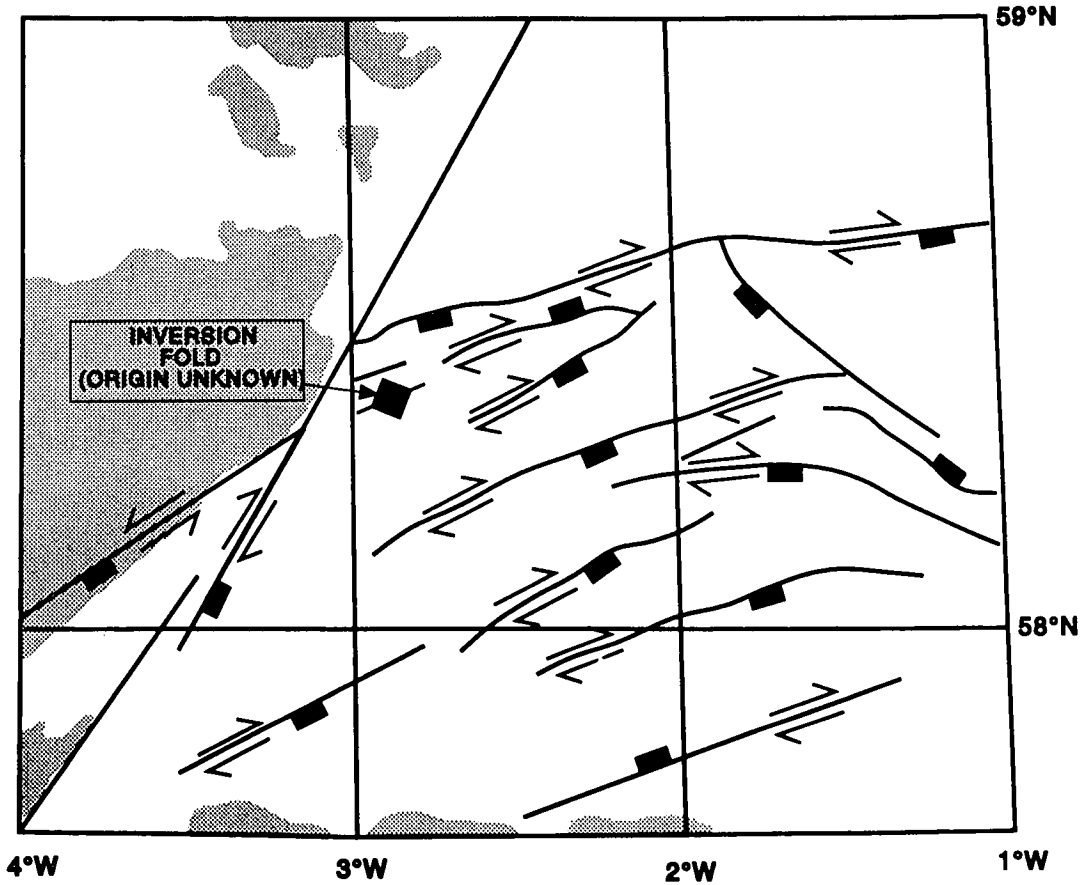

Figure 8.10 Proposed pattern of Tertiary structural reactivation in the Inner Moray Firth. An east-west to northeast-southwest orientated extensional vector could produce the extension on the major normal faults which are generally orientated east north east - west south west, a direction compatible with dextral oblique extension. Furthermore the stresses may be aligned in an appropriate direction to account for the strike-slip reactivation on the Great Glen Fault but does not seem able to generate the inversion seen in UKCS license block 12/16.

Inner Moray Firth problems arise. Where no post-Cretaceous sediments are present, there are no constraints on the uplift and erosion path and the vitrinite reflectance modelling (Chapter 5) shows that a variety of potential paths produce equally good results and the observations for the Scottish Highlands may hold for this area. Unfortunately, in the parts of the Inner Moray Firth where post-Cretaceous sediments are found, the data suggests that rapid subsidence needs to precede the rapid uplift in the Danian. This could be accounted for if the uplift in the area occurred slightly after the extensional reactivation so that accommodation space for the large volumes of sediment removed from the already uplifted areas to the north and west was available. In such a case the sediment could then be redistributed and deposited in the Inner Moray Firth to cause the overcompaction (documented in Chapter 3) and the rapid increase in subsidence prior to its removal by subsequent uplift. However, this still requires extremely high sedimentation and erosion rates **(Figure 8.11(a))** and this questions whether all the observed uplift in the Inner Moray Firth occurred during the Danian, particularly when a significant Neogene component has been proposed by Becker (1993) and has been documented in the surrounding areas (Booth et. al., 1993; Boldreel and Andersen, 1993; Japsen, 1993; Jensen and Schmidt, in press). Consequently, it appears possible, even highly probable, that Neogene uplift and erosion may have had a significant role to play in the evolution of the Inner Moray Firth and that maximum burial-depths were not achieved until after the Danian.

8.4.2 Compressional tectonics.

The two-layer compression model of Hillis (1992) at first sight appears capable of explaining many features of the uplift and structural reactivation history of the Inner Moray Firth. However, if regional uplift and erosion in the Inner Moray Firth occurred during a period of approximately 5ma during the Early Palaeocene and thermal re-equilibration following mantle lithospheric thickening drove the uplift, lithospheric warming must have occurred more rapidly following compression than it does cooling following lithospheric extension and thinning (which has a thermal time constant of 50-60ma). To overcome this problem Hillis (1992) suggests that the thermal boundary layer which separates the lithosphere from the asthenosphere may become unstable, and detach, if submersed in hot asthenosphere following lithospheric thickening (Houseman *et. al.*, 1981). Such detachment may cause rapid warming of the overlying mantle part of the lithosphere directly juxtaposed to convecting asthenosphere. However, the requirement of rapid uplift and the consequent invoking of the detachment of the

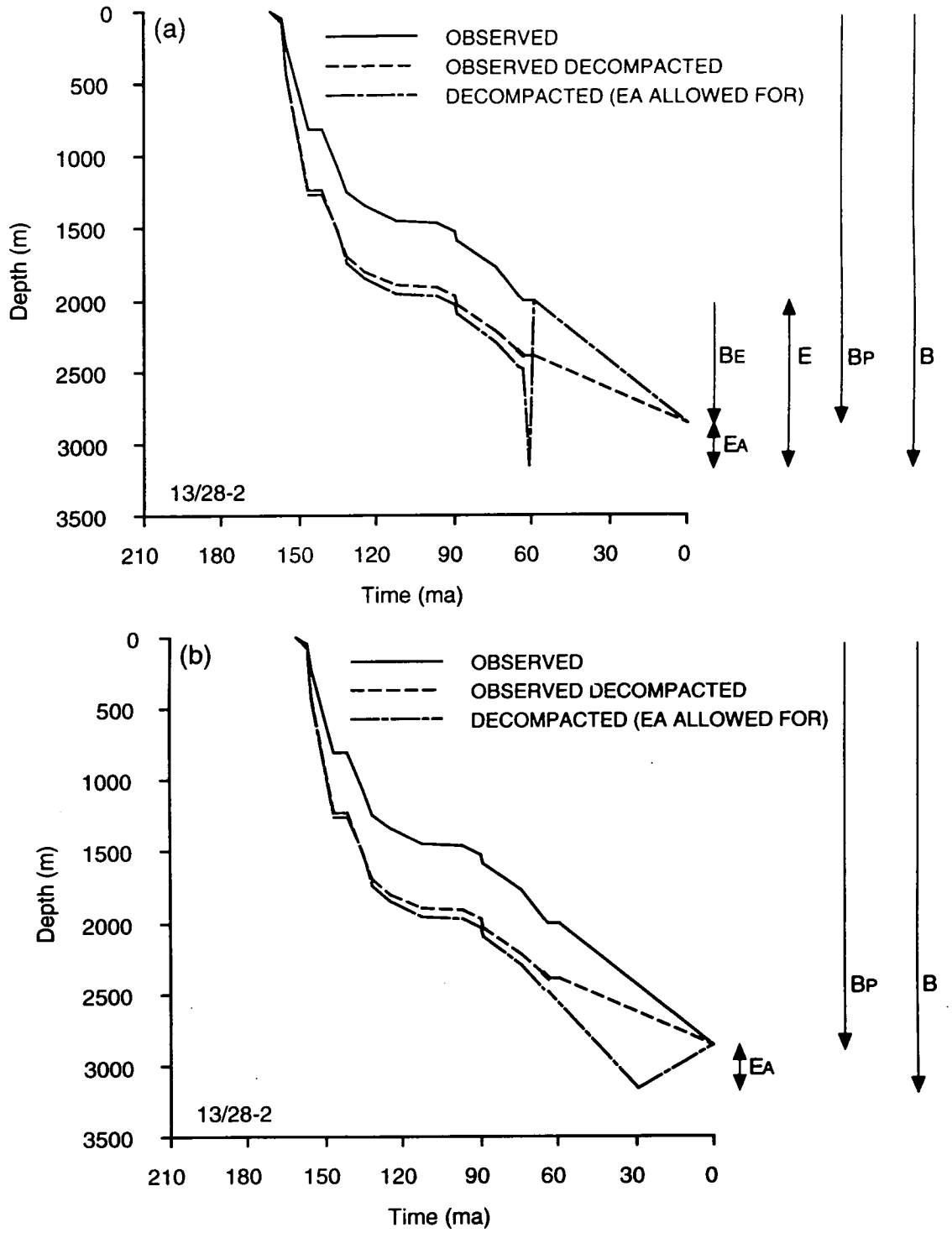

Figure 8.11 (a) Present observed (solid) and decompacted burial histories for the base Jurassic in well 13/28-2. The dashed plot is corrected for compactional effects without consideration of Palaeocene erosion, whereas the dash and dot plot has been corrected for compaction with allowance for Palaeocene erosion. (b) In this plot the Palaeocene erosion has been replaced with Neogene erosion and maximum burial-depth is assumed to have occurred after the Palaeocene. Note the reduction in the rates of subdience and uplift required at the time of erosion if it occurs in the Neogene and not the Palaeocene. The maximum burial-depth (B) equals present burial-depth (BP) plus apparent erosion (EA), i.e. B=EA+BP and erosion at the time of exhumation equals apparent erosion (EA) plus the post-erosional burial (BE). i.e. E=EA+BE.

thermal boundary layer is far from an ideal solution. Although the model can account for the structural reactivation, the subsidence and uplift it remains far from ideal and cannot be considered a viable proposal if maximum burial depths were achieved prior to Danian uplift. However, as there is evidence for Neogene uplift elsewhere (Japsen, 1993; Jensen and Schmidt, in press), and this time represented a major change in the plate boundary conditions, the mechanism could potentially work if the uplift and erosion was Neogene and not Danian.

The combined effect of the conclusion of the development of the Alpine Foredeep and Molasse Foreland Basin in the Western Alps by the Oligo-Miocene (Homewood *et. al.*, 1986; Pfiffner, 1986), and the imbrication of the Helvetic nappes, uplift of the external basement massifs and the folding of the Jura Mountains and external chains of the Western Alps in the Miocene and Pliocene, with the change in North Atlantic spreading direction from northwest-southeast in the Palaeocene to east-west in the Oligocene and Neogene (Becker, 1993) could have resulted in a change in the stress regime of northwestern Europe. It is possible that this alteration of the stress field in northwestern Europe resulted in the uplift and erosion seen in the Inner Moray Firth, possibly by the two-layer compression model of Hillis (1992). This would mean that although Danian uplift occurred it would have been smaller than previously thought as the exhumation would not have been from the maximum burial-depth measured in Chapter 3. Instead maximum burial-depths would have been achieved prior to the Neogene and consequently the rapid increase in subsidence which the Hillis (1992) model would need to produce would be smaller **(Figure 8.11)**. Additionally, the uplift phase of the Hillis (1992) model would not need to be as rapid as previously thought if uplift and erosion in the Inner Moray Firth was Neogene and not Danian. As no post-Neogene sediments are present in the area it is possible that the thermally driven uplift could have occurred with a thermal time constant of around 50-60ma (the same as during thermally driven subsidence) and this would remove the need to invoke the detachment of the thermal boundary layer. Furthermore, a gradual uplift using a thermal time constant of 50-60ma would explain why the Inner Moray Firth has not subsided since the erosion episode as the area would still be thermally re-equilibrating and consequently not prone to subsidence as yet.

If the Inner Moray Firth is seen as a flank to the North Sea rift system intraplate compression could generate tectonic uplift (Cloetingh *et. al.*, 1985; Kooi and Cloetingh, 1989; Cloetingh *et. al.*, 1990). However, this mechanism is only likely to generate up to 50 m of uplift as larger lithospheric deflections cannot be accommodated by the lithosphere (Cloetingh *et. al.*, 1985; Kooi and Cloetingh, 1989;

Cloetingh *et. al.*, 1990). Furthermore, the Inner Moray Firth is in itself a significant basin, being part of the North Sea triple rift system of the Viking Graben/Central Graben/Moray Firth. Hence, it is unlikely that the entire Inner Moray Firth would have been uplifted in response to intraplate compressional stresses *sensu* Cloetingh *et. al.* (1985). The Mesozoic depocentre of the Inner Moray Firth would be expected to subside in response to intraplate compression, and its flanks would be expected to be uplifted. Such a pattern does not account for the observed regional uplift of the Inner Moray Firth. Furthermore, the structural implications of compressional intraplate stresses are not compatible with the wide variety of structural reactivation patterns seen in the Inner Moray Firth. Although the compressional tectonic activity seen in the Inner Moray Firth could be expected when a basin is subjected to compressional intraplate stresses (Karner, 1986) and strike-slip deformation cannot be ruled out, extensional reactivation, which is by far the most common form of activity, seems incompatible. Consequently, it appears that intraplate compressive stress models (*sensu* Cloetingh *et. al.*, 1985) are incapable of producing most of the effects seen in the Inner Moray Firth and may be discounted as a likely mechanism.

8.5 Summary of the evidence for the timing of structural reactivation, uplift and erosion in the Inner Moray Firth and Scottish Highlands.

The above discussion seems to suggest that the increase in uplift and erosion rates over the Scottish Highlands from the Late Cretaceous/Early Tertiary onwards is compatible with the rifting of the North Atlantic at the same time. The large topographic anomaly would be expected to reach its maximum 10-20ma before the significant volcanism, and in this case this would suggest uplift reaching its peak during the latest Cretaceous and earliest Tertiary (Palaeocene) as the volcanism occurred in the latest Palaeocene and Early Eocene. The additional effects of thickening the crust with the products of the British Tertiary Igneous Province must also have played a role and may explain the westerly increase in erosion over the Scottish Highlands.

The large topographic anomaly caused be the Iceland "hot-spot" would have induced extension as it collapsed and this seems readily to explain the extensional and strike-slip faulting in the Inner Moray Firth which the data can only constrain has having occurred during the Tertiary. Consequently, although the possibility that the possible Neogene plate boundary changes caused the reactivation cannot be excluded

as yet, the most likely date for the tectonic reactivation is the Early Palaeocene when the dome reached its maximum extent.

Although the tectonic reactivation of the Inner Moray Firth seems compatible with an Early Palaeocene date, the uplift and erosion does not. If maximum burial-depths were achieved prior to the Danian then the subsidence immediately prior to uplift needs to be extremely rapid, as does the uplift itself **(Figure 8.11)**. None of the possible mechanisms which could have operated at this time are capable of generating the rapid subsidence except for the Hillis (1992) two-layer compression model. However, as the Hillis (1992) model requires special pleading for the thermodynamics which generate the rapid uplift the mid-late Danian unconformity does not seem to correlate with the major uplift and erosion episode in the basin, although some erosion must have occurred at this time. It appears more likely that the sediments in the Inner Moray Firth achieved their maximum burial-depth after the Danian and that Neogene uplift and erosion took place. This would require lower subsidence and erosion rates **(Figure 8.11)** and would correspond to the time of major changes in the spreading characteristics of the North Atlantic and the tectonics of the Alpine Orogeny. Additionally, this would reduce the amount of erosion that is required in the Inner Moray Firth as if uplift and erosion occurred after the Danian the total erosion estimates (Chapter 6) would be too large as the correction for post-erosional burial is incorrect **(Figure 6.2)**. Instead, the total erosion estimates would be the same as those for apparent erosion with uplift and erosion decreasing from a maximum of over 1km in the west to zero at the Inner Moray Firth-Outer Moray Firth transition **(Figure 6.2)**. As for the driving mechanism of any Neogene uplift and erosion it is as yet too poorly constrained to be definitive but models such as the Hillis (1992) two-layer compression model could possibly play a role, particularly when the need for rapid uplift and the consequent detachment of the thermal boundary layer is removed.

8.6 Conclusions.

(1) All the evidence documented suggests that the tectonic reactivation in the Inner Moray Firth and the uplift and erosion in both the Inner Moray Firth and Scottish Highlands occurred during the Cenozoic. As this time corresponds to a major tectonic reorganisation in the area, with North Atlantic rifting to the northwest and the Alpine Orogeny to the southeast, it appears likely that one or other of these events, or possibly the interplay between them, was responsible for the phenomena.

(2) Invoking the flexural effects of fluctuations in the level of intraplate stresses seems incompatible with the data. The magnitudes of such effects are an order of magnitude too small to account for the uplift and erosion documented, while the patterns of the vertical movements would not be the same as observed. In such models the margins of the Inner Moray Firth could be uplifted but the depocentres would be expected to subside which is in direct contradiction with the data.

(3) The effects of North Atlantic rifting in the Palaeocene appears to fit the data for the Scottish Highlands extremely well and may also explain the structural reactivation seen in the Inner Moray Firth. However, such a mechanism would appear incapable of accounting for the uplift and erosion of the Inner Moray Firth. If the Palaeocene effects were responsible for the uplift from maximum burial-depth of sediments in the Inner Moray Firth then a period of rapid subsidence is required immediately prior to uplift and the effects of North Atlantic rifting cannot account for this.

(4) Differential compression of the crust and lithosphere in the Palaeocene due to propagation of stresses from either the Alps and/or North Atlantic could potentially account for the uplift of the Scottish Highlands and the reactivation of the Inner Moray Firth, although the effects of the rifting over the "hot-spot" appear more likely. However, such a model would not appear feasible for the uplift of the Inner Moray Firth. However, if the major tectonic changes of the Neogene are invoked as the cause then such a model may be applied to the Inner Moray Firth, although this would then not account for the phenomena seen in the Scottish Highlands.

(5) The data as it stands seems to imply that the topographic anomaly associated with the Iceland "hot-spot" and the associated igneous under/overplating of the crust is responsible for the uplift of the Scottish Highlands and the reactivation of the Inner Moray Firth during the Palaeocene while Neogene compressional tectonics explain the uplift of the Inner Moray Firth. However, as the dating of some of the events is as yet too poorly constrained no definitive conclusions about this can as be drawn, but this raises the possibility that the two areas may have experienced different tectonic histories during the Cenozoic.

9. Summary and conclusions.

9.1 Introduction.

The primary aims of this project were to determine the timing and styles of Cenozoic structural reactivation in the Inner Moray Firth and the extent, timing and magnitude of Cenozoic uplift and erosion in both the Inner Moray Firth and Scottish Highlands. Once achieved, it was intended to place the areas in their Cenozoic regional context and attempt to determine the potential causes of these events.

In addition, the project had the subsidiary aim of examining the nature of the pre-Cenozoic tectonic evolution of the Inner Moray Firth. Particularly the relative roles of the major half-graben bounding faults and the Great Glen Fault in the development of the basin were of interest, that is an examination of the strike-slip versus extensional model for the formation of the basin was to be examined.

In this chapter the progress towards meeting these aims is discussed and where necessary recommendations for further research to solve the remaining problems are made.

9.2 Summary of the findings.

9.2.1 Compaction analysis.

As both the clastic Kimmeridge Clay and carbonate Hod and Tor formations show a steady decrease in porosity (as expressed by sonic slowness) with increasing burial-depth it appears most likely that the principal control on porosity, and its reduction, is burial-depth. As overburden increases, porosity is progressively reduced and the amount of overburden directly controls the amount of porosity reduction. When individual formations are analysed from all the wells where they are present the porosity values show a wide spread with burial-depth and a range of surface intercept values. Such a spread of porosity values suggests that the formations in the Inner Moray Firth are overcompacted with respect to their present burial-depth. Overcompaction can be interpreted as a result of uplift and erosion from maximum burial-depth resulting in the porosity-depth relation of the formation being displaced vertically from the normal trend. The widespread in porosity values for individual formations can then be attributed to varying degrees of

uplift and erosion in the Inner Moray Firth and as the Upper Cretaceous Chalk has been affected by uplift and erosion the erosive event must have occurred after its deposition (i.e. during the Tertiary).

Estimates of apparent erosion from the Inner Moray Firth show a general increase to the west reaching approximately 1.2 km. The general pattern also shows little influence from pre-existing structures suggesting that uplift and erosion was largely controlled by a more regional phenomenon. However, the local erosional maxima in the northwestern part of the basin resides over the only inversion structure of Tertiary age yet to be found in the basin. This may suggest that the higher values found in this area are directly related to the extra erosion caused by this local compressive event.

The similarity of apparent erosion estimates in the Kimmeridge Clay, Hod and Tor Formations, and their statistical significance suggests that the overcompaction they experienced must have been the result of a effect common to the history of all three formations. As both clastic and carbonate lithologies were examined it is unlikely that a common diagenetic process could have been involved. Additionally, the chances of a common sedimentological phenomenon having the same effect must be discounted. Consequently, uplift and erosion from maximum burial-depth appears to be the most probable explanation of the overcompaction.

9.2.2 Apatite fission track analysis.

Apatite fission track analysis of samples from the Scottish Highlands showed a dramatic reduction in apatite fission track ages compared to the stratigraphic ages of the samples, this combined with the reduction in track lengths suggests that thermal annealing was an important process in the history of the Scottish Highlands. As thermal annealing is primarily controlled by the maximum temperature experienced by the samples, the data suggest that these samples which are now at the surface have experienced significantly higher temperatures during their history. In the case of samples from the Isle of Skye the higher temperatures can be confidently related to the thermal effects of the Skye igneous centre. The remainder of the samples from the Scottish Highlands appear unaffected by Tertiary igneous activity and consequently the higher temperatures experienced by them can be confidently ascribed to burial at depths greater than currently observed. Consequently, as the samples are now at the surface they must have experienced uplift and erosion.

Fission track ages and modelling suggest that the Scottish Highlands experienced fairly continuous uplift and erosion since the Late Permian/Early Triassic with a slight increase in rates around the Late Cretaceous/Early Tertiary. Such an interpretation is consistent with the Scottish Highlands sourcing sediments for the North Sea and Sea of the Hebrides during the Mesozoic and Cenozoic. Indeed, the increase in uplift and erosion rates around the Late Cretaceous/Early Tertiary compares favourably with the rapid deposition of Tertiary fans and turbidites in the North Sea. Consequently, their appears to be a link between the rates of exhumation for the Scottish Highlands and the deposition in the North Sea.

Fission track modelling of the Late Cretaceous/Early Tertiary palaeotemperatures show a general increase to the west, similar to the uplift and erosion pattern observed for the Inner Moray Firth. Additionally these palaeotemperatures highlight the localised thermal effects of the Tertiary igneous centres which appear to only totally anneal samples within 10km of the centres. When Late Cretaceous/Early Tertiary palaeotemperatures are converted to uplift and erosion values their magnitudes can be shown to be of the same scale and regional trend as observed for the Inner Moray Firth. Along the margins of the Inner Moray Firth fission track estimates of 1-1.2km near the Wick/Great Glen Fault intersection are consistent with those seen offshore while to the west estimates increase to over 2km in the Outer Hebrides.

9.2.3 Geochemical analyses.

The geochemical data provides consistent evidence for uplift and erosion in the Inner Moray Firth after the Late Cretaceous. The variety of methods employed suggests that uplift and erosion was of the order of 100s of metres and in some cases suggests that it may have exceeded 1km. Although the results can differ significantly between the methods, the overall picture can be taken with some confidence.

Although capable of estimating the magnitude of uplift and erosion, modelling is unable to constrain the detailed uplift and erosion history of the basin. For example, the vitrinite reflectance modelling has shown that radically differing uplift and erosion paths can be fitted to the same dataset without the alteration of any other variables. Consequently, it is as yet not possible to determine the detailed history of uplift and erosion history of the basin and consequently suggest detailed models for its occurrence.

The greater range in uplift and erosion estimates derived from vitrinite reflectance compared to the other methods described in this and previous chapters shows that vitrinite reflectance must be used with caution and preferably in conjunction with other techniques. The variation in the vitrinite reflectance estimates is in all probability due to the fact that the models currently employed do not match the complexities which exist in reality. Unlike the analysis of geochemical marker molecules which have simple kinetics, the kinetics of vitrinite reflectance are more detailed and probably not fully understood at present.

9.2.4 Structural analyses.

Both seismic reflection profiles and field studies indicate that substantial structural modification of the Inner Moray Firth occurred after the Cretaceous, probably during the Early Tertiary. A variety of structural styles can be demonstrated involving extensional, compressional and strike-slip tectonics suggesting a complex interaction of the stress field with local pre-existing structures, many of which were reactivated.

Although compactional effects mask a substantial proportion of any extensional, tectonic reactivation of pre-existing half-graben bounding faults it appears likely that a tectonic component cannot be ruled out. This appears to be particularly reasonable when the existence of the extensional faults forming the Sinclair Horst is considered. As these faults are clearly new tectonic features and have the same general trend as the pre-existing extensional structures, reactivation of the older features would seem possible.

The presence of inversion geometries at the Wick/Great Glen Fault intersection attests to a period of compression within at least part of the Inner Moray Firth since the Cretaceous. Whether this period of compression was basin wide or a local expression of the regional stress field which caused contemporaneous extension and strike-slip movements on other faults remains unanswered. However, in the case of the inversion structure seen in UKCS license block 11/25 the compression which generated the folding can be ascribed with a high level of probability to the strike-slip activity of the Great Glen Fault.

Detailed examination of the Great Glen Fault can demonstrate that it was active after the Cretaceous and that the predominant style of movement was strike-slip. The sense of movement has a down to the southeast component and compressional

step-overs indicate that the lateral sense of movement was dextral. The dextral sense of movement is compatible with previous interpretations based on field mapping which suggest that during the Tertiary the fault experienced dextral strike-slip. Further evidence for dextral strike-slip activity on the Great Glen Fault comes from the folding seen in the Sutherland Terrace. The orientation of these folds is incompatible with them being generated as dip-slip inversion structures and they were probably the result of dextral movement on the Great Glen Fault and sinistral movement on the Helmsdale Fault. Such opposing slip senses would lead to compression in the Sutherland Terrace due to space problems and would be capable of generating the fold orientations observed.

The most widespread structural phenomenon in the Inner Moray Firth is the gentle tilting of the basin to the east and of all the structural styles it is probably the most regionally significant. The data shows a significant regional unconformity separating the Mesozoic and Cenozoic units which is dated as mid-late Danian. Consequently, it seems possible that the uplift and erosion may have occurred during the mid-late Danian.

9.2.5 Tectonic uplift and the extensional origin of the Inner Moray Firth: implications of the uplift and erosion data.

The large regional extent of the erosive episode at the Late Cretaceous/Early Tertiary unconformity would tend to imply that surface uplift and consequent erosion was responsible as opposed to a base level change. As surface uplift with respect to the geoid represents quantifiable work done against gravity it is necessary to invoke tectonic forces to drive it. Consequently, the erosive episode must have been tectonically driven. In order to remove 1km of sediment from the Inner Moray Firth and up to 2km from the Scottish Highlands the tectonically driven uplift must have been approximately $\frac{1}{3}$ km and up to $\frac{2}{3}$ km respectively.

As Upper Jurassic and Lower Cretaceous sediments are present at sea-bed and up to 1km of pre-Tertiary sediments were removed from the area, the removed sediments must have been Cretaceous in age. The preserved sediments of this age in both the Inner and Outer Moray Firth drape pre-existing topography and show prominent onlap patterns indicative of thermal subsidence deposits. Consequently, it can be assumed that the removed stratigraphy was probably deposited in a thermal subsidence regime and consequently the area must have contained in excess of 1km of thermal subsidence deposits. The presence of such a large thickness of thermal subsidence deposits combined with the knowledge that the basin lies on thinned crust and that the basin has structural geometries suggestive of extension on major half graben bounding faults is incompatible with the previously proposed strike-slip models for basin formation. Consequently, it appears most likely that the basin formed as result of extension and the consequent thermal subsidence provided space for the now missing stratigraphy.

9.2.6 Potential causes and timing of the phenomena.

As the tectonic reactivation in the Inner Moray Firth and the uplift and erosion in both the Inner Moray Firth and Scottish Highlands appears to have occurred during the Cenozoic and as this time corresponds to a major tectonic reorganisation in the area with North Atlantic rifting to the northwest and the Alpine Orogeny to the southeast, it appears likely that one or other of these events, or possibly the interplay between them, was responsible for the phenomena.

Invoking the flexural effects of fluctuations in the level of intraplate stresses as suggested by Cloetingh (1985) seems incompatible with the data. The magnitudes of such effects are an order of magnitude too small to account for the uplift and erosion documented, while the patterns of the vertical movements would not be the same as observed. In such models the margins of the Inner Moray Firth could be uplifted but the depot centres would be expected to subside which is in direct contradiction with the data.

The effects of North Atlantic rifting in the Palaeocene and in particular the topographic anomaly and the volcanics associated with the Iceland "hot-spot" (White, 1989) appears to fit the uplift and erosion data for the Scottish Highlands extremely well and may also explain the structural reactivation seen in the Inner Moray Firth. However, such a mechanism would appear incapable of accounting for the uplift and erosion of the Inner Moray Firth. If the Palaeocene effects were responsible for the

uplift from maximum burial-depth of sediments in the Inner Moray Firth, then a period of rapid subsidence is required immediately prior to uplift and the effects of North Atlantic rifting cannot account for this.

Differential compression of the crust and lithosphere (Hillis, 1992) in the Palaeocene due to propagation of stresses from either the Alps and/or North Atlantic could potentially account for the uplift of the Scottish Highlands and the reactivation of the Inner Moray Firth, although the effects of the rifting over the "hot-spot" appear more likely. However, such a model would not appear feasible for the uplift of the Inner Moray Firth. However, if the major tectonic changes of the Neogene are invoked as the cause then such a model may be applied to the Inner Moray Firth, although this would then not account for the phenomena seen in the Scottish Highlands. Consequently, the data seems to imply that the topographic anomaly associated with the Iceland "hot-spot" and the associated igneous under/overplating of the crust is responsible for the uplift of the Scottish Highlands and the reactivation of the Inner Moray Firth during the Palaeocene while Neogene compressional tectonics explain the uplift of the Inner Moray Firth. However, as the dating of some of the events is poorly constrained no definitive conclusions about this can as be drawn, but this raises the possibility that the two areas may have experienced different tectonic histories during the Cenozoic.

9.3 Unresolved issues and recommendations for future research.

Although some progress has been made towards understanding the Cenozoic evolution of the Inner Moray Firth and Scottish Highlands, and the potential driving mechanisms have been investigated, some problems still remain unsolved. In this section these problems shall be addressed and the future avenues of research highlighted.

(1) The timing of the phenomena in the Inner Moray Firth remains uncertain. Although it was originally thought that the uplift and erosion in the area was associated with the mid-late Danian unconformity this now appears doubtful. In order to resolve this problem a detailed investigation of the burial and exhumation histories of the wells in the area needs to carried out. Such a study should incorporate a detailed stratigraphic breakdown with a high resolution geochemical and apatite fission track analyses of the full section of wells. Combining all the possible geochemical analyses with apatite fission track results into a modelling package containing a detailed breakdown of the stratigraphy should allow the accurate

constraining of the magnitude and timing of any erosive period and consequently the distinction between Palaeocene and Neogene uplift. The presence of the mid-late Danian unconformity attests to a period of Palaeocene erosion in the basin but whether this was the main erosive period would be resolved by such a study. Ideally, such a study should extend into the Outer Moray Firth where younger stratigraphies are present which may allow the regional pattern of any erosive episode to be better constrained.

(2) The detailed dating of the tectonic reactivation in the Inner Moray Firth is difficult as the relevant stratigraphy needed to date the events is missing over most of the basin. Consequently, the only possible method to date the last time of movement on these faults would be to date the gouge or any cementation/mineralisation present on the fault planes. This is unlikely to occur as it would require the deliberate coring of boreholes through the fault planes in several places (an expensive undertaking) and the dating is most likely to be difficult to do accurately. Additionally, the dating of clay minerals is difficult to achieve with any accuracy as they expand and contract in response to hydration/dehydration and as they tend to change composition with depth. This leads to the escape of argon and as potassium-argon dating would probably be the dating method this would lead to inaccuracies. As cementation and mineralisation tends to exploit existing voids it generally fills small cavities between existing material and would use the fault plane only as the main conduit for transportation. Consequently, it would be difficult to isolate any material of interest from the country rock or other cements and this presents the possibility of contamination of the samples and inaccurate dating.

(3) The determination of the causes of the tectonic reactivation and uplift and erosion documented in this thesis should not be carried out in isolation. Before it is possible to produce a definitive model for the Inner Moray Firth and Scottish Highlands it would be desirable to carry out similar studies throughout northwestern Europe and its conjugate margin in North America and Greenland. Only by being aware of the timing and magnitude of events from the Alpine Front to the North Atlantic continental margin can the relative roles of both tectonic features be separated and this should aid the development of models to account for feature within areas such as the Inner Moray Firth. In addition, by examining the events in Greenland the actual true magnitude of North Atlantic rifting events can be determined as here no contemporaneous events like Alpine Orogeny took place to interfere with the North Atlantic phenomena. As a first stage towards fulfilling this samples have been collected from East Greenland for apatite fission track analysis in

order to constrain the burial and exhumation history of the area during North Atlantic rifting.

References.

Anderton, R., Bridges, P.H., Leeder, M.R. and Sellwood, B.W. (1979). *A dynamic stratigraphy of the British Isles.* George Allen and Unwin, London, pp. 301.

Andrews, I.J. and Brown, S. (1987). Statigraphic evolution of the Jurassic, Moray Firth. *In:* Brooks, J. and Glennie, K. (eds): *Petroleum Geology of North West Europe* Graham and Trotman, London, pp. 785-795.

Andrews, I.J., Long, D., Richards, P.C., Thomson, A.R., Brown, S., Chesher, J.A. and McCormac, M. (1990). British Geological Survey, United Kingdom Offshore Report. *The Geology of the Moray Firth*, HMSO, London, pp.96.

Arkell, W.J. (1933). *The Jurassic system in Great Britain.* Oxford University Press, Oxford, pp.601.

Astin, T.R. (1990). The Devonian lacustrine sediments of Orkney, Scotland: implications for climatic cyclicity, basin structure and maturation history. *Journal of the Geological Society,* London **147**, 141-151.

Arthur, T.J. (1993). Mesozoic structural evolution of the UK Southern North Sea: insights from analysis of fault systems. *In:* Parker, J.R. (ed): *Petroleum Geology of North West Europe.* Geological Society, London, 1269-1279.

Bailey, E.B. and Weir, J. (1932). Submarine Faulting in Kimmeridgian Times. *Transactions of the Royal Society of Edinburgh* **57**, 431-467.

Barker, C.E. and Pawlewicz, M.J. (1986). The correlation of vitrinite reflectance with maximum temperature in humic matter. *In:* Buntebarth, G. and Stegena, L. (eds): *Lecture notes in Earth Sciences, 5. Palaeogeothermics.* Springer-Verlag, Berlin, 79-93.

Barr, D. (1985). 3-D Palinspastic reconstruction of normal faults in the Inner Moray Firth: implications for extensional basin development. *Earth and Planetary Science Letters* **75**, 191-203.

Bartholomew, I.D., Peters, J.M. and Powell, C.M. (1993). Regional structural evolution of the North Sea: oblique slip and reactivation of basement lineaments. *In:* Parker, J.R. (ed): *Petroleum Geology of North West Europe.* Geological Society, London, 1109-1122.

Beach, A. (1987). A regional model for linked tectonics in north-west Europe. *In:* Brooks, J. and Glennie, K. (eds): *Petroleum Geology of North West Europe.* Graham and Trotman, London, pp. 43-48.

Becker, A. (1993). An attempt to define a "neotectonic period" for central and northern Europe. *Geologische Rundschau* **82**, 67-83.

Bevan, T.G. (1984). Tectonic evolution of the Isle of Wight: a Cenozoic stress history based on mesofractures. *Proceedings of the Geologists Association* **96**, 227-235.

Bird, T.J., Bell, A., Gibbs, A,D. and Nicholson, J. (1987). Aspects of strike-slip tectonics in the Inner Moray Firth basin, offshore Scotland. *Norsk Geologisk Tidsskrift* **67**, 353-369.

Boldreel, L.O. and Andersen, M.S. (1993). Late Paleocene to Miocene compression in the Faeroe-Rockall area. *In:* Parker, J.R. (ed): *Petroleum Geology of North West Europe.* Geological Society, London, 1025-1034.

Booth, J., Swiecicki, T. and Wilcockson, P. (1993). The tectono-stratigraphy of the Solan Basin, west of Shetland. *In:* Parker, J.R. (ed): *Petroleum Geology of North West Europe.* Geological Society, London, 987-998.

Bott, M.H.P. (1988). A new look at the causes and consequences of the Icelandic hot-spot. *In:* Parsons, A.C. and Parsons, L.M. (eds): *Early Tertiary Volcanism and the opening of the NE Atlantic.* Journal of the Geological Society, London, Special Publication **39**, 15-23.

Bray, R.J., Green, P.F. and Duddy, I.R. (1992). Thermal history reconstruction using apatite fission track analysis and vitrinite reflectance: a case study from the UK East Midlands and Southern North Sea. *In:* Hardman, R.F.P (ed): *Exploration Britain: Geological insights for the next decade.* Journal of the Geological Society, London, Special Publication **67**, 3-25.

Brown, R.W. (1991). Backstripping apatite fission-track "stratigraphy": A method for resolving the erosional and isostatic rebound components of tectonic uplift histories. *Geology* **19**, 74-77.

Brown, R.W., Summerfield, M.A. and Gleadow, A.J.W. (1993). Apatite fission track analysis: Its potential for the estimation of denudation rates and implications for models of long-term landscape development. *In:* Kirkby, M.J. (ed): *Theoretical Geomorphology.* Wiley, Chichester.

Bulat, J. and Stoker, S.J. (1987). Uplift determination from interval velocity studies. *In:* Brooks, J. and Glennie, K. (eds): *Petroleum Geology of North West Europe.* Graham and Trotman, London, pp. 293-305.

Burnham, A.K. and Sweeney, J.J. (1989). A chemical kinetic model of vitrinite maturation and reflectance. *Geochimica et Cosmochimica Acta* **53**, 2649-2657.

Campbell, I.H. and Griffiths, R.W. (1990). Implications of mantle plume structure for the evolution of flood basalts. *Earth and Planetary Science Letters* **99**, 79-93.

Cartwright, J.A. (1989). The kinematics of inversion in the Danish Central Graben. *In:* Cooper, M.A. and Williams, G.D. (eds): *Inversion Tectonics.* Journal of the Geological Society, London, Special Publication **44**, 153-175.

Chesher, J.A. and Bacon, M. (1975). *A deep seismic survey in the Moray Firth.* Institute of Geological Sciences Report 75/11.

Chesher, J.A., Ardus, D.A., Binns, P.E. and Fannin, N.G.T. (1972). *IGS drilling with m.v. Whitethorn in Scottish waters 1970-71.* Institute of Geological Sciences Report 72/10.

Chrisie-Blick, N. and Biddle, K.T. (1985). Deformation and basin formation along strike-slip faults. *Society of Economic Palaeontologists and Mineralogists Special Publication* **37**,1-27.

Cloetingh, S, McQueen, H., Lambeck, K. (1985). On a tectonic mechanism for regional sea level variations. *Earth and Planetary Science Letters* **75**, 157-166.

Cloetingh, S., Gradstein, F.M., Kooi, H., Grant, A.C. and Kaminski, M. (1990). Plate reorganisation: a cause of rapid late Neogene subsidence and sedimentation around the North Atlantic? *Journal of the Geological Society,* London **147**, 495-506.

Collette, B.J. (1960). The gravity field of the North Sea. *In:* Bruins, G.J. (ed): *Gravity expeditions 1948-58, Volume 5.* Netherlands Geodetic Commission, 47-96.

Cope, M.J. (1986). An Interpretation of Vitrinite Reflectance Data from the North Sea Basin. *In:* Brooks, J., Goff, J.C. and van Hoorn, B. (eds): *Habitat of Palaeozoic Gas in N.W. Europe.* Journal of the Geological Society, London, Special Publication **23**, pp.85-98.

Cornford, C. (1990). Source Rocks and Hydrocarbons of the North Sea. *In:* Glennie, K.W. (ed): *Introduction to the Petroleum Geology of the North Sea.* Blackwell Scientific Publications, Oxford, 294-361.

Coward, M.P., Enfield, M.A. and Fischer, M.W. (1989). Devonian Basins of Northern Scotland: extension and inversion related to Late Caledonian - Variscan tectonics. *In:* Cooper, M.A. and Williams, G.D. (eds): *Inversion Tectonics.* Journal of the Geological Society, London, Special Publication **44**, 275-308.

Crampton, C.B. and Carruthers, R.E. (1914). *The geology of Caithness (sheets 110 and 116 with parts of 109, 115 and 117).* Memoir of the Geological Survey, Scotland, pp.194.

Curtis, C.D. (1980). Diagenetic alteration in black shales. *Journal of the Geological Society,* London **137**, 189-194.

Deegan, C.E. and Scull, B.J. (1977). *A proposed standard lithostratigraphic nomenclature for the central and northern North Sea.* Report of the Institute of Geological Sciences **77/25**; Bulletin of the Norwegian Petroleum Directorate **1**, pp. 36.

Dimitropoulos, K. and Donato, J.A. (1981). The Inner Moray Firth Central Ridge, a geophysical interpretation. *Scottish Journal of Geology* **17**, 27-38.

Dixon, J.M. (1975). Finite strain and Progressive deformation in models of diapiric structures. *Tectonophysics* **28**, 89-124.

Donato, J.A. and Tully, M.C. (1981). A regional interpretation of North Sea gravity data. *In:* Illing, L.V. and Hobson, G.D. (eds): *Petroleum Geology of the Continental Shelf of North-West Europe.* Heyden, London, pp. 65-75.

Donovan, R.N., Foster,R.J. and Westoll, T.S. (1973). A Stratigraphic Revision of the Old Red Sandstone of North-eastern Caithness. *Transations of the Royal Society of Edinburgh* **69**, 167-201.

Donovan, R.N., Archer, A., Turner, P.and Tarling, D.H. (1976). Devonian palaeography of the Orcadian Basin and the Great Glen Fault. *Nature,* London, **259**, 550-551.

Duncan, A.D. (1986). Organic geochemistry applied to petroleum source potential and tectonic history of the Inner Moray Firth Basin. *Unpublished PhD Thesis* University of Aberdeen, UK.

England, R.W. (1988). The early Tertiary stress regime in NW Britain: evidence from the patterns of volcanic activity. *In:* Morton, A.C. and Parsons, L.M. (eds): *Early Tertiary Volcanism and the Opening of the NE Atlantic.* Journal of the Geological Society, London, Special Publication **39**, 381-389.

England, P. and Molnar, P. (1990). Surface uplift, uplift of rocks, and exhumation of rocks. *Geology* **18**, 1173-1177.

Faleide, J.I., Vagnes, E. and Gudlaugsson, S.T. (1993). Late Mesozoic-Cenozoic evolution of the southwestern Barents Sea. *In:* Parker, J.R. (ed): *Petroleum Geology of North West Europe.* Geological Society, London, 933-950.

Falvey, D.A. and Deighton, I. (1982). Recent advances in burial and thermal geohistory analysis. *Journal of the Australian Petroleum Exploration Association* **22** 65-81.

Frostick, L., Reid, I., Jarvis, J. and Eardley, H. (1988). Triassic sediments of the Inner Moray Firth, Scotland: early rift deposits. *Journal of the Geological Society,* London **145**, 235-248.

Galloway, W.E., Garber, J.L., Liu, X. and Sloan, B.J. (1993). Sequence stratigraphic and depositional framework of the Cenozoic fill, Central and Northern North Sea Basin Basin. *In:* Parker, J.R. (ed): *Petroleum Geology of North West Europe.* Geological Society, London, 33-43.

Gamond, J.F. (1987). Bridge structures as sense of displacement criteria in brittle fault zones. *Journal of Structural Geology* **9**, 609-620.

Garson, M.S. and Plant, J. (1972). Possible dextral movements on the Great Glen and Minch faults in Scotland. *Nature* **240**, 31-35.

Garson, M.S., Coats, J.S., Rock, N.M.S. and Deans, T. (1984). Fennites, breccia dykes, albitites and carbonatitic veins near the Great Glen Fault, Inverness, Scotland. *Journal of the Geological Society,* London **141**, 711-732.

George, T.N. (1966). Geomorphic evolution of Hebridean Scotland. *Scottish Journal of Geology* **2**, 1-34.

Gibbs, A.D. (1988). A Model for Linked Basin Development Around the British Isles. *In:* Tankard, A.J. and Balkwill, H.R. (eds): *Extensional tectonics and stratigraphy of the North Atlantic margins.* American Association of Petroleum Geologists Memoir **46**, 501-509.

Gleadow, A.J.W., Duddy, I.R., Green, P.F. and Lovering, J.F. (1986). Confined fission track lengths in apatite: A diagnostic tool for thermal history analysis. *Contributions to Mineralogy and Petrology* **94**, 405-415.

Glennie, K.W. (1990). North Sea history and structural framework. *In:* Glennie, K.W. (ed): *Introduction to the Petroleum Geology of the North Sea.* Blackwell Scientific Publications, Oxford, 34-77.

Glennie, K.W. and Boegner, P.L.E. (1981). Sole Pit inversion tectonics. *In:* Illing, L.V. and Hobson, G.D. (eds): *Petroleum Geology of the Continental Shelf of North-West Europe.* Heyden, London, pp. 110-120.

Gowers, M.B., Holtar, E. and Swensson, E. (1993). The structure of the Norwegian Central Trough (Central Graben area). *In:* Parker, J.R. (ed): *Petroleum Geology of North West Europe.* Geological Society, London, 1245-1254.

Green, P.F. (1986). On the thermo-tectonic evolution of Northern England: evidence from fission track analysis. *Geological Magazine* **123**, 493-506.

Green, P.F. (1988). The relationship between track shortening and fission track age reduction in apatite: combined influences of inherent instability, annealing anisotropy, length bias and system calibration. *Earth and Planetary Science Letters*, **89**, 335-352.

Green, P.F. (1989). Thermal and tectonic history of the East Midlands shelf (onshore UK) and surrounding regions assessed by apatite fission track analysis. *Journal of the Geological Society,* London **146**, 755-733.

Green, P.F., Duddy, I.R., Gleadow, A.J.W. and Lovering (1989a). Apatite fission track analysis as a palaeotemperature indicator for hydrocarbon exploration. *In:* Naeser, N.D. and McCulloch, T.H. (eds): *Thermal History of Sedimentary Basins: Methods and Case Histories.* Springer-Verlag, New York, 181-195.

Green, P.F., Duddy, I.R., Laslett, G.M., Hegarty, K.A., Gleadow, A.J.W. and Lovering (1989b). Thermal anealing of fission tracks in apatite, 4. Quantitative modelling techniques and extension to geological timescales. *Chemical Geology (Isotope Geoscience)*, **79**, 155-182.

Green, P.F., Duddy, I.R., Bray, R.J. and Lewis, C.L.E. (1993). Elevated palaeotemperatures prior to Early Tertiary cooling throughout the UK region: implications for hydrocarbon generation. *In:* Parker, J.R. (ed): *Petroleum Geology of North West Europe.* Geological Society, London, 1067-1074.

Griffiths, R.W. and Campbell, I.H (1991). Interaction of Mantle Plume Heads With the Earth's Surface and Onset of Small-Scale Convection. *Journal of Geophysical Research* **B96**, 18295-18310.

Hall, A.M. (1991). Pre-Quaternary landscape evolution in the Scottis Highlands. *Transactions of the Royal Society of Edinburgh* **82**, 1-26.

Hallam, A. (1965). Jurassic *In:* Craig, G.Y. (ed): *The geology of Scotland.* Oliver and Boyd, Edinburgh, 343-356.

Hallam, A. and Sellwood, B.W. (1976). Middle Mesozoic sedimentation in relation to tectonics in the British area. *Journal of Geology* **84**, 302-321.

Harding, T.P. (1990). Identification of Wrench Faults Using Subsurface Data: Criteria and Pitfalls. *American Association of Petroleum Geologists Bulletin* **74**, 1590-1609.

Harding, T.P., Vierbuchen, R.C. and Christie-Blick, N. (1985). Structural styles, plate-tectonic settings, and hydrocarbon traps of divergent (transtensional) wrench faults. *Society of Economic Palaeontologists and Mineralogists Special Publication* **37**, 51-77.

Hardman, M., Buchanan, P., Herrington, P. and Carr, A. (1993). Geochemical modelling of the East Irish Sea Basin: its influence on predicting hydrocarbon type and quality. *In:* Parker, J.R. (ed): *Petroleum Geology of North West Europe.* Geological Society, London, 809-821.

Harland, W.B., Armstrong, R.L., Cox, A.V., Craig, L.E., Smith, A.G., and Smith, D.G. (1989). *A Geological Time Scale.* Cambridge University Press, Cambridge, pp. 263.

Hartog Jager, D. Den, Giles, M.R. and Griffiths, G.R. (1993). Evolution of Palaeogene submarine fans of the North Sea in space and time. *In:* Parker, J.R. (ed): *Petroleum Geology of North West Europe.* Geological Society, London, 59-71.

Hillier, S. and Marshall, J.E.A. (1992). Organic maturation, thermal history and hydrocarbon generation in the Orcadian Basin, Scotland. *Journal of the Geological Society,* London **149**, 491-502.

Hillis, R.R. (1988). The Geology and Tectonic Evolution of the Western Approaches Trough. *Unpublished PhD Thesis.* University of Edinburgh, UK.

Hillis, R.R. (1991). Chalk porosity and Tertiary uplift, Western Approaches Trough, SW UK and NW French continental shelves. *Journal of the Geological Society,* London **148**, 669-679.

Hillis, R.R. (1992). A two-layer lithospheric compressional model for the Tertiary uplift of the southern United Kingdom. *Geophysical Research Letters*, **19**, 573-576.

Hinz, K., Eldholm, O., Block, M. and Skogseid, J. (1993). Evolution of North Atlantic volcanic continental margins. *In:* Parker, J.R. (ed): *Petroleum Geology of North West Europe.* Geological Society, London, 901-913.

Holgate, N. (1969). Palaeozoic and Tertiary transcurrent movements on the Great Glen Fault. *Scottish Journal of Geology* **5**, 97-139.

Homewood, P., Allem, P.A. and Williams, G.D. (1986). Dynamics of the Molasse Basin of western Switzerland. *In:* Allen, P.A. and Homewood, P. (eds): *Foreland Basins* International Association of Sedimentologists, Special Publication **8**, 199-217.

Houseman, G.A., McKenzie, D.P. and Molnar, P. (1981). Convective instability of a thickened boundary layer and its relevance for the thermal evolution of continental convergence belts. *Journal of Geophysical Research*, **B86**, 6115-6132.

Hower, J. (1981). Shale Diagenesis. *In:* Longstaffe, F.J. (ed): *Clay and Resource Geology.* Canadian Mineralogical Association Short Course Handbook **7**, 60-79.

Hurford, A.J. (1977). A preliminary fission track dating survey of Caledonian "Newer and Last Granites" from the Highlands of Scotland. *Scottish Journal of Geology* **13**, 271-284.

Hurford, A.J. and Green, P.F. (1983). A users' guide to fission track dating calibration. *Earth and Planetary Science Letters* **59**, 343-354.

Hurst, A. (1985). Mineralogy and diagenesis of Lower Jurassic sediments of the Lossiemouth borehole, north-east Scotland. *Proceedings of the Yorkshire Geological Society* **45**, 189-197.

Hurst, A. (1980). The diagenesis of Jurassic rocks of the Moray Firth, NE Scotland *Unpublished PhD Thesis.* University of Reading, UK.

Institute of Geological Sciences (1972). *Aeromagnetic map of Great Britain, Sheet 1. England, Scotland and Northern Ireland (north of National Grid line 500km N) 1:625000.* Ordnance Survey for the Institute of Geological Sciences, Chessington, Surrey.

Jankowsky, W. (1962). Diagenesis and oil accumulation as aids in the analysis of the structural history of the north-western German Basin. *Zeitschrift der Deutscher Geologischer Gesellschaft* **114**, 452-460.

Japsen, P. (1993). Influence of Lithology and Neogene Uplift on Seismic Velocities in Denmark: Implications for Depth Conversion Maps. *American Association of Petroleum Geologists Bulletin*, **77**, 194-211.

Jensen, L.N. and Schmidt (in press). Neogene uplift and erosion offshore Norway; magnitude and consequences for hydrocarbon exploration in the Farsund Basin. *In:* Spencer, A.M. (ed): *Generation, accumulation and production of Europe's hydrocarbons III.* European Association of Petroleum Geologists Special Publication **3**.

Karner, G.D. (1986). Effects of lithospheric in-plane stress on sedimentary basin stratigraphy. *Tectonics* **5**, 573-588.

Knipe, R.J., Cowan, G. and Balendran, V.S. (1993). The tectonic history of the East Irish Sea Basin with reference to the Morecambe Fields. *In:* Parker, J.R. (ed): *Petroleum Geology of North West Europe.* Geological Society, London, 857-866.

Knott, S.D., Burchell, M.T., Jolley, E.J. and Fraser, A.J. (1993). Mesozoic to Cenozoic plate reconstructions of the North Atlantic and hydrocarbon plays of the North Atlantic. *In:* Parker, J.R. (ed): *Petroleum Geology of North West Europe.* Geological Society, London, 953-974.

Kooi, H. and Cloetingh, S. (1987). Intraplate Stresses and the Tectono-Stratigraphic Evolution of the Central North Sea. *In:* Tankard, A.J. and Balkwill, H.R. (eds): *Extensional tectonics and stratigraphy of the North Atlantic margins.* American Association of Petroleum Geologists Memoir **46**, 541-558.

Koopman, A., Speksnijder, A. and Horsfield, W.T. (1987). Sandbox studies of inversion tectonics. *Tectonophysics* **137**, 379-388.

Kusznir, N.J. and Egan, S.S. (1989). Simple-Shear and Pure-Shear Models of Extensional Sedimentary Basin Formation: Application of the Jeanne d'Arc Basin, Grand Banks of Newfoundland. *In:* Tankard, A.J. and Balkwill, H.R. (eds): *Extensional tectonics and stratigraphy of the North Atlantic margins.* American Association of Petroleum Geologists Memoir **46**, 305-322.

Kusznir, N.J., Marsden, G. and Egan, S.S. (1991). A flexural-canterlever simple-shear/pure-shear model of continental lithosphere extension: applications to the Jeanne d'Arc Basin, Grand Banks and Viking Graben, North Sea. *In:* Roberts, A.M., Yielding, G., Freeman, B. (eds): *The Geometry of Normal Faults.* Geological Society, London, Special Publication **56**, 41-60.

Lang, J.R. (1978). The determination of prior depth of burial (uplift and erosion) using interval transit time. *Society of Professional Well Log Analysts Nineteenth Annual Logging Symposium* June 13-16, Paper B.

Lewis, C.L.E., Green, P.F., Carter, A. and Hurford, A.J. (1992a). Elevated K/T palaeotemperatures throughout Northwest England: three kilometres of Tertiary erosion? *Earth and Planetary Science Letters*, **112**, 131-145.

Lewis, C.L.E., Carter, A. and Hurford, A.J. (1992b). Low-temperature effects of the Skye Tertiary intrusions on Mesozoic sediments in the Sea of Hebridies Basin *In:* Parnell, J. (ed): *Basins on the Atlantic Seaboard: Petroleum Geology, Sedimentology and Basin Evolution.* Geological Society, London, Special Publication **62**, 175-188.

Little, T.A. (1992). Development of wrench folds along the Border Ranges fault system, southern Alaska, U.S.A. *Journal of Structural Geology* **14**, 343-359.

Lopatin, N.V. (1971). Temperature and geologic time as factors in coalification. *Akademiya Nauk SSSR, Serina Geologicheskya, Izvestiya* **3**, 95-106.

Magara, K. (1976). Thickness of removed sedimentary rocks, paleopore pressure, and paleotemperature, southwestern part of Western Canada Basin. *American Association of Petroleum Geologists Bulletin*, **60**, 554-565.

Marie, J.P.P. (1975). Rotliegendes Stratigraphy and diagenesis. *In:* Woodland, A.W. (ed): *Petroleum and the Continental Shelf of North-West Europe.* Applied Science Publishers, London, 205-211.

MacKenzie, A.S. and McKenzie, D. (1983). Isomerisation and aromatisation of hydrocarbons in sedimentary basins formed by extension. *Geological Magazine* **120**, 417-470.

MacDonald, A.C. (1985). Kimmeridgian and Volgian fault-margin sedimentation in the Northern North Sea area. *Unpublished PhD Thesis.* University of Strathclyde, UK.

McClay, K.R., Norton, M.G., Coney, P. and Davis, G.H. (1986). Collapse of the Caledonian orogen and the Old Red Sandstone. *Nature*, **323**,147-149.

McKenzie, D. (1978). Some remarks on the development of sedimentary basins. *Earth and Planetary Science Letters* **40**, 25-32.

McQuillin, R., Donato, J.A. and Tulstrup, J. (1982). Development of basins in the Inner Moray Firth and the North Sea by crustal extension and dextral displacement of the Great Glen Fault. *Earth and Planetary Science Letters* **60**, 127-139.

Merkel, R.H. (1981). *Well Log Formation Evaluation.* American Association of Petroleum Geologists Course Note Series **14**.

Miles, R.S. and Westoll, T.S. (1962). Two New Genera of Coccosteid Arthrodira from the Middle Old Red Sandstone of Scotland, and their Stratigraphic Distribution. *Transactions of the Royal Society of Edinburgh* **55**, 193-209.

Morton, A.C., Hallsworth, C.R. and Wilkinson, G.C. (1993). Stratigraphic evolution and sand provenance during Paleocene deposition in the Northern North Sea area. *In:* Parker, J.R. (ed): *Petroleum Geology of North West Europe.* Geological Society, London, 73-84.

Mykura, W. (1991). Old Red Sandstone. *In:* Craig, G.Y. (ed): *The geology of Scotland.* The Geological Society, London, 297-344.

Naylor, D., Haughey, N., Clayton, G. and Graham, J.R. (1993). The Kish Bank Basin, offshore Ireland. *In:* Parker, J.R. (ed): *Petroleum Geology of North West Europe.* Geological Society, London, 845-855.

Naylor, H., Turner, P., Vaughan, D.J. and Fallick, A.E. (1989). The Cherty Rock, Elgin: A petrographic and isotopic study of a Permo-Triassic calcrete. *Geological Journal* **24**, 205-221.

Naylor, M.A., Mandl, G. and Sijpesteijn, C.H.K. (1986). Fault geometries in basement-induced wrench faulting under different initial stress states. *Journal of Structural Geology* **8**, 737-752.

Norton, M.G., McClay, K.R. and Way, N.A. (1987). Tectonic evolution of Devonian basins in northern Scotland and southern Norway. *Norsk Geologisk Tidsskrift* **67**, 323-338.

Oudmayer, B.C. and de Jager, J. (1993). Fault reactivation and oblique-slip in the Southern North Sea. *In:* Parker, J.R. (ed): *Petroleum Geology of North West Europe.* Geological Society, London, 1281-1290.

Parker, J.R. (1975). Lower Tertiary sand development in the Central North Sea. *In:* Woodland, A.W. (ed): P*etroleum and the Continental Shelf of North West Europe.* Applied Science Publishers, London, 447-453.

Parnell, J. (1985). Hydrocarbon source rocks, reservoir rocks and migration in the Orcadian Basin. *Scottish Journal of Geology* **21**, 321-336.

Pearson, M.J. and Watkins, D. (1983). Organofacies and early maturation effects in the Upper Jurassic sediments from the Inner Moray Firth Basin, North sea. In: Brooks, J. (ed): *Petroleum Geochemistry and Exploration of Europe.* Geological Society, London, Special Publication **12**, 161-173.

Pfiffner, O.A. (1986). Evolution of the north Alpine foreland basin in the Central Alps. *In:* Allen, P.A. and Homewood, P. (eds): *Foreland Basins.* International Association of Sedimentologists, Special Publication **8**, 219-228.

Pickering, K.T. (1983). Small scale syn-sedimentary faults in the Upper Jurassic 'Boulder Beds'. *Scottish Journal of Geology* **19**, 169-181.

Prajoga, J. (1990). Thermal and Maturation History of the Inner Moray Firth Basin. *Unpublished MSc Thesis.* Royal Holloway and Bedford New College, University of London, UK.

Prosser, S.D. (1991). Syn-rift sequences: their recognition and significance in basin analysis. *Unpublished PhD Thesis.* University of Keele, UK.

Raiga-Clemenceau, J., Martin, J.P. and Nicoletis, S. (1988). The concept of acoustic formation factor for more accurate porosity determination from sonic transit time data. *The Log Analyst*, **January-February**, 54-59.

Rathbone, P.A. and Harris, A.L. (1980). Moine and Lewisian near the Great Glen Fault. *Scottish Journal of Geology* **16**, 51 -64.

Rattey, R.P. and Hayward, A.B. (1993). Sequence stratigraphy of a failed rift system: The Middle Jurassic to Early Cretaceous basin evolution of the Central and Northern North Sea. *In:* Parker, J.R. (ed): *Petroleum Geology of North West Europe.* Geological Society, London, 215-249.

Rawson, P.F. and Riley, L.A. (1982). Latest Jurassic - Early Cretaceous Events and the "Late Cimmerian Unconformity" in North Sea Area. *American Association of Petroleum Geologists Bulletin* **66**, 2628-2648.

Richardson, J.B. (1962). Spores with bifurcate processes from the Middle Old Red Sandstone of Scotland. *Palaeontology*, **5**, 171-194.

Richards, P.C. (1990). Devonian *In:* Glennie, K.W. (ed): *Introduction to the Petroleum Geology of the North Sea.* Blackwell Scientific Publications, Oxford, 78-89.

Roberts, A. (1989). Fold and thrust structures in the Kintradwell 'Boulder Beds', Moray Firth. *Scottish Journal of Geology* **25**, 173-186.

Roberts, A.M., Badley, M.E., Price, J.D. and Huck, I.W. (1990). The structural evolution of a transtensional basin: Inner Moray Firth , NE Scotland. *Journal of the Geological Society*, London **147**, 87-103.

Roberts, A.M. and Yielding, G. (1991). Deformation around basin-margin faults in the North Sea/mid-Norway rift. *In:* Roberts, A.M.,G. Yielding, G.,B. Freeman, B. (eds): *The Geometry of Normal Faults.* Geological Society, London, Special Publication **56**, 61-78.

Rochow, K.A. (1981). Seismic stratigraphy of the North Sea 'Paleocene' deposits. *In:* Illing, L.V. and Hobson, G.D. (eds):*Petroleum Geology of the Continental Shelf of North-West Europe.* Heyden, London, pp. 255-266.

Rogers, D.A. (1987). Devonian correlations, enviroments and tectonics across the Great Glen Fault. *Unpublished PhD thesis*, University of Cambridge.

Rogers, D.A., Marshall, J.E.A. and Astin, T.R. (1989). Devonian and later movements on the Great Glen fault system, Scotland. *Journal of the Geological Society*, London **146**, 369-372.

Rogers, J., Wehr, F.L. and Hunt, J.W. (1991). Tertiary uplift estimation from velocity data in the Eromanga Basin. *Exploration Geophysics*, **22**, 321-324.

Sandiford, M. and Powell, R. (1990). Some isostatic and thermal consequences of the vertical strain geometry in convergent orogens. *Earth and Planetary Science Letters* **98**, 154-165.

Schlumberger (1987). *Log Interpretation Principles/Applications*. Schlumberger Educational Services, Houston, Texas.

Scholle, P.A. (1977). Chalk diagenesis and it's relation to petroleum exploration : oil from chalks , a modern miracle ? *American Association of Petroleum Geologists Bulletin* **61**, 982-1009.

Sclater, J.G. and Christie, P.A.F. (1980). Continental stretching : an explanation of the post-mid-Cretaceous subsidence of the Central North Sea Basin. *Journal of Geophysical Research* **B85**, 3711-3739.

Scotchman, I.C. (1991). Kerogen facies and maturity of the Kimmeridge Clay Formation in southern and eastern England. *Marine and Petroleum Geology* **8**, 278-295.

Serranne, M. (1992). Devonian extensional tectonics versus Carboniferous inversion in the northern Orcadian basin. *Journal of the Geological Society,* London **149**, 27-37.

Smith, P.J. and Bott, M.H.P. (1975). Structure of the Crust Beneath the Caledonian Foreland and Caledonian Belt of the North Scottish Shelf Region. *Geophysical Journal of the Royal Astronomical Society* **40**, 187-205.

Speight, J.M. and Mitchell, J.G. (1979). The Permo-Carboniferous dyke-swarm of northern Argyll and its bearing on dextral displacement on the Great Glen Fault. *Journal of the Geological Society,* London **136**, 3-11.

Stephen, K.J., Underhill, J.R. , Partington, M. and Hedley, R.J. (1993). The sequence stratigraphy of the Hettangian to Oxfordian sedimentary succession, Inner Moray Firth. *In:* Parker, J.R. (ed): *Petroleum Geology of North West Europe.* Geological Society, London, 485-505.

Stewart, I.J. (1987). A revised stratigraphic interpretation of the Early Palaeogene of the central North Sea. *In:* Brooks, J. and Glennie, K. (eds): *Petroleum Geology of North West Europe.* Graham and Trotman, London, pp. 557-576.

Storetvedt, K.M. (1974). A possible large scale displacement along the Great Glen Fault in Scotland. *Geological Magazine* **111**, 23-30.

Sunderland, J. (1972). Deep sedimentary basin in the Moray Firth. *Nature*, London **236**, 24-25.

Surlyk, F. (1978). Submarine fan sedimentation along fault scarps on tilted fault blocks (Jurassic - Cretaceous boundary, East Greenland). *Gronlands Geologiske Undersogelse Bulletin*, **28**, 1-103.

Sweeney, J.J. (1990). Basimat Fortran Program Calculates Oil and Gas Generation Using a Distribution of Discrete Activation Energies. *Geobyte* **5**, 37-43.

Sweeney, J.J, Burnham, A.K. and Braun, R.L. (1987). A model of hydrocarbon generation from Type 1 kerogen: application to Uinta Basin, Utah. *American Association of Petroleum Geologists Bulletin* **71**, 967-985.

Sykes, R.M. (1975). The stratigraphy of the Callovian and Oxfordian stages (Middle-Upper Jurassic) in northern Scotland. *Scottish Journal of Geology* **11**, 51-78.

Sylvester, A.G. (1988). Strike-slip faults. *American Association of Petroleum Geologists Bulletin* **100**, 1666-1703.

Taylor, S.R. and Lapré, J.F. (1987). North Sea chalk diagenesis : its effect on reservoir location and properties. *In:* Brooks, J. and Glennie, K. (eds): *Petroleum Geology of North West Europe.* Graham and Trotman, London, 483-495.

Thomson, K. and Underhill, J.R. (1993). Controls on the development and evolution of structural styles in the Inner Moray Firth Basin. *In:* Parker, J.R. (ed): *Petroleum Geology of North West Europe.* Geological Society, London, 1167-1178.

Till, R. (1974). *Statistical Methods for the Earth Scientist.* MacMillan Press, London, 154pp.

Trewin, N.H. (1989). The petroleum potential of the Old Red Sandstone of northern Scotland. *Scottish Journal of Geology* **25**, 201-225.

Turner, C.C., Cohen, J.M., Connell, E.R. and Cooper, D.M. (1987). A depositional model for the South Brae oilfield. *In:* Brooks, J. and Glennie, K. (eds): *Petroleum Geology of North West Europe.* Graham and Trotman, London, pp. 853-864.

Underhill, J.R. (1991a). Implications of Mesozoic-Recent basin development in the western Inner Moray Firth, UK. *Marine and Petroleum Geology* **8**, 359-369.

Underhill, J.R. (1991b). Controls on Late Jurassic seismic sequences, Inner Moray Firth, UK North Sea: a critical test of a key segment of Exxon's original global cycle chart. *Basin Research* **3**, 79-98.

Underhill, J.R. and Brodie, J.A. (1993). A Re-Evaluation of the Structural Geology of the Easter Ross Peninsula: implications for the movement on the Great Glen fault zone. *Journal of the Geological Society,* London **150**, 515-527.

Underhill, J.R. and Partington, M.A. (1993a). Jurassic thermal doming and deflation in the North Sea: The Sequence Stratigraphic Evidence. *In:* Parker, J.R. (ed): *Petroleum Geology of North West Europe.* Geological Society, London, 337-345.

Underhill,J.R. and Partington, M. (1993b). Use of maximum flooding surfaces in determining a regional control on the Intra-Aalenian ("mid-Cimmerian") Sequence Boundary: Implications for North Sea basin development and Exxon's Sea Level Chart. *In:* Posamentier, H.W. & Wiemer, P. (eds): *Recent Advances in Sequence Stratigraphy* American Association of Petroleum Geologists Memoir.

Van der Voo, R. and Scotese, C. (1981). Palaeomagnetic evidence for a large (~ 2000km) sinistral offset along the Great Glen fault during Carboniferous time. *Geology* **9**, 583-589.

Waples, D.W. (1980). Time and Temperature in Petroleum Formation: Application of Lopatin's Method to Petroleum Exploration. *American Association of Petroleum Geologists Bulletin* **64**, 916-926.

Watson, J. (1985). Northern Scotland as an Atlantic-North Sea divide. *Journal of the Geological Society,* London **142**, 221-243.

Watts, N.L. (1983). Microfractures in chalk of Albuskjell Field, Norwegian sector, North Sea : possible origin and distribution. *American Association of Petroleum Geologists Bulletin* **67**, 201-234.

Weissel, J.K. and Karner, G.D. (1989). Flexural Uplift of Rift Flanks Due to Mechanical Unloading of the Lithosphere During Extension. *Journal of Geophysical Research* **94**, 13,919-13,950.

Wells, P.E. (1990). Porosities and seismic velocities of mudstones from Wairarapa and oil wells of North Island, New Zealand, and their use in determing burial history. *New Zealand Journal of Geology and Geophysics* **33**, 29-39.

Wernicke, B. (1985). Uniform-sense normal simple shear of the continental lithosphere. *Canadian Journal of Earth Science* **22**, 108-125.

White, R.S. (1988). A hot-spot model for early Tertiary volcanism in the N Atlantic. *In:* Morton, A.C. and Parsons, L.M. (eds): *Early Tertiary Volcanism and the Opening of the NE Atlantic.* Geological Society, London, Special Publication **39**, 3-13.

White, R.S. (1989). Initiation of the Iceland Plume and Opening of the North Atlantic. *In:* Tankard, A.J. and Balkwill, H.R. (eds): *Extensional tectonics and stratigraphy of the North Atlantic margins.* American Association of Petroleum Geologists Memoir **46**, 149-154.

White, R.S. (1992a). Magmatism during and after continental break-up. *In:* Storey, B.C., Alabaster, T and Pankhurst, R.J. (eds): *Magmatism and the Causes of Continental Break-up* Geological Society, London, Special Publication **68**, 1-16.

White, R.S. (1992b). Crustal structure and magmatism of the North Atlantic continental margins. *Journal of the Geological Society,* London **149**, 841-854.

Wignall, P.B. and Pickering, K.T. (1993). Palaeoecology and sedimentology across Jurassic fault scarp, NE Scotland. *Journal of the Geological Society,* London **150**, 323-340.

Winchester, J.A. (1973). Pattern of regional metamorphism suggests a sinistral displacement of 160Km along the Great Glen Fault. *Nature* **246**, 81-84.

Withjack, M.O. and Scheiner, C. (1982). Fault Patterns Associated with Domes-An Experimental and Analytical Study. *American Association of Petroleum Geologists Bulletin* **66**, 302-316.

Wyville, M.R.J., Gregory, A.R. and Gardener, G.H.F. (1956). Elastic wave velocities in heterogeneous and porous media. *Geophysics*, **21**, 41-70..

Ziegler, P.A. (1982). *Geological Atlas of Western and Central Europe*, Second Edition. Elsevier Scientific Publishing Co., Amsterdam.

Ziegler, P.A. (1987a). Compressional intra-plate deformations in the Alpine Foreland - an introduction. *Tectonophysics* **137**, 1-5.

Ziegler, P.A. (1987b). Late Cretaceous and Cenozoic intra-plate compressional deformations in the Alpine foreland - a geodynamic model. *Tectonophysics* **137**, 389-420.

Ziegler, P.A, (1989). Evolution of the Noth Atlantic - An Overview. *In:* Tankard, A.J. and Balkwill, H.R. (eds): *Extensional tectonics and stratigraphy of the North Atlantic margins.* American Association of Petroleum Geologists Memoir **46**, 111-129.

Appendix.

Copy of paper "Controls on the development and evolution of structural styles in the Inner Moray Firth Basin." by K. Thomson and J.R. Underhill. (1993). *In:* Parker, J.R. (ed): *Petroleum Geology of North West Europe.* Geological Society, London, 1167-1178.

Controls on the development and evolution of structural styles in the Inner Moray Firth Basin

K. THOMSON and J. R. UNDERHILL

Department of Geology and Geophysics, The University of Edinburgh, Grant Institute, King's Buildings, West Mains Road, Edinburgh EH9 3JW, UK

Abstract: Although it has generally been believed that structural styles in the Inner Moray Firth (IMF) have been largely controlled by strike-slip movements on the Great Glen Fault (GGF), integrated seismic and field studies suggest otherwise. Instead, most structural styles appear to have developed and evolved as a result of dip-slip extension and thermal subsidence consequent upon two phases of rifting during the Permo-Triassic and Late Jurassic and subsequent regional uplift and local inversion during the Tertiary. The integration of demonstrable thickening of Kimmeridgian–Portlandian intervals across the GGF with sedimentological information from onshore outcrops and cored wells suggests that the basin had a half-graben geometry during the Late Jurassic with a depocentre adjacent to the Helmsdale Fault, analogous to half-graben geometries which characterized other Late Jurassic sequences in Greenland and the South Viking Graben. Progressive marine onlap suggests that more gentle regional (thermal) subsidence took place in an underfilled basin, during subsequent Early Cretaceous deposition. However, the seismic data and subcrop information show that the geometries resulting from such classic rift- and thermally-driven phases of extension were modified by Cenozoic regional uplift and inversion in response to intraplate compression resulting from NE Atlantic (Thulean) and Alpine events. These events also appear to have effected minor strike-slip motion on the GGF, with the development of spectacular 'flower structure' and 'helicoidal' geometries, and caused limited oblique-slip reactivation of some extensional structures. The most notable modification of structural styles occurs in areas adjacent to the major basin-bounding faults. Particularly complex structural inversion geometries occur in the northwest corner of the basin adjacent to the Wick Fault while anomalously-trending folds developed in response to space problems in the Sutherland Terrace, between the Helmsdale Fault and the GGF, as a result of opposing senses of slip on these faults.

The Inner Moray Firth (IMF) lies adjacent to the Scottish mainland between the Grampian and East Sutherland coasts (Fig. 1). The continuity of structures and sequences offshore into adjacent coastal outcrops affords the opportunity to integrate field exposures into models of the basin's structural development (e.g. Underhill 1991*a*). Although well results have been largely disappointing, with only British Petroleum's Beatrice Field proving commercial to date, the data obtained from the IMF give important clues to the nature and timing of deformation in the NW European domain in general and other areas of the North Sea in particular.

Database

The database used in analysing the regional tectonics and local structural styles in the IMF consists of over 8000 km of offshore seismic data supplied by GECO, Horizon, Halliburton, Shelf Exploration, Shell, BP, Arco, Unocal and Esso. Additional onshore seismic was available over the Easter Ross peninsula courtesy of Fina and their partners in onshore licence EXL 208. The seismic data were tied to all released exploration wells in the area and additional confidential data. Use has been made of onshore exposures and electrical well log analyses to add a level of detail below that of seismic data. Additional sonic velocity, vitrinite reflectance and fission track information was integrated into the study in order to quantify some of the effects of relative uplift resulting from specific deformation events.

Structural interpretation

Interpretation of the large seismic database has led to a better understanding of the main controls on Late Paleozoic–Recent basin evolution and the recognition of significant tectonic events in the development of structural styles in the area. These significant events are now discussed in turn.

Late Paleozoic

Seismic data from the IMF highlight the occurrence of a significant unconformity within the Late Paleozoic successions (Fig. 2). It is largely defined by truncation of underlying reflectors and onlap of subsequent units previously identified by Roberts *et al.* (1990). Data from the Beatrice area and onshore analogues from Easter Ross suggest that the dominant structural style beneath this unconformity consists of eroded, thrust-bounded, hangingwall anticlines (Fig. 3; Underhill and Brodie in press). These apparently record a phase of Permo-Carboniferous ('Variscan') contractional deformation prior to partial peneplanation and Permian sedimentation (Fig. 4). As such, these structural styles are analogous to those formed during basin inversion in nearby areas (e.g. Coward *et al.* 1989; Astin 1990; Seranne 1992). Although the most well-defined data for this phase of deformation come from onshore exposures, some supporting evidence exists from recent, good-quality seismic data from the Beatrice area for the overlying succession draping a well-defined topography (Fig. 4), partially created by renewed Permian extension following the inversion episode.

It is likely that the early Devonian deformation in the IMF was controlled by active rifting. Field studies suggest that adjacent areas experienced syn-sedimentary fault activity (Rogers 1987) resulting from regional extensional collapse of the Caledonian orogen (Serrane 1992). Consequently, it is possible that many of the contractional features described above also represent reactivated normal faults. It remains unclear whether contractional deformation is always closely associated with syn-sedimentary faults and the extent to which truncation by the unconformity has occurred within the pre-Permian sequence; thus the exact stratigraphic level expected beneath the unconformity may be highly variable across the IMF and it is probable that significant amounts of Devonian and possibly thick Carboniferous sections will be found locally. Hence, Late Carboniferous successions are likely to be

From *Petroleum Geology of Northwest Europe: Proceedings of the 4th Conference* (edited by J. R. Parker).
© 1993 Petroleum Geology '86 Ltd. Published by The Geological Society, London, pp. 1167–1178.

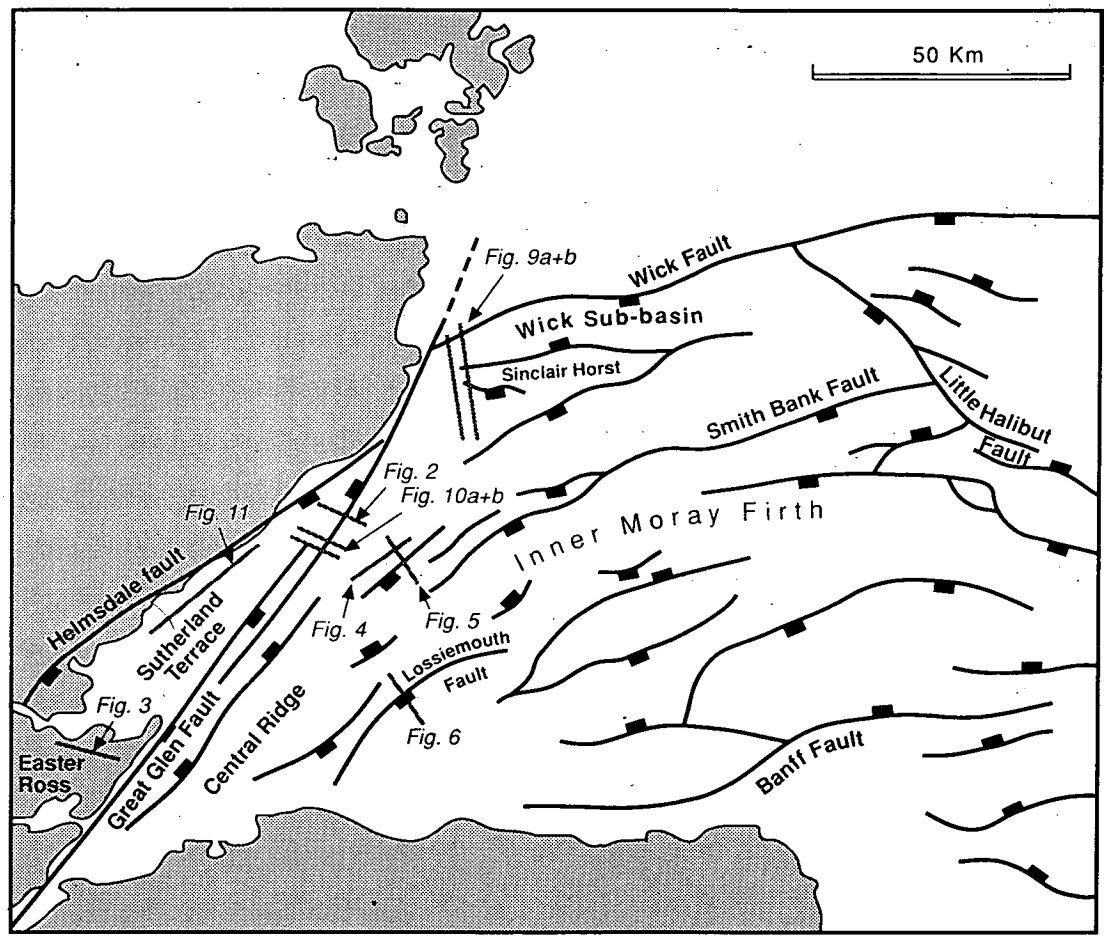

Fig. 1. Location map for the Inner Moray Firth showing the basin's main structural elements. Positions of the various seismic lines used in the article are shown.

preserved in some areas where the unconformity had significant topography or was underlain by pre-existing fault-controlled depocentres.

In contrast with most previous interpretations, there seems little reason to propose that the Great Glen Fault (GGF) played any significant role in the Devonian rift episode or the 'Variscan' or Pre-Permian phase of basin development because of the lack of demonstrable horizontal offset of structures. Indeed, as Rogers *et al.* (1989) have shown, no more that 25–29 km of dextral displacement appears to have affected Devonian sequences.

Permo-Triassic extension

Permian successions within the IMF are hard to separate from other red-bed sequences because of the lack of distinctive palaeontological markers and their lack of seismic character. Despite these limitations, the lowest units occurring above the prominent Permo-Carboniferous ('Variscan') unconformity show varying degrees of stratigraphic thickening on the seismic data. Although this can generally be explained by the passive infill of remnant (thrust-related hangingwall) topography, the occurrence of some thickening appears to occur adjacent to reactivated extensional faults (e.g. Fig. 4), indicating a minor component of early, syn-sedimentary tectonic control. Although this would also be consistent with regional extensional events elsewhere in the North Sea, further work is needed to test this hypothesis.

Latest Permian, Triassic and Early Jurassic thermal subsidence

The subdivison of later Permian and Triassic is hampered as Zechstein sequences are also often dominated by reddened sandstones similar to Triassic, Permian, Carboniferous and Devonian strata. Despite these problems, the seismic data show that Late Permian and Triassic sequences are largely dominated by concordant reflectors (layer-parallelism) and broad, basin-wide westerly thickening packages with little or no variation adjacent to faults (Underhill 1991*a*). In our opinion, and in contrast to Frostick *et al.* (1988), the data currently available from wells are too sparse to allow a detailed model to be proposed for Permo-Triassic tectonics and sedimentation. However, the Triassic sequences generally appear to have been laid down in a basin experiencing broad-based subsidence following an earlier extensional episode. As such, they probably represent a phase of thermal subsidence following the minor Permian rifting (contra Frostick *et al.* 1988). The absence of abrupt thickening across and along the GGF again suggests that it played a negligible role in controlling basin development at this time (contra Frostick *et al.* 1988).

The top of the Triassic succession is marked by the most prominent seismic reflector in the area. Its onshore equivalent is represented by the Stotfield Cherty Rock, a significant silcrete horizon marking a notable break in sedimentation (Naylor *et al.* 1989). Overlying Early Jurassic units also consist of relatively thin concordant sequences which show gradual

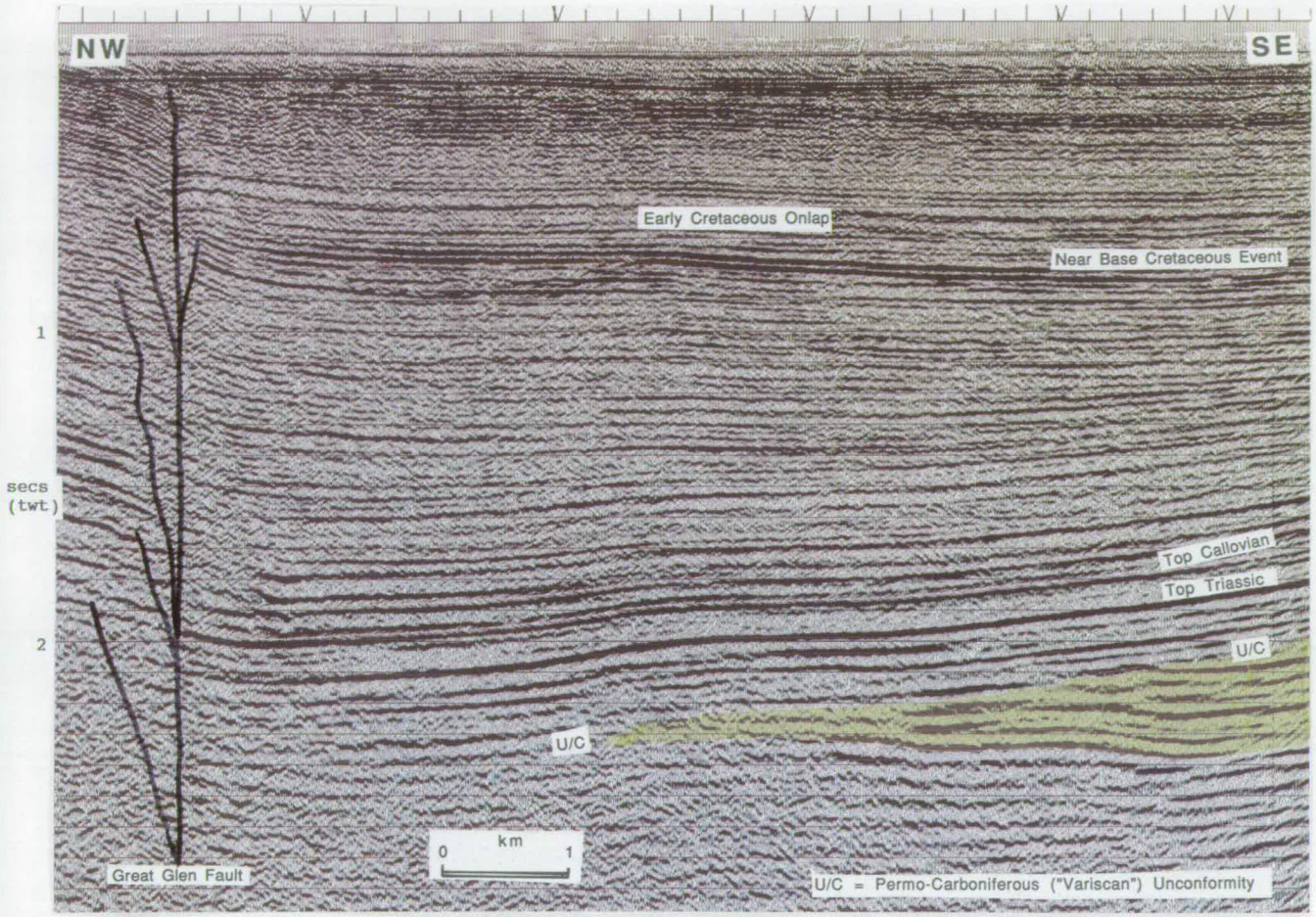

Fig. 2. Seismic line interpretation highlighting the occurrence of an intra-Late Paleozoic unconformity (u/c) defined largely by truncation of underlying strata which separates deformed Devonian sequences (highlighted in green) from overlying Permian red beds. Line shown courtesy of GECO-PRAKLA.

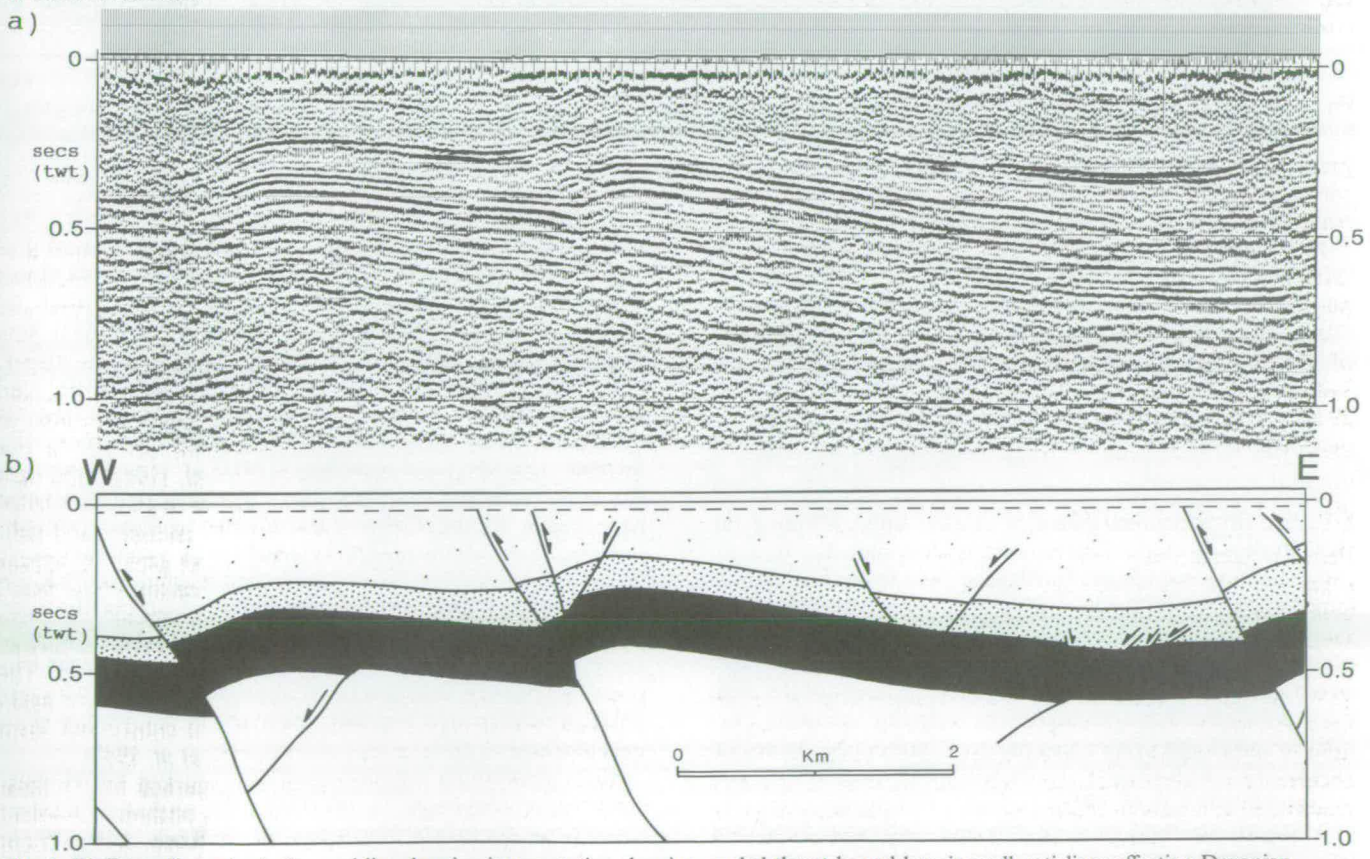

Fig. 3. W–E-trending seismic line and line drawing interpretation showing eroded thrust-bound hangingwall anticlines affecting Devonian sequences in Easter Ross, which are believed to have formed as a result of a phase of Permo-Carboniferous contraction and inversion. Key: open stipple: Late Devonian; close stipple: Top Middle Devonian; black: Middle Devonian fish beds. Line shown courtesy of Fina Exploration.

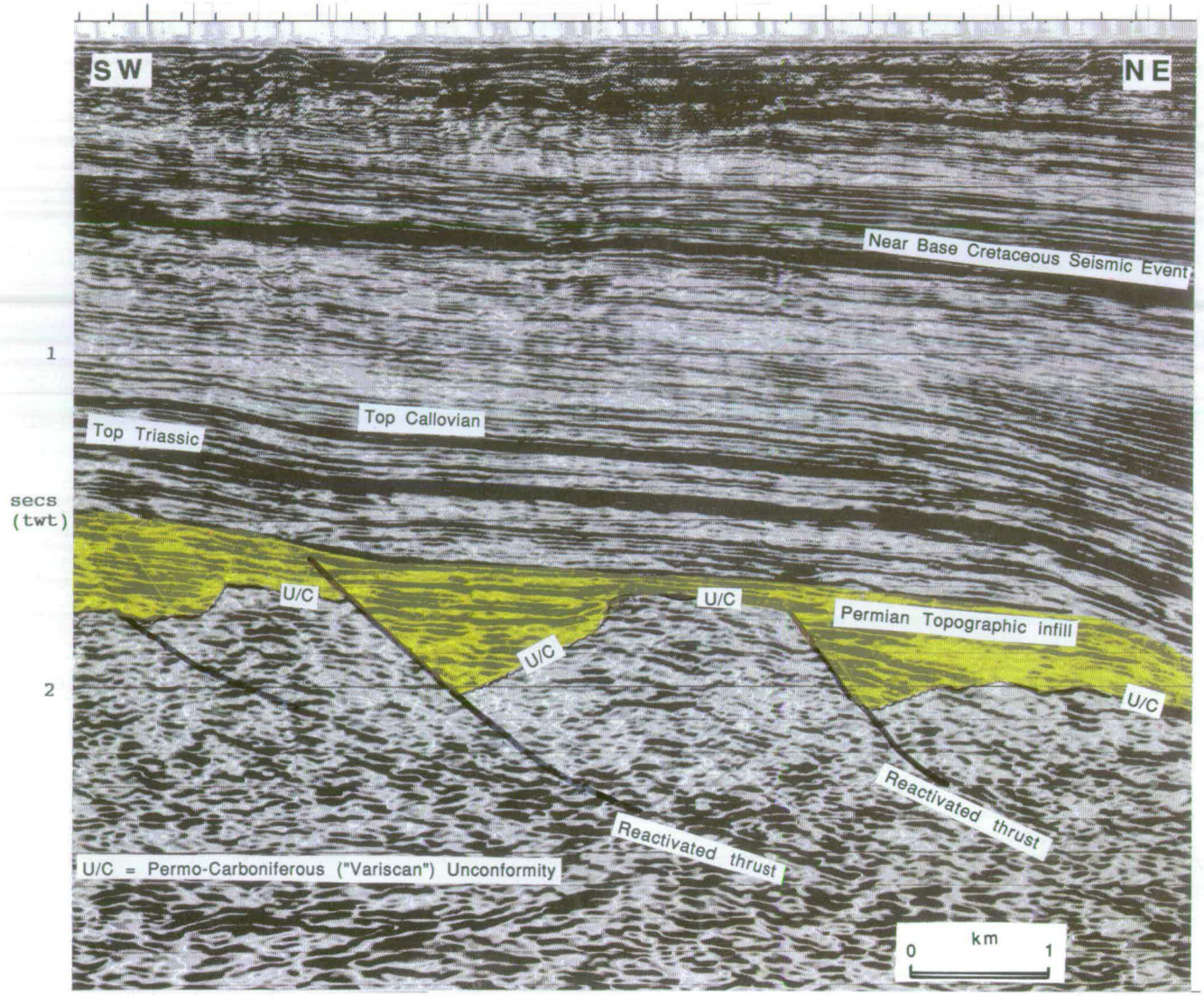

Fig. 4. Seismic line interpretation showing the topographic variation associated with the Permo-Carboniferous erosion surface highlighting the truncation of thrusted and folded Devonian sequences and their subsequent rejuvenation during the Permian as extensional features with a draped infill (highlighted in yellow). Line shown courtesy of BP Exploration.

thickening towards the Scottish mainland with maximum thicknesses occurring in the Sutherland Terrace area, between the GGF and Helmsdale Fault (Andrews and Brown 1987; Andrews *et al.* 1990; Underhill 1991*a,b*). These Early Jurassic sequences are interpreted to represent continued gentle, thermal (post-rift) subsidence following the Permian event.

Early–Middle Jurassic (Toarcian–Aalenian) regional uplift and Middle–Late Jurassic (Aalenian–Oxfordian) thermal subsidence

Evidence for a regional phase of relative uplift affecting the IMF during the Late Toarcian–Early Aalenian due to a regional doming event in the North Sea comes from stratigraphic information beyond the level of seismic resolution. These data show that a series of regional 'mid-Cimmerian' unconformities occur throughout the Middle Jurassic. The earliest and most significant of these unconformities occurs throughout the area, truncates Lower Jurassic successions including the Orrin Formation and shows progressive onlap of Bathonian–Oxfordian sequences towards the east (Underhill and Partington 1993 and in press; Stephen *et al.* 1993).

Although regional doming has not had any significant control on structural styles at a seismic scale, documentation and understanding of its cause and effects appear to have significance for the subsequent development of important structural styles (e.g. in the Late Jurassic rift episode). Regional mapping of the temporal and spatial variation of this event shows that similar relations exist over a wide area in the North Sea, which has been interpreted to be the result of regional doming ('Central North Sea Dome'; Hallam and Sellwood 1976; Ziegler 1982, 1990*a,b*) above a warm, diffuse and transient plume head (Underhill and Partington 1993 and in press). Evidence that progressive shallowing occurred during the Late Toarcian (i.e. the Orrin Formation in the IMF; Stephen *et al.* 1993) and sequences in other areas of Britain (i.e. Bridport Sands and Dunlin Group), suggests that uplift may have begun in the Lower Jurassic. Stratigraphic evidence suggests that the unconformity reached its maximum areal extent and hence, that the dome reached its climax during the Early Aalenian. Initial subsidence occurred during the Late Aalenian before subsiding gently during the Late Bajocian–Early Kimmeridgian (Underhill and Partington 1993 and in press), perhaps following a renewed phase of (Early Bajocian) uplift which created another relatively widespread erosive unconformity.

Most significantly for the subsequent development of diagnostic structural styles in the IMF, the stratigraphic data suggest that the trilete North Sea rift system already had an expression during the Middle Jurassic prior to the period of volcanism and most significant rifting. In the rift arms, significant deflection of the extent of maximum flooding may be seen

along each of the regions subsequently characterized by significant syn-sedimentary extension, suggesting that the IMF and Viking Graben formed topographic depressions prior to the onset of half-graben development (Underhill and Partington 1993 and in press). This suggests that lithospheric thinning and differential subsidence had already occurred along subsequent axes of deformation during uplift of the dome and persisted throughout the phase of subsidence resulting from the decay of this domal uplift.

Late Jurassic (Early Kimmeridgian–Late Portlandian) rifting

A drastic change in structural styles and basin architecture characterizes the Late Jurassic of the IMF. Seismic data demonstrate the development of numerous, classic half-graben across the area interpreted to result from dip-slip extension (Underhill 1991*a*,*b*). This phase of extension was the most significant for the development of potential hydrocarbon-bearing footwall structures adjacent to active extensional faults (e.g. Beatrice Field; Fig. 5).

Seismic mapping demonstrates that the dominant structural style of such extensional faults is as linear but discontinuous structures offshore. Onshore mapping gives additional insights into the potential significance of this structural discontinuity. The Helmsdale Fault is similar to the structures mapped on the seismic data in that it, too, is not one continuous fault as generally described, but consists of at least three sub-parallel en-échelon strands linked by overlapping relay ramps rather than transfer faults. Such zones appear to have been important conduits for sediment dispersal during the Late Jurassic (e.g. the early Kimmeridgian, Allt na Cuile Sandstone, Lothbeg Point). Accurate location of such syn-tectonic point sources may help locate additional reservoir sandstones offshore.

The duration of demonstrable syn-sedimentary fault activity may be gauged from the occurrence of divergent seismic reflector geometries and sedimentary evidence from onshore successions. These relations suggest that the area was initially deformed by continuous fault block rotation (Early Kimmeridgian) but was subsequently dominated by a passive sedimentary infill of topography created during discrete rift episodes (characterized by onlapping reflectors) during the Late Kimmeridgian–Late Portlandian (Underhill 1991*b*) in a similar fashion to that seen elsewhere (e.g. the Brae area in the South Viking Graben (Turner *et al.* 1987) and East Greenland (Surlyk 1978)).

Although these onlap relationships have previously been used by Exxon workers to derive their original eustatic curve purporting to show global sea-level changes (Vail and Todd 1981; Vail *et al.* 1984), recent analysis suggests that the onlap relationships are the result of syn-tectonic fault block rotation and limited sedimentary effects in a fully marine domain (*seismic marine onlap*, Underhill 1991*b*) and are not the direct result of global sea-level fluctuations in a coastal setting. It is also clear that the surfaces of onlap are not unconformities (*per se*), but are characterized by complete stratigraphic successions with no breaks. Hence, it seems likely that the surfaces of onlap are only recorded at seismic scale because they represent a considerable period of time. As such they probably represent condensed sections, analogous to those described by Partington *et al.* (1993).

Further complications to the dominantly extensional structural styles occur in association with Late Jurassic fault activity. Unusual structural geometries characterize several significant faults within the basin as exemplified by the Lossiemouth and Helmsdale faults (Figs 6 and 7). In both cases, hangingwall sequences dip steeply away from the fault before returning to the horizontal through a hangingwall synclinal structure. These are interpreted to form in response to differential compaction as a consequence of varying hangingwall and footwall depositional fills and as a result of a buttressing effect created by the underlying rigid footwall.

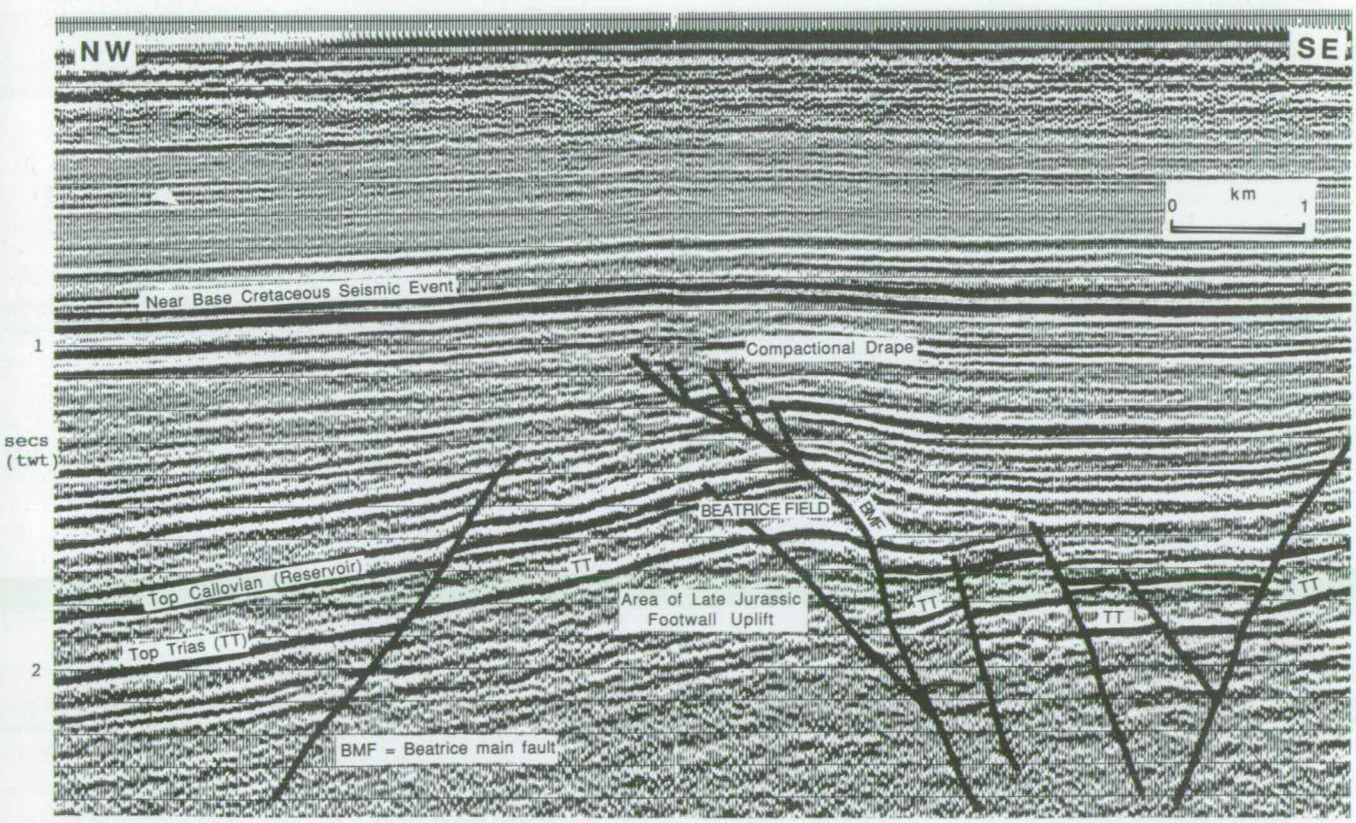

Fig. 5. NW–SE-trending cross-section of Beatrice Field showing the area of Late Jurassic footwall uplift associated with Beatrice Main Fault (BMF) which also shows a compactional drape geometry similar to other examples in the area such as the Lossiemouth (Fig. 6) and Helmsdale (Fig. 7) faults.

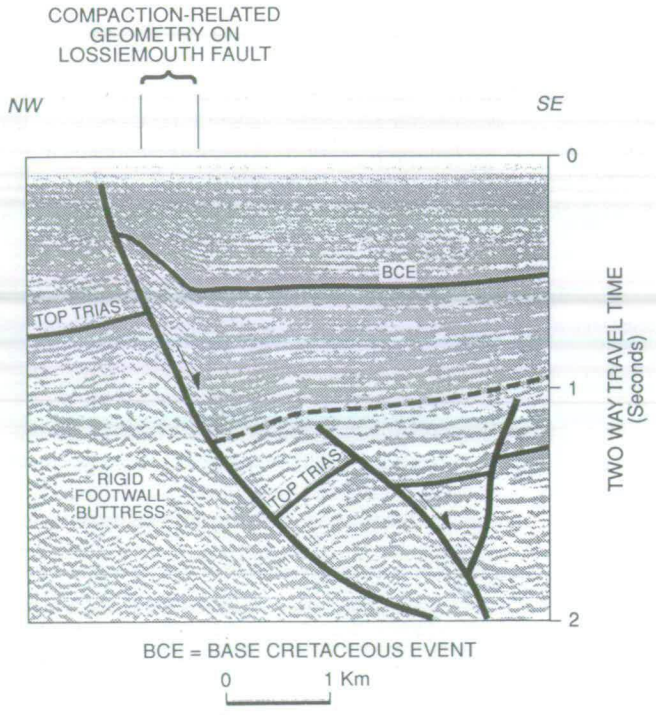

Fig. 6. Seismic line across the Lossiemouth Fault characterizing the unusual increase in depositional dips adjacent to extensional structures in the IMF and interpreted to result from the effects of compactional drape above.

The Late Jurassic sequences are capped by the second most prominent seismic reflector seen in the area: the 'Base Cretaceous Event'. As such, it is convenient to use this regional marker to define a distinct seismic package. However, in reality, this event does not appear to represent an unconformity but rather a condensed section (Rawson and Riley 1982), which lies beyond the level of seismic resolution. Furthermore, it appears to have formed in response to a drastic change in water circulation patterns (Rattey and Hayward 1993), rather than a particularly significant change in tectonic deformation and structural styles.

Cretaceous thermal subsidence

Early Cretaceous sequences are preserved and well-imaged above the 'Base Cretaceous Event'. They are largely characteized by well-defined onlapping reflectors, which show progressive onlap towards the basin's margins. Passive infill of well-defined Jurassic half-grabens occurred with evidence for significant shifts in depocentre location (compared to the Kimmeridgian) to areas adjacent to the Wick and Little Halibut faults (Andrews *et al.* 1990; Roberts *et al.* 1990). The Upper Cretaceous Chalk sequence can similarly be seen to drape most of the pre-existing topography and although commonly demonstrating progressive onlap onto basement highs, it is only occasionally interrupted by unconformities (Andrews *et al.* 1990).

The lack of evidence for divergent reflectors within the Cretaceous seismic sequences is suggestive of a passive infill of a pre-existing topography. Such an interpretation is supported by palaeontological evidence which suggests that the basin was underfilled at this time (BP proprietary data). Consequently, it seems most plausible that the area was undergoing a phase of thermal subsidence following the Late Jurassic rift episode.

This suggestion contrasts with many previous interpretations which have suggested that the IMF did not undergo Mesozoic thermal subsidence on account of its being interpreted as an isostatically uncompensated strike-slip basin (McQuillin *et al.* 1982; Barr 1985; Bird *et al.* 1987; Roberts *et al.* 1990). This suggestion was based on the regional gravity interpretation of the North Sea by Donato and Tully (1981) which shows a residual negative anomaly over the IMF which in turn has been taken to imply that the basin lies on unthinned lithosphere and formed as a result of upper crustal extension. Although the presence of such an anomaly cannot be disputed, the interpretation is open to question particularly in the light of seismic refraction studies which indicate that the area has experienced significant crustal thinning (Smith and Bott 1975; also see discussion at the end of this article). Indeed, the negative anomaly could be accounted for by the presence of a low density basement of Moine rocks and Caledonian granites beneath the IMF similar to those seen at outcrop on the Scottish Mainland. Although other possibilities also exist such as an heterogeneous stretching model for the IMF with isostatic compensation being offset laterally, the influence of unusual basement density variations may also explain why the negative anomaly can be seen to extend over much of the Scottish Mainland as well as the IMF.

Post-Cretaceous structural history

Regional structural styles

Although no Tertiary sequences occur within the Inner Moray Firth, it is still possible to deduce the basin development of the area during this period using regional tectonic and sedimentary analysis and local seismic evidence. Examination of sea bed

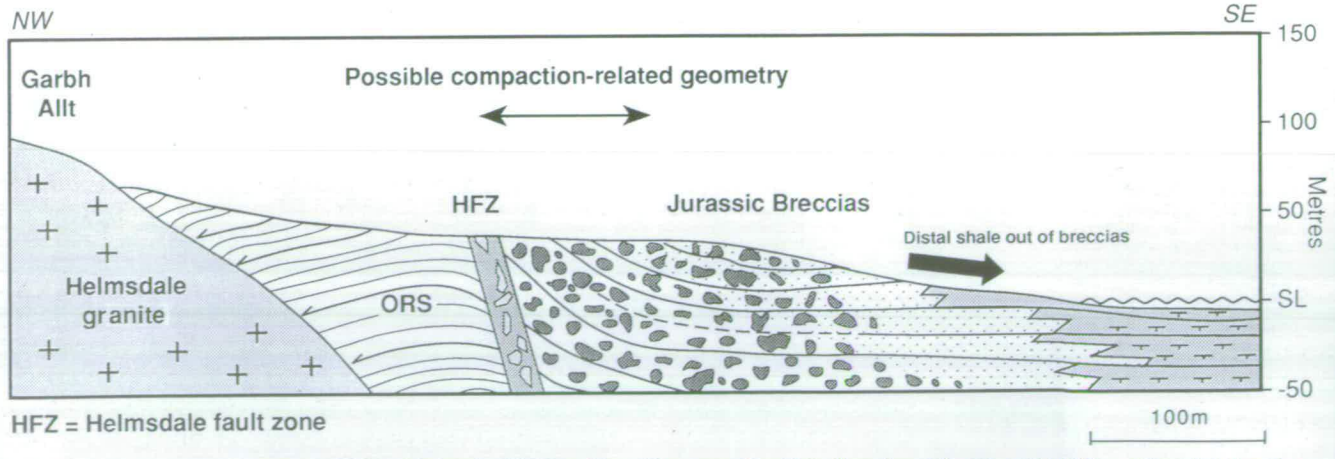

Fig. 7. W–E Cross-section across the Helmsdale Fault (HFZ) at Dun Glas, near Navidale (based on MacDonald 1985) and highlighting the increase in unusually steep dip to beds immediately adjacent to the fault, which are also believed to be the result of compactional drape adjacent to the Helmsdale Granite footwall buttress (cf. Fig. 6). ORS: Old Red Sandstone.

geological maps and seismic reflection profiles, which preserve rotated half-graben sequences, indicate that the IMF has been uplifted and tilted down to the east (Underhill 1991*a*). Integration of sonic velocity (Fig. 8), vitrinite reflectance and fission track data further suggest that relative uplift exceeded 1 km in the west of the basin and shows a gradual decrease eastwards to zero near the IMF–Outer Moray Firth transition (e.g. Hillis *et al.* 1992). Once corrected for post-erosional sedimentation, the total erosion values show little variation across the IMF with values of the order of 1 km suggesting that the area experienced significant regional tectonism.

The relative dating of the erosional event can be made using compaction data, evidence of depositional sequences in eastern parts of the Moray Firth and apatite fission track analysis. All imply that relative uplift occurred after the deposition of the Chalk Group (i.e. during the Tertiary). Although Tertiary sediments are only found in the extreme east of the IMF, the areas still further to the east contain large quantities of such sediments. Indeed, the deposition of prograding Paleocene deltaic sequences close to the Inner Moray Firth–Outer Moray Firth transition passing distally eastwards into slope fans and turbidites (Parker 1975; Rochow 1981) is consistent with the uplift and erosion of the Scottish Mainland, East Shetland Platform and the IMF during the Paleocene.

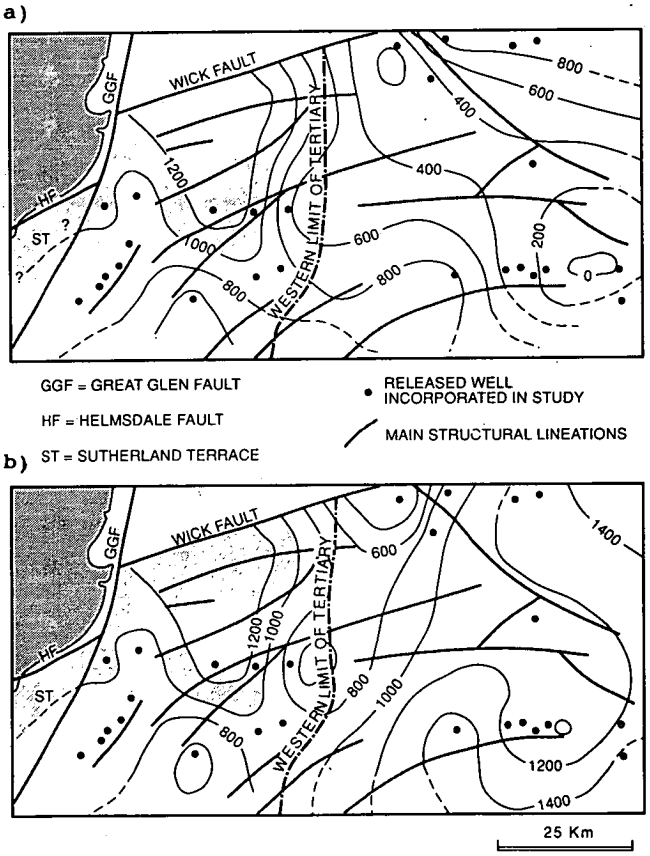

Fig. 8. Maps recording uplift and erosion: (**a**) apparent erosion; and (**b**) total erosion in the Inner Moray Firth, which suggest that the whole area has undergone at least 250 m of uplift after the Cretaceous. The most pronounced uplift appears to characterize the NW corner of the basin where figures exceed 1 km of uplift. The regional uplift is interpreted to result from intra-plate compression. Although only released well locations are shown, additional data from confidential wells have been incorporated into the diagrams.

Local Tertiary structural styles

Several local structural styles appear also to have resulted from Tertiary uplift. Many are highly localized to the NW corner of the basin and have not previously been described. For example, in the area of UKCS Block 12/16, close to the point where the Wick Fault terminates against the GGF, previously undocumented inversion structures can be found which affect Early Cretaceous sediments. These structures include a hangingwall anticline developed adjacent to the Wick Fault as a result of contractional reactivation (Fig. 9a). A spectacular 'short-cut fault' developed in association with the hangingwall anticline probably in response to increasing compressional stress as a result of buttressing against the Wick Fault.

In the region adjacent to the Wick Fault, numerous normal offsets can be seen on faults displacing Early Cretaceous sediments (e.g. Fig. 9b). However, such movement is not localized to the Wick fault area but can be found to have reactivated older extensional faults in the IMF such as the Smith Bank, Banff, Buckie and Halibut Horst Boundary faults (Roberts *et al.* 1990; Underhill 1991*a*), suggesting that the whole area experienced tectonic rejuvenation perhaps as a local expression of the regional deformation.

The most significant Tertiary fault activity within the IMF Basin occurs along the narrow Great Glen Fault zone (Fig. 10). Stratigraphic relations on seismic reflection profiles demonstrate that it was active after the Early Cretaceous. It displays typical 'flower structures' (*sensu* Harding 1990) with 'helicoidal' geometries similar to those described from sandbox experiments (Naylor *et al.* 1986) and suggestive of strike-slip movement (Fig. 10). The overall sense of movement can be shown to have a down to the east/southeast component. Although the sense of strike-slip movement cannot be determined directly from seismic profiles, isopach maps of the Mesozoic basin-fill suggest that any subsequent net strike-slip displacement was small, dextral and perhaps less than 10 km (Underhill 1991*a*).

Independent evidence for there being a period of Tertiary movement affecting the GGF can be found from onshore localities. Numerous dextral offsets of Tertiary dykes can be found adjacent to the Great Glen Fault zone on the island of Mull. This is consistent with the proposed dextral movement suggested by Holgate (1969) during the Tertiary and consistent with the dextral and down to the southeast-Permo-Carboniferous movement proposed by Speight and Mitchell (1979).

Tertiary movement on the GGF may also have contributed to the fold generation evident in the Sutherland Terrace between the Helmsdale and Great Glen faults from both offshore seismic reflection profiles (Fig. 11) and onshore exposures (Fig. 12). Onshore mapping demonstrates that these folds plunge northwest and southeast, at high angles ($>50°$ and which possibly increase with amount of rotation) adjacent to the Helmsdale Fault. Such fold orientations discount the possibility that they are classical inversion folds due to the hangingwall moving up the Helmsdale Fault and imply that fault-sub-parallel compression occurred in the Sutherland Terrace. It seems likely that dextral movement on the GGF would have created space problems in the Sutherland Terrace as it was compressed into the smaller area to the northeast where the faults merge (Fig. 12). The consequence of such movement was northeast–southwest compression and generation of northwest–southeast-orientated folds. It appears likely that the footwall to the Helmsdale Fault acted as a fixed buttress on which there was a limited amount of sinistral displacement (Fig. 12).

Regional Tertiary events responsible for the structures in the IMF

The proposed Tertiary structures are thought to have formed as a result of the combined effects of rifting of the North Atlantic Ocean and collision of the Alpine system. Together they caused the NW European domain to experience intra-plate deformation. The presence of a mantle 'hot-spot' at the

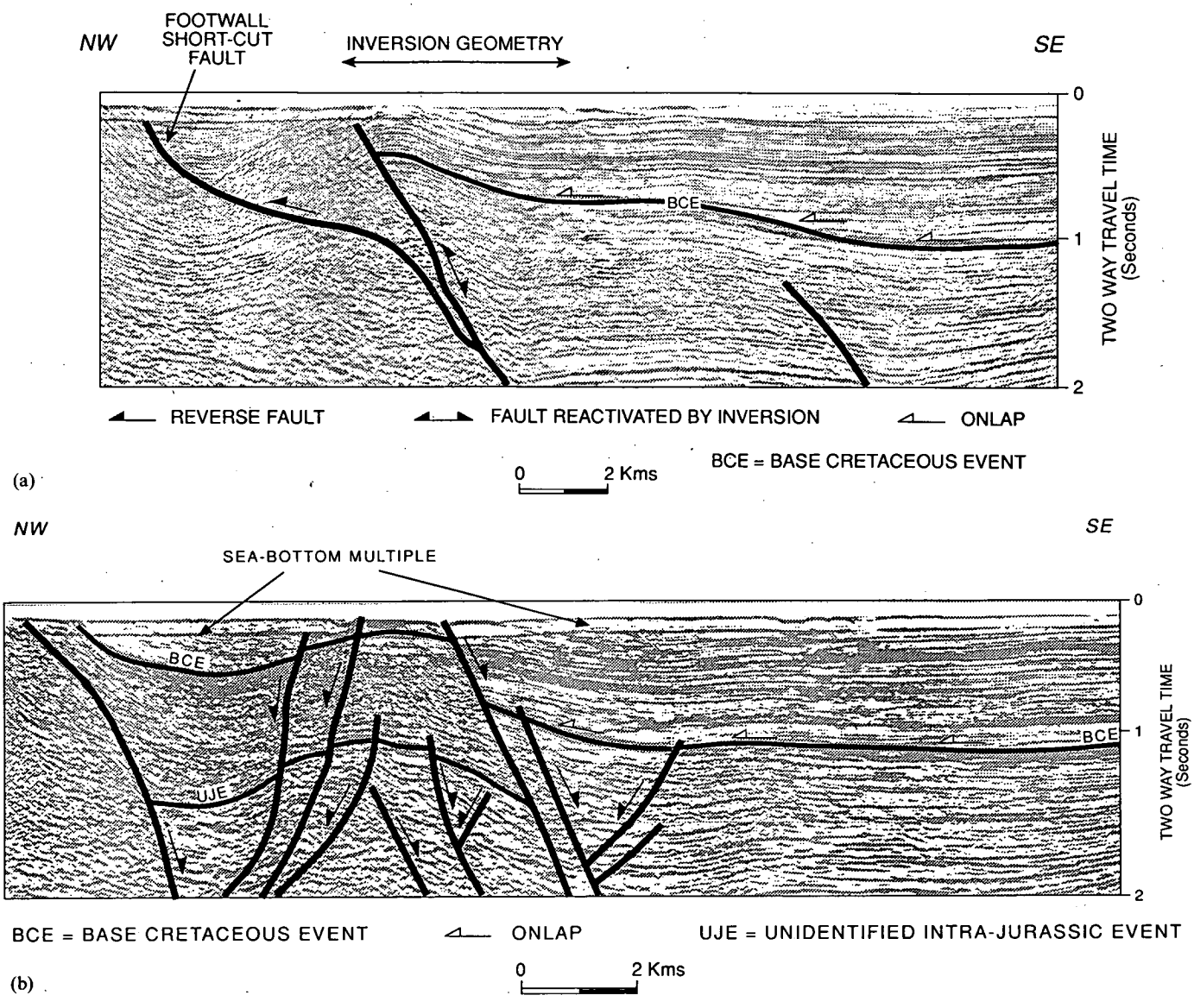

Fig. 9. Seismic line showing: (**a**) an inversion-related hangingwall anticline and associated short-cut fault developed adjacent to the Wick/Great Glen Fault intersection in the NW corner of the basin which is characterized by the greatest amounts of relative uplift and severest late-stage deformation; and (**b**) late horst-block geometries in the area of the Wick Fault probably formed in response to extensional stress related to doming and NE Atlantic opening.

time of rifting (White 1988, 1989) caused a broad bathymetric swell together with gravity and geoidal anomalies of approximate wavelength 2000 km and the production of large quantities of Tertiary volcanics (White 1989).

It is likely that the initial doming would produce extension at the surface, the magnitude of which would decrease radially away from the hot-spot. It is possible that the IMF would have experienced minor amounts of extension by virtue of its position at the margins of the dome (as witnessed by the post-Early Cretaceous extension around the Wick Fault). According to experimental studies (e.g. Dixon 1975; Withjack and Schiener 1982), strike-slip faulting might be expected in association with such domes, and may possibly account for the movements on the GGF and the Helmsdale Fault and hence, initiation of the folding in the Sutherland Terrace.

Upon rifting, the continental margins would not subside but remain relatively elevated due to continued hot-spot activity and the isostatic response of crust thickened by Tertiary volcanics. The consequences would be that the continental margins would experience minor amounts of compression as the margins were tilted back away from the newly formed rift. This compression would be the probable cause of the inversion seen around the Wick Fault and may have initiated movement of the Great Glen–Helmsdale fault system and its associated folding in the Sutherland Terrace. The evidence of westward-increasing uplift as seen in the IMF could, therefore, be interpreted as a direct consequence of doming and rift shoulder uplift. The highest amounts of relative uplift might, therefore, be expected in Western Scotland or beyond.

However, this model does not explain two major facts which are consequences of the total erosion exceeding the apparent erosion (Fig. 8). Firstly, in the IMF the total erosion shows no marked decrease from west to east. This would require unrealistic amounts of pre-rift doming and post-rift flexure of the rift shoulder. Secondly, decompacted burial curves for wells in the IMF with stratigraphy preserved into the Early Paleocene and in the Late Tertiary require an initial rapid subsidence phase followed by equally rapid uplift in order to satisfy the requirements of both erosion estimates and stratigraphy. Such a rapid burial cannot be easily accounted for by the North Atlantic active rifting model.

In order to explain the Tertiary features of the IMF and be

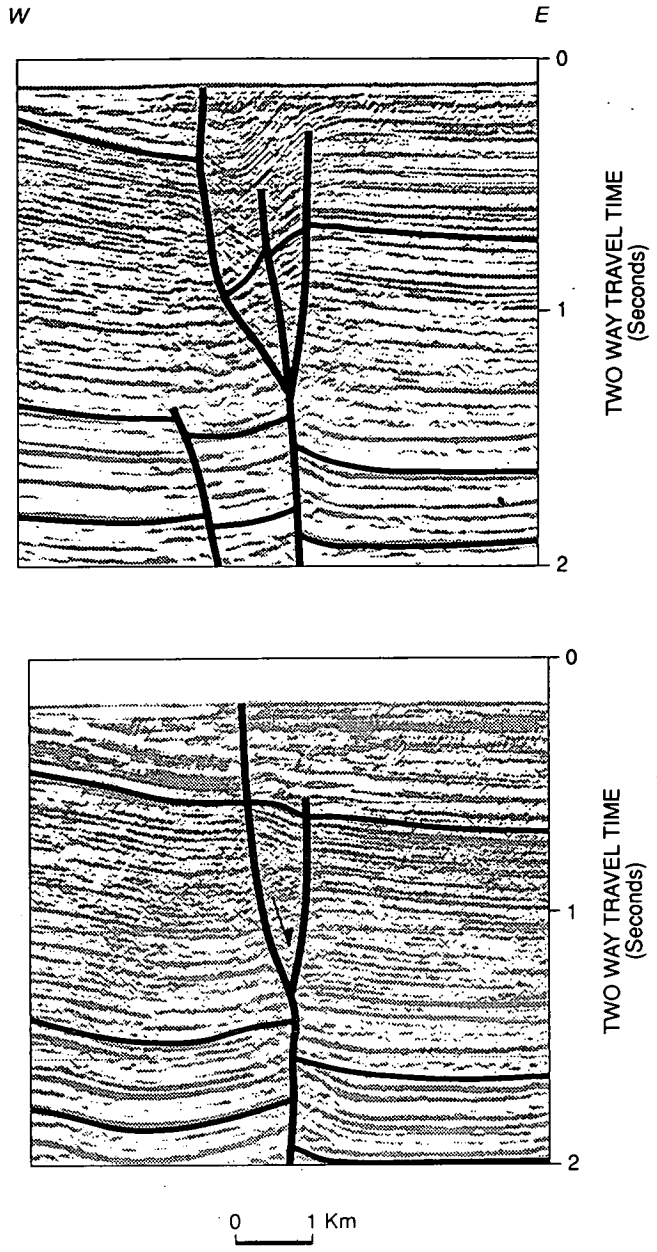

Fig. 10. Seismic lines to highlight the geometry associated with the Great Glen Fault and the nature of the 'negative flower' structure along strike believed to be the result of limited dextral strike-slip motion on the feature during the Tertiary.

consistent with the history of other areas of the northwestern European plate, it may be necessary to have recourse to alternative models which take the presence of the Alpine orogeny at the southern continental margin into account. The opening of the northeastern Atlantic in conjunction with the Alpine orogeny would result in intra-plate compressive stress (Ziegler 1987; Ziegler and Van Hoorn 1989). The orientation of such a compressive stress would be northwest–southeast. This would be consistent with that of England (1988) from the NW–SE and NNW–SSE orientation of Tertiary dyke swarms and Late Cenozoic mesofractures due to lateral escape (extension) in the foreland to the Alpine front (Bevan and Hancock 1986; Hancock and Bevan 1987).

Such a compressive stress regime could possibly account for the inversion seen in the NW corner of the basin (e.g. UKCS Block 12/16) and the dextral strike-slip motion on the Great Glen Fault. In addition, it would allow the explanation of the rapid burial and uplift observed in the IMF during the Tertiary to be explained in terms of differential compression between the crust and lithosphere. As stresses are transmitted with greater efficiency through the lithosphere compared to the crust this will allow heterogeneous compression, with the lithosphere thickening to a greater extent than the crust (Kusznir and Karner 1985; Hillis 1992). If the lithosphere thickens to a greater degree than the crust, rapid subsidence follows with rapid uplift following during the thermal re-equilibration phase. Furthermore, such a lithospheric mechanism for stress transmission through the plate allows the explanation of the differences in timing of Tertiary inversion throughout the plate (Ziegler, 1987). Consequently, it appears possible to integrate the Tertiary history of the IMF with that of other Mesozoic basins in Europe into a compressive intra-plate setting developed in response to North Atlantic rifting over a mantle plume to the northwest and the Alpine collisional events to the south.

Conclusions

(1) Structural styles in the Inner Moray Firth appear to be largely the result of three phases of extensional activity punctuated by periods of contraction, regional uplift and inversion.

(2) Onshore analogues suggest that active rifting which occurred during the Devonian was followed by more broad-based thermal subsidence prior to a phase of Permo-Carboniferous ('Variscan') contraction and inversion.

(3) Renewed extension characterized the Permian with the reactivation of some contractional structures as normal faults. Subsequent Permo-Triassic and Early Jurassic deposition occurred in a broad basin driven by thermal subsidence with little evidence for syn-sedimentary activity.

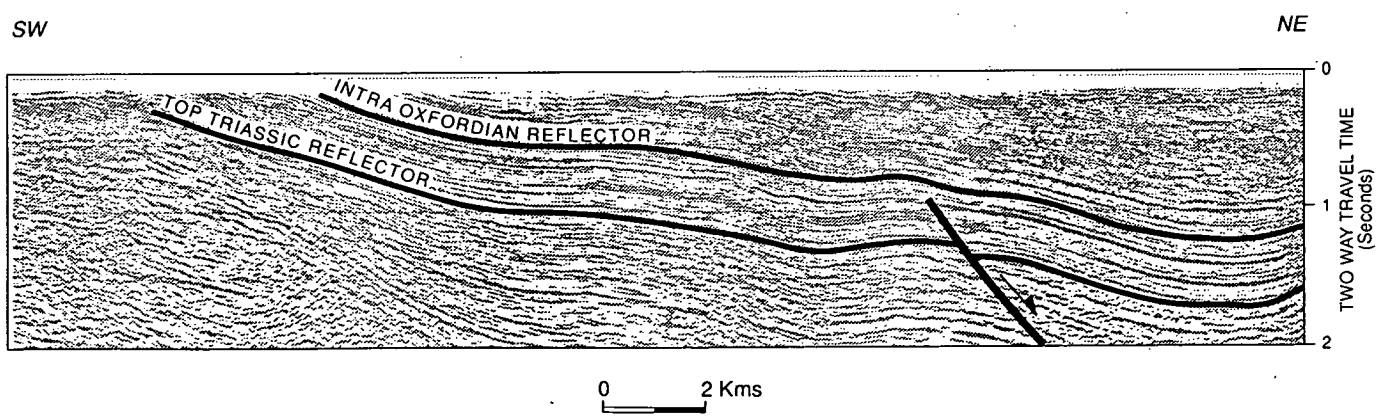

Fig. 11. Offshore SW–NE-trending seismic line from the Sutherland Terrace demonstrating the nature of large-scale folding interpreted to result from opposed senses of strike-slip motion on its bounding Helmsdale and Great Glen faults.

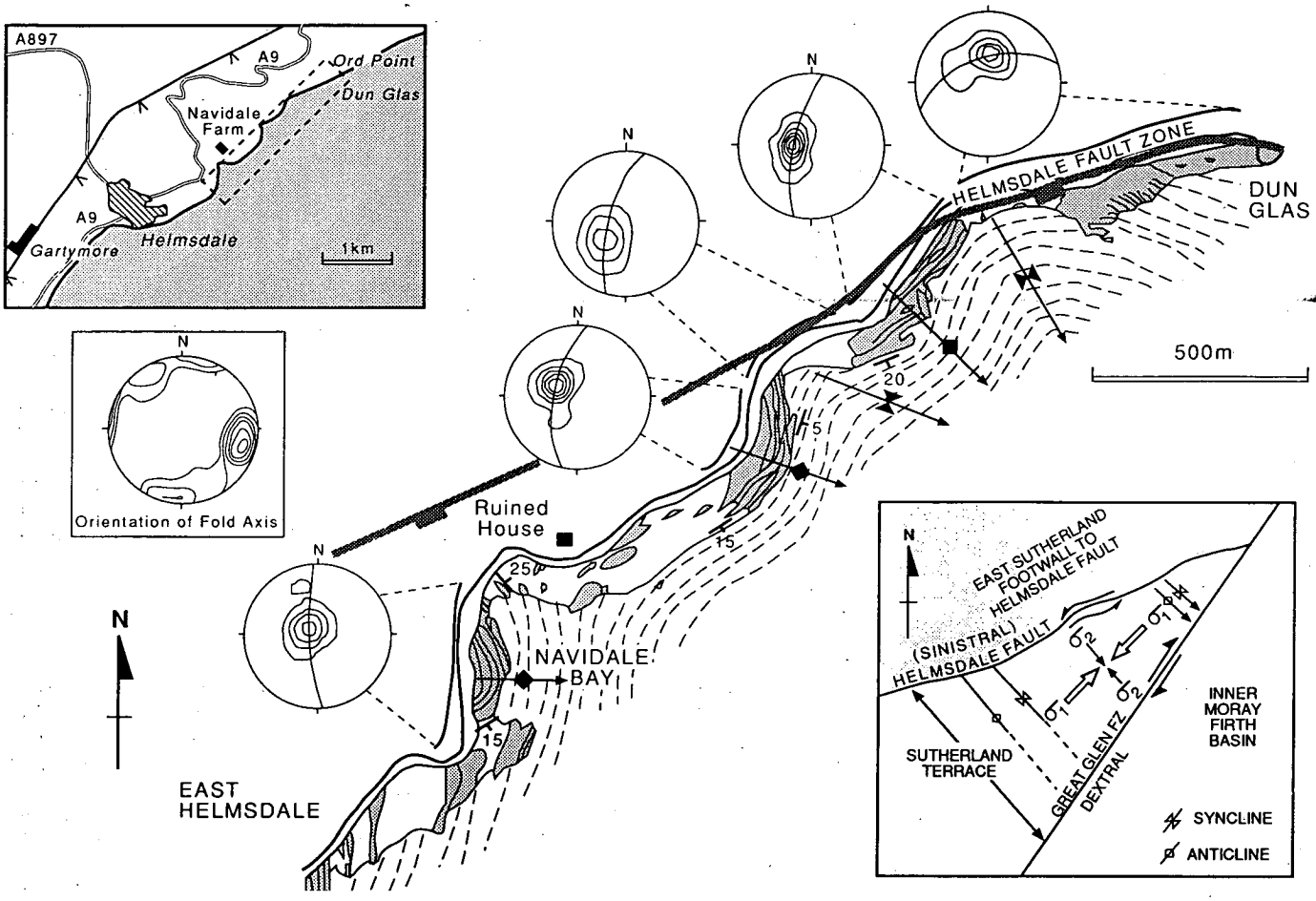

Fig. 12. Onshore map with stereonets showing the nature of individual, gently plunging folds formed at relatively high angles to the Helmsdale Fault. Inserts summarize all available stereonet data from folds along the whole length of the fault and show a cartoon depicting the stress regime interpreted to cause the structural styles in the Sutherland Terrace.

(4) Toarcian–Aalenian regional doming interrupted Early Jurassic gentle subsidence as a result of the rise of a warm and diffuse, transient plume head below the North Sea triple junction. Although its effects lie below seismic resolution, well-based stratigraphic studies show that it led to sublithospheric thinning in the Inner Moray Firth, which had major significance for later Jurassic extensional tectonism.

(5) Differential subsidence characterized Aalenian–Late Oxfordian times prior to the onset of significant Early Kimmeridgian–Portlandian extension, which largely followed the course of the earlier thinned crust and created numerous, syn-sedimentary half-graben analogous to those seen in the Viking Graben and Greenland.

(6) Subsequent Early Cretaceous sedimentation appears to have occurred in a gently subsiding, underfilled basin with progressive onlap onto its margin, which is interpreted to be the result of thermal subsidence which probably continued into Late Cretaceous times.

(7) The Inner Moray Firth area was characterized by significant Tertiary tectonism resulting from its intra-plate setting between the North East Atlantic rift and the Alpine fold-and-thrust belt which led to regional- and local-scale complex deformation.

(8) Although little evidence exists for strike-slip control on regional structural styles, limited dextral motions appear to characterize the Great Glen Fault during the (Permo-Carboniferous and more particularly Cenozoic) periods of contraction and inversion and caused the development of spectacular 'flower' geometries.

(9) Unusual structural geometries in the Sutherland Terrace area between the Great Glen Fault and the Helmsdale Fault appear to be the result of local transpression resulting from minor, opposed strike-slip motion on these faults during the Tertiary.

KT and JRU acknowledge the help of Shell, Esso, British Petroleum, Halliburton, Intera, GEOTRACK, GECO, Shelf Exploration, Arco, Horizon, Mobil and Unocal in providing data for the work. We thank Roger Scrutton, John Dixon, Richard Hillis, Sarah Prosser, Jon Turner and Al Fraser for useful discussion and Larry Wakefield, John Parker, Griff Cordey and Ceri Powell (Shell) for logistic support. Ceri Powell and Iain Bartholomew are thanked for providing information and constructive reviews. Mark Cattanach is acknowledged for drafting the diagrams. KT is sponsored by a Shell/Esso Studentship. JRU's relevant research was supported by NERC Grant GR9/692.

References

ANDREWS, I. J. AND BROWN, S. 1987. Stratigraphic evolution of the Jurassic, Moray Firth. *In*: BROOKS, J. AND GLENNIE, K. (eds) *Petroleum Geology of North-West Europe*. Graham & Trotman, London, 785–795.

——, LONG, D., RICHARDS, P. C., THOMSON, A. R., BROWN, S., CHESHER, J. A. AND MCCORMAC, M. 1990. *The Geology of the Moray Firth*, British Geological Survey, United Kingdom Offshore Report, HMSO, London.

ASTIN, T. R. 1990. The Devonian lacustrine sediments of Orkney, Scotland; implications for climatic cyclicity, basin structure and maturation history. *Journal of the Geological Society, London*, **147**, 105–120.

BARR, D. 1985. 3-D Palinspastic reconstruction of normal faults in the Inner Moray Firth: implications for extensional basin development. *Earth and Planetary Science Letters*, **75**, 191–203.

BARTHOLOMEW, I. D., PETERS, J. M. AND POWELL, C. M. 1993. Regional structural evolution of the North Sea: oblique-slip and the reactivation of basement lineaments. *In*: PARKER, J. R. (ed.) *Petroleum Geology of Northwest Europe: Proceedings of the 4th Conference*. Geological Society, London, 1109–1122.

BEVAN, T. G. AND HANCOCK, P. L. 1986. A late Cenozoic regional mesofracture system in southern England and northern France. *Journal of the Geological Society, London*, **143**, 355–362.

BIRD, T. J., BELL, A., GIBBS, A. D. AND NICHOLSON, J. 1987. Aspects of strike-slip tectonics in the Inner Moray Firth basin, offshore Scotland. *Norsk Geologisk Tidsskrift*, **67**, 353–369.

COWARD, M. P., ENFIELD, M. A., FISCHER, M. W. 1989. Devonian basins of Northern Scotland: extension and inversion related to Late Caledonian–Variscan tectonics. *In*: COOPER, M. A. AND WILLIAMS, G. D. (eds) *Inversion Tectonics*, Geological Society, London, Special Publication, **44**, 275–308.

DIMITROPOULOS, K. AND DONATO, J. A. 1981. The Inner Moray Firth Central Ridge, a geophysical interpretation. *Scottish Journal of Geology*, **17**, 27–38.

DIXON, J. M. 1975. Finite strain and progressive deformation in models of diapiric structures. *Tectonophysics*, **28**, 89–124.

DONATO, J. A. AND TULLY, M. C. 1981. A regional interpretation of North Sea gravity data. *In*: ILLING, L. V. AND HOBSON, G. D. (eds) *Petroleum Geology of the Continental Shelf of North-West Europe*, Heyden, London, 65–75.

ENGLAND, R. W. 1988. The early Tertiary stress regime in NW Britain: evidence from the patterns of volcanic activity. *In*: MORTON, A. C. AND PARSONS, L. M. (eds). *Early Tertiary Volcanism and the Opening of the NE Atlantic*, Geological Society, London, Special Publication, **39**, 381–389.

FROSTICK, L., REID, I., JARVIS, J. AND EARDLEY, H. 1988. Triassic sediments of the Inner Moray Firth, Scotland: early rift deposits. *Journal of the Geological Society, London*, **145**, 235–248.

HALLAM, A. AND SELLWOOD, B. W. 1976. Middle Mesozoic sedimentation in relation to tectonics in the British area. *Journal of Geology*, **84**, 301–321.

HANCOCK, P. L. AND BEVAN, T. G. 1987. Brittle modes of foreland extension. *In*: COWARD, M. P., DEWEY, J. F. AND HANCOCK, P. L. (eds). *Continental Extensional Tectonics*, Geological Society, London, Special Publication, **28**, 127–137.

HARDING, T. P. 1990. Identification of wrench faults using subsurface structural data: criteria and pitfalls. *American Association of Petroleum Geologists Bulletin*, **74**, 1590–1609.

HILLIS, R. R. 1992. A two-layer lithospheric compressional model for the Tertiary uplift of the southern United Kingdom. *Geophysical Research Letters*, **19**, 573–576.

——, THOMSON, K. AND UNDERHILL, J. R. Quantification of Tertiary erosion in the Inner Moray Firth by sonic velocity data from the Chalk and the Kimmeridge Clay. *Marine and Petroleum Geology*, (in press).

HOLGATE, N. 1969. Palaeozoic and Tertiary transcurrent movement on the Great Glen Fault. *Scottish Journal of Geology*, **5**, 97–139.

KUSZNIR, N. J. AND KARNER, G. 1985. Dependence of the flexural rigidity of the continental lithosphere on rheology and temperature. *Nature*, **316**, 138–142.

MACDONALD, A. C. 1985. *Kimmeridgian and Volgian fault-margin sedimentation in the Northern North Sea area*. PhD thesis, University of Strathclyde.

MCQUILLIN, R., DONATO, J. A. AND TULSTRUP, J. 1982. Development of basins in the Inner Moray Firth and the North Sea by crustal extension and dextral displacement of the Great Glen Fault. *Earth and Planetary Science Letters*, **60**, 127–139.

NAYLOR, H., TURNER, P., VAUGHAN, D. J. AND FALLICK, A. E. 1989. The Cherty Rock, Elgin: A petrographic and isotopic study of a Permo-Triassic calcrete. *Geological Journal*, **24**, 205–221.

NAYLOR, M. A., MANDL, G. AND SIJPESTEIJN, C. H. K. 1986. Fault geometries in basement-induced wrench faulting under different initial stress states. *Journal of Structural Geology*, **8**, 737–752.

PARKER, J. R. 1975. Lower Tertiary sand development in the Central North Sea. *In*: WOODLAND, A. W. (ed.) *Petroleum and the Continental Shelf of North West Europe*. Applied Science Publishers, London, 447–453.

PARTINGTON, M. A., MITCHENER, B. C., MILTON, N. J. AND FRASER, A. J. 1993. Genetic sequence stratigraphy for the North Sea Late Jurassic and Early Cretaceous: distribution and prediction of Kimmeridgian–Late Ryazanian reservoirs in the North Sea and adjacent areas. *In*: PARKER, J. R. (ed.) *Petroleum Geology of Northwest Europe: Proceedings of the 4th Conference*. Geological Society, London, 347–370.

RATTEY, R. P. AND HAYWARD, A. B. 1993. Sequence stratigraphy of a failed rift system: the Middle Jurassic to Early Cretaceous basin evolution of the Central and Northern North Sea. *In*: PARKER, J. R. (ed.) *Petroleum Geology of Northwest Europe: Proceedings of the 4th Conference*. Geological Society, London, 215–249.

RAWSON, P. F. AND RILEY, L. 1982. Latest Jurassic–Early Cretaceous Events and the 'Late Cimmerian Unconformity' in North Sea Area. *American Association of Petroleum Geologists Bulletin*, **66**, 2628–2648.

ROBERTS, A. M., BADLEY, M. E., PRICE, J. D. AND HUCK, I. W. 1990. The structural evolution of a transtensional basin: Inner Moray Firth, NE Scotland. *Journal of the Geological Society, London*, **147**, 87–103.

ROCHOW, K. A. 1981. Seismic stratigraphy of the North Sea 'Paleocene' deposits. *In*: ILLING, L. V. AND HOBSON, G. D. (eds) *Petroleum Geology of the Continental Shelf of NW Europe*. Heyden, London, 255–266.

ROGERS, D. A. 1987. *Devonian correlations, environments and tectonics across the Great Glen Fault*. PhD thesis, University of Cambridge.

——, MARSHALL, J. E. A. AND ASTIN, T. R. (1989). Devonian and later movements on the Great Glen fault system, Scotland. *Journal of the Geological Society, London*, **146**, 369–372.

SERANNE, M. 1992. Devonian extensional tectonics versus Carboniferous inversion in the northern Orcadian basin. *Journal of the Geological Society, London*, **149**, 27–37.

SMITH, P. J. AND BOTT, M. H. P. 1975. Structure of the Crust beneath the Caledonian Foreland and Caledonian Belt of the North Scottish Shelf Region. *Geophysics Journal of the Royal Astronomical Society*, **40**, 187–205.

SPEIGHT, J. M. AND MITCHELL, J. G. 1979. The Permo-Carboniferous dyke swarm of northern Argyll and its bearing on dextral displacement on the Great Glen Fault. *Journal of the Geological Society, London*, **1365**, 3–12.

STEPHEN, K. J., UNDERHILL, J. R., PARTINGTON, M. A. AND HEDLEY, R. J. 1993. The genetic sequence stratigraphy of the Hettangian to Oxfordian succession, Inner Moray Firth. *In*: PARKER, J. R. (ed.) *Petroleum Geology of Northwest Europe: Proceedings of the 4th Conference*. Geological Society, London, 485–505.

SURLYK, F. 1978. Submarine fan sedimentation along fault scarps on tilted fault blocks (Jurassic–Cretaceous boundary, East Greenland). *Gronlands Geologiske undersogelse Bulletin*, **28**, 1–103.

TURNER, C. C., COHEN, J. M., CONNELL, E. R. AND COOPER, D. M. 1987. A depositional model for the South Brae oilfield. *In*: BROOKS, J. AND GLENNIE, K. (eds) *Petroleum Geology of North-West Europe*. Graham & Trotman, London, 853–864.

UNDERHILL, J. R. 1991*a*. Implications of Mesozoic-Recent basin development in the western Inner Moray Firth, UK. *Marine and Petroleum Geology*, **8**, 359–369.

—— 1991*b*. Controls on Late Jurassic seismic sequences, Inner Moray Firth, UK North Sea: a critical test of a key segment of Exxon's original global cycle chart. *Basin Research*, **3**, 79–98.

—— AND BRODIE, J. A. A Re-evaluation of the Structural Geology of the Easter Ross Peninsula. *Journal of the Geological Society, London* (in press).

—— AND PARTINGTON, M. A. 1993. Jurassic thermal doming and deflation in the North Sea: implications of the sequence stratigraphic evidence. *In*: PARKER, J. R. (ed.) *Petroleum Geology of Northwest Europe: Proceedings of the 4th Conference*. Geological Society, London, 337–345.

—— AND —— Use of maximum flooding surfaces in determining a regional control on the Intra-Aalenian ('mid-Cimmerian') Sequence Boundary: Implications for North Sea basin development and Exxon's Sea Level Chart. *In*: POSAMENTIER, H. W. AND WIEMER, P. J. (eds) *Recent Advances in Sequence Stratigraphy*.

American Association of Petroleum Geologists Memoir (in press).

VAIL, P. R., HARDENBOL, J. AND TODD, R. G. 1984. Jurassic unconformities, chronostratigraphy, and sea-level changes from seismic stratigraphy and biostratigraphy. *In*: SCHLEE, J. S. (ed.) *International Unconformities and Hydrocarbon Accumulation.* American Association of Petroleum Geologists Memoir, **36**, 129–144.

—— AND TODD, R. G. 1981. Northern North Sea Jurassic unconformities, chronostratigraphy and sea-level changes from seismic stratigraphy. *In*: ILLING, L. V. AND HOBSON, G. D. (eds) *Petroleum Geology of the Continental Shelf of North-west Europe.* Heyden, London, 216–235.

WHITE, R. S. 1988. A hot-spot model for early Tertiary volcanism in the N Atlantic. *In*: MORTON, A. C. AND PARSONS, L. M. (eds) *Early Tertiary Volcanism and the Opening of the N.E. Atlantic.* Geological Society, London, Special Publication, **39**, 3–13.

—— 1989. Initiation of the Iceland Plume and Opening of the North Atlantic. *In*: TANKARD, A. J. AND BALKWILL, H. R. (eds) *Extensional tectonics and stratigraphy of the North Atlantic margins.* American Association of Petroleum Geologists Memoir, **46**, 149–154.

WITHJACK, M. O. AND SCHIENER, C. 1982. Fault Patterns Associated with Domes—An Experimental and Analytical Study. *American Association of Petroleum Geologists Bulletin*, **66**, 302–316.

ZIEGLER, P. A. 1982. *Geological Atlas of Western and Central Europe.* Elsevier, Amsterdam.

—— 1987. Late Cretaceous and Cenozoic intra-plate compressional deformations in the Alpine foreland—a geodynamic model. *Tectonophysics*, **137**, 389–420.

—— 1990*a*. Tectonic and palaeogeographic development of the North Sea rift system. *In*: BLUNDELL, D. J. AND GIBBS, A. D. (eds) *Tectonic Evolution of the North Sea Rifts.* Clarendon Press, Oxford, 1–36.

—— 1990*b*. *Geological Atlas of Western and Central Europe*, Second edition. Shell Internationale Petroleum Maapascappij B.V., Netherlands.

—— AND VAN HOORN, B. 1989. Evolution of North Sea Rift system. *In*: TANKARD, A. J. AND BALKWILL, H. R. (eds) *Extensional Tectonics and Stratigraphy of North Atlantic Margins.* American Association of Petroleum Geologists Memoir, **46**, 471–500.

Discussion

Question (A. Roberts, Badley Ashton, Winceby, Lincs)

In two previous papers I, together with my co-authors, suggested that the opening of the Moray Firth Basin was controlled by strike-slip motion on the Great Glen Fault. In the light of Dr Underhill's recent work I recognize that this suggestion was probably wrong and that extensional movement on the Helmsdale Fault was the dominant control on the architecture of the Inner Moray Firth. Rather than the Helmsdale Fault being a purely dip-slip structure, however, would Dr Underhill be able to reconcile his observations with an overall *c.* N–S extension direction in the Inner and Outer Moray Firth basins? Such an extension direction would be orthogonal to the large, uplifted Halibut Horst in the centre of the basin and would maintain an extensional (but not necessarily dip-slip) framework throughout the arcuate fault pattern of the Moray Firth. A N–S extension direction would, in addition, maintain kinematic compatibility with dominantly orthogonal opening of the Viking and Central Graben.

Answer (J. R. Underhill)

I would like to thank Alan for his statement and question Although Ken and I cannot rule out a minor component of oblique-slip on the Helmsdale Fault, our field observations do actually imply that the feature was of purely dip-slip origin in the Jurassic. Hence, we would still conclude that the folds which characterize regions adjacent to the fault and complicate interpretations are the result of syn-sedimentary compactional drape and subsequent minor sinistral transpression probably resulting from Tertiary reactivation and inversion.

As a result of our structural interpretations, our best estimates of the overall extensional direction during the Late Jurassic remain NW–SE or NNW–SSE in the local area. However, on the database currently available and analysed for our studies, we cannot rule out the possibility of different local extensional directions affecting *other areas* such as the Outer Moray Firth and beyond. Given the contrast in directions indicated in this question and by Bartholomew *et al.* 1993, resolution of the more regional stress field seems likely to stir considerable debate for some time to come.

Question (D. O'Driscoll, Texaco Ltd, Knightsbridge, London)

Can you comment on previously published models which refer to anomalously thinned continental crust under the Outer Moray Firth, Central Graben and South Viking Graben as opposed to thick, competent continental crust under the Inner Moray Firth, and on potential implications for dip-slip/extensional tectonics in the Inner Moray Firth?

Answer (J. R. Underhill and K. Thomson)

We welcome the opportunity to expand upon this important point. It seems that the idea that the Inner Moray Firth is underlain by anomalously thick continental crust is entrenched in the literature and has clouded many workers' thinking about basin development in the area. We agree that the most plausible explanation for the gravity data (originally given in Donato and Tulley 1981) is that the IMF consists of a thick Paleozoic and Mesozoic sedimentary succession, which is underlain by contrasting basement lithologies and local granitic intrusions (Dimitropoulos and Donato 1981) and hence, has highly variable basement densities. Although further interpretation of the gravity data has been taken to imply that no crustal thinning has occurred across the whole area and rather that basin development has occurred under the influence of thick-skinned, strike-slip tectonics, it is worth stressing that the evidence for unthinned crust must be restricted to western parts of the basin. Moreover, valid alternative interpretations of the raw data can be made which are compatible with the seismic data and field evidence for an extensional origin. Indeed, Smith and Bott (1975) have shown (in a rarely-quoted paper) that the results of a crustal refraction study can be used to demonstrate that although 'the [Inner Moray Firth] region lies within the Caledonian belt, it appears that substantial crustal thinning has subsequently occurred, probably contemporaneously with the formation of the sedimentary basin'. Furthermore, they are able to use the data to suggest that the thinning has reduced the crustal thickness to around 23 km beneath the basin (a similar figure to that beneath the Witch Ground Graben; Andrews *et al.* 1990). Thus, we believe that there is sufficient evidence to show that the Inner Moray Firth demonstrates crustal thinning of similar aspect to that described for the South Viking Graben and Central Graben and hence, was probably also controlled by extensional tectonics. Consequently, although there is a clear difference in detailed gravity signatures shown beneath western parts of the Inner Moray Firth (IMF) and these areas, perhaps implying that the actual amounts of stretching vary across the basin, independent evidence demonstrates that the IMF as a whole experienced crustal thinning. Hence, we think that many previously published interpretations, which have been biased towards the regional gravity data, without taking into account either its non-uniqueness, any local detailed variations or the independent evidence, are likely to be misleading and should be treated with caution.